Fluctuations and correlations of a biased tracer in a hardcore lattice gas

Pierre Illien

THÈSE DE DOCTORAT
DE L'UNIVERSITÉ PIERRE-ET-MARIE-CURIE

Spécialité : Physique
Ecole doctorale : Physique en Île-de-France

réalisée au

Laboratoire de Physique Théorique de la Matière Condensée

présentée par

Pierre ILLIEN

pour obtenir le grade de

DOCTEUR DE L'UNIVERSITÉ PIERRE-ET-MARIE-CURIE

Sujet de la thèse :

Fluctuations and correlations of a biased tracer in a hardcore lattice gas

Fluctuations et corrélations d'un traceur biaisé dans un gaz de coeurs durs

soutenue le 26 juin 2015

devant le jury composé de :

Ludovic BERTHIER	*Rapporteur*
David DEAN	*Rapporteur*
Leticia CUGLIANDOLO	*Examinatrice*
Kirone MALLICK	*Examinateur*
Andrea PARMEGGIANI	*Examinateur*
Olivier BÉNICHOU	*Directeur de thèse*
Raphaël VOITURIEZ	*Invité*

Contents

CHAPTER 0

Main results

This Chapter presents the main results of this thesis, and can be read independently.

0.1 Introduction

In various physical and biological systems, one encounters the situation when either an active particle or a particle subject to an external force travels through a quiescent host medium. A few stray examples include self-propelled particles in crowded environments, such as molecular motors, motile living cells or bacteria [83, 31], biased intruders in granular systems [27] or in colloidal suspensions [51]. Determining the dynamics of such a driven particle – called the tracer particle (TP) in what follows – in a host medium which hinders its motion is a challenging problem with important applications. For example, this question is central in the field of active microrheology, in which the properties of a medium are studied through the response of a probe to an external force [110, 102], and which have become a powerful experimental tool to study colloidal suspensions [51, 87], complex fluids [30, 29], live cells [10, 74] or actin networks [48, 122].

From a theoretical point of view, the difficulty lies in the modeling of the environment of the TP, which is constituted of a large number of interacting bath particles. In most approaches the microscopic structure of the bath is not taken into account explicitly, and the response functions are determined instead by using some effective bath dynamics [84]. While these approaches are rather efficient, they cannot account for the detailed correlations between the tracer particle and the fluctuating density profiles of the bath particles. In particular, when the tracer is biased, a jam of bath particles forms in front of it, and the density profiles become strongly asymmetric. This aspect becomes crucial when the probe and the medium particles have comparable sizes. In this regime, the fluctuations of the probe cannot be described correctly if the medium is treated as a continuous bath.

In this thesis, we consider the model where the TP is driven in a bath of Brownian hardcore particles performing symmetric random walks on a lattice (Fig. 1). More precisely, we consider a regular hypercubic lattice, which is populated by particles performing nearest-neighbor symmetric random walks, with a characteristic time τ^*. We also introduce a tracer particle, which performs a biased random walk, with a characteristic time τ. We assume that all the particles interact via hardcore interactions, which means that there is at most one particle per site.

In this model, the evolution of the mean position of the TP has been studied previously [15, 14, 13]. However, the behavior of its fluctuations and of the distribution of its position have not been studied yet. This lattice description is particularly adapted in the context presented above, as it allows to take into account explicitly the dynamics of the bath, and to study the statistical properties of the TP position. Moreover, lattice models of interacting particles are paradigmatic in nonequilibrium statistical mechanics and have received a lot of attention in the past decades [42, 82].

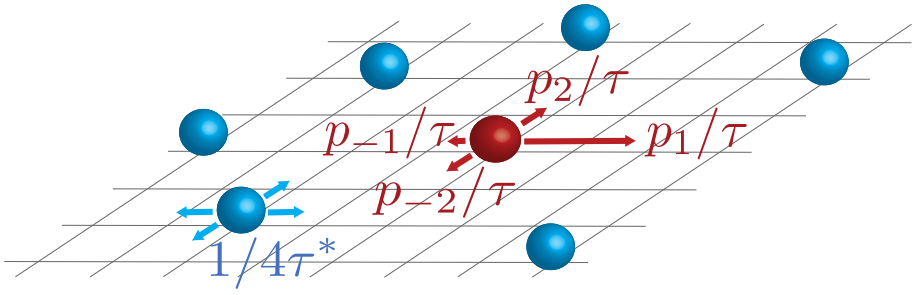

Figure 1: Biased tracer in a hardcore lattice gas. In this Figure, we represent the particular case of a two-dimensional lattice.

In the particular case where the bath of particles is very dense, exact results at leading order in the density of vacancies on the lattice are obtained. The analysis of these solutions reveals anomalous behaviors of the fluctuations of the position of the TP and of its mean position in confined geometries. For arbitrary density, one faces a complex N-body problem, for which we obtain approximate values of the mean, fluctuations and distribution of the position of the TP using a mean-field-type approximation. This approximation is shown to give exact results in the limits of a very dilute or very dense lattice gas.

0.2 Biased tracer diffusion in a high-density lattice gas

0.2.1 General method

We present here the general model of a biased tracer in a hardcore lattice gas. We consider a hypercubic lattice of arbitrary dimension. The lattice sites are occupied by hardcore particles performing symmetric random walks with a mean waiting time τ^*, with the restriction that the occupancy number for each site is at most equal to one. The fraction of occupied sites is denoted as ρ, whereas the vacancy density is denoted as ρ_0 (with $\rho_0 = 1 - \rho$). A tracer particle (TP) is also present on the lattice, and performs a nearest-neighbor biased random walk with a mean waiting time τ (in what follows, we will consider the particular case where $\tau = \tau^*$). The probability for the TP to make one step in direction $\boldsymbol{e}_\nu$ will be denoted by p_ν ($\nu \in \{\pm 1, \ldots, \pm d\}$). Although our results will be valid for any choice of the probabilities p_ν, it will be convenient to assume that the bias originates from an external force $\boldsymbol{F} = F\boldsymbol{e}_1$, so that the jump probability in direction ν is written

$$p_\nu = \frac{\mathrm{e}^{\beta\sigma \boldsymbol{F}\cdot\boldsymbol{e}_\nu/2}}{\sum_{\mu\in\{\pm 1,\ldots\pm d\}} \mathrm{e}^{\beta\sigma \boldsymbol{F}\cdot\boldsymbol{e}_\mu/2}}, \tag{1}$$

where the lattice spacing σ and the inverse temperature β are taken equal to one. Note that this choice of the jump probabilities fulfills the detailed balance condition.

In the high-density limit, the motion of the TP is mediated by the diffusion of the vacancies: the TP can move only if a vacancy visits one of its neighboring sites. In this situation, it is easier to describe the dynamics of the vacancies rather than the dynamics of the whole bath of particles. We adopt a discrete-time description, and at each time step, each vacancy moves according to the following rules: (i) if the TP is not adjacent to the vacancy, one neighbor is randomly selected and exchanges its position

with the vacancy; (ii) otherwise, if the TP is at position $\boldsymbol{X}$ and the vacancy at position $\boldsymbol{X}+\boldsymbol{e}_\nu$, the TP exchanges its position with the vacancy with probability $p_\nu = /[1-1/(2d)+p_\nu]$ and with probability $1/(2d-1+2dp_\nu)$ with any of the $2d-1$ other neighbors. We aim to obtain results at leading order in the density of vacancies ρ_0. Consequently, as the events involving two vacancies at the same site or on neighboring sites are of order $\mathcal{O}({\rho_0}^2)$, they do not contribute in the limit we consider and are not taken into account.

In the spirit of [22, 23], where tracer diffusion in the *absence* of bias was studied, we first consider an auxiliary problem involving a single vacancy, starting from site $\boldsymbol{Y}_0$. The TP, initially at site $\mathbf{0}$, can move only by exchanging its position with the vacancy. For the sake of simplicity, we first present in detail the particular case where the applied force is strong enough for the TP motion to be directed, so that $p_1 = 1$ and $p_\nu = 0$ for $\nu \neq 1$. Results in the general case of an arbitrary force, obtained along the same method, will be given next. We define the single-vacancy propagator $P_t^{(1)}(\boldsymbol{X}|\boldsymbol{Y}_0)$ as the probability for the TP to be at site $\boldsymbol{X} = n\boldsymbol{e}_1$ at time t knowing that the vacancy started from site $\boldsymbol{Y}_0$. An expression for this quantity can be obtained by summing over the number of steps taken by the TP up to time t, over the directions of these steps, and over the length of the time intervals elapsed between consecutive steps. The single-vacancy propagator can then be written as :

$$P_t^{(1)}(\boldsymbol{X}|\boldsymbol{Y}_0) = \delta_{n,0}\left(1-\sum_{j=0}^{t} F_j(\boldsymbol{Y}_0)\right) + \sum_{m_1=1}^{+\infty}\cdots\sum_{m_n=1}^{+\infty}\sum_{m_{n+1}=0}^{+\infty}\delta_{m_1+\ldots+m_{n+1},t}\left(1-\sum_{j=0}^{m_{n+1}} F_j(-\boldsymbol{e}_1)\right)F_{m_n}(-\boldsymbol{e}_1)\ldots F_{m_2}(-\boldsymbol{e}_1)F_{m_1}(\boldsymbol{Y}_0), \tag{2}$$

where $F_t(\boldsymbol{Y}_0)$ is the probability that the vacancy, which starts its random walk at the site $\boldsymbol{Y}_0$, arrives at the origin $\mathbf{0}$ for the first time at the time step t, and where the second sum in (2) is equal to zero if $n \leq 0$. The first term in the right- hand side of (2) represents the event that at time t, the TP has not been visited by the vacancy, while the second one results from a partition on the waiting times m_j between the successive visits of the TP by the vacancy. The Fourier-Laplace transform of the single-vacancy propagator is then easily found to be given by :

$$\widehat{\widetilde{P}}^{(1)}(\boldsymbol{k}|\boldsymbol{Y}_0;\xi) = \frac{1}{1-\xi}\left[1+\frac{\widehat{F}(\boldsymbol{Y}_0;\xi)(\mathrm{e}^{\mathrm{i}k_1}-1)}{1-\mathrm{e}^{ik_1}\widehat{F}(\boldsymbol{e}_{-1};\xi)}\right], \tag{3}$$

where the discrete Laplace transform (or generating function) of a time-dependent function $\phi(t)$ has been denoted by $\widehat{\phi}(\xi) = \sum_{t=0}^{\infty}\phi(t)\xi^t$ and the Fourier transform of a space-dependent function $\psi(\boldsymbol{r})$ by $\widetilde{\psi}(\boldsymbol{k}) = \sum_{\boldsymbol{r}}\mathrm{e}^{\mathrm{i}\boldsymbol{k}\cdot\boldsymbol{r}}\psi(\boldsymbol{r})$. Note that the single-vacancy propagators are only determined in terms of the first-passage time densities (FPTD) $F_t(\mathbf{Y_0})$.

The second step of the calculation consists in reducing in the dense limit $\rho_0 \to 0$ the full problem to the single-vacancy problem. This is conveniently done by starting from a finite number M of vacancies, of initial positions $\boldsymbol{Y}_0^{(1)},\cdots,\boldsymbol{Y}_0^{(M)}$ on a finite lattice of N sites. The key point is that, in the limit $\rho_0 = M/N \to 0$, the vacancies contribute independently to the motion of the TP, so that the full

propagator can be written at leading order in ρ_0 in terms of the single vacancy propagator:

$$P_t(\boldsymbol{X}|\boldsymbol{Y}_0^{(1)},\cdots,\boldsymbol{Y}_0^{(M)}) \underset{\rho_0\to 0}{\sim} \sum_{\boldsymbol{X}_0^{(1)}} \cdots \sum_{\boldsymbol{X}_0^{(M)}} \delta_{\boldsymbol{X},\boldsymbol{X}_0^{(1)}+\cdots+\boldsymbol{X}_0^{(M)}} \prod_{j=1}^{M} P_t^{(1)}(\boldsymbol{X}_0^{(j)}|\boldsymbol{Y}_0^{(j)}). \tag{4}$$

Averaging next over the initial positions of the vacancies, taking the Fourier transform and finally going to the thermodynamic limit ($M,N\to\infty$ with $M/N=\rho_0$ fixed), the logarithm of the Fourier transform of the propagator can be written at leading order in ρ_0 as $\ln \widetilde{P}_t(\boldsymbol{k}) \sim_{\rho_0\to 0} -\rho_0\Omega_t(\boldsymbol{k})$, where

$$\widehat{\Omega}(\boldsymbol{k};\xi) = \left[\frac{1}{1-\xi} - \mathrm{e}^{ik_1}\widehat{\widetilde{P}}^{(1)}(\boldsymbol{k}|\boldsymbol{e}_{-1};\xi)\right] \sum_{\boldsymbol{Y}\neq 0} \widehat{F}(\boldsymbol{Y};\xi). \tag{5}$$

The function $\widehat{\Omega}(\boldsymbol{k};\xi)$ is simply related to the cumulant generating function $\ln\left\langle \mathrm{e}^{\mathrm{i}\boldsymbol{k}\cdot\boldsymbol{X}_t}\right\rangle$, so that the cumulants of $\boldsymbol{X}_t$ are given by the successive derivatives of Ω_t:

$$\boldsymbol{\kappa}^{(n)}(t) \sim -\frac{\rho_0}{\mathrm{i}^n}\sum_{\nu=1}^{d}\left(\left.\frac{\partial^n\Omega_t}{\partial {k_\nu}^n}\right|_{\boldsymbol{k}=\boldsymbol{0}}\right)\boldsymbol{e}_\nu. \tag{6}$$

Consequently, the determination of the function $\widehat{\Omega}(\boldsymbol{k};\xi)$ and therefore of the cumulants of the position of the TP only relies on the FPTD $F_t(\boldsymbol{Y}_0)$ (probability for a vacancy to visit the origin for the first-time at time t starting from site $\boldsymbol{Y}_0$).

When the tracer is no longer directed and undergoes an arbitrary bias, we show that the single-vacancy propagators and the ultimate expression of $\widehat{\Omega}(\boldsymbol{k};\xi)$ only depends on conditional FPTD $F_t^*(\boldsymbol{0}|\boldsymbol{e}_\mu|\boldsymbol{Y}_0)$ (probability for a vacancy to visit the origin for the first-time at time t starting from $\boldsymbol{Y}_0$ and being at site $\boldsymbol{e}_\mu$ at time $t-1$). These conditional FPTD are relative to the random walk of a vacancy on a lattice in presence of a biased TP that locally modifies the evolution rules of the vacancy. The vacancy then performs a symmetric random walk on every sites of the lattice, excepted on the neighboring sites of the TP, on which the evolution rules of the vacancies are perturbed because of the bias experienced by the TP. The conditional FPTD are computed using standard techniques for random walks on lattices with defectives site [58], and written in terms of the propagators associated to the simple symmetric random walk on the considered structure. These calculations yield explicit expressions for the conditional FPTD but are very lengthy, so that the help from a computer algebra software is required.

In this framework, we will study the fluctuations of the position of the TP as well as the other cumulants of its position. The dependence of these quantities on the different parameters of the problem (time, force, density, lattice dimension) are shown to be non-trivial. We first consider the case of a one-dimensional lattice, for which we determine the probability distribution of the TP position. We consider higher-dimensional lattices, and study the fluctuations and mean of the position of the TP. We then study the higher-order cumulants of the distribution, and show that there exists universal formulae to describe their behavior in terms of the properties of a simple random walk on the considered structures. Finally, we provide a simplified description that correctly captures the physical mechanisms at stake.

0.2.2 One-dimensional lattice

We first consider the case of a one-dimensional lattice. The transport properties of a biased TP in a one-dimensional hardcore lattice gas are related to the well-known problem of single-file diffusion. In

this paradigmatic model, all the particles are identical and perform symmetric nearest-neighbor random walks with the hardcore exclusion constraint. In the absence of a bias, it has been shown that the fluctuations of a tagged particle are anomalous and that they grow subdiffusively as $\sqrt{t}$ [54, 4]. The situation where the tagged particle is biased also raised some attention. In this case, the mean position itself has a nontrivial behavior, and it was shown that it was growing as $\sqrt{t}$ with a prefactor that is a function of the bias and which was given as the implicit solution of an equation [25, 72].

In the presence of a bias, the fluctuations of the position of the TP and its distribution have not been studied yet. In the high-density limit, we use the general framework presented in the previous section. We express the cumulant generating function of the TP position in terms of the first-passage time densities (FPTD) associated to the random walk of the vacancies. These FPTD are calculated with standard methods from the theory of random walks on lattices. It is shown that all the odd cumulants on the one hand, and all the even cumulants on the other hand are identical in the long-time limit, and scale as $\sqrt{t}$:

$$\lim_{\rho_0\to 0} \frac{\kappa^{(\mathrm{odd})}(t)}{\rho_0} \underset{t\to\infty}{\sim} (p_1 - p_{-1})\sqrt{\frac{2t}{\pi}}, \tag{7}$$

$$\lim_{\rho_0\to 0} \frac{\kappa^{(\mathrm{even})}(t)}{\rho_0} \underset{t\to\infty}{\sim} \sqrt{\frac{2t}{\pi}}. \tag{8}$$

In particular, we observe that fluctuations of the TP position grow subdiffusively as $\sqrt{t}$ and are independent of the bias. Finally, the distribution of the TP position is shown to be given by the Skellam distribution:

$$\mathcal{P}_t(X) \underset{\rho_0\to 0}{\sim} \exp\left(-\kappa^{(\mathrm{even})}(t)\right) \left(\frac{\kappa^{(\mathrm{even})}(t) + \kappa^{(\mathrm{odd})}(t)}{\kappa^{(\mathrm{even})}(t) - \kappa^{(\mathrm{odd})}(t)}\right)^{X/2} \mathrm{I}_X\left(\sqrt{\kappa^{(\mathrm{even})}(t)^2 - \kappa^{(\mathrm{odd})}(t)^2}\right), \tag{9}$$

where $\mathrm{I}_n(\cdot)$ is a modified Bessel function of the first kind. The rescaled variable $(X_t - \langle X_t\rangle)/\sqrt{\mathrm{Var}(X_t)}$ is shown to be distributed accordingly to a Gaussian distribution.

The one-dimensional geometry yields an anomalous evolution of the cumulants of the position of the TP. In particular, the fluctuations of the TP position are shown to grow subdiffusively. Indeed, because of the exclusion interactions and of the geometry of the lattice, the particles cannot bypass each other, and the displacement of a given particle on progressively larger distances requires the motion of more and more particles in the same direction. Then, the motion of the particles becomes strongly correlated, and the fluctuations of the TP are subdiffusive.

0.2.3 Confinement-induced superdiffusion

We now consider higher-dimensional lattices. As it was emphasized in Section 0.2.1, an important technical point is that for small values of the density of vacancies ρ_0, the dynamics of the TP can be deduced from analyzing the joint dynamics of the TP and a single isolated vacancy. Exact asymptotic expressions of the fluctuations of the TP position in the direction of the force, denoted by $\kappa_1^{(2)}(t)$, are obtained for various geometries and for arbitrary values of the jump probabilities p_ν (probability for the TP to make a jump in direction ν). These are valid at large times and low vacancy densities, and are summarized below.

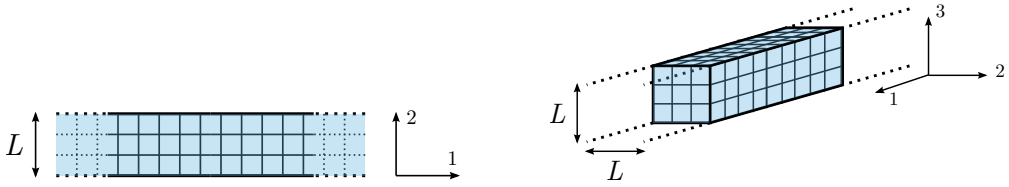

Figure 2: Stripe-like (left) and capillary-like (right) geometries. The lattice is infinite in the first direction (which will be the direction of the external force imposed on the TP), and finite of width L with periodic boundary conditions in the other directions.

Superdiffusive regime. First, our approach predicts the following large-t behaviour of the variance $\kappa_1^{(2)}(t)$ in the leading order of ρ_0 for different lattices:

$$\lim_{\rho_0\to 0}\frac{\kappa_1^{(2)}(t)}{\rho_0}\underset{t\to\infty}{=}2a_0^2\times\begin{cases}(4/3\sqrt{\pi}L)\,t^{3/2} & \text{2D stripe,}\\ (2\sqrt{2/3\pi}/L^2)\,t^{3/2} & \text{3D capillary,}\\ \pi^{-1}t\ln(t) & \text{2D lattice,}\\ \left[A+\frac{1}{2a_0}\frac{p_1-p_{-1}}{p_1+p_{-1}}\right]t & \text{3D lattice,}\end{cases} \tag{10}$$

where 2D stripes and 3D capillaries are quasi-one-dimensional geometries, which are infinite in the direction of $\boldsymbol{e}_1$ and finite of width L in the other directions (Fig. 2). In (10), the coefficient a_0 depends on the bias

$$a_0 \;=\; \frac{p_1-p_{-1}}{1+\frac{2d\alpha}{2d-\alpha}(p_1+p_{-1})}, \tag{11}$$

$A=\widehat{P}(\mathbf{0}|\mathbf{0};1)+2(13\alpha-6)/[(2+\alpha)(\alpha-6)]$, d is the system dimension, $\alpha=\lim_{\xi\to 1^-}[\widehat{P}(\mathbf{0}|\mathbf{0};\xi)-\widehat{P}(2\boldsymbol{e}_1|\mathbf{0};\xi)]$ and $\widehat{P}(\boldsymbol{r}|\boldsymbol{r}_0;\xi)$ is the generating function (discrete Laplace transform) of the propagator of a symmetric random walk on the considered lattice. These surprisingly simple exact expressions unveil the dependence of the variance on time, width L of the stripe or of the capillary, and on the bias. A number of important conclusions can be drawn from this result:

- Strong superdiffusion with exponent $3/2$ takes place in confined, quasi-1D geometries, those being, infinitely long 3D capillaries and 2D stripes. This result is quite counterintuitive: indeed, in the absence of driving force it is common to encounter diffusive, or even subdiffusive growth of the fluctuations of the TP position in such crowded environments, however not superdiffusion.

- The superdiffusion in such systems emerges beyond (and therefore can not be reproduced within) the linear response-based approaches. If the bias originates from an external force F and if the jump probabilities of the TP are given by (1), the prefactor in the superdiffusive law is proportional to F^2 when $F\to 0$. Despite the presence of the superdiffusion, the Einstein relation is nonetheless valid for systems of arbitrary geometry due to subdominant (in time) terms whose prefactor is proportional to F.

- In unbounded 3D systems $\kappa_1^{(2)}(t)$ grows diffusively and not superdiffusively.

- Finally, this shows that superdiffusion is geometry-induced and the recurrence of the random walk performed by a vacancy is a necessary condition in order for superdiffusion to occur. However, this condition is not sufficient. Indeed, on one-dimensional lattices, although the random walk of a vacancy is recurrent, the behavior of the TP is not superdiffusive (see Section 0.2.2).

Giant diffusion regime. The exact analytical result in (10) provides explicit criteria for superdiffusion to occur. Technically, this yields the behavior of the variance when the limit $\rho_0 \to 0$ is taken before the large-t limit. It however does not allow us, due to the nature of the limits involved, to answer the question whether the superdiffusion is the ultimate regime (or just a transient), which requires the determination of $\lim_{t\to\infty} \kappa_1^{(2)}(t)$ at fixed ρ_0. Importantly, we find that the order in which these limits are taken is crucial in confined geometries and show that $\lim_{t\to\infty} \lim_{\rho_0\to 0} \kappa_1^{(2)}(t) \neq \lim_{\rho_0\to 0} \lim_{t\to\infty} \kappa_1^{(2)}(t)$. In fact, the effective bias experienced by a vacancy between two consecutive interactions with the TP, originating from a non zero velocity of the TP, dramatically affects the ultimate long-time behavior of the variance in confined geometries.

More precisely, we show that the superdiffusive regime is always transient for an experimentally relevant system with ρ_0 fixed, while the long-time behavior obeys

$$\lim_{t\to\infty} \frac{\kappa_1^{(2)}(t)}{t} \underset{\rho_0\to 0}{=} \begin{cases} B & \text{quasi-1D,} \\ 4a_0^2\pi^{-1}\rho_0 \ln({\rho_0}^{-1}) & \text{2D lattice,} \\ 2a_0^2\left[A + \frac{1}{2a_0}\frac{p_1-p_{-1}}{p_1-p_{-1}}\right]\rho_0 & \text{3D lattice,} \end{cases} \tag{12}$$

i.e., is always diffusive. The constant B only depends on the driving force F: this long-time diffusive behavior is particularly remarkable in quasi-1D systems, in which the variance is independent of ρ_0.

Full dynamics: scaling regime and cross-over. Finally, our approach provides the complete time evolution of the variance in the regime corresponding to $\rho_0 \ll 1$ and at a sufficiently large time t, that interpolates between the two limiting regimes of superdiffusion and giant diffusion listed above. In this regime, it is found that

$$\kappa_1^{(2)}(t) \sim \begin{cases} t\widetilde{f}(\rho_0^2 t)/L^{d-1} & \text{quasi-1D,} \\ -\frac{2a_0^2}{\pi}\rho_0 t \ln\left((\rho_0 a_0)^2 + 1/t\right) & \text{2D lattice,} \\ 2a_0^2\left[A + \frac{1}{2a_0}\frac{p_1-p_{-1}}{p_1-p_{-1}}\right]\rho_0 t & \text{3D lattice,} \end{cases} \tag{13}$$

where the scaling function $\widetilde{f}$ is explicitly calculated and satisfies

$$\widetilde{f}(x) \propto \begin{cases} x^{1/2} & \text{when } x \ll 1, \\ \text{constant} & \text{when } x \gg 1. \end{cases} \tag{14}$$

On quasi-one-dimensional and two-dimensional lattices, the crossover times between the two regimes scales as $1/{\rho_0}^2$, so that superdiffusion is very long-lived in these systems. On Fig. 3, we present results from Monte-Carlo numerical simulations performed on a two-dimensional stripe of width $L = 3$, in the case where the TP is directed. The fluctuations of the position of the TP divided by time are plotted as a function of a rescaled time $\tau = {a_0'}^2{\rho_0}^2 t$ (where a_0' is a function of the bias which will be introduced explicitly in the next section) for different values of the density of vacancy ρ_0. For small values of the rescaled time ($\tau \ll 1$), the fluctuations grow superdiffusively as $t^{3/2}$. At long times ($\tau \gg 1$), the

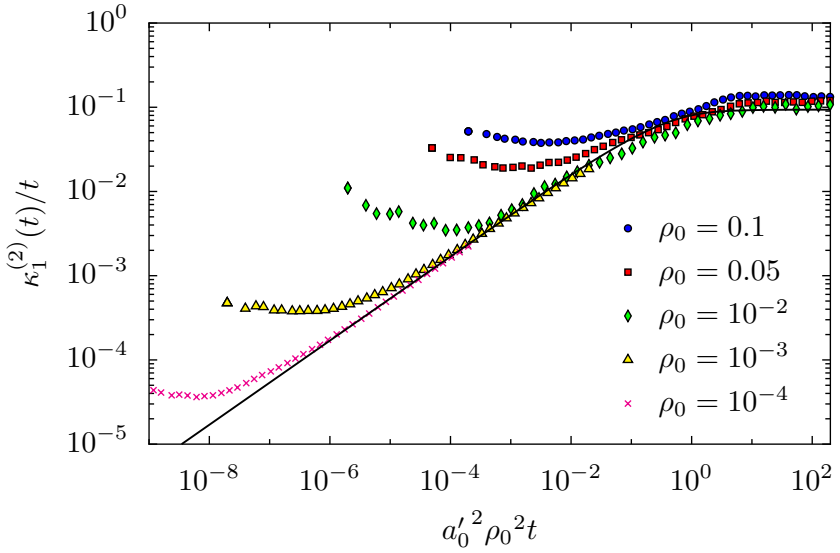

Figure 3: Rescaled variance $\kappa_1^{(2)}(t)/t$ as a function of $\tau = a_0'^2\rho_0^2 t$ obtained from numerical simulations of tracer diffusion on a 2D stripe of width $L = 3$ with different densities. The external force is $F = \infty$, which implies $p_1 = 1$ and $p_\mu = 0$ for $\mu \neq 1$.

fluctuations cross over to a diffusive regime. The scaling function $\widetilde{f}(\tau)/L$ is also plotted (black line). We verify that it constitutes a good description of both regimes and of the transition between them.

The superdiffusive behavior of the biased TP was also observed in off-lattice systems. The behavior of a driven TP in an continuous-space bath of Brownian particles was studied by numerical simulations in two types of system: (i) a colloidal fluid of identical particles interacting via a purely repulsive potential (simulations performed by A. Law and D. Chakraborty, Universität Stuttgart), (ii) a dissipative granular fluid (simulations performed by A. Bodrova, Moscow State University). In both algorithms, a biased intruder is submitted to an external force. In stripe-like geometries, the simulations reveal a superdiffusive behavior of the position of the TP, with fluctuations growing as $t^{3/2}$. This suggests that confinement-induced superdiffusion could be a generic feature of the dynamics of a biased intruder in a crowded medium.

0.2.4 Velocity anomaly in quasi-one-dimensional geometries

We found that in quasi-one-dimensional and two-dimensional systems there exists a long-lived superdiffusive behavior of the fluctuations of the position of the TP, crossing-over to a diffusive behavior after a time $t_\times \sim 1/\rho_0^2$. The complete time behavior of the variance was found to display a scaling behavior as a function of the rescaled variable $\rho_0^2 t$. We show that, actually, the behavior of the *mean* itself of the position of the TP displays a striking anomaly in quasi-one-dimensional geometries. This unexpected behavior, obtained from Monte-Carlo numerical simulations in a quasi-1D stripe, is plotted in Fig. 4 for several vacancy densities ρ_0, as a function of the rescaled variable $\tau = a_0'^2\rho_0^2 t$, suggested by the scaling behavior of the variance. A scaled form of the mean-position is found which, very surprisingly, after a long-lived plateau drops to a lower ultimate value. The transition from the "high" velocity to

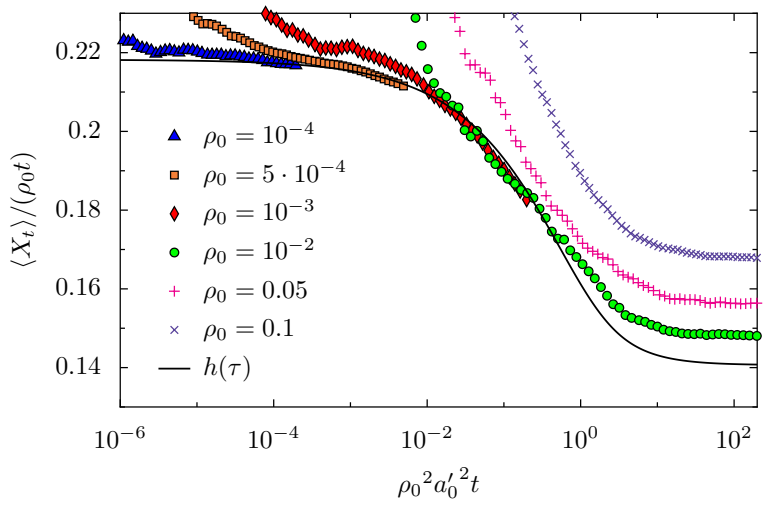

Figure 4: Rescaled mean position (velocity) $\langle X_t\rangle/(\rho_0 t)$ as a function of $\tau = {a'_0}^2{\rho_0}^2 t$ obtained from numerical simulations of tracer diffusion on a 2D stripe of width $L = 3$ with different densities. The external force is $F = \infty$, which implies $p_1 = 1$ and $p_\mu = 0$ for $\mu \neq 1$.

the ultimate regime of "low" velocity takes place at a time scale of the order of the cross-over time $t_\times \sim 1/{\rho_0}^2$ involved in the time evolution of the variance, suggesting that the anomaly of the variance and that of the mean could be linked.

Using again the general formalism valid at leading order in ρ_0 presented in Section 0.2.1, we study analytically the mean position of the TP. One can obtain the expression of the mean position of the TP in terms of the conditional FPTD associated to the random walks of the vacancies, which have been computed for the study of the fluctuations of the TP. On quasi-one-dimensional lattices, it is found that

$$\lim_{\rho_0\to 0} \frac{\langle X_t\rangle}{\rho_0} \underset{t\to\infty}{\sim} a_0 t, \tag{15}$$

with

$$a_0 \equiv \frac{p_1 - p_{-1}}{1 + \frac{2d\alpha}{2d-\alpha}(p_1 + p_{-1})}. \tag{16}$$

The value of a_0 corresponds to the long-lived plateau displayed by the velocity of the TP at short times. In order to describe the ultimate regime corresponding to the "low" velocity we now need to analyze the regime where the large time limit is taken first and the small density limit next, in contrast to the regime considered in (15). The formalism described above can actually be extended to analyze this second limit. The key difference with the previous case is that for a *fixed* small ρ_0 the random walk performed by the vacancy between two successive visits of the lattice site occupied by the TP is a *biased* random walk in the reference frame of the TP, due to the interactions of the TP with the other vacancies. More precisely, this bias originates from the non zero mean displacement of the TP in the $\boldsymbol{e}_1$ direction. The method presented above can then be applied, provided that the symmetric propagators describing the random walk of a given vacancy are replaced by biased propagators. In the dense limit $\rho_0 \to 0$, the bias is proportional to the vacancy density ρ_0, and thus vanishes when ρ_0 goes to zero. The explicit expression

of the bias is not needed to determine the velocity at leading order, and is determined self-consistently afterwards. It is finally found that:

$$\lim_{t\to\infty} \frac{\langle X_t \rangle}{t} \underset{\rho_0\to 0}{\sim} \rho_0 a_0', \tag{17}$$

where

$$a_0' = \frac{p_1 - p_{-1}}{1 + \frac{2d\alpha}{2d-\alpha}(p_1 + p_{-1}) + \frac{4d^2}{L^{d-1}(2d-\alpha)}(p_1 - p_{-1})}. \tag{18}$$

Several comments are in order. (i) In quasi-1D systems, the transverse width L is finite, so that the ultimate velocity $\rho_0 a_0'$ is always lower than the first high velocity $\rho_0 a_0$. The theoretical expressions (15) and (17) quantitatively account for the velocity anomaly numerically evidenced in Fig. 4 ; (ii) If the bias originates from an external force F and if the jump probabilities of the TP are given by (1), this velocity jump $\rho_0(a_0 - a_0')$ can be shown to scale as F^2 for small applied force F, so that this anomaly emerges only beyond linear response analysis. In turn, to linear order in F, there is a single velocity which can be shown to fulfill the Einstein relation; (iii) In systems unbounded in the transverse direction, i.e. such that $L \to \infty$, $a_0' = a_0$ meaning that no velocity anomaly occurs. In particular, in infinite 2D systems, superdiffusion takes place but no velocity anomaly is observed.

On quasi-one-dimensional lattices, we also considered the joint limit where $\rho_0 \to 0$ and $t \to \infty$ simultaneously with the appropriate scaling $t \sim 1/{\rho_0}^2$. We obtain $\langle X_t \rangle / (\rho_0 t)$ as an explicit function of the rescaled variable $\tau = {a_0'}^2 {\rho_0}^2 t$, which is plotted on Fig. 4 (black solid line). This approach correctly describes the velocity anomaly, and the transition from the initial "high" plateau to the ultimate "low" value.

0.2.5 Universal formula for the cumulants

In the previous Sections, we presented the expressions of the mean and fluctuations of the position of a biased TP in a hardcore lattice gas, in different geometries. These expressions only involve the propagators associated to simple random walks on the considered structures. Although the behavior of the TP is strongly affected by the geometry of the lattice, we can show that there exist general expressions of the first cumulants of the position of the TP that hold for every geometries. We extend these results to higher-order cumulants, and we also study the cumulants of the position of the TP in the direction perpendicular to the bias. These universal expressions are used to predict the behavior of the TP on more complex structures such as fractal lattices.

0.2.6 Simplified description

In the previous Sections, we showed that the transport properties of a biased TP in a dense hardcore lattice gas were closely related to the properties of the random walks performed by the vacancies on the considered structure. In particular, the recurrence (or transience) of these random walks appeared to be key property controlling the behavior of the fluctuations of the TP. Here we consider a simplified model that unveils the physical mechanism controlling the statistical properties of the position of the TP.

The TP is assumed to be directed, so that it jumps in the direction of the bias every time it is visited by a vacancy. Its position at time t is then exactly equal to the the number of time steps during which the TP location was occupied by at least one vacancy up time to t. Defining the random variable η_τ, which is equal to 1 if there is at least one vacancy at the origin at time t and 0 otherwise, the position of the TP

is written $X_t = \sum_{\tau=1}^{t} \eta_\tau$. Using a continuous-time description for simplicity, the second moment of X_t reads

$$\left\langle {X_t}^2 \right\rangle = 2 \int_0^t \mathrm{d}\tau' \int_0^{\tau'} \mathrm{d}\tau \left\langle \eta_\tau \eta_{\tau'} \right\rangle . \tag{19}$$

The correlation function $\langle \eta_\tau \eta_{\tau'} \rangle$ is formally the probability to have at least one vacancy at the origin at time τ and at time τ'. At leading order in ρ_0, it can be written in terms of a single-vacancy propagator:

$$\langle \eta_\tau \eta_{\tau'} \rangle \underset{\rho_0 \to 0}{=} \rho_0 p(\mathbf{0}, \tau' - \tau | \mathbf{0}, 0) + \mathcal{O}({\rho_0}^2), \tag{20}$$

where $p(\boldsymbol{r}, t|\mathbf{0}, 0)$ is the propagator associated to the *biased* random walk of a vacancy which starts from site $\mathbf{0}$ and arrives at site $\boldsymbol{r}$. Indeed, for a fixed value of ρ_0, the random walk performed by a given vacancy between two successive visits to the location of the TP is biased due to the net displacement of the TP in the direction of the force originating from its interactions with other vacancies. The bias experienced by the vacancies is in the direction opposite to that of the TP displacement, is taken equal to $V\rho_0$ (where V is a constant), and then vanishes when $\rho_0 \to 0$.

Equations (19) and (20) then give a simple relation between the fluctuations of the TP position and the properties of the random walk of vacancy. In the particular case of a stripe-like geometry, and using a continuous-space description for simplicity, the propagators p can be written explicitly, and we finally obtain the Laplace transform of the second moment:

$$\mathcal{L}\left[\left\langle {X_t}^2 \right\rangle\right](s) = \frac{2\rho_0}{s^2} \frac{1}{L\sqrt{4sD + {\rho_0}^2 V^2}}, \tag{21}$$

where D is the diffusion coefficient of the vacancy far from the TP. In the limit where ρ_0 is taken first, and taking the inverse Laplace transform, we get the following expression for the variance

$$\lim_{\rho_0 \to 0} \frac{\left\langle {X_t}^2 \right\rangle}{\rho_0} \underset{t \to \infty}{\sim} \frac{4}{3L\sqrt{D\pi}} t^{3/2}. \tag{22}$$

We then retrieve qualitatively the time-dependence of the variance which was obtained with the exact approach (10). In the limit where t is going to infinity for a fixed value of ρ_0, which is equivalent to take the limit $s \to 0$ in Laplace space, we obtain after an inverse Laplace transform

$$\lim_{t \to \infty} \frac{\left\langle {X_t}^2 \right\rangle}{t} \underset{\rho_0 \to 0}{\sim} \frac{2}{LV} \tag{23}$$

which is in qualitative agreement with the exact computation (12).

Consequently, with a simplified description of the problem where the TP is directed and where the properties of the random walk performed by the vacancies are described using propagators in continuous space and time, we obtain the nontrivial behaviors obtained through the exact analytical treatment of the problem. This shows that superdiffusion is a single-vacancy effect: in low-dimensional systems, the return statistics of a vacancy to the location of the TP is anomalous and yields an anomalous behavior of the TP fluctuations. At large times, the random walk performed by a vacancy between two successive visits to the location of the TP is biased, due to the net displacement of the TP caused by its interactions with other vacancies. This biased random walk is not recurrent anymore, and the TP has a diffusive behavior in the long-time limit.

This approach can be extended to retrieve the superdiffusive behavior observed on the two-dimensional lattice, and the anomalous subdiffusion obtained in the case of the one-dimensional lattice. However, this simplified description does not predict the emergence of the velocity anomaly in quasi-1D geometries presented in Section 0.2.4. Further work could result in a more accurate description that would take into account the anticorrelations effects between the TP and a single vacancy, that would describe more subtle effects.

0.3 Biased tracer diffusion in a hardcore lattice gas of arbitrary density

0.3.1 General formalism

The situation where the density of the bath of particles is no longer close to 1 and is arbitrary is more complex. In this case, the motion of the TP cannot be simply related to the diffusion of independent vacancies on the lattice, and we face a highly correlated N-body problem: when the TP moves forward, it perturbs the repartition of the bath particles, and in turn the reorganization of the bath particles around the TP controls the evolution of its position.

The resolution method presented below allows us to consider a more general situation than the one considered so far: we consider the model of a driven tracer in a bath of hardcore Brownian particles on a lattice (of dimension d and spacing σ) in contact with a reservoir of particles (Fig. 5). We adopt a continuous-time description, and we assume that the particles in the reservoir may adsorb onto vacant lattice sites at a fixed rate f/τ^*. The adsorbed particles may move randomly along the lattice by hopping at a rate $1/(2d\tau^*)$ to any of $2d$ neighboring lattice sites, which process is constrained by a hard-core exclusion preventing multiple occupancy. The adsorbed particles may desorb from the lattice back to the reservoir at rate g/τ^*. This so-called "Langmuir kinetics" has been shown to be relevant in several experimental contexts, and in particular to model transport in biological media.

The occupancy of lattice sites is described by the time-dependent Boolean variable $\eta_{\boldsymbol{r}}$, which takes two values: 1, if the site $\boldsymbol{r}$ is occupied by an adsorbed particle, and 0, otherwise. Note that the mean density of the bath particles, $\langle \eta_{\boldsymbol{r}} \rangle$, approaches as $t \to \infty$ a constant value $\rho = f/(f+g)$ but the number of particles on the lattice is not explicitly conserved in such a dynamics. The case where the number of particles on the lattice is conserved can be retrieved by taking the limits $f \to 0$ and $g \to 0$ with a fixed value of the density $\rho = f/(f+g)$.

We also introduce a tracer particle (TP), whose position at time t is a time-dependent random variable denoted as $\boldsymbol{X}_t$. The TP dynamics is different from that of the adsorbed particles in two aspects: first, it can not desorb from the lattice and second, it is subject to an external driving force, which favors its jumps along the direction corresponding to the unit vector $\boldsymbol{e}_1$ of the lattice. The TP dynamics is defined as follows: we suppose that the tracer, which occupies the site $\boldsymbol{X}_t$ at time t, waits an exponentially distributed time with mean τ, and then attempts to hop onto one of the $2d$ neighboring sites, $\boldsymbol{X}_t + \boldsymbol{e}_\mu$, where $\boldsymbol{e}_\mu$ is one of the $2d$ unit vectors. The jump direction is chosen according to the probability p_ν. It can be convenient to assume that the bias originates from an external force $\boldsymbol{F} = F\boldsymbol{e}_1$ (see Section 0.2.1). After the direction of the jump has been chosen, the hop is instantaneously fulfilled if the target site is vacant at this moment of time; otherwise, i.e., if the target site is occupied by any adsorbed particle, the jump is rejected and the tracer remains at its position. This model was studied before [14, 13, 15], but the results were limited to the behavior of the mean position of the TP. We aim to study the fluctuations of the position of the TP, and more generally the distribution of its position.

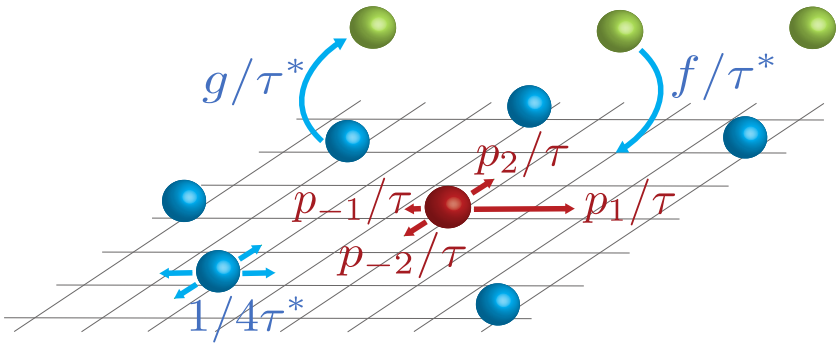

Figure 5: Model and notations in the two-dimensional (2D) case.

Defining $P(\boldsymbol{X},\eta;t)$ as the joint probability of finding at time t the TP at the site $\boldsymbol{X}$ and all adsorbed particles in the configuration $\eta=\{\eta_{\boldsymbol{r}}\}$, we write the master equation verified by $P(\boldsymbol{X},\eta;t)$:

$$\begin{aligned}2d\tau^*\partial_t P(\boldsymbol{X},\eta;t) =& \sum_{\mu=1}^{d}\sum_{\boldsymbol{r}\neq\boldsymbol{X}-\boldsymbol{e}_\mu,\boldsymbol{X}}\left[P(\boldsymbol{X},\eta^{\boldsymbol{r},\mu};t)-P(\boldsymbol{X},\eta;t)\right]\\ &+\frac{2d\tau^*}{\tau}\sum_{\mu}p_\mu\left[(1-\eta_{\boldsymbol{X}})\,P(\boldsymbol{X}-\boldsymbol{e}_{\boldsymbol{\mu}},\eta;t)-\left(1-\eta_{\boldsymbol{X}+\boldsymbol{e}_\mu}\right)P(\boldsymbol{X},\eta;t)\right]\\ &+2dg\sum_{\boldsymbol{r}\neq\boldsymbol{X}}\left[(1-\eta_{\boldsymbol{r}})\,P(\boldsymbol{X},\hat{\eta}^{\boldsymbol{r}};t)-\eta_{\boldsymbol{r}}P(\boldsymbol{X},\eta;t)\right]\\ &+2df\sum_{\boldsymbol{r}\neq\boldsymbol{X}}\left[\eta_{\boldsymbol{r}}P(\boldsymbol{X},\hat{\eta}^{\boldsymbol{r}};t)-(1-\eta_{\boldsymbol{r}})\,P(\boldsymbol{X},\eta;t)\right].\end{aligned}\tag{24}$$

where $\eta^{\boldsymbol{r},\nu}$ is a configuration obtained from η by the exchange of the occupation variables of two neighboring sites $\boldsymbol{r}$ and $\boldsymbol{r}+\boldsymbol{e}_\nu$, and $\hat{\eta}^{\boldsymbol{r}}$ is a configuration obtained from the original η by the replacement $\eta_{\boldsymbol{r}}\to 1-\eta_{\boldsymbol{r}}$.

From this master equation, one obtains the following equation verified by the mean position of the TP in the direction of the force ($X_t=\boldsymbol{X}_t\cdot\boldsymbol{e}_1$):

$$\frac{\mathrm{d}}{\mathrm{d}t}\langle X_t\rangle=\frac{\sigma}{\tau}\left[p_1\left(1-k_{\boldsymbol{e}_1}\right)-p_{-1}\left(1-k_{\boldsymbol{e}_{-1}}\right)\right],\tag{25}$$

where we define the density profiles in the reference frame of the TP $k_{\boldsymbol{r}}\equiv\langle\eta_{\boldsymbol{X}_t+\boldsymbol{r}}\rangle$. The equations verified by the density profiles $k_{\boldsymbol{r}}$ are also obtained from the master equation, and are not closed with respect to $k_{\boldsymbol{r}}$, as they involve correlation functions of the form $\left\langle\eta_{\boldsymbol{X}_t+\boldsymbol{r}}\eta_{\boldsymbol{X}_t+\boldsymbol{e}_\mu}\right\rangle$. The evolution equations for such correlation functions involve higher-order correlation functions, so that the master equation yields an infinite hierarchy of equations that needs to be closed with an approximation. We use a mean-field-type approximation, which consists in writing the occupation variables as $\eta_{\boldsymbol{R}}=\langle\eta_{\boldsymbol{R}}\rangle+\delta\eta_{\boldsymbol{R}}$, and discarding the terms of order $(\delta\eta_{\boldsymbol{R}})^2$. This yields the approximation

$$\left\langle\eta_{\boldsymbol{X}_t+\boldsymbol{r}}\eta_{\boldsymbol{X}_t+\boldsymbol{e}_\mu}\right\rangle\simeq\langle\eta_{\boldsymbol{X}_t+\boldsymbol{r}}\rangle\left\langle\eta_{\boldsymbol{X}_t+\boldsymbol{e}_\mu}\right\rangle,\tag{26}$$

and we finally obtain a closed set of equations verified by the density profiles $k_{\boldsymbol{r}}$.

We can extend this method to get the evolution equation of the fluctuations of the TP position from the master equation (24):

$$\frac{\mathrm{d}}{\mathrm{d}t}\left(\langle {X_t}^2\rangle - \langle X_t\rangle^2\right) = -\frac{2\sigma}{\tau}\left[p_1\widetilde{g}_{\boldsymbol{e}_1} - p_{-1}\widetilde{g}_{\boldsymbol{e}_{-1}}\right] + \frac{\sigma^2}{\tau}\left[p_1(1-k_{\boldsymbol{e}_1}) + p_{-1}(1-k_{\boldsymbol{e}_{-1}})\right], \tag{27}$$

where we define the cross-correlation functions

$$\widetilde{g}_{\boldsymbol{r}} \equiv \langle \delta X_t(\eta_{\boldsymbol{X}_t+\boldsymbol{r}} - \langle \eta_{\boldsymbol{X}_t+\boldsymbol{r}}\rangle)\rangle, \tag{28}$$

with $\delta X_t = X_t - \langle X_t\rangle$. The evolution equations for $\widetilde{g}_{\boldsymbol{r}}$ obtained from the master equation (24) involve higher-order correlation functions of the form $\left\langle \delta X_t \eta_{\boldsymbol{X}_t+\boldsymbol{r}}\eta_{\boldsymbol{X}_t+\boldsymbol{e}_\mu}\right\rangle$. The hierarchy of equations is closed by extending the mean-field-type decoupling approximation and neglecting again the quadratic terms in the variations of the occupations variables $\eta_{\boldsymbol{R}}$:

$$\left\langle \delta X_t \eta_{\boldsymbol{X}_t+\boldsymbol{r}}\eta_{\boldsymbol{X}_t+\boldsymbol{e}_\mu}\right\rangle \simeq k_{\boldsymbol{r}}\widetilde{g}_{\boldsymbol{e}_\mu} + k_{\boldsymbol{e}_\mu}\widetilde{g}_{\boldsymbol{r}}. \tag{29}$$

We finally obtain a closed set of equations whose solutions are the correlation functions $\widetilde{g}_{\boldsymbol{r}}$, and the fluctuations of the TP position can be obtained from (27).

The methods presented for the mean and the fluctuations of the position of the TP can be extended to compute the behavior of the cumulant generating function associated to the position of the TP $\Psi(t) \equiv \ln\left\langle \mathrm{e}^{\mathrm{i}uX_t}\right\rangle$. Note that the distribution of the position of the TP can easily be deduced from the cumulant generating function. It is found that

$$\frac{\mathrm{d}\Psi}{\mathrm{d}t} = \frac{p_1}{\tau}\left(\mathrm{e}^{\mathrm{i}u\sigma}-1\right)\left(1-\widetilde{w}_{\boldsymbol{e}_1}\right) + \frac{p_{-1}}{\tau}\left(\mathrm{e}^{-\mathrm{i}u\sigma}-1\right)\left(1-\widetilde{w}_{\boldsymbol{e}_{-1}}\right), \tag{30}$$

where $\widetilde{w}_{\boldsymbol{r}} \equiv \left\langle \mathrm{e}^{\mathrm{i}uX_t}\eta_{\boldsymbol{X}_t+\boldsymbol{r}}\right\rangle / \left\langle \mathrm{e}^{\mathrm{i}uX_t}\right\rangle$. Once again, we obtain a closed set of equations verified by the correlation functions $\widetilde{w}_{\boldsymbol{r}}$ by extending the mean-field-type decoupling approximation.

We then obtain approximated equations verified by the correlation functions $k_{\boldsymbol{r}}$, $\widetilde{g}_{\boldsymbol{r}}$ and $\widetilde{w}_{\boldsymbol{r}}$, which are involved in the evolution equations of the mean, the fluctuations and the cumulant generating function of the position of the TP.

0.3.2 One-dimensional situation

We consider the particular case of a one-dimensional lattice in contact with a reservoir of particles. Note that the presence of a reservoir of particles strongly affects the dynamics of the TP in this geometry. The behavior of the cumulants of its position are shown to be qualitatively very different than what was obtained in the case of a lattice gas with a conserved number of bath particles. In particular we show that the mean and fluctuations of the TP position are no longer anomalous, and grow linearly with time. Starting from the general formalism presented in Section 0.3.1, we compute the stationary solutions of the equations verified by the correlation functions $k_{\boldsymbol{r}}$, $\widetilde{g}_{\boldsymbol{r}}$ and $\widetilde{w}_{\boldsymbol{r}}$, and we deduce the stationary values of the velocity, the diffusion coefficient and of the distribution of position.

We first obtain the solutions of the equations verified by the mean density profiles $k_{\boldsymbol{r}} = \langle \eta_{\boldsymbol{r}}\rangle$, already presented in [15]. In particular, the quantities $k_{\boldsymbol{e}_{\pm 1}}$, involved in the expression of the TP velocity, are the solutions of an implicit system of equations, that can be solved numerically for a given set of parameters.

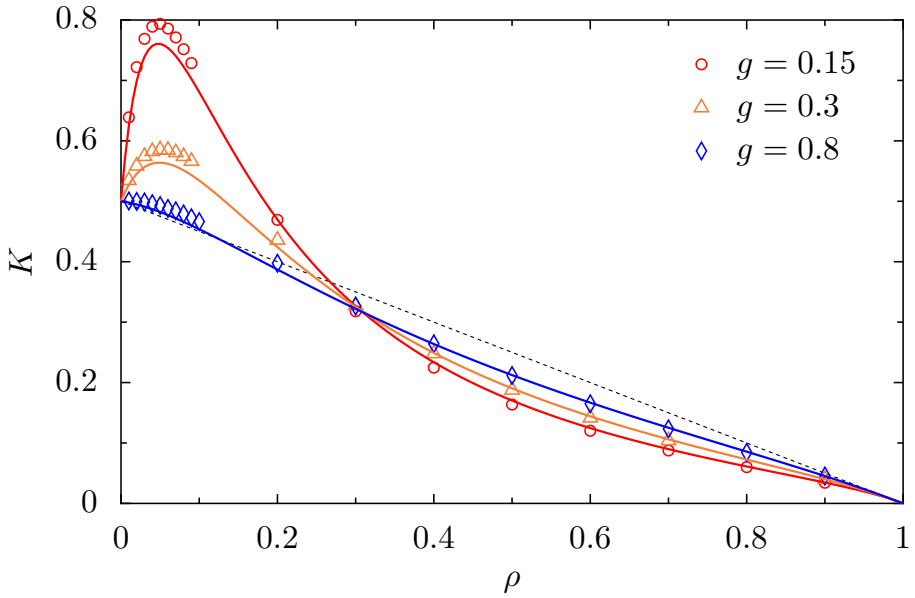

Figure 6: Stationary diffusion coefficient K of the TP as a function of the density for different values of the desorption rate g obtained from numerical simulations (symbols) and from the decoupling approximation (lines). The bias is $p_1 - p_{-1} = 0.96$, the waiting times are $\tau = \tau^* = 1$. The dashed line is the trivial mean-field solution $K = \frac{\sigma^2}{2\tau}(1-\rho)$.

The general solution for the TP velocity is confronted to Monte-Carlo simulations, which exactly sample the master equation of the problem. The agreement between the numerical simulations and the solution from the decoupling approximation is very good.

We study the solutions of the equations verified by the cross-correlation functions $\widetilde{g}_{\boldsymbol{r}} = \langle \delta X_t (\eta_{\boldsymbol{X}_t+\boldsymbol{r}} - \langle \eta_{\boldsymbol{X}_t+\boldsymbol{r}} \rangle) \rangle$, and obtain in particular an expression for the quantities $\widetilde{g}_{\boldsymbol{e}_{\pm 1}}$, involved in the computation of the diffusion coefficient of the TP, in terms of the density profiles $k_{\boldsymbol{r}}$. It is then possible to obtain the value of the diffusion coefficient for a given set of parameters. The analysis of this general solution shows that the diffusion coefficient is a nonmonotonic function of the density as soon as the bias is strong enough. Indeed, surprisingly, the diffusion coefficient may be increased by the presence of bath particles on the lattice for a wide range of parameters. This nonmonotonicity is not an artifact of the decoupling approximation, and we show that its existence is confirmed by Monte-Carlo simulations, which confirm the accuracy of the approximation (Fig. 6). This effect can be related to an anomaly in the profiles of the cross-correlations $\widetilde{g}_{\boldsymbol{r}}$, which are shown to be nonmonotonic functions of the distance to the TP for values of the parameters similar to the ones leading to the existence of a maximum value for the diffusion coefficient. This enhanced diffusion coefficient could be investigated in experimental realizations, and lead to interesting applications.

We also study the solutions of the equations governing the correlation functions $\widetilde{w}_{\boldsymbol{e}_{\pm 1}}$, involved in the computation of the cumulant generating function of X_t and therefore in its distribution. We show that the quantities $\widetilde{w}_{\boldsymbol{e}_{\pm 1}}$ are implicit solutions of a system of equations, so that the distribution of X_t can be determined numerically and confronted to numerical simulations with a good agreement. Finally, we deduce from that behavior of the cumulant generating function that the rescaled variable

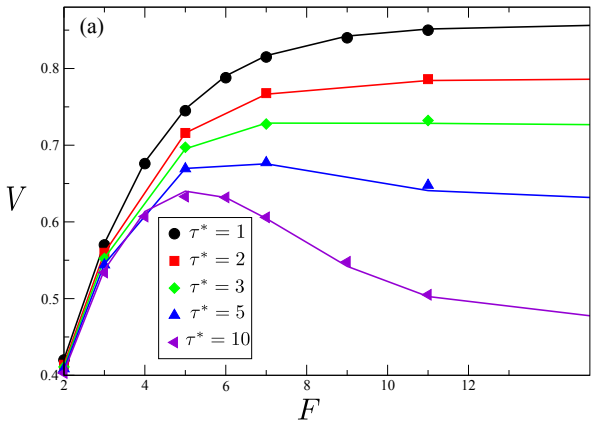

Figure 7: Velocity V of the TP as a function of the force F for a density of bath particles $\rho = 0.05$. τ is taken equal to 1 and τ^* varies. Results obtained from numerical simulations (symbols) are confronted with the predictions from the decoupling approximation. Numerical simulations performed by Alessandro Sarracino (postdoc in the group).

$(X_t - \langle X_t \rangle)/\sqrt{\mathrm{Var}(X_t)}$ is expected to be distributed accordingly to a Gaussian distribution in the long-time limit.

0.3.3 Higher-dimensional lattices

The evolution equations verified by the correlation functions $k_{\boldsymbol{r}}$ and $\widetilde{g}_{\boldsymbol{r}}$ are also solved on higher-dimensional lattices. We show that the quantities $k_{\boldsymbol{e}_\nu}$ and $\widetilde{g}_{\boldsymbol{e}_\nu}$ are solutions of closed set of equations that can be solved numerically. This gives a method to obtain the value of the velocity and of the diffusion coefficient for a given set of parameters.

The analysis of these solutions yields several interesting results. In particular, we study the dependence of the terminal velocity of the TP on the applied force. If the bath particles are slow enough (i.e. if their mean waiting time τ^* is large enough), we show that the velocity can be a nonmonotonic function of the applied force, and that it may decrease for increasing values of the force. This counterintuitive effect is known in other domains as *negative differential mobility* (NDM). It can be explained by the following simple physical arguments: increasing the applied force on the TP reduces its travel time between successive encounters with the bath particles, but increases the escape time from traps created by the bath particles when they are slow enough. The competition between these two effects controls the emergence of NDM. Our approach gives a new microscopic explanation to this phenomenon. The analytical predictions are confirmed by Monte-Carlo simulations, which also confirm the accuracy of the decoupling approximation in a wide range of parameters (Fig. 7).

We also show that in the extreme density regimes $\rho \to 0$ and $\rho \to 1$, the equations verified by the density profiles $k_{\boldsymbol{r}}$ and $\widetilde{g}_{\boldsymbol{r}}$ are no longer implicit and have explicit solutions. The decoupling approximation then yields explicit expressions for the velocity and the diffusion coefficient of the TP in these

limits. The high-density limit, in the case where the lattice is not in contact with a reservoir, was studied using an exact approach, from which we obtained exact results for the mean position (Section 0.2.4) and the fluctuations (Section 0.2.3) of the TP at leading order in the density of vacancy ρ_0 . We show that the results from the decoupling approximation perfectly match the results obtained from the exact approach in the limit $\rho \to 1$. The opposite limit, where $\rho \to 0$, was studied by other authors [77] who obtained the velocity of the TP at leading order in the density of bath particles ρ. We show that our decoupling approximation yields the same result. Importantly, this shows that the decoupling approximation is *exact* in both limits of very high and very low densities.

0.4 Conclusion

We studied the general model of a biased tracer particle (TP) in a bath of Brownian particles on a lattice. The bath particles perform symmetric nearest-neigbor random walks, whereas the TP performs a biased nearest-neighbor random walk, where the bias can originate from an external force applied on the TP. This model has been studied in the past, but the results were limited to the behavior of the mean position of the TP and to the determination of the force-velocity relation. The aim of this thesis was to go beyond the force-velocity relation, and to study the fluctuations of the position of the TP, and more generally its whole distribution.

We first studied the diffusion of a biased tracer in a very dense lattice gas. In this situation, the motion of the TP is mediated by the diffusion of the vacancies. At leading order in the density of vacancies, the propagator associated to the random walk of the TP can be written using the first-passage time densities associated to the random walk of a vacancy on the considered structure. In the case of a one-dimensional lattice, we determined the distribution of the position of the TP, and showed that the mean and the fluctuations of the position of the TP grow sublinearly. On higher-dimensional confined geometries (quasi-one-dimensional and two-dimensional lattices), we show that the fluctuations of the TP position are superdiffusive, and cross over to a diffusive behavior after a very long time. In quasi-one-dimensional lattices, this is associated to an anomaly in the velocity of the TP which saturates to a "high"-value before crossing over to its ultimate lower value at large times. We give a simple description of the problem, unveiling the physical origin of these anomalous behaviors.

In the situation of an arbitrary density of bath particles on a lattice in contact with a reservoir of particles, we face a complex N-body problem described by a master equation. The computation of the velocity and diffusion coefficient of the TP yields an infinite hierarchy of equations that needs to be closed in order to be solved. We use a mean-field-type decoupling approximation which gives approximate equations verified by the velocity and diffusion coefficient of the TP. This approximation is extended to obtain the equations verified by the distribution of the position of the TP. The accuracy of this mean-field-type approximation is verified with Monte-Carlo simulations. In the limits of a very dilute and very dense bath of particles, the equations verified by the first cumulants of the position of the TP have explicit expressions, which match the exact expressions obtained in these limits.

CHAPTER 1

Introduction

In various physical and biological systems, one encounters the situation when either an active particle or a particle subject to an external force travels through a quiescent host medium. A few stray examples include self-propelled particles in crowded environments, such as molecular motors, motile living cells or bacteria [83, 31], biased intruders in granular systems [27] or in colloidal suspensions [51]. Determining the dynamics of such a driven particle – called the tracer particle (TP) in what follows – in a host medium which hinders its motion is a challenging problem with important applications.

From a theoretical point of view, the difficulty lies in the modeling of the environment of the TP, which is constituted of a large number of interacting bath particles. The resulting stochastic dynamics of the whole system is a many-body problem which is difficult or even impossible to solve in practice. Formally, the one-particle distribution function is determined in terms of a two-particle distribution function and so on. The exact description of the system then yields an infinite hierarchy of equations, that must be closed in order to be solved. The Boltzmann equation [28] represents a first attempt to obtain an equation for the one-particle distribution function, assuming that the particles undergo binary collisions and that their velocities are uncorrelated before each encounter. This equation was extensively studied to describe classical dilute gases.

The study of Brownian motion – the erratic motion of a heavy particle in a solvent constituted of much lighter particles – inspired another description of the bath of particles. This phenomenon is usually described by a Langevin equation [40, 73], which involves a random force modeling the effect of the bath. In its most simple form, the random force is uncorrelated and memoryless. To provide a more faithful description of a real bath, the Langevin equation was generalized to more complex random forces, taking into account memory effects [71].

In most approaches the microscopic structure of the bath is not considered explicitly, and the response functions are determined instead by using some effective bath dynamics [84]. While these approaches are rather efficient, they cannot account for the detailed correlations between the tracer particle and the fluctuating density profiles of the bath particles. In particular, when the tracer is biased, a jam of bath particles forms in front of it, and the density profiles become strongly asymmetric. This aspect becomes crucial when the probe and the medium particles have comparable sizes. In this regime, fluctuations of the probe can not be described correctly if the medium is treated as a continuous bath.

These questions have received a growing interest in the previous years, and are central in active microrheology experiments, in which the properties of a medium are studied through the response of a probe to an external force [110, 102]. This experimental technique has become a powerful tool for the analysis of such diverse systems as colloidal suspensions [51, 87], complex fluids [30, 29], live cells [10, 74] or actin networks [48, 122]. So far, the available theoretical descriptions of such systems relied on hydrodynamic descriptions of the host fluid [109, 116], or on mode-coupling theories [46, 18, 45]. Recently, the limit of very soft bath particles was investigated and the dynamics of the bath was considered explicitly, using the Dean equation [36] to describe the bath as a large number of interacting

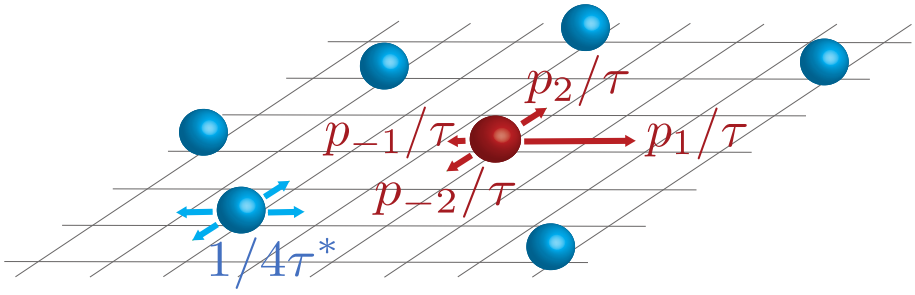

Figure 1.1: Biased tracer in a hardcore lattice gas. In this figure, we represent the particular case of a two-dimensional lattice.

Langevin processes [38, 37].

In this thesis, we consider the model where the TP is driven in a bath of Brownian hardcore particles performing symmetric random walks on a lattice. In this context, the evolution of the mean position of the TP has been studied [14, 13, 15]. However, the behavior of its fluctuations and of its position distribution has not been studied yet. This lattice description is particularly adapted in the context presented above, as it allows to take into account explicitly the dynamics of the bath, and to study the statistical properties of the TP position. Moreover, lattice models of interacting particles are paradigmatic in nonequilibrium statistical mechanics and have received a lot of attention in the past decades [42, 82]. Finally, this approach is not perturbative in the external force applied on the TP, and allows the study of the nonlinear response regime, which has been shown to be prevalent in experimental systems [102].

We consider a regular hypercubic lattice, which is populated by particles performing nearest-neighbor symmetric random walks, with a characteristic time τ^* (Fig 1.1). The density of particles on the lattice is denoted by ρ. We also introduce a tracer particle, which performs a nearest-neighbor symmetric or biased random walk, with a characteristic time τ. We assume that all the particles interact *via* hardcore interactions, which means that there is at most one particle per site. From a probabilistic point view, the joint process describing the position of the TP and the entire configuration of the bath particles is a Markov process. However, the motion of the TP only is no longer a Markov process.

This system has motivated a large amount of analytical work, and was also investigated by numerical simulations in the past [63]. In what follows, we review the results obtained in the two situations where the TP is symmetric and where it is biased.

We first present the case where a symmetric TP moves in a lattice gas of dimension equal or greater than two, with the additional assumption that the TP is identical to the untagged particle ($\tau^* = \tau$). In the particular case where the density ρ is close to one, the lattice actually contains very few vacant sites, that we will call *vacancies*, and whose density $\rho_0 = 1 - \rho$ is close to zero. Consequently, the TP may move only when a vacancy visits a site in its vicinity. The fact that the random walk of the TP is correlated may be understood as follows: after the TP has exchanged its position with a given vacancy, the vacancy remains in its vicinity, and there is a large probability that the TP exchanges its position with the same vacancy again. At leading order in the density of vacancies ρ_0, the diffusion coefficient of the TP then writes $D = \rho_0 f D_0$, where D_0 is the TP diffusion coefficient in the absence of interactions, and f is a correlation factor which was first computed in [75]. Further on, this situation was studied by a large

number of authors in the past decades [22, 23, 66, 60, 88, 105].

The opposite situation where the density ρ goes to zero has been particularly studied in the case where the bath particles are fixed (i.e. in the limit $\tau^* \to \infty$) and where they are called "obstacles". This model, often designated as the lattice Lorentz gas, has been studied by Nieuwenhuizen et al. [95, 96, 41], who obtained an exact expression of the diffusion coefficient of the TP at leading order in the density of obstacles ρ. These predictions were verified later on by numerical simulations [44].

The diffusion properties of the TP are less understood when the lattice concentration is not close to the values 0 and 1 anymore: the problem is then a N-body problem that only admits approximated solutions. Note that in this situation, the physical reason for the correlation effects used in the limit $\rho \to 1$ still holds: when the TP jumps to a vacant site, it leaves behind a vacant site, whereas the other neighboring sites are occupied with probability ρ. It is then more likely to jump back on its previous position than on any other. In this system, the diffusion coefficient of the TP becomes $D = (1-\rho)f(\rho)D_0$, and the difficulty lies in the determination of the correlation factor $f(\rho)$ which is now a function of the gas density. This question was first addressed by numerical simulations, which allowed several authors to obtain estimations of $f(\rho)$ on different types of lattices [35, 91, 64]. From a theoretical point of view, the first derivation of $f(\rho)$ was introduced by Sankey and Fedders [103], who used a complex diagrammatic approach, valid in the situation where $\tau^* = \tau$. A more general approach, valid for arbitrary values of the characteristic times, was proposed by Nakazato and Kitahara [92] who obtained an approximate expression of $f(\rho)$, which has been shown to be exact in the limits $\rho \to 0$ and $\rho \to 1$. We also mention the work of Tahir-Kheli and Elliot [112], who used a mean-field-like approximation to close the infinite hierarchy of master equations in order to compute $f(\rho)$.

Exclusion interactions on lattices in dimension at least equal to two then modify the TP transport properties in the sense that it cannot wander as far as in free diffusion. However, the mean square displacement (MSD) still grows linearly with time, and the interactions only affect the prefactor and make the diffusion coefficient concentration-dependent. In one-dimension, exclusion interactions lead to an anomalous behavior of the TP mean square displacement, which was shown to grow as $t^{1/2}$. This sub-diffusive behavior can be understood as follows: in one dimension and with exclusion interactions, the initial order of the particles is conserved, so that the motion of the TP on progressively larger distances requires the displacement of more and more particles in the same direction, so that the movement of individuals particles becomes strongly correlated. If the TP mean waiting time is identical to that of the bath particles ($\tau = \tau^*$), the long-time behavior of the variance of the TP position X_t is given by the exact expression

$$\mathrm{Var}(X_t) \underset{t\to\infty}{\sim} \frac{(1-\rho)}{\rho}\sqrt{\frac{2t}{\tau^*\pi}} \tag{1.1}$$

which was obtained by several authors who used different methods [54, 78, 3, 4, 80, 7].

The more general case where the TP is biased, which will be considered in this thesis, has received less attention. In this situation, note that the mean position of the TP itself is a nontrivial quantity and deserves attention. Technically, the analytical determination of the TP transport properties is difficult as it is a highly correlated problem: when the TP moves forward, it perturbs the repartition of the bath particles, and in turn the reorganization of the bath particles around the TP controls the evolution of its position.

The first attempt to address this problem was to consider the case of a directed TP in a one-dimensional symmetric gas [26]. It was shown that the mean position of the TP was growing as $t^{1/2}$, whose evolution is considerably slower that the linear growth expected for an isolated biased particle. Later on, the same authors extended their results to the case of an arbitrary value of the bias [25]. This result was confirmed by an exact probabilistic treatment of the problem [72].

This problem was extended to the case of a d-dimensional hypercubic lattice, in the general case where exchanges of particles with a reservoir can also take place. In this model, particles may adsorb on vacant lattice sites, and the bath particles may desorb back to the reservoir. A biased TP is also introduced on the lattice. The mean position of the TP was computed using a mean-field-type approximation, used to decouple relevant correlation functions and to close the infinite hierarchy of equations arising from the exact description of the problem. This resolution was first applied to one-dimensional systems [15] and generalized to lattices of arbitrary dimension [13, 14]. It was shown that this decoupling approximation was very accurate in a wide range of parameters. As the Einstein relation was rigorously shown to hold in this system [67], the diffusion coefficient of the TP in the case where $F = 0$ was deduced from the expression of the mean position of the TP experiencing an arbitrary bias in the limit $F \to 0$. This approach allowed the authors to retrieve the results obtained by Nakazato and Kitahara [92], known to be exact in the extreme density regimes.

The particular case of a very dense environment deserved a particular treatment [17], relying on an extension of the framework initially introduced by Brummelhuis and Hilhorst [22, 23]. The mean position of the TP was computed analytically at leading order in the density of vacancies, in the case of a two-dimensional lattice.

Although the mean position of a biased TP in a lattice gas has motivated a lot of work, the question of its fluctuations – and more generally of the distribution of its position – has not been considered. In this thesis, we address this problem, using two different but complementary analytical resolution schemes.

- The first part of this thesis is devoted to the particular case where the density of particles is high. In this situation, the TP may only move when a vacancy visits one of its neighboring sites. Its motion is then mediated by the diffusion of vacancies. At leading order in the density of vacancies ρ_0, each vacancy contributes independently to the motion of the TP. The distribution of position of the TP in the case where there is only one vacancy on the lattice can be expressed in terms of the first-passage time densities of a vacancy. When ρ_0 is arbitrarily small, the TP position distribution may be written in terms of the single-vacancy propagators. This method yields *exact* results at leading order in ρ_0, and is presented in detail in Chapter 2. It is first applied to study the case of a one-dimensional system, for which the distribution of the TP position is completely determined (Chapter 3). Then, this formalism is applied to compute the fluctuations of the TP position in higher dimensions (Chapter 4). They are shown to have many striking features, and a nontrivial dependence on all the parameters of the problem (time, applied force, density of particles). In particular, in confined geometries, the fluctuations of the TP display a long-lived superdiffusive evolution, and an ultimate crossover to a diffusive state. In Chapter 5, we show that the mean position itself has an anomalous behavior in confined geometries, as it displays a long-lived high plateau before a drop to its ultimate value. These results are shown to be general, and are recast in more universal formulae, which also give the expressions of the higher-order cumulants in the high-density limit (Chapter 6). These general formulae are used to describe the behavior of the

TP on fractal lattices. Finally, in Chapter 7, we give a simplified picture of the problem, which correctly captures the physical mechanisms governing the behavior of the TP.

- In the second part of this thesis, we study the general case where the density of particles on the lattice is arbitrary, so that the motion of the TP cannot be easily related to the diffusion of vacancies anymore. Starting from the master equation describing exactly the problem and using a mean-field-type decoupling approximation of the tracer-bath particles correlation functions, we derive equations verified by relevant correlation functions involved in the computation of the TP fluctuations. This decoupling approximation also allows us to obtain an implicit expression of the cumulant generating function of the TP position, and therefore of its distribution (Chapter 8). In Chapter 9, these equations are solved in the particular case of a one-dimensional lattice in contact with a reservoir of particles. Surprisingly, the diffusion coefficient of the TP is shown to be non-monotonous with the density of particles on the lattice. Finally, in Chapter 10, we give a resolution scheme of the equations derived in Chapter 8 for lattices of higher dimensions. We show that the velocity of the TP may be a non-monotonic function of the applied force, and provide a microscopic description of this phenomenon known in other contexts as negative differential mobility. In the particular limit of a high density of particles, we retrieve the results for the fluctuations and the mean position of the TP, obtained by the exact approach at leading order in the density of vacancies. In the low density limit, we retrieve recent exact results [77] obtained at leading order in the density ρ. This shows that the decoupling approximation is exact in the low-density limit, and in the high-density limit.

Part I

Biased tracer diffusion in a high-density lattice gas

CHAPTER 2

Motivation and general presentation

Contents

We present the model of a biased tracer particle (TP) in a hardcore lattice gas, in the high-density limit, where the density of vacancies ρ_0 is small. In this limit, the motion of the TP is mediated by the diffusion of the vacancies on the lattice, which perform symmetric nearest-neighbor random walk, perturbed in the vicinity of the TP. We consider the auxiliary problem where there is only one vacancy on the lattice, and write the propagator associated to the position of the TP in terms of the first-passage time densities (FPTD) of the vacancy. At leading order in the density of vacancies, each vacancy contributes independently to the motion of the TP, so that the propagator associated to the TP position in the limit $\rho_0 \to 0$ is written in terms of the single-vacancy propagators. Finally, we deduce the expression of the cumulants of the distribution of the TP position in terms of the FPTD associated to the random walk of the vacancies.

2.1 Introduction

2.1.1 Statement of the problem

We consider a hybercubic lattice of arbitrary dimension, on which particles perform symmetric nearest-neighbor random walks, with the restriction that there is at most one particle per site. The density of particles on the lattice is denoted by ρ. We select at random a particle, an study its position $\boldsymbol{X}_t$. This particle will be called the tracer particle in what follows. The TP can either be identical to the other particles, or be submitted to an external force, so that is performs a biased nearest-neighbor random walk. In this Chapter, we study the limit where the density of particles is close to 1, so that there are very few vacant sites on the lattice.

We first consider the case where each site of the lattice is occupied by a particle, except one, which will be called the vacancy. Consequently, the only particles that are likely to move are the one located in the vicinity of the vacancy. In this situation, it is easier to describe the dynamics of the vacancy rather than the dynamics of the TP. The vacancy performs a symmetric nearest-neighbor random walk, whereas the dynamics of the TP is more complicated: it will only change its position when visited by the vacancy. Moreover, its successive steps are correlated: after it exchanges its position with that of the vacancy, it is more likely to go back to its initial position than to move to any other neighboring site. The statistical properties of the tracer position may then display non-trivial and unexpected features. This problem is known as "vacancy-mediated diffusion" or "slaved diffusion".

The case where the number of vacant sites is not equal to one, but is very small compared to the number of lattice sites (i.e. when the vacancy density $\rho_0 = 1 - \rho$ is close to zero) may be studied from this approach. At lowest order in ρ_0, each vacancy performs a symmetric nearest-neighbor random walk, as the events where two vacancies are adjacent or have common neighbors only contribute to order $\mathcal{O}({\rho_0}^2)$. The evolution rules established for the single-vacancy problem are still valid, and the total TP displacement may be written as the sum of all the displacements $\Delta\boldsymbol{X}_j$ due to its interactions with the j-th vacancy.

In what follows, we give a brief review of the experimental and theoretical results obtained on the problem of vacancy-mediated diffusion, in the case where the TP is not biased.

2.1.2 Experimental works

Vacancy-mediated diffusion (VMD) was investigated experimentally at the atomic scale. Depositing atoms of indium on a copper surface, it was observed that the intruders were surprisingly mobile and could travel as far a five lattice spacings [114, 113]. It was shown that this "jumps" were induced by the diffusion of surface vacancies.

This mechanism is then highly important in solid-state physics, as it may be the dominant effect by which atoms or more complex entities can be transported in a medium. VMD is then used to dope semi-conductors [2]. The study of complex materials, for instance the determination of self-diffusion constants, is possible by tracking radioactive tracers which diffuse thanks to VMD. This was applied to quasicrystals [20], amorphous metallic alloys [65], or aluminides [119].

2.1.3 Theoretical descriptions

In addition to these experimental observations, the question of VMD has motivated many theoretical approaches. On a three-dimensional lattice and with a single vacancy, the Pólya theorem [101] ensures that the vacancy will encounter the tracer particle only a finite number of times on average, so that the equilibrium distribution of the tracer position is reached in a finite time. This equilibrium distribution was computed by Sholl [105]. The general problem of tracer diffusion in a concentrated lattice gas adsorbed on a three-dimensional lattice has been first investigated numerically by Kehr and Binder [64] and confronted with analytical predictions obtained within a mean-field approximation.

The one-dimensional situation has also raised a lot of interest, as it is related to the well-known problem of single-file diffusion. This case will be presented with more details in the introduction of Chapter 3.

Brummelhuis and Hilhorst considered the two-dimensional lattice formulation of the problem, and obtained an exact expression of the TP position probability distribution, both in the case where there is only one vacancy on the lattice [22], and in the case where there is an asymptotically small vacancy density [23]. Interestingly, the single-vacancy situation gives rise to non-Gaussian fluctuations of the TP position.

Finally, continuous-space descriptions of the problem were also studied. We cite in particular the work of Newman [94], who proposed a coarse-grained description of the VMD problem, and retrieved the results obtained from the exact lattice formulations.

2.1.4 Objectives

All the approaches presented above focused on situations where the TP is identical to the others particles, and can be chosen at random among them. As it was emphasized in the introduction of this thesis, the case where the TP is biased is interesting in different experimental fields.

From a theoretical perspective, the VMD of a biased tracer is a difficult problem: the tracer has anisotropic hopping probabilities, and depending on the relative position of the vacancy and the TP, this latter will have a higher (or lower) probability to exchange its positions with that of the vacancy compared to the surrounding unbiased particles.

This Chapter is an introduction to the first part of this thesis. We first introduce the model rules and notations. Then, we study the single-vacancy situation, and the case of a very small density of vacancies. The cumulant generating function of the TP position is expressed in terms of simpler quantities that will be computed explicitly in the next chapters. This method was first introduced in [17], and is an extension to the case of a biased TP of the formulation proposed by Brummelhuis and Hilhorst [22, 23].

2.2 Presentation of the model

2.2.1 Model

We consider a hypercubic lattice in dimension d. The lattice sites are occupied by hard-core particles performing symmetrical random walks, with the restriction that the occupancy number for each site is at most equal to one. The fraction of occupied sites is denoted as ρ, whereas the vacancy density is denoted as ρ_0 (so that $\rho + \rho_0 = 1$). A tracer particle (denoted as TP in what follows) is also present

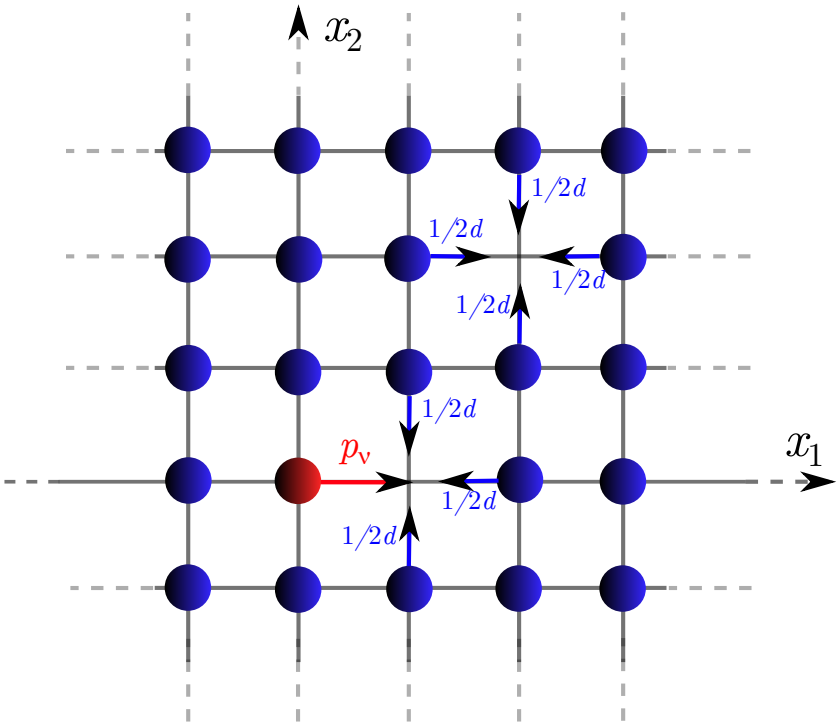

Figure 2.1: Dynamics of the particles on a generic d-dimensional lattice (represented in two dimensions for clarity). The bath particles (in blue) perform nearest-neighbor symmetric random walks, the tracer particle (in red) is biased and jumps in direction ν with probability p_ν.

on the lattice, and performs a biased random walk. The probability for the TP to make one step in direction $\boldsymbol{e}_\nu$ will be denoted p_ν ($\nu \in \{\pm 1, \ldots, \pm d\}$). We assume that the bias experienced by the TP only affects its jump probabilities in direction 1, so that the probabilities $p_{\pm 2}, \ldots, p_{\pm d}$ are identical and will be denoted by p_2. A normalization condition imposes $p_1 + p_{-1} + 2(d-1)p_2 = 1$. We then write $p_2 = (1 - p_1 - p_{-1})/[2(d-1)]$, so that the only relevant quantities do describe the TP asymmetry are p_1 and p_{-1}. We represent the evolution rules of the particles on Fig. 2.1.

Although our computations are valid for any choice of p_1 and p_{-1}, it will be convenient to assume that the bias originates from an external force $\boldsymbol{F} = F\boldsymbol{e}_1$ applied on the TP. In this situation, the probability for the TP to have its first coordinate equal to x in the stationary state is given by the Boltzmann distribution:

$$P_{\text{stat}}(x) = \frac{1}{\mathcal{Z}} \mathrm{e}^{-\beta F x} \tag{2.1}$$

where $\mathcal{Z}$ is a normalization constant, and where $\beta = 1/(k_{\text{B}}T)$ is the inverse temperature. Denoting by $p(\boldsymbol{r} \to \boldsymbol{r}_0)$ the probability for the TP to jump from site $\boldsymbol{r}$ to site $\boldsymbol{r}_0$ in a single step, the detailed balance condition imposes

$$P_{\text{stat}}(0)p(\boldsymbol{0} \to \boldsymbol{e}_1) = P_{\text{stat}}(1)p(\boldsymbol{e}_1 \to \boldsymbol{0}), \tag{2.2}$$

and, using (2.1), one gets

$$\frac{p_1}{p_{-1}} = \mathrm{e}^{-\beta F}. \tag{2.3}$$

Then, to fulfill the detailed balance condition, the jump probability of the TP in direction ν is given by

$$p_\nu = \frac{\mathrm{e}^{\frac{1}{2}\beta \boldsymbol{F}\cdot\boldsymbol{e}_\nu}}{\sum_{\mu\in\{\pm1,\dots\pm d\}} \mathrm{e}^{\frac{1}{2}\beta \boldsymbol{F}\cdot\boldsymbol{e}_\mu}} \tag{2.4}$$

The inverse temperature β will be taken equal to one.

The probability for the TP to be on site $\boldsymbol{X}$ at time step t is denoted by $\mathcal{P}_t(\boldsymbol{X})$. The position of the TP at time t is a random variable denoted by $\boldsymbol{X}_t$. The first component of $\boldsymbol{X}_t$ (i.e. the position of the TP in the direction of the bias) is denoted by X_t.

2.2.2 Evolution rules

In the high-density limit, the TP only moves when a vacancy visits one of its neighboring sites. In this Section, we present the evolution rules of a vacancy on the lattice. At each step of a discrete time t, a vacancy moves according to the following rules (see Fig. 2.2):

- if the TP is not adjacent to the vacancy, one of the $2d$ neighboring particles is randomly selected and exchanges its position with the vacancy.
- otherwise, if the TP is at position $\boldsymbol{X}$ and the vacancy at position $\boldsymbol{X}+\boldsymbol{e}_\nu$, the vacancy exchanges its position with the TP with a probability proportional to p_ν. It exchanges its position with one of the $2d-1$ neighboring bath particles with a probability proportional to $1/(2d)$. Consequently, if we denote by q_μ the probability for the vacancy to make a jump in direction μ, we get

$$q_\mu = \begin{cases} Z_\nu p_\nu & \text{if } \mu = -\nu, \\ Z_\nu/(2d) & \text{otherwise.} \end{cases} \tag{2.5}$$

  where Z_ν is some normalization factor. Using the normalization condition $\sum_{\mu\in\{\pm1,\dots\pm d\}} q_\mu = 1$, we find

$$Z_\nu = \left(p_\nu + \frac{2d-1}{2d}\right)^{-1}. \tag{2.6}$$

  Finally, the jump probabilities q_μ are

$$q_\mu = \begin{cases} \frac{p_\nu}{p_\nu+\frac{2d-1}{2d}} & \text{if } \mu = -\nu, \\ \frac{1}{2d\left(p_\nu+\frac{2d-1}{2d}\right)} & \text{otherwise.} \end{cases} \tag{2.7}$$

Note that these expressions of q_μ are only valid in the specific case where the vacancy performs a Pólya walk [1] everywhere on the lattice except in the vicinity of the TP. These evolution rules will be shown to be consistent with a continuous-time description of the system, which will be presented in the second part of this thesis.

[1] A Pólya walk is a lattice nearest-neighbor random walk for which there is no directional bias and for which all allowed steps are equally likely [58].

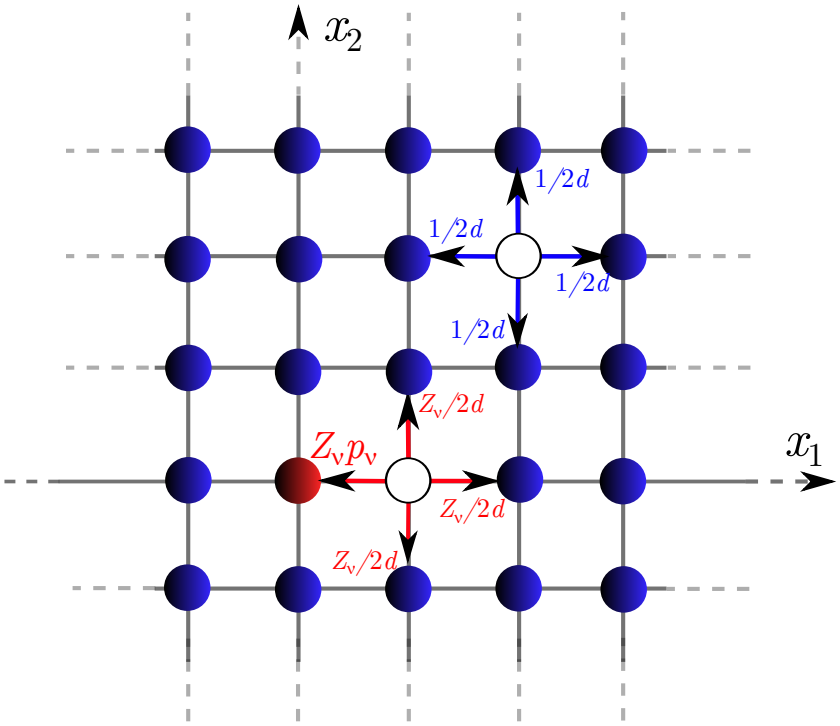

Figure 2.2: Dynamics of the vacancies on a generic d-dimensional lattice (represented in two dimensions for clarity). If the vacancy is not adjacent to the TP, it exchanges its position with any of the neighbors equiprobably. If the TP is at position $\boldsymbol{X}$ and the vacancy at position $\boldsymbol{X} + \boldsymbol{e}_\nu$, the jump probabilites are given by the quantities q_ν defined in the text.

2.3 Single-vacancy situation

2.3.1 Single-vacancy propagator

Following the procedure first introduced by Brummelhuis and Hilhorst [22], we consider the problem where there is only one vacancy on the lattice, whose position is denoted by $\boldsymbol{Y}$ (its initial position is $\boldsymbol{Y}_0$). The TP is initially at the origin of the lattice. We introduce the following notations :

- $P_t^{(1)}(\boldsymbol{X}|\boldsymbol{Y}_0)$ is the probability that the TP is at site $\boldsymbol{X}$ at time moment t given that the vacancy was initially at site $\boldsymbol{Y}_0$.
- $F_t(\mathbf{0}|\boldsymbol{Y}_0)$ is the probability that the vacancy, which started its random walk at site $\boldsymbol{Y}_0$, arrives at the origin $\mathbf{0}$ for the first time at time t.
- $F_t^*(\mathbf{0}|\boldsymbol{e}_\nu|\boldsymbol{Y}_0)$ is the conditional probability that the vacancy, which started its random walk at site $\boldsymbol{Y}_0$, appears at the origin for the first time at time t, being at site $\boldsymbol{e}_\nu$ at time $t-1$.

With these notations, following [22], an expression for $P_t^{(1)}(\boldsymbol{X}|\boldsymbol{Y}_0)$ can be obtained by summing over the number of steps p of the TP, over the directions $\nu_1,\dots,\nu_p$ of these p steps, and over the length of the time intervals m_j elapsed between the $(j-1)$-th step and the j-th step. We also sum over the time elapsed since the last step occured m_{p+1}. One obtains:

$$\begin{aligned} P_t^{(1)}(\boldsymbol{X}|\boldsymbol{Y}_0) &= \delta_{\boldsymbol{X},\mathbf{0}}\left(1-\sum_{j=0}^{t}F_j(\mathbf{0}|\boldsymbol{Y}_0)\right) \\ &+ \sum_{p=1}^{\infty}\sum_{m_1=1}^{\infty}\cdots\sum_{m_p=1}^{\infty}\sum_{m_{p+1}=0}^{\infty}\delta_{m_1+\ldots+m_{p+1},t}\sum_{\nu_1}\cdots\sum_{\nu_p}\delta_{\mathbf{e}_{\nu_1}+\ldots+\mathbf{e}_{\nu_p},\boldsymbol{X}} \\ &\times \left(1-\sum_{j=0}^{m_{p+1}}F_j(\mathbf{0}|-\boldsymbol{e}_{\nu_p})\right)F_{m_p}^*(\mathbf{0}|\boldsymbol{e}_{\nu_p}|-\boldsymbol{e}_{\nu_{p-1}})\ldots F_{m_2}^*(\mathbf{0}|\boldsymbol{e}_{\nu_2}|-\boldsymbol{e}_{\nu_1})F_{m_1}^*(\mathbf{0}|\boldsymbol{e}_{\nu_1}|\boldsymbol{Y}_0). \end{aligned} \tag{2.8}$$

The first term of the sum in the right-hand side of (2.8) corresponds to the event that the TP has not moved yet at time t. This equation in conveniently analyzed in Fourier-Laplace space. For any time-dependent function ϕ_t, we define the associated generating function (or discrete Laplace transform) by

$$\widehat{\phi}(\xi)=\sum_{t=0}^{\infty}\phi_t\xi^t. \tag{2.9}$$

For any space-dependent function $\psi(\boldsymbol{r})$, we define its Fourier transform by

$$\widetilde{\psi}(\boldsymbol{k})=\sum_{\boldsymbol{r}}\psi(\boldsymbol{r})\mathrm{e}^{\mathrm{i}\boldsymbol{k}\cdot\boldsymbol{r}}, \tag{2.10}$$

where the sum over $\boldsymbol{r}$ runs over every lattice sites. We then get

$$\widehat{\widetilde{P}}^{(1)}(\boldsymbol{k}|\boldsymbol{Y}_0;\xi)=\frac{1}{1-\xi}\left(1+\mathcal{D}^{-1}(\boldsymbol{k};\xi)\sum_{\mu}U_\mu(\boldsymbol{k};\xi)F^*(\mathbf{0}|\boldsymbol{e}_\mu|\boldsymbol{Y}_0;\xi)\right). \tag{2.11}$$

In (2.11), the function $\mathcal{D}(\boldsymbol{k};\xi)$ stands for the determinant of the following $2d \times 2d$ matrix,

$$\mathcal{D}(\boldsymbol{k};\xi) \equiv \det[\mathbf{1} - \boldsymbol{T}(\boldsymbol{k};\xi)], \tag{2.12}$$

where $\mathbf{1}$ is the identity of size $2d$ and the matrix $\boldsymbol{T}(\boldsymbol{k};\xi)$ has the entries $[\boldsymbol{T}(\boldsymbol{k};\xi)]_{\mu,\nu}$ defined by

$$[\boldsymbol{T}(\boldsymbol{k};\xi)]_{\mu,\nu} = \mathrm{e}^{\mathrm{i}\boldsymbol{k}\cdot\boldsymbol{e}_\mu} F^*(\mathbf{0}|\boldsymbol{e}_\mu|\boldsymbol{e}_{-\nu};\xi), \tag{2.13}$$

$$= \mathrm{e}^{\mathrm{i}\boldsymbol{k}\cdot\boldsymbol{e}_\mu} \sum_{t=0}^{\infty} F_t^*(\mathbf{0}|\boldsymbol{e}_\mu|\boldsymbol{e}_{-\nu})\xi^t. \tag{2.14}$$

Lastly, the matrix $U_\mu(\boldsymbol{k};\xi)$ in (2.11) is given by

$$U_\mu(\boldsymbol{k};\xi) \equiv \mathcal{D}(\boldsymbol{k};\xi) \sum_\nu \left[1 - \mathrm{e}^{-\mathrm{i}\boldsymbol{k}\cdot\boldsymbol{e}_\nu}\right] \left\{[\mathbf{1} - \boldsymbol{T}(\boldsymbol{k};\xi)]^{-1}\right\}_{\nu,\mu} \mathrm{e}^{\mathrm{i}\boldsymbol{k}\cdot\boldsymbol{e}_\mu}. \tag{2.15}$$

Consequently, the Fourier-Laplace transform of the single-vacancy propagator $\widehat{\widetilde{P}}^{(1)}(\boldsymbol{k}|\boldsymbol{Y}_0;\xi)$ may be calculated if the generating functions associated to the conditional first-passage time densities $F_t^*(\mathbf{0}|\boldsymbol{e}_\mu|\boldsymbol{e}_\nu)$ are known.

2.3.2 Calculation of the conditional first-passage time densities F^*

The conditional first-passage time densities F^* are relative to the random walk of a vacancy on a lattice populated by bath particles and a tracer particle. The conditional first-passage time densities can be formally computed as follows: we assume that the site at the origin of the lattice is absorbing, and we denote by $P_t^\dagger(\boldsymbol{r}|\boldsymbol{r}_0)$ the probability for the vacancy to be at site $\boldsymbol{r}$ at time t knowing that it started from site $\boldsymbol{r}_0$ at time $t = 0$. Let $p^\dagger(\boldsymbol{r}|\boldsymbol{r}_0)$ be the probability to jump from site $\boldsymbol{r}_0$ to site $\boldsymbol{r}$ in one step exactly. Let the symbols $\mathcal{E}$, $\mathcal{A}$ and $\mathcal{B}$ define the following three events:

- the event $\mathcal{E}$: the vacancy, which has started its random walk at the site $\boldsymbol{e}_\nu$, visits the origin $\mathbf{0}$ for the first time at the t-th step exactly, being at the site $\boldsymbol{e}_\mu$ at the previous step $t-1$;
- the event $\mathcal{A}$: the vacancy, which started its random walk at the site $\boldsymbol{e}_\nu$, is at the site $\boldsymbol{e}_\mu$ at the time moment $t-1$ and the origin $\mathbf{0}$ has not been visited during the $t-1$ first steps of its walk;
- the event $\mathcal{B}$: the vacancy jumps from the neighboring to the origin site $\boldsymbol{e}_\mu$ to the site $\mathbf{0}$ at the t-th step exactly.

Evidently, by definition, the desired first visit probability $F_t^*(\mathbf{0}|\boldsymbol{e}_\mu|\boldsymbol{e}_\nu)$ is just the probability of the $\mathcal{E}$ event

$$F_t^*(\mathbf{0}|\boldsymbol{e}_\mu|\boldsymbol{e}_\nu) = \mathrm{Prob}(\mathcal{E}). \tag{2.16}$$

To calculate $\mathrm{Prob}(\mathcal{E})$ we note first that the probabilities of such three events obey:

$$\mathrm{Prob}(\mathcal{E}) = \mathrm{Prob}(\mathcal{A} \cap \mathcal{B}) = \mathrm{Prob}(\mathcal{A})\mathrm{Prob}(\mathcal{B}). \tag{2.17}$$

On the other hand, we have that

$$\mathrm{Prob}(\mathcal{A}) = P_{t-1}^\dagger(\boldsymbol{e}_\mu|\boldsymbol{e}_\nu), \tag{2.18}$$

and

$$\mathrm{Prob}(\mathcal{B}) = p^{\dagger}(\mathbf{0}|\boldsymbol{e}_{\mu}). \tag{2.19}$$

Hence, in virtue of (2.16), (2.17), (2.18) and (2.19), the generating functions associated to the conditional first-passage time densities $F_t^*(\mathbf{0}|\boldsymbol{e}_{\mu}|\boldsymbol{e}_{\nu})$ are given explicitly by

$$\widehat{F}^*(\mathbf{0}|\boldsymbol{e}_{\mu}|\boldsymbol{e}_{\nu};\xi) = \xi p^{\dagger}(\mathbf{0}|\boldsymbol{e}_{\mu})\widehat{P}^{\dagger}(\boldsymbol{e}_{\mu}|\boldsymbol{e}_{\nu};\xi). \tag{2.20}$$

Therefore, the calculation of the conditional first-passage time densities $F_t^*(\mathbf{0}|\boldsymbol{e}_{\mu}|\boldsymbol{e}_{\nu})$ amounts to the evaluation of the probability distribution $P_t^{\dagger}(\boldsymbol{r}|\boldsymbol{r}_0)$ of the vacancy random walk in the presence of an absorbing site placed at the lattice origin.

By definition, the quantities $P_t^{\dagger}(\boldsymbol{r}|\boldsymbol{r}_0)$ are the propagators associated to the random walk of a vacancy in presence of a TP. As it was specified in Section 2.2.2, if the vacancy is not adjacent to the TP, it exchanges its position with any of the neighbors equiprobably, which means that its random walk is actually symmetric. Otherwise, if it is on a site adjacent to the TP, its evolution rules are modified. The propagators $P_t^{\dagger}(\boldsymbol{r}|\boldsymbol{r}_0)$ may be obtained starting from the propagators of a simple symmetric random walk $P_t(\boldsymbol{r}|\boldsymbol{r}_0)$ and assuming that there are $2d+1$ defective sites (the $2d$ neighbors of the origin and the origin itself, which is an absorbing site). Technically, the relation between $P_t^{\dagger}(\boldsymbol{r}|\boldsymbol{r}_0)$ and $P_t(\boldsymbol{r}|\boldsymbol{r}_0)$ is obtained by a usual method [89, 58], which results in a simple matrix relation:

$$\boldsymbol{P}^{\dagger} = (\mathbf{1} - \boldsymbol{A})^{-1}\boldsymbol{P}, \tag{2.21}$$

in which $\mathbf{1}$ is the $(2d+1)$-dimensional identity matrix, and $\boldsymbol{P}$, $\boldsymbol{P}^{\dagger}$ and $\boldsymbol{A}$ stand for the $(2d+1)\times(2d+1)$ matrices with the entries defined by

$$\boldsymbol{P}_{i,j} = \widehat{P}(\boldsymbol{s}_i|\boldsymbol{s}_j;\xi) \tag{2.22}$$

$$\boldsymbol{P}^{\dagger}{}_{i,j} = \widehat{P}^{\dagger}(\boldsymbol{s}_i|\boldsymbol{s}_j;\xi) \tag{2.23}$$

$$\boldsymbol{A}_{i,j} = A(\boldsymbol{s}_i|\boldsymbol{s}_j;\xi) \equiv \xi \sum_{\boldsymbol{r}} \widehat{P}(\boldsymbol{s}_i|\boldsymbol{r};\xi)\left[p^{\dagger}(\boldsymbol{r}|\boldsymbol{s}_j) - p(\boldsymbol{r}|\boldsymbol{s}_j)\right] \tag{2.24}$$

where the sum over $\boldsymbol{r}$ runs over all lattice sites, and where the $2d+1$ sites are the defective sites:

$$(\boldsymbol{s}_1, \ldots, \boldsymbol{s}_{2d+1}) = (\mathbf{0}, \boldsymbol{e}_1, \boldsymbol{e}_{-1}, \ldots, \boldsymbol{e}_d, \boldsymbol{e}_{-d}). \tag{2.25}$$

We also introduced the quantities $p(\boldsymbol{r}|\boldsymbol{r}_0)$, which are the elementary jump probabilities from $\boldsymbol{r}_0$ to $\boldsymbol{r}$ associated to a simple symmetric random walk on the considered structure.

For a specific lattice, one can then readily express $\boldsymbol{A}$ and $\boldsymbol{P}$, deduce $\boldsymbol{P}^{\dagger}$ from (2.21), and finally the conditional first-passage time densities F^* from (2.20). The single-vacancy propagator can therefore be deduced from (2.11).

2.4 Finite low vacancy density

2.4.1 Average over the initial positions of the vacancies

In order to study the situation where there are several vacancies on the lattice, we start from a finite d-dimensional hypercubic lattice of N sites with a finite number M of vacancies. The vacancy density

is $\rho_0 = M/N$ and is supposed to be very small, $\rho_0 \ll 1$, so that we will restrain our analysis to the leading order in ρ_0. The TP is initially at the origin and the initial positions of the vacancies are denoted by $\boldsymbol{Y}_1, \ldots, \boldsymbol{Y}_M$. At each time step, all the vacancies exchange their positions with one of the neighboring particles, such that each vacancy makes a jump at each time step. We follow here a method first presented in [23]. The general expression of $\mathcal{P}_t(\boldsymbol{X}|\boldsymbol{Y}_1, \ldots, \boldsymbol{Y}_M)$, which denotes the probability of finding at time step t the TP at position $\boldsymbol{X}$ as a result of its interactions with all M vacancies is

$$\mathcal{P}_t(\boldsymbol{X}|\boldsymbol{Y}_1, \ldots, \boldsymbol{Y}_M) = \sum_{\boldsymbol{X}_1} \cdots \sum_{\boldsymbol{X}_M} \delta_{\boldsymbol{X}, \boldsymbol{X}_1 + \ldots + \boldsymbol{X}_M} \mathcal{P}_t(\boldsymbol{X}_1, \ldots, \boldsymbol{X}_M|\boldsymbol{Y}_1, \ldots, \boldsymbol{Y}_M) \tag{2.26}$$

where $\mathcal{P}_t(\boldsymbol{X}_1, \ldots, \boldsymbol{X}_M|\boldsymbol{Y}_1, \ldots, \boldsymbol{Y}_M)$ denotes the conditional probability that within the time interval t the TP has displaced from a quantity $\boldsymbol{X}_j$ due to its interactions with the j-th vacancy.

It may appear that two vacancies are adjacent or on the same site. Implementing the evolution of such situations would require additional dynamic rules, which are in fact unnecessary as such events would contribute only to order $\mathcal{O}({\rho_0}^2)$ in the calculation. Consequently, at leading order in ρ_0, each vacancy contributes independently to the TP displacement, and discarding the events involving two or more vacancies, the quantity $\mathcal{P}_t(\boldsymbol{X}|\boldsymbol{Y}_1, \ldots, \boldsymbol{Y}_M)$ can be approximated as a product of two-particle distribution functions:

$$\mathcal{P}_t(\boldsymbol{X}|\boldsymbol{Y}_1, \ldots, \boldsymbol{Y}_M) \simeq \prod_{j=1}^{M} P_t^{(1)}(\boldsymbol{X}_j|\boldsymbol{Y}_j), \tag{2.27}$$

where the quantities $P^{(1)}$ are the single-vacancy propagators (for a lattice of N sites) calculated in the previous section. Combining these two equations, and averaging over the initial positions of the vacancies (this average being denoted by an overline), we get

$$\overline{\mathcal{P}_t(\boldsymbol{X}|\boldsymbol{Y}_1, \ldots, \boldsymbol{Y}_M)} \simeq \sum_{\boldsymbol{X}_1} \cdots \sum_{\boldsymbol{X}_M} \delta_{\boldsymbol{X}, \boldsymbol{X}_1 + \ldots + \boldsymbol{X}_M} \prod_{j=1}^{M} \overline{P_t^{(1)}(\boldsymbol{X}_j|\boldsymbol{Y}_j)}. \tag{2.28}$$

The averages involved in the right-hand side of (2.28) can be expressed as

$$\overline{P_t^{(1)}(\boldsymbol{X}_j|\boldsymbol{Y})} = \frac{1}{N-1} \sum_{\boldsymbol{Y} \neq \boldsymbol{0}} P_t^{(1)}(\boldsymbol{X}_j|\boldsymbol{Y}). \tag{2.29}$$

We then define the following Fourier transforms:

$$\widetilde{\mathcal{P}}_t(\boldsymbol{k}) \equiv \sum_{\boldsymbol{X}} \mathrm{e}^{\mathrm{i}\boldsymbol{k}\cdot\boldsymbol{X}} \overline{\mathcal{P}_t(\boldsymbol{X}|\boldsymbol{Y}_1, \ldots, \boldsymbol{Y}_M)} \tag{2.30}$$

$$\widetilde{P}_t^{(1)}(\boldsymbol{k}) \equiv \sum_{\boldsymbol{X}} \mathrm{e}^{\mathrm{i}\boldsymbol{k}\cdot\boldsymbol{X}} \overline{P_t^{(1)}(\boldsymbol{X}|\boldsymbol{Y})} = \frac{1}{N-1} \sum_{\boldsymbol{Y} \neq \boldsymbol{0}} \widetilde{P}_t^{(1)}(\boldsymbol{k}|\boldsymbol{Y}). \tag{2.31}$$

Using these definitions and writing the Fourier transform of (2.28), one gets

$$\widetilde{\mathcal{P}}_t(\boldsymbol{k}) \simeq \left[\widetilde{P}_t^{(1)}(\boldsymbol{k})\right]^M. \tag{2.32}$$

This expression formally gives the relation between the propagator $\mathcal{P}_t$ and the single-vacancy propagators $P_t^{(1)}$. Before taking the thermodynamic limit of this expression, we obtain a more suitable writing

of (2.32) by relating the single-vacancy propagators $P_t^{(1)}(\boldsymbol{X}|\boldsymbol{Y})$ to the conditional first-passage time densities $F_t^*(\mathbf{0}|\boldsymbol{e}_\nu|\boldsymbol{Y}_0)$. We write the following recurrence relation on the quantities $P_t^{(1)}$, obtained by partitioning over the first step of the walk of the vacancy:

$$P_t^{(1)}(\boldsymbol{X}|\boldsymbol{Y}) = \delta_{\boldsymbol{X},\mathbf{0}}\left(1-\sum_{j=0}^{t}F_j(\mathbf{0}|\boldsymbol{Y})\right)+\sum_{j=0}^{t}\sum_{\nu=\pm1,\ldots,\pm d}P_{t-j}^{(1)}(\boldsymbol{X}-\boldsymbol{e}_\nu|-\boldsymbol{e}_\nu)F_t^*(\mathbf{0}|\boldsymbol{e}_\nu|\boldsymbol{Y}). \quad (2.33)$$

Fourier transforming this expression, and averaging over the initial positions, we find

$$\widetilde{P}_t^{(1)}(\boldsymbol{k}) = 1-\frac{1}{N-1}\sum_{j=0}^{t}\sum_{\nu=\pm1,\ldots,\pm d}\left[1-\widetilde{P}_{t-j}^{(1)}(\boldsymbol{k}|-\boldsymbol{e}_\nu)\mathrm{e}^{\mathrm{i}\boldsymbol{k}\cdot\boldsymbol{e}_\nu}\right]\sum_{\boldsymbol{Y}\neq\mathbf{0}}F^*(\mathbf{0}|\boldsymbol{e}_\nu|\boldsymbol{Y}), \quad (2.34)$$

and finally,

$$\widetilde{\mathcal{P}}_t(\boldsymbol{k}) \simeq \left\{1-\frac{1}{N-1}\sum_{j=0}^{t}\sum_{\nu=\pm1,\ldots,\pm d}\left[1-\widetilde{P}_{t-j}^{(1)}(\boldsymbol{k}|-\boldsymbol{e}_\nu)\mathrm{e}^{\mathrm{i}\boldsymbol{k}\cdot\boldsymbol{e}_\nu}\right]\sum_{\boldsymbol{Y}\neq\mathbf{0}}F_t^*(\mathbf{0}|\boldsymbol{e}_\nu|\boldsymbol{Y})\right\}^M \quad (2.35)$$

The computation of the propagators $\mathcal{P}_t$ then relies on the determination of the single-vacancy propagators (see Section 2.3.1), and of the quantities $\sum_{\boldsymbol{Y}\neq\mathbf{0}}F_t^*(\mathbf{0}|\boldsymbol{e}_\nu|\boldsymbol{Y})$. We define the associated generating functions:

$$F'_\nu(\xi) \equiv \sum_{\boldsymbol{Y}\neq\mathbf{0}}\widehat{F}^*(\mathbf{0}|\boldsymbol{e}_\nu|\boldsymbol{Y};\xi), \quad (2.36)$$

and present a method to compute them in what follows.

2.4.2 Computation of the quantities F'_ν

The quantities F'_ν involve conditional first-passage time densities of the form $\widehat{F}^*(\mathbf{0}|\boldsymbol{e}_\nu|\boldsymbol{Y};\xi)$. Extending the relation (2.20), to an arbitrary starting point, we get

$$\widehat{F}^*(\mathbf{0}|\boldsymbol{e}_\nu|\boldsymbol{Y};\xi) = \xi p^\dagger(\mathbf{0}|\boldsymbol{e}_\nu)\widehat{P}^\dagger(\boldsymbol{e}_\mu|\boldsymbol{Y};\xi). \quad (2.37)$$

Recalling the matrix definition of $\boldsymbol{P}^\dagger$ (2.21), we get

$$F'_\nu = \xi p^\dagger(\mathbf{0}|\boldsymbol{e}_\nu)\sum_{\boldsymbol{Y}\neq\mathbf{0}}\widehat{P}^\dagger(\boldsymbol{e}_\mu|\boldsymbol{Y};\xi) \quad (2.38)$$

$$= \xi p^\dagger(\mathbf{0}|\boldsymbol{e}_\nu)\mathcal{B}_\nu{}^\top(\mathbf{1}-\boldsymbol{A})^{-1}\sum_{\boldsymbol{Y}\neq\mathbf{0}}\mathcal{B}(\boldsymbol{Y};\xi) \quad (2.39)$$

where $\mathcal{B}$ is a vector of elements

$$[\mathcal{B}(\boldsymbol{Y};\xi)]_j = \widehat{P}(\boldsymbol{s}_j|\boldsymbol{Y};\xi), \quad (2.40)$$

and the basis vectors $\mathcal{B}_\nu$ are

$$\mathcal{B}_0=\begin{pmatrix}1\\0\\0\\\vdots\\0\\0\end{pmatrix},\mathcal{B}_1=\begin{pmatrix}0\\1\\0\\\vdots\\0\\0\end{pmatrix},\mathcal{B}_{-1}=\begin{pmatrix}0\\0\\1\\\vdots\\0\\0\end{pmatrix},\ldots,\mathcal{B}_d=\begin{pmatrix}0\\0\\0\\\vdots\\1\\0\end{pmatrix},\mathcal{B}_{-d}=\begin{pmatrix}0\\0\\0\\\vdots\\0\\1\end{pmatrix}. \quad (2.41)$$

The sum over $\boldsymbol{Y}$ may be explicated in the case where lattice is homogeneous[2]. Indeed, in this case

$$\left[\sum_{\boldsymbol{Y}\neq\boldsymbol{0}} \mathcal{B}(\boldsymbol{Y};\xi)\right]_j = \sum_{\boldsymbol{Y}\neq\boldsymbol{0}} \widehat{P}(\boldsymbol{s}_j|\boldsymbol{Y};\xi) \tag{2.42}$$

$$= \sum_{\boldsymbol{Y}\neq\boldsymbol{0}} \widehat{P}(\boldsymbol{Y}|\boldsymbol{s}_j;\xi) \tag{2.43}$$

$$= \sum_{\boldsymbol{Y}} \widehat{P}(\boldsymbol{Y}|\boldsymbol{s}_j;\xi) - \widehat{P}(\boldsymbol{0}|\boldsymbol{s}_j;\xi) \tag{2.44}$$

The sum over $\boldsymbol{Y}$ can be computed using the following normalization condition

$$\sum_{\boldsymbol{Y}} P_t(\boldsymbol{Y}|\boldsymbol{s}_j) = 1, \tag{2.45}$$

and the associated generating function

$$\sum_{\boldsymbol{Y}} \widehat{P}(\boldsymbol{Y}|\boldsymbol{s}_j;\xi) = \frac{1}{1-\xi}. \tag{2.46}$$

Finally, we get the simple relation

$$\left[\sum_{\boldsymbol{Y}\neq\boldsymbol{0}} \mathcal{B}(\boldsymbol{Y};\xi)\right]_j = \frac{1}{1-\xi} - \widehat{P}(\boldsymbol{0}|\boldsymbol{s}_j;\xi). \tag{2.47}$$

Consequently, using (2.39), the quantities F'_ν are explicitly given in terms of the generating functions $\widehat{P}$ and of the matrix $\boldsymbol{A}$.

2.4.3 Thermodynamic limit and expression of the cumulants

Since we consider lattice geometries where the number of sites is infinite, we now turn to the thermodynamic limit of (2.35) ($M, N \to \infty$ with fixed ratio $M/N = \rho_0$), and we get

$$\widetilde{\mathcal{P}}_t(\boldsymbol{k}) \underset{\rho_0\to 0}{\sim} \exp\left[-\rho_0 \Omega_t(\boldsymbol{k})\right] \tag{2.48}$$

where we define

$$\Omega_t(\boldsymbol{k}) \equiv \sum_{j=0}^{t} \sum_{\nu=\pm 1,\ldots,\pm d} \left[1 - \widetilde{P}^{(1)}_{t-j}(\boldsymbol{k}|-\boldsymbol{e}_\nu)\mathrm{e}^{\mathrm{i}\boldsymbol{k}\cdot\boldsymbol{e}_\nu}\right] \sum_{\boldsymbol{Y}\neq\boldsymbol{0}} F^*_t(\boldsymbol{0}|\boldsymbol{e}_\nu|\boldsymbol{Y}). \tag{2.49}$$

In order to deduce the cumulants of the random variable $\boldsymbol{X}_t$, we notice that, by definition of the Fourier transform,

$$\widetilde{\mathcal{P}}_t(\boldsymbol{k}) = \left\langle \mathrm{e}^{\mathrm{i}\boldsymbol{k}\cdot\boldsymbol{X}_t} \right\rangle \tag{2.50}$$

[2] A lattice is *homogeneous*, if for two arbitrary sites $\boldsymbol{r}_1$ and $\boldsymbol{r}_2$, the relation $P_t(\boldsymbol{r}_1|\boldsymbol{r}_2) = P_t(\boldsymbol{r}_2 - \boldsymbol{r}_1|\boldsymbol{0})$ stands for any time t.

Consequently, the cumulant generating function, defined by $\Psi_t(\boldsymbol{k}) = \ln \left\langle \mathrm{e}^{\mathrm{i}\boldsymbol{k}\cdot\boldsymbol{X}_t} \right\rangle$, is

$$\Psi_t(\boldsymbol{k}) \underset{\rho_0 \to 0}{\sim} -\rho_0 \Omega_t(\boldsymbol{k}). \tag{2.51}$$

The cumulants of $\boldsymbol{X}_t$ are defined as the coefficients of the expansion of $\Psi_t(\boldsymbol{k})$ in powers of $\boldsymbol{k}$, and they are written:

$$\boldsymbol{\kappa}^{(n)}(t) = \frac{1}{\mathrm{i}^n} \sum_{\nu=1}^{d} \left(\left. \frac{\partial^n \Psi_t}{\partial {k_\nu}^n} \right|_{\boldsymbol{k}=\boldsymbol{0}} \right) \boldsymbol{e}_\nu. \tag{2.52}$$

Using (6.36), one gets

$$\lim_{\rho_0 \to 0} \frac{\boldsymbol{\kappa}^{(n)}(t)}{\rho_0} = -\frac{1}{\mathrm{i}^n} \sum_{\nu=1}^{d} \left(\left. \frac{\partial^n \Omega_t}{\partial {k_\nu}^n} \right|_{\boldsymbol{k}=\boldsymbol{0}} \right) \boldsymbol{e}_\nu. \tag{2.53}$$

It will often be more convenient to compute the generating functions associated to these quantities. We will then use the expression

$$\lim_{\rho_0 \to 0} \frac{\widehat{\boldsymbol{\kappa}}^{(n)}(\xi)}{\rho_0} = -\frac{1}{\mathrm{i}^n} \sum_{\nu=1}^{d} \left(\left. \frac{\partial^n \widehat{\Omega}}{\partial {k_\nu}^n} \right|_{\boldsymbol{k}=\boldsymbol{0}} \right) \boldsymbol{e}_\nu, \tag{2.54}$$

with

$$\widehat{\Omega}(\boldsymbol{k};\xi) = \sum_{\nu=\pm 1,\dots,\pm d} \left[\frac{1}{1-\xi} - \widehat{\widetilde{P}}^{(1)}(\boldsymbol{k}|-\boldsymbol{e}_\nu;\xi) \mathrm{e}^{\mathrm{i}\boldsymbol{k}\cdot\boldsymbol{e}_\nu} \right] \sum_{\boldsymbol{Y}\neq\boldsymbol{0}} \widehat{F}^*(\boldsymbol{0}|\boldsymbol{e}_\nu|\boldsymbol{Y};\xi). \tag{2.55}$$

Finally, the determination of the function $\widehat{\Omega}(\boldsymbol{k};\xi)$ and therefore of the cumulants $\boldsymbol{\kappa}^{(n)}(t)$ only relies on the determination of the following quantities:

- the sums $F'_\nu = \sum_{\boldsymbol{Y}\neq\boldsymbol{0}} \widehat{F}^*(\boldsymbol{0}|\boldsymbol{e}_\nu|\boldsymbol{Y};\xi)$, with the method given in Section 2.4.2.
- the single-vacancy propagators $\widehat{\widetilde{P}}^{(1)}(\boldsymbol{k}|-\boldsymbol{e}_\nu;\xi)$. In Section 2.3.1, we wrote these propagators in terms of the conditional first-passage time densities $F^*_t(\boldsymbol{0}|\boldsymbol{e}_\mu|\boldsymbol{e}_\nu)$, which can be computed using the method presented in Section 2.3.2.

2.5 Conclusion

In this Chapter, we presented the model of a biased TP in a d-dimensional hypercubic lattice gas of symmetric particles, constrained by hardcore interactions. In the limit where the density is high (i.e. if the vacancy density $\rho_0 = 1 - \rho$ goes to zero), it is more convenient to follow the dynamics of the vacancies than the dynamics of the particles. Indeed, the TP may move only when a vacancy visits one of its neighboring sites. At leading order in ρ_0, the vacancies contribute independently to the motion of the TP, so that the propagator associated to the TP random walk can be expressed in terms of single-vacancy propagators. These single-vacancy propagators can be formally written in terms of conditional first-passage time densities related to the random walk of a vacancy. These quantities can be studied by noticing that the random walk of a vacancy on the lattice is symmetric on every lattice site except on the $2d$ neighboring sites of the TP, on which the evolution rules of the vacancy are anisotropic. Then, the propagators of a vacancy random walk, and therefore the conditional first-passage time densities,

can be expressed in terms of the propagators of a simple symmetric random walk using a defective sites method. Thus, these propagators are the only missing quantities to obtain an explicit expression of the cumulants of the TP position. In the following Chapters, we will study different geometries:

- the one-dimensional geometry, on which we obtain an explicit expression of the probability density function of the TP position (Chapter 3).
- infinite lattices and capillary-like geometries in two and three dimensions, on which we study extensively the behavior of the fluctuations of the TP position (Chapter 4) and of its mean position (Chapter 5). This analysis yields striking observations: in confined geometries, the fluctuations of the TP exhibit a long-lived superdiffusive regime, and its mean position displays a surprising anomaly.

We also study higher-order cumulants and propose a universal formula which correctly accounts for the behavior of the TP in the different situations we considered (Chapter 6). Finally, we propose in Chapter 7 a simplified continuous description, which allows to retrieve qualitatively all the nontrivial features obtained through the exact approach.

CHAPTER 3

One-dimensional geometry

Contents

We study the transport of a biased TP in a one-dimensional hardcore lattice gas, in the limit where the density is high and where the motion of the TP is mediated by the diffusion of a small number of vacancies. Following the general method presented in Chapter 2, we express the cumulant generating function of the TP position in terms of the first-passage time densities (FPTD) associated to the random walk of the vacancies. These FPTD are calculated with standard methods from the theory of random walks on lattices. It is shown that all the odd cumulants on the one hand, and all the even cumulants on the other hand are identical in the long-time limit, and scale as $\sqrt{t}$. In particular, the fluctuations of the TP grow subdiffusively, and the classical results on single-file diffusion are retrieved in the limit of a symmetric TP. Finally, the distribution of the TP position is shown to converge to a Gaussian distribution.

Results from this Chapter were published in [P3].

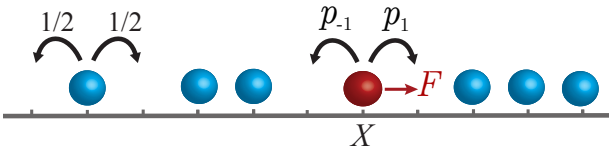

Figure 3.1: Dynamics of a biased TP in a bath of symmetric particles in one dimension

3.1 Introduction

3.1.1 Single-file diffusion

Single-file diffusion refers to strictly one-dimensional random motion of interacting particles in naturally occurring or man-made pores, which are so narrow that particles cannot bypass each other. Clearly, in such a geometry the initial order of particles remains the same over time, and the movements of individual particles become strongly correlated: the displacement of any given tracer particle (TP) on progressively larger distances necessitates the motion of more and more other particles in the same direction. This results in a subdiffusive growth of the TP mean-square displacement in the long-time limit: $\langle {X_t}^2 \rangle \propto \sqrt{t}$. This anomalous behavior has been evidenced by passive microrheological experimental studies of diffusion in molecular sieves [50], zeolites [52], or diffusion of confined colloidal particles in circular [115] or straight channels [79]. Nowadays, a single-file diffusion, prevalent in many physical, chemical and biological processes, provides a paradigmatic example of anomalous diffusion in *equilibrium* systems, which emerges due to a cooperative many-particle behavior.

From a theoretical point of view, this remarkable result has been first discovered analytically in 1965. Considering Brownian walkers on a line interacting via elastic collisions, Harris provided the rigorous proof that for a given particle, its position X_t was a random variable such that $X_t/(2t/\pi)^{1/4}$ was normally distributed with mean 0 and standard deviation 1 [54]. A discrete approach of this problem on a one-dimensional lattice allowed Arratia [4] to show that

$$\mathrm{Var}(X_t) \underset{t\to\infty}{\sim} \frac{1-\rho}{\rho}\sqrt{\frac{2t}{\pi}}, \tag{3.1}$$

where ρ is the fraction of occupied sites on the lattice. This result was reproduced using different approaches by many other authors [78, 3, 80, 7]. Recently, using macroscopic fluctuation theory, the cumulant generating function of the tracer position was derived for different initial conditions [69].

3.1.2 Case of a biased TP

Less attention has been paid to the case where the TP is pulled with a constant force F through a single-file system of unbiased diffusive particles. Such dynamics, represented in Fig. 3.1, provides a minimal model of active transport in crowded single-file environments, which mimics situations as varied as the active transport of a vesicle in a crowded axone [81], directed cellular movements in crowded channels [55], or active microrheology in capillaries [117].

The only available theoretical results concern the time evolution of the mean displacement $\langle X_t \rangle$ of a biased TP in a single-file lattice gas of hard-core particles undergoing symmetric exclusion process. It was realized that $\langle X_t \rangle$ grows sub-linearly with time, $\langle X_t \rangle \sim \alpha_F(\rho)\sqrt{t}$, which signifies that in single

files the frictional force exerted on the TP by the gas particles exhibits an unbounded growth [25]. As a matter of fact, the biased TP drives the gas to a *non-equilibrium* state with an asymmetric distribution of the gas particles around it: the gas particle accumulate in front of the TP increasing the frictional force and are depleted behind. The characteristic extents of these two perturbed regions both grow as $\sqrt{t}$.

The coefficient $\alpha_F(\rho)$ results from an interplay between the bias, formation of non-equilibrium density profiles and backflow effects of the medium on the TP, and is implicitly defined as the solution of a certain transcendental equation. Such an equation has been first evaluated in [26] for $F = \infty$, (so that the TP performs a directed random walk), in which case the model can be mapped onto the directional solidification process. Then, $\alpha_F(\rho)$ has been defined in [25] for arbitrary F and ρ using simple physical arguments, which result has been confirmed by a rigorous probabilistic calculation in [72]. Finally, it was shown that the Einstein relation between the mobility and the diffusivity holds also in this case.

3.1.3 Objectives of this chapter

We focus on the standard situation where the TP only is subject to a constant force F, which favors its motion in a preferential direction, while the gas particles perform unbiased diffusions. We will focus on the high-density limit and use the method presented in Chapter 2. At leading order in the density of vacancies, we will answer the following questions:

- What is the force and time dependance of the cumulants of the position $\kappa^{(j)}(t)$ of arbitrary order j?
- What is the probability distribution function $P_t(X)$ of the TP position?

We will show that for such dense systems all even cumulants are equal to each other for any time t, and so do all odd cumulants. Further on, we will show that all cumulants grow in proportion to $\sqrt{t}$ in the leading order in t, and, curiously enough, this leading large-t behavior of the cumulants is *independent* of F when j is even, and does depend on F for odd j. Finally, we prove that the distribution of the TP displacement converges in the limit $t \to \infty$ to a Gaussian distribution centered at the mean position $\langle X \rangle = \alpha_F(\rho)\sqrt{t}$ and with the variance which grows asymptotically as $\sqrt{t}$ and is independent of F.

3.2 Resolution

3.2.1 Model

Consider a one-dimensional lattice infinite in both directions, populated by hard-core particles present at mean density ρ. The mean density of "vacant" sites is thus equal to $\rho_0 = 1 - \rho$. The TP is initially placed at the origin. Each lattice site is occupied by at most one particle. The jump direction is chosen with probability $1/2$ for the gas particles, while the TP chooses to hop in along the bias with probability p_1, and in the opposite direction - with probability p_{-1} (see Fig. 3.1).

3.2.2 Cumulant generating function

From now on we focus on the limit $\rho_0 \ll 1$. In this limit it is more convenient to follow the vacancies, rather than the particles, and we thus reformulate the dynamics of the systems in terms of vacancies. As it was proposed in Chapter 2, we start with an auxiliary problem in which the system contains just

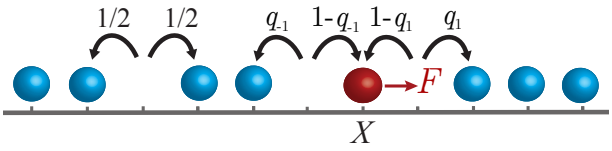

Figure 3.2: Dynamics of the vacancies, far from the tracer and in its vicinity.

a single vacancy initially at position Z. Clearly, in such a system the vacancy will perform a standard Pólya random walk stepping at each time step on the nearest-neighboring sites with probability $1/2$, except for the case when the vacancy arrives to a site adjacent to the tracer particle. In this case, the evolution rules are the following:

(i) if the vacancy occupies the site to the right of the TP, it has a probability $q_1 = 1/(2p_1+1)$ to jump to the right and $1-q_1$ to jump to the left.

(ii) if the vacancy occupies the site to the left of the TP, it has a probability $q_{-1} = 1/(2p_{-1}+1)$ to jump to the left and $1-q_{-1}$ to jump to the right.

The dynamics of the vacancies is represented on Fig. 3.2. These rules are the discrete counterpart of a continuous time version of the model, as shown in [17]. In the continuous time model, waiting times of particles are exponentials with mean 1. In that case, q_1 is in fact the probability that the adjacent bath particle jumps onto the vacancy before the TP.

Further on, for this situation with a single vacancy, let $P_t^{(1)}(X|Y)$ denote the probability of having the TP at site X at time moment t, given that the vacancy commenced its random walk at Y. In order to express this propagator, we use its generic expression (2.8). The one-dimensional geometry introduces an important simplification for the conditional return probabilities F^*. Indeed, as the lattice is not looped[1], the last site visited by a vacancy before it reaches the origin will be $\mathrm{sgn}(Y)$, where sgn is the sign function. Consequently, we have the relations

$$F_t^*(0|\nu|Y) = \begin{cases} F_t(0|Y) & \text{if } \nu = \mathrm{sgn}(Y)\ , \\ 0 & \text{otherwise.} \end{cases} \tag{3.2}$$

For this geometry, (2.8) then simplifies to

$$\begin{aligned} P_t^{(1)}(X|Y) &= \delta_{X,0}\left(1-\sum_{j=0}^{t} F_t(0|Y)\right) \\ &+ \sum_{p=1}^{+\infty}\sum_{m_1,m_2,\ldots,m_p=1}^{+\infty}\sum_{m_{p+1}=0}^{+\infty} \delta_{m_1+\ldots+m_{p+1},n}\delta_{X,\frac{\mathrm{sgn}(Z)+(-1)^{p+1}}{2}} \\ &\times \left(1-\sum_{j=0}^{m_{p+1}} F_j(0|(-1)^p)\right) \times F_{m_p}(0|(-1)^{p+1})\ldots F_{m_2}(0|-1)F_{m_1}(0|Y). \end{aligned} \tag{3.3}$$

[1] A *looped* lattice is rigorously defined as follows. Let $\mathbf{x}$ and $\mathbf{y}$ be two distinct sites of the considered lattice. Let us define the distance $d(\mathbf{x},\mathbf{y})$ as the minimal length of a path connecting $\mathbf{x}$ and $\mathbf{y}$. A lattice is *looped* is there exists two or more distinct paths of length $d(\mathbf{x},\mathbf{y})$.

According to (2.49), the computation of the cumulant generating function of X_t relies on the single-vacancy propagators $\widetilde{P}_t^{(1)}(k|\pm 1)$. We deduce from (3.3) the generating function associated to these single-vacancy propagators:

$$\widehat{P}^{(1)}(X|\pm 1;\xi) = \frac{\delta_{X,0}(1-\widehat{F}_{\pm 1}) + \delta_{X,\pm 1}\widehat{F}_{\pm 1}(1-\widehat{F}_{\mp 1})}{(1-\widehat{F}_1\widehat{F}_{-1})(1-\xi)} \tag{3.4}$$

where we define for the sake of simplicity:

$$\widehat{F}_{\pm 1} = \widehat{F}(0|\pm 1;\xi). \tag{3.5}$$

We then deduce the Fourier-Laplace transform:

$$\widehat{\widetilde{P}}^{(1)}(k|\pm 1;\xi) = \frac{1-\widehat{F}_{\pm 1} + \mathrm{e}^{\pm \mathrm{i}k}\widehat{F}_{\pm 1}(1-\widehat{F}_{\mp 1})}{(1-\widehat{F}_1\widehat{F}_{-1})(1-\xi)}. \tag{3.6}$$

Then, using (2.55), we find the auxiliary function

$$\widehat{\Omega}(\boldsymbol{k};\xi) = \sum_{\nu=\pm 1}\left[\frac{1}{1-\xi} - \widehat{\widetilde{P}}^{(1)}(k|-\nu;\xi)\mathrm{e}^{\mathrm{i}\nu k}\right]\sum_{Y\neq 0}\widehat{F}^*(0|\nu|Y;\xi) \tag{3.7}$$

$$= \sum_{\nu=\pm 1}\left[\frac{1}{1-\xi} - \frac{1-\widehat{F}_{-\nu} + \mathrm{e}^{-\mathrm{i}\nu k}\widehat{F}_{-\nu}(1-\widehat{F}_{\nu})}{(1-\widehat{F}_1\widehat{F}_{-1})(1-\xi)}\mathrm{e}^{\mathrm{i}\nu k}\right]\sum_{Y=1}^{\infty}\widehat{F}(0|\nu Y;\xi). \tag{3.8}$$

Before expanding this function in powers of k in order to get the expressions of the cumulants, we give explicit expressions of the first-passage time densities $\widehat{F}_{\pm 1}$ and of the quantity $h_\nu(\xi) \equiv \sum_{Y=1}^{\infty}\widehat{F}(0|\nu Y;\xi)$.

3.2.3 Calculation of $\widehat{F}_{\pm 1}$

We denote by $f_t(0|x)$ the first-passage time density at the origin at time t of a symmetric one-dimensional Pólya random walk starting at time 0 at site x. We get an equation for $F_t(0|\pm 1)$ by partitioning over the first time when the sites adjacent to the origin are reached:

$$F_t(0|\pm 1) = (1-q_{\pm 1})\delta_{t,1} + q_{\pm 1}\sum_{j=1}^{t} f_{j-1}(0|1)F_{t-j}(0|\pm 1), \tag{3.9}$$

Multiplying by ξ^t and summing for t going from 0 to infinity, we find

$$\widehat{F}(0|\pm 1;\xi) = (1-q_{\pm 1})\xi + q_{\pm 1}\xi\widehat{f}(0|1;\xi)\widehat{F}(0|\pm 1;\xi). \tag{3.10}$$

Using the result for one-dimensional Pólya walks [58],

$$\widehat{f}(0|x;\xi) = \left(\frac{1-\sqrt{1-\xi^2}}{\xi}\right)^{|x|}, \tag{3.11}$$

we finally get

$$\widehat{F}(0|\pm 1;\xi) = \widehat{F}_{\pm 1} = \frac{(1-q_{\pm 1})\xi}{1-q_{\pm 1}(1-\sqrt{1-\xi^2})}. \tag{3.12}$$

3.2.4 Calculation of $h_\nu(\xi)$

Similarly, noticing that

$$F_t(0|Y) = \begin{cases} \sum_{j=1}^{t} f_j(0|Y-1)F_{t-j}(0|1) & \text{if } Y > 0, \\ \sum_{j=1}^{t} f_j(0|-1-Y)F_{t-j}(0|-1) & \text{if } Y < 0. \end{cases} \tag{3.13}$$

The associated generating functions are

$$\widehat{F}(0|Y;\xi) = \begin{cases} \xi\widehat{f}(0|Y-1;\xi)\widehat{F}(0|1;\xi) & \text{if } Y > 0, \\ \xi\widehat{f}(0|-1-Y;\xi)\widehat{F}(0|-1;\xi) & \text{if } Y < 0. \end{cases} \tag{3.14}$$

Using again (3.11), we finally obtain

$$\sum_{Y=1}^{\infty} \widehat{F}(0|\nu Y;\xi) = h_\nu(\xi) = \frac{\widehat{F}_\nu}{1-(1-\sqrt{1-\xi^2})/\xi}. \tag{3.15}$$

3.2.5 Expression of the cumulants

Using (3.15) in (3.8), we obtain

$$\begin{aligned} \widehat{\Omega}(k;\xi) &= \frac{1}{1-\xi}\frac{1}{1-(1-\sqrt{1-\xi^2})/\xi}\frac{1}{1-\widehat{F}_1\widehat{F}_{-1}}\left[\widehat{F}_1(1-\widehat{F}_{-1})(1-\mathrm{e}^{\mathrm{i}k}) + \widehat{F}_{-1}(1-\widehat{F}_1)(1-\mathrm{e}^{-\mathrm{i}k})\right] \\ &= \frac{1}{1-\xi}\frac{1}{1-(1-\sqrt{1-\xi^2})/\xi}\frac{1}{1-\widehat{F}_1\widehat{F}_{-1}}\sum_{n=1}^{\infty}\frac{(\mathrm{i}k)^n}{n!}\left[\widehat{F}_1(1-\widehat{F}_{-1}) + (-1)^n\widehat{F}_{-1}(1-\widehat{F}_1)\right] \end{aligned} \tag{3.16}$$

It is then straightforward to obtain the cumulants using (2.54):

$$\widehat{\kappa}^{(n)}(\xi) \underset{\rho_0\to 0}{\sim} \rho_0 \frac{\widehat{F}_1(1-\widehat{F}_{-1}) + (-1)^n\widehat{F}_{-1}(1-\widehat{F}_1)}{(1-\xi)[1-(1-\sqrt{1-\xi^2})/\xi](1-\widehat{F}_1\widehat{F}_{-1})}. \tag{3.17}$$

Recalling that the functions $\widehat{F}_{\pm 1}$ are explicitly given in terms of the bias with (3.12), this equation gives an expression of the cumulants of arbitrary order, which constitute the key result of this Chapter. Note that this expression is valid for any ξ, i.e. for any time moment. It then gives access to the full statistics of the TP.

3.3 Results

3.3.1 Cumulants in the long-time limit

The first conclusion we can draw from (3.17) is that for arbitrary F (including $F = 0$) all odd cumulants have the same generating function $\widehat{\kappa}^{(\mathrm{odd})}(\xi)$, and all even cumulants have the same generating function $\widehat{\kappa}^{(\mathrm{even})}(\xi)$. This means that at any moment of time and for any F all cumulants $\kappa^{(j)}(t)$ with arbitrary odd $j = 2m+1$ are equal to each other, $\kappa^{(2m+1)}(t) = \kappa^{(\mathrm{odd})}(t)$, and so do all cumulants with arbitrary even $j = 2m$, $\kappa^{(2m)}(t) = \kappa^{(\mathrm{even})}(t)$.

Using (3.17) together with (3.12), we find the following results:

(i) the expansion in powers of $(1-\xi)$ (which is equivalent to the large-time limit in Laplace space) of the odd cumulants is

$$\lim_{\rho_0\to 0}\frac{\widehat{\kappa}^{(\mathrm{odd})}(\xi)}{\rho_0}\underset{\xi\to 1}{=}\frac{p_1-p_{-1}}{\sqrt{2}}\frac{1}{(1-\xi)^{3/2}}-\frac{2p_1p_{-1}(p_1-p_{-1})}{(1-\xi)}+\mathcal{O}\left(\frac{1}{\sqrt{1-\xi}}\right) \tag{3.18}$$

Using a Tauberian theorem [2], we finally obtain the long-time behavior of the odd cumulants:

$$\boxed{\lim_{\rho_0\to 0}\frac{\kappa^{(\mathrm{odd})}(t)}{\rho_0}\underset{t\to\infty}{=}(p_1-p_{-1})\sqrt{\frac{2t}{\pi}}-2p_1p_{-1}(p_1-p_{-1})+o(1).} \tag{3.22}$$

(ii) similarly, for the even cumulants, we get

$$\lim_{\rho_0\to 0}\frac{\widehat{\kappa}^{(\mathrm{even})}(\xi)}{\rho_0}\underset{\xi\to 1}{=}\frac{\sqrt{2}}{2}\frac{1}{(1-\xi)^{3/2}}+\mathcal{O}\left(\frac{1}{\sqrt{1-\xi}}\right), \tag{3.23}$$

and, using a Tauberian theorem,

$$\boxed{\lim_{\rho_0\to 0}\frac{\kappa^{(\mathrm{even})}(t)}{\rho_0}\underset{t\to\infty}{=}\sqrt{\frac{2t}{\pi}}+o(1).} \tag{3.24}$$

Equations (3.22) and (3.24) signifiy that, remarkably, the leading in time behavior of all even cumulants is independent of the bias, while the leading in time behavior of all odd cumulants does depend on the bias. The asymptotic expression of $\kappa^{\mathrm{even}}(t)$ reveals in particular that the variance of the TP grows as $\sqrt{t}$, which the same time-dependance as in single-file diffusion. This subdiffusive behavior is explained by the fact that the hardcore interactions force the particles to remain in the same order, so that the displacement of a given particle on large distances – and in particular of the TP – requires the displacement of many particles in the same direction.

In addition, for the standard choice of the transition probabilities fulfilling the detailed balance condition such that $p_1=1-p_{-1}$ and $p_1/p_{-1}=\exp(\beta F)$, where β is the inverse temperature, and for the specific case $j=0$, we check from (3.22) that

$$\lim_{\rho_0\to 0}\frac{\langle X_t\rangle}{\rho_0}=\tanh(\beta F/2)\sqrt{\frac{2t}{\pi}}+O(1), \tag{3.25}$$

[2] In this thesis, we will use several times the following Tauberian theorem (see [43] for a demonstration). We consider a time-dependent function $\phi(t)$, and we define the associated generating function $\widehat{\phi}(\xi)=\sum_{n=0}^{\infty}\phi(t)\xi^t$. If the expansion of $\widehat{\phi}(\xi)$ in powers of $(1-\xi)$ has the form

$$\widehat{\phi}(\xi)\underset{\xi\to 1}{\sim}\frac{1}{(1-\xi)^{\alpha}}\Phi\left(\frac{1}{1-\xi}\right), \tag{3.19}$$

then the long-time of $\phi(t)$ is given by

$$\phi(t)\underset{t\to\infty}{\sim}\frac{1}{\Gamma(\alpha)}t^{\alpha-1}\Phi(t), \tag{3.20}$$

where Γ is the usual gamma function. This relation holds if $\alpha>0$, $\phi(t)>0$, $\phi(t)$ is monotonic and Φ is slowly varying in the sense that

$$\lim_{x\to\infty}\frac{\Phi(\lambda x)}{\Phi(x)}=1 \tag{3.21}$$

for any $\lambda>0$.

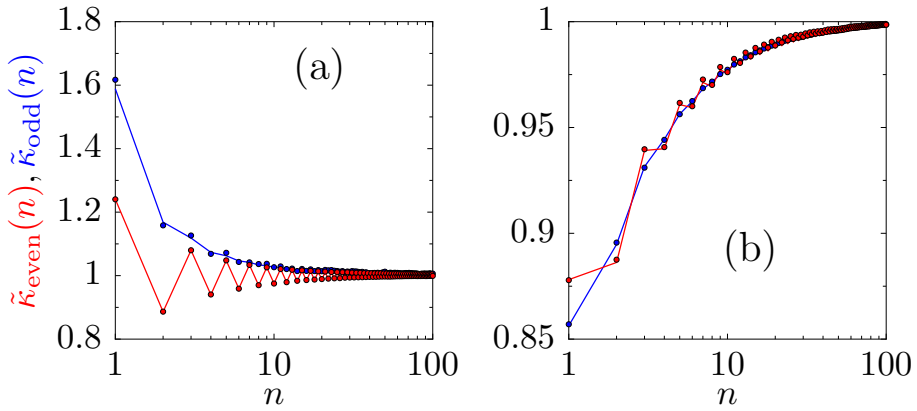

Figure 3.3: Reduced cumulants $\widetilde{\kappa}^{(\rm even)}(t) = \kappa^{(\rm even)}(t)/\sqrt{2t/\pi}$ and $\widetilde{\kappa}^{(\rm odd)}(t) = \kappa^{(\rm odd)}(t)/[(p_1-p_{-1})\sqrt{2t/\pi} - 2p_1p_{-1}(p_1-p_{-1})]$ vs time t for $\rho_0 = 0.01$ and (a) $p_1 = 0.6$ and (b) $p_1 = 0.98$. Solid lines give the results of the inversion of Eq. 3.17, while symbols are the results from numerical simulations.

which reproduces the results of [25, 72]. In the particular, in the limit $F \to 0$, (3.25) together with the expression of the even cumulants (3.24) (and thus of the variance) yield

$$\lim_{F\to 0}\left(\frac{1}{F}\lim_{\rho_0\to 0}\frac{\langle X_t\rangle}{\rho_0}\right) = \frac{1}{2\beta}\lim_{\rho_0\to 0}\frac{\mathrm{Var}(X_t)}{\rho_0}, \tag{3.26}$$

which constitutes a verification of the validity of the Einstein relation in this system.

Finally, note that (3.24) contains the particular case of the variance of a TP in single-file diffusion in the limit of $\rho \to 1$ (3.1).

3.3.2 Numerical simulations

We perform Monte-Carlo simulations of this process. Starting from a lattice of L sites (L will be taken large enough to consider the lattice as infinite), we place N vacancies on randomly chosen sites (the origin being excluded). At each simulation time step, each vacancy is moved according to the evolution rules prescribed in Section 3.2.2. The position of the TP is then averaged for a large number of relalizations.

In Fig. 3.3, we plot our theoretical predictions for the time evolution of the cumulants obtained by the inversion of Eq. 3.17, for different values of the force and at a fixed density ρ_0. We observe a perfect agreement between theory and simulations. Note that for small fields, the reduced odd cumulants approach 1 from above while for strong fields from below.

Finally, the regime of validity of our expressions with respect to the density ρ_0 is tested in Fig. 3.4, where we compare our theoretical predictions for the cumulants against the results of numerical simulations for different values of the density ρ_0 of the vacancies, for different forces F and a fixed time moment $t = 100$. We observe a very good agreement for very small values of ρ_0 and conclude that, in general, the approach developed here provides a very accurate description of the TP dynamics for $\rho_0 \lesssim 0.1$.

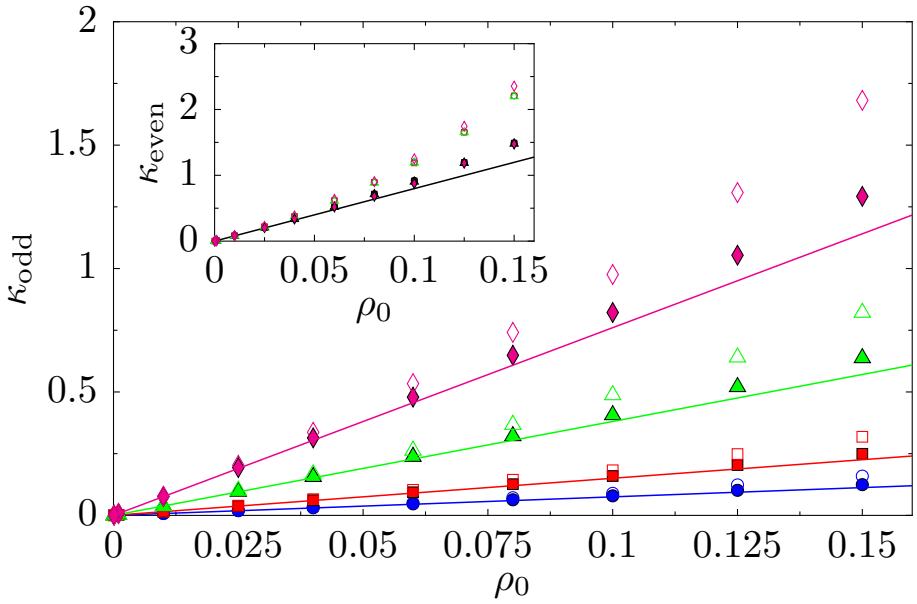

Figure 3.4: Odd cumulants at time $t = 100$ vs ρ_0. The straight lines define our predictions in (3.17) for different values of p_1, while the filled and empty symbols are the results of numerical simulations for the first and third cumulants, respectively. Circles are results for $p_1 = 0.55$, squares for $p_1 = 0.6$, triangles for $p_1 = 0.75$, and diamonds for $p_1 = 0.98$. The inset shows analogous results for the second and fourth cumulants.

3.3.3 Case of a symmetric TP

In the particular case where the TP is symmetric (i.e. $F = 0$), one has $q_1 = q_{-1} = 1/2$ and

$$\widehat{F}_1 = \widehat{F}_{-1} = \frac{\xi}{1 + \sqrt{1 - \xi^2}}. \tag{3.27}$$

As expected, this leads to $\widehat{\kappa}^{(\mathrm{odd})}(\xi) = 0$ and

$$\lim_{\rho_0 \to 0} \frac{\widehat{\kappa}^{(\mathrm{even})}(\xi)}{\rho_0} = \frac{\xi}{(1-\xi)\sqrt{1-\xi^2}}. \tag{3.28}$$

The time-dependance of the even cumulants can be retrieved by expanding $\widehat{\kappa}^{(\mathrm{even})}(\xi)$ in powers of ξ and using the definition

$$\widehat{\kappa}^{(\mathrm{even})}(\xi) = \sum_{t=0}^{\infty} \kappa^{(\mathrm{even})}(t) \xi^t. \tag{3.29}$$

We start from the known expansion

$$\frac{1}{\sqrt{1-4\xi}} = \sum_{k=0}^{\infty} \binom{2k}{k} \xi^k \tag{3.30}$$

and deduce

$$\lim_{\rho_0 \to 0} \frac{\widehat{\kappa}^{(\mathrm{even})}(\xi)}{\rho_0} = \frac{1}{1-\xi} \sum_{k=0}^{\infty} 2 \binom{2k}{k} \left(\frac{\xi}{2}\right)^{2k+1}. \tag{3.31}$$

With a Cauchy product, we get

$$\lim_{\rho_0 \to 0} \frac{\widehat{\kappa}^{(\mathrm{even})}(\xi)}{\rho_0} = \sum_{t=0}^{\infty} \left(\sum_{k=0}^{\lfloor \frac{t-1}{2} \rfloor} \binom{2k}{k} \frac{1}{2^{2k}} \right) \xi^t \tag{3.32}$$

and

$$\lim_{\rho_0 \to 0} \frac{\kappa^{(\mathrm{even})}(t)}{\rho_0} = \sum_{k=0}^{\lfloor \frac{t-1}{2} \rfloor} \binom{2k}{k} \frac{1}{2^{2k}} = \rho_0 \frac{1+N}{2^{1+2N}} \binom{2(1+N)}{1+N}, \tag{3.33}$$

where we introduced $N = \lfloor \frac{t-1}{2} \rfloor$. We use the following expression of the central binomial coefficient and introduce the Gamma function:

$$\binom{2m}{m} = \frac{2^m (2m-1)!!}{m!} = \frac{2^{2m}}{m! \sqrt{\pi}} \Gamma\left(m + \frac{1}{2}\right) \tag{3.34}$$

to finally obtain the simple relation

$$\lim_{\rho_0 \to 0} \frac{\kappa^{(\mathrm{even})}(t)}{\rho_0} = \frac{2}{\sqrt{\pi}} \frac{\Gamma\left(\lfloor \frac{t-1}{2} \rfloor + \frac{3}{2}\right)}{\left(\lfloor \frac{t-1}{2} \rfloor\right)!} \tag{3.35}$$

where Γ is the usual Gamma function and $\lfloor \cdot \rfloor$ the floor function. The time-dependent expression of $\kappa^{(\mathrm{even})}$ from (3.35) is represented on Fig 3.5 and compared to numerical simulations. Note that this expression is not restricted to the limit $t \to \infty$, and gives the expression of the even cumulant for any time, which was not known up to now.

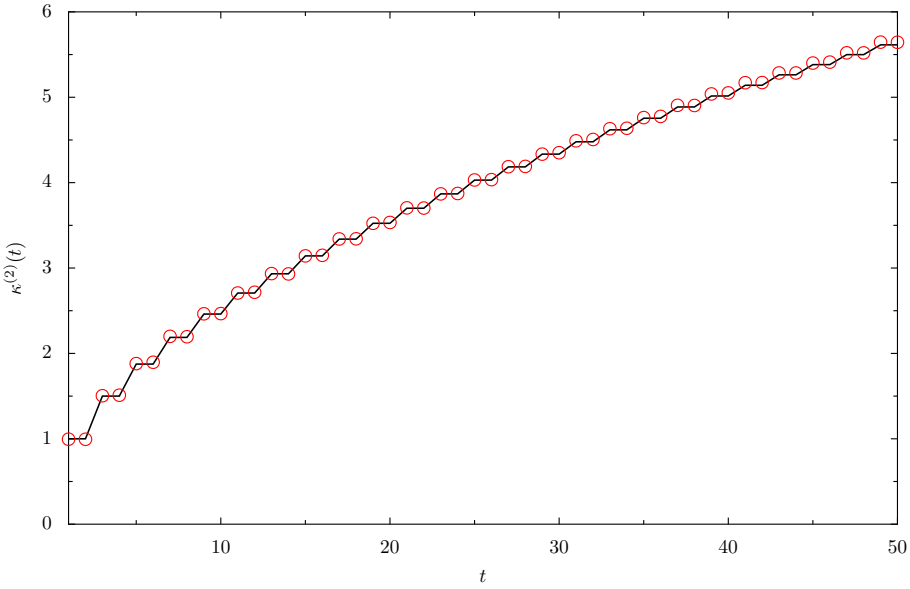

Figure 3.5: Second cumulant obtained from numerical simulations (red circles) compared to the expression from Eq. 3.35 (solid line) for a vacancy density $\rho_0 = 10^{-2}$.

3.3.4 Full distribution

We finaly provide an explicit expression of the full distribution function $\mathcal{P}_t(X)$ for any t. As a matter of fact, the equality at leading order in ρ_0 of cumulants of the same parity proved above shows that the distribution associated to these cumulants is of Skellam type [106], so that

$$\mathcal{P}_t(X) \underset{\rho_0 \to 0}{\sim} \exp\left(-\kappa^{(\mathrm{even})}(t)\right) \left(\frac{\kappa^{(\mathrm{even})}(t) + \kappa^{(\mathrm{odd})}(t)}{\kappa^{(\mathrm{even})}(t) - \kappa^{(\mathrm{odd})}(t)}\right)^{X/2} \mathrm{I}_X\left(\sqrt{\kappa^{(\mathrm{even})}(t)^2 - \kappa^{(\mathrm{odd})}(t)^2}\right), \tag{3.36}$$

where $\mathrm{I}_n(\cdot)$ is a modified Bessel function of the first kind [1]. Importantly, we find that despite the known asymmetry of the concentration profil of the bath particles [25], the rescaled variable

$$Z_t = \frac{X_t - \kappa^{(\mathrm{odd})}(t)}{\sqrt{\kappa^{(\mathrm{even})}(t)}} \tag{3.37}$$

is asymptotically distributed accordingly to a Gaussian distribution.

The explicit expression of the p.d.f. of X_t can be compared to histograms obtained from the numerical simulations described above, with a very good agreement (see Fig. 3.6).

3.4 Conclusion

In this Chapter, we studied the diffusion of a TP with asymmetric jump probabilities (Fig. 3.1) on a one-dimensional lattice populated by hardcore particles performing symmetric random walks. This system constitutes a minimal model of active transport in a crowded single-file environment, relevant

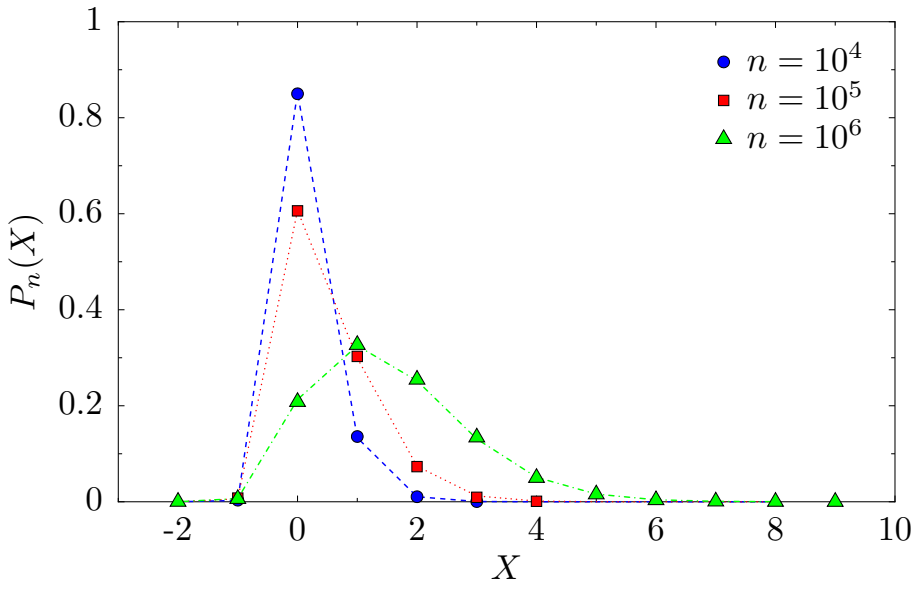

Figure 3.6: The distribution $\mathcal{P}_t(X)$ for $\rho_0 = 2 \cdot 10^{-3}$ and $p_1 = 0.98$. The dashed lines are our theoretical predictions from Eq. 3.36, while the symbols are the results of numerical simulations.

to describe different experimental situations. In the limit where the density of particles is close to 1, we applied the general formalism presented in Chapter 2, and we computed the cumulant generating function associated to the TP position. We showed that the odd cumulants are all identical, and are given by $\rho_0(p_1 - p_{-1})\sqrt{2t/\pi}$ in the limit $\rho_0 \to 0$ and $t \to \infty$. In the same limit, the even cumulants are also shown to be identical, and are independent of the bias, with the asymptotic expression $\rho_0\sqrt{2t/\pi}$. In particular, the variance of the TP position grows subdiffusively as $\sqrt{t}$. As all the cumulants of the same parity are equal, the distribution of the TP position is given by a Skellam distribution, and the distribution of the rescaled variable $(X_t - \langle X_t \rangle)/\sqrt{\mathrm{Var}(X_t)}$ converges to a Gaussian distribution in the long-time limit.

In a future work, we would like to study the case of an arbitrary density of particles, for which the results are limited to the mean position of the TP, which was computed by an approximated approach [25] and confirmed by a rigorous treatment [72]. These works could be extended in order to obtain the higher-order cumulants of the TP distribution, and in particular the variance, whose time and force dependence is still an open question.

CHAPTER 4

Confinement-induced superdiffusion

Contents

We study the fluctuations of the position a biased tracer particle (TP) in a dense hardcore lattice gas. In the limit where the density of vacancies ρ_0 goes to zero, following the method presented in Chapter 2, the fluctuations of the TP position are expressed in terms of the first-passage time densities associated to the random walk of the vacancies. We find that in confined geometries, such as quasi-one-dimensional stripe-like and capillary-like lattices or a two-dimensional lattice, the fluctuations of the TP position grow superdiffusively, and that this effect emerges beyond the linear response of the system. We show that this superdiffusive evolution is a transient long-lived regime, which crosses over to a diffusive regime after a time which scales as $1/{\rho_0}^2$. We finally compute the scaling functions describing both regimes. Off-lattice numerical simulations suggest that superdiffusion could be a generic feature of driven crowded systems.

Results from this Chapter were published in [P2] and [P4].

4.1 Introduction

4.1.1 Context

As it was emphasized in the general introduction of this thesis, determining the response of a medium to a perturbation created by a driven particle in a host medium which hinders its motion has become a key problem in statistical physics. In particular, it constitues a recurrent question of nonequilibrium statistical mechanics, arising in the quest of fundamental fluctuation-dissipation relations [84, 34]. A considerable amount of knowledge has been gathered on the forms of the so-called force-velocity relation, i.e. the dependence of the TP velocity v on the value of the applied force F, both in the linear and the nonlinear response regimes.

Behavior beyond the force-velocity relation was recently addressed numerically in the pioneering work [118], which studied via Molecular Dynamics (MD) simulations the dynamics of an externally driven, or biased TP in a glass-forming liquid (a dense binary Yukawa liquid). It was recognized that while the TP moves ballistically, i.e. $\langle X_t \rangle \sim vt$, the variance $\sigma_x^2 = \left\langle (X_t - \langle X_t \rangle)^2 \right\rangle$ of the TP position X_t along the bias grows surprisingly in a superdiffusive manner with respect to time t, so that $\sigma_x^2 \sim t^\lambda$, where λ is within the range $1.3 - 1.5$. For such systems, this effect was found *only* in the close vicinity of the glass transition while regular diffusion was recovered away from the transition [53], suggesting that such anomalous behavior could be a distinct feature of being close to the glass transition.

This as of yet unexplained finding of superdiffusion in an active microrheological set-up is counter-intuitive: indeed, in passive microrheology it is common to encounter diffusive, or even subdiffusive growth of the fluctuations of the TP position in such crowded molecular environments [56], however not superdiffusion.

The very existence of this intriguing superdiffusion remains however a matter of some debate and the available MD simulations lead to apparently conflicting results. In particular, recent MD simulations [104] investigating the dynamics of a biased TP in a dense, binary Lennard-Jones liquid, which is another glass-former, showed that the superdiffusion, if any, is only a transient and that ultimately the asymptotic behavior is diffusive.

A number of attempts has been made to explain these findings, based either on a random trap model [118], mode coupling theory [53], or continuous-time random walks (CTRWs) [104] based on previous studies of kinetically constrained models [19, 61]. All of these approaches rely on the notion of a complex energy landscape and thereby assume that the system is close to the glass transition. However, they do not provide a quantitative nor qualitative understanding of the superdiffusive behaviour. In particular, the question whether superdiffusion is the ultimate regime or only a transient is still open [118, 104].

4.1.2 Objectives of this Chapter

In this Chapter, we show that superdiffusion in active microrheology settings can appear away from the glass transition, and even *independently* of glassy properties. Based on a simple model that does not involve any complex energy landscape or kinetic constraints, we demonstrate that superdiffusion emerges generically in confined crowded systems. We fully quantify this superdiffusion, show that it is long-lived and highlight the key role of the geometry of the system.

In order to achieve this, we will investigate the high-density limit of the lattice gas model presented in Chapter 2. In particular, we will compute the second cumulant of the position X_t of the TP along the direction of the bias, defined by

$$\kappa_1^{(2)}(t) = \left\langle {X_t}^2 \right\rangle - \left\langle X_t \right\rangle^2 , \tag{4.1}$$

and we will investigate the influence of three parameters:

- the time t,
- the density of vacancies ρ_0,
- the external force F applied on the TP.

Indeed, our approach correctly captures the dependences on these parameters, which appear to be non-trivial. Before giving a complete picture of our analytical treatment, we present in the following Section a summary of the main results.

4.2 Main results of this Chapter

We consider the lattice gas model presented in Chapter 2, where the particles in the medium perform symmetric random walks on a d-dimensional lattice constrained by hard-core interactions between the particles, so that there is at most one particle per lattice site. The TP performs a random walk biased by an external force $\boldsymbol{F} = F\boldsymbol{e}_1$, so that its probability to jump in direction ν is proportional to $\mathrm{e}^{\frac{1}{2}\boldsymbol{F}\cdot\boldsymbol{e}_\nu}$. All the particles on the lattice interact via hardcore interactions. We consider several different geometries:

two-dimensional and three-dimensional infinite lattices, as well as confined quasi-one-dimensional geometries, which are infinite in the direction of $\boldsymbol{e}_1$ and finite with periodic boundary conditions in the other directions. The latter will be called "stripes" (in 2D) and "capillaries" (in 3D).

As it was emphasized in Chapter 2, an important technical point is that for small values of the density of vacancies ρ_0, the dynamics of the TP can be deduced from analyzing the joint dynamics of the TP and a single isolated vacancy. Exact asymptotic expressions of the variance $\kappa_1^{(2)}(t)$ are obtained for various geometries and for arbitrary values of the jump probabilities p_ν (probability for the TP to make a jump in direction ν). These are valid at large times and low vacancy densities, and are summarized below.

Superdiffusive regime. First, our approach predicts the following large-t behaviour of the variance $\kappa_1^{(2)}(t)$ in the leading order of ρ_0:

$$\lim_{\rho_0\to 0}\frac{\kappa_1^{(2)}(t)}{\rho_0} \underset{t\to\infty}{=} 2a_0^2 \times \begin{cases} (4/3\sqrt{\pi}L)\, t^{3/2} & \text{2D stripe,} \\ (2\sqrt{2/3\pi}/L^2)\, t^{3/2} & \text{3D capillary,} \\ \pi^{-1} t \ln(t) & \text{2D lattice,} \\ \left[A + \frac{1}{2a_0}\frac{p_1-p_{-1}}{p_1+p_{-1}}\right] t & \text{3D lattice,} \end{cases} \tag{4.2}$$

where a_0 depends on the bias

$$a_0 \;=\; \frac{p_1 - p_{-1}}{1 + \frac{2d\alpha}{2d-\alpha}(p_1+p_{-1})}, \tag{4.3}$$

$A = \widehat{P}(\mathbf{0}|\mathbf{0};1) + 2(13\alpha-6)/[(2+\alpha)(\alpha-6)]$, d is the system dimension, $\alpha = \lim_{\xi\to 1^-}[\widehat{P}(\mathbf{0}|\mathbf{0};\xi) - \widehat{P}(2\boldsymbol{e}_1|\mathbf{0};\xi)]$ and $\widehat{P}(\boldsymbol{r}|\boldsymbol{r}_0;\xi)$ is the generating function (discrete Laplace transform) of the propagator of a symmetric simple random walk. These surprisingly simple exact expressions unveil the dependence of the variance on time, width L of the stripe or of the capillary, and on the external force F. A number of important conclusions can be drawn from this result:

- Strong superdiffusion with exponent $3/2$ takes place in confined, quasi-1D geometries, those being, infinitely long 3D capillaries and 2D stripes. This result is quite counterintuitive: indeed, in the absence of driving force it is common to encounter diffusive, or even subdiffusive growth of the fluctuations of the TP position but not superdiffusion.

- The superdiffusion in such systems emerges beyond (and therefore can not be reproduced within) the linear-response-based approaches: the prefactor in the superdiffusive law is proportional to F^2 when $F \to 0$. Despite the presence of the superdiffusion, the Einstein relation is nonetheless valid for systems of arbitrary geometry due to subdominant (in time) terms whose prefactor is proportional to F.

- In unbounded 3D systems, $\kappa_1^{(2)}(t)$ grows diffusively and not superdiffusively.

- Finally, this shows that superdiffusion is geometry-induced and the recurrence of the random walk performed by a vacancy is a necessary condition in order for superdiffusion to occur. However, this condition is not sufficient. Indeed, on one-dimensional lattices, although the random walk of a vacancy is recurrent, the behavior of the TP is not superdiffusive (see Chapter 3).

Giant diffusion regime. The exact analytical result in (4.2) provides explicit criteria for superdiffusion to occur. Technically, this yields the behavior of the variance when the limit $\rho_0 \to 0$ is taken before the large-t limit. It however does not allow us, due to the nature of the limits involved, to answer the question whether the superdiffusion is the ultimate regime (or just a transient), which requires the determination of $\lim_{t\to\infty} \kappa_1^{(2)}(t)$ at fixed ρ_0. Importantly, we find that the order in which these limits are taken is crucial in confined geometries and show that $\lim_{t\to\infty} \lim_{\rho_0\to 0} \kappa_1^{(2)}(t) \neq \lim_{\rho_0\to 0} \lim_{t\to\infty} \kappa_1^{(2)}(t)$. In fact, the effective bias experienced by a vacancy between two consecutive interactions with the TP, originating from a non-zero velocity of the TP, dramatically affects the ultimate long-time behavior of the variance in confined geometries.

More precisely, we show that the superdiffusive regime is always transient for an experimentally relevant system with ρ_0 fixed, while the long-time behaviour obeys

$$\lim_{t\to\infty} \frac{\kappa_1^{(2)}(t)}{t} \underset{\rho_0\to 0}{=} \begin{cases} B & \text{quasi-1D,} \\ 4a_0^2\pi^{-1}\rho_0 \ln(\rho_0^{-1}) & \text{2D lattice,} \\ 2a_0^2\left[A + \frac{1}{2a_0}\frac{p_1-p_{-1}}{p_1-p_{-1}}\right]\rho_0 & \text{3D lattice,} \end{cases} \tag{4.4}$$

i.e., is always diffusive. The constant B only depends on the driving force F: this long-time diffusive behaviour is particularly remarkable in quasi-1D systems, in which the variance is independent of ρ_0.

Full dynamics: scaling regime and cross-over. Finally, our approach provides the complete time evolution of the variance in the regime corresponding to $\rho_0 \ll 1$ and at a sufficiently large time t, that interpolates between the two limiting regimes of superdiffusion and giant diffusion listed above. In this regime, it is found that

$$\kappa_1^{(2)}(t) \sim \begin{cases} t\widetilde{f}(\rho_0^2 t)/L^{d-1} & \text{quasi-1D,} \\ -\frac{2a_0^2}{\pi}\rho_0 t \ln\left((\rho_0 a_0)^2 + 1/t\right) & \text{2D lattice,} \\ 2a_0^2\left[A + \frac{1}{2a_0}\frac{p_1-p_{-1}}{p_1-p_{-1}}\right]\rho_0 t & \text{3D lattice,} \end{cases} \tag{4.5}$$

where the scaling function $\widetilde{f}$ is explicitly given and satisfies

$$\widetilde{f}(x) \propto \begin{cases} x^{1/2} & \text{when } x \ll 1, \\ \text{constant} & \text{when } x \gg 1. \end{cases} \tag{4.6}$$

On quasi-1D geometries an 2D lattice, the crossover time between the two regimes scales as $1/{\rho_0}^2$, so that superdiffusion is therefore very long-lived in such systems. Despite its transient feature, we thus expect superdiffusion to be a robust characteristic of confined crowded systems.

In what follows, we give a derivation of the results presented in this summary. We first present with details the case of a two-dimensional stripe-like geometry. The method can be extended to other geometries, for which we give a less detailed outline of the calculation.

4.3 Stripe-like geometry

We first study the case of a stripe-like lattice, which is two-dimensional, infinite in the direction of the applied force (chosen to be direction 1) and finite (of size L) with periodic boundary conditions in

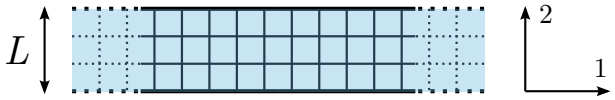

Figure 4.1: Stripe-like geometry. The lattice is infinite in the first direction (which will be the direction of the external force imposed on the TP), and finite of width L with periodic boundary conditions in the other direction.

the other direction (see Fig. 4.1). This geometry actually constitutes a minimal quasi-one-dimensional system. The evolution of the TP is given *a priori* by four jump probabilities: $p_{\pm 1}$, $p_{\pm 2}$. We assume that the bias only affects direction 1, so that $p_{-2} = p_2$. Using a normalization condition, we will write p_2 as

$$p_2 = \frac{1}{2}(1 - p_1 - p_{-1}). \tag{4.7}$$

A detailed derivation of the second cumulant in the longitudinal direction is given below for this geometry, following the method presented in Chapter 2. It will be extended to other geometries afterwards.

4.3.1 Expression of $\widehat{\Omega}(k_1;\xi)$

We follow the method described in Chapter 2. We first intend to compute the single-vacancy propagators $P_t^{(1)}(\boldsymbol{X}|\boldsymbol{Y}_0)$, and we use the notations defined previously. In this Chapter, we focus on the statistical properties of the TP position in the direction of the force $\boldsymbol{X}\cdot\boldsymbol{e}_1 \equiv X$. We then take $\boldsymbol{k} = (k_1, 0)$, and all functions of $\boldsymbol{k}$ will actually be functions of k_1. The matrix $\boldsymbol{T}(k_1;\xi)$, defined by (2.13), can be written

$$\boldsymbol{T}(k_1;\xi) = \begin{pmatrix} \mathrm{e}^{\mathrm{i}k_1}\widehat{F}^*_{1,-1}(\xi) & \mathrm{e}^{\mathrm{i}k_1}\widehat{F}^*_{1,1}(\xi) & \mathrm{e}^{\mathrm{i}k_1}\widehat{F}^*_{1,2}(\xi) & \mathrm{e}^{\mathrm{i}k_1}\widehat{F}^*_{1,-2}(\xi) \\ \mathrm{e}^{-\mathrm{i}k_1}\widehat{F}^*_{-1,-1}(\xi) & \mathrm{e}^{-\mathrm{i}k_1}\widehat{F}^*_{-1,1}(\xi) & \mathrm{e}^{-\mathrm{i}k_1}\widehat{F}^*_{-1,2}(\xi) & \mathrm{e}^{-\mathrm{i}k_1}\widehat{F}^*_{-1,-2}(\xi) \\ \widehat{F}^*_{2,-1}(\xi) & \widehat{F}^*_{2,1}(\xi) & \widehat{F}^*_{2,2}(\xi) & \widehat{F}^*_{2,-2}(\xi) \\ \widehat{F}^*_{-2,-1}(\xi) & \widehat{F}^*_{-2,1}(\xi) & \widehat{F}^*_{-2,2}(\xi) & \widehat{F}^*_{-2,-2}(\xi) \end{pmatrix} \tag{4.8}$$

where we introduced the simplified notations

$$\widehat{F}^*_{\mu,\nu}(\xi) \equiv \widehat{F}^*(\boldsymbol{0}|\boldsymbol{e}_\mu|\boldsymbol{e}_\nu;\xi), \tag{4.9}$$

and where $\widehat{F}^*(\boldsymbol{0}|\boldsymbol{e}_\mu|\boldsymbol{e}_\nu;\xi)$ are the generating functions associated to the probability for a vacancy to reach the origin for the first time a time t, being at $\boldsymbol{e}_\mu$ at time $t-1$ and starting from $\boldsymbol{e}_\nu$. For symmetry reasons, we have the following relations:

$$\widehat{F}^*_{\pm 1,-2}(\xi) = \widehat{F}^*_{\pm 1,2}(\xi) \tag{4.10}$$
$$\widehat{F}^*_{-2,\pm 1}(\xi) = \widehat{F}^*_{2,\pm 1}(\xi) \tag{4.11}$$
$$\widehat{F}^*_{-2,2}(\xi) = \widehat{F}^*_{2,-2}(\xi) \tag{4.12}$$
$$\widehat{F}^*_{-2,-2}(\xi) = \widehat{F}^*_{2,2}(\xi) \tag{4.13}$$

Introducing these relations in (4.8), it is straightforward to compute the determinant $\mathcal{D}(k_1;\xi)$,

$$\mathcal{D}(k_1;\xi) = \det[\boldsymbol{1} - \boldsymbol{T}(k_1;\xi)] \tag{4.14}$$
$$= -b_-\left(\mathcal{D}_0 + \mathcal{D}_1\mathrm{e}^{ik_1} + \mathcal{D}_{-1}\mathrm{e}^{-ik_1}\right) \tag{4.15}$$

where

$$\mathcal{D}_0 = \left(\widehat{F}^*_{-1,-1}\widehat{F}^*_{1,1} - \widehat{F}^*_{-1,1}\widehat{F}^*_{1,-1} - 1\right) b_+ + 2\left(\widehat{F}^*_{2,-1}b_1 + \widehat{F}^*_{2,1}b_{-1}\right) \tag{4.16}$$

$$\mathcal{D}_{\pm 1} = \widehat{F}^*_{\pm 1,\mp 1}b_+ - 2\widehat{F}^*_{2,\mp 1}\widehat{F}^*_{\pm 1,2} \tag{4.17}$$

and

$$b_\pm = \widehat{F}^*_{2,-2} \pm \widehat{F}^*_{2,2} - 1 \tag{4.18}$$

$$b_{\pm 1} = \widehat{F}^*_{\mp 1,\pm 1}\widehat{F}^*_{\pm 1,2} - \widehat{F}^*_{\pm 1,\pm 1}\widehat{F}^*_{\mp 1,2} \tag{4.19}$$

Expressing $U_\mu(k_1;\xi)$ from its definition (2.15), and using the expression of the Fourier-Laplace transform of $P_t^{(1)}(\boldsymbol{X}|\boldsymbol{Y}_0)$ (2.11), we find

$$\widehat{\widetilde{P}}^{(1)}(k_1|\boldsymbol{Y}_0;\xi) = \frac{1}{1-\xi}\frac{\mathcal{D}_0 - \sigma_1(\boldsymbol{Y}_0) - \sigma_{-1}(\boldsymbol{Y}_0) + [\mathcal{D}_1 + \sigma_1(\boldsymbol{Y}_0)]\,\mathrm{e}^{ik_1} + [\mathcal{D}_{-1} + \sigma_{-1}(\boldsymbol{Y}_0)]\,\mathrm{e}^{-ik_1}}{\mathcal{D}_0 + \mathcal{D}_1\mathrm{e}^{ik_1} + \mathcal{D}_{-1}\mathrm{e}^{-ik_1}} \tag{4.20}$$

with

$$\begin{aligned}\sigma_{\pm 1}(\boldsymbol{Y}_0) &= \widehat{F}^*_{\pm 1,\boldsymbol{Y}_0}[-b_+\widehat{F}^*_{\mp 1,\mp 1}b_+ - 2\widehat{F}^*_{2,\mp 1}\widehat{F}^*_{\mp 1,2}] + \widehat{F}^*_{\mp 1,\boldsymbol{Y}_0}[-\widehat{F}^*_{\pm 1,\mp 1}b_+ + 2\widehat{F}^*_{2,\mp 1}\widehat{F}^*_{\pm 1,2}] \\ &+ (\widehat{F}^*_{\pm 1,2} + b_{\mp 1})\left(\sum_{\mu\neq\pm 1}\widehat{F}^*_{\mu,\boldsymbol{Y}_0}\right),\end{aligned} \tag{4.21}$$

and

$$\widehat{F}^*_{\mu,\boldsymbol{Y}_0} = \widehat{F}^*(\boldsymbol{0}|\boldsymbol{e}_\mu|\boldsymbol{Y}_0;\xi). \tag{4.22}$$

Finally, recalling that the definition of $\Omega(k_1;\xi)$ (2.55), we get

$$\begin{aligned}\widehat{\Omega}(k_1;\xi) = \frac{1}{1-\xi}\sum_\nu \left(\sum_{\boldsymbol{Y}\neq\boldsymbol{0}}\widehat{F}^*(\boldsymbol{0}|\boldsymbol{e}_\nu|\boldsymbol{Y};\xi)\right) \\ \times\left\{1 - \mathrm{e}^{\mathrm{i}\boldsymbol{k}\cdot\boldsymbol{e}_\nu}\frac{\mathcal{D}_0 - \sigma_1(\boldsymbol{e}_{-\nu}) - \sigma_{-1}(\boldsymbol{e}_{-\nu}) + [\mathcal{D}_1 + \sigma_1(\boldsymbol{e}_{-\nu})]\,\mathrm{e}^{\mathrm{i}k_1} + [\mathcal{D}_{-1} + \sigma_{-1}(\boldsymbol{e}_{-\nu})]\,\mathrm{e}^{-\mathrm{i}k_1}}{\mathcal{D}_0 + \mathcal{D}_1\mathrm{e}^{\mathrm{i}k_1} + \mathcal{D}_{-1}\mathrm{e}^{-\mathrm{i}k_1}}\right\}.\end{aligned} \tag{4.23}$$

From this expression, and recalling the relation between $\widehat{\Omega}$ and the generating functions associated to the cumulants (2.54), we find

$$\lim_{\rho_0\to 0}\frac{\widehat{\kappa}_1^{(2)}(\xi)}{\rho_0} = \left.\frac{\partial^2\widehat{\Omega}}{\partial {k_1}^2}\right|_{\boldsymbol{k}=\boldsymbol{0}} \tag{4.24}$$

$$\begin{aligned}&= \big\{F_1'\left[(3\mathcal{D}_0 + \mathcal{D}_1 + 5\mathcal{D}_{-1})\sigma_1(\boldsymbol{e}_{-1}) + (-\mathcal{D}_0 + \mathcal{D}_1 - 3\mathcal{D}_{-1})\sigma_{-1}(\boldsymbol{e}_{-1})\right] \\ &\quad + F_{-1}'\left[(-\mathcal{D}_0 - 3\mathcal{D}_1 + \mathcal{D}_{-1})\sigma_1(\boldsymbol{e}_1) + (3\mathcal{D}_0 + 5\mathcal{D}_1 + \mathcal{D}_{-1})\sigma_{-1}(\boldsymbol{e}_1)\right] \\ &\quad + F_2'\left[(\mathcal{D}_0 - \mathcal{D}_1 + 3\mathcal{D}_{-1})\sigma_1(\boldsymbol{e}_{-2}) + (\mathcal{D}_0 + 3\mathcal{D}_1 - \mathcal{D}_{-1})\sigma_{-1}(\boldsymbol{e}_{-2})\right] \\ &\quad + F_{-2}'\left[(\mathcal{D}_0 - \mathcal{D}_1 + 3\mathcal{D}_{-1})\sigma_1(\boldsymbol{e}_2) + (\mathcal{D}_0 + 3\mathcal{D}_1 - \mathcal{D}_{-1})\sigma_{-1}(\boldsymbol{e}_2)\right]\big\} \\ &\quad \times\frac{1}{[(1-\xi)(\mathcal{D}_0 + \mathcal{D}_1 + \mathcal{D}_{-1})^2]} + \frac{F_1' + F_{-1}'}{1-\xi}\end{aligned} \tag{4.25}$$

where we defined

$$F'_\nu(\xi) = \sum_{\boldsymbol{Y}\neq\boldsymbol{0}} \widehat{F}^*(\boldsymbol{0}|\boldsymbol{e}_\nu|\boldsymbol{Y};\xi). \tag{4.26}$$

Using the symmetry relations

$$\begin{aligned} F'_{-2} &= F'_2 && (4.27)\\ \sigma_1(\boldsymbol{e}_{-2}) &= \sigma_1(\boldsymbol{e}_2) && (4.28)\\ \sigma_{-1}(\boldsymbol{e}_{-2}) &= \sigma_{-1}(\boldsymbol{e}_2) && (4.29) \end{aligned}$$

we obtain the simplified expression

$$\begin{aligned} \lim_{\rho_0\to 0}\frac{\widehat{\kappa}_1^{(2)}(\xi)}{\rho_0} &= \big\{F'_1\left[(3\mathcal{D}_0+\mathcal{D}_1+5\mathcal{D}_{-1})\sigma_1(\boldsymbol{e}_{-1})+(-\mathcal{D}_0+\mathcal{D}_1-3\mathcal{D}_{-1})\sigma_{-1}(\boldsymbol{e}_{-1})\right]\\ &\quad +F'_{-1}\left[(-\mathcal{D}_0-3\mathcal{D}_1+\mathcal{D}_{-1})\sigma_1(\boldsymbol{e}_1)+(3\mathcal{D}_0+5\mathcal{D}_1+\mathcal{D}_{-1})\sigma_{-1}(\boldsymbol{e}_1)\right]\\ &\quad +2F'_2\left[(\mathcal{D}_0-\mathcal{D}_1+3\mathcal{D}_{-1})\sigma_1(\boldsymbol{e}_{-2})+(\mathcal{D}_0+3\mathcal{D}_1-\mathcal{D}_{-1})\sigma_{-1}(\boldsymbol{e}_{-2})\right]\big\}\\ &\quad \times\frac{1}{[(1-\xi)(\mathcal{D}_0+\mathcal{D}_1+\mathcal{D}_{-1})^2]}+\frac{F'_1+F'_{-1}}{1-\xi} \end{aligned} \tag{4.30}$$

Therefore, recalling the definitions of $\mathcal{D}_k$ and $\sigma_{\pm1}(\boldsymbol{e}_\mu)$, one notices that the generating function associated to the second cumulant is expressed only in terms of

- the conditional first-passage time densities (FPTD) $F^*(\boldsymbol{0}|\boldsymbol{e}_\mu|\boldsymbol{e}_\nu)$,
- the sums $F'_\nu(\xi)=\sum_{\boldsymbol{Y}\neq\boldsymbol{0}}\widehat{F}^*(\boldsymbol{0}|\boldsymbol{e}_\nu|\boldsymbol{Y};\xi)$.

In what follows, we give a method to derive these quantities explicitly.

4.3.2 Calculation of the conditional FPTD F^*

Using the results from Chapter 2, we recall that the condition FPTD F^* are obtained using the expression

$$\widehat{F}^*(\boldsymbol{0}|\boldsymbol{e}_\mu|\mathbf{e_\nu};\xi) = \xi p^\dagger(\boldsymbol{0}|\boldsymbol{e}_\mu)\widehat{P}^\dagger(\mathbf{e}_\mu|\boldsymbol{e}_\nu;\xi). \tag{4.31}$$

where the dagger $\dagger$ is relative to the random walk of a vacancy with an absorbing site at the origin (see Fig. 2.2 for the definition of the evolution rules of the vacancies). The quantities $\widehat{P}^\dagger$ are given by the matrix relation (2.21), that we recall here:

$$\boldsymbol{P}^\dagger = (\mathbf{1}-\boldsymbol{A})^{-1}\boldsymbol{P} \tag{4.32}$$

In what follows, we give explicit expressions of the matrices $\boldsymbol{P}$ and $\boldsymbol{A}$.

4.3.2.1 Expression of $\boldsymbol{A}$

The elements of $\boldsymbol{A}$ were in Section 2.3.2 defined as

$$\boldsymbol{A}_{i,j} = A(\boldsymbol{s}_i|\boldsymbol{s}_j;\xi) = \xi\sum_{\boldsymbol{r}}\widehat{P}(\boldsymbol{s}_i|\boldsymbol{r};\xi)\underbrace{\left[p^\dagger(\boldsymbol{r}|\boldsymbol{s}_j)-p(\boldsymbol{r}|\boldsymbol{s}_j)\right]}_{\equiv p'(\boldsymbol{r}|\boldsymbol{s}_j)}. \tag{4.33}$$

In what follows, we compute $A(\boldsymbol{s}_i|\boldsymbol{s}_j;\xi)$ in the two cases: $\boldsymbol{s}_j=\boldsymbol{0}$ and $\boldsymbol{s}_j\neq\boldsymbol{0}$.

(i) if $\boldsymbol{s}_j = \mathbf{0}$:

The elementary jump probabilities can be written:

$$p(\boldsymbol{r}|\mathbf{0}) = \begin{cases} 1/4 & \text{if } \boldsymbol{r} = \boldsymbol{e}_\mu \ , \\ 0 & \text{otherwise.} \end{cases} \tag{4.34}$$

$$p^\dagger(\boldsymbol{r}|\mathbf{0}) = \begin{cases} 1 & \text{if } \boldsymbol{r} = \mathbf{0} \ , \\ 0 & \text{otherwise.} \end{cases} \tag{4.35}$$

so that

$$p'(\boldsymbol{r}|\mathbf{0}) = \begin{cases} 1 & \text{if } \boldsymbol{r} = \mathbf{0} \ , \\ -1/4 & \text{if } \boldsymbol{r} = \boldsymbol{e}_\mu, \\ 0 & \text{otherwise.} \end{cases} \tag{4.36}$$

We deduce an expression for $A(\boldsymbol{s}_i|\mathbf{0};\xi)$:

$$A(\boldsymbol{s}_i|\mathbf{0};\xi) = \xi \left[\widehat{P}(\boldsymbol{s}_i|\mathbf{0};\xi) - \frac{1}{4} \sum_{\mu=\pm1,\pm2} \widehat{P}(\boldsymbol{s}_i|\boldsymbol{e}_\mu;\xi) \right]. \tag{4.37}$$

In order to simplify this equation, we write the following relation between the propagators $\widehat{P}$, obtained by partitioning over the first step of the walk:

$$P_{t+1}(\boldsymbol{r}|\boldsymbol{r}_0) = \sum_{\mu=\pm1,\pm2} p(\boldsymbol{r}_0 + \boldsymbol{e}_\mu|\boldsymbol{r}_0) P_t(\boldsymbol{r}|\boldsymbol{r}_0 + \boldsymbol{e}_\mu). \tag{4.38}$$

Writing the associated generating functions (i.e. multiplying by ξ^t and summing for t going from 0 to infinity), we get:

$$\frac{1}{\xi}\left[\widehat{P}(\boldsymbol{r}|\boldsymbol{r}_0;\xi) - \delta_{\boldsymbol{r},\boldsymbol{r}_0}\right] = \sum_{\mu=\pm1,\pm2} p(\boldsymbol{r}_0 + \boldsymbol{e}_\mu|\boldsymbol{r}_0)\widehat{P}(\boldsymbol{r}|\boldsymbol{r} + \boldsymbol{e}_\mu;\xi), \tag{4.39}$$

or, equivalently

$$\widehat{P}(\boldsymbol{r}|\boldsymbol{r}_0;\xi) = \delta_{\boldsymbol{r},\boldsymbol{r}_0} + \frac{\xi}{4} \sum_{\mu=\pm1,\pm2} \widehat{P}(\boldsymbol{r}|\boldsymbol{r}_0 + \boldsymbol{e}_\mu;\xi). \tag{4.40}$$

Using (4.40) in (4.37), we obtain

$$A(\boldsymbol{s}_i|\mathbf{0};\xi) = \delta_{i,0} - (1-\xi)\widehat{P}(\boldsymbol{s}_i|\mathbf{0};\xi). \tag{4.41}$$

(ii) if $\boldsymbol{s}_j = \boldsymbol{e}_\nu$ ($\nu \in \{\pm1, \pm2\}$)

The elementary jump probabilities write:

$$p(\boldsymbol{r}|\boldsymbol{e}_\nu) = \begin{cases} 1/4 & \text{if } \boldsymbol{r} = \boldsymbol{e}_\nu + \boldsymbol{e}_\mu \ , \\ 0 & \text{otherwise.} \end{cases} \tag{4.42}$$

$$p^\dagger(\boldsymbol{r}|\boldsymbol{e}_\nu) = \begin{cases} \frac{p_\nu}{p_\nu+3/4} & \text{if } \boldsymbol{r} = \mathbf{0} \ , \\ \frac{1/4}{p_\nu+3/4} & \text{if } \boldsymbol{r} = \boldsymbol{e}_\nu + \boldsymbol{e}_\mu, \, \mu \neq -\nu, \\ 0 & \text{otherwise.} \end{cases} \tag{4.43}$$

so that

$$p'(\boldsymbol{r}|\boldsymbol{e}_\nu) = \begin{cases} \frac{p_\nu}{p_\nu+3/4} - \frac{1}{4} & \text{if } \boldsymbol{r} = \boldsymbol{0}\,, \\ \frac{1/4}{p_\nu+3/4} - \frac{1}{4} & \text{if } \boldsymbol{r} = \boldsymbol{e}_\nu + \boldsymbol{e}_\mu,\, \mu \neq -\nu, \\ 0 & \text{otherwise.} \end{cases} \tag{4.44}$$

We then obtain an expression for $A(\boldsymbol{s}_i|\boldsymbol{e}_\nu;\xi)$:

$$\begin{aligned} A(\boldsymbol{s}_i|\boldsymbol{e}_\nu;\xi) &= \xi \left[\left(\frac{p_\nu}{p_\nu+3/4} - \frac{1}{4} \right) \widehat{P}(\boldsymbol{s}_i|\boldsymbol{0};\xi) + \sum_{\mu\neq-\nu} \left(\frac{1/4}{p_\nu+3/4} - \frac{1}{4} \right) \widehat{P}(\boldsymbol{s}_i|\boldsymbol{e}_\nu+\boldsymbol{e}_\mu;\xi) \right] \\ &= \xi \left[\frac{p_\nu - 1/4}{p_\nu+3/4} \widehat{P}(\boldsymbol{s}_i|\boldsymbol{0};\xi) + \frac{1}{4} \left(\frac{1}{p_\nu+3/4} - 1 \right) \sum_{\mu=\pm1,\pm2} \widehat{P}(\boldsymbol{s}_i|\boldsymbol{e}_\nu+\boldsymbol{e}_\mu;\xi) \right] \end{aligned}$$

Finally, using again (4.40), we get

$$A(\boldsymbol{s}_i|\boldsymbol{e}_\nu;\xi) = \left(\frac{1}{p_\nu+3/4} - 1 \right) \left[\widehat{P}(\boldsymbol{s}_i|\boldsymbol{e}_\nu;\xi) - \delta_{i,\nu} - \xi \widehat{P}(\boldsymbol{s}_i|\boldsymbol{0};\xi) \right] \tag{4.45}$$

These two cases then lead to the general expression

$$A(\boldsymbol{s}_i|\boldsymbol{s}_j;\xi) = \begin{cases} \delta_{i,0} - (1-\xi)\widehat{P}(\boldsymbol{s}_i|\boldsymbol{0};\xi) & \text{if } \boldsymbol{s}_j = \boldsymbol{0}\,, \\ \left(\frac{1}{p_\nu+3/4} - 1 \right) \left[\widehat{P}(\boldsymbol{s}_i|\boldsymbol{e}_\nu;\xi) - \delta_{i,\nu} - \xi \widehat{P}(\boldsymbol{s}_i|\boldsymbol{0};\xi) \right] & \text{if } \boldsymbol{s}_j = \boldsymbol{e}_\nu. \end{cases} \tag{4.46}$$

Finally, the entries of the matrix $\boldsymbol{A}$ are simply expressed in terms of the propagators $\widehat{P}(\boldsymbol{s}_i|\boldsymbol{s}_j)$, i.e. the entries of the matrix $\boldsymbol{P}$. In what follows, we give an expression of the matrix $\boldsymbol{P}$, and simplify it using symmetry relations.

4.3.2.2 Expression of $\boldsymbol{P}$

The elements of $\boldsymbol{P}$ are the propagators $\widehat{P}(\boldsymbol{s}_i|\boldsymbol{s}_j;\xi)$, relative to the random walk of a vacancy without perturbation at the origin. Note that this random walk is equivalent to a Pólya walk of a single walker on a stripe-like lattice. The expression of $\boldsymbol{P}$ is

$$\boldsymbol{P} = \begin{pmatrix} \widehat{P}(\boldsymbol{0}|\boldsymbol{0};\xi) & \widehat{P}(\boldsymbol{0}|\boldsymbol{e}_1;\xi) & \widehat{P}(\boldsymbol{0}|\boldsymbol{e}_{-1};\xi) & \widehat{P}(\boldsymbol{0}|\boldsymbol{e}_2;\xi) & \widehat{P}(\boldsymbol{0}|\boldsymbol{e}_{-2};\xi) \\ \widehat{P}(\boldsymbol{e}_1|\boldsymbol{0};\xi) & \widehat{P}(\boldsymbol{e}_1|\boldsymbol{e}_1;\xi) & \widehat{P}(\boldsymbol{e}_1|\boldsymbol{e}_{-1};\xi) & \widehat{P}(\boldsymbol{e}_1|\boldsymbol{e}_2;\xi) & \widehat{P}(\boldsymbol{e}_1|\boldsymbol{e}_{-2};\xi) \\ \widehat{P}(\boldsymbol{e}_{-1}|\boldsymbol{0};\xi) & \widehat{P}(\boldsymbol{e}_{-1}|\boldsymbol{e}_1;\xi) & \widehat{P}(\boldsymbol{e}_{-1}|\boldsymbol{e}_{-1};\xi) & \widehat{P}(\boldsymbol{e}_{-1}|\boldsymbol{e}_2;\xi) & \widehat{P}(\boldsymbol{e}_{-1}|\boldsymbol{e}_{-2};\xi) \\ \widehat{P}(\boldsymbol{e}_2|\boldsymbol{0};\xi) & \widehat{P}(\boldsymbol{e}_2|\boldsymbol{e}_1;\xi) & \widehat{P}(\boldsymbol{e}_2|\boldsymbol{e}_{-1};\xi) & \widehat{P}(\boldsymbol{e}_2|\boldsymbol{e}_2;\xi) & \widehat{P}(\boldsymbol{e}_2|\boldsymbol{e}_{-2};\xi) \\ \widehat{P}(\boldsymbol{e}_{-2}|\boldsymbol{0};\xi) & \widehat{P}(\boldsymbol{e}_{-2}|\boldsymbol{e}_1;\xi) & \widehat{P}(\boldsymbol{e}_{-2}|\boldsymbol{e}_{-1};\xi) & \widehat{P}(\boldsymbol{e}_{-2}|\boldsymbol{e}_2;\xi) & \widehat{P}(\boldsymbol{e}_{-2}|\boldsymbol{e}_{-2};\xi) \end{pmatrix} \tag{4.47}$$

This matrix involves 25 distinct propagators. The considered lattice has several properties which will be useful to simplify the expression of $\boldsymbol{P}$:

- the lattice is translation invariant:

$$\widehat{P}(\boldsymbol{r}|\boldsymbol{r}_0;\xi) = \widehat{P}(\boldsymbol{r}-\boldsymbol{r}_0|\boldsymbol{0};\xi). \tag{4.48}$$

- the random walk is symmetric with respect to each coordinate:

$$\widehat{P}(r_1\boldsymbol{e}_1 + r_2\boldsymbol{e}_2|\mathbf{0};\xi) = \widehat{P}(-r_1\boldsymbol{e}_1 + r_2\boldsymbol{e}_2|\mathbf{0};\xi), \tag{4.49}$$

$$\widehat{P}(r_1\boldsymbol{e}_1 + r_2\boldsymbol{e}_2|\mathbf{0};\xi) = \widehat{P}(r_1\boldsymbol{e}_1 - r_2\boldsymbol{e}_2|\mathbf{0};\xi), \tag{4.50}$$

Using these properties, $\boldsymbol{P}$ reduces to

$$\boldsymbol{P} = \begin{pmatrix} \widehat{P}(\mathbf{0}|\mathbf{0};\xi) & \widehat{P}(\boldsymbol{e}_1|\mathbf{0};\xi) & \widehat{P}(\boldsymbol{e}_1|\mathbf{0};\xi) & \widehat{P}(\boldsymbol{e}_2|\mathbf{0};\xi) & \widehat{P}(\boldsymbol{e}_2|\mathbf{0};\xi) \\ \widehat{P}(\boldsymbol{e}_1|\mathbf{0};\xi) & \widehat{P}(\mathbf{0}|\mathbf{0};\xi) & \widehat{P}(2\boldsymbol{e}_1|\mathbf{0};\xi) & \widehat{P}(\boldsymbol{e}_1+\boldsymbol{e}_2|\mathbf{0};\xi) & \widehat{P}(\boldsymbol{e}_1+\boldsymbol{e}_2|\mathbf{0};\xi) \\ \widehat{P}(\boldsymbol{e}_1|\mathbf{0};\xi) & \widehat{P}(2\boldsymbol{e}_1|\mathbf{0};\xi) & \widehat{P}(\mathbf{0}|\mathbf{0};\xi) & \widehat{P}(\boldsymbol{e}_1+\boldsymbol{e}_2|\mathbf{0};\xi) & \widehat{P}(\boldsymbol{e}_1+\boldsymbol{e}_2|\mathbf{0};\xi) \\ \widehat{P}(\boldsymbol{e}_2|\mathbf{0};\xi) & \widehat{P}(\boldsymbol{e}_1+\boldsymbol{e}_2|\mathbf{0};\xi) & \widehat{P}(\boldsymbol{e}_1+\boldsymbol{e}_2|\mathbf{0};\xi) & \widehat{P}(\mathbf{0}|\mathbf{0};\xi) & \widehat{P}(2\boldsymbol{e}_2|\mathbf{0};\xi) \\ \widehat{P}(\boldsymbol{e}_2|\mathbf{0};\xi) & \widehat{P}(\boldsymbol{e}_1+\boldsymbol{e}_2|\mathbf{0};\xi) & \widehat{P}(\boldsymbol{e}_1+\boldsymbol{e}_2|\mathbf{0};\xi) & \widehat{P}(2\boldsymbol{e}_2|\mathbf{0};\xi) & \widehat{P}(\mathbf{0}|\mathbf{0};\xi) \end{pmatrix}. \tag{4.51}$$

This matrix only involves six distinct propagators, corresponding to random walks starting from the origin and arriving at sites $\mathbf{0}$, $\boldsymbol{e}_1$, $\boldsymbol{e}_2$, $2\boldsymbol{e}_1$, $2\boldsymbol{e}_2$ and $\boldsymbol{e}_1+\boldsymbol{e}_1$. A detailed calculation of these propagators, as well as their expansions in the long-time limit ($\xi \to 1$) is given in Appendix A.

Using the symmetry relations of the propagators $\widehat{P}$ and the expressions of the entries of $\boldsymbol{A}$ (4.46), we find

$$\boldsymbol{A} = \begin{pmatrix} 1-(1-\xi)\widehat{P}_{0,0} & r_1(\widehat{P}_{1,0}-\xi\widehat{P}_{0,0}) & r_{-1}(\widehat{P}_{1,0}-\xi\widehat{P}_{0,0}) & r_2(\widehat{P}_{0,1}-\xi\widehat{P}_{0,0}) & r_2(\widehat{P}_{0,1}-\xi\widehat{P}_{0,0}) \\ -(1-\xi)\widehat{P}_{1,0} & r_1(\widehat{P}_{0,0}-1-\xi\widehat{P}_{1,0}) & r_{-1}(\widehat{P}_{2,0}-\xi\widehat{P}_{1,0}) & r_2(\widehat{P}_{1,1}-\xi\widehat{P}_{1,0}) & r_2(\widehat{P}_{1,1}-\xi\widehat{P}_{1,0}) \\ -(1-\xi)\widehat{P}_{1,0} & r_1(\widehat{P}_{2,0}-\xi\widehat{P}_{1,0}) & r_{-1}(\widehat{P}_{0,0}-1-\xi\widehat{P}_{1,0}) & r_2(\widehat{P}_{1,1}-\xi\widehat{P}_{1,0}) & r_2(\widehat{P}_{1,1}-\xi\widehat{P}_{1,0}) \\ -(1-\xi)\widehat{P}_{0,1} & r_1(\widehat{P}_{1,1}-\xi\widehat{P}_{0,1}) & r_{-1}(\widehat{P}_{1,1}-\xi\widehat{P}_{0,1}) & r_2(\widehat{P}_{0,0}-1-\xi\widehat{P}_{0,1}) & r_2(\widehat{P}_{0,2}-\xi\widehat{P}_{0,1}) \\ -(1-\xi)\widehat{P}_{0,1} & r_1(\widehat{P}_{1,1}-\xi\widehat{P}_{0,1}) & r_{-1}(\widehat{P}_{1,1}-\xi\widehat{P}_{0,1}) & r_2(\widehat{P}_{0,2}-\xi\widehat{P}_{0,1}) & r_2(\widehat{P}_{0,0}-1-\xi\widehat{P}_{0,1}) \end{pmatrix} \tag{4.52}$$

where we used the simplified notations $r_\nu = \frac{1}{p_\nu+3/4} - 1$ and $\widehat{P}_{r_1,r_2} = \widehat{P}(r_1\boldsymbol{e}_1 + r_2\boldsymbol{e}_2|\mathbf{0};\xi)$.

Finally, using the matrix relation (2.21) and the definitions of $\boldsymbol{P}$ (4.51) and $\boldsymbol{A}$ (4.52), the propagators $\widehat{P}^\dagger(\mathbf{e}_\mu|\boldsymbol{e}_\nu;\xi)$ are readily expressed in terms of the propagators $\widehat{P}(\mathbf{e}_\mu|\boldsymbol{e}_\nu;\xi)$. One deduces from (2.20) and from the values of $p^\dagger$ (4.43) the expressions of $\widehat{F}^*(\mathbf{0}|\boldsymbol{e}_\mu|\boldsymbol{e}_\nu;\xi)$ in terms of the propagators $\widehat{P}$. These expressions are straightforward to obtain, but are cumbersome as they rely on the inversions and products of 5×5 matrices. In practice, the determination of the conditional FPTD requires the use of a computer algebra software.

4.3.3 Calculation of the quantities F'_ν

Recalling the method given in Section 2.4.2, the quantities F'_ν may be computed straightforwardly using a computer algebra software with (2.39) and (2.47), and using the expressions of $\boldsymbol{A}$ (4.52) and the propagators $\widehat{P}(\mathbf{0}|\boldsymbol{s}_j;\xi)$ (Appendix A).

4.3.4 Expression of the second cumulant in the long-time limit

In what follows, we give an explicit derivation of the leading order term of $\widehat{\kappa}_1^{(2)}(\xi)$ in the $\xi \to 1$ limit. Using the expansion of the propagators $\widehat{P}$ (see Appendix A and the equations (A.36)-(A.41)), we first notice that at leading order in $(1-\xi)$, the quantities $\sigma_{\pm1}(\boldsymbol{e}_{\pm\nu})$ involved in the expression of the second cumulant (4.30) are independent of ν, and can be written

$$\sigma_{\pm1}(\boldsymbol{e}_\nu) \underset{\xi\to1}{\sim} -\frac{1}{\mathcal{S}} p_{\pm1}(\alpha-4)(4+\alpha-4\beta), \tag{4.53}$$

with

$$\begin{aligned}\mathcal{S} \equiv\ & 8\alpha(\alpha-4\beta+2)(p_1+p_{-1})^3-4(3\alpha-4)(\alpha-4\beta+2)(p_1+p_{-1})^2\\ &+\left[6\alpha^2-24\alpha\beta+64\beta-32-8\alpha(\alpha-4\beta+2)(p_1-p_{-1})^2\right](p_1+p_{-1})\\ &+2\alpha(3\alpha-12\beta+4)(p_1-p_{-1})^2-(\alpha-4)(4+\alpha-4\beta),\end{aligned} \tag{4.54}$$

where we have introduced the useful quantities α and β, defined by

$$\alpha = \lim_{\xi\to 1}\left[\widehat{P}(\mathbf{0}|\mathbf{0};\xi)-\widehat{P}(2\boldsymbol{e}_1|\mathbf{0};\xi)\right]=8(1-S^{(2)}_{L,1}-S^{(2)}_{L,3}) \tag{4.55}$$

$$\beta = \lim_{\xi\to 1}\left[\widehat{P}(\mathbf{0}|\mathbf{0};\xi)-\widehat{P}(\boldsymbol{e}_1|\mathbf{0};\xi)\right]=2(1-S^{(2)}_{L,1}) \tag{4.56}$$

and the quantities $S^{(2)}_{L,n}$

$$S^{(2)}_{L,n}\equiv\frac{1}{L}\sum_{k_2=1}^{L-1}\frac{\sin^n(\pi k_2/L)}{\sqrt{1+\sin^2(\pi k_2/L)}}. \tag{4.57}$$

(see Appendix A for details). Furthermore, one obtains the leading order of the quantities $\mathcal{D}_j$ and $\mathcal{D}_0+\mathcal{D}_1+\mathcal{D}_{-1}$ involved in the expression of the second cumulant (4.30):

$$\mathcal{D}_0 \underset{\xi\to1}{\sim} -\frac{1}{\mathcal{S}}(p_1+p_{-1})(\alpha-4)(4+\alpha-4\beta), \tag{4.58}$$

$$\mathcal{D}_{\pm1} \underset{\xi\to1}{\sim} \frac{1}{\mathcal{S}}p_{\pm1}(\alpha-4)(4+\alpha-4\beta), \tag{4.59}$$

$$\mathcal{D}_0+\mathcal{D}_1+\mathcal{D}_{-1} \underset{\xi\to1}{\sim} \frac{1}{\mathcal{S}}(4+\alpha-4\beta)[4-\alpha+4\alpha(p_1+p_{-1})]L\sqrt{1-\xi}. \tag{4.60}$$

With these expansions, we find an intermediate expression of the second cumulant

$$\lim_{\rho_0\to0}\frac{\widehat{\kappa}^{(2)}_1(\xi)}{\rho_0}\underset{\xi\to1}{\sim}\frac{1}{1-\xi}\left[\frac{2(p_1-p_{-1})^2(\alpha-4)^2}{L^2(1-\xi)(4+\alpha+4\alpha(p_1+p_{-1}))^2}\sum_\nu F'_\nu+(F'_1+F'_{-1})\right] \tag{4.61}$$

Finally, the expansions of $F'_1+F'_{-1}$ and of the sum $\sum_\nu F'_\nu$ are

$$\begin{aligned}F'_1+F'_{-1} &\underset{\xi\to1}{\sim} \frac{1}{\mathcal{S}}\frac{L}{\sqrt{1-\xi}}[8\alpha p_1p_{-1}-(\alpha-4)(p_1+p_{-1})][2(\alpha-6\beta+4)(p_1+p_{-1})-\alpha+8\beta-4]\\ \sum_\nu F'_\nu(\xi) &\underset{\xi\to1}{\sim} \frac{L}{\sqrt{1-\xi}}\end{aligned} \tag{4.62}$$

Combining these results in the expression of the second cumulant from (4.61), we get

$$\lim_{\rho_0\to0}\frac{\widehat{\kappa}^{(2)}_1(\xi)}{\rho_0}\underset{\xi\to1}{\sim}\frac{2}{L}\left[\frac{p_1-p_{-1}}{1+\frac{4\alpha}{4-\alpha}(p_1+p_{-1})}\right]^2\frac{1}{(1-\xi)^{5/2}}. \tag{4.63}$$

Finally, using a Tauberian theorem and introducing the quantity

$$a_0\equiv\frac{p_1-p_{-1}}{1+\frac{4\alpha}{4-\alpha}(p_1+p_{-1})}, \tag{4.64}$$

we get the long-time behavior of the second cumulant in the limit of a low vacancy density:

$$\boxed{\lim_{\rho_0\to0}\frac{\kappa^{(2)}_1(t)}{\rho_0}\underset{t\to\infty}{\sim}\frac{8{a_0}^2}{3\sqrt{\pi}L}t^{3/2}} \tag{4.65}$$

4.3.5 Comments

- In stripe-like geometries, the fluctuations of the position of the TP are superdiffusive and grow as $t^{3/2}$. This anomalous behavior is counterintuitive, as the fluctuations would grow linearly with time in the absence of driving force.
- Superdiffusion emerges beyond (and therefore can not be reproduced within) the linear-response-based approaches. Indeed, if the transition probabilities are assumed to be related to some driving force ($p_\mu \propto \mathrm{e}^{\frac{1}{2}\boldsymbol{F}\cdot\boldsymbol{e}_\mu}$, with an appropriate normalization), it is straightforward to show that

$$ {a_0}^2 \underset{F\to 0}{=} \mathcal{O}(F^2), \tag{4.66} $$

  so that the prefactor computed above vanishes when $F \to 0$ but proportionally to F^2. However, it can be shown that the subdominant terms in time cancels as F, and that an Einstein relation is valid in this system.
- In Chapter 7, we will present a simplified description of the system, unveiling the physical mechanism at the origin of this anomalous behavior.

4.3.6 Numerical simulations

To simulate our lattice gas system on a stripe-like geometry, we performed Monte-Carlo simulations of M vacancies on an N-site lattice ($\rho_0 = M/N$) of size $L_x \times L$, including periodic boundary conditions. For a fixed value of ρ_0, L_x is chosen so that the number of vacancies is at least of a few tens. For the different sets of parameters, we checked that increasing L_x has no impact on the results, so that L_x is large enough to consider the system as infinite. This remark holds for all the simulation results presented in this Chapter and in Chapter 5.

At each time step, each of the N vacancies exchanges its position with one of the neighboring particles according to the rules defined previously. Consequently, the TP may move as a result of the vacancies displacements. We keep track of the time evolution of its position, compute the first moments of the distribution of X_t, and deduce the cumulants.

The elementary jump probabilities p_μ of the TP are assumed to be controlled by a single parameter, namely an external force $\boldsymbol{F} = F\boldsymbol{e}_1$ ($F > 0$), such that

$$ p_\mu \propto \mathrm{e}^{\frac{1}{2}\boldsymbol{F}\cdot\boldsymbol{e}_\mu}. \tag{4.67} $$

With an appropriate normalization, we get

$$ p_1 = \frac{\mathrm{e}^{F/2}}{2[1+\cosh(F/2)]} \tag{4.68} $$

$$ p_{-1} = \frac{\mathrm{e}^{-F/2}}{2[1+\cosh(F/2)]} \tag{4.69} $$

$$ p_{\pm 2} = \frac{1}{2[1+\cosh(F/2)]} \tag{4.70} $$

We present on Fig. 4.2 the results from numerical simulations on a two-dimensional stripe. For different values of L and F, the rescaled variance $[3\sqrt{\pi}L\kappa_1^{(2)}(t)]/(8{a_0}^2\rho_0)$ is plotted and compared to the

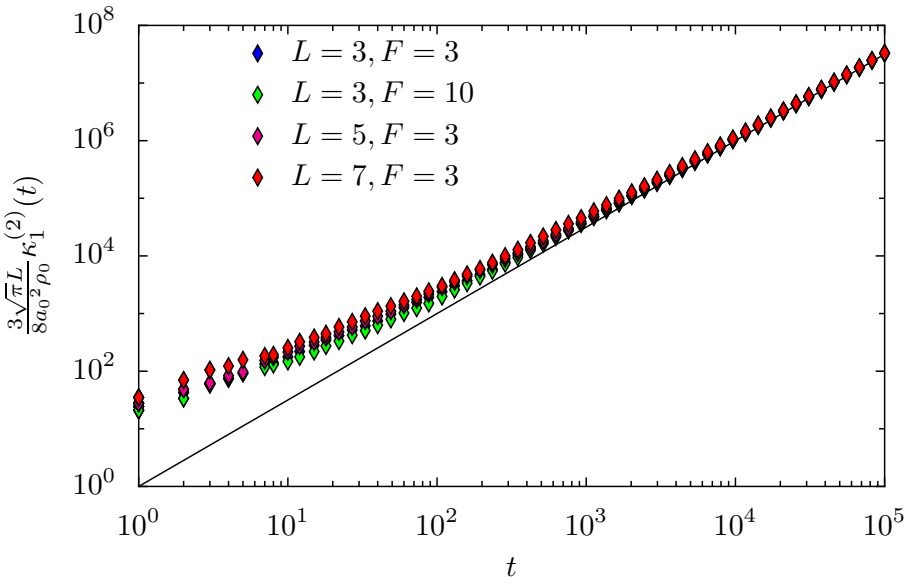

Figure 4.2: Rescaled variance obtained from numerical simulations of tracer diffusion on a stripe with different sizes L and external forces F. The vacancy density is $\rho_0 = 10^{-5}$. The black line is $t^{3/2}$.

analytical prediction. At large times, we observe a good collapse of the simulations results obtained for different values of the parameters on the prediction from (4.65). Our analytical treatment of the problem correctly captures the dependence of the TP fluctuations with all the parameters (time, applied force, width of the stripe).

4.4 Capillary-like geometry

4.4.1 Introduction

A more realistic description of a quasi-one-dimensional system would be the extension of the stripe-like lattice to three dimensions, that we will call a capillary-like geometry (represented on Fig. 4.3). This lattice is infinite in the direction of the applied force, and finite of width L with periodic boundary conditions in the other directions. The evolution of the TP is given *a priori* by six jump probabilities: $p_{\pm 1}, p_{\pm 2}, p_{\pm 3}$. As previously, we will assume that the bias experienced by the TP only affects directions $\boldsymbol{e}_{\pm 1}$, so that $p_{-3} = p_3 = p_{-2} = p_2$. Using a normalization condition, we will write p_2 as

$$p_2 = \frac{1}{4}(1 - p_1 - p_{-1}). \tag{4.71}$$

The calculation presented below closely follows the one presented in the case of stripe-like geometries. We recall the main steps leading to the expression of the fluctuations of the TP position, and give the main intermediate results.

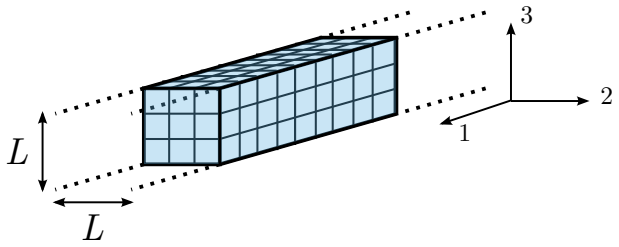

Figure 4.3: Capillary-like geometry. The lattice is infinite in the first direction (which will be the direction of the external force imposed on the TP), and finite of width L with periodic boundary conditions in the other directions.

4.4.2 Expression of $\widehat{\Omega}(k_1;\xi)$

We follow the same procedure as the one used for the stripe-like geometry in Section 4.3. First of all, the matrix $\boldsymbol{T}$ becomes

$$\boldsymbol{T}(k_1;\xi) = \begin{pmatrix} \mathrm{e}^{\mathrm{i}k_1}\widehat{F}^*_{1,-1} & \mathrm{e}^{\mathrm{i}k_1}\widehat{F}^*_{1,1} & \mathrm{e}^{\mathrm{i}k_1}\widehat{F}^*_{1,2} & \mathrm{e}^{\mathrm{i}k_1}\widehat{F}^*_{1,2} & \mathrm{e}^{\mathrm{i}k_1}\widehat{F}^*_{1,2} & \mathrm{e}^{\mathrm{i}k_1}\widehat{F}^*_{1,2} \\ \mathrm{e}^{-\mathrm{i}k_1}\widehat{F}^*_{-1,-1} & \mathrm{e}^{-\mathrm{i}k_1}\widehat{F}^*_{-1,1} & \mathrm{e}^{-\mathrm{i}k_1}\widehat{F}^*_{-1,2} & \mathrm{e}^{-\mathrm{i}k_1}\widehat{F}^*_{-1,2} & \mathrm{e}^{-\mathrm{i}k_1}\widehat{F}^*_{-1,2} & \mathrm{e}^{-\mathrm{i}k_1}\widehat{F}^*_{-1,2} \\ \widehat{F}^*_{2,-1} & \widehat{F}^*_{2,1} & \widehat{F}^*_{2,-2} & \widehat{F}^*_{2,2} & \widehat{F}^*_{2,3} & \widehat{F}^*_{2,3} \\ \widehat{F}^*_{2,-1} & \widehat{F}^*_{2,1} & \widehat{F}^*_{2,2} & \widehat{F}^*_{2,-2} & \widehat{F}^*_{2,3} & \widehat{F}^*_{2,3} \\ \widehat{F}^*_{2,-1} & \widehat{F}^*_{2,1} & \widehat{F}^*_{2,3} & \widehat{F}^*_{2,3} & \widehat{F}^*_{2,-2} & \widehat{F}^*_{2,2} \\ \widehat{F}^*_{2,-1} & \widehat{F}^*_{2,1} & \widehat{F}^*_{2,3} & \widehat{F}^*_{2,3} & \widehat{F}^*_{2,2} & \widehat{F}^*_{2,-2} \end{pmatrix}, \tag{4.72}$$

where we used the symmetry relations (4.10)-(4.13) and the additional relations related to the third coordinate:

$$\widehat{F}^*_{\pm 2,\pm 3} = \widehat{F}^*_{2,3}, \tag{4.73}$$

$$\widehat{F}^*_{\pm 3,\pm 2} = \widehat{F}^*_{2,3}. \tag{4.74}$$

$$\tag{4.75}$$

We finally obtain an expression for the function $\widehat{\Omega}(k_1;\xi)$ (see Appendix D.1 for details and for the expressions of the quantities $\mathcal{D}_j$ and $\sigma_{\pm 1}(\boldsymbol{e}_\nu)$)

$$\widehat{\Omega}(k_1;\xi) = \frac{1}{1-\xi}\sum_\nu \left(\sum_{\boldsymbol{Y}\neq\boldsymbol{0}} F^*(\boldsymbol{0}|\boldsymbol{e}_\nu|\boldsymbol{Y};\xi)\right) \times \left\{1 - \mathrm{e}^{i\boldsymbol{k}\cdot\boldsymbol{e}_\nu}\frac{\mathcal{D}_0 - \sigma_1(-\boldsymbol{e}_\nu) - \sigma_{-1}(-\boldsymbol{e}_\nu) + [\mathcal{D}_1 + \sigma_1(-\boldsymbol{e}_\nu)]\,\mathrm{e}^{ik_1} + [\mathcal{D}_{-1} + \sigma_{-1}(-\boldsymbol{e}_\nu)]\,\mathrm{e}^{-ik_1}}{\mathcal{D}_0 + \mathcal{D}_1\mathrm{e}^{ik_1} + \mathcal{D}_{-1}\mathrm{e}^{-ik_1}}\right\}. \tag{4.76}$$

We define again $F'_\nu = \sum_{\boldsymbol{Y}\neq\boldsymbol{0}} F^*(\boldsymbol{0}|\boldsymbol{e}_\nu|\boldsymbol{Y};\xi)$, and derivating twice $\widehat{\Omega}$ and using the symmetry relations

$$F'_{\pm 2} = F'_{\pm 3} = F'_2, \tag{4.77}$$

$$\sigma_1(\boldsymbol{e}_{\pm 2}) = \sigma_1(\boldsymbol{e}_{\pm 3}) = \sigma_1(\boldsymbol{e}_2), \tag{4.78}$$

$$\sigma_{-1}(\boldsymbol{e}_{\pm 2}) = \sigma_{-1}(\boldsymbol{e}_{\pm 3}) = \sigma_{-1}(\boldsymbol{e}_2), \tag{4.79}$$

we obtain the following expression for the generating function associated to the second cumulant:

$$\begin{aligned}\lim_{\rho_0\to 0}\frac{\widehat{\kappa}_1^{(2)}(\xi)}{\rho_0} &= \rho_0\left\{F_1'\left[(3\mathcal{D}_0+\mathcal{D}_1+5\mathcal{D}_{-1})\sigma_1(\boldsymbol{e}_{-1})+(-\mathcal{D}_0+\mathcal{D}_1-3\mathcal{D}_{-1})\sigma_{-1}(\boldsymbol{e}_{-1})+(\mathcal{D}_0+\mathcal{D}_1+\mathcal{D}_{-1})^2\right]\right.\\ &+F_{-1}'\left[(-\mathcal{D}_0-3\mathcal{D}_1+\mathcal{D}_{-1})\sigma_1(\boldsymbol{e}_1)+(3\mathcal{D}_0+5\mathcal{D}_1+\mathcal{D}_{-1})\sigma_{-1}(\boldsymbol{e}_1)+(\mathcal{D}_0+\mathcal{D}_1+\mathcal{D}_{-1})^2\right]\\ &\left.+4F_2'\left[(\mathcal{D}_0-\mathcal{D}_1+3\mathcal{D}_{-1})\sigma_1(\boldsymbol{e}_2)+(\mathcal{D}_0+3\mathcal{D}_1-\mathcal{D}_{-1})\sigma_{-1}(\boldsymbol{e}_2)\right]\right\}/\left[(1-\xi)(\mathcal{D}_0+\mathcal{D}_1+\mathcal{D}_{-1})^2\right].\end{aligned} \tag{4.80}$$

As previously, the quantities $\mathcal{D}_j$ and $\sigma_{\pm1}(\boldsymbol{e}_\nu)$ only depends on the conditional FPTD $\widehat{F}^*$, and the sums F_ν'.

4.4.3 Conditional FPTD $\widehat{F}^*$ and sums F_ν'

The conditional FPTD are computed using (2.20), and the expression of the modified elementary jumps $p^\dagger(\mathbf{0}|\boldsymbol{e}_\mu)$ are:

$$p^\dagger(\mathbf{0}|\boldsymbol{e}_\mu)=\frac{p_\mu}{p_\mu+\frac{5}{6}}. \tag{4.81}$$

The propagators $\widehat{P}^\dagger$ are computed through the usual matrix relation (2.21). As there are now 7 defective sites to take into account ($\mathbf{0}, \boldsymbol{e}_{\pm1}, \boldsymbol{e}_{\pm2}$ and $\boldsymbol{e}_{\pm3}$,), the matrix $\boldsymbol{P}$ is a 7×7 matrix which can be simplified using symmetry relations. The final expression of $\boldsymbol{P}$ is given in Appendix D (Section D.2). Some useful propagators $\widehat{P}(\boldsymbol{r}|\mathbf{0};\xi)$ and their detailed derivations are given in Appendix B.

Extending the calculation from Section 4.3.2.1, we obtain an analogous expression for the coefficients of $\boldsymbol{A}$:

$$A(\boldsymbol{s}_i|\mathbf{0};\xi) = \delta_{i,0}-(1-\xi)\widehat{P}(\boldsymbol{s}_i|\mathbf{0};\xi) \tag{4.82}$$

$$A(\boldsymbol{s}_i|\boldsymbol{e}_\nu;\xi) = \left(\frac{1}{p_\nu+5/6}-1\right)\left[\widehat{P}(\boldsymbol{s}_i|\boldsymbol{e}_\nu;\xi)-\delta_{i,\nu}-\xi\widehat{P}(\boldsymbol{s}_i|\mathbf{0};\xi)\right] \tag{4.83}$$

An explicit expression of $\boldsymbol{A}$ where the symmetry properties of the propagators $\widehat{P}$ have been taken into account is given in Appendix D (Section D.3). Finally, using a computer algebra software, one may deduce from the matrix relation (2.21) and expression of the matrix $\boldsymbol{P}^\dagger$, whose entries are the propagators $\widehat{P}^\dagger$. Finally, with the relation (2.20), one obtains expressions of the conditional FPTD.

Recalling the method given in Section 2.4.2, the quantities F_ν' may be computed straightforwardly using a computer algebra software with (2.39) and (2.47), and using the expressions of $\boldsymbol{A}$ and the propagators $\widehat{P}(\mathbf{0}|\boldsymbol{s}_j;\xi)$.

4.4.4 Expression of the second cumulant in the long time limit

Using the long-time limit expansion of the propagators $\widehat{P}(\boldsymbol{r}|\mathbf{0};\xi)$ (see Appendix B and equations (B.26)-(B.32)), we expand the quantities $\sigma_{\pm1}(\boldsymbol{e}_\nu)$, $\mathcal{D}_j$ and $F_{\pm1}'$ (see Appendix F, Section F.1) involved in the computation of the second cumulant (4.80). This leads to the following expression of the second cumulant at leading order in $\rho_0\to 0$ and $\xi\to 1$:

$$\lim_{\rho_0\to 0}\frac{\widehat{\kappa}_1^{(2)}(\xi)}{\rho_0}\underset{\xi\to1}{\sim}\frac{\sqrt{6}}{L^2}\left[\frac{p_1-p_{-1}}{1+\frac{6\alpha}{6-\alpha}(p_1+p_{-1})}\right]^2\frac{1}{(1-\xi)^{5/2}} \tag{4.84}$$

where we defined as previously

$$\alpha = \lim_{\xi \to 1} \left[\widehat{P}(\mathbf{0}|\mathbf{0};\xi) - \widehat{P}(2\boldsymbol{e}_1|\mathbf{0};\xi) \right]. \tag{4.85}$$

In the case of a three-dimensional capillary, the quantities α can be written (see Appendix B and relations (B.26) and (B.29))

$$\alpha = 18 - 16 S^{(3)}_{L,0} + 12 S^{(3)}_{L,1} - 2 S^{(3)}_{L,2} \tag{4.86}$$

with

$$S^{(3)}_{L,n} = \frac{1}{L^2} \sum_{\substack{k_2,k_3=0 \\ (k_2,k_3)\neq(0,0)}} \frac{[\cos(2\pi k_2/L) + \cos(2\pi k_3/L)]^n}{\sqrt{\left(1 + \frac{1}{3}[\cos(2\pi k_2/L) + \cos(2\pi k_3/L)]\right)^2 - \frac{1}{9}}}. \tag{4.87}$$

Finally, using a Tauberian theorem and defining:

$$a_0 = \frac{p_1 - p_{-1}}{1 + \frac{6\alpha}{6-\alpha}(p_1 + p_{-1})} \tag{4.88}$$

one gets

$$\boxed{\lim_{\rho_0 \to 0} \frac{\kappa^{(2)}_1(t)}{\rho_0} \underset{t\to\infty}{\sim} \frac{4{a_0}^2}{L^2}\sqrt{\frac{2}{3\pi}}t^{3/2}} \tag{4.89}$$

As in the case of the stripe-like geometry, it appears that the fluctuations of the TP are superdiffusive, as they grow as $t^{3/2}$. Once again, it seems that this effect emerges beyond linear response, as the coefficient ${a_0}^2$ is equivalent to F^2 when the driving force F goes to zero.

4.4.5 Numerical simulations

We present on Fig. 4.4 results from numerical simulations on a three-dimensional capillary. For different values of L and F, a rescaled variance is plotted and compared to the analytical prediction. The jump probabilities of the TP are now

$$p_1 = \frac{\mathrm{e}^{F/2}}{2[2 + \cosh(F/2)]} \tag{4.90}$$

$$p_{-1} = \frac{\mathrm{e}^{-F/2}}{2[2 + \cosh(F/2)]} \tag{4.91}$$

$$p_{\pm 2} = p_{\pm 3} = \frac{1}{2[2 + \cosh(F/2)]} \tag{4.92}$$

For different values of L and F, the rescaled variance $[\sqrt{3\pi}L^2\kappa^{(2)}_1(t)]/(4\sqrt{2}{a_0}^2\rho_0)$ is plotted and compared to the analytical prediction. At large times, we observe a good collapse of the simulations results obtained for different values of the parameters on the prediction from (4.65). Our analytical treatment of the problem correctly captures the dependence of the TP fluctuations with all the parameters (time, applied force, width of the stripe).

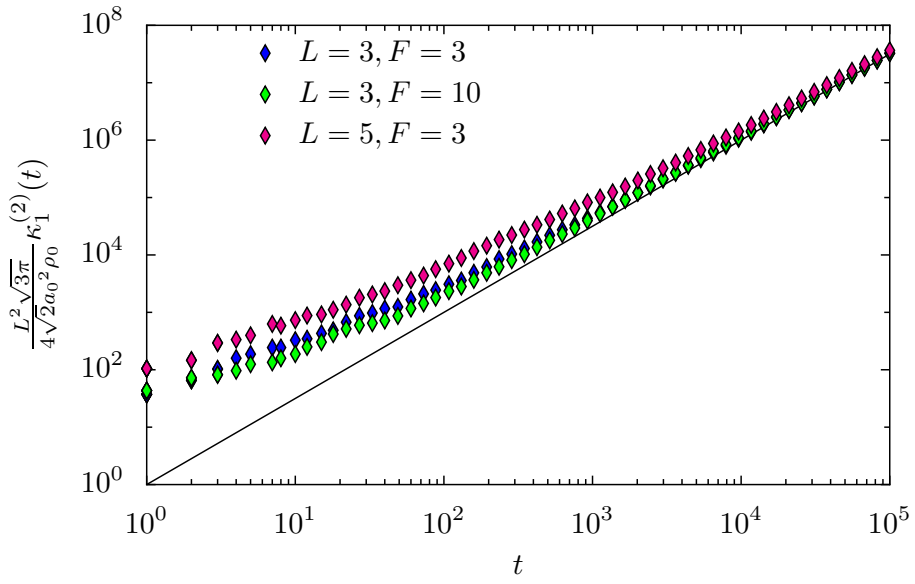

Figure 4.4: Rescaled variance obtained from numerical simulations of tracer diffusion on a capillary with different sizes L and external forces F. The vacancy density is $\rho_0 = 10^{-5}$. The black line is $t^{3/2}$.

4.5 Two-dimensional infinite lattice

4.5.1 Computation of the second cumulant

We now consider the case of a two-dimensional infinite lattice. This situation cannot be obtained starting from the results obtained on the stripe-like geometry and taking $L \to \infty$. In particular, one needs to use the propagators of a random walk on a two-dimensional lattice, that cannot be obtained as a limit of the propagators on a stripe-like lattice.

The expression of $\lim_{\rho_0 \to 0} \widehat{\kappa}_1^{(2)}(\xi)/\rho_0$ obtained for the two-dimensional stripe (4.30) is still valid, but the conditional FPTD must be computed for the specific case of a two-dimensional lattice. As the lattice is now rotation-invariant (i.e. directions 1 and 2 are equivalent), we add the following symmetry relations on the propagators $\widehat{P}$:

$$\widehat{P}(\boldsymbol{e}_2|\boldsymbol{0};\xi) = \widehat{P}(\boldsymbol{e}_1|\boldsymbol{0};\xi) \tag{4.93}$$

$$\widehat{P}(2\boldsymbol{e}_2|\boldsymbol{0};\xi) = \widehat{P}(2\boldsymbol{e}_1|\boldsymbol{0};\xi) \tag{4.94}$$

The matrix $\boldsymbol{P}$ then simplifies to

$$\boldsymbol{P} = \begin{pmatrix} \widehat{P}(\boldsymbol{0}|\boldsymbol{0};\xi) & \widehat{P}(\boldsymbol{e}_1|\boldsymbol{0};\xi) & \widehat{P}(\boldsymbol{e}_1|\boldsymbol{0};\xi) & \widehat{P}(\boldsymbol{e}_1|\boldsymbol{0};\xi) & \widehat{P}(\boldsymbol{e}_1|\boldsymbol{0};\xi) \\ \widehat{P}(\boldsymbol{e}_1|\boldsymbol{0};\xi) & \widehat{P}(\boldsymbol{0}|\boldsymbol{0};\xi) & \widehat{P}(2\boldsymbol{e}_1|\boldsymbol{0};\xi) & \widehat{P}(\boldsymbol{e}_1+\boldsymbol{e}_2|\boldsymbol{0};\xi) & \widehat{P}(\boldsymbol{e}_1+\boldsymbol{e}_2|\boldsymbol{0};\xi) \\ \widehat{P}(\boldsymbol{e}_1|\boldsymbol{0};\xi) & \widehat{P}(2\boldsymbol{e}_1|\boldsymbol{0};\xi) & \widehat{P}(\boldsymbol{0}|\boldsymbol{0};\xi) & \widehat{P}(\boldsymbol{e}_1+\boldsymbol{e}_2|\boldsymbol{0};\xi) & \widehat{P}(\boldsymbol{e}_1+\boldsymbol{e}_2|\boldsymbol{0};\xi) \\ \widehat{P}(\boldsymbol{e}_1|\boldsymbol{0};\xi) & \widehat{P}(\boldsymbol{e}_1+\boldsymbol{e}_2|\boldsymbol{0};\xi) & \widehat{P}(\boldsymbol{e}_1+\boldsymbol{e}_2|\boldsymbol{0};\xi) & \widehat{P}(\boldsymbol{0}|\boldsymbol{0};\xi) & \widehat{P}(2\boldsymbol{e}_1|\boldsymbol{0};\xi) \\ \widehat{P}(\boldsymbol{e}_1|\boldsymbol{0};\xi) & \widehat{P}(\boldsymbol{e}_1+\boldsymbol{e}_2|\boldsymbol{0};\xi) & \widehat{P}(\boldsymbol{e}_1+\boldsymbol{e}_2|\boldsymbol{0};\xi) & \widehat{P}(2\boldsymbol{e}_1|\boldsymbol{0};\xi) & \widehat{P}(\boldsymbol{0}|\boldsymbol{0};\xi) \end{pmatrix}. \tag{4.95}$$

and the matrix $\boldsymbol{A}$ becomes

$$\boldsymbol{A} = \begin{pmatrix} 1-(1-\xi)\widehat{P}_{0,0} & r_1(\widehat{P}_{1,0}-\xi\widehat{P}_{0,0}) & r_{-1}(\widehat{P}_{1,0}-\xi\widehat{P}_{0,0}) & r_2(\widehat{P}_{1,0}-\xi\widehat{P}_{0,0}) & r_2(\widehat{P}_{1,0}-\xi\widehat{P}_{0,0}) \\ -(1-\xi)\widehat{P}_{1,0} & r_1(\widehat{P}_{0,0}-1-\xi\widehat{P}_{1,0}) & r_{-1}(\widehat{P}_{2,0}-\xi\widehat{P}_{1,0}) & r_2(\widehat{P}_{1,1}-\xi\widehat{P}_{1,0}) & r_2(\widehat{P}_{1,1}-\xi\widehat{P}_{1,0}) \\ -(1-\xi)\widehat{P}_{1,0} & r_1(\widehat{P}_{2,0}-\xi\widehat{P}_{1,0}) & r_{-1}(\widehat{P}_{0,0}-1-\xi\widehat{P}_{1,0}) & r_2(\widehat{P}_{1,1}-\xi\widehat{P}_{1,0}) & r_2(\widehat{P}_{1,1}-\xi\widehat{P}_{1,0}) \\ -(1-\xi)\widehat{P}_{1,0} & r_1(\widehat{P}_{1,1}-\xi\widehat{P}_{1,0}) & r_{-1}(\widehat{P}_{1,1}-\xi\widehat{P}_{1,0}) & r_2(\widehat{P}_{0,0}-1-\xi\widehat{P}_{1,0}) & r_2(\widehat{P}_{2,0}-\xi\widehat{P}_{1,0}) \\ -(1-\xi)\widehat{P}_{1,0} & r_1(\widehat{P}_{1,1}-\xi\widehat{P}_{1,0}) & r_{-1}(\widehat{P}_{1,1}-\xi\widehat{P}_{1,0}) & r_2(\widehat{P}_{2,0}-\xi\widehat{P}_{1,0}) & r_2(\widehat{P}_{0,0}-1-\xi\widehat{P}_{1,0}) \end{pmatrix} \tag{4.96}$$

The expansions of the propagators $\widehat{P}(\mathbf{0}|\mathbf{0};\xi)$, $\widehat{P}(\boldsymbol{e}_1|\mathbf{0};\xi)$, $\widehat{P}(2\boldsymbol{e}_1|\mathbf{0};\xi)$ and $\widehat{P}(\boldsymbol{e}_1+\boldsymbol{e}_2|\mathbf{0};\xi)$ are given in Appendix C (Section C.1). The expansions of the quantities $\mathcal{D}_j$ and $\sigma_{\pm1}(\boldsymbol{e}_\nu)$, necessary to compute the expansion of the second cumulant with (4.30), are given in Appendix G (Section G.1).

4.5.2 Long-time expansion

We finally obtain the leading order term of the second cumulant in the limit of $\rho_0 \to 0$ and $\xi \to 1$:

$$\lim_{\rho_0\to 0} \frac{\widehat{\kappa}^2(\xi)}{\rho_0} \underset{\xi\to 1}{=} \frac{2{a_0}^2}{(1-\xi)^2}\frac{1}{\pi}\ln\frac{1}{1-\xi} + \mathcal{O}\left(\frac{1}{(1-\xi)^2}\right) \tag{4.97}$$

where we define

$$a_0 = \frac{p_1 - p_{-1}}{1+\frac{4\alpha}{4-\alpha}(p_1+p_{-1})} \tag{4.98}$$

and

$$\alpha = \lim_{\xi\to 1}\left[\widehat{P}(\mathbf{0}|\mathbf{0};\xi) - \widehat{P}(2\boldsymbol{e}_1|\mathbf{0};\xi)\right]. \tag{4.99}$$

In the case of a two-dimensional lattice, the quantity α is shown to be given by

$$\alpha = 4 - \frac{8}{\pi} \tag{4.100}$$

(see Appendix C and the relations (C.12) and (C.13)). Then, using a Tauberian theorem, one gets

$$\lim_{\rho_0\to 0} \frac{\kappa_1^{(2)}(t)}{\rho_0} \underset{t\to\infty}{=} \frac{2{a_0}^2}{\pi} t\ln t + \mathcal{O}(t). \tag{4.101}$$

As a remark, we show that the value of α obtained for the two-dimensional lattice may be retrieved from its expression on a stripe-like geometry, which is a function of the width L, by taking the limit $L\to\infty$. On stripe-like lattices, we had the expression $\alpha = 8\left[1 - S_{L,1}^{(2)} - S_{L,3}^{(2)}\right]$ where $S_{L,n}^{(2)}$ is defined in (4.57). This may be rewritten as

$$8\left[1 - S_{L,1}^{(2)} - S_{L,3}^{(2)}\right] = 8\left[1 - \frac{1}{L}\sum_{k=1}^{L-1}\sin\frac{\pi k}{L}\sqrt{1+\sin^2\frac{\pi k}{L}}\right] \tag{4.102}$$

$$= 8\left[1 - \frac{1}{L}\sum_{k=1}^{L}\sin\frac{\pi k}{L}\sqrt{1+\sin^2\frac{\pi k}{L}}\right] \tag{4.103}$$

The sum over k may be estimated as a Riemann sum in the limit $L \to \infty$. We get

$$\lim_{L\to\infty}\left[1 - S^{(2)}_{L,1} - S^{(2)}_{L,3}\right] = 8\left[1 - \int_0^1 \mathrm{d}x\, \sin(\pi x)\sqrt{1+\sin^2(\pi x)}\right] \tag{4.104}$$

$$= 8\left[1 - \left(\frac{1}{2} + \frac{1}{\pi}\right)\right] \tag{4.105}$$

$$= 4 - \frac{8}{\pi} \tag{4.106}$$

which was the value obtained by evaluating $\lim_{\xi\to 1}\left[\widehat{P}(\mathbf{0}|\mathbf{0};\xi) - \widehat{P}(2\boldsymbol{e}_1|\mathbf{0};\xi)\right]$ using (C.12) and (C.13). However, this remark is not sufficient to obtain the behavior of the TP on a 2D lattice as a limit of the stripe-like geometry situation. Indeed, the expression of the fluctuations of the TP position (4.97) also depends on the divergence of the propagators $\widehat{P}$, which cannot be obtained as a limit of the propagators of a random walk on as stripe-like lattice.

4.5.3 Subdominant term

From (4.101), we observe that the leading order term (proportional to $t\ln t$) is only logarithmically larger than the subdominant term (proportional to t). Thus, the subdominant term is not negligible if we aim to compare this expression to our numerical simulations. Computing the second term in the expansion of the cumulant, we get

$$\lim_{\rho_0\to 0}\frac{\widehat{\kappa}^{(2)}_1(\xi)}{\rho_0} \underset{\xi\to 1}{=} \frac{2{a_0}^2}{(1-\xi)^2}\frac{1}{\pi}\ln\frac{1}{1-\xi} + \frac{1}{(1-\xi)^2}\left[2{a_0}^2\left(\frac{\ln 8}{\pi} + \frac{2(5\alpha-4)}{\alpha(\alpha-4)}\right) + a_1\right] + \dots \tag{4.107}$$

where we define

$$a_1 = \frac{p_1 + p_{-1}}{1 + \frac{4\alpha}{4-\alpha}(p_1+p_{-1})}. \tag{4.108}$$

We now determine the time-dependence of the second cumulant. Using a Tauberian theorem, the term proportional to $1/(1-\xi)^2$ will give a term proportional to t. The inversion of the term $\frac{1}{(1-\xi)^2}\ln\frac{1}{1-\xi}$ requires some attention, as it may give rise to a term growing as $t\ln t$ and a subdominant term growing as t, that we may not discard. We first recall the definition of the harmonic numbers:

$$\mathrm{H}_n = \sum_{k=1}^{n}\frac{1}{k}. \tag{4.109}$$

A generating function of this sequence is

$$\frac{1}{1-\xi}\ln\frac{1}{1-\xi} = \sum_{t=0}^{\infty}\mathrm{H}_t\,\xi^t. \tag{4.110}$$

Derivating this expression, one gets

$$\frac{1}{(1-\xi)^2}\ln\frac{1}{1-\xi} = \sum_{n=0}^{\infty}(t+1)\mathrm{H}_{t+1}\xi^t - \frac{1}{(1-\xi)^2} \tag{4.111}$$

$$= \sum_{n=0}^{\infty}\left[(t+1)(\mathrm{H}_{t+1}-1)\right]\xi^t \tag{4.112}$$

Finally, we use the expansion

$$\mathrm{H}_t \underset{t\to\infty}{=} \ln t + \gamma + \dots \tag{4.113}$$

where $\gamma = 0.577215...$ is the Euler-Mascheroni constant, to obtain the time-dependence of the second cumulant:

$$\boxed{\lim_{\rho_0\to 0} \frac{\kappa_1^{(2)}(t)}{\rho_0} \underset{t\to\infty}{=} \frac{2{a_0}^2}{\pi} t\ln t + \left[2{a_0}^2\left(\frac{\ln 8+\gamma-1}{\pi} + \frac{2(5\alpha-4)}{\alpha(\alpha-4)}\right) + a_1\right] t + \mathcal{O}(1)} \tag{4.114}$$

On a two-dimensional lattice, the fluctuations grow superdiffusively. However, the leading order of the second cumulant is proportional to $t\ln t$, and is only logarithmically faster than a linear growth. This superdiffusion is not as strong as in the case of quasi-one-dimensional lattice for which the variance was growing as $t^{3/2}$.

As in the case of quasi-one-dimensional systems, the prefactor ${a_0}^2$ cancels when $F \to 0$ but proportionally to F^2, which again indicates that this superdiffusive behavior emerges beyond linear response of the system.

4.5.4 Remarks and numerical simulations

We present on Fig. 4.5 results from numerical simulations on a two-dimensional lattice. The lattice is of size ${L_x}^2$, and L_x is large enough to make sure that no finite-size effects appear. We define a rescaled variance:

$$\phi(t) \equiv \frac{\pi}{2{a_0}^2}\left\{\frac{\kappa_1^{(2)}(t)}{\rho_0 t} - \left[2{a_0}^2\left(\frac{\ln 8+\gamma-1}{\pi} + \frac{2(5\alpha-4)}{\alpha(\alpha-4)}\right) + a_1\right]\right\}, \tag{4.115}$$

which is expected to be equivalent to $\ln t$ in the long time limit. We observe a good agreement between the numerical results and the theoretical prediction, for different values of the driving force F.

4.6 Three-dimensional infinite lattice

In this Section, we study the case of a three-dimensional infinite lattice. The propagators of a random walk on a three-dimensional lattice cannot be deduced as a limit of the propagators on a capillary when its width L goes to infinity. We then need to write the matrices $\boldsymbol{A}$ and $\boldsymbol{P}$ with the specific propagators associated to the three-dimensional lattice. We give in what follows the main steps of the calculation.

The expression of $\lim_{\rho_0\to 0} \widehat{\kappa}_1^{(2)}(\xi)/\rho$ obtained for the three-dimensional capillary (4.80) is still valid. In order to compute the conditional FPTD F^* in the case of a three-dimensional lattice, we use again their definition (2.20) as well as the matrix relation (2.21). The generic expression of the matrix $\boldsymbol{P}$ in three dimensions (Appendix D, Section D.2) may be simplified using the following symmetry relations:

$$\widehat{P}(\boldsymbol{e}_2|\boldsymbol{0};\xi) = \widehat{P}(\boldsymbol{e}_1|\boldsymbol{0};\xi), \tag{4.116}$$

$$\widehat{P}(\boldsymbol{e}_2+\boldsymbol{e}_3|\boldsymbol{0};\xi) = \widehat{P}(\boldsymbol{e}_1+\boldsymbol{e}_2|\boldsymbol{0};\xi), \tag{4.117}$$

$$\widehat{P}(2\boldsymbol{e}_2|\boldsymbol{0};\xi) = \widehat{P}(2\boldsymbol{e}_1|\boldsymbol{0};\xi), \tag{4.118}$$

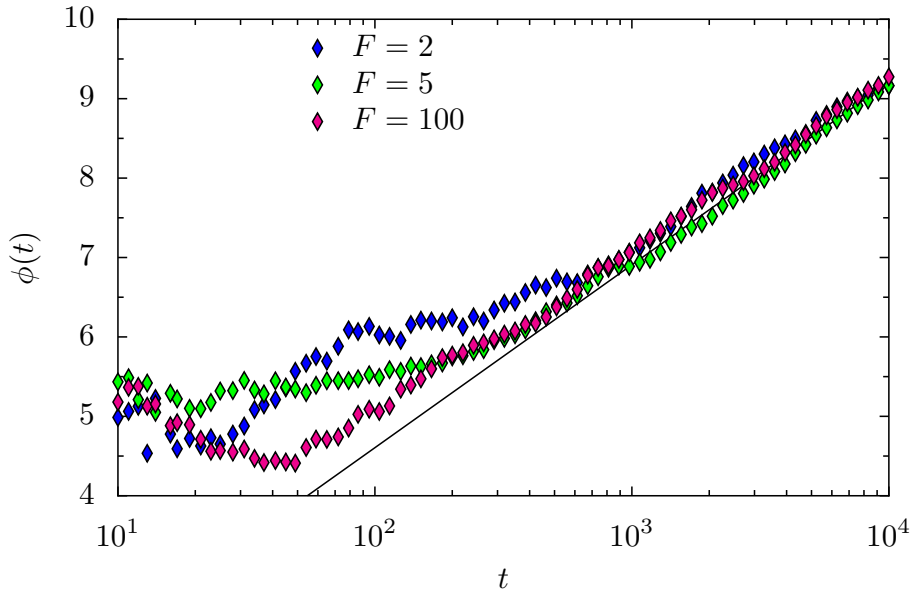

Figure 4.5: Rescaled variance obtained from numerical simulations of tracer diffusion on a two-dimensional lattice for different external forces F. The vacancy density is $\rho_0 = 10^{-5}$. The black line is $\ln t$.

and has the following form:

$$\boldsymbol{P} = \begin{pmatrix} \widehat{P}_{0,0,0} & \widehat{P}_{1,0,0} & \widehat{P}_{1,0,0} & \widehat{P}_{1,0,0} & \widehat{P}_{1,0,0} & \widehat{P}_{1,0,0} & \widehat{P}_{1,0,0} \\ \widehat{P}_{1,0,0} & \widehat{P}_{1,0,0} & \widehat{P}_{2,0,0} & \widehat{P}_{1,1,0} & \widehat{P}_{1,1,0} & \widehat{P}_{1,1,0} & \widehat{P}_{1,1,0} \\ \widehat{P}_{1,0,0} & \widehat{P}_{2,0,0} & \widehat{P}_{0,0,0} & \widehat{P}_{1,1,0} & \widehat{P}_{1,1,0} & \widehat{P}_{1,1,0} & \widehat{P}_{1,1,0} \\ \widehat{P}_{1,0,0} & \widehat{P}_{1,1,0} & \widehat{P}_{1,1,0} & \widehat{P}_{0,0,0} & \widehat{P}_{2,0,0} & \widehat{P}_{1,1,0} & \widehat{P}_{1,1,0} \\ \widehat{P}_{1,0,0} & \widehat{P}_{1,1,0} & \widehat{P}_{1,1,0} & \widehat{P}_{2,0,0} & \widehat{P}_{0,0,0} & \widehat{P}_{1,1,0} & \widehat{P}_{1,1,0} \\ \widehat{P}_{1,0,0} & \widehat{P}_{1,1,0} & \widehat{P}_{1,1,0} & \widehat{P}_{1,1,0} & \widehat{P}_{1,1,0} & \widehat{P}_{0,0,0} & \widehat{P}_{2,0,0} \\ \widehat{P}_{1,0,0} & \widehat{P}_{1,1,0} & \widehat{P}_{1,1,0} & \widehat{P}_{1,1,0} & \widehat{P}_{1,1,0} & \widehat{P}_{2,0,0} & \widehat{P}_{0,0,0} \end{pmatrix}. \tag{4.119}$$

It involves four distinct propagators: $\widehat{P}(\mathbf{0}|\mathbf{0};\xi)$, $\widehat{P}(\boldsymbol{e}_1|\mathbf{0};\xi)$, $\widehat{P}(2\boldsymbol{e}_1|\mathbf{0};\xi)$ and $\widehat{P}(\boldsymbol{e}_1+\boldsymbol{e}_2|\mathbf{0};\xi)$. The relation between the propagators $\widehat{P}(\boldsymbol{r}|\boldsymbol{r}_0;\xi)$ (4.40) which was established for two-dimensional lattices can be extended in three dimensions:

$$\widehat{P}(\boldsymbol{r}|\boldsymbol{r}_0;\xi) = \delta_{\boldsymbol{r},\boldsymbol{r}_0} + \frac{\xi}{6} \sum_{\mu=\pm1,\ldots,\pm3} \widehat{P}(\boldsymbol{r}|\boldsymbol{r}_0+\boldsymbol{e}_\mu;\xi), \tag{4.120}$$

in order to obtain the following relations:

$$\widehat{P}(\mathbf{0}|\mathbf{0};\xi) = 1 + \xi \widehat{P}(\boldsymbol{e}_1|\mathbf{0};\xi), \tag{4.121}$$

$$\widehat{P}(\boldsymbol{e}_1|\mathbf{0};\xi) = \xi \left[\widehat{P}(2\boldsymbol{e}_1|\mathbf{0};\xi) + \widehat{P}(\mathbf{0}|\mathbf{0};\xi) + 4\widehat{P}(\boldsymbol{e}_1+\boldsymbol{e}_2|\mathbf{0};\xi) \right]. \tag{4.122}$$

We note that we can finally express the results in terms of two propagators only: $\widehat{P}(\mathbf{0}|\mathbf{0};\xi)$ and $\widehat{P}(2\boldsymbol{e}_1|\mathbf{0};\xi)$. For a random walker on a d-dimensional lattice, the propagator $\widehat{P}(\boldsymbol{r}|\mathbf{0};\xi)$ is known to

be given by [58]:

$$\widehat{P}(\boldsymbol{r}|\mathbf{0};\xi) = \int_0^\infty \mathrm{e}^{-t} \prod_{j=1}^{d} \mathrm{I}_{|r_j|}\left(\frac{t\xi}{d}\right) \tag{4.123}$$

where I_n is the modified Bessel function of the first kind of integer order n. At leading order in $(1-\xi)$, it is found that

$$\widehat{P}(\mathbf{0}|\mathbf{0};\xi=1) = \frac{\sqrt{6}}{284\pi^3}\Gamma\left(\frac{1}{24}\right)\Gamma\left(\frac{5}{24}\right)\Gamma\left(\frac{7}{24}\right)\Gamma\left(\frac{11}{24}\right) \simeq 1.516386 \tag{4.124}$$

$$\widehat{P}(2\boldsymbol{e}_1|\mathbf{0};\xi=1) \simeq 0.257335 \tag{4.125}$$

The entries of the matrix $\boldsymbol{A}$ are expressed using (4.83). Finally, using a computer algebra software, we deduce the expression of the conditional FPTD $\widehat{F}^*$ and deduce the fluctuations of the TP position with (4.80). We finally obtain:

$$\lim_{\rho_0\to 0} \frac{\widehat{\kappa}_1^{(2)}(\xi)}{\rho_0} \underset{\xi\to 1}{\sim} \frac{1}{(1-\xi)^2}\left[2{a_0}^2\left(G + \frac{2(13\alpha-6)}{(\alpha+2)(\alpha-6)}\right) + a_1\right] \tag{4.126}$$

where we defined as previously

$$a_0 = \frac{p_1 - p_{-1}}{1 + \frac{6\alpha}{6-\alpha}(p_1+p_{-1})} \tag{4.127}$$

$$a_1 = \frac{p_1+p_{-1}}{p_1-p_{-1}} a_0 \tag{4.128}$$

$$G_0 = \lim_{\xi\to 1} \widehat{P}(\mathbf{0}|\mathbf{0};\xi) \simeq 1.516386 \tag{4.129}$$

$$\alpha = \lim_{\xi\to 1}\left[\widehat{P}(\mathbf{0}|\mathbf{0};\xi) - \widehat{P}(2\boldsymbol{e}_1|\mathbf{0};\xi)\right] \simeq 1.259051. \tag{4.130}$$

Using a Tauberian theorem, we get

$$\boxed{\lim_{\rho_0\to 0} \frac{\kappa^{(2)}(t)}{\rho_0} \underset{t\to\infty}{\sim} \left[2{a_0}^2\left(G + \frac{2(13\alpha-6)}{(\alpha+2)(\alpha-6)}\right) + a_1\right] t.} \tag{4.131}$$

Consequently, on a three-dimensional lattice, the fluctuations of the TP are diffusive, and not superdiffusive as it was obtained for quasi-one-dimensional and two-dimensional lattices. Geometrical confinement then induces the apparition of superdiffusive fluctuations.

We compare these results with numerical simulations performed on a three-dimensional lattice (Fig. 4.6). We plot the quantity $\kappa_1^{(2)}(t)/D_{3\mathrm{D}}$ where we define

$$D_{3\mathrm{D}} \equiv \rho_0\left[2{a_0}^2\left(G + \frac{2(13\alpha-6)}{(\alpha+2)(\alpha-6)}\right) + a_1\right]. \tag{4.132}$$

The agreement between numerical simulations and the theoretical prediction is very good, and confirmed for different values of the driving force F.

As a remark, we emphasize the fact that the interactions between the TP and in a single-vacancy are strongly influenced by the dimension of the lattice. On the "confined" geometries (quasi-one-dimensional and two-dimensional), we give the leading order term of the generating functions $\widehat{P}(\mathbf{0}|\mathbf{0};\xi)$

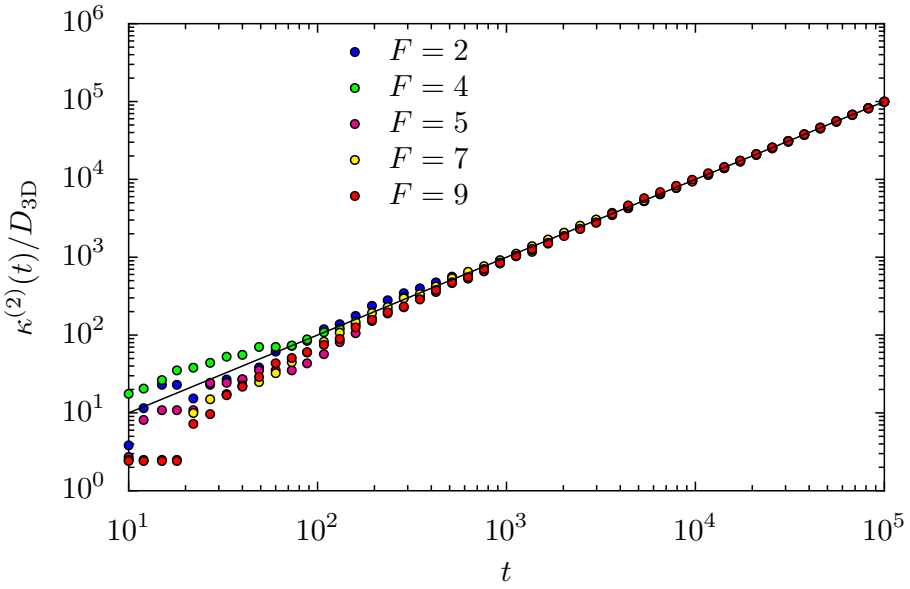

Figure 4.6: Rescaled variance obtained from numerical simulations of tracer diffusion on a 3D lattice with different external forces F. The vacancy density is $\rho_0 = 10^{-6}$. The black line is t.

in the limit where $\xi \to 1$ (i.e. in the long-time limit) which are presented in Appendices A (A.36), B (B.26) and C (C.12):

$$\widehat{P}(\mathbf{0}|\mathbf{0};\xi) \underset{\xi\to 1}{\sim} \begin{cases} \dfrac{1}{L\sqrt{1-\xi}} & \text{on a 2D stripe,} \\ \dfrac{\sqrt{6}}{2L^2\sqrt{1-\xi}} & \text{on a 3D capillary,} \\ \dfrac{1}{\pi}\ln\dfrac{1}{1-\xi} & \text{on a 2D lattice.} \end{cases} \tag{4.133}$$

These propagators have a common feature: they diverge when $\xi \to 1$. This means [58] that the random walk of a vacancy on this structure is recurrent, i.e. that a vacancy will interact an infinite number of times with the TP. However, on the 3D lattice, the propagator $\widehat{P}(\mathbf{0}|\mathbf{0};\xi)$ tend to the constant G_0 and does not diverge. This means that the random walk of a vacancy is transient, i.e. the vacancy will only interact with the TP a finite number of times, before wandering off to infinity. Then, the recurrence of the random walk of vacancy is a necessary condition to allow the emergence of superdiffusion. However, this condition is not sufficient: on the one-dimensional lattice, although the random walk of a vacancy is recurrent, the motion of the TP is not superdiffusive. It is actually subdiffusive, as shown in Chapter 3. In Chapter 7, we will give a simplified description of the problem, explaining the emergence of the superdiffusive regime with simple physical mechanisms.

Finally, we summarize the results from this section in the following table:

Geometry	$\lim_{\rho_0\to 0}\kappa^{(2)}(t)/\rho_0$ **in the long-time limit**
2D stripe	$\dfrac{8{a_0}^2}{3\sqrt{\pi}L}t^{3/2}+\dots$
3D capillary	$\dfrac{4{a_0}^2}{L^2}\sqrt{\dfrac{2}{3\pi}}t^{3/2}+\dots$
2D infinite lattice	$\dfrac{2{a_0}^2}{\pi}t\ln t+\left[2{a_0}^2\left(\dfrac{\ln 8+\gamma-1}{\pi}+\dfrac{2(5\alpha-4)}{\alpha(\alpha-4)}\right)+a_1\right]t+\dots$
3D infinite lattice	$\left[2{a_0}^2\left(G+\dfrac{2(13\alpha-6)}{(\alpha+2)(\alpha-6)}\right)+a_1\right]t+\dots$

4.7 Crossover to diffusion – Stripe-like geometry

4.7.1 Introduction

The exact analytical results from the previous part provide explicit criteria for superdiffusion to occur. Technically, this yields the behavior of the variance when the limit $\rho_0\to 0$ is taken before the large-time limit. However, it does not allow us, due to the nature of the limits involved, to answer the question of whether the superdiffusion is the ultimate regime (or just a transient), which requires the determination of $\lim_{t\to\infty}\kappa_1^{(2)}(t)$ at fixed ρ_0. Importantly, we show in what follows that the order in which these limits are taken is crucial in confined geometries, in which the limits cannot be inverted:

$$\lim_{t\to\infty}\lim_{\rho_0\to 0}\kappa_1^{(2)}(t)\neq\lim_{\rho_0\to 0}\lim_{t\to\infty}\kappa_1^{(2)}(t) \tag{4.134}$$

The key difference with the previous case is that for a *fixed* small ρ_0 the random walk performed by the vacancy between two successive visits of the lattice site occupied by the TP is a *biased* random walk in the reference frame of the TP, due to the interactions of the TP with the other vacancies. More precisely, this bias ε undergone by a vacancy originates from the non zero mean displacement of the TP in the $\boldsymbol{e}_1$ direction. This bias is directed towards direction $\boldsymbol{e}_{-1}$, and its value is equal to the TP velocity.

The method to compute the fluctuations of the TP presented above can then be applied, provided that the symmetric propagators P describing the symmetric random walk of a vacancy are replaced by the propagators $\mathcal{P}$ describing the *biased* random walk of a vacancy. These propagators can be explicitly evaluated, and are formally functions of the bias ε. Note that P and $\mathcal{P}$ are related through:

$$P_t(\boldsymbol{r}|\boldsymbol{r}_0)=\mathcal{P}_t(\boldsymbol{r}|\boldsymbol{r}_0;\varepsilon=0) \tag{4.135}$$

Quite surprisingly, this effective bias, even if arbitrarily small in the $\rho_0\to 0$ limit, dramatically affects the ultimate long-time behavior of the variance in confined geometries. In this Section, we present a detailed method to compute the fluctuations of the TP position in the limit where $t\to\infty$ is taken first, in the particular case of a stripe-like geometry. We then give a less detailed outline of the calculation for the other geometries.

4.7.2 Determination of the conditional FPTD

4.7.2.1 Evolution rules of a vacancy

In order to take into account the displacement of the TP due to its interactions with other vacancies, we modify that evolution rules of each vacancy as presented on Fig. 4.7. The new jump probabilities are

denoted by $\widetilde{p}_\mu$ (probability for a vacancy to jump from $\boldsymbol{r}$ to $\boldsymbol{r}+\boldsymbol{e}_\mu$ in a single step). The bias is chosen as follows: $\widetilde{p}_{-1}$ is proportional to $1/4+\varepsilon$, where ε is a positive quantity. With an appropriate normalization we get

$$\widetilde{p}_{-1} = \frac{1}{1+\varepsilon}\left(\frac{1}{4}+\varepsilon\right) \tag{4.136}$$

$$\widetilde{p}_1 = \widetilde{p}_{\pm 2} = \frac{1}{4(1+\varepsilon)} \tag{4.137}$$

The bias undergone by a vacancy is

$$\widetilde{p}_{-1} - \widetilde{p}_1 = \frac{\varepsilon}{1+\varepsilon} \underset{\varepsilon\to 0}{\sim} \varepsilon. \tag{4.138}$$

This bias, equal to ε at leading order, is equal to the velocity of the TP. It implies that ε goes to zero when the vacancy density ρ_0 goes to 0. The explicit determination of ε is not necessary to compute the expression of the mean position of the TP (see Chapter 5). The condition $\lim_{\rho_0\to 0}\varepsilon = 0$ suffices to determine the velocity of the TP and then the expression of ε self-consistently. The evolution rules (4.136) and (4.136) will be shown to be compatible with an alternative approach of the problem presented in Chapter 10.

The general expression of the variance (4.80) still holds as it was obtained independently of the evolution rules of the vacancies. The conditional FPTD $\widehat{\mathcal{F}}^*$ are now functions of the bias ε and write

$$\widehat{\mathcal{F}}^*(\mathbf{0}|\boldsymbol{e}_\mu|\boldsymbol{e}_\nu;\xi,\varepsilon) = \xi\widetilde{p}^\dagger(\mathbf{0}|\boldsymbol{e}_\mu)\widehat{\mathcal{P}}^\dagger(\boldsymbol{e}_\mu|\boldsymbol{e}_\nu;\xi,\varepsilon) \tag{4.139}$$

The quantity $\widetilde{p}^\dagger(\mathbf{0}|\boldsymbol{e}_\mu)$ must be computed using the appropriate normalization corresponding to the new transition probabilities:

$$\widetilde{p}^\dagger(\mathbf{0}|\boldsymbol{e}_\mu) = \frac{p_\mu}{p_\mu + \sum_{\eta\neq -\mu}\widetilde{p}_\eta}. \tag{4.140}$$

We define the generating functions $\widehat{\mathcal{P}}(\boldsymbol{r}|\boldsymbol{r}_0;\xi,\varepsilon)$ associated to the biased random walk of a vacancy with the rules presented on Fig. 4.7, in the absence of a biased TP. The generating functions $\widehat{\mathcal{P}}^\dagger$ are obtained starting from the generating functions $\widehat{\mathcal{P}}$ and adding five defective sites at $\{\mathbf{0},\boldsymbol{e}_{\pm 1},\boldsymbol{e}_{\pm 2}\}$. The corresponding matrix relation is still

$$\boldsymbol{\mathcal{P}}^\dagger = (\mathbf{1}-\boldsymbol{\mathcal{A}})^{-1}\boldsymbol{\mathcal{P}}, \tag{4.141}$$

where

$$\boldsymbol{\mathcal{P}}_{i,j} = \widehat{\mathcal{P}}(\boldsymbol{s}_i|\boldsymbol{s}_j;\xi) \tag{4.142}$$

$$\boldsymbol{\mathcal{P}}^\dagger_{i,j} = \widehat{\mathcal{P}}^\dagger(\boldsymbol{s}_i|\boldsymbol{s}_j;\xi) \tag{4.143}$$

$$\boldsymbol{\mathcal{A}}_{i,j} = \mathcal{A}(\boldsymbol{s}_i|\boldsymbol{s}_j;\xi) = \xi\sum_{\boldsymbol{r}}\widehat{\mathcal{P}}(\boldsymbol{s}_i|\boldsymbol{r};\xi)\left[\widetilde{p}^\dagger(\boldsymbol{r}|\boldsymbol{s}_j) - \widetilde{p}(\boldsymbol{r}|\boldsymbol{s}_j)\right] \tag{4.144}$$

In what follows, we give explicit expressions of the matrices $\boldsymbol{\mathcal{P}}$ and $\boldsymbol{\mathcal{A}}$.

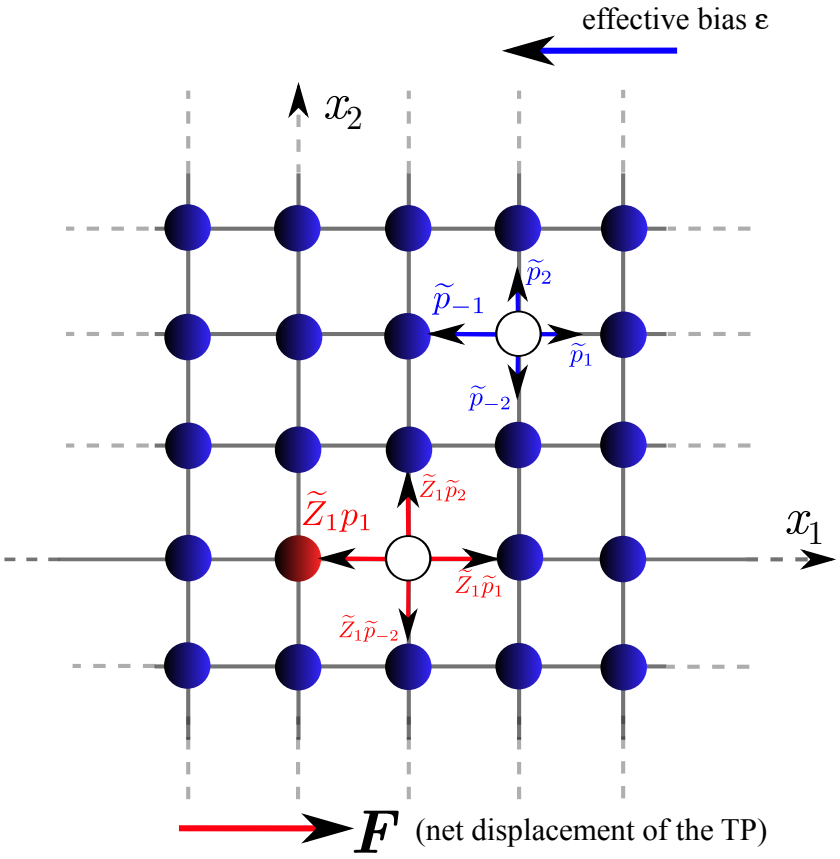

Figure 4.7: Dynamics of the vacancies on a two-dimensional lattice with the effective bias ε in direction -1 (case of a two-dimensional lattice). The jump probabilities $\widetilde{p}_\mu$ are defined in the text. The normalization $\widetilde{Z}_\nu$ is defined as $\widetilde{Z}_\nu = \left[p_\nu + \sum_{\eta\neq-\mu}\widetilde{p}_\eta\right]^{-1}$.

4.7.2.2 Expression of $\boldsymbol{\mathcal{P}}$

The matrix $\boldsymbol{\mathcal{P}}$ contains *a priori* 25 elements. In spite of the bias experienced by the vacancies and of the more complex structure of the associated propagators, it is still possible to simplify $\boldsymbol{\mathcal{P}}$. Indeed, the lattice is still translation invariant and symmetric with respect to the second coordinate. Finally, $\boldsymbol{\mathcal{P}}$ is expressed in terms of nine distinct propagators:

$$\boldsymbol{\mathcal{P}} = \begin{pmatrix} \widehat{\mathcal{P}}_{0,0} & \widehat{\mathcal{P}}_{-1,0} & \widehat{\mathcal{P}}_{1,0} & \widehat{\mathcal{P}}_{0,1} & \widehat{\mathcal{P}}_{0,1} \\ \widehat{\mathcal{P}}_{1,0} & \widehat{\mathcal{P}}_{0,0} & \widehat{\mathcal{P}}_{2,0} & \widehat{\mathcal{P}}_{1,1} & \widehat{\mathcal{P}}_{1,1} \\ \widehat{\mathcal{P}}_{-1,0} & \widehat{\mathcal{P}}_{-2,0} & \widehat{\mathcal{P}}_{0,0} & \widehat{\mathcal{P}}_{-1,1} & \widehat{\mathcal{P}}_{-1,1} \\ \widehat{\mathcal{P}}_{0,1} & \widehat{\mathcal{P}}_{-1,1} & \widehat{\mathcal{P}}_{1,1} & \widehat{\mathcal{P}}_{0,0} & \widehat{\mathcal{P}}_{0,2} \\ \widehat{\mathcal{P}}_{0,1} & \widehat{\mathcal{P}}_{-1,1} & \widehat{\mathcal{P}}_{1,1} & \widehat{\mathcal{P}}_{0,2} & \widehat{\mathcal{P}}_{0,0} \end{pmatrix} \tag{4.145}$$

where we introduced the short notations $\widehat{\mathcal{P}}_{r_1,r_2} \equiv \widehat{\mathcal{P}}(r_1\boldsymbol{e}_1 + r_2\boldsymbol{e}_2|\boldsymbol{0};\xi,\varepsilon)$. An explicit derivation of the propagators $\widehat{\mathcal{P}}$ is given in Appendix A.

4.7.2.3 Expression of $\boldsymbol{\mathcal{A}}$

The elements of $\boldsymbol{\mathcal{A}}$ are the quantities

$$\mathcal{A}(\boldsymbol{s}_i|\boldsymbol{s}_j;\xi,\varepsilon) = \xi \sum_{\boldsymbol{r}} \widehat{\mathcal{P}}(\boldsymbol{s}_i|\boldsymbol{r};\xi) \underbrace{\left[\widetilde{p}^{\dagger}(\boldsymbol{r}|\boldsymbol{s}_j) - \widetilde{p}(\boldsymbol{r}|\boldsymbol{s}_j)\right]}_{\equiv \widetilde{p}'(\boldsymbol{r}|\boldsymbol{s}_j)}. \tag{4.146}$$

The principle of the computation carried out in Section 4.3.2.1 in the case of non-biased vacancies is still valid, and we give here its extension to the case of biased vacancies. In order to compute $\mathcal{A}(\boldsymbol{s}_i|\boldsymbol{s}_j;\xi,\varepsilon)$, we consider two cases separately:

(i) if $\boldsymbol{s}_j = \boldsymbol{0}$:

The elementary jump probabilities write:

$$\widetilde{p}(\boldsymbol{r}|\boldsymbol{0}) = \begin{cases} \widetilde{p}_\mu & \text{if } \boldsymbol{r} = \boldsymbol{e}_\mu\,, \\ 0 & \text{otherwise.} \end{cases} \tag{4.147}$$

$$\widetilde{p}^{\dagger}(\boldsymbol{r}|\boldsymbol{0}) = \begin{cases} 1 & \text{if } \boldsymbol{r} = \boldsymbol{0}\,, \\ 0 & \text{otherwise.} \end{cases} \tag{4.148}$$

so that

$$\widetilde{p}'(\boldsymbol{r}|\boldsymbol{0}) = \begin{cases} 1 & \text{if } \boldsymbol{r} = \boldsymbol{0}\,, \\ -\widetilde{p}_\mu & \text{if } \boldsymbol{r} = \boldsymbol{e}_\mu, \\ 0 & \text{otherwise.} \end{cases} \tag{4.149}$$

We deduce the expression for $A(\boldsymbol{s}_i|\boldsymbol{0};\xi)$:

$$\mathcal{A}(\boldsymbol{s}_i|\boldsymbol{0};\xi,\varepsilon) = \xi \left[\widehat{\mathcal{P}}(\boldsymbol{s}_i|\boldsymbol{0};\xi,\varepsilon) - \sum_{\mu=\pm1,\pm2} \widetilde{p}_\mu \widehat{\mathcal{P}}(\boldsymbol{s}_i|\boldsymbol{e}_\mu;\xi,\varepsilon)\right]. \tag{4.150}$$

The extension of (4.40) to the case of a non-symmetric random walk is

$$\widehat{\mathcal{P}}(\boldsymbol{r}|\boldsymbol{r}_0;\xi,\varepsilon) = \delta_{\boldsymbol{r},\boldsymbol{r}_0} + \xi \sum_{\mu} \widetilde{p}_\mu \widehat{\mathcal{P}}(\boldsymbol{r}|\boldsymbol{r}_0 + \boldsymbol{e}_\mu;\xi,\varepsilon) \tag{4.151}$$

Using (4.151) in (4.150), we obtain

$$A(\boldsymbol{s}_i|\boldsymbol{0};\xi) = \delta_{i,0} - (1-\xi)\widehat{\mathcal{P}}(\boldsymbol{s}_i|\boldsymbol{0};\xi) \tag{4.152}$$

(ii) if $\boldsymbol{s}_j = \boldsymbol{e}_\nu$ ($\nu \in \{\pm 1, \pm 2\}$)

The elementary jump probabilities write:

$$p(\boldsymbol{r}|\boldsymbol{e}_\nu) = \begin{cases} \widetilde{p}_\mu & \text{if } \boldsymbol{r} = \boldsymbol{e}_\nu + \boldsymbol{e}_\mu \ , \\ 0 & \text{otherwise.} \end{cases} \tag{4.153}$$

$$p^\dagger(\boldsymbol{r}|\boldsymbol{e}_\nu) = \begin{cases} \frac{p_\nu}{p_\nu + \sum_{\eta \neq -\nu} \widetilde{p}_\eta} & \text{if } \boldsymbol{r} = \boldsymbol{0} \ , \\ \frac{\widetilde{p}_\mu}{p_\nu + \sum_{\eta \neq -\nu} \widetilde{p}_\eta} & \text{if } \boldsymbol{r} = \boldsymbol{e}_\nu + \boldsymbol{e}_\mu, \, \mu \neq -\nu, \\ 0 & \text{otherwise.} \end{cases} \tag{4.154}$$

so that

$$\widetilde{p}'(\boldsymbol{r}|\boldsymbol{e}_\nu) = \begin{cases} \frac{p_\nu}{p_\nu + \sum_{\eta \neq -\nu} \widetilde{p}_\eta} - \widetilde{p}_{-\nu} & \text{if } \boldsymbol{r} = \boldsymbol{0} \ , \\ \frac{\widetilde{p}_\mu}{p_\nu + \sum_{\eta \neq -\nu} \widetilde{p}_\eta} - \widetilde{p}_\mu & \text{if } \boldsymbol{r} = \boldsymbol{e}_\nu + \boldsymbol{e}_\mu, \, \mu \neq -\nu, \\ 0 & \text{otherwise.} \end{cases} \tag{4.155}$$

Using the relation $\sum_{\eta \neq -\mu} \widetilde{p}_\eta = 1 - \widetilde{p}_{-\nu}$, we then obtain an expression for $A(\boldsymbol{s}_i|\boldsymbol{e}_\nu;\xi)$:

$$\begin{aligned} \mathcal{A}(\boldsymbol{s}_i|\boldsymbol{e}_\nu;\xi,\varepsilon) &= \xi \left[\left(\frac{p_\nu}{p_\nu - \widetilde{p}_{-\nu} + 1} - \widetilde{p}_{-\nu} \right) \widehat{P}(\boldsymbol{s}_i|\boldsymbol{0};\xi,\varepsilon) \right. \\ &\quad \left. + \left(\frac{1}{p_\nu - \widetilde{p}_{-\nu} + 1} - 1 \right) \sum_{\mu \neq -\nu} \widetilde{p}_\mu \widehat{\mathcal{P}}(\boldsymbol{s}_i|\boldsymbol{e}_\nu + \boldsymbol{e}_\mu;\xi,\varepsilon) \right] \qquad (4.156) \\ &= \xi \left[\left(\frac{p_\nu}{p_\nu - \widetilde{p}_{-\nu} + 1} - \widetilde{p}_{-\nu} \right) \widehat{\mathcal{P}}(\boldsymbol{s}_i|\boldsymbol{0};\xi,\varepsilon) \right. \\ &\quad \left. + \left(\frac{1}{p_\nu - \widetilde{p}_{-\nu} + 1} - 1 \right) \left(\sum_{\mu} \widetilde{p}_\mu \widehat{\mathcal{P}}(\boldsymbol{s}_i|\boldsymbol{e}_\nu + \boldsymbol{e}_\mu;\xi,\varepsilon) - \widetilde{p}_{-\nu} \widehat{\mathcal{P}}(\boldsymbol{s}_i|\boldsymbol{0};\xi,\varepsilon) \right) \right] \qquad (4.157) \end{aligned}$$

Finally, using again (4.151), we get

$$\mathcal{A}(\boldsymbol{s}_i|\boldsymbol{e}_\nu;\xi,\varepsilon) = \left(\frac{1}{p_\nu - \widetilde{p}_{-\nu} + 1} - 1 \right) \left[\widehat{\mathcal{P}}(\boldsymbol{s}_i|\boldsymbol{e}_\nu;\xi,\varepsilon) - \delta_{i,\nu} - \xi \widehat{\mathcal{P}}(\boldsymbol{s}_i|\boldsymbol{0};\xi,\varepsilon) \right] \tag{4.158}$$

These two cases then lead to the general equation

$$\mathcal{A}(\boldsymbol{s}_i|\boldsymbol{s}_j;\xi) = \begin{cases} \delta_{i,0} - (1-\xi)\widehat{\mathcal{P}}(\boldsymbol{s}_i|\boldsymbol{0};\xi,\varepsilon) & \text{if } \boldsymbol{s}_j = \boldsymbol{0}\,, \\ \left(\frac{1}{p_\nu - \widetilde{p}_{-\nu}+1} - 1\right)\left[\widehat{\mathcal{P}}(\boldsymbol{s}_i|\boldsymbol{e}_\nu;\xi,\varepsilon) - \delta_{i,\nu} - \xi\widehat{\mathcal{P}}(\boldsymbol{s}_i|\boldsymbol{0};\xi,\varepsilon)\right] & \text{if } \boldsymbol{s}_j = \boldsymbol{e}_\nu. \end{cases} \tag{4.159}$$

Using the definitions of $\boldsymbol{\mathcal{A}}$ and $\boldsymbol{\mathcal{P}}$, the matrix $\boldsymbol{\mathcal{P}}^\dagger$ is deduced from (4.141), and an expression of the FPTD $\widehat{\mathcal{F}}^*$ is deduced in terms of the propagators $\widehat{\mathcal{P}}$.

Similarly, the quantities $\mathcal{F}'_\nu$, defined here by

$$\mathcal{F}'_\nu = \xi\widetilde{P}^\dagger(\boldsymbol{0}|\boldsymbol{e}_\nu)\mathcal{B}_\nu^\top(\boldsymbol{1}-\boldsymbol{A})^{-1}\sum_{\boldsymbol{Y}\neq\boldsymbol{0}}\mathcal{B}(\boldsymbol{Y};\xi), \tag{4.160}$$

with

$$\left[\sum_{\boldsymbol{Y}\neq\boldsymbol{0}}\mathcal{B}(\boldsymbol{Y};\xi)\right]_j = \frac{1}{1-\xi} - \widehat{\mathcal{P}}(\boldsymbol{0}|\boldsymbol{s}_j;\xi), \tag{4.161}$$

are readily expressed in terms of the quantities $\widehat{\mathcal{P}}$.

4.7.3 Propagators

The exact expression of the propagators $\widehat{\mathcal{P}}(\boldsymbol{r}|\boldsymbol{r}_0;\xi,\varepsilon)$ is given in Appendix A (Section A.3). These propagators are functions of the Laplace variable ξ and of the bias ε. We are interested in the limit where we first take $t\to\infty$ (equivalent in Laplace to $\xi\to 1$) and $\rho_0\to 0$. Recalling the ε is equal to the velocity of the TP and vanishes when $\rho_0\to 0$, we thus need to consider the expansions close to $\varepsilon\to 0$ of the propagators $\widehat{\mathcal{P}}(\boldsymbol{r}|\boldsymbol{r}_0;\xi,\varepsilon)$ evaluated at $\xi=1$. The important point is that this expansion is easily deduced from the expression of the non-biased propagators $\widehat{P}$ with the relation

$$\widehat{\mathcal{P}}(\boldsymbol{r}|\boldsymbol{0};\xi=1,\varepsilon) \underset{\varepsilon\to 0}{=} \frac{1}{L\varepsilon} + \frac{1}{L} - \frac{2|r_1|}{L} - S^{(2)}_{L,-1} - \Delta(\boldsymbol{r}) + \mathcal{O}(\varepsilon), \tag{4.162}$$

where

$$\Delta(\boldsymbol{r}) = \lim_{\xi\to 1}\left[\widehat{P}(\boldsymbol{0}|\boldsymbol{0};\xi) - \widehat{P}(\boldsymbol{r}|\boldsymbol{0};\xi)\right]. \tag{4.163}$$

The quantities $\Delta(\boldsymbol{r})$ can be computed using the expansions of the propagators $\widehat{P}$ (A.36)-(A.41). Using a computer algebra software, we then obtain the expansion of the quantities $\sigma_{\pm1}(\boldsymbol{e}_\nu)$, $\mathcal{D}_0$, $\mathcal{D}_{\pm1}$ and F'_ν involved in the expression of $\widehat{\kappa}_1^{(2)}(\xi)$ (4.30). These expansions are given in Appendix E (Section E.2).

4.7.4 Ultimate expression of the second cumulant

Using (4.30), we finally obtain the following expression of the second cumulant in the limit where we first take $\xi\to 1$ and $\varepsilon\to 0$. We obtain:

$$\lim_{\xi\to 1}\left[(1-\xi)^2\widehat{\kappa}_1^{(2)}(\xi)\right] \underset{\varepsilon\to 0}{\sim} \rho_0\frac{2{a'_0}^2}{L\varepsilon}, \tag{4.164}$$

where

$$a'_0 = \frac{p_1 - p_{-1}}{1 + \frac{4\alpha}{4-\alpha}(p_1+p_{-1}) + \frac{16}{L(4-\alpha)}(p_1-p_{-1})}. \tag{4.165}$$

The expression of ε is deduced from the expression of the TP velocity. The Laplace transform of the first cumulant $\kappa_1^{(1)}(t) = \langle X_t \rangle$ will be shown in the next Chapter to be given by

$$\lim_{\xi \to 1} \left[(1-\xi)^2 \widehat{\kappa}_1^{(1)}(\xi) \right] \underset{\varepsilon \to 0}{\sim} \rho_0 a_0' \tag{4.166}$$

Using a Tauberian theorem, we then find

$$\lim_{t \to \infty} \frac{\kappa^{(1)}(t)}{t} \underset{\rho_0 \to 0}{\sim} \rho_0 a_0'. \tag{4.167}$$

The velocity of the TP is then equal to $\rho_0 a_0'$, which leads to the expression of the bias $\varepsilon = \rho_0 a_0'$. Finally, replacing ε in (4.164) and using a Tauberian theorem, we get

$$\boxed{\lim_{t \to \infty} \frac{\kappa^{(2)}(t)}{t} \underset{\rho_0 \to 0}{\sim} \frac{2a_0'}{L}} \tag{4.168}$$

A few comments follow from this result:

- first, we observe that in the ultimate regime reached by the TP, its fluctuations grow linearly with time, which means that its behavior eventually becomes *diffusive*.
- the crossover time $t_\times$ between the two regimes (4.65) and (4.168) verifies

$$\frac{8{a_0}^2}{3\sqrt{\pi}L} \rho_0 {t_\times}^{3/2} \sim \frac{2a_0'}{L} t_\times. \tag{4.169}$$

  Consequently, the scaling between $t_\times$ and ρ_0 is given by

$$t_\times \sim \frac{1}{{\rho_0}^2}. \tag{4.170}$$

  This crossover time diverges when $\rho_0 \to 0$. The superdiffusive regime, even though it is transient, may then be long-lived if the vacancy density is small enough.

- surprisingly, in this regime, the expression of $\kappa_1^{(2)}(t)$ is independent from ρ_0. This is not contradictory with the fact the the fluctuations should decrease when there are less and less vacancies on the lattice: the crossover to the ultimate regime occurs for infinitely long times when $\rho_0 \to 0$ as $t_\times \sim 1/{\rho_0}^2$. We will present in Chapter 7 a simplified description which qualitatively accounts for this observation.

4.7.5 Scaling function

We showed that the second cumulant had two limiting behaviors, given by:

$$\lim_{\rho_0 \to 0} \frac{\kappa^2(t)}{\rho_0} \underset{t \to \infty}{\sim} \frac{8{a_0}^2}{3\sqrt{\pi}L} t^{3/2} \tag{4.171}$$

$$\lim_{t \to \infty} \frac{\kappa^{(2)}(t)}{t} \underset{\rho_0 \to 0}{\sim} \frac{2a_0'}{L} \tag{4.172}$$

Mathematically, the existence of these two regimes rely on the non-interversion of the limits $\rho_0 \to 0$ and $t \to \infty$. In this Section, we aim to compute the scaling function where the $\rho_0 \to 0$ and $t \to \infty$ limits are taken simultaneously with the appropriate scaling between the variables:

$$t \sim \frac{1}{{\rho_0}^2}, \tag{4.173}$$

suggested by the expression of the crossover time $t_\times$ (4.170).

The method given above to compute the conditional return probabilites $\widehat{\mathcal{F}}^*$ and the sums $\mathcal{F}'_\nu$ for arbitrary values of ξ and ε are still valid. We then give the expansions of the propagators $\widehat{\mathcal{P}}$ in the joint limit of $\xi \to 1$ and $\varepsilon \to 0$, with the scaling

$$1 - \xi \sim \varepsilon^2 \tag{4.174}$$

With no loss of generality, we choose to eliminate the parameter ε, by introducing a quantity $\lambda = \mathcal{O}(1)$ such that:

$$\varepsilon = \frac{1}{\lambda}\sqrt{1-\xi}. \tag{4.175}$$

In Appendix A (Section A.3.2), we show that in this limit the expansion of the propagators $\widehat{\mathcal{P}}$ can still be expressed in terms if the non-biased propagators with the formula:

$$\widehat{\mathcal{P}}(\boldsymbol{r}|\boldsymbol{0};\xi,\varepsilon) \underset{\substack{\varepsilon\sim\sqrt{1-\xi}\\ \xi\to 1}}{=} \frac{\lambda}{L\sqrt{1+\lambda^2}\sqrt{1-\xi}} - \frac{2r_1}{L}\frac{1}{\sqrt{1+\lambda^2}} + \frac{1}{2L\sqrt{1+\lambda^2}}\frac{2-\lambda^2}{1+\lambda^2} + S^{(2)}_{L,-1} - \Delta(\boldsymbol{r}) + \mathcal{O}(\sqrt{1-\xi}) \tag{4.176}$$

where the quantities $\Delta(\boldsymbol{r})$ were defined in (4.163), and can be computed using the expansions of the propagators $\widehat{P}$ given by (A.36)-(A.41). We obtain the expansions of the quantities $\sigma_{\pm 1}(\boldsymbol{e}_\nu)$, $\mathcal{D}_0$, $\mathcal{D}_{\pm 1}$ and F'_ν involved in the expression of $\widehat{\kappa}^{(2)}_1(\xi)$ (4.80). These expansions are given in Appendix E (Section E.3). In this joint limit, we finally obtain:

$$\widehat{\kappa}^{(2)}_1(\xi) \underset{\substack{\varepsilon\sim\sqrt{1-\xi}\\ \xi\to 1}}{\sim} \frac{2\rho_0 L\lambda\sqrt{1+\lambda^2}}{(1-\xi)^{5/2}} \frac{(p_1-p_{-1})^2(\alpha-4)^2}{\left\{16(p_1-p_{-1}) + L\sqrt{1+\lambda^2}\left[4-\alpha+4\alpha(p_1+p_{-1})\right]\right\}^2} \tag{4.177}$$

Recalling the definitions of a_0 (4.64) and a'_0 (4.165), replacing λ by $\sqrt{1-\xi}/\varepsilon$ and relacing ε by $\rho_0 a'_0$, one gets the expression:

$$\widehat{\kappa}^{(2)}_1(\xi) \underset{\substack{\varepsilon\sim\sqrt{1-\xi}\\ \xi\to 1}}{\sim} \frac{2}{(1-\xi)^2 a'_0 L} \frac{{a_0}^2\sqrt{1+\frac{1-\xi}{\varepsilon^2}}}{\sqrt{1+\frac{1-\xi}{\varepsilon^2}} + \frac{16}{L}\frac{a_0}{4-\alpha}}. \tag{4.178}$$

In the long-time limit, the discrete-time description we used so far can be conveniently replaced by a continuous-time description. Denoting by s the Laplace variable associated to the continuous-time variable t, we then aim to invert the Laplace transform:

$$\widehat{\kappa}^{(2)}(s) \underset{\substack{\varepsilon\sim\sqrt{s}\\ s\to 0}}{\sim} \frac{2}{s^2 a'_0 L} \frac{{a_0}^2\sqrt{1+\frac{s}{\varepsilon^2}}}{\sqrt{1+\frac{s}{\varepsilon^2}} + \frac{16}{L}\frac{a_0}{4-\alpha}} \tag{4.179}$$

Using tabulated inverse Laplace transforms, we obtain the following scaling function for the quantity $\kappa_1^{(2)}(t)/t$:

$$\begin{aligned}\frac{\kappa_1^{(2)}(t)}{t} &\sim \frac{{a_0}^2}{La_0'\tau(b^2-1)^3}\left\{2\mathrm{e}^{-\tau}(b^2-1)(3b^2+1)\sqrt{\frac{\tau}{\pi}}-4b^3+(2b^4\tau+b^4+6b^2-2\tau+1)\mathrm{erf}(\sqrt{\tau})\right.\\ &\left.+4b\left[(-b^4\tau+b^2\tau+b^2+1)\mathrm{e}^{-(1-b^2)\tau}\mathrm{erfc}(b\sqrt{\tau})-1\right]-4\tau b(b^2-1)\right\} \qquad (4.180)\end{aligned}$$

where we used the relation $\varepsilon = \rho_0 a_0'$, and where we defined the following quantities:

- the rescaled time $\tau \equiv {a_0'}^2{\rho_0}^2 t$,
- the parameter $b \equiv \frac{a_0}{a_0'} - 1 = \frac{16a_0}{L(4-\alpha)}$.

The error functions an complementary error functions are defined in the usual fashion:

$$\mathrm{erf}(x) = \frac{2}{\sqrt{\pi}}\int_0^x \mathrm{e}^{-t^2}\mathrm{d}t, \qquad (4.181)$$

$$\mathrm{erfc}(x) = 1-\mathrm{erf}(x). \qquad (4.182)$$

We define the scaling function $g(\tau)$ as follows:

$$\begin{aligned}g(\tau) &\equiv \frac{{a_0}^2}{a_0'\tau(b^2-1)^3}\left\{2\mathrm{e}^{-\tau}(b^2-1)(3b^2+1)\sqrt{\frac{\tau}{\pi}}-4b^3+(2b^4\tau+b^4+6b^2-2\tau+1)\mathrm{erf}(\sqrt{\tau})\right.\\ &\left.+4b\left[(-b^4\tau+b^2\tau+b^2+1)\mathrm{e}^{-(1-b^2)\tau}\mathrm{erfc}(b\sqrt{\tau})-1\right]\right\} \qquad (4.183)\end{aligned}$$

so that

$$\frac{\kappa_1^{(2)}(t)}{t} \sim \frac{g(\tau)}{L}. \qquad (4.184)$$

The limiting behaviors of $g(\tau)$ are

$$g(\tau) \sim \begin{cases}\frac{8}{3}\frac{{a_0}^2}{a_0'}\sqrt{\frac{\tau}{\pi}} & \text{when } \tau \to 0,\\ 2a_0' & \text{when } \tau \to \infty.\end{cases} \qquad (4.185)$$

We now check that the limiting behaviors of (4.180) allow us to retrieve the results from the previous calculations:

1. when the rescaled time τ goes to 0 (which is equivalent to the limit where ρ_0 is going to zero first), we find

$$\frac{\kappa_1^{(2)}(t)}{t} \sim \frac{8}{3}\frac{a_0^2}{a_0' L}\sqrt{\frac{\tau}{\pi}} \qquad (4.186)$$

Replacing τ by ${\rho_0}^2{a_0'}^2 t$, we finally obtain

$$\kappa_1^{(2)}(t) \sim \frac{8{a_0}^2}{3\sqrt{\pi}L}t^{3/2}, \qquad (4.187)$$

which corresponds to (4.65).

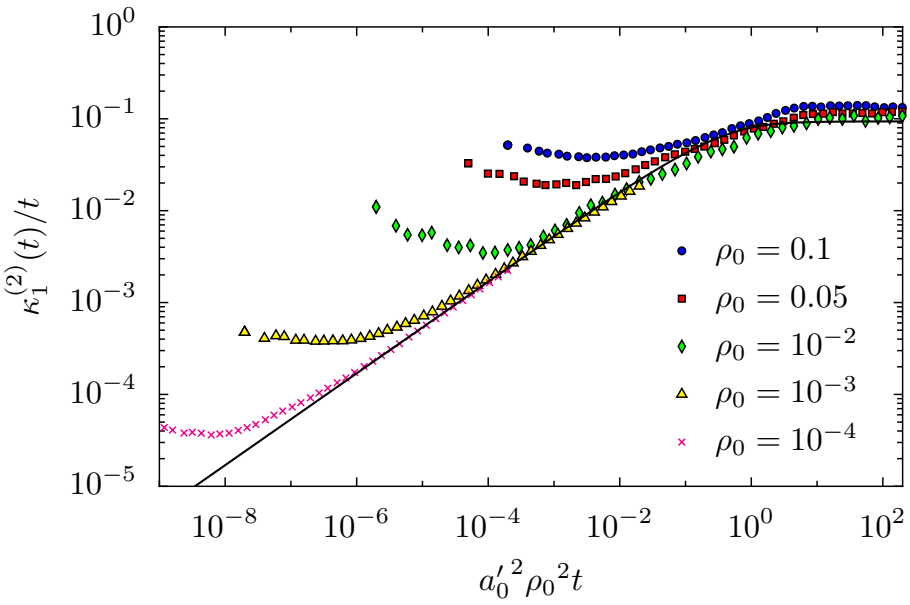

Figure 4.8: Rescaled variance $\kappa_1^{(2)}(t)/t$ as a function of $\tau = {a_0'}^2\rho_0^2 t$ obtained from numerical simulations of tracer diffusion on a 2D stripe of width $L = 3$ with different densities. The external force is $F = \infty$, which implies $p_1 = 1$ and $p_\mu = 0$ for $\mu \neq 1$. The black line is the function from (4.180).

2. when the rescaled time τ goes to infinity (which is equivalent to the limit where t is going to infinity first), we find

$$\frac{\kappa_1^{(2)}(t)}{t} \sim \frac{2{a_0}^2}{La_0'} \frac{1}{(b+1)^2} \tag{4.188}$$

Using the definition of b, we finally obtain

$$\kappa_1^{(2)}(t) \sim \frac{2a_0'}{L} t, \tag{4.189}$$

which corresponds to (4.168).

On Fig. 4.8, we confront the expression of the scaling function (4.180) with the results from numerical simulations. The rescaled variance $\kappa_1^{(2)}(t)$ is plotted as a function of the rescaled time $\tau = {a_0'}^2\rho_0^2 t$, for different values of the vacancy density and for an infinite external force (which is equivalent to taking $p_1 = 1$ and $p_\mu = 0$ for $\mu \neq 1$). The scaling function, represented in black, is a good description of both regimes and of the crossover between them.

4.8 Crossover to diffusion – Capillary-like geometry

4.8.1 Introduction

The calculation presented in the case of the stripe-like geometry in the previous section is now extended to the case a capillary. The elementary jump probabilities of the vacancies away from the TP are given

by

$$\widetilde{p}_{-1} = \frac{1}{1+\varepsilon}\left(\frac{1}{6}+\varepsilon\right), \tag{4.190}$$

$$\widetilde{p}_1 = \widetilde{p}_{\pm 2} = \widetilde{p}_{\pm 3} = \frac{1}{6(1+\varepsilon)}, \tag{4.191}$$

where the bias ε is equal to the velocity of the TP in the ultimate regime. The method to compute the FPTD $\mathcal{F}^*$ and the sums $\mathcal{F}'$ relative to vacancies undergoing an effective bias, which was presented for the case of a two-dimensional stripe in Section 4.7.2, is extended to the three-dimensional capillary. The propagators associated to the biased random walk of the vacancies are computed in Appendix B (Section B.2). They are found to be simply expressed in terms of the non-biased propagators, through the formula

$$\widehat{\mathcal{P}}(\boldsymbol{r}|\mathbf{0};\xi=1,\varepsilon) \underset{\varepsilon\to 0}{=} \frac{1}{L^2\varepsilon} + \frac{1}{L^2} - \frac{3r_1}{L^2} + S^{(3)}_{L,0} - \Delta(\boldsymbol{r}) \tag{4.192}$$

with

$$\Delta(\boldsymbol{r}) = \lim_{\xi\to 1}\left[\widehat{P}(\mathbf{0}|\mathbf{0};\xi) - \widehat{P}(\boldsymbol{r}|\mathbf{0};\xi)\right]. \tag{4.193}$$

The quantities $\Delta(\boldsymbol{r})$ can be computed using the expansions of the propagators $\widehat{P}$ (B.26)-(B.32). We then obtain the expansion of the quantities $\sigma_{\pm 1}(\boldsymbol{e}_\nu)$, $\mathcal{D}_0$, $\mathcal{D}_{\pm 1}$ and F'_ν involved in the expression of $\widehat{\kappa}^{(2)}_1(\xi)$ (4.80). These expansions are presented in the particular case of a directed TP ($p_1 = 1$ and $p_\mu = 0$ for $\mu \neq 1$) in Appendix F (Section F.2). In principle, these expansions can also be computed for an arbitrary value of the bias. However, the computation is too cumbersome to be handled, even with a computer algebra software. An alternative approach to the problem (see Chapter 10) will give an expression of the second cumulant for an arbitrary value of the bias.

4.8.2 Ultimate expression of the second cumulant

We obtain the following limit behavior of the second cumulant in this limit:

$$\lim_{\xi\to 1}\left[(1-\xi)^2\widehat{\kappa}^{(2)}_1(\xi)\right] \underset{\varepsilon\to 0}{\sim} \rho_0 \frac{2{a'_0}^2}{L^2\varepsilon} \tag{4.194}$$

with

$$a'_0 = \frac{1}{1+\frac{6\alpha}{6-\alpha}+\frac{36}{L^2(6-\alpha)}} \tag{4.195}$$

The expression of ε is deduced from the expression of the TP velocity. The Laplace transform of the first cumulant $\kappa^{(1)}_1(t) = \langle X_t\rangle$ will be shown in the next Chapter to be given by

$$\lim_{\xi\to 1}\left[(1-\xi)^2\widehat{\kappa}^{(1)}_1(\xi)\right] \underset{\varepsilon\to 0}{\sim} \rho_0 a'_0 \tag{4.196}$$

Using a Tauberian theorem, we then find

$$\lim_{t\to\infty}\frac{\kappa^{(1)}_1(t)}{t} \underset{\rho_0\to 0}{\sim} \rho_0 a'_0. \tag{4.197}$$

The velocity of the TP is then given by $\rho_0 a_0'$, which leads to the expression of the bias $\varepsilon = \rho_0 a_0'$. Finally, replacing ε in (4.194) and using a Tauberian theorem, we get

$$\boxed{\lim_{t\to\infty} \frac{\kappa_1^{(2)}(t)}{t} \underset{\rho_0\to 0}{\sim} \frac{2a_0'}{L^2}} \tag{4.198}$$

4.8.3 Scaling function

As in the case of the stripe-like geometry, the comparison of the expressions of the fluctuations of the TP position in the two regimes (4.89) and (4.198) shows that the crossover time $t_\times$ scales as:

$$t_\times \sim \frac{1}{{\rho_0}^2}. \tag{4.199}$$

The calculation presented in this Section is then very similar to the one presented in the case of the stripe-like geometry. We expand the propagators $\widehat{\mathcal{P}}$ in the joint limit $\xi \to 1$ and $\varepsilon \to 0$ with the scaling

$$1-\xi \sim \varepsilon^2. \tag{4.200}$$

With no loss of generality, we choose to eliminate the parameter ε, by introducing a quantity $\lambda = \mathcal{O}(1)$ such that:

$$\varepsilon = \frac{1}{\lambda}\sqrt{1-\xi} \tag{4.201}$$

In Appendix B (Section B.2.3), we show that in this limit the expansion of the propagators $\widehat{\mathcal{P}}$ can still be expressed in terms if the non-biased propagators with the formula:

$$\widehat{\mathcal{P}}(\boldsymbol{r}|\boldsymbol{0};\varepsilon) \underset{\varepsilon\to 0}{=} \frac{\lambda}{L^2\sqrt{1+2\lambda^2/3}\sqrt{1-\xi}} - \frac{3r_1}{L^2}\frac{1}{\sqrt{1+2\lambda^2/3}} + \frac{1}{L^2\sqrt{1+2\lambda^2/3}}\frac{3-2\lambda^2}{3+2\lambda^2} + S_{L,0}^{(3)} - \Delta(\boldsymbol{r}) + \mathcal{O}(\sqrt{1-\xi}) \tag{4.202}$$

where the quantities $\Delta(\boldsymbol{r})$ were defined in (4.163), and can be computed using the expansions of the propagators $\widehat{P}$ (B.26)-(B.32). We obtain the expansions of the quantities $\sigma_{\pm 1}(\boldsymbol{e}_\nu)$, $\mathcal{D}_0$, $\mathcal{D}_{\pm 1}$ and F_ν' involved in the expression of $\widehat{\kappa}_1^{(2)}(\xi)$ (4.80). These expansions are given in Appendix F (Section F.3). In this joint limit, and in the particular case of a directed TP, we finally obtain:

$$\widehat{\kappa}_1^{(2)}(\xi) \underset{\substack{\varepsilon\sim\sqrt{1-\xi}\\ \xi\to 1}}{\sim} \frac{2\rho_0 L^2 \lambda\sqrt{1+2\lambda^2/3}}{(1-\xi)^{5/2}} \frac{(6-\alpha)^2}{\left[36 + L^2\sqrt{1+2\lambda^2/3}\,(6-\alpha+6\alpha)\right]^2} \tag{4.203}$$

Recalling the definitions of a_0 (4.88) and a_0' (4.195), replacing λ by $\sqrt{1-\xi}/\varepsilon$ and finally using the definition of $\varepsilon = \rho_0 a_0'$, one gets the expression:

$$\widehat{\kappa}_1^{(2)}(\xi) \underset{\substack{\varepsilon\sim\sqrt{1-\xi}\\ \xi\to 1}}{\sim} \frac{2}{(1-\xi)^2 a_0' L^2} \frac{{a_0}^2\sqrt{1+\frac{2}{3}\frac{1-\xi}{\varepsilon^2}}}{\sqrt{1+\frac{2}{3}\frac{1-\xi}{\varepsilon^2}} + \frac{36}{L^2}\frac{a_0}{6-\alpha}} \tag{4.204}$$

In the long-time limit, the discrete-time description we used so far can be conveniently replaced by a continuous-time description. Denoting by s the Laplace variable associated to the continuous-time

variable t, we then aim to invert the Laplace transform:

$$\widehat{\kappa}^{(2)}(s) \underset{\substack{\varepsilon\sim\sqrt{s}\\ p\to 0}}{\sim} \frac{2}{s^2 a_0' L} \frac{{a_0}^2\sqrt{1+\frac{2}{3}\frac{s}{\varepsilon^2}}}{\sqrt{1+\frac{2}{3}\frac{s}{\varepsilon^2}}+\frac{36}{L^2}\frac{a_0}{6-\alpha}} \tag{4.205}$$

The scaling function we are computing is then simply related to the scaling function g already computed for the stripe-like geometry (4.183):

$$\frac{\kappa^{(2)}(t)}{t} \sim \frac{1}{L^2} g\left(\frac{3}{2}\tau\right), \tag{4.206}$$

where the values of a_0 and a_0' used in the expression of g are replaced by the ones computed for the capillary-like geometry. Using the asymptotic expansions of g (4.185), we show that the limiting behaviors of (4.206) allow us to retrieve the results from the previous calculations:

1. when the rescaled time τ goes to 0 (which is equivalent to the limit where ρ_0 is going to zero first), we find
$$\frac{\kappa^{(2)}(t)}{t} \sim 4\sqrt{\frac{2}{3\pi}}\frac{a_0^2}{a_0' L^2}\sqrt{\tau} \tag{4.207}$$
Replacing τ by ${\rho_0}^2{a_0'}^2 t$, we finally obtain
$$\kappa^{(2)}(t) \sim \frac{4{a_0}^2}{L^2}\sqrt{\frac{2}{3\pi}}t^{3/2}, \tag{4.208}$$
which corresponds to (4.89).

2. when the rescaled time τ goes to infinity (which is equivalent to the limit where t is going to infinity first), we find
$$\frac{\kappa^{(2)}(t)}{t} \sim \frac{2a_0'}{L^2}t \tag{4.209}$$
which corresponds to (4.198).

4.9 Crossover to diffusion – Two-dimensional lattice

4.9.1 Ultimate expression of the second cumulant

We finally study the ultimate regime reached by the TP in the case of a two-dimensional lattice. To this purpose, the computation presented in the case of two-dimensional stripe (Section 4.7.2) can be extended. The evolution rules of the vacancies with the set of biased jump probabilities $\widetilde{p}_\mu$ are given by (4.136) and (4.137). The expression of the entries of the matrix $\boldsymbol{\mathcal{A}}$ (4.159), as well as the expression of $\boldsymbol{\mathcal{P}}$ (4.145) are valid as well. Consequently, the FPTD $\widehat{\mathcal{F}}^*$ and the sums $\mathcal{F}_\nu'$ are computed in the usual way. The propagators $\widehat{\mathcal{P}}$ are shown to take the simple expansion (see Appendix C)

$$\widehat{\mathcal{P}}(\boldsymbol{r}|\boldsymbol{0};\xi,\varepsilon) \underset{\varepsilon\to 0}{=} \frac{2}{\pi}\ln\frac{1}{\varepsilon} + \frac{\ln 8}{\pi} - \Delta(\boldsymbol{r}) + \mathcal{O}(\varepsilon\ln\varepsilon) \tag{4.210}$$

where $\Delta(\boldsymbol{r})$ is defined as a function of the non-biased propagators $\widehat{P}$ (4.163), which were computed for a two-dimensional lattice in Appendix C (Section C.2). The expression of the quantities involved in the expression of the second cumulant (4.30) are given in Appendix G (Section G.2). Using these expansions, we obtain:

$$\lim_{\xi\to 1}\left[(1-\xi)^2\widehat{\kappa}_1^{(2)}(\xi)\right] \underset{\varepsilon\to 0}{=} \rho_0\left[a_1 + 2{a_0}^2\left(\frac{2}{\pi}\ln\frac{1}{\varepsilon} + \frac{\ln 8}{\pi} + \frac{\pi(5-2\pi)}{2\pi-4}\right)\right] \tag{4.211}$$

The expression of ε is deduced from the expression of the TP velocity. The Laplace transform of the first cumulant $\kappa_1^{(1)}(t) = \langle X_t\rangle$ will be shown in the next Chapter to be given by

$$\lim_{\xi\to 1}\left[(1-\xi)^2\widehat{\kappa}_1^{(1)}(\xi)\right] \underset{\varepsilon\to 0}{\sim} \rho_0 a_0 \tag{4.212}$$

Using a Tauberian theorem, we then find

$$\lim_{t\to\infty}\frac{\kappa_1^{(1)}(t)}{t} \underset{\rho_0\to 0}{\sim} \rho_0 a_0. \tag{4.213}$$

The velocity of the TP is then given by $\rho_0 a_0$, which leads to the expression of the bias $\varepsilon = \rho_0 a_0$. Finally, replacing ε in (4.211) and using a Tauberian theorem, we get

$$\boxed{\lim_{t\to\infty}\frac{\kappa_1^{(2)}(t)}{t} \underset{\rho_0\to 0}{=} \rho_0\left[a_1 + 2{a_0}^2\left(\frac{2}{\pi}\ln\frac{1}{\rho_0 a_0} + \frac{\ln 8}{\pi} + \frac{\pi(5-2\pi)}{2\pi-4}\right)\right]} \tag{4.214}$$

We conclude that on a two-dimensional lattice, the TP finally reaches a diffusive regime. Contrary to the case of quasi-one-dimensional lattices, the diffusion coefficient now depends on the vacancy density ρ_0, and goes to zero as $\rho_0\ln(1/\rho_0)$. The crossover time between the two regimes may be deduced by equalizing the leading order terms of (4.114) and (4.214):

$$\frac{4{a_0}^2}{\pi}\rho_0 t\ln\rho_0 = \frac{2{a_0}^2}{\pi}\rho_0 t\ln t \tag{4.215}$$

which leads to the crossover time

$$t_\times = \frac{1}{{\rho_0}^2}. \tag{4.216}$$

The crossover time scales as $1/{\rho_0}^2$, which the same scaling as the one obtained for quasi-one-dimensional geometries. This behavior then seems to be independent of the lattice geometry.

4.9.2 Scaling function

As in the case of a two-dimensional stripe, we want to compute the scaling function describing both the superdiffusive and the diffusive regime. Mathematically, it may be obtained by taking simultaneously the limits $t\to\infty$ (i.e. $\xi\to 1$) and $\varepsilon\to 0$ with the scaling

$$1-\xi \sim \varepsilon^2. \tag{4.217}$$

The expansions of the propagators in this joint limit are calculated in Appendix C (Section C.2.4). The variable ε is taken equal to $\sqrt{1-\xi}/\lambda$. The propagators are found to be given by

$$\widehat{\mathcal{P}}(\boldsymbol{r}|\boldsymbol{0};\xi,\varepsilon) \underset{\substack{\varepsilon\sim\sqrt{1-\xi}\\ \xi\to 1}}{=} \frac{1}{\pi}\ln\frac{1}{1-\xi+\varepsilon^2}+\frac{\ln 8}{\pi}-\Delta(\boldsymbol{r})+\dots, \tag{4.218}$$

where the quantities $\Delta(\boldsymbol{r})$ are defined by (4.163). In this joint limit, the variance is

$$\widehat{\kappa}_1^{(2)}(\xi) \underset{\substack{\varepsilon\sim\sqrt{1-\xi}\\ \xi\to 1}}{\sim} \frac{\rho_0}{(1-\xi)^2}\left[\frac{2{a_0}^2}{\pi}\ln\left(\frac{1}{1-\xi}\frac{\lambda^2}{1+\lambda^2}\right)+a_1+\frac{2{a_0}^2}{\pi}\left(\ln 8+\frac{\pi(5-2\pi)}{2\pi-4}\right)+\dots\right]. \tag{4.219}$$

We now aim to retrieve the time dependence of the cumulant. The term proportional to $1/(1-\xi)^2$ will give a term growing linearly with time. Recalling the definition of λ, we get

$$\frac{1}{(1-\xi)^2}\ln\left(\frac{1}{1-\xi}\frac{\lambda^2}{1+\lambda^2}\right)=\frac{1}{(1-\xi)^2}\ln\frac{1}{\varepsilon^2}+\frac{1}{(1-\xi)^2}\ln\frac{1}{1+\frac{1-\xi}{\varepsilon^2}}. \tag{4.220}$$

Using a Tauberian theorem, we get the time-dependent term at leading order when $t\to\infty$:

$$t\ln\frac{t}{1+\varepsilon^2 t}. \tag{4.221}$$

Finally, replacing ε with $\rho_0 a_0$, we obtain the following scaling behavior

$$\boxed{\kappa_1^{(2)}(t)\sim\rho_0 t\left[\frac{2{a_0}^2}{\pi}\ln\frac{t}{1+{\rho_0}^2{a_0}^2 t}+a_1+\frac{2{a_0}^2}{\pi}\left(\ln 8+\gamma-1+\frac{\pi(5-2\pi)}{2\pi-4}\right)\right]} \tag{4.222}$$

We then verify that this scaling function allows us to retrieve the two limiting behaviors predicted above:

1. when we take the limit where ρ_0 is going to zero first, we find

$$\kappa_1^{(2)}(t)\sim\rho_0 t\left[\frac{2{a_0}^2}{\pi}\ln t+a_1+2{a_0}^2\frac{\pi(5-2\pi)}{2\pi-4}+\frac{2{a_0}^2}{\pi}(\ln 8+\gamma-1)\right] \tag{4.223}$$

   which is equivalent to (4.114).

2. when we take the limit where t is going to ∞ first), we find

$$\kappa_1^{(2)}(t)\sim\rho_0 t\left[a_1+2{a_0}^2\frac{\pi(5-2\pi)}{2\pi-4}+\frac{2{a_0}^2}{\pi}\left(\ln 8+\gamma-1+\ln\frac{1}{{\rho_0}^2{a_0}^2}\right)\right] \tag{4.224}$$

   which is equivalent to (4.214).

In order to confront these analytical predictions with numerical simulations, we study the following function of the variance:

$$\psi(t)=\frac{\kappa^{(2)}(t)}{\rho_0 t}-\frac{2{a_0}^2}{\pi}\ln\frac{1}{{\rho_0}^2{a_0}^2}. \tag{4.225}$$

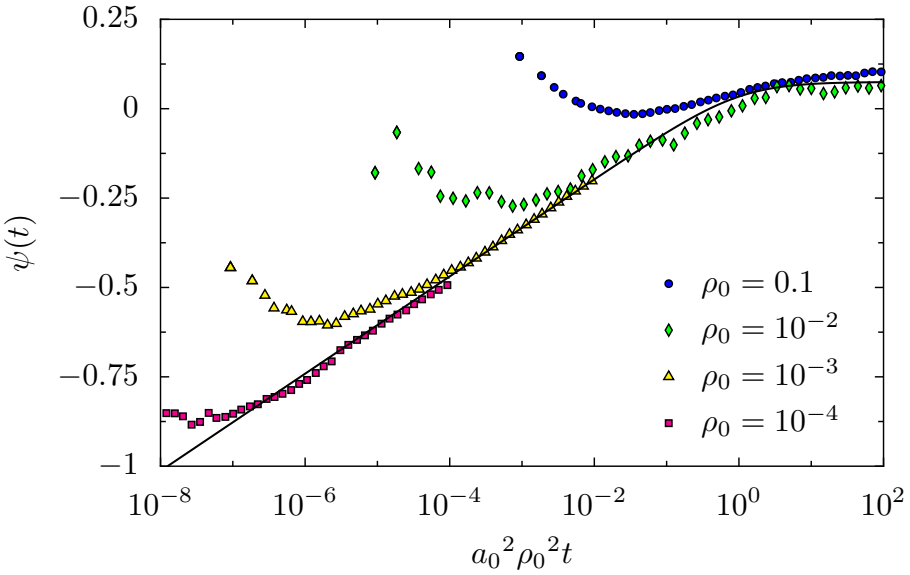

Figure 4.9: Rescaled function of the variance $\psi(t)$ (see text) as a function of $\tau = {a_0}^2{\rho_0}^2 t$ obtained from numerical simulations of tracer diffusion on a 2D lattice with different densities. The external force is $F = \infty$, which implies $p_1 = 1$ and $p_\mu = 0$ for $\mu \neq 1$. The black line is the function $g_{2\mathrm{D}}(\tau)$ (4.226).

It is then expected to be described by the scaling function

$$g_{2\mathrm{D}}(\tau) \equiv \frac{2{a_0}^2}{\pi} \ln \frac{\tau}{1+\tau} + a_1 + 2{a_0}^2 \frac{\pi(5-2\pi)}{2\pi-4} + \frac{2{a_0}^2}{\pi}(\ln 8 + \gamma - 1), \tag{4.226}$$

where $\tau = {\rho_0}^2{a_0}^2 t$ is a rescaled time variable

On Fig. 4.9, we confront the expression of the scaling function $g_{2\mathrm{D}}$ (4.226) with the results from the value of $\psi(t)$ defined in (4.225) computed from numerical simulations. $\psi(t)$ is plotted as a function of the rescaled time $\tau = {a_0}^2{\rho_0}^2 t$, for different values of the vacancy density and for an infinite external force (which is equivalent to taking $p_1 = 1$ and $p_\mu = 0$ for $\mu \neq 1$). The scaling function, represented in black, is a good description of both regimes and of the crossover between them.

4.10 Conclusion

In this Chapter, we studied the fluctuations of the position of a driven TP in a lattice gas, in the limit where the density of bath particles goes to 1. We applied the formalism presented in Chapter 2, which consists in considering that each vacancy contributes independently to the motion of the TP in the limit where the density of vacancies ρ_0 is very small. In confined geometries, it was shown that the behavior of the TP was superdiffusive. Indeed, in quasi-one-dimensional geometries (such as 2D stripes and 3D capillaries), the fluctuations of the TP position grow as $t^{3/2}$, and as $t \ln t$ on a two-dimensional lattice. We also show that this effect appears beyond the linear response of the system, and so it could not be obtained by a simpler linear-response approach. Finally, this effect is not observed on a three-dimensional lattice, on which the fluctuations are normal and grow linearly with time.

In confined geometries, we showed that superdiffusion is actually a long-lived transient regime, which crosses over to an ultimate diffusive regime after a time $t_\times \sim 1/{\rho_0}^2$ which diverges when the vacancy density goes to zero. This implies that the initial superdiffusive regime may be long-lived if the density of vacancies is very small. We will give a more physical insight into this observation with a simplified description presented in Chapter 7. Technically, the ultimate regime of the system can be obtained by taking the limit $t \to \infty$ for a fixed value of the vacancy density ρ_0. Indeed, we show that the two limits $\rho_0 \to 0$ and $t \to \infty$ cannot be inverted. The physical origin of this phenomenon is the following: between two successive visits of a vacancy to the TP position, the TP moves due to its interactions with other vacancies, so that the random walk of a vacancy is actually biased, with a bias that vanishes when the density of vacancies goes to zero. We finally obtain explicitly the expression of the diffusion coefficient in the ultimate regime. Surprisingly, this diffusion coefficient is independent of the vacancy density ρ_0 in quasi-one-dimensional lattices. Finally, we obtained the expression of the scaling functions describing both regimes, by taking simultaneously the limits $\rho_0 \to 0$ and $t \to \infty$ with the scaling $t \sim 1/{\rho_0}^2$.

The emergence of confinement-induced superdiffusion in a minimal model a driven TP in a hardcore lattice gas suggests that this effect is not restricted to the glassy systems presented in the introduction of this Chapter [118, 104], and could be a generic feature of driven dynamics in confined crowded systems.

The robustness of the results we obtained on the lattice description was tested on two types of off-lattice systems with Molecular Dynamics simulations:

- a colloidal fluid (CF) of identical particles interacting *via* a purely repulsive potential (collaboration with Adam Law and Dipanjan Chakraborty, Universität Stuttgart).
- a dissipative granular fluid (GF) (collaboration with Anna Bodrova, Moscow State University).

In both algorithms, a biased intruder is submitted to an external force. Its fluctuations as a function of time are computed for different values of the parameters: applied force f and stripe width L for the CF; applied force f, stripe width L and restitution parameter e for the GF. For both systems, a value of the density close to the packing fraction is chosen.

In order to collapse all data, we need to rescale the variance $\kappa_1^{(2)}(t)$. It will be shown in Chapter 5 that the velocity of the TP is proportional to the vacancy density and to the coefficient a_0, which contains the force-dependence of the variance. A good function to plot is then $L\kappa_1^{(2)}(t)/v^2$, where the velocity v is also computed from the simulations. The results are presented on Fig. 4.10.

This validates the time, width, and driving force dependences that feature in our analytical expression also for off-lattice systems. This suggests that superdiffusion may be a generic property of a driven TP in a confined environment. With future work and collaborations, we could test the robustness of this observation in other numerical simulations involving more complex interactions, or in experimental realizations.

In the next Chapter, we study the behavior of the mean position of the TP. We show that its behavior also displays an anomaly in confined geometries.

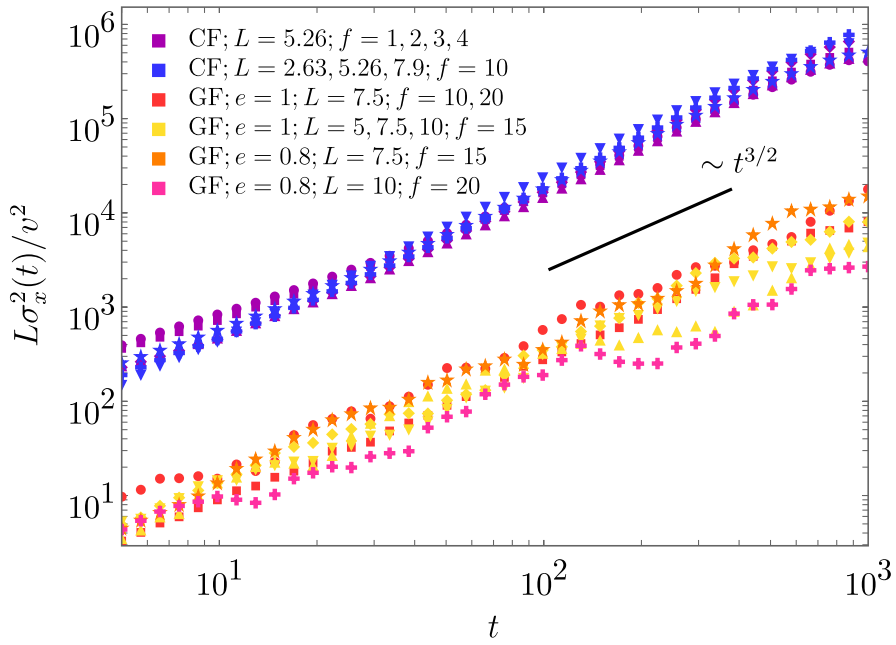

Figure 4.10: Rescaled variance $L\kappa_1^{(2)}(t)/v^2$ as a function of time obtained from off-lattice simulations for different widths of stripes L and forces f. CF: molecular dynamics of colloidal fluids in confined strip-like geometries. GF: simulations of dense monodisperse granular fluid in confined strip-like geometries; e stands for the restitution parameter. The black line is $t^{3/2}$.

CHAPTER 5

Velocity anomaly in quasi-one-dimensional geometries

Contents

We studied in Chapter 4 the fluctuations of the position of a biased TP in a dense lattice gas. It was found that in 2D and quasi-1D systems such as stripes or capillaries, there exists a long-lived superdiffusion crossing over to a diffusive behavior after a time scaling as $1/{\rho_0}^2$. We show that in confined geometries not only the variance but already the mean of the TP displacement displays a striking anomaly. In quasi-1D systems, we find that the temporal evolution of the TP velocity consists of two distinct, clearly separated regimes: after a short transient the velocity attains first a long-lived "high" constant value which persists up to times of order of $1/{\rho_0}^2$ and then rather abruptly drops to a terminal "low" constant value.

Results from this Chapter were published in [P5].

5.1 Introduction

In the previous Chapter a superdiffusive growth of the variance of a biased TP in a crowded environment was established analytically in a simple discrete model. In this model, the tracer performs a random walk biased by an external force, in a dense bath of particles performing symmetric random walks constrained by hard-core interactions. In the high-density limit, the motion of the TP is mediated by successive visits of vacancies whose density is denoted $\rho_0 = 1 - \rho$, where ρ is the density of bath particles. It was found that in 2D and quasi-1D systems such as stripes or capillaries there exists a long-lived superdiffusion, crossing-over to a diffusive behavior after a time $t_\times \sim 1/{\rho_0}^2$. The complete time evolution of the variance was found to display a scaling behavior as a function of the scaled variable ${\rho_0}^2 t$ (see Fig. 4.8).

On the basis of such model of a driven tracer in a dense lattice gas, we show here that the behavior of the *mean* itself of the TP position displays a striking anomaly in confined geometries, which apparently has been left aside up to now. This unexpected behavior, obtained from Monte-Carlo numerical

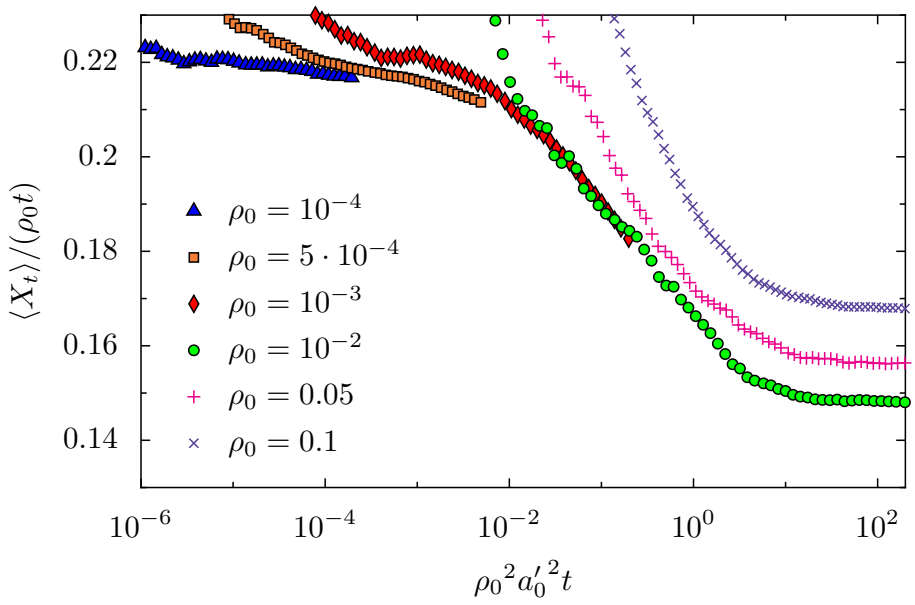

Figure 5.1: Rescaled mean position (velocity) $\langle X_t \rangle / (\rho_0 t)$ as a function of $\tau = a_0'{}^2 \rho_0{}^2 t$ obtained from numerical simulations of tracer diffusion on a 2D stripe of width $L = 3$ with different densities. The external force is $F = \infty$, which implies $p_1 = 1$ and $p_{\mu \neq 1} = 0$.

simulations in a quasi-1D stripe, is plotted in Fig. 5.1 for several vacancy densities ρ_0, as a function of the rescaled variable $\tau = a_0'{}^2 \rho_0{}^2 t$, suggested by the scaling behavior of the variance (Section 4.7.5). A scaled form of the mean-position is found which, very surprisingly, after a long-lived plateau drops to a lower ultimate value. The transition from the "high" velocity to the ultimate regime of "low" velocity takes place at a time scale of the order of the cross-over time $t_\times \sim 1/\rho_0{}^2$ involved in the time evolution of the variance, suggesting that the anomaly of the variance and that of the mean could be linked. In this Chapter, we (i) calculate analytically the mean position of the TP in quasi-1D systems like stripes and capillaries in the dense limit $\rho_0 \to 0$, (ii) quantitatively account for the intriguing velocity anomaly reported above numerically and (iii) show that such velocity anomaly occurs only in quasi-1D systems in contrast to superdiffusion which is observed in both quasi-1D and 2D systems, revealing that the velocity anomaly and superdiffusion are not controlled by the same criteria.

5.2 Quasi-one-dimensional geometries

5.2.1 Stripe-like geometry

In order to compute the mean position of the TP (i.e. the first cumulant of its distribution) in the high-density limit, we start from the general expression of the cumulants (2.54) established in Chapter 2 in order to obtain

$$\lim_{\rho_0 \to 0} \frac{\widehat{\kappa}_1^{(1)}(\xi)}{\rho_0} = \mathrm{i} \left. \frac{\partial \widehat{\Omega}(k_1; \xi)}{\partial k_1} \right|_{k_1 = 0}, \tag{5.1}$$

where the first cumulant $\kappa_1^{(1)}(t)$ is the mean position of the TP in the direction of the bias $\langle X_t \rangle$, and where the function $\widehat{\Omega}(k_1;\xi)$ is defined in (2.55). In the particular case of a two-dimensional stripe-like geometry, we use the general expression of $\widehat{\Omega}(k_1;\xi)$ (4.23) as well as the symmetry relations (4.27), (4.28) and (4.29) in order to write the first cumulant as a function of the quantities previously defined:

$$\lim_{\rho_0\to 0} \frac{\widehat{\kappa}_1^{(1)}(\xi)}{\rho_0} = \frac{1}{1-\xi}\frac{1}{\mathcal{D}_0+\mathcal{D}_1+\mathcal{D}_{-1}}\left\{(F_1'-F_{-1}')(\mathcal{D}_0+\mathcal{D}_1+\mathcal{D}_{-1})+F_1'[\sigma_1(\boldsymbol{e}_{-1})-\sigma_{-1}(\boldsymbol{e}_{-1})]\right.$$
$$\left.+F_{-1}'[\sigma_1(\boldsymbol{e}_1)-\sigma_{-1}(\boldsymbol{e}_1)]+2F_2'[\sigma_1(\boldsymbol{e}_2)-\sigma_{-1}(\boldsymbol{e}_2)]\right\}. \tag{5.2}$$

We recall that the quantities $\mathcal{D}_0$, $\mathcal{D}_{\pm 1}$ and $\sigma_{\pm 1}(\boldsymbol{e}_\nu)$, which were defined in Section 4.3.1, only depend on the conditional first-passage time densities (FPTD) $\widehat{F}^*$ associated to the random walk of a vacancy, which are determined using the methods presented in Section 4.3.2. The computation of the conditional FPTD then allows us to find the expansion of the quantities $\sigma_{\pm 1}(\boldsymbol{e}_\nu)$, $\mathcal{D}_0+\mathcal{D}_1+\mathcal{D}_{-1}$ and F_ν' involved in the expression of the first cumulant (5.2). These expansions are given in Appendix E (Section E.1). Using these expansions in the expression of the first cumulant (5.2), we finally obtain at leading order

$$\lim_{\rho_0\to 0} \frac{\widehat{\kappa}_1^{(1)}(\xi)}{\rho_0} \underset{\xi\to 1}{\sim} \frac{1}{(1-\xi)^2}\frac{p_1-p_{-1}}{1+\frac{4\alpha}{4-\alpha}(p_1+p_{-1})}. \tag{5.3}$$

Using a Tauberian theorem, one obtains

$$\boxed{\lim_{\rho_0\to 0} \frac{\kappa_1^{(1)}(t)}{\rho_0} \underset{t\to\infty}{\sim} a_0 t,} \tag{5.4}$$

where we defined again

$$a_0 \equiv \frac{p_1-p_{-1}}{1+\frac{4\alpha}{4-\alpha}(p_1+p_{-1})}, \tag{5.5}$$

and where α is a function of the width of the stripe only and is defined by (4.55).

In order to describe the ultimate regime corresponding to the low velocity, we now need to analyze the regime where the large time limit is taken first and the small density limit next, in contrast to the regime considered in (5.4). The formalism described above can actually be extended to analyze this second limit. The key difference with the previous case is that for a fixed small ρ_0 the random walk performed by the vacancy between two successive visits of the lattice site occupied by the TP is a biased random walk in the reference frame of the TP, due to the interactions of the TP with the other vacancies. The method presented above can then be applied, provided that the FPTD F^* computed for the symmetric walk of a vacancy are replaced by the FPTD $\mathcal{F}^*$ corresponding to the random walk of a vacancy undergoing a bias in the direction opposite to the TP displacement. This bias, denoted by ε, vanishes in the limit $\rho_0 \to 0$. Its explicit expression is not needed and will be obtained self-consistently. The method to compute the FPTD $\mathcal{F}^*$ was given in Section 4.7.2. The expansions of the quantities $\sigma_{\pm 1}(\boldsymbol{e}_\nu)$, $\mathcal{D}_0+\mathcal{D}_1+\mathcal{D}_{-1}$ and F_ν' involved in the expression of the first cumulant (5.2) are given in Appendix E (Section E.2). Using these expansions in the expression of the first cumulant (5.2), we obtain at leading order

$$\lim_{\xi\to 1}\left[(1-\xi)^2\widehat{\kappa}_1^{(1)}(\xi)\right] \underset{\rho_0\to 0}{\sim} \rho_0 a_0' \tag{5.6}$$

where

$$a_0' = \frac{p_1 - p_{-1}}{1 + \frac{4\alpha}{4-\alpha}(p_1 + p_{-1}) + \frac{16}{L(4-\alpha)}(p_1 - p_{-1})}. \tag{5.7}$$

Finally, using a Tauberian theorem, we get

$$\boxed{\lim_{t\to\infty} \frac{\kappa_1^{(1)}(t)}{t} \underset{\rho_0\to 0}{\sim} \rho_0 a_0'} \tag{5.8}$$

A few comments follow from these calculations:

- the mean position of the TP grows linearly with time in both regimes. This is in contrast with the situation observed in the one-dimensional geometry, in which the mean position of the TP was found to grow as $\sqrt{t}$, i.e. sublinearly.
- the relation (5.8) indicates that in the ultimate regime reached by the TP, its velocity is $\rho_0 a_0'$. This gives in a self-consistent way the value of the bias $\varepsilon = \rho_0 a_0'$ undergone by a vacancy between two successive visits to the location of the TP.
- we notice that $a_0' < a_0$. Indeed, it can be checked numerically that α, which is a function of L only (4.55), is smaller than 4 for any value of $L \geq 2$. This implies $\frac{16}{L(4-\alpha)}(p_1 - p_{-1}) > 0$ and therefore $a_0' < a_0$. The ultimate velocity $\rho_0 a_0'$ is then always lower than the first velocity $\rho_0 a_0$.
- we define the velocity jump Δv as

$$\Delta v \equiv \rho_0(a_0 - a_0') \tag{5.9}$$

$$= \frac{\frac{16(p_1-p_{-1})^2}{L(4-\alpha)}}{\left(1 + \frac{4\alpha}{4-\alpha}(p_1 + p_{-1})\right)^2 + \frac{64\alpha}{L(4-\alpha)^2}({p_1}^2 - {p_{-1}}^2)} \tag{5.10}$$

With the usual choice of the jump probabilities $p_{\pm 1} \propto \exp(\pm F/2)$, we find in the small-force limit:

$$\Delta v \underset{F\to 0}{=} \frac{1}{L}\frac{4-\alpha}{(4+\alpha)^2}F^2 + \mathcal{O}(F^3). \tag{5.11}$$

The velocity jump then vanishes when the applied force goes to zero, but proportionally to F^2. It means that this anomaly emerges beyond the linear response of the system.

Finally, we are interested in the joint limit where $\rho_0 \to 0$ and $t \to \infty$ simultaneously. We use the scaling $t \sim 1/{\rho_0}^2$ which was suggested by the study of the variance of the TP (see Section 4.7.5). The expansions in the joint limit of the quantities $\sigma_{\pm 1}(\boldsymbol{e}_\nu)$, $\mathcal{D}_0 + \mathcal{D}_1 + \mathcal{D}_{-1}$ and F_ν' involved in the expression of the first cumulant (5.2) are given in Appendix E (Section E.3). Using these expansions in the expression of the first cumulant (5.2), we obtain at leading order

$$\widehat{\kappa}_1^{(1)}(\xi) \underset{\substack{\varepsilon\sim\sqrt{1-\xi}\\ \xi\to 1}}{\sim} \frac{\rho_0}{(1-\xi)^2} \frac{(p_1 - p_{-1})L\sqrt{1 + \frac{1-\xi}{\varepsilon^2}}}{L\sqrt{1 + \frac{1-\xi}{\varepsilon^2}} + \frac{16}{4-\alpha}(p_1 - p_{-1}) + \frac{4\alpha}{4-\alpha}L\sqrt{1 + \frac{1-\xi}{\varepsilon^2}}(p_1 + p_{-1})}. \tag{5.12}$$

Recalling the definitions of a_0 (5.5) one gets the expression:

$$\widehat{\kappa}_1^{(1)}(\xi) \underset{\substack{\varepsilon\sim\sqrt{1-\xi}\\ \xi\to 1}}{\sim} \frac{\rho_0 a_0}{(1-\xi)^2} \frac{\sqrt{1+\frac{1-\xi}{\varepsilon^2}}}{\sqrt{1+\frac{1-\xi}{\varepsilon^2}}+\frac{16}{L}\frac{a_0}{4-\alpha}}. \tag{5.13}$$

The time-dependence of the first cumulant can be retrieved by replacing the discrete Laplace variable ξ by $1-s$, where s is a continuous Laplace variable. With usual inverse Laplace transforms, we obtain the dependance of the quantity $\kappa_1^{(1)}(t)/(\rho_0 t)$ in terms of a rescaled variable $\tau = {a_0'}^2 {\rho_0}^2 t$:

$$\begin{aligned}\frac{\langle X_t\rangle}{\rho_0 t} &\sim a_0\Big\{\frac{b}{b^2-1}\left[\mathrm{erf}(\sqrt{\tau})+\frac{\mathrm{e}^{-\tau}}{\sqrt{\pi\tau}}\right]+\frac{1}{\tau}\left(\frac{b}{b^2-1}\right)^2\left[\mathrm{e}^{(b^2-1)\tau}[1-\mathrm{erf}(b\sqrt{\tau})]-1\right]\\ &\quad +\frac{b}{2}\frac{b^2+1}{(b^2-1)^2}\frac{\mathrm{erf}(\sqrt{\tau})}{\tau}-\frac{1}{b^2-1}\Big\} \qquad (5.14)\\ &\equiv h(\tau) \qquad (5.15)\end{aligned}$$

where we defined $b = a_0/a_0' - 1$. We verify that this scaling function gives the right limit behaviors:

1. in the case where the limit $\rho_0 \to 0$ is taken first (i.e. when τ goes to 0), we get

$$\lim_{\tau\to 0} h(\tau) = a_0, \tag{5.16}$$

   which leads to $\langle X_t\rangle \sim \rho_0 a_0 t$ and which corresponds to (5.4).

2. in the case where the limit $t \to \infty$ is taken first (i.e. when τ goes to ∞), we get

$$\lim_{\tau\to\infty} h(\tau) = \frac{a_0}{1+b} = a_0', \tag{5.17}$$

   which leads to $\langle X_t\rangle \sim \rho_0 a_0' t$ and which corresponds to (5.8).

This scaling function is compared to results from numerical simulations, for two different values of the bias (Figs. 5.2 and 5.3). Note that the theoretical low value is reached only in the limit $\rho_0 \to 0$, which explains the observed discrepancy between the theoretical and numerical values, that decreases when $\rho_0 \to 0$.

5.2.2 Capillary-like geometry

We now extend the calculation presented in the case of stripe-like geometries to the case of capillary-like geometries. Starting again from the general expression of the first cumulant (5.1), and with the general expression of $\widehat{\Omega}(k_1;\xi)$ (2.55), we get

$$\begin{aligned}\lim_{\rho_0\to 0}\frac{\widehat{\kappa}_1^{(1)}(\xi)}{\rho_0} &= \frac{1}{1-\xi}\frac{1}{\mathcal{D}_0+\mathcal{D}_1+\mathcal{D}_{-1}}\Big\{(F_1'-F_{-1}')(\mathcal{D}_0+\mathcal{D}_1+\mathcal{D}_{-1})+F_1'[\sigma_1(\boldsymbol{e}_{-1})-\sigma_{-1}(\boldsymbol{e}_{-1})]\\ &\quad +F_{-1}'[\sigma_1(\boldsymbol{e}_1)-\sigma_{-1}(\boldsymbol{e}_1)]+4F_2'[\sigma_1(\boldsymbol{e}_2)-\sigma_{-1}(\boldsymbol{e}_2)]\Big\}, \qquad (5.18)\end{aligned}$$

where the quantities $\sigma_{\pm 1}(\boldsymbol{e}_\nu)$, $\mathcal{D}_0+\mathcal{D}_1+\mathcal{D}_{-1}$ and F_ν' are defined in Appendix D (Section D.1). These quantities are expressed in terms of the FPTD F^*, whose computation in the case of capillary-like

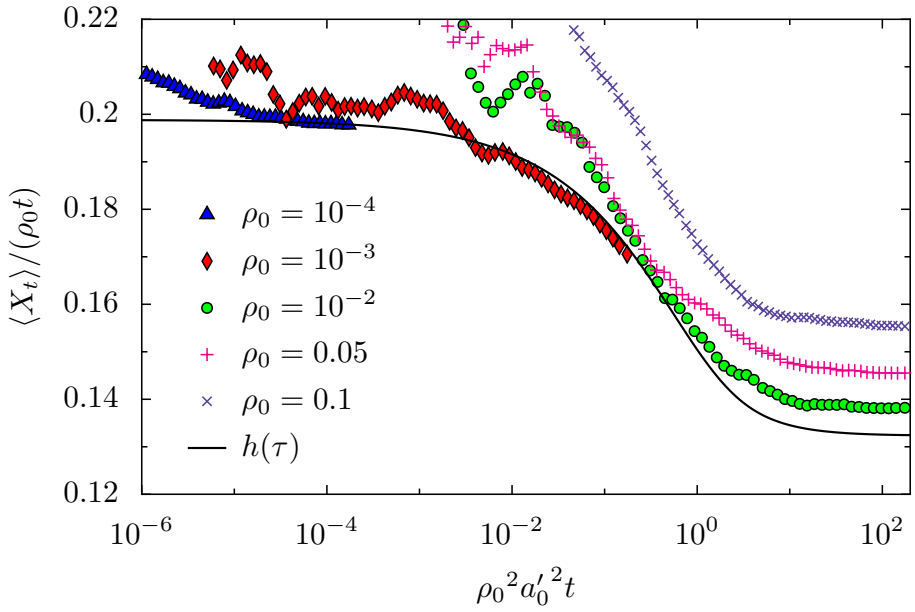

Figure 5.2: Rescaled mean position (velocity) $\langle X_t\rangle/(\rho_0 t)$ as a function of $\tau = {a'_0}^2{\rho_0}^2 t$ obtained from numerical simulations of tracer diffusion on a 2D stripe of width $L = 3$ with different densities of vacancies. The external force is $F = 4$, and the jump probabilities of the TP are $p_\mu \propto \mathrm{e}^{\frac{1}{2}\boldsymbol{F}\cdot\boldsymbol{e}_\mu}$. The black line is the scaling function from (5.14).

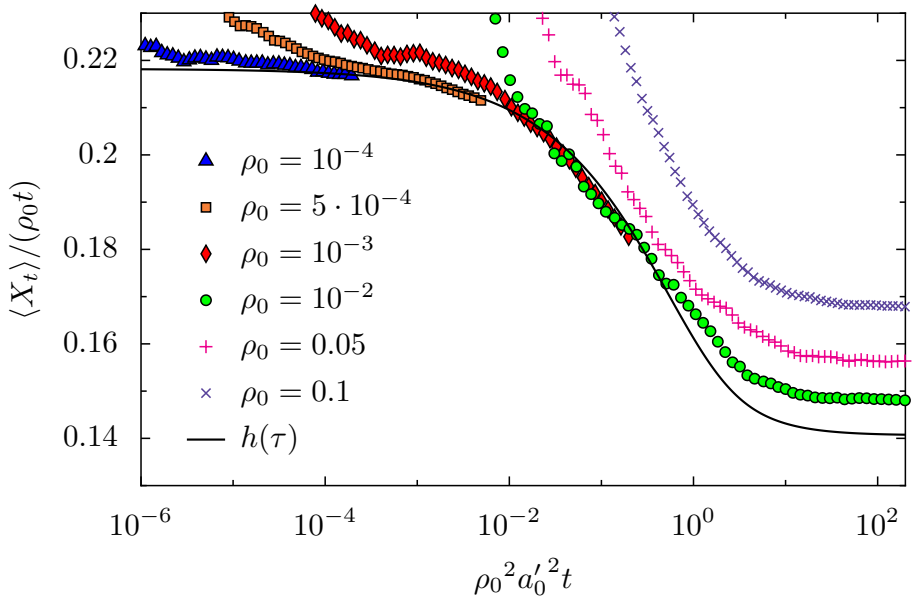

Figure 5.3: Rescaled mean position (velocity) $\langle X_t\rangle/(\rho_0 t)$ as a function of $\tau = {a'_0}^2{\rho_0}^2 t$ obtained from numerical simulations of tracer diffusion on a 2D stripe of width $L = 3$ with different densities of vacancies. The external force is $F = \infty$, which implies $p_1 = 1$ and $p_\mu = 0$ for $\mu \neq 1$. The black line is the scaling function from (5.14).

lattices is presented in Section 4.4.3. Recalling the expansions of the intermediate quantities $\sigma_{\pm 1}(\boldsymbol{e}_\nu)$, $\mathcal{D}_0 + \mathcal{D}_1 + \mathcal{D}_{-1}$ and F'_ν from Appendix F (Section F.1), we obtain the expression of the first cumulant in the limit where $\rho_0 \to 0$ is taken first:

$$\boxed{\lim_{\rho_0 \to 0} \frac{\kappa_1^{(1)}(t)}{\rho_0} \underset{t \to \infty}{\sim} a_0 t.} \tag{5.19}$$

where

$$a_0 \equiv \frac{p_1 - p_{-1}}{1 + \frac{6\alpha}{6-\alpha}(p_1 + p_{-1})}, \tag{5.20}$$

and where α is a function of the width of the capillary only and is defined by (4.86).

In order to obtain the ultimate regime, the FPTD associated to the random walk of vacancy must be replaced by the FPTD $\mathcal{F}^*$, introduced in Section 4.8.1. We perform the computation in the particular case where the TP is directed, i.e. where it can only jump direction in the direction of the bias. Using the expansions of the intermediate quantities $\sigma_{\pm 1}(\boldsymbol{e}_\nu)$, $\mathcal{D}_0 + \mathcal{D}_1 + \mathcal{D}_{-1}$ and F'_ν involved in the expression of the first cumulant (5.18), which are given in Appendix F (Section F.2) we obtain the expression of the second cumulant:

$$\boxed{\lim_{t \to \infty} \frac{\kappa_1^{(1)}(t)}{t} \underset{\rho_0 \to 0}{\sim} \rho_0 a'_0} \tag{5.21}$$

where

$$a'_0 = \frac{1}{1 + \frac{6\alpha}{6-\alpha} + \frac{36}{L^2(6-\alpha)}} \tag{5.22}$$

Finally, we extend the calculation presented in the case of a stripe-like geometry to study the joint limit where $\rho_0 \to 0$ and $t \to \infty$ simultaneously. We use the scaling $t \sim 1/{\rho_0}^2$ which was suggested by the study of the variance of the TP (see Section 4.8.3). The expansions in the joint limit of the quantities $\sigma_{\pm 1}(\boldsymbol{e}_\nu)$, $\mathcal{D}_0 + \mathcal{D}_1 + \mathcal{D}_{-1}$ and F'_ν involved in the expression of the first cumulant (5.18) are given in Appendix F (Section F.3). Using these expansions in the expression of the first cumulant (5.18), we finally obtain at leading order, and in the particular case of a biased TP,

$$\widehat{\kappa}_1^{(1)}(\xi) \underset{\substack{\varepsilon \sim \sqrt{1-\xi} \\ \xi \to 1}}{\sim} \frac{\rho_0}{(1-\xi)^2} \frac{L\sqrt{1 + \frac{1-\xi}{\varepsilon^2}}}{L^2\sqrt{1 + \frac{2}{3}\frac{1-\xi}{\varepsilon^2}} + \frac{36}{6-\alpha} + \frac{6\alpha}{6-\alpha} L^2 \sqrt{1 + \frac{2}{3}\frac{1-\xi}{\varepsilon^2}}} \tag{5.23}$$

Recalling the definitions of a_0 (5.20), one gets the expression:

$$\widehat{\kappa}_1^{(1)}(\xi) \underset{\substack{\varepsilon \sim \sqrt{1-\xi} \\ \xi \to 1}}{\sim} \frac{\rho_0 a_0}{(1-\xi)^2} \frac{\sqrt{1 + \frac{2}{3}\frac{1-\xi}{\varepsilon^2}}}{\sqrt{1 + \frac{2}{3}\frac{1-\xi}{\varepsilon^2}} + \frac{36}{L^2}\frac{a_0}{6-\alpha}} \tag{5.24}$$

The time-dependence of the first cumulant can be retrieved by replacing the discrete Laplace variable ξ by $1 - s$, where s is the usual continuous Laplace variable. Using usual inverse Laplace transforms, we obtain the dependance of the quantity $\langle X_t \rangle / (\rho_0 t)$ in terms of a rescaled variable $\tau = {a'_0}^2 {\rho_0}^2 t$ and of the function h defined in the case of stripe-like geometry (5.14):

$$\frac{\langle X_t \rangle}{\rho_0 t} \sim h\left(\frac{3}{2}\tau\right) \tag{5.25}$$

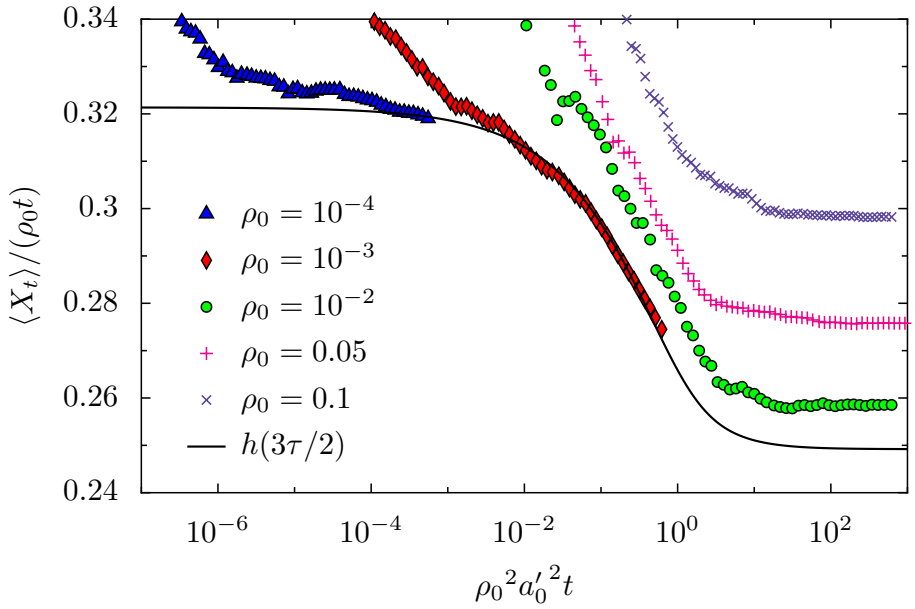

Figure 5.4: Rescaled mean position (velocity) $\langle X_t \rangle / (\rho_0 t)$ as a function of $\tau = a_0'^2 \rho_0^2 t$ obtained from numerical simulations of tracer diffusion on a 3D capillary of width $L = 3$ with different densities. The external force is $F = \infty$, which implies $p_1 = 1$ and $p_{\mu \neq 1} = 0$. The black line is the scaling function from (5.14).

Recalling the limit behaviors of h:

$$\lim_{\tau \to 0} h(\tau) = a_0, \tag{5.26}$$

$$\lim_{\tau \to \infty} h(\tau) = a_0', \tag{5.27}$$

we show that the scaling function $h\left(\frac{3}{2}\tau\right)$ allows to retrieve the limiting behaviors of the first cumulant (5.19) and (5.21).

5.3 Two-dimensional lattice

We finally study the case of a two-dimensional lattice. In the limit where $\rho_0 \to 0$ is taken first, the mean position of the TP may be computed from the expression (5.2). The intermediate quantities $\sigma_{\pm 1}(\boldsymbol{e}_\nu)$, $\mathcal{D}_0 + \mathcal{D}_1 + \mathcal{D}_{-1}$ and F'_ν involved in the expression of the first cumulant (5.2) are given in Appendix G (Section G.1). Using these expansions in the expression of the first cumulant (5.2), and using a Tauberian theorem, we finally obtain

$$\lim_{\rho_0 \to 0} \frac{\kappa_1^{(1)}(t)}{\rho_0} \underset{t \to \infty}{\sim} a_0 t, \tag{5.28}$$

where

$$a_0 \equiv \frac{p_1 - p_{-1}}{1 + \frac{4\alpha}{4-\alpha}(p_1 + p_{-1})}, \tag{5.29}$$

and

$$\alpha = 4 - \frac{8}{\pi}. \tag{5.30}$$

The ultimate regime is obtained by considering the new FPTD corresponding to the biased random walk of a vacancy. Using the expansions of the quantities $\sigma_{\pm 1}(\boldsymbol{e}_\nu)$, $\mathcal{D}_0 + \mathcal{D}_1 + \mathcal{D}_{-1}$ and F'_ν in the limit where $t \to \infty$ is taken first (Appendix G, Section G.2), we obtain

$$\lim_{t\to\infty} \frac{\kappa_1^{(1)}(t)}{t} \underset{\rho_0\to 0}{\sim} \rho_0 a_0. \tag{5.31}$$

These results show that the limits $\rho_0 \to 0$ and $t \to \infty$ can be inverted in the computation of the TP mean position on a two-dimensional lattice. This implies that there is no velocity anomaly in 2D, and that the mean position of the TP scales as $\rho_0 a_0 t$. Results from numerical simulations confirming the absence of a velocity jump in this geometry are given on Fig. 5.5. Recalling the expression of the velocity jump on a two-dimensional stripe (5.11), we see explicitly that it vanishes when $L \to \infty$, which is consistent with the results obtained by the exact treatment of the two-dimensional lattice.

This also shows that the emergence of superdiffusive fluctuations and of the velocity anomaly are not controlled by the same criteria. Mathematically, the criterion for superdiffusion to occur is that the limits $\varepsilon \to 0$ and $\xi \to 1$ of the biased propagators $\widehat{\mathcal{P}}(\boldsymbol{r}|\boldsymbol{r}_0;\xi,\varepsilon)$ do not commute, which is the case in 2D and quasi-1D systems (see Appendices A, B and C). The condition for velocity anomaly is in contrast that the limits $\varepsilon \to 0$ and $\xi \to 1$ of $\widehat{\mathcal{P}}(\boldsymbol{0}|\boldsymbol{0};\xi,\varepsilon) - \widehat{\mathcal{P}}(2\boldsymbol{e}_1|\boldsymbol{0};\xi,\varepsilon)$ do not commute, which is in fact more constraining, and is satisfied in quasi-1D but not in 2D systems. Parenthetically, we note that this non-commutation of the limits for $\widehat{\mathcal{P}}(\boldsymbol{0}|\boldsymbol{0};\xi,\varepsilon) - \widehat{\mathcal{P}}(2\boldsymbol{e}_1|\boldsymbol{0};\xi,\varepsilon)$ is a general property which holds for any biased random-walk in quasi-1D systems, and could potentially have implications in other contexts.

5.4 Conclusion

In conclusion, on the basis of a simple model of a driven diffusive tracer in a crowded environment, our analysis has revealed the emergence of a striking velocity anomaly in confined geometries. Namely, we have shown that in quasi-1D systems such as stripes or capillaries, the TP velocity displays a long-lived plateau before ultimately dropping to a lower value. We have developed an analytical solution that quantitatively accounts for this intriguing behavior. This anomaly is also shown to emerge beyond the linear response of the system. A subtle point, quantified by the expression (5.11) is that this velocity jump is actually strictly equal to zero in infinite 2D systems. In particular, velocity anomaly occurs only in quasi-1D systems, in contrast with the superdiffusive growth of the variance of the TP position, which is observed in both quasi-1D and 2D systems.

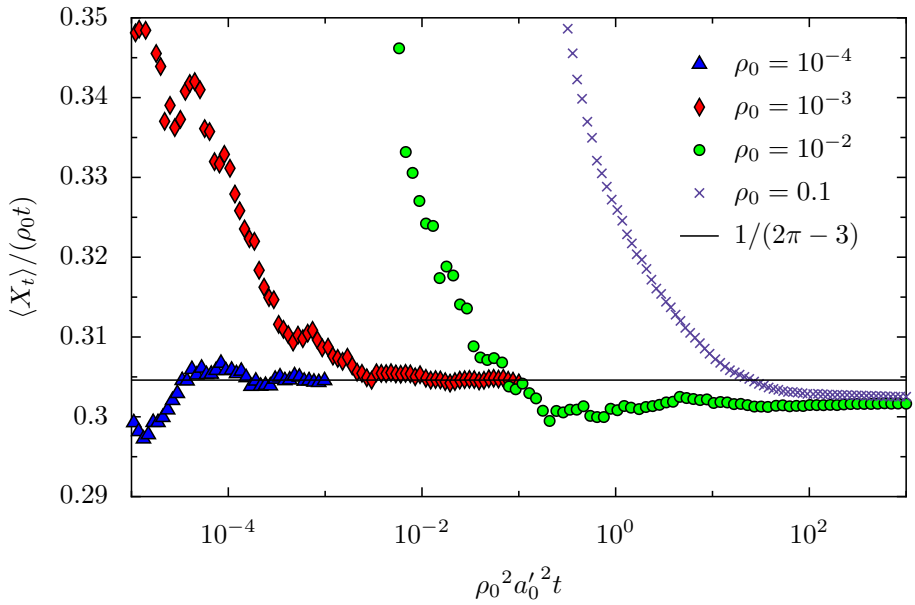

Figure 5.5: Rescaled mean position (velocity) $\langle X_t \rangle / (\rho_0 t)$ as a function of $\tau = {a'_0}^2 {\rho_0}^2 t$ obtained from numerical simulations of tracer diffusion on a 2D lattice with different densities. The external force is $F = \infty$, which implies $p_1 = 1$ and $p_\mu = 0$ for $\mu \neq 1$. In this situation, with (5.29), we obtain $\langle X_t \rangle \sim \frac{4-\alpha}{4+3\alpha} \rho_0 t$, and, with the expression of α in the case of a 2D lattice, we get $\langle X_t \rangle \sim \frac{\rho_0 t}{2\pi - 3}$. The value of $1/(2\pi - 3)$ is represented by the black line.

CHAPTER 6

Universal formulae for the cumulants

Contents

In the previous Chapters, we obtained the expressions of the mean and fluctuations of the position of a biased TP in a hardcore lattice gas, in different geometries. These expressions only involve the propagators associated to simple random walks on the considered structures. Although the behavior of the TP is strongly affected by the geometry of the lattice, we show in this Chapter that there exist general expressions of the first cumulants of the position of the TP that hold for every geometries. We extend these results to higher-order cumulants, and we also study the cumulants of the position of the TP in the direction perpendicular to the bias. Finally, these universal expressions are used to predict the behavior of the TP on fractal structures.

6.1 Introduction

In the previous Chapters, we studied the position of a biased TP in a hardcore lattice gas, in the limit where the density is very high. We first studied the fluctuations of the TP position, and showed that they had the following behaviors, depending on the lattice geometry:

- on a one-dimensional lattice, the fluctuations are shown to be subdiffusive and to grow as $\sqrt{t}$ (Chapter 3).

- in higher-dimensional confined geometries (quasi-one-dimensional lattices, two-dimensional infinite lattice), there exists a superdiffusive behavior of the TP position. On quasi-one-dimensional lattices, the fluctuations of the TP position grow as $t^{3/2}$. On a two-dimensional lattice, they grow as $t \ln t$. However, this superdiffusive regime is transient, and crosses over to an ultimate diffusive regime. The crossover time between the two regimes scales as $1/{\rho_0}^2$, which indicates that the initial superdiffusive regime is actually long-lived in the limit where $\rho_0 \to 0$ (Chapter 4).
- on a three-dimensional lattice, the fluctuations of the TP are normal and grow linearly with time (Chapter 4).

We also studied the mean position of the TP. In one dimension, it grows as $\sqrt{t}$, i.e. slower than linearly (Chapter 3). In higher-dimension lattices, the mean position of the TP always grows linearly with time, but there exists a velocity anomaly in quasi-one-dimensional lattices such as stripe-like and capillary-like geometries: before reaching its ultimate value, the velocity of the TP saturates to a higher long-lived plateau. The crossover to the final value occurs at a time that scales as $1/{\rho_0}^2$ (Chapter 5).

The mean of the position of the TP and its fluctuations then display a large variety of behaviors, depending on the considered geometry. In the high-density limit, the motion of the TP is mediated by the diffusion of the vacancies on the considered lattice, so that the properties of the random walk of the TP are closely related to that of the vacancies. In confined geometries (one-dimensional, quasi-one-dimensional, two-dimensional) the random walk (RW) of a vacancy is *recurrent*, i.e. the eventual return to its starting point is certain. On the contrary, on a three-dimensional lattice, the eventual return of a vacancy to its starting point is not certain, and its RW is *transient* [58]. In Chapter 4, we showed that the recurrence of the vacancy RW was a necessary condition to allow the emergence of superdiffusive fluctuations, but that it was not a sufficient condition. Indeed, on a one-dimensional lattice, the behavior of the TP is qualitatively different compared to quasi-one-dimensional and two-dimensional lattices. The main difference between these geometries is the fact that the quasi-one-dimensional and two-dimensional lattices are *looped*, which means that there exists several distinct paths linking two given vertices of the lattice, whereas the one-dimensional lattice is *non-looped* (or *tree-like*). Consequently, the presence of loops on the considered lattice also seems to control the behavior of the TP.

More precisely, the first step of the general method presented in Chapter 2 is the study of the situation where there is only one vacancy on the lattice, which depends on the lattice dimension. In one dimension, because of the tree-like structure of the lattice, the TP can only reach two distinct sites if it interacts with only one vacancy. In confined geometries (quasi-1D, 2D), the random walk of the vacancy is recurrent, and it can transport the TP to arbitrarily large distances. In three dimensions, the vacancy only visits the location of the TP a finite number of times, so that the TP can only travel to finite distances. The outcome of this single-vacancy problem is then strongly affected by the dimension of the lattice.

In this Chapter, we show that, in spite of these differences, the first cumulants (mean and fluctuations) of the TP position are described by universal formulae, which are expressed in terms of the propagators of symmetric nearest-neighbor RWs on the considered structure. These expressions are remarkably simple, and account for the variety of behaviors reminded above. These results are extended in several

other directions: (i) we study the higher-order cumulants of the TP position in the direction of the bias; (ii) we also study the cumulants of the TP position in the transverse direction; (iii) finally, these universal properties are used to predict the behavior of the TP on fractal lattices.

6.2 First cumulants of the TP position

6.2.1 Mean position of the TP

In Chapter 5, we obtained the following scaling function for the generating function associated to the mean position of the TP in the direction of the bias on quasi-one-dimensional lattices:

$$\widehat{\kappa}_1^{(1)}(\xi) \sim \frac{\rho_0 a_0}{(1-\xi)^2} \frac{1}{1+\frac{4d^2}{L^{d-1}}\frac{a_0}{2d-\alpha}\frac{1}{\sqrt{1+\frac{1-\xi}{\rho_0^2 {a'_0}^2}}}} \tag{6.1}$$

where the quantities a_0 and a'_0 are defined by

$$a_0 = \frac{p_1 - p_{-1}}{1+\frac{2d\alpha}{2d-\alpha}(p_1+p_{-1})}, \tag{6.2}$$

$$a'_0 = \frac{p_1 - p_{-1}}{1+\frac{2d\alpha}{2d-\alpha}(p_1+p_{-1})+\frac{4d^2}{L^{d-1}(2d-\alpha)}(p_1-p_{-1})}, \tag{6.3}$$

with

$$\alpha = \lim_{\xi\to 1}\left[\widehat{P}(\mathbf{0}|\mathbf{0};\xi) - \widehat{P}(2\boldsymbol{e}_1|\,\mathbf{0};\xi)\right], \tag{6.4}$$

where is $\widehat{P}(\boldsymbol{r}|\boldsymbol{r}_0;\xi)$ is the generating function associated to the propagator of a symmetric nearest-neighbor random walk starting from $\boldsymbol{r}_0$ and arriving at $\boldsymbol{r}$. The scaling function (6.1) describes both the long-lived transient regime and the ultimate regime reached by the mean position of the TP at large times. Mathematically, the existence of these two regimes rely on a non-interversion of the long-time ($\xi \to 1$) and low-vacancy-density ($\rho_0 \to 0$) limits:

- in the limit where $\rho_0 \to 0$ is taken first, we obtain from (6.1):

$$\lim_{\rho_0\to 0}\frac{\widehat{\kappa}_1^{(1)}(\xi)}{\rho_0} \sim \frac{a_0}{(1-\xi)^2}, \tag{6.5}$$

  and, using a Tauberian theorem,

$$\lim_{\rho_0\to 0}\frac{\kappa^{(1)}(t)}{\rho_0} \sim a_0 t \tag{6.6}$$

  which corresponds to the expression for the stripe-like (5.4) and capillary-like (5.19) geometries.

- the ultimate regime is obtained by taking first the limit $\xi \to 1$ for a given value of the vacancy density ρ_0. We obtain from (6.1):

$$\lim_{\xi\to 1}\left[(1-\xi)^2\widehat{\kappa}_1^{(1)}(\xi)\right] \underset{\rho_0\to 0}{\sim} \frac{\rho_0 a_0}{1+\frac{4d^2}{L^{d-1}}\frac{a_0}{2d-\alpha}} = \rho_0 a'_0, \tag{6.7}$$

and, using a Tauberian theorem,

$$\lim_{t\to\infty} \frac{\kappa_1^{(1)}(t)}{t} \underset{\rho_0\to 0}{\sim} \rho_0 a_0' \tag{6.8}$$

which corresponds to the expression for the stripe-like (5.8) and capillary-like (5.21) geometries.

In what follows, we show that this formula is general and also covers the cases of the two-dimensional, three-dimensional and one-dimensional lattices on which the behavior of the mean position of the TP is qualitatively different.

- The general equation (6.1) written in the case of a two-dimensional lattice (with $d = 2$ and in the limit $L \to \infty$) yields

$$\widehat{\kappa}^{(1)}(\xi) \sim \frac{\rho_0 a_0}{(1-\xi)^2}. \tag{6.9}$$

Consequently, we retrieve the fact that the limits $\rho_0 \to 0$ and $t \to \infty$ commute in the case of a two-dimensional lattice, so that there is no velocity anomaly in two dimensions. With a Tauberian theorem, we retrieve the expression (5.31) obtained in Section 5.3:

$$\lim_{\rho_0\to 0} \frac{\kappa_1^{(1)}(t)}{\rho_0} \underset{t\to\infty}{\sim} a_0 t. \tag{6.10}$$

- Using the properties associated to an infinite three-dimensional lattice presented in Section 4.6 as well as the general expression for the mean position of the TP in terms of the first-passage time densities of the vacancies random walk (5.18), one can show that there is no velocity anomaly in three-dimensions, and that the long-time limit of the first cumulant is also given by (6.10). The general expression (6.1) also holds for a three-dimensional lattice.

- We finally extend the general expression (6.1) to the case of a biased TP in a one-dimensional lattice gas. In this situation, the quantity α is not a constant at leading order in $(1-\xi)$. We replace it by the expansion of $\widehat{P}(\mathbf{0}|\mathbf{0};\xi) - \widehat{P}(2\boldsymbol{e}_1|\mathbf{0};\xi)$, given by the usual expressions of the propagators of a symmetric nearest-neighbor random walk on a one-dimensional lattice [58]:

$$\widehat{P}(\mathbf{0}|\mathbf{0};\xi) - \widehat{P}(2\boldsymbol{e}_1|\mathbf{0};\xi) = \frac{1}{\sqrt{1-\xi^2}} - \frac{1}{\sqrt{1-\xi^2}} \left(\frac{1-\sqrt{1-\xi^2}}{\xi} \right)^2 \tag{6.11}$$

$$\underset{\xi\to 1}{=} 2 - 2\sqrt{2}\sqrt{1-\xi} + \mathcal{O}(1-\xi) \tag{6.12}$$

The coefficients a_0 and a_0', defined through (6.2) and (6.3), then become functions of ξ, and at leading order in $(1-\xi)$, we get

$$a_0(\xi) \underset{\xi\to 1}{\sim} \frac{p_1 - p_{-1}}{\sqrt{2}} \sqrt{1-\xi}, \tag{6.13}$$

$$a_0'(\xi) \underset{\xi\to 1}{\sim} \frac{p_1 - p_{-1}}{2\sqrt{2}p_1} \sqrt{1-\xi}. \tag{6.14}$$

Finally, (6.1) yields

$$\lim_{\rho_0\to 0} \frac{\widehat{\kappa}_1^{(1)}(\xi)}{\rho_0} \underset{\xi\to 1}{\sim} \frac{p_1 - p_{-1}}{\sqrt{2}} \frac{1}{(1-\xi)^{3/2}}, \tag{6.15}$$

and, using a Tauberian theorem,

$$\lim_{\rho_0 \to 0} \frac{\kappa_1^{(1)}(t)}{\rho_0} \underset{t\to\infty}{\sim} (p_1 - p_{-1})\sqrt{\frac{2t}{\pi}}, \tag{6.16}$$

which is equivalent to the expression (3.22) obtain in Chapter 3.

Finally, we conclude that the behavior of the mean position of the TP, although it is strongly affected by the lattice dimension, is always given by the general relation (6.1), which is written in terms of the propagators associated to a symmetric nearest-neighbor random walk on the considered lattice.

6.2.2 Fluctuations of the position of the TP

The fluctuations of the position of the TP were studied in Chapter 4. In the cases of the stripe-like and capillary-like geometries, the calculation lead to the leading order term of the expansion of $\lim_{\rho_0\to 0} \widehat{\kappa}_1^{(2)}(\xi)$ in powers of $(1-\xi)$ (see equations (4.63) and (4.84)). In the case of the two-dimensional geometry, we obtained the leading order term and the first correction, given by (4.107). The calculation of the subdominant terms can be extended to obtain the first correction in the case of the quasi-one-dimensional geometries. We obtain the general formula

$$\boxed{\lim_{\rho_0\to 0} \frac{\widehat{\kappa}_1^{(2)}(\xi)}{\rho_0} \underset{\xi\to 1}{=} \frac{2{a_0}^2}{(1-\xi)^2}\left[G_0(\xi) + \left(G_1 + c + \frac{a_1}{2{a_0}^2} + 2c_1'\right) + \dots\right]} \tag{6.17}$$

where we define

$$a_1 = \frac{p_1 + p_{-1}}{p_1 - p_{-1}} a_0 \tag{6.18}$$

$$\alpha = \lim_{\xi\to 1}\left[\widehat{P}(\mathbf{0}|\mathbf{0};\xi) - \widehat{P}(2\boldsymbol{e}_1|\,\mathbf{0};\xi)\right] \tag{6.19}$$

$$\beta = \lim_{\xi\to 1}\left[\widehat{P}(\mathbf{0}|\mathbf{0};\xi) - \widehat{P}(\boldsymbol{e}_1|\,\mathbf{0};\xi)\right] \tag{6.20}$$

$$c = \frac{2[(2d^2 - 2d\beta + \beta^2)\alpha - 2d\beta^2]}{(\alpha - 2d)(\alpha + 2d - 4\beta)} + \frac{d+1}{2}\frac{1}{L^{2(d-1)}} \quad \text{for stripes and capillaries} \tag{6.21}$$

$$= \frac{2[(2d^2 - 2d + 1)\alpha - 2d]}{(\alpha - 2d)(\alpha + 2d - 4)} \quad \text{for infinitely extended lattices} \tag{6.22}$$

$$c_1' = \frac{4(\alpha(\alpha-4)(p_1 - p_{-1})^2 - 32(p_1 + p_{-1}))}{L^2(\alpha-4)(4\alpha(p_1+p_{-1}) - \alpha + 4)} \quad \text{for the stripe-like geometry} \tag{6.23}$$

$$= \frac{3}{2L^4}\frac{5\alpha - 24\alpha - 468}{(\alpha-6)(5\alpha+6)} \quad \text{for the capillary-like geometry and } p_1 = 1 \tag{6.24}$$

$$= 0 \quad \text{for infinitely extended lattices} \tag{6.25}$$

and where the coefficients $G_0(\xi)$ and G_1 are the first terms of the expansion of the propagator $\widehat{P}(\mathbf{0}|\mathbf{0};\xi)$ in the long-time limit ($\xi \to 1$):

$$\widehat{P}(\mathbf{0}|\mathbf{0};\xi) \underset{\xi\to 1}{=} G_0(\xi) + G_1 + o(1). \tag{6.26}$$

We recall the expressions of $G_0(\xi)$ and G_1 for the different lattices we considered in the following table (see Appendices A, B and C):

Lattice	$G_0(\xi)$	G_1
2D stripe	$\frac{1}{L\sqrt{1-\xi}}$	$S^{(2)}_{L,-1}$
3D capillary	$\frac{\sqrt{6}}{2L^2\sqrt{1-\xi}}$	$S^{(3)}_{L,0}$
2D infinite	$\frac{1}{\pi}\ln\frac{1}{1-\xi}$	$\frac{\ln 8}{\pi}$

Using the expression of $G_0(\xi)$ in (6.17) and using a Tauberian theorem to obtain the time-dependence of the fluctuations, we retrieve the fact that they grow superdiffusively in these geometries. The superdiffusive behavior of the TP was shown to be a long-lived transient regime which crosses over to regular diffusion after a time that scales as $1/{\rho_0}^2$. Mathematically, this ultimate regime is obtained by taking first the limit where $t \to \infty$ and ultimately the limit $\rho_0 \to 0$. The ultimate regime was shown to be diffusive, and the leading order term of the second cumulant in this regimes was given in Chapter 4 (see equations (4.168), (4.198) and (4.214)). These equations can be recast under the form

$$\boxed{\lim_{t\to\infty}\frac{\kappa_1^{(2)}(t)}{t}\underset{\rho_0\to 0}{\sim} 2\rho_0 {a_0'}^2 \mathcal{G}(\rho_0 a_0')} \tag{6.27}$$

where $\mathcal{G}(\varepsilon)$ is such that

$$\widehat{\mathcal{P}}(\mathbf{0}|\mathbf{0};\xi=1,\varepsilon)\underset{\varepsilon\to 0}{\sim}\mathcal{G}(\varepsilon), \tag{6.28}$$

where we denote by $\widehat{\mathcal{P}}(\boldsymbol{r}|\boldsymbol{r}_0;\xi,\varepsilon)$ the generating function of a nearest-neighbor random walk starting from $\boldsymbol{r}_0$ and arriving at $\boldsymbol{r}$, with the jump probabilities defined in Section 4.7.2.1. The expression of $\mathcal{G}(\varepsilon)$ in the different geometries we considered is given in the table below (see Appendices A, B and C).

Lattice	$\mathcal{G}(\varepsilon)$
2D stripe	$\frac{1}{L\varepsilon}$
3D capillary	$\frac{1}{L^2\varepsilon}$
2D infinite	$\frac{2}{\pi}\ln\frac{1}{\varepsilon}$

Note that the functions $\mathcal{G}$ and G_0 are related by

$$\mathcal{G}(\rho_0 a_0') = G_0\left(1-(\rho_0 a_0')^2\right). \tag{6.29}$$

In what follows, we show that the expression (6.17) is also valid to describe the fluctuations of the TP on the three-dimensional lattice (which was considered in Chapter 4, Section 4.6) and the one-dimensional lattice (which was considered in Chapter 3).

- On a three-dimensional lattice, the leading order term of the propagator $\widehat{P}(\mathbf{0}|\mathbf{0};\xi)$ was shown to be constant at leading order in $(1-\xi)$ and given by (4.124). The first correction G_1 then vanishes when $\xi \to 1$. The coefficient c_1' is taken equal to zero as the lattice in infinitely extended. Finally, specifying the general definition of c (6.22) to 3D, we get the expression

$$\lim_{\rho_0\to 0}\frac{\widehat{\kappa}_1^{(2)}(\xi)}{\rho_0}\underset{\xi\to 1}{=}\frac{2{a_0}^2}{(1-\xi)^2}\left[G_0+\frac{2(13\alpha-6)}{(\alpha+2)(\alpha-6)}+\frac{a_1}{2{a_0}^2}+\dots\right] \tag{6.30}$$

  which corresponds to the expression (4.126). The general expression for the generating function associated to the second cumulant (6.17) is also valid in the case of a three-dimensional lattice.

- Extending the calculation presented in Section 4.6, we studied the fluctuations of the TP on higher-dimensional infinite lattices. Using a computer algebra software, we can show that the formula (6.17) holds up to $d = 6$, with $c_1' = 0$ and c given by (6.22).
- On a one-dimensional lattice, the expansion of the propagator $\widehat{P}(\mathbf{0}|\mathbf{0};\xi)$ is given by

$$\widehat{P}(\mathbf{0}|\mathbf{0};\xi) = \frac{1}{\sqrt{1-\xi^2}}, \tag{6.31}$$

$$\underset{\xi\to 1}{=} \frac{1}{\sqrt{2}\sqrt{1-\xi}} + \frac{1}{2^{5/2}}\sqrt{1-\xi} + \mathcal{O}(1-\xi). \tag{6.32}$$

$$\tag{6.33}$$

Thus $G_0(\xi) = 1/\sqrt{2}\sqrt{1-\xi}$ and $G_1 = 0$. Finally, specifying the general definition of c (6.22) to 1D, we get the expression

$$\lim_{\rho_0\to 0} \frac{\widehat{\kappa}_1^{(2)}(\xi)}{\rho_0} \underset{\xi\to 1}{=} \frac{2{a_0}^2}{(1-\xi)^2}\left[G_0(\xi) + \frac{2}{\alpha(\xi)-2} + \frac{a_1}{2{a_0}^2} + \dots\right], \tag{6.34}$$

and using (6.11) and (6.13), we obtain at leading order in $\xi \to 1$

$$\lim_{\rho_0\to 0} \frac{\widehat{\kappa}_1^{(2)}(\xi)}{\rho_0} \underset{\xi\to 1}{=} \frac{1}{\sqrt{2}}\frac{1}{(1-\xi)^{3/2}} \tag{6.35}$$

which is equivalent to (3.23). The general expression for the generating function associated to the second cumulant (6.17) is also valid in the case of a one-dimensional lattice.

Finally, although the geometries we considered yield very different results, the quantity $\lim_{\rho_0\to 0}\widehat{\kappa}_1^{(2)}(\xi)/\rho_0$ is always given by the general relation (6.17). In the particular case where the limits $\rho_0 \to 0$ and $t \to \infty$ do not commute, the ultimate regime reached by the TP is given by (6.27).

In what follows, we give several extensions to the results presented in this Section: (i) we obtain the expression of the higher-order cumulants of the position of the TP in the direction of the bias (called the *longitudinal* direction hereafter) in the two situations where the random walk of a vacancy on the considered structure is *recurrent* (quasi-one-dimensional and two-dimensional lattices) and in the case where it is *transient* (three-dimensional lattice); (ii) we perform the same calculation to obtain the cumulants of the position of the TP in a direction which is perpendicular to that of the bias (called the *transverse* direction hereafter).

6.3 Higher-order cumulants in the longitudinal direction

6.3.1 Method

It was shown in Chapter 2 that the cumulants of the position of the TP can be obtained as the successive derivatives of the function $\widehat{\Omega}(\boldsymbol{k};\xi)$ (2.54), which is the generating function associated to $\Omega_t(\boldsymbol{k})$ related to the cumulant generating function of the position of the TP $\boldsymbol{X}_t$:

$$\Omega_t(\boldsymbol{k}) \underset{\rho_0\to 0}{\sim} -\frac{1}{\rho_0}\ln\left\langle \mathrm{e}^{\mathrm{i}\boldsymbol{k}\cdot\boldsymbol{X}_t}\right\rangle. \tag{6.36}$$

In Chapter 2, we showed that $\widehat{\Omega}(\boldsymbol{k};\xi)$ could be written in terms of the conditional first-passage time densities (FPTD) associated to the random walk of a vacancy $F_t^*(\mathbf{0}|\boldsymbol{e}_\mu|\boldsymbol{Y}_0)$ (probability to reach the origin for the first time at time t, starting from $\boldsymbol{Y}_0$ and being at site $\boldsymbol{e}_\mu$ at time $t-1$).

The cumulants of the position of the TP in the direction of the bias are obtained by derivating $\widehat{\Omega}(\boldsymbol{k};\xi)$ with respect to k_1 and by taking $\boldsymbol{k}=\mathbf{0}$ afterwards (see (2.54)). It then suffices to determine the dependence of $\widehat{\Omega}$ on the first component of the Fourier variable k_1. The explicit expression of $\widehat{\Omega}(k_1;\xi)$ in terms of the conditional FPTD is given in Appendix H (Section H.1). Starting from this expression, we study separately the cases of recurrent and transient lattices.

6.3.2 Recurrent lattices

We give here a general presentation of the procedure we followed to compute the higher-order cumulants. The calculation is given explicitly for the case of a stripe-like geometry in Appendix I (Section I.1.2), and can be extended to the cases of a three-dimensional capillary and of a two-dimensional lattice.

We start from the general expression of $\widehat{\Omega}(k_1;\xi)$ in terms of the conditional FPTD (H.11) (Appendix H). The latter are computed using the methods presented in Chapter 4 (see Section 4.3.2 for the specific case of the stripe-like geometry). Using a computer algebra software, we perform a joint expansion of $\widehat{\Omega}(k_1;\xi)$ in the variables k_1 and $(1-\xi)$ with an appropriate scaling between these variables. Using the relation between the cumulants and the function $\widehat{\Omega}(k_1;\xi)$

$$\lim_{\rho_0\to 0}\frac{\widehat{\kappa}_1^{(n)}(\xi)}{\rho_0}=-\frac{1}{\mathrm{i}^n}\left.\frac{\partial^n\widehat{\Omega}(k_1;\xi)}{\partial {k_1}^n}\right|_{k_1=0}, \tag{6.37}$$

we obtain the first two terms of $\lim_{\rho_0\to 0}\widehat{\kappa}_1^{(n)}(\xi)/\rho_0$ in its expansion in powers of $(1-\xi)$. Remarkably, this expansion takes the same form for the different geometries we consider, and is given by

$$\boxed{\lim_{\rho_0\to 0}\frac{\widehat{\kappa}_1^{(n)}(\xi)}{\rho_0}\underset{\xi\to 1}{=}\frac{a_0^n n!}{(1-\xi)^2}\left\{G_0(\xi)^{n-1}+(n-1)\left[G_1+\frac{a_1}{2a_0^2}+c+\frac{n}{n-1}c_1'\right]G_0(\xi)^{n-2}+\cdots\right\},} \tag{6.38}$$

where a_0, a_1, G_0, G_1, c and c_1' are defined as in Section 6.2. Note that the time-dependence of the n-th cumulant at leading order when $t\to\infty$ is not trivial. For instance, in quasi-one-dimensional geometries, as $G_0(\xi)\underset{\xi\to 1}{=}\mathcal{O}(1/\sqrt{1-\xi})$, the leading order term in (6.38) is of order $1/(1-\xi)^{(n+3)/2}$. A Tauberian theorem then allows to retrieve the time evolution of the n-th cumulant, which grows as $t^{(n+1)/2}$. If we consider the centered and reduced random variable $Z_t\equiv(X_t-\langle X_t\rangle)/\sqrt{\langle {X_t}^2\rangle-\langle X_t\rangle^2}$, we can show that the n-th moment of its distribution scales as $t^{1/2-n/4}$, so that all the moments of order greater than 2 vanish in the long-time limit. This shows that the rescaled variable Z_t is distributed accordingly to a Gaussian distribution in the long-time limit. This result cannot be expected *a priori*, provided that the biased TP drives the system in a nonequilibrium state.

As it was shown in Chapter 4, in these geometries, the limits $t\to\infty$ (i.e. $\xi\to 1$) and $\rho_0\to 0$ cannot be inverted. Indeed, between two successive visits of a vacancy to the TP location, the TP actually has a net displacement due to its interactions with other vacancies. The ultimate regime reached by the cumulants of the TP position (i.e. their long-time limit for a fixed value of ρ_0) is obtained by assuming that the vacancies do not perform symmetric random walks anymore, but undergo an effective bias equal

to the velocity of the TP, which depends on ρ_0 and vanishes when $\rho_0 \to 0$ (see Chapter 4, Section 4.7.2.1 for a more precise definition of the evolution rules of the vacancies).

In this situation, the expression of $\widehat{\Omega}(k_1;\xi)$ in terms of the conditional FPTD given in Appendix H (Section H.1) is still valid, but the conditional FPTD must be replaced by the ones computed with the new evolution rules of the vacancies. Consequently, $\widehat{\Omega}$ is now a function of k_1, ξ and ρ_0. Using the following relation between the cumulants and $\widehat{\Omega}(k_1;\xi)$:

$$\lim_{\xi\to 1}\left[(1-\xi)^2\widehat{\kappa}_1^{(n)}(\xi)\right] = -\frac{1}{\mathrm{i}^n}\frac{\partial^n}{\partial {k_1}^n}\lim_{\xi\to 1}\left[(1-\xi)^2\widehat{\Omega}_1(k_1;\xi,\rho_0)\right]\Big|_{k_1=0}, \tag{6.39}$$

we can obtain the ultimate behavior of the cumulants with the help of a computer algebra software. The details of the computation in the case of a stripe-like geometry are given in Appendix I (Section I.1.3). These can be extended straightforwardly to other geometries. We finally obtain

$$\boxed{\lim_{t\to\infty}\frac{\kappa_1^{(n)}(t)}{t} \underset{\rho_0\to 0}{\sim} \rho_0 n! {a_0'}^n \mathcal{G}(\rho_0 a_0')^{n-1}} \tag{6.40}$$

where $\mathcal{G}(\varepsilon)$ was defined by (6.28). The relation (6.40) indicate that all the cumulants grow linearly with time in the ultimate regime.

The relations (6.38) and (6.40) are remarkable as they give universal expressions of the higher-order cumulants of the position of the TP in the longitudinal direction in terms of the propagators of the simple random walks (symmetric or biased) on the considered structure.

6.3.3 Transient lattices

We now study the case of the three-dimensional lattice. We start from the expression of $\widehat{\Omega}(k_1;\xi)$ in terms of the conditional FPTD given in Appendix H (Section H.1). The method to compute the conditional FPTD associated to the random walk of a vacancy was presented in Section 4.6. Using a computer algebra software, one can show that at leading order in $(1-\xi)$, $\widehat{\Omega}(k_1;\xi)$ has the expansion

$$\widehat{\Omega}(k_1;\xi) \underset{\xi\to 1}{\sim} \frac{\rho_0}{(1-\xi)^2}\frac{p_1(\mathrm{e}^{ik_1}-1)+p_{-1}(\mathrm{e}^{-ik_1}-1)}{(G_0+c)\left[p_1(\mathrm{e}^{ik_1}-1)+p_{-1}(\mathrm{e}^{-ik_1}-1)\right]-\frac{p_1-p_{-1}}{a_0}} \tag{6.41}$$

where G_0 is given by (4.124), c by (6.22) and a_0 by (6.2). The expansion of $\widehat{\Omega}(k_1;\xi)$ in powers of k_1 is non-trivial but the coefficient of the series and, consequently, using (6.47), the cumulants, may still be defined recursively:

$$\kappa_1^{(n)}(\xi) \underset{\xi\to 1}{\sim} \frac{\rho_0 a_0}{(1-\xi)^2}\frac{p_1+(-1)^n p_{-1}}{p_1-p_{-1}}\left[1+\frac{(1-\xi)^2}{\rho_0}(G_0+c)\sum_{k=0}^{n-1}\binom{n}{k}\kappa_1^{(k)}(\xi)\frac{p_1+(-1)^{n-k}p_{-1}}{p_1+(-1)^n p_{-1}}\right] \tag{6.42}$$

for $n \geq 1$ and with $\kappa_1^{(0)}(\xi) = 0$. We can then obtain the expressions for the first cumulants recursively and, using a Tauberian theorem, one gets the leading order behavior of the first four cumulants:

$$\kappa_1^{(1)}(t) \underset{t\to\infty}{\sim} \rho_0 a_0 t \tag{6.43}$$

$$\kappa_1^{(2)}(t) \underset{t\to\infty}{\sim} \rho_0 a_0 \left[\frac{p_1+p_{-1}}{p_1-p_{-1}} + 2a_0(G_0+c)\right] t \tag{6.44}$$

$$\kappa_1^{(3)}(t) \underset{t\to\infty}{\sim} \rho_0 a_0 \left[1 + 6\frac{p_1+p_{-1}}{p_1-p_{-1}} a_0(G_0+c) + 6a_0^2(G_0+c)^2\right] t \tag{6.45}$$

$$\begin{aligned}\kappa_1^{(4)}(t) \underset{t\to\infty}{\sim} \rho_0 a_0 \Bigg[&\frac{p_1+p_{-1}}{p_1-p_{-1}} + 2a_0(G_0+c)\frac{7{p_1}^2 - 2p_1p_{-1} + 7{p_{-1}}^2}{(p_1-p_{-1})^3} \\ &+36{a_0}^2(G_0+c)^2\frac{p_1+p_{-1}}{p_1-p_{-1}} + 24{a_0}^3(G_0+c)^3\Bigg] t\end{aligned} \tag{6.46}$$

All the cumulants are linear in time in the long-time limit. The prefactors are not trivial and are obtained recursively.

6.4 Cumulants in the transverse direction

6.4.1 Method

We now study the cumulants of the position of the TP in the other directions. For symmetry reasons, the cumulants of the position of the TP are identical in all the directions $2, \ldots, d$. In each of this direction, for symmetry reasons, all the cumulants of odd order are null. The other ones are obtained by derivating $\widehat{\Omega}(\boldsymbol{k};\xi)$ with respect to k_2 and taking $\boldsymbol{k} = \mathbf{0}$ afterwards (see (2.54)). It then suffices to determine the dependence of $\widehat{\Omega}$ in the first component of the Fourier variable k_2. The explicit expression of $\widehat{\Omega}(k_2;\xi)$ in terms of the conditional FPTD is given in Appendix H (Section H.2). Starting from this expression, we study separately the cases of recurrent and transient lattices, as they were defined previously.

6.4.2 Recurrent lattices

We give here a general presentation of the procedure we followed to compute the cumulants in the transverse direction. The calculation is given explicitly for the case of a stripe-like geometry in Appendix I (Section I.2.1), and can be extended to the case of a two-dimensional lattice.

We start from the general expression of $\widehat{\Omega}(k_2;\xi)$ in terms of the conditional FPTD. The latter are computed using the methods presented in Chapter 4 (see Section 4.3.2 for the specific case of the stripe-like geometry). Using a computer algebra software, we perform a joint expansion of $\widehat{\Omega}(k_2;\xi)$ in the variables k_2 and $(1-\xi)$ with an appropriate scaling between these variables. Using the relation between the cumulants and the function $\widehat{\Omega}(k_2;\xi)$

$$\lim_{\rho_0\to 0} \frac{\widehat{\kappa}_2^{(2n)}(\xi)}{\rho_0} = -\frac{1}{\mathrm{i}^n} \left.\frac{\partial^n \widehat{\Omega}(k_2;\xi)}{\partial {k_2}^n}\right|_{k_2=0}, \tag{6.47}$$

we obtain the first two terms of $\lim_{\rho_0\to 0} \widehat{\kappa}_2^{(n)}(\xi)/\rho_0$ in its expansion in powers of $(1-\xi)$. Remarkably,

this expansion takes the form for the different geometries we consider, and is given by

$$\boxed{\lim_{\rho_0\to 0}\frac{\widehat{\kappa}_2^{(2n)}(\xi)}{\rho_0}\underset{\xi\to 1}{=}\frac{(2n)!}{(1-\xi)^2}\left(\frac{a_2}{2}\right)^n\left\{G_0(\xi)^{n-1}+(n-1)\left[G_1+\frac{1}{6a_2}+c+\frac{n}{n-1}c_2'\right]G_0(\xi)^{n-2}+\cdots\right\}.} \tag{6.48}$$

where

$$a_2=\frac{2p_2}{1+\frac{2d\alpha_2}{2d-\alpha_2}2p_2} \tag{6.49}$$

with

$$\alpha_2=\lim_{\xi\to 1}\left[\widehat{P}(\mathbf{0}|\mathbf{0};\xi)-\widehat{P}(2\boldsymbol{e}_2|\mathbf{0};\xi)\right], \tag{6.50}$$

and where the coefficient c_2' is given by

$$c_2'=\frac{4(\alpha_2-8\beta_2+8)(p_1-p_{-1})^2}{L^2[4(\alpha_2-8\beta_2+8)(p_1+p_{-1})-\alpha_2+8\beta_2-4]} \tag{6.51}$$

for a two-dimensional stripe, and vanishes in the case of a two-dimensional lattice. The coefficient β_2 is defined as

$$\beta_2=\lim_{\xi\to 1}\left[\widehat{P}(\mathbf{0}|\mathbf{0};\xi)-\widehat{P}(\boldsymbol{e}_2|\mathbf{0};\xi)\right], \tag{6.52}$$

and G_0, G_1, c are defined as in Section 6.2. Note that the time-dependence of the $(2n)$-th cumulant at leading order when $t\to\infty$ is not trivial. For instance, in quasi-one-dimensional geometries, as $G_0(\xi)=\mathcal{O}(1/\sqrt{1-\xi})$, the leading order term in (6.38) is of order $1/(1-\xi)^{(n+3)/2}$. A Tauberian theorem then allows to retrieve the time evolution of the $(2n)$-th cumulant, which grows as $t^{(n+1)/2}$.

As it was shown in Chapter 4, in these geometries, the limits $t\to\infty$ (i.e. $\xi\to 1$) and $\rho_0\to 0$ cannot be inverted. The ultimate regime, where the limit $t\to\infty$ is taken first, is obtained by considering new evolution rules of the vacancies, which perform biased random walks (see Chapter 4, Section 4.7.2.1 for a more precise definition of the evolution rules of the vacancies).

In this situation, the expression of $\widehat{\Omega}(k_2;\xi)$ in terms of the conditional FPTD given in Appendix H (Section H.1) is still valid, but the conditional FPTD must be replaced by the ones computed with the new evolution rules of the vacancies. Consequently, $\widehat{\Omega}$ is now a function of k_1, ξ and ρ_0. Using the following relation between the cumulants and $\widehat{\Omega}(k_1;\xi)$:

$$\lim_{\xi\to 1}\left[(1-\xi)^2\widehat{\kappa}_2^{(2n)}(\xi)\right]=-\frac{1}{\mathrm{i}^n}\frac{\partial^n}{\partial {k_2}^n}\lim_{\xi\to 1}\left[(1-\xi)^2\widehat{\Omega}(k_2;\xi,\rho_0)\right]\Big|_{k_1=0}, \tag{6.53}$$

to obtain the ultimate behavior of the cumulants with the help of a computer algebra software. The details of the computation in the case of a stripe-like geometry are given in Appendix I (Section I.2.2). These can be extended straightforwardly to other geometries. We finally obtain

$$\boxed{\lim_{t\to\infty}\frac{\kappa_2^{(2n)}(t)}{t}\underset{\rho_0\to 0}{\sim}\rho_0(2n)!\left(\frac{a_2'}{2}\right)^n\mathcal{G}(\rho_0 a_0')^{n-1}} \tag{6.54}$$

where $\mathcal{G}(\varepsilon)$ is was defined by (6.28). In the ultimate regime, all the cumulants grow linearly with time.

Note that, in the particular case of quasi-one-dimensional lattices, we study here the cumulative displacement of the TP in the transverse direction, which is not counted modulo the width of the lattice in the transverse direction. This is the reason why the cumulants of the TP position in the transverse direction diverge even for quasi-one-dimensional lattices. Rigorously, these expressions would only be valid at short times, i.e. as long as the distribution is not affected by the periodic boundary conditions in the transverse direction.

Finally, we obtained the These relations (6.48) and (6.54) are remarkable as they give the expressions of the cumulants of the position of the TP in the transverse direction in terms of the propagators of the simple random walks on the considered structure.

6.4.3 Transient lattices

We now study the case of the three-dimensional lattice. We start from the expression of $\widehat{\Omega}(k_2;\xi)$ in terms of the conditional FPTD given in Appendix H (Section H.2). The method to compute the conditional FPTD associated to the random walk of a vacancy was presented in Section 4.6. Using a computer algebra software, one can show that at leading order in $(1-\xi)$, $\widehat{\Omega}(k_2;\xi)$ has the expansion

$$\widehat{\Omega}(k_2;\xi) \underset{\xi\to 1}{\sim} \frac{\rho_0}{(1-\xi)^2}\frac{\cos k_2 - 1}{(G_0+c)(\cos k_2 - 1) - \frac{1}{a_2}} \tag{6.55}$$

where G_0 is given by (4.124), c by (6.22) and a_0 by (6.2). The expansion of $\widehat{\Omega}(k_2;\xi)$ in powers of k_2 is non-trivial but the coefficient of the series and, using (6.47), the cumulants, may still be defined recursively:

$$\widehat{\kappa}_2^{(2n)}(\xi) \underset{\xi\to 1}{=} \frac{\rho_0 a_2}{(1-\xi)^2} + (G_0+c)a_2 \sum_{k=0}^{n-1} \binom{2n}{2k} \widehat{\kappa}_2^{(2k)}(\xi) \tag{6.56}$$

for $n \geq 1$ and $\kappa_1^{(0)}(\xi) = 0$. In particular, using a Tauberian theorem, we obtain the following expressions for the first cumulants :

$$\kappa_2^{(2)}(t) \underset{t\to\infty}{\sim} \rho_0 a_2 t \tag{6.57}$$

$$\kappa_2^{(4)}(t) \underset{t\to\infty}{\sim} \rho_0 a_2 \left[1 + 6(G_0+c)a_2\right] t \tag{6.58}$$

$$\kappa_2^{(6)}(t) \underset{t\to\infty}{\sim} \rho_0 a_2 \left[1 + 30(G_0+c)a_2 + 90(G_0+c)^2 {a_2}^2\right] t. \tag{6.59}$$

All the cumulants of the TP position in the transverse direction are linear in time, and the their prefactor can be obtained recursively.

6.5 Extension to fractal lattices

The results we obtained in Sections 6.3 and 6.4 are remarkable: the cumulants of the position of the TP in the longitudinal and transverse directions have simple expressions, which only depend on the propagators of a simple random walk on the considered structure. These relations have been demonstrated in the particular case of hypercubic lattices, and we would like to test the universality of these formulae

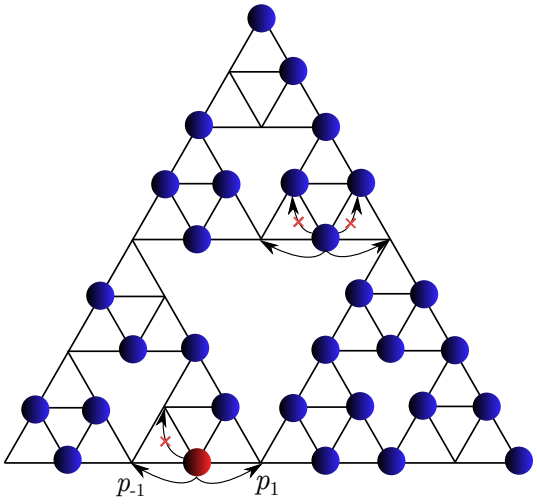

Figure 6.1: Tracer and bath particles on a Sierpinski gasket (represented here after 3 generations for simplicity).

on more complex structures. Indeed, the propagators of a simple random walk are known explicitly on many different geometries (triangular, hexagonal, fractals...) [90, 59, 58].

In this Section, we aim to study the case of a fractal lattice, on the example of the Sierpinski gasket. Fractal lattices are commonly used in statistical physics in order to model diffusion in disordered media [11]. We will compare results from numerical simulations with the predictions from the expression (6.38), which gives the generating functions associated to the cumulants of the position of the TP in terms of the propagators of a simple random walk.

For simplicity, we represent on Fig. 6.1 the Sierpinski gasket obtained after three generations. The lattice is populated by hardcore bath particles performing nearest-neighbor symmetric random walks. We assume that TP stays on one external side of the lattice. Mathematically, this condition is equivalent to taking $p_\mu = 0$ if $\mu \neq \pm 1$. On such a lattice, the generating function $\widehat{P}(\mathbf{0}|\mathbf{0};\xi)$ is known to have the long-time behavior [58]

$$\widehat{P}(\mathbf{0}|\mathbf{0};\xi) \underset{\xi\to 1}{\sim} \text{constant} \times (1-\xi)^{H/2-1}, \tag{6.60}$$

where H is the harmonic dimension of the Sierpinski gasket,

$$H = \frac{2\ln 3}{\ln 5} \simeq 1.365\,212\cdots \tag{6.61}$$

Note that the prefactor in (6.60) is not known, so that we will only give the time dependence of the cumulants and not their prefactor. The generalization of (6.38) to the Sierpinski gasket reads

$$\lim_{\rho_0\to 0} \frac{\widehat{\kappa}_1^{(n)}(\xi)}{\rho_0} \underset{\xi\to 1}{\propto} \frac{1}{(1-\xi)^2} G_0(\xi)^{n-1} \tag{6.62}$$

$$\underset{\xi\to 1}{\propto} \frac{1}{(1-\xi)^2} [(1-\xi)^{H/2-1}]^{n-1} \tag{6.63}$$

$$\underset{\xi\to 1}{\propto} (1-\xi)^{(n-1)(H/2-1)-2}. \tag{6.64}$$

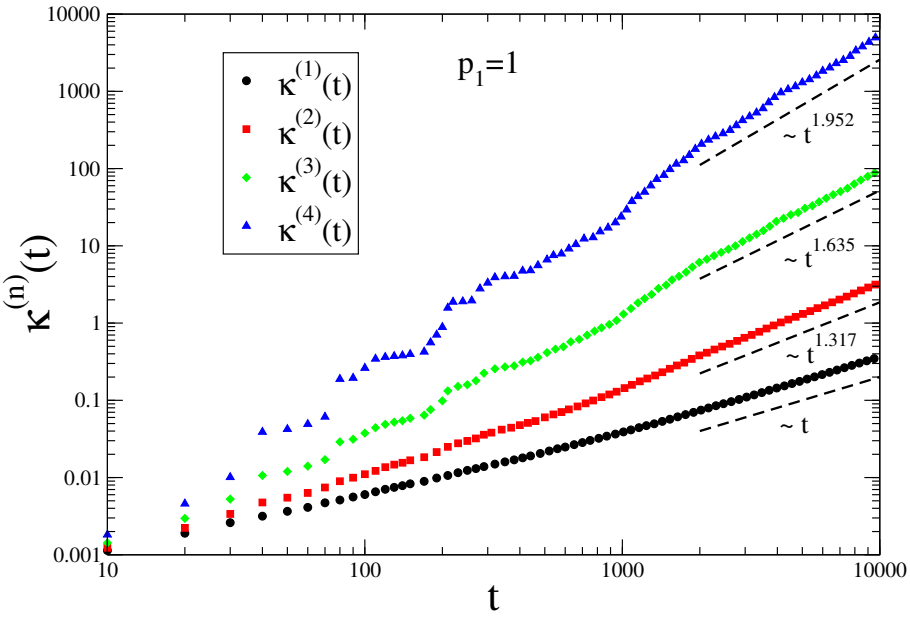

Figure 6.2: Results from simulations on a Sierpinski gasket of generation 15, with vacancy density $\rho_0 = 10^{-5}$ (symbols). The TP is completely directed ($p_1 = 1$). The dashed lines represent the exponents predicted by our theory. These simulations were realized by Alessandro Sarracino (postdoc in the group).

Using a Tauberian theorem, we get

$$\lim_{\rho_0 \to 0} \frac{\kappa_1^{(n)}(t)}{\rho_0} \underset{t\to\infty}{\propto} t^{(n-1)(1-H/2)+1}. \tag{6.65}$$

The numerical value of the first exponents of t are given in the table below:

n	exponent
1	1
2	1.3174
3	1.6348
4	1.9522

The cumulants then grow with anomalous exponents that were not observed before. Defining again the rescaled variable $Z_t \equiv (X_t - \langle X_t \rangle)/\sqrt{\langle {X_t}^2 \rangle - \langle X_t \rangle^2}$, one can show that its n-th moment scales as $t^{\frac{H}{2}\left(1-\frac{n}{2}\right)}$, so that all the moments of order greater than two vanish in the long-time limit. This shows that the rescaled variable Z_t in distributed accordingly to a Gaussian distribution.

We compare these analytical predictions with results from numerical simulations (Fig. 6.2), where the first four cumulants of the position of the TP in the direction of the bias were calculated. The time-dependence of the cumulants predicted by (6.65) is in correct agreement with the result from numerical simulations. This suggests that the relation (6.38) correctly predicts the behavior of a biased TP in a hardcore lattice gas in a structure that would be more complicated than the hypercubic lattice. This

seems to indicate that the relation (6.65) is a universal description of the cumulants of the TP position, for different types of lattices.

This universality could be confirmed by studying with numerical simulations the cumulants of the position of the TP in other complex lattices (triangular, hexagonal, other fractals...).

6.6 Conclusion

In this Chapter, we showed that the expressions obtained in Chapters 4 and 5 for the fluctuations and mean of the position of the TP could be recast under simple formulae that only involve the properties of a simple random walk on the considered structures: quasi-one-dimensional geometries, two-dimensional lattice, three-dimensional lattice. We showed that these expressions were also valid in the case of the one-dimensional lattice. This result is surprising, as the properties of the random walks performed by the vacancies are strongly affected by the geometry of the considered structure. In spite of these very different behaviors, there exist universal formulae describing the behavior of the TP.

We extended the computation to the higher-order cumulants of the position of the TP in the longitudinal direction, and the cumulants in the transverse direction. Considering separately the case of recurrent and transient lattices, we obtained again simple expressions that only involve the properties of simple random walks on the considered structures.

Finally, the general expression for the cumulants of the position of the TP in the longitudinal direction was used to predict the behavior of a biased tracer in a hardcore lattice gas adsorbed on a Sierpinski gasket. We extended to this fractal lattice the general expression we obtained from the study of hypercubic lattices, and showed that it correctly predicts the time-dependence of the cumulants obtained from numerical simulations. This suggests that the expressions we obtained in this Chapter are very general, and could allow us to study biased tracer diffusion in a hardcore lattice gas on more complex structures.

CHAPTER 7

Simplified continuous description

Contents

In this Chapter, we give a simplified description of the interactions of the TP with the vacancies present on the lattice, in the particular case where the TP is completely directed. The fluctuations of the position of the TP are simply related to the propagators associated to the random walk of the vacancies on the considered structure, and we can retrieve qualitatively the main features obtained through the exact approach presented in Chapter 4. We finally adapt our simplified description to the particular case of a one-dimensional lattice, which was studied exactly in Chapter 3. This simplified approach unveils the physical mechanisms at stake in the problem.

7.1 Introduction

In this Chapter, we consider a simplified model that unveils the physical mechanisms controlling the statistical properties of the position of the TP. The relation between the properties of the random walks performed by the vacancies and the behavior of the position of the TP is made explicit by considering a simple model where the TP is directed, so that it jumps in the direction of the bias every time it is visited by a vacancy. The position of the TP at time t is then exactly equal to the number of time steps during which the TP location was occupied by at least one vacancy up to time t. For the sake of simplicity, the random walk of the vacancies is described in continuous space and time.

We first present the general formalism of this calculation, and present afterwards the results we obtain in the cases of a two-dimensional lattice and of a stripe-like lattice. We show that this simplified approach qualitatively describes the exact results we obtained in Chapter 4, and correctly captures the physical mechanisms of the problem. This formalism is adapted to the particular case of a one-dimensional lattice in order to retrieve with a straightforward calculation the results exactly obtained in Chapter 3.

7.2 General formalism

We start from the model of a biased tracer in a hardcore lattice gas, in the high-density limit, presented in Chapter 2 (Section 2.2). We assume that the TP is completely directed (i.e. $p_1 = 1$ and $p_\nu = 0$ for $\nu \neq 1$) so that the TP may only jump in the direction of the unitary vector $\boldsymbol{e}_1$. As previously, $\boldsymbol{X}_t$ is the random variable representing the position of the TP at time t, and X_t its projection on the direction of the bias. We also assume that when a vacancy is at position $\boldsymbol{X}_t + \boldsymbol{e}_1$ at time t, then the TP instantly jumps to position $\boldsymbol{X}_t + \boldsymbol{e}_1$, exchanging its position with the vacancy.

We denote as N_t the number of time steps during which the origin of the lattice has been occupied by at least one vacancy between times 1 and t. Under the previous assumption, we conclude that the random variables X_t and N_t have the same properties. We can then study the TP position by describing N_t. We will focus on the leading order in the density of vacancies ρ_0, so that the events where two vacancies are on adjacent sites or at the same site only contribute to order $\mathcal{O}({\rho_0}^2)$ and will be discarded. We define the random variable η_τ as follows:

- if there is at least one vacancy at the origin of the lattice at time τ, then $\eta_\tau = 1$,
- otherwise $\eta_\tau = 0$.

Then, the quantities N_t and X_t can be represented as

$$X_t = N_t = \sum_{\tau=1}^{t} \eta_\tau. \tag{7.1}$$

From this expression we deduce the variance of X_t:

$$\begin{aligned}
\mathrm{Var}(X_t) &= \left\langle (X_t - \langle X_t \rangle)^2 \right\rangle && (7.2)\\
&= \left\langle {X_t}^2 \right\rangle - \langle X_t \rangle^2 && (7.3)\\
&= \left\langle \left(\sum_{\tau=1}^{t} \eta_\tau \right)^2 \right\rangle - \left(\sum_{\tau=1}^{t} \langle \eta_\tau \rangle \right)^2 && (7.4)\\
&= \sum_{\tau=1}^{t} \langle \eta_\tau \rangle \left(1 - \langle \eta_\tau \rangle^2 \right) + 2 \sum_{\tau' > \tau} \left[\langle \eta_{\tau'} \eta_\tau \rangle - \langle \eta_{\tau'} \rangle \langle \eta_\tau \rangle \right] && (7.5)
\end{aligned}$$

where we used the property ${\eta_\tau}^2 = \eta_\tau$. In what follows, we derive the expressions of $\langle \eta_\tau \rangle$ and $\langle \eta_{\tau'} \eta_\tau \rangle$ at leading order in ρ_0. We assume that the lattice has N sites and is populated by M vacancies, with $\rho_0 = M/N$. We define the auxiliary random variable $\delta_{m,\tau}$, which is equal to 1 if the m-th vacancy is at the origin at time τ and 0 otherwise. At leading order in ρ_0 and averaging over the initial position of the vacancies, one has

$$\begin{aligned}
\langle \eta_\tau \rangle &= \sum_{m=1}^{M} \langle \delta_{m,\tau} \rangle + \mathcal{O}({\rho_0}^2) && (7.6)\\
&= M \langle \delta_{1,\tau} \rangle + \mathcal{O}({\rho_0}^2) && (7.7)\\
&= \frac{M}{N} \sum_{\boldsymbol{Z}} p(\boldsymbol{0}, \tau | \boldsymbol{Z}, 0) + \mathcal{O}({\rho_0}^2) && (7.8)
\end{aligned}$$

where we defined $p(\boldsymbol{r}_2, t_2|\boldsymbol{r}_1, t_1)$ as the probability for a vacancy to be at site $\boldsymbol{r}_2$ at time t_2 knowing that it was at site $\boldsymbol{r}_1$ at time t_1 ($t_1 < t_2$). Using the normalization condition $\sum_{\boldsymbol{Z}} p(\boldsymbol{0}, \tau|\boldsymbol{Z}, 0) = 1$, and taking the thermodynamic limit where M and N go to infinity with a fixed ratio M/N, one obtains

$$\langle \eta_\tau \rangle = \rho_0 + \mathcal{O}({\rho_0}^2). \tag{7.9}$$

The correlation functions $\langle \eta_{\tau'} \eta_\tau \rangle$ are calculated in a similar way:

$$\langle \eta_{\tau'} \eta_\tau \rangle = \sum_{m=1}^{M} \sum_{m'=1}^{M} \left\langle \delta_{m,\tau} \delta_{m',\tau'} \right\rangle + \mathcal{O}({\rho_0}^2) \tag{7.10}$$

$$= \sum_{m=1}^{M} \left\langle \delta_{m,\tau} \delta_{m,\tau'} \right\rangle + 2 \sum_{m=1}^{M-1} \sum_{m'=m+1}^{M} \left\langle \delta_{m,\tau} \right\rangle \left\langle \delta_{m',\tau'} \right\rangle + \mathcal{O}({\rho_0}^2) \tag{7.11}$$

The first term is evaluated introducing $p(\boldsymbol{r}_3, t_3|\boldsymbol{r}_2, t_2|\boldsymbol{r}_1, t_1)$ (probability for a vacancy to be at $\boldsymbol{r}_3$ at time t_3, being at site $\boldsymbol{r}_2$ at time t_2 and at site $\boldsymbol{r}_1$ at time t_1, with $t_1 < t_2 < t_3$). The second term is of order $\mathcal{O}({\rho_0}^2)$. Averaging over the initial positions, we finally obtain

$$\langle \eta_{\tau'} \eta_\tau \rangle = \sum_{m=1}^{M} \left\langle \delta_{m,\tau} \delta_{m,\tau'} \right\rangle + \mathcal{O}({\rho_0}^2) \tag{7.12}$$

$$= M \left\langle \delta_{1,\tau} \delta_{1,\tau'} \right\rangle + \mathcal{O}({\rho_0}^2) \tag{7.13}$$

$$= \frac{M}{N} \sum_{\boldsymbol{Z}} p(\boldsymbol{0}, \tau|\boldsymbol{0}, \tau'|\boldsymbol{Z}, 0) + \mathcal{O}({\rho_0}^2). \tag{7.14}$$

Using again a normalization condition, and using the Markovianity of the vacancy random walk, we obtain in the thermodynamic limit

$$\langle \eta_{\tau'} \eta_\tau \rangle = \rho_0 p(\boldsymbol{0}, \tau' - \tau|\boldsymbol{0}, 0) + \mathcal{O}({\rho_0}^2) \tag{7.15}$$

Finally, using Eqs. (7.9) and (7.15) in Eq. (7.5), we find that the variance of X_t is simply expressed in terms of the single-vacancy propagators:

$$\mathrm{Var}(X_t) = \rho_0 t + 2\rho_0 \sum_{\tau' > \tau} p(\boldsymbol{0}, \tau' - \tau|\boldsymbol{0}, 0) + \mathcal{O}({\rho_0}^2) \tag{7.16}$$

For simplicity, we consider the equivalent expression in continuous time:

$$\boxed{\mathrm{Var}(X_t) = \rho_0 t + 2\rho_0 \int_0^t \mathrm{d}\tau' \int_0^{\tau'} \mathrm{d}\tau \, p(\boldsymbol{0}, \tau' - \tau|\boldsymbol{0}, 0) + \mathcal{O}({\rho_0}^2)} \tag{7.17}$$

Equivalenty, defining the Laplace transform (LT) of a time-dependent function $f(t)$ as

$$\mathcal{L}[f](s) = \widehat{f}(s) = \int_0^\infty \mathrm{e}^{-st} f(t) \mathrm{d}t, \tag{7.18}$$

we get

$$\boxed{\mathcal{L}\left[\mathrm{Var}(X_t)\right](s) = \frac{\rho_0}{s^2} + \frac{2\rho_0}{s^2} \int_0^\infty \mathrm{e}^{-s\tau} p(\boldsymbol{0}, \tau|\boldsymbol{0}, 0) \mathrm{d}\tau,} \tag{7.19}$$

where we used twice the usual property of the LT:

$$\mathcal{L}\left[\int_0^t f(t')\mathrm{d}t'\right](s) = \frac{1}{s}\mathcal{L}[f](s). \tag{7.20}$$

The simple formula (7.19) explicitly gives the relation between the propagator associated to the random walk of a vacancy and the fluctuations of the position of the TP. If the random walk performed by the vacancy is *transient*, the LT of $p(\mathbf{0}, \tau|\mathbf{0}, 0)$ is a constant at leading order in the long-time limit, and the inverse LT of (7.19) yields a linear growth of the fluctuations of the TP. On the contrary, if the random walk performed by the vacancy is *recurrent*, the LT of $p(\mathbf{0}, \tau|\mathbf{0}, 0)$ is not constant at leading order in the long-time limit (it diverges when $s \to 0$), and the behavior of $\mathrm{Var}(X_t)$ is superlinear.

This is consistent with the behavior of the TP fluctuations in confined geometries (quasi-one-dimensional, two-dimensional) that was studied in Chapter 4. On such structures, the random walk of a vacancy is recurrent, which yields a superdiffusive evolution of the TP fluctuations. At sufficiently long times, the random walk of a vacancy between two successive visits to the TP location is in fact biased, because of the net displacement of the TP due to its interactions with the other vacancies. This bias is in the opposite direction of the TP mean displacement, and equal to the velocity of the TP. Such a random walk is transient, and the fluctuations of the TP cross over to a diffusive regime.

In what follows, we give an expression for the single-vacancy propagators p in the stripe-like and two-dimensional geometries, and deduce the expression of the variance. For simplicity, we give the equations verified by the propagators in a continuous-space description. We include in these equations a drift term in the direction -1 representing the effective bias experienced by a vacancy, that originates from the net displacement of the TP in the direction $+1$. The diffusion equation verified by the propagators p reads:

$$\begin{cases} \dfrac{\partial}{\partial t}p(\boldsymbol{r}, t|\mathbf{0}, 0) & = D\Delta p + v\dfrac{\partial}{\partial x}p(\boldsymbol{r}, t|\mathbf{0}, 0) \\ p(\boldsymbol{r}, 0|\mathbf{0}, 0) & = \delta(\boldsymbol{r}) \end{cases} \tag{7.21}$$

where v is positive and vanishes when the vacancy density ρ_0 goes to zero. We will write $v = V\rho_0$, where V is a positive numerical constant. In what follows, we solve the diffusion equation (7.21) on the two-dimensional and stripe-like lattices, and deduce the expression of $\mathrm{Var}(X_t)$ using (7.17).

7.3 Two-dimensional lattice

In two dimensions, the diffusion equation (7.21) writes

$$\begin{cases} \dfrac{\partial}{\partial t}p(x, y, t|\mathbf{0}, 0) & = D\left(\dfrac{\partial^2}{\partial x^2} + \dfrac{\partial^2}{\partial y^2}\right)p(x, y, t|\mathbf{0}, 0) + v\dfrac{\partial}{\partial x}p(x, y, t|\mathbf{0}, 0) \\ p(x, y, 0|\mathbf{0}, 0) & = \delta(x)\delta(y) \end{cases} \tag{7.22}$$

The Fourier transform of the diffusion equation then writes

$$\frac{\partial}{\partial t}\widetilde{p}(\boldsymbol{k}, t|\mathbf{0}, 0) = (\mathrm{i}vk_1 - D\boldsymbol{k}^2)\widetilde{p}(\boldsymbol{k}, t|\mathbf{0}, 0). \tag{7.23}$$

The Fourier transform of the initial condition is $\widetilde{p}(\boldsymbol{k}, 0|\mathbf{0}, 0) = 1$, so that we get

$$\widetilde{p}(\boldsymbol{k}, t|\mathbf{0}, 0) = \mathrm{e}^{(\mathrm{i}vk_1 - D\boldsymbol{k}^2)t}. \tag{7.24}$$

Computing the inverse Fourier transform, we finally get the expression for the propagator $p(\boldsymbol{r}, t|\mathbf{0}, 0)$:

$$p(\boldsymbol{r}, t|\mathbf{0}, 0) = \frac{1}{(2\pi)^2} \int_{-\infty}^{\infty} \mathrm{d}k_1 \int_{-\infty}^{\infty} \mathrm{d}k_2 \, \mathrm{e}^{(\mathrm{i}vk_1 - D\boldsymbol{k}^2)t} \mathrm{e}^{\mathrm{i}\boldsymbol{k}\cdot\,\boldsymbol{r}} \tag{7.25}$$

$$= \frac{1}{4\pi Dt} \mathrm{e}^{-\frac{(x+vt)^2}{4Dt}} \mathrm{e}^{-\frac{y^2 t}{4D}} \tag{7.26}$$

In order to apply (7.19) to the two-dimensional case, we need to compute the integral of $\mathrm{e}^{-s\tau} p(\mathbf{0}, \tau|\mathbf{0}, 0)$ for t going from 0 to ∞. As this integral is not defined, we introduce a cutoff value ε, compute the integral, and take the limit $\varepsilon \to 0$ afterwards. This yields

$$\int_{\varepsilon}^{\infty} \mathrm{e}^{-s\tau} \frac{1}{4\pi D\tau} \mathrm{e}^{-\frac{v^2\tau}{4D}} \mathrm{d}\tau = \frac{1}{4\pi D} \int_{s+\frac{v^2}{4D}}^{\infty} \frac{\mathrm{e}^{-u}}{u} \mathrm{d}u \tag{7.27}$$

$$= -\mathrm{Ei}\left[-\left(s + \frac{v^2}{4D} \right) \varepsilon \right] \tag{7.28}$$

where Ei is the exponential integral function, defined by

$$\mathrm{Ei}(x) = -\int_{-x}^{\infty} \frac{\mathrm{e}^{-t}}{t} \mathrm{d}t \tag{7.29}$$

and has the equivalent [1]

$$\mathrm{Ei}(x) \underset{x\to 0}{\sim} \ln x. \tag{7.30}$$

As we will consider the large time and small density (i.e. small v) limits, we obtain

$$\int_{\varepsilon}^{\infty} \mathrm{e}^{-s\tau} \frac{1}{4\pi D\tau} \mathrm{e}^{-\frac{v^2\tau}{4D}} \mathrm{d}\tau \sim -\ln\left(s + \frac{v^2}{4D} \right), \tag{7.31}$$

which is independent of the cutoff ε, and finally, using (7.19) and the relation $v = V\rho_0$,

$$\boxed{\mathcal{L}\left[\mathrm{Var}(X_t)\right](s) = \frac{\rho_0}{s^2} - \frac{2\rho_0}{s^2} \ln\left(s + \frac{V^2{\rho_0}^2}{4D} \right).} \tag{7.32}$$

In the limit where ρ_0 is taken first, we get the following expression for the variance

$$\lim_{\rho_0 \to 0} \frac{\mathcal{L}\left[\mathrm{Var}(X_t)\right](s)}{\rho_0} = \frac{1 - 2\ln s}{s^2}, \tag{7.33}$$

whose inverse Laplace transform is

$$\lim_{\rho_0 \to 0} \frac{\mathrm{Var}(X_t)}{\rho_0} = 2t\ln t + (2\gamma - 1)t, \tag{7.34}$$

$$\underset{t\to\infty}{\sim} 2t \ln t. \tag{7.35}$$

We then retrieve qualitatively the time-dependence of the variance which was obtained with the exact approach (see (4.114)). In the limit where t is going to infinity for a fixed value of ρ_0, which is equivalent to take the limit $s \to 0$ in Laplace space, we get

$$\lim_{s\to 0} \left\{ s^2 \mathcal{L}\left[\mathrm{Var}(X_t)\right](s) \right\} = \rho_0 \left(1 - 2\ln \frac{V^2{\rho_0}^2}{4D} \right), \tag{7.36}$$

whose inverse Laplace transform yields, at leading order in ρ_0,

$$\lim_{t\to\infty} \frac{\mathrm{Var}(X_t)}{t} \underset{\rho_0\to 0}{\sim} 4\rho_0 \ln\frac{1}{\rho_0} \tag{7.37}$$

which is in qualitative agreement with the exact computation (4.214). This simplified continuous-time random walk approach then allows to retrieve the dependences in t and ρ_0 of the variance of the TP position in the two regimes. We also retrieve with (7.32) the scaling behavior of the variance in the joint limit of $\rho_0 \to 0$ and $t \to \infty$ with the scaling $t \sim 1/{\rho_0}^2$, which corresponds to the function obtained from the exact approach (4.222).

This simplified approach reveals the physical mechanisms at the origin of the superdiffusive behavior of the TP, and of the crossover towards a diffusive regime:

- on a two-dimensional lattice, the random walk performed by a vacancy on the lattice is recurrent. The return statistics of a vacancy to the location of the TP is then anomalous and leads to a superlinear evolution of the fluctuations of the TP.
- at large times, the random walk performed by a vacancy between two visits to the location of the TP is in fact *biased*, as the TP has a net displacement due to its interactions with other vacancies. This random walk is no longer recurrent, and the return statistics of a given vacancy to the TP location is no longer anomalous. The fluctuations of the TP become diffusive.

7.4 Stripe-like lattice

We now focus on the case of a strip-like lattice of width L, which corresponds to the domain $\mathbb{R} \times [-L/2; L/2]$. We then solve (7.22) with the periodic boundary condition:

$$p(x, L/2, t|\mathbf{0}, 0) = p(x, -L/2, t|\mathbf{0}, 0) \tag{7.38}$$

for any values of x and t. We try to find solutions under the form

$$p(x, y, t|\mathbf{0}, 0) = \sum_{n=-\infty}^{\infty} q_n(x, t)\mathrm{e}^{\frac{2\mathrm{i}\pi n y}{L}}. \tag{7.39}$$

The functions $q_n(x, t)$ are then the solution of the equation

$$\frac{\partial q_n}{\partial t} = D\frac{\partial^2 q_n}{\partial x^2} - v\frac{\partial q_n}{\partial x} - \frac{4\pi^2 n^2}{L^2} q_n. \tag{7.40}$$

Writing the Fourier transform with respect to the coordinate x, one finally obtains

$$q_n(x, t) = \frac{1}{L}\frac{1}{\sqrt{4\pi D t}}\mathrm{e}^{-\frac{4\pi^2 n^2}{L^2}Dt}\mathrm{e}^{-\frac{(x+vt)^2}{4Dt}}. \tag{7.41}$$

The propagator p then writes

$$p(x, y, t|\mathbf{0}, 0) = \frac{1}{L}\frac{1}{\sqrt{4\pi D t}}\mathrm{e}^{-\frac{(x+vt)^2}{4Dt}} \sum_{n=-\infty}^{\infty} \mathrm{e}^{-\frac{4\pi^2 n^2}{L^2}Dt} \cos\frac{2\pi n y}{L}. \tag{7.42}$$

The sum over n is equivalent to 1 for large times, we will then focus on the part which depends on x and approximate the propagator as:

$$p(x,y,t|\mathbf{0},0) \simeq \frac{1}{L}\frac{1}{\sqrt{4\pi D t}}\mathrm{e}^{-\frac{(x+vt)^2}{4Dt}}. \tag{7.43}$$

(7.19) then becomes

$$\mathcal{L}\left[\mathrm{Var}(X_t)\right](s) = \frac{\rho_0}{s^2} + \frac{2\rho_0}{s^2}\int_0^\infty \mathrm{e}^{-s\tau} p(\mathbf{0},\tau|\mathbf{0},0)\mathrm{d}\tau \tag{7.44}$$

$$= \frac{\rho_0}{s^2} + \frac{2\rho_0}{s^2}\int_0^\infty \mathrm{e}^{-s\tau}\frac{1}{L}\frac{1}{\sqrt{4\pi D\tau}}\mathrm{e}^{-\frac{v^2\tau}{4D}}\mathrm{d}\tau. \tag{7.45}$$

Using the usual Laplace transform $\mathcal{L}[\exp(-at)/\sqrt{t}](s) = \sqrt{\pi}/\sqrt{s+a}$ (for $a > 0$) and the relation $v = \rho_0 V$, we obtain

$$\boxed{\mathcal{L}\left[\mathrm{Var}(X_t)\right](s) = \frac{\rho_0}{s^2} + \frac{2\rho_0}{s^2}\frac{1}{L\sqrt{4sD + {\rho_0}^2V^2}}.} \tag{7.46}$$

In the limit where ρ_0 is taken first, we get the following expression for the variance

$$\lim_{\rho_0\to 0}\frac{\mathcal{L}\left[\mathrm{Var}(X_t)\right](s)}{\rho_0} = \frac{1}{L\sqrt{D}s^{5/2}}, \tag{7.47}$$

whose inverse Laplace transform is

$$\lim_{\rho_0\to 0}\frac{\mathrm{Var}(X_t)}{\rho_0} = \frac{4}{3L\sqrt{D\pi}}t^{3/2}. \tag{7.48}$$

We then retrieve qualitatively the time-dependence of the variance which was obtained with the exact approach (4.65). In the limit where t is going to infinity for a fixed value of ρ_0, which is equivalent to the limit $s \to 0$ in Laplace space, we get

$$\lim_{s\to 0}\left\{s^2\mathcal{L}\left[\mathrm{Var}(X_t)\right](s)\right\} = \rho_0 + \frac{2}{LV}, \tag{7.49}$$

whose inverse Laplace transform yields, at leading order in ρ_0,

$$\lim_{t\to\infty}\frac{\mathrm{Var}(X_t)}{t} \underset{\rho_0\to 0}{\sim} \frac{2}{LV} \tag{7.50}$$

which is in qualitative agreement with the exact computation (4.168). In particular, we retrieve the fact that the diffusion coefficient of the TP in the long-time limit is independent of the density of vacancies on the lattice. We also retrieve with (7.46) the scaling behavior of the variance in the joint limit of $\rho_0 \to 0$ and $t \to \infty$ with the scaling $t \sim 1/{\rho_0}^2$, which is the equivalent of the function obtained from the exact approach (4.179).

Finally, as in the case of a two-dimensional lattice, we showed that the superdiffusive behavior of the TP iq due to the anomalous return statistics of the vacancies to the location of the TP. In the long-time limit, the random walks performed by the vacancies are in fact biased due to the net displacement of the TP. This modifies the return statistics of the vacancies to the TP location, and its fluctuations become diffusive.

7.5 One-dimensional lattice

The approach presented in this Chapter allowed us to retrieve the results we obtained on the stripe-like and two-dimensional geometries. We now extend them to the case of a one-dimensional lattice. This situation is different from the ones we studied so far. In two dimensions (and higher), the same vacancy may interact many times with the TP. This is in contrast with the case of a directed TP on a one-dimensional lattice, in which each vacancy can only interact once with the TP. The number of steps performed by the TP up to time t is then equal to the number of vacancies which were initially to the right of the TP and which are to its left at time t. Indeed, as the TP is completely directed, a vacancy cannot go back to the right of the TP after it arrived to its left. We define a random variable $\zeta_i(t)$, which is equal to 1 if the i-th vacancy went from right to left before time t, and 0 otherwise. Assuming that they are M vacancies on a finite lattice of N sites (with $\rho_0 = M/N$), the position of the TP then writes

$$X_t = \sum_{i=1}^{M} \zeta_i(t). \tag{7.51}$$

In the particular case where the TP is directed, it was shown in Chapter 3 that all the cumulants were equal at leading order in $\rho_0 \to 0$ and $t \to \infty$ (see equations (3.22) and (3.24)). It is then sufficient to compute the first one in order to get the leading behaviors of the other cumulants. Averaging over the initial positions and writing all the quantities in continuous space for simplicity, we get

$$\langle X_t \rangle = \sum_{i=1}^{M} \langle \zeta_i(t) \rangle \tag{7.52}$$

$$= M \langle \zeta_1(t) \rangle \tag{7.53}$$

$$= M \frac{1}{L} \int_0^L \mathrm{d}z \int_0^t \mathrm{d}t' \, F(0, t'|z, 0), \tag{7.54}$$

where $F(0, t'|z, 0)$ is the probability for a vacancy to reach the origin for the first time at time t' knowing that it started from site z at time 0. In the thermodynamic limit where $M, N \to \infty$ with a fixed density $\rho_0 = M/N$, we obtain

$$\langle X_t \rangle = \rho_0 \int_0^\infty \mathrm{d}z \int_0^t \mathrm{d}t' \, F(0, t'|z, 0). \tag{7.55}$$

For convenience, we compute the Laplace transform of this quantity, which becomes

$$\mathcal{L}[\langle X_t \rangle](s) = \frac{\rho_0}{s} \int_0^\infty \mathrm{d}z \int_0^\infty \mathrm{d}t \, \mathrm{e}^{-st} F(0, t|z, 0) \tag{7.56}$$

$$= \frac{\rho_0}{s} \int_0^\infty \mathrm{d}z \, \widehat{F}(0, p|z, 0). \tag{7.57}$$

The next step is to express the first-passage densities $F(0, t'|z, 0)$ characterizing the random walk of a vacancy on the lattice. We assume that the vacancies undergo an effective bias in direction -1. By analogy with the cases of the stripe and 2D lattices, this effective bias would be due to the net displacement of the TP in the direction of the force and could eventually cause the apparition of an ultimate regime, different from the one we calculated so far. This bias will be denoted v, and we will assume that it vanishes when ρ_0 goes to zero, so that there exists a constant V such that $v = V\rho_0$.

Denoting by $p(x,t|x_0,0)$ the probability for a vacancy to be at site x at time t starting from x_0 at time 0, this quantity is the solution of the diffusion equation

$$\begin{cases} \dfrac{\partial}{\partial t}p(x,t|x_0,0) &= D\dfrac{\partial^2}{\partial x^2}p(x,t|x_0,0) + v\dfrac{\partial}{\partial x}p(x,t|x_0,0) \\ p(x,0|x_0,0) &= \delta(x-x_0), \end{cases} \tag{7.58}$$

so that we get

$$p(x,t|x_0,0) = \frac{1}{\sqrt{4\pi Dt}}\mathrm{e}^{-\frac{(x-x_0+vt)^2}{4Dt}}. \tag{7.59}$$

The first-passage densities are related to the Laplace transforms of the propagators with the renewal equation [58]

$$\widehat{F}(0,s|z,0) = \frac{\widehat{p}(0,s|z,0)}{\widehat{p}(0,s|0,0)}, \tag{7.60}$$

and the expression of $\mathcal{L}[\langle X_t\rangle](s)$ then writes

$$\mathcal{L}[\langle X_t\rangle](s) = \frac{\rho_0}{s}\frac{1}{\widehat{p}(0,s|0,0)}\int_0^\infty \mathrm{d}z\,\widehat{p}(0,s|z,0). \tag{7.61}$$

We first compute $\widehat{p}(0,s|0,0)$:

$$\widehat{p}(0,s|0,0) = \frac{1}{\sqrt{4\pi D}}\int_0^\infty \mathrm{d}t\,\mathrm{e}^{-st}\mathrm{e}^{-\frac{V^2t}{4D}} \tag{7.62}$$

$$= \frac{1}{\sqrt{4sD+{\rho_0}^2V^2}}. \tag{7.63}$$

We finally compute the integral over the initial positions:

$$\int_0^\infty \mathrm{d}z\,\widehat{p}(0,s|z,0) = \frac{1}{\sqrt{4\pi D}}\int_0^\infty \mathrm{d}t\,\frac{\mathrm{e}^{-st}}{\sqrt{t}}\int_0^\infty \mathrm{d}z\mathrm{e}^{-\frac{(z-vt)^2}{4Dt}} \tag{7.64}$$

$$= \frac{1}{2s}\left(1+\frac{\rho_0 V}{\sqrt{4sD+{\rho_0}^2V^2}}\right) \tag{7.65}$$

Finally, the Laplace transform of the mean position writes

$$\boxed{\mathcal{L}[\langle X_t\rangle](s) = \frac{\rho_0}{2s^2}\sqrt{4sD+{\rho_0}^2V^2}\left(1+\frac{\rho_0 V}{\sqrt{4sD+{\rho_0}^2V^2}}\right).} \tag{7.66}$$

In the limit where $\rho_0 \to 0$ is taken first, we find the following leading order behavior

$$\mathcal{L}[\langle X_t\rangle](s) \sim \frac{\rho_0\sqrt{D}}{s^{3/2}}, \tag{7.67}$$

which yields, using a Tauberian theorem,

$$\langle X_t\rangle \sim \rho_0\frac{D}{\pi}\sqrt{t} \tag{7.68}$$

This is qualitatively equivalent to the expression we obtained from the exact approach (3.22). In the limit where we first take $p \to 0$, we get

$$\mathcal{L}[\langle X_t \rangle](s) \sim \frac{D}{s} \tag{7.69}$$

so that $\langle X_t \rangle$ tends to a constant when t goes to infinity. This is not compatible with the hypothesis that the tracer reaches a regime where it has a non-zero velocity. Then, there is only one regime in this situation. It was computed through the exact approach in Chapter 3, and retrieved by our simplified approach (7.68).

7.6 Conclusion

In this Chapter, we proposed a simplified description of the vacancy-mediated diffusion of a biased tracer in a hardcore lattice gas. We focused on the case of a directed TP which can only jump in the direction of the bias. The TP jumps each time it is visited by a vacancy, and its position at time t is then exactly equal to the number of time steps during which the location of the TP was occupied by at least one vacancy up to time t. In a simplified continuous time and space approach, the variance of the position of the TP is simply expressed in terms of the propagator associated to the random walk of a vacancy. If the random walk performed by a vacancy is recurrent, we show that the the variance of the position of the TP is anomalous and superlinear in time. On the contrary, if the vacancy performs a transient random walk, the variance of the position of the TP grows linearly with time. We retrieve the superdiffusive effect observed in confined geometries as well as the crossover to a diffusive behavior, that were demonstrated with a complete analytical treatment in Chapter 4.

This simplified description is extended to the case of directed TP in a one-dimensional hardcore lattice gas. As this lattice is non-looped, each vacancy can interact with the tracer only once: the number of steps taken by the TP at time t is equal to the number of vacancies that were initially at the right of the TP and passed to its left between times 0 and t. The position of the TP is then written in terms of the first-passage time densities associated to the random walks of the vacancies initially located to the right of the TP. With a continuous description in time and space, the cumulants of the position of the TP are computed, and successfully compared to the results from the exact calculation at leading order in ρ_0 presented in Chapter 3.

The approach we presented in this Chapter is much simpler than the exact description detailed before, and correctly accounts for the qualitative features we highlighted. This approach also makes explicit the relation between the properties of the vacancies random walks and the statistical properties of the position of the TP. However, this simplified description does not predict the emergence of the velocity anomaly in quasi-1D geometries presented in Chapter 5. Further work could result in a more accurate description that would take into account the anticorrelations effects between the TP and a single vacancy, that would describe more subtle effects.

Part II

Biased tracer diffusion in a lattice gas of arbitrary density

CHAPTER 8

General formalism and decoupling approximation

Contents

We present the model of a biased tracer particle (TP) in a hardcore lattice gas in contact with a reservoir of particles. The bath particles perform symmetric nearest-neighbor random walks, with a mean waiting time τ^*, and may desorb back to the reservoir. Particles from the reservoir may adsorb onto vacant lattice sites. The TP performs a biased random walk with a mean waiting time τ. The dynamics is constrained with hardcore interactions. Starting from the master equation on the joint probability of the TP position and the bath configuration, and resorting to a mean-field type approximation, we express the mean position of the TP position and its fluctuations in terms of correlations functions which are given as solutions of a set of equations. The decoupling approximation is extended to write the evolution of the cumulant generating function of the TP position in terms of generalized correlation functions, whose governing equations are determined.

8.1 Introduction

In the first part of this thesis, we studied the transport properties of a biased TP in a hardcore lattice gas, in the limit where the density of particles is very high. In this limit, the motion of the TP is mediated by

the diffusion of vacancies on the lattice, and we could obtain exact results at leading order in the density of vacancies. In the second part of this thesis, we study the more general situation where the density of particles is *arbitrary*. We briefly present the model and the objectives of this study.

Our analysis relies on a model of driven tracer diffusion in a hard-core lattice gas, which appears as a minimal model that explicitly takes into account the dynamics of a bath of discrete particles: a TP driven by an external force performs a biased random walk in a bath of hardcore particles, which themselves perform symmetric random walks with the restriction that there it at most one particle per site. The resolution method introduced in this Chapter allows us to consider a more general situation than the one considered in the first part of this thesis. We assume that the lattice is in contact with a reservoir of particles, so that the bath particles present on the lattice may desorb back to the reservoir, and particles from the reservoir may adsorb onto vacant lattice sites. This so-called *Langmuir kinetics* is relevant to describe situations where a gas or a vapor is brought in contact with a solid surface, on which the gas particles may form an adsorbed layer. The transport properties of the adsorbed particles have been shown to control many different processes, such as spreading of molecular films on solid surfaces [24] or dewetting [97, 100]. The particular case where the Langmuir kinetics is coupled to a Totally Asymmetric Exclusion Process was investigated theoretically [98, 99], and has been show to be relevant to describe the directional motion of molecular motors on a cytoskeletal filament, with random attachment and detachment of the motors [57, 70].

The situation where a TP is biased in a bath of symmetric hardcore particles on a lattice in contact with a reservoir was first investigated in [14, 13, 15]. Studying the transport properties of the biased TP is actually a complex N-body problem, that cannot be solved exactly. Using a mean-field-type approximation consisting in the decoupling of relevant correlation functions, the authors proposed a method to compute the mean position of the TP in the long-time limit. Using an Einstein relation that was established rigorously [67], the diffusion coefficient of a symmetric TP was deduced in the limit of a small bias.

In this Chapter, we present an extension of the decoupling approximation allowing us to determine the equations verified by the fluctuations of the TP position for an arbitrary value of the bias. We also show that the approximation can be extended to obtain the distribution of the position of the TP. These equations will then be solved in the case of a one-dimensional lattice (Chapter 9) and in the case of higher-dimensional lattices (Chapter 10).

8.2 Model and master equation

8.2.1 Model

We consider a d-dimensional hypercubic lattice of spacing σ in contact with a reservoir of particles (see Fig. 8.1). We adopt a continuous-time description of the system. We assume that the particles in the reservoir may adsorb onto vacant lattice sites at a fixed rate f/τ^*. The adsorbed particles may move randomly along the lattice by hopping at a rate $1/(2d\tau^*)$ to any of $2d$ neighboring lattice sites, which process is constrained by a hard-core exclusion preventing multiple occupancy of any of the sites. The adsorbed particles may desorb from the lattice back to the reservoir at rate g/τ^*. The occupancy of lattice sites is described by the time-dependent Boolean variable $\eta_{\boldsymbol{r}}$, which takes two values, 1, if the site $\boldsymbol{r}$ is occupied by an adsorbed particle, and 0, otherwise. Note that the mean density of the bath

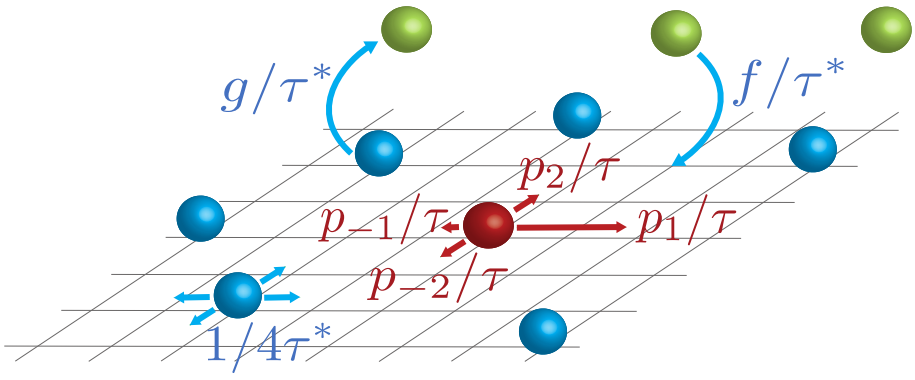

Figure 8.1: Model and notations in the two-dimensional (2D) case.

particles, $\langle \eta_{\boldsymbol{r}} \rangle$, approaches as $t \to \infty$ a constant value $\rho = f/(f+g)$ but the number of particles on the lattice is not explicitly conserved in such a dynamics. The case where the number of particles on the lattice is conserved can be retrieved by taking the limits $f \to 0$ and $g \to 0$ with a fixed value of the density $\rho = f/(f+g)$.

We also introduce a tracer particle (TP), whose position at time t is a time-dependent random variable denoted as $\boldsymbol{X}_t$. The TP dynamics is different from that of the adsorbed particles in two aspects: first, it can not desorb from the lattice and second, it is subject to an external driving force, which favors its jumps along the direction corresponding to the unit vector $\boldsymbol{e}_1$ of the lattice.

The TP dynamics is defined as follows: we suppose that the tracer, which occupies the site $\boldsymbol{X}_t$ at time t, waits an exponentially distributed time with mean τ, and then attempts to hop onto one of the $2d$ neighboring sites, $\boldsymbol{X}_t + \boldsymbol{e}_\mu$, where $\boldsymbol{e}_\mu$ is one of the $2d$ unit vectors $\{\boldsymbol{e}_{\pm 1}, \cdots, \boldsymbol{e}_{\pm d}\}$. For simplicity, we use the notation $\boldsymbol{e}_{-\nu} \equiv -\boldsymbol{e}_\nu$. The jump direction is chosen according to the probability p_ν. The model is valid for any choice of the jump probabilities. It can be convenient to assume that the bias originates from an external force $\boldsymbol{F} = F\boldsymbol{e}_1$, so that the jump probability in direction ν writes (see Section 2.2.1)

$$p_\nu = \frac{\mathrm{e}^{\frac{1}{2}\beta \boldsymbol{F}\cdot\boldsymbol{e}_\nu}}{\sum_{\mu\in\{\pm 1,\ldots\pm d\}} \mathrm{e}^{\frac{1}{2}\beta \boldsymbol{F}\cdot\boldsymbol{e}_\mu}} \tag{8.1}$$

where $\beta = 1/(k_{\mathrm{B}}T)$ is the inverse temperature, and will be taken equal to one. This choice of p_ν fulfills the detailed balance condition.

After the direction of the jump has been chosen, it is instantaneously fulfilled if the target site is vacant at this moment of time; otherwise, i.e., if the target site is occupied by any adsorbed particle, the jump is rejected and the tracer remains at its position.

8.2.2 Master equation

We begin by introducing some auxiliary definitions. Let $\eta \equiv \{\eta_{\boldsymbol{r}}\}$ denote the entire set of the occupation variables, which defines the instantaneous configuration of the adsorbed particles on the lattice at a given time moment. Next, let $P(\boldsymbol{X}, \eta; t)$ stand for the joint probability of finding at time t the TP at the site $\boldsymbol{X}$ and all adsorbed particles in the configuration η. Then, denoting as $\eta^{\boldsymbol{r},\nu}$ a configuration obtained from η by the Kawasaki-type [62] exchange of the occupation variables of two neighboring sites $\boldsymbol{r}$ and

$\boldsymbol{r}+\boldsymbol{e}_\nu$, and as $\hat{\eta}^{\boldsymbol{r}}$ - a configuration obtained from the original η by the replacement $\eta_{\boldsymbol{r}} \to 1-\eta_{\boldsymbol{r}}$, which corresponds to the Glauber-type [49] flip of the occupation variable due to the adsorption/desorption events, we have that the time evolution of the configuration probability $P(\boldsymbol{X},\eta;t)$ obeys the following master equation :

$$\begin{aligned} 2d\tau^*\partial_t P(\boldsymbol{X},\eta;t) = &\sum_{\mu=1}^{d}\sum_{\boldsymbol{r}\neq\boldsymbol{X}-\boldsymbol{e}_\mu,\boldsymbol{X}}\left[P(\boldsymbol{X},\eta^{\boldsymbol{r},\mu};t)-P(\boldsymbol{X},\eta;t)\right] \\ &+\frac{2d\tau^*}{\tau}\sum_{\mu}p_\mu\left[\left(1-\eta_{\boldsymbol{X}}\right)P(\boldsymbol{X}-\boldsymbol{e}_\mu,\eta;t)-\left(1-\eta_{\boldsymbol{X}+\boldsymbol{e}_\mu}\right)P(\boldsymbol{X},\eta;t)\right] \\ &+2dg\sum_{\boldsymbol{r}\neq\boldsymbol{X}}\left[\left(1-\eta_{\boldsymbol{r}}\right)P(\boldsymbol{X},\hat{\eta}^{\boldsymbol{r}};t)-\eta_{\boldsymbol{r}}P(\boldsymbol{X},\eta;t)\right] \\ &+2df\sum_{\boldsymbol{r}\neq\boldsymbol{X}}\left[\eta_{\boldsymbol{r}}P(\boldsymbol{X},\hat{\eta}^{\boldsymbol{r}};t)-\left(1-\eta_{\boldsymbol{r}}\right)P(\boldsymbol{X},\eta;t)\right]. \end{aligned} \tag{8.2}$$

The first term of the right-hand-side of (8.2) describes the diffusion of adsorbed particles, the second term corresponds to the diffusion of the TP, and the third and fourth terms are associated to the desorption and adsorption events of the bath particles.

If no otherwise specified, the sum over an index μ runs over the $2d$ elements $\{\pm1,\cdots,\pm d\}$. In what follows, the brackets $\langle\cdot\rangle$ denote an average over the TP position and bath particles configurations with weight $P(\boldsymbol{X},\eta;t)$, and $X_t=\boldsymbol{X}_t\cdot\boldsymbol{e}_1$ denotes the position of the TP along the direction of the external force.

8.3 Equations verified by the first cumulants

8.3.1 Mean position

The time evolution of the first moment $\langle X_t\rangle$ of the TP can be obtained by multiplying both sides of (8.2) by $(\boldsymbol{X}_t\cdot\boldsymbol{e}_1)$ and summing over all possible configurations $(\boldsymbol{X}_t,\eta)$. An alternative way to compute $\langle X_t\rangle$ is to write that during an infinitesimal time interval Δt, the TP position X_t evolves according to

$$X_{t+\Delta t}=\begin{cases} X_t+\sigma & \text{with probability } p_1(1-\eta_{\boldsymbol{X}_t+\boldsymbol{e}_1})\frac{\Delta t}{\tau}, \\ X_t-\sigma & \text{with probability } p_{-1}(1-\eta_{\boldsymbol{X}_t+\boldsymbol{e}_{-1}})\frac{\Delta t}{\tau}, \\ X_t & \text{with probability } 1-p_1(1-\eta_{\boldsymbol{X}_t+\boldsymbol{e}_1})\frac{\Delta t}{\tau}-p_{-1}(1-\eta_{\boldsymbol{X}_t+\boldsymbol{e}_{-1}})\frac{\Delta t}{\tau}, \end{cases} \tag{8.3}$$

and take the average of this equation. Both methods result in the following exact equation:

$$\frac{\mathrm{d}}{\mathrm{d}t}\langle X_t\rangle=\frac{\sigma}{\tau}\left[p_1\left(1-k_{\boldsymbol{e}_1}\right)-p_{-1}\left(1-k_{\boldsymbol{e}_{-1}}\right)\right], \tag{8.4}$$

where $k_{\boldsymbol{r}}\equiv\langle\eta_{\boldsymbol{X}_t+\boldsymbol{r}}\rangle$ is the probability of having at time t an adsorbed particle at position $\boldsymbol{r}$, defined in the frame of reference moving with the TP. In other words, $k_{\boldsymbol{r}}$ can be thought of as being the density profile in the adsorbed monolayer as seen from the moving TP. The trivial mean-field approximation of the expression of the derivative of $\langle X_t\rangle$ (8.4) is obtained by replacing all the local average densities $k_{\boldsymbol{r}}$ by the global density ρ. One obtains

$$\frac{\mathrm{d}}{\mathrm{d}t}\langle X_t\rangle=\frac{\sigma}{\tau}(p_1-p_{-1})(1-\rho). \tag{8.5}$$

A more accurate determination of the evolution of the mean position of the TP then relies on the calculation of the quantities $k_{\boldsymbol{e}_{\pm 1}}$, which are the mean density of bath particles at the sites in the vicinity of the TP. This actually requires the computation of the density profile $k_{\boldsymbol{r}}$ for arbitrary $\boldsymbol{r}$. The evolution equations for $k_{\boldsymbol{r}}$ may be obtained by multiplying the master equation (8.2) by $\eta_{\boldsymbol{X}+\boldsymbol{r}}$ and summing over all the configurations of $(\boldsymbol{X}, \eta)$. We get the following equation :

$$2d\tau^* \partial_t k_{\boldsymbol{r}} = \sum_{\mu} \left(\nabla_\mu - \delta_{\boldsymbol{r},\boldsymbol{e}_\mu} \nabla_{-\mu}\right) k_{\boldsymbol{r}} - 2d(f+g)k_{\boldsymbol{r}} + 2df + \frac{2d\tau^*}{\tau} \sum_{\nu} p_\nu \left\langle (1 - \eta_{\boldsymbol{X}_t+\boldsymbol{e}_\nu}) \nabla_\nu \eta_{\boldsymbol{X}_t+\boldsymbol{r}} \right\rangle, \tag{8.6}$$

where we define the operator ∇_μ acting on any space-dependent function f:

$$\nabla_\mu f(\boldsymbol{r}) = f(\boldsymbol{r} + \boldsymbol{e}_\mu) - f(\boldsymbol{r}). \tag{8.7}$$

(8.6) is not closed with respect to $k_{\boldsymbol{r}}$, but involves correlation functions $\left\langle \eta_{\boldsymbol{X}_t+\boldsymbol{e}_\mu} \eta_{\boldsymbol{X}_t+\boldsymbol{r}} \right\rangle$. Evolution equations for such correlation functions actually involve higher-order correlation functions. Consequently, we face the problem of solving an infinite hierarchy of coupled equations for the correlation functions. We then resort to a decoupling approximation, obtained by writing the occupation variables as $\eta_{\boldsymbol{R}} = \langle \eta_{\boldsymbol{R}} \rangle + \delta\eta_{\boldsymbol{R}}$, and by discarding the terms of order $(\delta\eta_{\boldsymbol{R}})^2$. We obtain

$$\begin{aligned} \left\langle \eta_{\boldsymbol{X}_t+\boldsymbol{r}} \eta_{\boldsymbol{X}_t+\boldsymbol{e}_\mu} \right\rangle &= \left\langle (\langle \eta_{\boldsymbol{X}_t+\boldsymbol{r}} \rangle + \delta\eta_{\boldsymbol{X}_t+\boldsymbol{r}})(\left\langle \eta_{\boldsymbol{X}_t+\boldsymbol{e}_\mu} \right\rangle + \delta\eta_{\boldsymbol{X}_t+\boldsymbol{e}_\mu}) \right\rangle & (8.8) \\ &\simeq \langle \eta_{\boldsymbol{X}_t+\boldsymbol{r}} \rangle \left\langle \eta_{\boldsymbol{X}_t+\boldsymbol{e}_\mu} \right\rangle & (8.9) \\ &\simeq k_{\boldsymbol{r}} k_{\boldsymbol{e}_\mu}, & (8.10) \end{aligned}$$

which is valid for $\boldsymbol{r} \neq \boldsymbol{e}_\mu$. This approximation then relies on the *decoupling* of the correlation functions $\left\langle \eta_{\boldsymbol{X}_t+\boldsymbol{r}} \eta_{\boldsymbol{X}_t+\boldsymbol{e}_\mu} \right\rangle$. It can be seen as a mean-field type approximation, and is the key assumption we use in our method for evaluating the cumulants of the TP position. This approximation will be shown to be very accurate in what follows.

Using this approximation in (8.6), we obtain

$$2d\tau^* \partial_t k_{\boldsymbol{r}} = \widetilde{L} k_{\boldsymbol{r}} + 2df, \tag{8.11}$$

if $\boldsymbol{r} \neq \boldsymbol{e}_\nu$. For the special sites $\boldsymbol{r} = \boldsymbol{e}_\nu$ with $\nu = \{\pm 1, \pm 2, \ldots, \pm d\}$ we find

$$2d\tau^* \partial_t k_{\boldsymbol{e}_\nu} = (\widetilde{L} + A_\nu) k_{\boldsymbol{e}_\nu} + 2df, \tag{8.12}$$

where $\widetilde{L}$ is the operator

$$\widetilde{L} \equiv \sum_{\mu} A_\mu \nabla_\mu - 2d(f+g), \tag{8.13}$$

and the coefficients A_μ are the quantities

$$A_\mu \equiv 1 + \frac{2d\tau^*}{\tau} p_\mu (1 - k_{\boldsymbol{e}_\mu}). \tag{8.14}$$

The occupation number of the origin is taken equal to zero by convention. Note that (8.12) represents, from the mathematical point of view, the boundary conditions for the general evolution equation (8.11), imposed on the sites in the immediate vicinity of the TP. (8.11) and (8.12) together with (8.14) thus constitute a closed system of equations which suffices for computation of all quantities of interest. These

equations were first obtained by Bénichou and collaborators, and solved in the case of a one-dimensional lattice [15] and of higher-dimensional lattices [14, 13].

The fluctuations of the TP position have not been studied yet in this context. In what follows, we give an extension of the decoupling approximation (8.10) which will allow us to find the equations verified by the fluctuations of the TP position.

8.3.2 Fluctuations of the TP position

The time evolution of the second moment $\langle {X_t}^2 \rangle$ is obtained by multiplying the master equation by $(\boldsymbol{X}_t \cdot \boldsymbol{e}_1)^2$, and averaging over the TP position and the bath configuration; or, alternatively, averaging the balance equation (8.3). The details of this calculation are given in Appendix J (Section J.1). We get

$$\begin{aligned} \frac{\mathrm{d}}{\mathrm{d}t}\langle {X_t}^2 \rangle &\equiv \frac{\mathrm{d}}{\mathrm{d}t}\left\langle (\boldsymbol{X}_t \cdot \boldsymbol{e}_1)^2 \right\rangle \\ &= \frac{2\sigma}{\tau}\left[p_1\left(\langle X_t \rangle - g_{\boldsymbol{e}_1}\right) - p_{-1}\left(\langle X_t \rangle - g_{\boldsymbol{e}_{-1}}\right)\right] \\ &\quad + \frac{\sigma^2}{\tau}\left[p_1\left(1 - k_{\boldsymbol{e}_1}\right) + p_{-1}\left(1 - k_{\boldsymbol{e}_{-1}}\right)\right], \end{aligned} \tag{8.15}$$

where $g_{\boldsymbol{r}} \equiv \langle X_t \, \eta_{\boldsymbol{X}_t + \boldsymbol{r}} \rangle$. Knowing that

$$\frac{\mathrm{d}}{\mathrm{d}t}\langle X_t \rangle^2 = 2\langle X_t \rangle \left(\frac{\mathrm{d}}{\mathrm{d}t}\langle X_t \rangle \right), \tag{8.16}$$

and using (8.4), we can deduce an expression for the second cumulant of the TP position in the first direction:

$$\frac{\mathrm{d}}{\mathrm{d}t}\left(\langle {X_t}^2 \rangle - \langle X_t \rangle^2 \right) = -\frac{2\sigma}{\tau}\left[p_1 \widetilde{g}_{\boldsymbol{e}_1} - p_{-1}\widetilde{g}_{\boldsymbol{e}_{-1}}\right] + \frac{\sigma^2}{\tau}\left[p_1(1 - k_{\boldsymbol{e}_1}) + p_{-1}(1 - k_{\boldsymbol{e}_{-1}})\right], \tag{8.17}$$

where

$$\widetilde{g}_{\boldsymbol{r}} \equiv \langle \delta X_t \delta \eta_{\boldsymbol{X}_t + \boldsymbol{r}} \rangle = \langle \delta X_t (\eta_{\boldsymbol{X}_t + \boldsymbol{r}} - \langle \eta_{\boldsymbol{X}_t + \boldsymbol{r}} \rangle) \rangle, \tag{8.18}$$

and where $\delta X_t \equiv X_t - \langle X_t \rangle$. In the simplest mean-field approximation, one has $k_{\boldsymbol{r}} = \rho$ and $\widetilde{g}_{\boldsymbol{r}} = 0$ for any $\boldsymbol{r}$. (8.17) then reduces to

$$\frac{\mathrm{d}}{\mathrm{d}t}\left(\langle {X_t}^2 \rangle - \langle X_t \rangle^2 \right) = \frac{\sigma^2}{\tau}(p_1 + p_{-1})(1 - \rho). \tag{8.19}$$

A more accurate determination of the evolution of the second cumulant then relies on the determination of the functions $\widetilde{g}_{\boldsymbol{e}_{\pm 1}}$. The evolution equations for $\widetilde{g}_{\boldsymbol{r}}$ may be obtained by multiplying the master equation (8.2) by $\delta X_t \eta_{\boldsymbol{X}_t + \boldsymbol{r}}$ and summing over all the configurations of $(\boldsymbol{X}_t, \eta)$. The details of the calculation are given in Appendix J (Section J.2). We get the following equation

$$\begin{aligned} 2d\tau^* \partial_t \widetilde{g}_{\boldsymbol{r}} = &\sum_{\mu} \left(\nabla_\mu - \delta_{\boldsymbol{r}, \boldsymbol{e}_\mu} \nabla_{-\mu} \right) \widetilde{g}_{\boldsymbol{r}} - 2d(f + g)\widetilde{g}_{\boldsymbol{r}} \\ &+ \frac{2d\tau^*}{\tau} \sum_{\mu} p_\mu \left\langle \delta X_t (1 - \eta_{\boldsymbol{X}_t + \boldsymbol{e}_\mu}) \nabla_\mu \eta_{\boldsymbol{X}_t + \boldsymbol{r}} \right\rangle \\ &+ \frac{2d\tau^*}{\tau} \sigma \left[p_1 \left\langle (1 - \eta_{\boldsymbol{X}_t + \boldsymbol{e}_1}) \eta_{\boldsymbol{X}_t + \boldsymbol{r} + \boldsymbol{e}_1} \right\rangle - p_{-1} \left\langle (1 - \eta_{\boldsymbol{X}_t + \boldsymbol{e}_{-1}}) \eta_{\boldsymbol{X}_t + \boldsymbol{r} + \boldsymbol{e}_{-1}} \right\rangle \right] \\ &- \frac{2d\tau^*}{\tau} \sigma \left[p_1(1 - k_{\boldsymbol{e}_1}) - p_{-1}(1 - k_{\boldsymbol{e}_{-1}}) \right] k_{\boldsymbol{r}}. \end{aligned} \tag{8.20}$$

We then notice that this evolution equation involves higher-order correlation functions, of the form $\left\langle \delta X_t \eta_{\boldsymbol{X}_t+\boldsymbol{r}} \eta_{\boldsymbol{X}_t+\boldsymbol{e}_\mu} \right\rangle$. As previously, their computation leads to an infinite hierarchy of coupled equations. We then write an extension of the decoupling approximation (8.10), obtained by writing $\eta_{\boldsymbol{R}} = \langle \eta_{\boldsymbol{R}} \rangle + \delta\eta_{\boldsymbol{R}}$ and discarding the terms of order $(\delta\eta_{\boldsymbol{R}})^2$. We find

$$\begin{aligned} \left\langle \delta X_t \eta_{\boldsymbol{X}_t+\boldsymbol{r}} \eta_{\boldsymbol{X}_t+\boldsymbol{e}_\mu} \right\rangle &\simeq \langle \eta_{\boldsymbol{X}_t+\boldsymbol{r}} \rangle \left\langle \delta X_t \eta_{\boldsymbol{X}_t+\boldsymbol{e}_\mu} \right\rangle + \langle \delta X_t \eta_{\boldsymbol{X}_t+\boldsymbol{r}} \rangle \left\langle \eta_{\boldsymbol{X}_t+\boldsymbol{e}_\mu} \right\rangle, & (8.21) \\ &= k_{\boldsymbol{r}} \widetilde{g}_{\boldsymbol{e}_\mu} + k_{\boldsymbol{e}_\mu} \widetilde{g}_{\boldsymbol{r}}, & (8.22) \end{aligned}$$

which is valid for $\boldsymbol{r} \neq \boldsymbol{e}_\nu$. Using this approximation in (8.20), we finally get the equation

$$2d\tau^* \partial_t \widetilde{g}_{\boldsymbol{r}} = \widetilde{L}\widetilde{g}_{\boldsymbol{r}} + \frac{2d\tau^*}{\tau}\sigma \left\{ p_1(1-k_{\boldsymbol{e}_1})\nabla_1 k_{\boldsymbol{r}} - p_{-1}(1-k_{\boldsymbol{e}_{-1}})\nabla_{-1} k_{\boldsymbol{r}} \right\} - \frac{2d\tau^*}{\tau} \sum_\mu p_\mu \widetilde{g}_{\boldsymbol{e}_\mu} \nabla_\mu k_{\boldsymbol{r}}, \tag{8.23}$$

which holds for all $\boldsymbol{r}$, except for $\boldsymbol{r} = \{\boldsymbol{0}, \boldsymbol{e}_{\pm 1}, \ldots, \boldsymbol{e}_{\pm d}\}$. On the other hand, for the special sites $\boldsymbol{r} = \boldsymbol{e}_\nu$ with $\nu = \{\pm 1, \ldots, \pm d\}$, we find

$$\begin{aligned} 2d\tau^* \partial_t \widetilde{g}_{\boldsymbol{e}_\nu} =& (\widetilde{L} + A_\nu)\widetilde{g}_{\boldsymbol{e}_\nu} + \frac{2d\tau^*}{\tau}\sigma \left\{ p_1(1-k_{\boldsymbol{e}_1})\nabla_1 k_{\boldsymbol{e}_\nu} - p_{-1}(1-k_{\boldsymbol{e}_{-1}})\nabla_{-1} k_{\boldsymbol{e}_\nu} \right\} \\ &- \frac{2d\tau^*}{\tau} p_\nu \widetilde{g}_{\boldsymbol{e}_\nu} k_{\boldsymbol{e}_\nu} - \frac{2d\tau^*}{\tau} \sum_\mu p_\mu \widetilde{g}_{\boldsymbol{e}_\mu} \nabla_\mu k_{\boldsymbol{e}_\nu}. \end{aligned} \tag{8.24}$$

(8.23) and (8.24) then form a closed system of equations for the quantities $\widetilde{g}_{\boldsymbol{r}}$, provided that the quantities $k_{\boldsymbol{e}_\nu}$ are known. The quantities $\widetilde{g}_{\boldsymbol{e}_{\pm 1}}$ can be deduced from these equations, and one can compute the evolution of the fluctuations of the TP position using (8.17).

8.3.3 Stationary values

We turn to the limit $t \to \infty$. We assume that the quantities $k_{\boldsymbol{r}}$ and $\widetilde{g}_{\boldsymbol{r}}$ have stationary values, so that

$$\begin{aligned} \lim_{t\to\infty} \partial_t k_{\boldsymbol{r}} &= 0, & (8.25) \\ \lim_{t\to\infty} \partial_t \widetilde{g}_{\boldsymbol{r}} &= 0. & (8.26) \end{aligned}$$

We will use the simplified notations:

$$\begin{aligned} k_{\boldsymbol{r}} &= \lim_{t\to\infty} k_{\boldsymbol{r}}(t), & (8.27) \\ \widetilde{g}_{\boldsymbol{r}} &= \lim_{t\to\infty} \widetilde{g}_{\boldsymbol{r}}(t), & (8.28) \\ A_\mu &= \lim_{t\to\infty} A_\mu(t). & (8.29) \end{aligned}$$

We also define the observables:

$$\begin{aligned} V &\equiv \lim_{t\to\infty} \frac{\mathrm{d}}{\mathrm{d}t} \langle X_t \rangle, & (8.30) \\ K &\equiv \lim_{t\to\infty} \frac{1}{2d} \frac{\mathrm{d}}{\mathrm{d}t} \left(\left\langle {X_t}^2 \right\rangle - \langle X_t \rangle^2 \right) & (8.31) \end{aligned}$$

so that V and K represent respectively the velocity and the dispersion coefficient of the TP in the stationary state. Using (8.4), V can be written in terms of functions $k_{\boldsymbol{r}}$ and $\widetilde{g}_{\boldsymbol{r}}$:

$$V = \frac{\sigma}{\tau} \left\{ p_1 \left(1 - k_{\boldsymbol{e}_1}\right) - p_{-1} \left(1 - k_{\boldsymbol{e}_{-1}}\right) \right\}. \tag{8.32}$$

Similarly, using (8.17),

$$K = \frac{\sigma^2}{2d\tau}\left[p_1\left(1-k_{\boldsymbol{e}_1}\right)+p_{-1}\left(1-k_{\boldsymbol{e}_{-1}}\right)\right]-\frac{\sigma}{d\tau}\left(p_1\widetilde{g}_{\boldsymbol{e}_1}-p_{-1}\widetilde{g}_{\boldsymbol{e}_{-1}}\right). \tag{8.33}$$

Consequently, the existence of stationary values for $k_{\boldsymbol{r}}$ and $\widetilde{g}_{\boldsymbol{r}}$, that will be demonstrated later on by the study of the equations they verify, implies that the mean and the fluctuations of the position of the TP grow linearly with time in the long-time limit.

The quantities $k_{\boldsymbol{r}}$ are determined by the stationary limit of (8.11) and (8.12) :

$$\begin{cases} \widetilde{L}k_{\boldsymbol{r}}+2df=0 & \text{for } \boldsymbol{r}\notin\{\boldsymbol{0},\boldsymbol{e}_{\pm1},\dots,\boldsymbol{e}_{\pm d}\} \\ (\widetilde{L}+A_\nu)k_{\boldsymbol{e}_\nu}+2df=0 & \text{for } \nu\in\{\pm1,\dots,\pm d\}. \end{cases} \tag{8.34}$$

Similarly, using (8.23) and (8.24), the quantities $\widetilde{g}_{\boldsymbol{r}}$ obey the stationary equations

$$\widetilde{L}\widetilde{g}_{\boldsymbol{r}}+\frac{2d\tau^*}{\tau}\sigma\left\{p_1(1-k_{\boldsymbol{e}_1})\nabla_1 k_{\boldsymbol{r}}-p_{-1}(1-k_{\boldsymbol{e}_{-1}})\nabla_{-1}k_{\boldsymbol{r}}\right\}-\frac{2d\tau^*}{\tau}\sum_\mu p_\mu\widetilde{g}_{\boldsymbol{e}_\mu}\nabla_\mu k_{\boldsymbol{r}}=0 \tag{8.35}$$

for $\boldsymbol{r}\notin\{\boldsymbol{0},\boldsymbol{e}_{\pm1},\dots,\boldsymbol{e}_{\pm d}\}$, and :

$$(\widetilde{L}+A_\nu)\widetilde{g}_{\boldsymbol{e}_\nu}+\frac{2d\tau^*}{\tau}\sigma\left\{p_1(1-k_{\boldsymbol{e}_1})\nabla_1 k_{\boldsymbol{e}_\nu}-p_{-1}(1-k_{\boldsymbol{e}_{-1}})\nabla_{-1}k_{\boldsymbol{e}_\nu}\right\} \tag{8.36}$$

$$-\frac{2d\tau^*}{\tau}p_\nu\widetilde{g}_{\boldsymbol{e}_\nu}k_{\boldsymbol{e}_\nu}-\frac{2d\tau^*}{\tau}\sum_\mu p_\mu\widetilde{g}_{\boldsymbol{e}_\mu}\nabla_\mu k_{\boldsymbol{e}_\nu}=0 \tag{8.37}$$

for $\nu=\{\pm1,\dots,\pm d\}$.

Note that these equations are valid in the stationary limit, for any dimension, and allow to compute the velocity and dispersion coefficient of the TP under the approximations (8.10) and (8.22) presented above. Their solutions will be presented in the case of a one-dimensional system (Chapter 9) and in higher dimensions (Chapter 10).

8.4 Cumulant generating function

8.4.1 Governing equations

In the previous Sections, using a decoupling approximation, we were able to determine the stationary equations verified by the quantities $k_{\boldsymbol{r}}=\langle\eta_{\boldsymbol{r}}\rangle$ and $\widetilde{g}_{\boldsymbol{r}}=\langle\delta X_t\delta\eta_{X_t+\boldsymbol{r}}\rangle$, which are involved in the expression of the stationary velocity V (8.32) and of the stationary diffusion coefficient K (8.33) of the TP. We also aim to calculate the higher-order cumulants of X_t, defined by

$$\kappa_1^{(n)}(t)\equiv\frac{1}{\mathrm{i}^n}\left.\frac{\partial^n\Psi(t)}{\partial u^n}\right|_{u=0} \tag{8.38}$$

where the quantity

$$\Psi(t)\equiv\ln\left\langle\mathrm{e}^{\mathrm{i}uX_t}\right\rangle \tag{8.39}$$

is known as the second characteristic function (or cumulant generating function) of X_t. The index 1 in the notation $\kappa_1^{(n)}(t)$ indicates that we study the projection of the TP position $\boldsymbol{X}_t$ in the direction of the bias. Using the balance equation (8.3), we get the relation

$$\begin{aligned}\left\langle \mathrm{e}^{\mathrm{i}uX_{t+\Delta t}}\right\rangle &= \left\langle \mathrm{e}^{\mathrm{i}u(X_t+\sigma)}\frac{\Delta t}{\tau}p_1(1-\eta_{\boldsymbol{X}_t+\boldsymbol{e}_1})\right\rangle + \left\langle \mathrm{e}^{\mathrm{i}u(X_t-\sigma)}\frac{\Delta t}{\tau}p_{-1}(1-\eta_{\boldsymbol{X}_t+\boldsymbol{e}_{-1}})\right\rangle \\ &+ \left\langle \mathrm{e}^{\mathrm{i}uX_t}\left[1-\frac{\Delta t}{\tau}(p_1(1-\eta_{\boldsymbol{X}_t+\boldsymbol{e}_1})+p_{-1}(1-\eta_{\boldsymbol{X}_t+\boldsymbol{e}_{-1}})\right]\right\rangle . \end{aligned} \tag{8.40}$$

Note that this equation involves two different averages: an average over the direction of the step taken by the TP, and an average the realizations. (8.40) leads to

$$\frac{\mathrm{d}}{\mathrm{d}t}\left\langle \mathrm{e}^{\mathrm{i}uX_t}\right\rangle = \frac{p_1}{\tau}\left(\mathrm{e}^{\mathrm{i}u\sigma}-1\right)\left\langle \mathrm{e}^{\mathrm{i}uX_t}(1-\eta_{\boldsymbol{X}_t+\boldsymbol{e}_1})\right\rangle + \frac{p_{-1}}{\tau}\left(\mathrm{e}^{-\mathrm{i}u\sigma}-1\right)\left\langle \mathrm{e}^{\mathrm{i}uX_t}(1-\eta_{\boldsymbol{X}_t+\boldsymbol{e}_{-1}})\right\rangle , \tag{8.41}$$

and, using the definition of $\Psi(t)$:

$$\frac{\mathrm{d}\Psi}{\mathrm{d}t} = \frac{1}{\left\langle \mathrm{e}^{\mathrm{i}uX_t}\right\rangle}\frac{\mathrm{d}}{\mathrm{d}t}\left\langle \mathrm{e}^{\mathrm{i}uX_t}\right\rangle \tag{8.42}$$

$$= \frac{p_1}{\tau}\left(\mathrm{e}^{\mathrm{i}u\sigma}-1\right)\left[1-\frac{\left\langle \mathrm{e}^{\mathrm{i}uX_t}\eta_{\boldsymbol{X}_t+\boldsymbol{e}_1}\right\rangle}{\left\langle \mathrm{e}^{\mathrm{i}uX_t}\right\rangle}\right] + \frac{p_{-1}}{\tau}\left(\mathrm{e}^{-\mathrm{i}u\sigma}-1\right)\left[1-\frac{\left\langle \mathrm{e}^{\mathrm{i}uX_t}\eta_{\boldsymbol{X}_t+\boldsymbol{e}_{-1}}\right\rangle}{\left\langle \mathrm{e}^{\mathrm{i}uX_t}\right\rangle}\right]. \tag{8.43}$$

We define

$$w_{\boldsymbol{r}} \equiv \left\langle \mathrm{e}^{\mathrm{i}uX_t}\eta_{\boldsymbol{X}_t+\boldsymbol{r}}\right\rangle \quad \text{and} \quad \widetilde{w}_{\boldsymbol{r}} \equiv \frac{\left\langle \mathrm{e}^{\mathrm{i}uX_t}\eta_{\boldsymbol{X}_t+\boldsymbol{r}}\right\rangle}{\left\langle \mathrm{e}^{\mathrm{i}uX_t}\right\rangle}. \tag{8.44}$$

Finally,

$$\frac{\mathrm{d}\Psi}{\mathrm{d}t} = \frac{p_1}{\tau}\left(\mathrm{e}^{\mathrm{i}u\sigma}-1\right)\left(1-\widetilde{w}_{\boldsymbol{e}_1}\right) + \frac{p_{-1}}{\tau}\left(\mathrm{e}^{-\mathrm{i}u\sigma}-1\right)\left(1-\widetilde{w}_{\boldsymbol{e}_{-1}}\right). \tag{8.45}$$

Assuming that the quantities $\widetilde{w}_{\boldsymbol{e}_1}$ and $\widetilde{w}_{\boldsymbol{e}_{-1}}$ reach stationary values when $t\to\infty$ (see 8.4.2 for a presentation of the evolution equations verified by $\widetilde{w}_{\boldsymbol{r}}$), the second characteristic function has the following asymptotic behavior :

$$\Psi(t) \underset{t\to\infty}{\sim} \Phi(u)t \tag{8.46}$$

with

$$\Phi(u) = \frac{p_1}{\tau}\left(\mathrm{e}^{\mathrm{i}u\sigma}-1\right)\left(1-\widetilde{w}_{\boldsymbol{e}_1}\right) + \frac{p_{-1}}{\tau}\left(\mathrm{e}^{-\mathrm{i}u\sigma}-1\right)\left(1-\widetilde{w}_{\boldsymbol{e}_{-1}}\right). \tag{8.47}$$

The relation (8.46) indicates that all the cumulants of X_t are linear with time in the long-time limit. In particular, this implies that the n-th moment of the rescaled variable $Z_t = (X_t - \langle X_t\rangle)/\sqrt{\langle {X_t}^2\rangle - \langle X_t\rangle^2}$ scales as $t^{1-n/2}$ in the long-time limit. All the moments of Z_t of order greater than 2 vanish when $t\to\infty$, and Z_t is distributed accordingly to a Gaussian distribution at large times.

In addition, our calculation allows us to compute the full distribution of X_t in the long-time limit. Assuming that the u-dependance of $\widetilde{w}_{\boldsymbol{e}_{\pm1}}$ is known (see Section 8.4.2), we can derive from these equations the probability density function $P_t(x) \equiv \mathrm{Prob}[X_t = x]$ as follows. The quantity $\left\langle \mathrm{e}^{\mathrm{i}uX_t}\right\rangle = \mathrm{e}^{\Psi(t)}$ is defined by

$$\left\langle \mathrm{e}^{\mathrm{i}uX_t}\right\rangle = \sum_{x=-\infty}^{\infty} P_t(x)\mathrm{e}^{\mathrm{i}ux}. \tag{8.48}$$

$\mathrm{e}^{\Psi(t)}$ is then the Fourier transform of the p.d.f. $P_t(x)$, which can be obtained by the inverse Fourier transform:

$$P_t(x) = \int_{-\pi}^{\pi} \frac{\mathrm{d}u}{2\pi} \mathrm{e}^{-\mathrm{i}ux} \mathrm{e}^{\Psi(t)}, \tag{8.49}$$

and, using the expression of $\Psi(t)$ of the long-time limit (8.46) and (8.47),

$$P_t(x) \underset{t\to\infty}{\sim} \int_{-\pi}^{\pi} \frac{\mathrm{d}u}{2\pi} \exp\left\{ \frac{p_1 t}{\tau}(\mathrm{e}^{\mathrm{i}u\sigma} - 1)(1 - \widetilde{w}_{\boldsymbol{e}_1}) + \frac{p_{-1} t}{\tau}(\mathrm{e}^{-\mathrm{i}u\sigma} - 1)(1 - \widetilde{w}_{\boldsymbol{e}_{-1}}) - \mathrm{i}ux \right\}. \tag{8.50}$$

Consequently, it suffices to determine the u-dependance of $\widetilde{w}_{\pm 1}$ to obtain the p.d.f. of the TP position. In what follows, we establish the evolution equations for the quantities $\widetilde{w}_{\boldsymbol{r}}$ starting again from the master equation (8.2).

8.4.2 Evolution equations of the quantities $\widetilde{w}_{\boldsymbol{r}}$

The evolution equation of $w_{\boldsymbol{r}}$ (defined by (8.44)) can be obtained by multiplying both sides of the master equation (8.2) by the quantity $\eta_{\boldsymbol{X}_t+\boldsymbol{r}}\mathrm{e}^{\mathrm{i}uX_t}$ and averaging with respect to η and $\boldsymbol{X}_t$. Extending the method used to derive the evolution equations of the correlation functions $\widetilde{g}_{\boldsymbol{r}}$ starting from the master equation (8.2) (see Appendix J, Section J.2), it is found that $w_{\boldsymbol{r}}$ obeys the following exact equation:

$$\begin{aligned} 2d\tau^* \partial_t w_{\boldsymbol{r}} = &\left(\sum_\mu \nabla_\mu - \delta_{\boldsymbol{r},\boldsymbol{e}_\mu} \nabla_{-\mu} \right) w_{\boldsymbol{r}} - 2d(f+g) w_{\boldsymbol{r}} + 2df \left\langle \mathrm{e}^{\mathrm{i}uX_t} \right\rangle \\ &+ \frac{2d\tau^*}{\tau} \sum_\mu p_\mu \left\langle \mathrm{e}^{\mathrm{i}uX_t} (1 - \eta_{\boldsymbol{X}_t+\boldsymbol{e}_\mu}) \nabla_\mu \eta_{\boldsymbol{X}_t+\boldsymbol{r}} \right\rangle \\ &+ \frac{2d\tau^*}{\tau} p_1 \left(\mathrm{e}^{\mathrm{i}u\sigma} - 1\right) \left\langle \mathrm{e}^{\mathrm{i}uX_t} (1 - \eta_{\boldsymbol{X}_t+\boldsymbol{e}_1}) \eta_{\boldsymbol{X}_t+\boldsymbol{r}+\boldsymbol{e}_1} \right\rangle \\ &+ \frac{2d\tau^*}{\tau} p_{-1} \left(\mathrm{e}^{-\mathrm{i}u\sigma} - 1\right) \left\langle \mathrm{e}^{\mathrm{i}uX_t} (1 - \eta_{\boldsymbol{X}_t+\boldsymbol{e}_{-1}}) \eta_{\boldsymbol{X}_t+\boldsymbol{r}+\boldsymbol{e}_1} \right\rangle. \end{aligned} \tag{8.51}$$

We then make the following decoupling hypothesis:

$$\begin{aligned} \left\langle \left(\mathrm{e}^{\mathrm{i}uX_t} - \left\langle \mathrm{e}^{\mathrm{i}uX_t} \right\rangle\right) \eta_{\boldsymbol{X}_t+\boldsymbol{r}} \eta_{\boldsymbol{X}_t+\boldsymbol{e}_\mu} \right\rangle \simeq &\left\langle \left(\mathrm{e}^{\mathrm{i}uX_t} - \left\langle \mathrm{e}^{\mathrm{i}uX_t} \right\rangle\right) \eta_{\boldsymbol{X}_t+\boldsymbol{r}} \right\rangle \left\langle \eta_{\boldsymbol{X}_t+\boldsymbol{e}_\mu} \right\rangle \\ &+ \left\langle \left(\mathrm{e}^{\mathrm{i}uX_t} - \left\langle \mathrm{e}^{\mathrm{i}uX_t} \right\rangle\right) \eta_{\boldsymbol{X}_t+\boldsymbol{e}_\mu} \right\rangle \left\langle \eta_{\boldsymbol{X}_t+\boldsymbol{r}} \right\rangle, \end{aligned} \tag{8.52}$$

which is valid for $\boldsymbol{r} \neq \boldsymbol{e}_\nu$. This is equivalent to

$$\left\langle \mathrm{e}^{\mathrm{i}uX_t} \eta_{\boldsymbol{X}_t+\boldsymbol{r}} \eta_{\boldsymbol{X}_t+\boldsymbol{r}'} \right\rangle \simeq w_{\boldsymbol{r}} k_{\boldsymbol{r}'} + k_{\boldsymbol{r}} w_{\boldsymbol{r}'} - \left\langle \mathrm{e}^{\mathrm{i}uX_t} \right\rangle k_{\boldsymbol{r}} k_{\boldsymbol{r}'}. \tag{8.53}$$

This decoupling approximation is an extension of the approximations (8.10) and (8.22): it is obtained by writing the occupation variables as $\eta_{\boldsymbol{R}} = \langle \eta_{\boldsymbol{R}} \rangle + \delta\eta_{\boldsymbol{R}}$, and discarding the terms of order $(\delta\eta_{\boldsymbol{R}})^2$. Developing (8.53) at order 0 and 1 in u, one notices that it allows to retrieve the decoupling approximations made for the correlation functions $\left\langle \eta_{\boldsymbol{X}_t+\boldsymbol{r}} \eta_{\boldsymbol{X}_t+\boldsymbol{e}_\mu} \right\rangle$ (8.10) and $\left\langle \delta X_t \eta_{\boldsymbol{X}_t+\boldsymbol{r}} \eta_{\boldsymbol{X}_t+\boldsymbol{e}_\mu} \right\rangle$ (8.22). Using

this approximation in equation (8.51), we obtain for $\boldsymbol{r} \neq \boldsymbol{e}_\nu$,

$$\begin{aligned} 2d\tau^*\partial_t w_{\boldsymbol{r}} &= \widetilde{L} w_{\boldsymbol{r}} + 2df\left\langle \mathrm{e}^{\mathrm{i}uX_t}\right\rangle + \frac{2d\tau^*}{\tau}\sum_\mu p_\mu\left(k_{\boldsymbol{e}_\mu}\left\langle \mathrm{e}^{\mathrm{i}uX_t}\right\rangle - w_{\boldsymbol{e}_\mu}\right)\nabla_\mu k_{\boldsymbol{r}} \\ &+ \frac{2d\tau^*}{\tau}p_1\left(\mathrm{e}^{\mathrm{i}u\sigma}-1\right)\left[w_{\boldsymbol{r}+\boldsymbol{e}_1}(1-k_{\boldsymbol{e}_1}) + k_{\boldsymbol{r}+\boldsymbol{e}_1}\left(\left\langle \mathrm{e}^{\mathrm{i}uX_t}\right\rangle k_{\boldsymbol{e}_1} - w_{\boldsymbol{e}_1}\right)\right] \\ &+ \frac{2d\tau^*}{\tau}p_{-1}\left(\mathrm{e}^{-\mathrm{i}u\sigma}-1\right)\left[w_{\boldsymbol{r}+\boldsymbol{e}_{-1}}(1-k_{\boldsymbol{e}_{-1}}) + k_{\boldsymbol{r}+\boldsymbol{e}_{-1}}\left(\left\langle \mathrm{e}^{\mathrm{i}uX_t}\right\rangle k_{\boldsymbol{e}_{-1}} - w_{\boldsymbol{e}_{-1}}\right)\right]. \end{aligned} \tag{8.54}$$

For $\boldsymbol{r} = \boldsymbol{e}_\nu$, the evolution equation becomes :

$$\begin{aligned} 2d\tau^*\partial_t w_{\boldsymbol{e}_\nu} &= (\widetilde{L} + A_\nu) w_{\boldsymbol{e}_\nu} + 2df\left\langle \mathrm{e}^{\mathrm{i}uX_t}\right\rangle + \frac{2d\tau^*}{\tau}\sum_{\mu\neq\pm\nu} p_\mu\left(k_{\boldsymbol{e}_\mu}\left\langle \mathrm{e}^{\mathrm{i}uX_t}\right\rangle - w_{\boldsymbol{e}_\mu}\right)\nabla_\mu k_{\boldsymbol{e}_\nu} \\ &+ \frac{2d\tau^*}{\tau}p_\nu\left(k_{\boldsymbol{e}_\nu}\left\langle \mathrm{e}^{\mathrm{i}uX_t}\right\rangle - w_{\boldsymbol{e}_\nu}\right)k_{2\boldsymbol{e}_\nu} - \frac{2d\tau^*}{\tau}p_{-\nu}\left(k_{\boldsymbol{e}_\nu}\left\langle \mathrm{e}^{\mathrm{i}uX_t}\right\rangle - w_{\boldsymbol{e}_\nu}\right)k_{\boldsymbol{e}_\nu} \\ &+ \frac{2d\tau^*}{\tau}p_1\left(\mathrm{e}^{\mathrm{i}u\sigma}-1\right)\left[w_{\boldsymbol{e}_\nu+\boldsymbol{e}_1}(1-k_{\boldsymbol{e}_1}) + k_{\boldsymbol{e}_\nu+\boldsymbol{e}_1}\left(\left\langle \mathrm{e}^{\mathrm{i}uX_t}\right\rangle k_{\boldsymbol{e}_1} - w_{\boldsymbol{e}_1}\right)\right] \\ &+ \frac{2d\tau^*}{\tau}p_{-1}\left(\mathrm{e}^{-\mathrm{i}u\sigma}-1\right)\left[w_{\boldsymbol{e}_\nu+\boldsymbol{e}_{-1}}(1-k_{\boldsymbol{e}_{-1}}) + k_{\boldsymbol{e}_\nu+\boldsymbol{e}_{-1}}\left(\left\langle \mathrm{e}^{\mathrm{i}uX_t}\right\rangle k_{\boldsymbol{e}_{-1}} - w_{\boldsymbol{e}_{-1}}\right)\right]. \end{aligned} \tag{8.55}$$

In order to write these equations in terms of the variable $\widetilde{w}$, we notice that :

$$\begin{aligned} \frac{\partial \widetilde{w}_{\boldsymbol{r}}}{\partial t} &= \frac{1}{\left\langle \mathrm{e}^{\mathrm{i}uX_t}\right\rangle}\frac{\partial w_{\boldsymbol{r}}}{\partial t} - \frac{w_{\boldsymbol{r}}}{\left\langle \mathrm{e}^{\mathrm{i}uX_t}\right\rangle}\frac{1}{\left\langle \mathrm{e}^{\mathrm{i}uX_t}\right\rangle}\frac{\partial\left\langle \mathrm{e}^{\mathrm{i}uX_t}\right\rangle}{\partial t} \\ &= \frac{1}{\left\langle \mathrm{e}^{\mathrm{i}uX_t}\right\rangle}\frac{\partial w_{\boldsymbol{r}}}{\partial t} - \widetilde{w}_{\boldsymbol{r}}\frac{\partial \Psi}{\partial t} \\ &= \frac{1}{\left\langle \mathrm{e}^{\mathrm{i}uX_t}\right\rangle}\frac{\partial w_{\boldsymbol{r}}}{\partial t} - \widetilde{w}_{\boldsymbol{r}}\left[\frac{p_1}{\tau}\left(\mathrm{e}^{\mathrm{i}u\sigma}-1\right)(1-\widetilde{w}_{\boldsymbol{e}_1}) + \frac{p_{-1}}{\tau}\left(\mathrm{e}^{-\mathrm{i}u\sigma}-1\right)(1-\widetilde{w}_{\boldsymbol{e}_1})\right]. \end{aligned} \tag{8.56}$$

Finally, we divide the evolution equations (8.54) and (8.55) by $\left\langle \mathrm{e}^{\mathrm{i}uX_t}\right\rangle$ and obtain the evolution equations for $\widetilde{w}_{\boldsymbol{r}}$, for $\boldsymbol{r} \neq \mathbf{e_\nu}$:

$$\begin{aligned} 2d\tau^*\partial_t \widetilde{w}_{\boldsymbol{r}} &= \widetilde{L}\widetilde{w}_{\boldsymbol{r}} + 2df + \frac{2d\tau^*}{\tau}\sum_\mu p_\mu\left(k_{\boldsymbol{e}_\mu} - \widetilde{w}_{\boldsymbol{e}_\mu}\right)\nabla_\mu k_{\boldsymbol{r}} \\ &+ \frac{2d\tau^*}{\tau}p_1\left(\mathrm{e}^{\mathrm{i}u\sigma}-1\right)\left[\nabla_1\widetilde{w}_{\boldsymbol{r}} - k_{\boldsymbol{e}_1}(\widetilde{w}_{\boldsymbol{r}+\boldsymbol{e}_1} - k_{\boldsymbol{r}+\boldsymbol{e}_1}) - \widetilde{w}_{\boldsymbol{e}_1}(k_{\boldsymbol{r}+\boldsymbol{e}_1} - \widetilde{w}_{\boldsymbol{r}})\right] \\ &+ \frac{2d\tau^*}{\tau}p_1\left(\mathrm{e}^{-\mathrm{i}u\sigma}-1\right)\left[\nabla_{-1}\widetilde{w}_{\boldsymbol{r}} - k_{\boldsymbol{e}_{-1}}(\widetilde{w}_{\boldsymbol{r}+\boldsymbol{e}_{-1}} - k_{\boldsymbol{r}+\boldsymbol{e}_{-1}}) - \widetilde{w}_{\boldsymbol{e}_{-1}}(k_{\boldsymbol{r}+\boldsymbol{e}_{-1}} - \widetilde{w}_{\boldsymbol{r}})\right], \end{aligned} \tag{8.57}$$

and for $\boldsymbol{r} = \mathbf{e_\nu}$:

$$
\begin{aligned}
2d\tau^* \partial_t \widetilde{w}_{\boldsymbol{e}_\nu} &= (\widetilde{L} + A_\nu)\widetilde{w}_{\boldsymbol{e}_\nu} + 2df + \frac{2d\tau^*}{\tau} \sum_{\mu \neq \pm\nu} p_\mu \left(k_{\boldsymbol{e}_\mu} - \widetilde{w}_{\boldsymbol{e}_\mu}\right) \nabla_\mu k_{\boldsymbol{e}_\nu} \\
&+ \frac{2d\tau^*}{\tau} p_\nu \left(k_{\boldsymbol{e}_\nu} - \widetilde{w}_{\boldsymbol{e}_\nu}\right) k_{2\boldsymbol{e}_\nu} - \frac{2d\tau^*}{\tau} p_{-\nu} \left(k_{\boldsymbol{e}_\nu} - \widetilde{w}_{\boldsymbol{e}_\nu}\right) k_{\boldsymbol{e}_\nu} \\
&+ \frac{2d\tau^*}{\tau} p_1 \left(\mathrm{e}^{\mathrm{i}u\sigma} - 1\right) \left[\nabla_1 \widetilde{w}_{\boldsymbol{e}_\nu} - k_{\boldsymbol{e}_1}(\widetilde{w}_{\boldsymbol{e}_\nu + \boldsymbol{e}_1} - k_{\boldsymbol{e}_\nu + \boldsymbol{e}_1}) - \widetilde{w}_{\boldsymbol{e}_1}(k_{\boldsymbol{e}_\nu + \boldsymbol{e}_1} - \widetilde{w}_{\boldsymbol{e}_\nu})\right] \\
&+ \frac{2d\tau^*}{\tau} p_1 \left(\mathrm{e}^{-\mathrm{i}u\sigma} - 1\right) \left[\nabla_{-1} \widetilde{w}_{\boldsymbol{e}_\nu} - k_{\boldsymbol{e}_{-1}}(\widetilde{w}_{\boldsymbol{e}_\nu + \boldsymbol{e}_{-1}} - k_{\boldsymbol{e}_\nu + \boldsymbol{e}_{-1}}) - \widetilde{w}_{\boldsymbol{e}_{-1}}(k_{\boldsymbol{e}_\nu + \boldsymbol{e}_{-1}} - \widetilde{w}_{\boldsymbol{e}_\nu})\right] .
\end{aligned}
\tag{8.58}
$$

These equations can in principle be solved in the stationary limit where $\lim_{t\to\infty} \widetilde{w}_{\boldsymbol{r}}$, by setting $\partial_t \widetilde{w}_{\boldsymbol{r}} = 0$ in (8.57) and (8.58) and obtaining the values of $\widetilde{w}_{\boldsymbol{r}}$ satisfying these equations. In particular, this allows us to obtain the u-dependance of the functions $\widetilde{w}_{\boldsymbol{e}_{\pm 1}}$ and to deduce $P_t(x)$ from (8.50). This will be made explicit in the case of a one-dimensional lattice in Chapter 9. We also notice that the computation of the functions $\widetilde{w}_{\boldsymbol{r}}$ can be used to compute higher-order cumulants. In particular, we give in the next Section the evolution equation verified by the third cumulant of the position of the TP.

8.4.3 Application: Third-order cumulant

We now use (8.57) and (8.58) describing the evolution of $\widetilde{w}_{\boldsymbol{r}}$ to calculate the third order cumulant. We define the coefficient γ by the relation :

$$
\gamma \equiv \lim_{t\to\infty} \frac{1}{6} \frac{\mathrm{d}}{\mathrm{d}t} \Big\langle (X_t - \langle X_t \rangle)^3 \Big\rangle . \tag{8.59}
$$

Recalling the definition of $\Psi(t)$ (8.39), we get the following expansion in powers of u:

$$
\Psi(t) \underset{u\to 0}{=} \mathrm{i}u \langle X_t \rangle + \frac{(\mathrm{i}u)^2}{2} \Big\langle (X_t - \langle X_t \rangle)^2 \Big\rangle + \frac{(\mathrm{i}u)^3}{6} \Big\langle (X_t - \langle X_t \rangle)^3 \Big\rangle + \dots . \tag{8.60}
$$

In the long-time limit, and using the definitions of V (8.30), K (8.33) and γ (8.59), one gets

$$
\lim_{t\to\infty} \frac{\mathrm{d}\Psi}{\mathrm{d}t} = \mathrm{i}uV + (\mathrm{i}u)^2 dK + (\mathrm{i}u)^3 \gamma + \dots \tag{8.61}
$$

We define $\widetilde{m}_{\boldsymbol{r}}$ by the relation

$$
\widetilde{m}_{\boldsymbol{r}} \equiv \left\langle (X_t - \langle X_t \rangle)^2 \eta_{\boldsymbol{X}_t + \boldsymbol{r}} \right\rangle - k_{\boldsymbol{r}} \left[\left\langle {X_t}^2 \right\rangle - \langle X_t \rangle^2 \right] . \tag{8.62}
$$

so that the expansion of $\widetilde{w}$ in powers of u writes

$$
\widetilde{w}_{\boldsymbol{r}} = k_{\boldsymbol{r}} + iu\widetilde{g}_{\boldsymbol{r}} + \frac{(iu)^2}{2} \widetilde{m}_{\boldsymbol{r}} + \mathcal{O}\left(u^3\right) , \tag{8.63}
$$

where we used the definitions of $k_{\boldsymbol{r}} = \langle \eta_{\boldsymbol{X}_t + \boldsymbol{r}} \rangle$ and $\widetilde{g}_{\boldsymbol{r}} = \langle \delta X_t \delta \eta_{\boldsymbol{X}_t + \boldsymbol{r}} \rangle$. Developing both sides of equation (8.45) up to order 3 in u in the limit $t \to \infty$ and using (8.61), one gets the following expression for γ :

$$
\gamma = \frac{p_1 \sigma}{\tau} \left[\frac{1}{6}\sigma^2 (1 - k_{\boldsymbol{e}_1}) - \frac{1}{2}\sigma \widetilde{g}_{\boldsymbol{e}_1} - \frac{1}{2} \widetilde{m}_{\boldsymbol{e}_1} \right] - \frac{p_{-1}\sigma}{\tau} \left[\frac{1}{6}\sigma^2 (1 - k_{\boldsymbol{e}_{-1}}) + \frac{1}{2}\sigma \widetilde{g}_{\boldsymbol{e}_{-1}} - \frac{1}{2} \widetilde{m}_{\boldsymbol{e}_{-1}} \right] \tag{8.64}
$$

According to (8.63), the general evolution equations for $\widetilde{w}$ (8.57) and (8.58) developed at order 2 in u then give the evolution equations of $\widetilde{m}$. We get:

- for $\boldsymbol{r} \neq \mathbf{e_\nu}$:

$$\begin{aligned} 2d\tau^*\partial_t\widetilde{m}_{\boldsymbol{r}} &= \widetilde{L}\widetilde{m}_{\boldsymbol{r}} - \frac{2d\tau^*}{\tau}\sum_\mu p_\mu \widetilde{m}_{\boldsymbol{e}_\mu}\nabla_\mu k_{\boldsymbol{r}} \\ &+ \frac{2d\tau^*}{\tau}p_1\sigma\left\{2\left[(1-k_{\boldsymbol{e}_1})\nabla_1\widetilde{g}_{\boldsymbol{r}} - \widetilde{g}_{\boldsymbol{e}_1}\nabla_1 k_{\boldsymbol{r}}\right] + \sigma(1-k_{\boldsymbol{e}_1})\nabla_1 k_{\boldsymbol{r}}\right\} \\ &+ \frac{2d\tau^*}{\tau}p_{-1}\sigma\left\{-2\left[(1-k_{\boldsymbol{e}_{-1}})\nabla_{-1}\widetilde{g}_{\boldsymbol{r}} - \widetilde{g}_{\boldsymbol{e}_{-1}}\nabla_{-1}k_{\boldsymbol{r}}\right] + \sigma(1-k_{\boldsymbol{e}_{-1}})\nabla_{-1}k_{\boldsymbol{r}}\right\}. \end{aligned} \quad (8.65)$$

- for $\boldsymbol{r} = \boldsymbol{e}_\nu$:

$$\begin{aligned} 2d\tau^*\partial_t\widetilde{m}_{\boldsymbol{e}_\nu} &= (\widetilde{L}+A_\nu)\widetilde{m}_{\boldsymbol{e}_1} - \frac{2d\tau^*}{\tau}\sum_{\mu\neq\pm\nu} p_\mu\widetilde{m}_{\boldsymbol{e}_\mu}\nabla_\mu k_{\boldsymbol{e}_1} \\ &- \frac{2d\tau^*}{\tau}p_\nu\widetilde{m}_{\boldsymbol{e}_\nu}k_{2\boldsymbol{e}_\nu} + \frac{2d\tau^*}{\tau}p_{-\nu}\widetilde{m}_{\boldsymbol{e}_{-\nu}}k_{\boldsymbol{e}_\nu} \\ &+ \frac{2d\tau^*}{\tau}p_1\sigma\left\{2\left[(1-k_{\boldsymbol{e}_1})\nabla_1\widetilde{g}_{\boldsymbol{e}_\nu} - \widetilde{g}_{\boldsymbol{e}_1}\nabla_1 k_{\boldsymbol{e}_\nu}\right] + \sigma(1-k_{\boldsymbol{e}_1})\nabla_1 k_{\boldsymbol{e}_\nu}\right\} \\ &+ \frac{2d\tau^*}{\tau}p_{-1}\sigma\left\{-2\left[(1-k_{\boldsymbol{e}_{-1}})\nabla_{-1}\widetilde{g}_{\boldsymbol{e}_\nu} - \widetilde{g}_{\boldsymbol{e}_{-1}}\nabla_{-1}k_{\boldsymbol{e}_\nu}\right] + \sigma(1-k_{\boldsymbol{e}_{-1}})\nabla_{-1}k_{\boldsymbol{e}_\nu}\right\} \end{aligned} \quad (8.66)$$

These equations can be solved in the stationary limit, in order to obtain an expression of $\widetilde{m}_{\boldsymbol{e}_{\pm1}}$ and then an expression of γ from (8.64). This will be made explicit in the case of a one-dimensional lattice in Chapter 9.

8.5 Conclusion

In this Chapter, we studied the model of a biased TP in a lattice gas in contact with a reservoir of particles. This model has been studied in previous works: an evolution equation for the mean position of the TP was obtained, involving the mean density profiles $k_{\boldsymbol{r}} = \langle \eta_{\boldsymbol{X}_t+\boldsymbol{r}}\rangle$. The quantities $k_{\boldsymbol{r}}$ could be given as the solutions of a closed set of equations by resorting to a mean-field-type decoupling approximation.

We generalized this method and obtained an evolution equation for the fluctuations of the TP, written in terms of the correlation functions $\widetilde{g}_{\boldsymbol{r}} = \langle \delta X_t \delta\eta_{\boldsymbol{X}_t+\boldsymbol{r}}\rangle$. Extending the decoupling approximation, we obtained a closed set of equations governing the correlations functions $\widetilde{g}_{\boldsymbol{r}}$. We finally extended the decoupling approximation in order to obtain the evolution equations of the quantities $\widetilde{w}_{\boldsymbol{r}} = \left\langle \mathrm{e}^{\mathrm{i}uX_t}\eta_{\boldsymbol{X}_t+\boldsymbol{r}}\right\rangle / \left\langle \mathrm{e}^{\mathrm{i}uX_t}\right\rangle$, involved in the expression of the cumulant generating function. We deduced from this function an evolution equation for the third cumulant of the position of the TP.

Consequently, with the solutions of the equations verified by $k_{\boldsymbol{r}}$, $\widetilde{g}_{\boldsymbol{r}}$ and $\widetilde{w}_{\boldsymbol{r}}$, one can compute the velocity of the TP, its diffusion coefficient, and the distribution of its position. In the next Chapter, we solve these equations in the particular case of a one-dimensional lattice in contact with a reservoir.

CHAPTER 9

One-dimensional lattice in contact with a reservoir

Contents

We show that the equations verified by the correlation functions involved in the calculation of the first three cumulants of the TP position can be solved in the stationary limit, in the particular situation where the lattice is one-dimensional. The analysis of these solutions leads to striking observations. In a wide range of parameters, the diffusion coefficient of the TP is a nonmonotonic function of the density, and may actually be greater in the presence of bath particles than at zero density. We also show that the distribution of the TP can be negatively skewed. Finally, we obtain the implicit equations involving the functions $\widetilde{w}_r$, allowing the computation of the distribution of the TP position. All these analytical predictions are compared with Monte-Carlo simulations.

Some results from this Chapter were published in [P1].

9.1 Introduction

In the previous Chapter, we studied a general d-dimensional lattice in contact with a reservoir of particles. Two types of particles were present on the lattice:

- bath particles, contained in a reservoir, which may adsorb on vacant lattice sites with a fixed rate f/τ^*. They move randomly on the lattice, and jump on each of the $2d$ neighboring sites at a rate $1/(2d\tau^*)$, with the restriction that each site is occupied by at most one particle. These particles may desorb and go back to the reservoir with a rate g/τ^*.
- a tracer particle, which waits an exponentially distributed time with mean τ, and which jumps on the neighboring sites with asymmetric jump probabilities $(p_\nu)_{\nu\in\{\pm1,\dots,\pm d\}}$.

The position of the tracer $\boldsymbol{X}_t$ is a random variable, and we denote by $X_t = \boldsymbol{X}_t \cdot \boldsymbol{e}_1$ its projection in the direction of the applied force. In the previous Chapter, using a mean-field type approximation, we obtained the expressions of the first cumulants of the TP:

- the first cumulant of the distribution $\langle X_t\rangle$, which is related to the TP velocity V, defined by

$$V \equiv \lim_{t\to\infty} \frac{\mathrm{d}}{\mathrm{d}t} \langle X_t\rangle = \frac{\sigma}{\tau}\left[p_1\left(1-k_{\boldsymbol{e}_1}\right) - p_{-1}\left(1-k_{\boldsymbol{e}_{-1}}\right)\right], \tag{9.1}$$

  where the quantities $k_{\boldsymbol{r}} = \langle \eta_{\boldsymbol{X}_t+\boldsymbol{r}}\rangle$ are the solutions of (8.11) and (8.12).

- the second cumulant of the distribution $\left\langle (X_t - \langle X_t\rangle)^2\right\rangle$, which is related to the TP diffusion coefficient K, defined by

$$K \equiv \lim_{t\to\infty} \frac{1}{2d}\frac{\mathrm{d}}{\mathrm{d}t}\left(\left\langle {X_t}^2\right\rangle - \langle X_t\rangle^2\right) \tag{9.2}$$

$$= \frac{\sigma^2}{2d\tau}\left[p_1(1-k_{\boldsymbol{e}_1}) + p_{-1}(1-k_{\boldsymbol{e}_{-1}})\right] - \frac{\sigma}{d\tau}\left[p_1\widetilde{g}_{\boldsymbol{e}_1} - p_{-1}\widetilde{g}_{\boldsymbol{e}_{-1}}\right], \tag{9.3}$$

  where we defined the correlation functions $\widetilde{g}_{\boldsymbol{r}} = \langle \delta X_t(\eta_{\boldsymbol{X}_t+\boldsymbol{r}} - \langle \eta_{\boldsymbol{X}_t+\boldsymbol{r}}\rangle)\rangle$, which are the solutions of (8.23) and (8.24).

- the third cumulant $\left\langle (X_t - \langle X_t\rangle)^3\right\rangle$, from which we may compute the skewness of the distribution, and for which we define the coefficient γ:

$$\gamma = \lim_{t\to\infty} \frac{1}{6}\frac{\mathrm{d}}{\mathrm{d}t}\left\langle (X_t - \langle X_t\rangle)^3\right\rangle \tag{9.4}$$

$$= \frac{p_1\sigma}{\tau}\left[\frac{1}{6}\sigma^2(1-k_{\boldsymbol{e}_1}) - \frac{1}{2}\sigma\widetilde{g}_{\boldsymbol{e}_1} - \frac{1}{2}\widetilde{m}_{\boldsymbol{e}_1}\right] - \frac{p_{-1}\sigma}{\tau}\left[\frac{1}{6}\sigma^2(1-k_{\boldsymbol{e}_{-1}}) + \frac{1}{2}\sigma\widetilde{g}_{\boldsymbol{e}_{-1}} - \frac{1}{2}\widetilde{m}_{\boldsymbol{e}_{-1}}\right] \tag{9.5}$$

  where the coefficients $\widetilde{m}_{\boldsymbol{r}}$ are defined by $\widetilde{m}_{\boldsymbol{r}} = \left\langle (\delta X_t)^2(\eta_{\boldsymbol{X}_t+\boldsymbol{r}} - \langle \eta_{\boldsymbol{X}_t+\boldsymbol{r}}\rangle)\right\rangle$ and are the solutions of (8.65) and (8.66).

We also determined the expression of the TP distribution function $P_t(x) = \mathrm{Prob}[X_t = x]$ (8.50), as a function of the quantities $\widetilde{w}_{\boldsymbol{r}} \equiv \left\langle \mathrm{e}^{\mathrm{i}uX_t}\eta_{\boldsymbol{X}_t+\boldsymbol{r}}\right\rangle / \left\langle \mathrm{e}^{\mathrm{i}uX_t}\right\rangle$, solutions of (8.57) and (8.58).

In this Chapter, we focus on the one-dimensional version of this model. In this situation, we solve the equations verified by the quantities $k_{\boldsymbol{r}}$, $\widetilde{g}_{\boldsymbol{r}}$, $\widetilde{m}_{\boldsymbol{r}}$ and $\widetilde{w}_{\boldsymbol{r}}$. We then obtain the expression of the first three cumulants of X_t in the long-time limit, as well as an expression of its probability distribution function. We show that the dependence on the different parameters of the first cumulants is not trivial, and gives rise to surprising effects. In particular, the diffusion coefficient K is shown to be a nonmonotonic function of the density ρ, and reaches a maximum for a nonzero value of ρ. These observations are confirmed by numerical simulations, which also allow us to discuss the validity of the decoupling approximation.

9.2 First cumulants of the TP position in one dimension

9.2.1 Solution of the equation on k_r in one dimension

The solutions of the equations verified by $k_{\boldsymbol{r}}$ have already been presented [15] and we recall it here for completeness. In one dimension, we adopt the simplified notation $k_{\boldsymbol{r}} = k_{n\boldsymbol{e}_1} \equiv k_n$. The system verified by $k_{\boldsymbol{r}}$ (8.34) is then a second order recurrence relation on the quantities k_n. Its solution has the following form:

$$k_n = \begin{cases} \rho + K_+ {r_1}^n & \text{for } n > 0, \\ \rho + K_- {r_2}^n & \text{for } n < 0. \end{cases} \tag{9.6}$$

where

$$r_1 = \frac{A_1 + A_{-1} + 2(f+g) - \sqrt{\Big(A_1 + A_{-1} + 2(f+g)\Big)^2 - 4A_1A_{-1}}}{2A_1}, \tag{9.7}$$

and

$$r_2 = \frac{A_1 + A_{-1} + 2(f+g) + \sqrt{\Big(A_1 + A_{-1} + 2(f+g)\Big)^2 - 4A_1A_{-1}}}{2A_1}, \tag{9.8}$$

while the amplitudes $K_\pm$ are given respectively by

$$K_+ = \rho \frac{A_1 - A_{-1}}{A_{-1} - A_1 r_1}, \tag{9.9}$$

and

$$K_- = \rho \frac{A_1 - A_{-1}}{A_{-1}/r_2 - A_1}. \tag{9.10}$$

Note that $r_2 > r_1$, and consequently, the local density past the TP approaches its non-perturbed value ρ slower than in front of it; this signifies that correlations between the TP position and particle distribution are stronger past the TP. Next, K_+ is always positive, while K_- is always negative; this means that the density profile is characterized by a jammed region in front of the TP, in which the local density is higher than ρ, and a depleted region past the TP in which the density is lower than ρ.

One obtains a system of two closed-form non-linear equations determing implicitly the unknown parameters A_1 and A_{-1}, which allows to compute the TP terminal velocity, related to $A_{\pm 1}$ through

$$V = \frac{\sigma}{2\tau^*}(A_1 - A_{-1}). \tag{9.11}$$

Substituting (9.6) into the definition of A_μ (8.14), we find

$$A_1 = 1 + \frac{2p_1\tau^*}{\tau}\left[1-\rho-\rho\frac{A_1-A_{-1}}{A_{-1}/r_1 - A_1}\right], \tag{9.12}$$

$$A_{-1} = 1 + \frac{2p_{-1}\tau^*}{\tau}\left[1-\rho-\rho\frac{A_1-A_{-1}}{A_{-1} - A_1 r_2}\right]. \tag{9.13}$$

For a given set of parameters (f, g, σ, τ, τ^* and p_1), the numerical resolution of this system leads to the values of A_1 and A_{-1} and then, using (9.11), to the value of the stationary velocity of the TP. This approximated value of the stationary velocity will be compared to numerical simulations in Section 9.3.2.

9.2.2 Solution of the equation on $\widetilde{g}_r$ in one dimension

We now go one step further and determine the dispersion coefficient K. This in turn requires the knowledge of the $\widetilde{g}_r$ function. For simplicity, we adopt the notations $\widetilde{g}_{\boldsymbol{\lambda}} = \widetilde{g}_{ne_1} = \widetilde{g}_n$. Using the expressions of k_n (9.6) , the general equations satisfied by $\widetilde{g}_n$ (8.23) and (8.24) become:

- for $n > 1$:

$$\begin{aligned} & A_1(\widetilde{g}_{n+1}-\widetilde{g}_n) + A_{-1}(\widetilde{g}_{n-1}-\widetilde{g}_n) - 2(f+g)\widetilde{g}_n \\ + \;& \frac{2\tau^*}{\tau}\sigma\left\{p_1 K_+ r_1^n\left(1-\rho-K_+r_1-\frac{\widetilde{g}_1}{\sigma}\right)(r_1-1)\right. \\ - \;& \left. p_{-1}K_+r_1^n\left(1-\rho-K_+r_1+\frac{\widetilde{g}_{-1}}{\sigma}\right)(r_1^{-1}-1)\right\} = 0, \end{aligned} \tag{9.14}$$

- for $n < -1$:

$$\begin{aligned} & A_1(\widetilde{g}_{n+1}-\widetilde{g}_n) + A_{-1}(\widetilde{g}_{n-1}-\widetilde{g}_n) - 2(f+g)\widetilde{g}_n \\ + \;& \frac{2\tau^*}{\tau}\sigma\left\{p_1 K_- r_2^n\left(1-\rho-K_+r_1-\frac{\widetilde{g}_1}{\sigma}\right)(r_2-1)\right. \\ - \;& \left. p_{-1}K_-r_2^n\left(1-\rho-K_+r_1+\frac{\widetilde{g}_{-1}}{\sigma}\right)(r_2^{-1}-1)\right\} = 0, \end{aligned} \tag{9.15}$$

- $\widetilde{g}_1$ and $\widetilde{g}_{-1}$ may be computed using the following boundary conditions:

$$\begin{aligned} & A_1\widetilde{g}_2 - \widetilde{g}_1\left(A_{-1}+2(f+g)+\frac{2\tau^*}{\tau}p_1(\rho+K_+r_1^2)\right) + \frac{2\tau^*}{\tau}p_{-1}(\rho+K_+r_1)\widetilde{g}_{-1} \\ = \;& -\frac{2\tau^*}{\tau}\sigma p_1(1-\rho-K_+r_1)(\rho+K_+r_1^2) \\ + \;& \frac{2\tau^*}{\tau}\sigma(p_1(1-\rho-K_+r_1)-p_{-1}(1-\rho-K_-r_2^{-1}))(\rho+K_+r_1), \end{aligned} \tag{9.16}$$

$$\begin{aligned} & A_{-1}\widetilde{g}_{-2} - \widetilde{g}_{-1}\left(A_1+2(f+g)+\frac{2\tau^*}{\tau}p_{-1}(\rho+K_-r_2^{-2})\right) + \frac{2\tau^*}{\tau}p_1(\rho+K_-r_2^{-1})\widetilde{g}_1 \\ = \;& \frac{2\tau^*}{\tau}\sigma p_{-1}(1-\rho-K_-r_2^{-1})(\rho+K_-r_2^{-2}) \\ + \;& \frac{2\tau^*}{\tau}\sigma(p_1(1-\rho-K_+r_1)-p_{-1}(1-\rho-K_-r_2^{-1}))(\rho+K_-r_2^{-1}). \end{aligned} \tag{9.17}$$

The general solution of (9.14) and (9.15) can be written:

$$\widetilde{g}_n = \alpha r_1^n - \frac{W}{A_1 r_1 - A_{-1} r_1^{-1}} n r_1^n \quad \text{for } n > 0, \tag{9.18}$$

and

$$\widetilde{g}_n = \beta r_2^n - \frac{W'}{A_1 r_2 - A_{-1} r_2^{-1}} n r_2^n \quad \text{for } n < 0, \tag{9.19}$$

where α and β are constants to be determined, and where

$$W \equiv K_+ \frac{2\tau^*}{\tau}\sigma \left\{ p_1 \left(1 - \rho - K_+ r_1 - \frac{\widetilde{g}_1}{\sigma}\right)(r_1 - 1) - p_{-1}\left(1 - \rho - K_+ r_1 + \frac{\widetilde{g}_{-1}}{\sigma}\right)(r_1^{-1} - 1)\right\} \tag{9.20}$$

$$W' \equiv K_- \frac{2\tau^*}{\tau}\sigma \left\{ p_1 \left(1 - \rho - K_+ r_1 - \frac{\widetilde{g}_1}{\sigma}\right)(r_2 - 1) - p_{-1}\left(1 - \rho - K_+ r_1 + \frac{\widetilde{g}_{-1}}{\sigma}\right)(r_2^{-1} - 1)\right\}. \tag{9.21}$$

Substituting (9.18) into (9.16), (9.19) into (9.17) on the one hand, and writing (9.18) for $n = 1$ and (9.19) for $n = -1$ on the other hand, leads to a linear system of four equations satisfied by the four unknowns α, β, $\widetilde{g}_1$ and $\widetilde{g}_{-1}$, which is straightforward to solve. The explicit expressions of $\widetilde{g}_1$ and $\widetilde{g}_{-1}$ are given in Appendix K (Section K.1). Note that they rely on the determination of the quantities $K_\pm$ and r_1, r_2, which can be determined numerically for a given set of parameters with the method detailed in Section 9.2.1. Finally, for a given set of parameter, one can deduce the values of $\widetilde{g}_{\pm 1}$ and the value of the diffusion coefficient using (9.3). Note that this calculation also gives access to the behavior of the cross-correlations functions $\widetilde{g}_{\boldsymbol{r}}$ through (9.18) and (9.19).

In Section 9.3.3, we investigate the dependence of K in the different parameters of the problem. We confront the analytical prediction from the decoupling approximation to results from numerical simulations.

9.2.3 Solution of the equation on $\widetilde{m}_{\boldsymbol{r}}$ in one dimension

We finally present a method to compute the correlation functions $\widetilde{m}_{\boldsymbol{e}_{\pm 1}}$ (8.62) involved in the computation of the stationary limit of the coefficient γ, defined in (9.5). Starting from the general equations verified by $\widetilde{m}_{\boldsymbol{r}}$ and valid in any dimension (8.65) and (8.66), we study the one-dimensional case. For simplicity, we write $\widetilde{m}_{\boldsymbol{r}} = \widetilde{m}_{n\boldsymbol{e}_1} = \widetilde{m}_n$. The quantities $\widetilde{m}_n$ are the solutions of the equation presented below:

- for $\boldsymbol{\lambda} \neq \boldsymbol{r}$, i.e. using (8.65) one gets :

$$A_1(\widetilde{m}_{n+1} - \widetilde{m}_n) + A_{-1}(\widetilde{m}_{n-1} - \widetilde{m}_n) - 2(f+g)\widetilde{m}_n = S(n) \tag{9.22}$$

  where $S(n)$ can be expressed explicitly in terms of the functions k_n and $\widetilde{g}_n$, determined respectively in Sections 9.2.1 and 9.2.2. For $n > 0$, we write $S(n)$ under the following form :

$$S(n) = (C_1^+ + nC_2^+) r_1^n \tag{9.23}$$

with

$$\begin{aligned}
C_1^+ &= \frac{2\tau^*}{\tau}\left[p_1\widetilde{m}_1K_+(r_1-1)+p_{-1}\widetilde{m}_{-1}K_+(r_1^{-1}-1)\right]\\
&- \frac{2\tau^*}{\tau}p_1\sigma\left\{2[(1-k_1)(\alpha r_1-\alpha' r_1-\alpha)-\widetilde{g}_1K_+(r_1-1)]+\sigma(1-k_1)K_+(r_1-1)\right\}\\
&- \frac{2\tau^*}{\tau}p_{-1}\sigma\left\{-2[(1-k_{-1})(\alpha r_1^{-1}+\alpha' r_1^{-1}-\alpha)-\widetilde{g}_{-1}K_+(r_1^{-1}-1)]+\sigma(1-k_{-1})K_+(r_1^{-1}-1)\right\}\\
&\equiv \frac{2\tau^*}{\tau}\left[p_1\widetilde{m}_1K_+(r_1-1)+p_{-1}\widetilde{m}_{-1}K_+(r_1^{-1}-1)\right]+\psi_+, \qquad (9.24)\\
C_2^+ &= -\frac{4\tau^*}{\tau}\sigma\alpha'[p_1(1-k_1)(1-r_1)-p_{-1}(1-k_{-1})(1-r_1^{-1})]. \qquad (9.25)
\end{aligned}$$

Consequently, the solution of (9.22) reads:

$$\widetilde{m}_n = \gamma r_1^n + (a_+n^2+b_+n)r_1^n, \qquad (9.26)$$

with

$$\begin{aligned}
a_+ &= \frac{1}{2}\frac{C_2^+}{A_1r_1-A_{-1}r_1^{-1}}, \qquad (9.27)\\
b_+ &= \frac{1}{A_1r_1-A_{-1}r_1^{-1}}[C_1^+-a_+(A_1r_1+A_{-1}r_1^{-1}]. \qquad (9.28)
\end{aligned}$$

For $n<0$, a similar resolution leads to:

$$\widetilde{m}_n = \delta r_2^n + (a_-n^2+b_-n)r_2^n, \qquad (9.29)$$

with

$$\begin{aligned}
a_- &= \frac{1}{2}\frac{C_2^-}{A_1r_2-A_{-1}r_2^{-1}}, \qquad (9.30)\\
b_- &= \frac{1}{A_1r_2-A_{-1}r_2^{-1}}[C_1^--a_-(A_1r_2+A_{-1}r_2^{-1}], \qquad (9.31)
\end{aligned}$$

and

$$\begin{aligned}
C_1^- &= \frac{2\tau^*}{\tau}\left[p_1\widetilde{m}_1K_-(r_2-1)+p_{-1}\widetilde{m}_{-1}K_-(r_2^{-1}-1)\right]\\
&- \frac{2\tau^*}{\tau}p_1\sigma\left\{2[(1-k_1)(\beta r_2-\beta' r_2-\beta)-\widetilde{g}_1K_-(r_2-1)]+\sigma(1-k_1)K_-(r_2-1)\right\}\\
&- \frac{2\tau^*}{\tau}p_{-1}\sigma\left\{-2[(1-k_{-1})(\beta r_2^{-1}+\beta' r_2^{-1}-\beta)-\widetilde{g}_{-1}K_-(r_2^{-1}-1)]+\sigma(1-k_{-1})K_-(r_2^{-1}-1)\right\}\\
&\equiv \frac{2\tau^*}{\tau}\left[p_1\widetilde{m}_1K_-(r_2-1)+p_{-1}\widetilde{m}_{-1}K_-(r_2^{-1}-1)\right]+\psi_-, \qquad (9.32)\\
C_2^- &= -\frac{4\tau^*}{\tau}\sigma\beta'[p_1(1-k_1)(1-r_2)-p_{-1}(1-k_{-1})(1-r_2^{-1})]. \qquad (9.33)
\end{aligned}$$

- for $\boldsymbol{r} = \boldsymbol{e}_1$:

$$0 = A_1\widetilde{m}_2 - \widetilde{m}_1\left(A_{-1} + 2(f+g) + \frac{2\tau^*}{\tau}p_1k_2\right) + \frac{2\tau^*}{\tau}p_{-1}\widetilde{m}_{-1}k_1 + \varphi_1, \tag{9.34}$$

with

$$\begin{aligned}\varphi_1 &= \frac{2d\tau^*}{\tau}p_1\left\{2\sigma\left[(\widetilde{g}_2-\widetilde{g}_1)(1-k_1)-\widetilde{g}_1(k_2-k_1)\right]+\sigma^2(k_2-k_1)(1-k_1)\right\}\\ &+ \frac{2d\tau^*}{\tau}p_{-1}\left\{-2\sigma\left[-\widetilde{g}_1(1-k_{-1})+\widetilde{g}_{-1}k_1\right]-\sigma^2k_1(1-k_{-1})\right\}.\end{aligned} \tag{9.35}$$

- for $\boldsymbol{r} = \boldsymbol{e}_{-1}$:

$$0 = A_{-1}\widetilde{m}_{-2} - \widetilde{m}_{-1}\left(A_1 + 2(f+g) + \frac{2\tau^*}{\tau}p_{-1}k_{-2}\right) + \frac{2\tau^*}{\tau}p_1\widetilde{m}_1k_{-1} + \varphi_{-1}, \tag{9.36}$$

with

$$\begin{aligned}\varphi_{-1} &= \frac{2d\tau^*}{\tau}p_{-1}\left\{-2\sigma\left[-\widetilde{g}_{-1}(1-k_1)+\widetilde{g}_1k_{-1}\right]-\sigma^2k_{-1}(1-k_1)\right\}\\ &+ \frac{2d\tau^*}{\tau}p_{-1}\left\{2\sigma\left[(\widetilde{g}_{-2}-\widetilde{g}_{-1})(1-k_{-1})-\widetilde{g}_{-1}(k_{-2}-k_{-1})\right]+\sigma^2(k_{-2}-k_{-1})(1-k_{-1})\right\}.\end{aligned} \tag{9.37}$$

Writing (9.26) for $n = 1$, (9.29) for $n = -1$, and considering (9.34) and (9.36) leads to a linear system of four equations with unknowns $\widetilde{m}_1$, $\widetilde{m}_{-1}$, γ and δ :

$$\begin{bmatrix} r_1 & 0 & M_{13} & M_{14} \\ 0 & r_2^{-1} & M_{23} & M_{24} \\ A_1r_1^2 & 0 & M_{33} & M_{34} \\ 0 & A_{-1}r_2^{-2} & M_{43} & M_{44} \end{bmatrix} \begin{bmatrix} \gamma \\ \delta \\ \widetilde{m}_1 \\ \widetilde{m}_{-1} \end{bmatrix} = \begin{bmatrix} Y_1 \\ Y_2 \\ Y_3 \\ Y_4 \end{bmatrix} \tag{9.38}$$

where the expressions of the quantities M_{ij} and Y_j are given in Appendix K.3. Finally:

$$\begin{aligned}\widetilde{m}_1 =& \frac{1}{\det M}\left[(M_{44}M_{22}-M_{42}M_{24})(M_{11}Y_3+M_{31}Y_1)\right.\\ &\left.+(M_{34}M_{11}-M_{31}M_{14})(M_{42}Y_2+M_{22}Y_4)\right],\end{aligned} \tag{9.39}$$

$$\begin{aligned}\widetilde{m}_{-1} =& \frac{1}{\det M}\left[(M_{43}M_{22}-M_{42}M_{23})(M_{11}Y_3+M_{31}Y_1)\right.\\ &\left.+(M_{33}M_{11}-M_{13}M_{31})(M_{42}Y_2+M_{22}Y_4)\right].\end{aligned} \tag{9.40}$$

The procedure to compute the coefficient γ for a given set of parameters is the following. With the method presented in Section 9.2.1, one can compute numerically the quantities $K_\pm$, r_1, r_2 and $k_{\pm1}$ for a given set of parameters. Using the expressions of $\widetilde{g}_{\pm1}$ given in Appendix K (Section K.1), one deduces the values cross-correlation functions $\widetilde{g}_{\pm1}$. Finally, with (9.39) and (9.40), we obtain $\widetilde{m}_{\pm1}$. The coefficient γ is deduced from its definition (9.5).

In the next Section, we use the methods presented above to compute the velocity V, the diffusion coefficient K and the coefficient γ to study their dependence on the different parameters of the problem. These results, which were obtained using a mean-field-type approximation, are confronted to numerical simulations which exactly sample the master equation of the problem (8.2).

9.3 Results and discussion

9.3.1 Algorithm and numerical methods

In order to verify the accuracy of the approximation involved in the computation of the TP cumulants, we perform numerical simulations. We use a kinetic Monte-Carlo (or Gillespie) algorithm [120, 47] in order to get an exact sampling of the master equation (8.2) describing the dynamics of the system. This method consists in generating a sequence of random numbers (τ, x, μ) with the joint probability density function $p(\tau, x, \mu)$ where $p(\tau, x, \mu)\mathrm{d}\tau$ is the probability at time t that the next event occurs in the infinitesimal time interval $[t+\tau, t+\tau+\mathrm{d}\tau]$, at site x, and is of type μ (i.e. a diffusion event, an absorption event or a desorption event). We write

$$p(\tau, x, \mu) = p_1(\tau)p_2(x|\tau)p_3(\mu|, x, \tau) \tag{9.41}$$

where

- $p_1(\tau)\mathrm{d}\tau$ is the probability at time t that the next event occurs in the time interval $[t+\tau, t+\tau+\mathrm{d}\tau]$.
- $p_2(x|\tau)\mathrm{d}\tau$ is the probability that the next event occurs at site x, knowing that it occurs during the time interval $[t+\tau, t+\tau+\mathrm{d}\tau]$.
- $p_3(\mu|, x, \tau)\mathrm{d}\tau$ is the probability that the next event is of type μ knowing that it occurs during the time interval $[t+\tau, t+\tau+\mathrm{d}\tau]$ and at site x.

Writing $c_{x,\mu}$ the transition rate of event μ at site x, we define

$$r_x \equiv \sum_\mu c_{x,\mu}, \tag{9.42}$$

$$R \equiv \sum_x r_x. \tag{9.43}$$

r_x is then the total rate of the events at site x, and R is the total rate of all the events on all lattice sites. The quantities τ, x and μ are then respectively drawn from the following distributions:

$$p_1(\tau) = R\mathrm{e}^{-R\tau}, \tag{9.44}$$

$$p_2(x|\tau) = \frac{r_x}{R}, \tag{9.45}$$

$$p_3(\mu|x, \tau) = \frac{c_{x,\mu}}{r_x}. \tag{9.46}$$

The algorithm is as follows. We build a lattice of length $2L+1$ (the spacing of the lattice σ is taken equal to 1). The boundary conditions are periodic, and L is chosen to be large enough so that we can consider the lattice as infinite (in the results presented below, $L = 250$). The initial condition is the following: the TP is initially at the origin and at each site different from the origin, a particle is set with probability ρ. We chose a final simulation time $t_{\max}$. At each step of the simulation, and as long as $t < t_{\max}$, the algorithm follows these steps:

1. Set $R = 0$.
2. For each $x \in [0, 2L+1]$, compute r_x:

- if the site x is occupied by a bath particle, three events are possible : a jump to the left, a jump to the right, or a desorption event (respectively labeled by 1, 2 and 3). The associate rates $c_{x,\mu}$ are

$$c_{x,1} = \frac{1}{2}(1-g)(1-\eta_{x-1}) \quad (9.47)$$

$$c_{x,2} = \frac{1}{2}(1-g)(1-\eta_{x+1}) \quad (9.48)$$

$$c_{x,3} = g \quad (9.49)$$

  so that $r_x = \frac{1}{2}(1-g)(1-\eta_{x-1}) + \frac{1}{2}(1-g)(1-\eta_{x+1}) + g$.
- if the site x is occupied by the TP, two events are possible : a jump to the left, or a jump to the right. The local rate is then $r_x = (1-p_1)(1-\eta_{x-1}) + p_1(1-\eta_{x+1})$.
- if the site is empty, the only possible event is an absorption event, and $r_x = f$.

3. Compute the total rate $R = \sum_x r_x$.
4. Draw τ from the distribution $p_1(\tau) = R\mathrm{e}^{-R\tau}$.
5. Draw x from the distribution $p_2(x|\tau) = r_x/R$.
6. Draw the event μ from the distribution $p_3(\mu|x,\tau) = c_{x,\mu}/r_x$.
7. Update the lattice occupation after the realization of the event (note that such an algorithm is rejection-free).
8. Increase the time $t \leftarrow t + \tau$.

We finally keep track of the TP position X_t with time. With a large number of realizations, we then sample the p.d.f. of X_t.

9.3.2 Velocity

For completeness, we present results for the velocity of the TP, which had already been presented in [15]. We study here the terminal velocity reached by the TP as a function of the density ρ, for different values of the bias. As ρ is in fact fixed by the values of f and g, we decide to vary f for different values of g in order to explore the whole range of parameters. Results are presented on Fig. 9.1. As expected, the velocity of the TP is a decreasing function of the bath density. We also confront the result from our decoupling approximation to the trivial mean-field solution (dashed line).

The discrepancy between the results from numerical simulations, which correspond to an exact sampling of the master equation (8.2), and the solution obtained using the decoupling approximation (8.10) is very small, and the agreement is particularly good close to $\rho = 0$ and $\rho = 1$. The decoupling approximation is then very accurate for the estimation of the velocity of the TP.

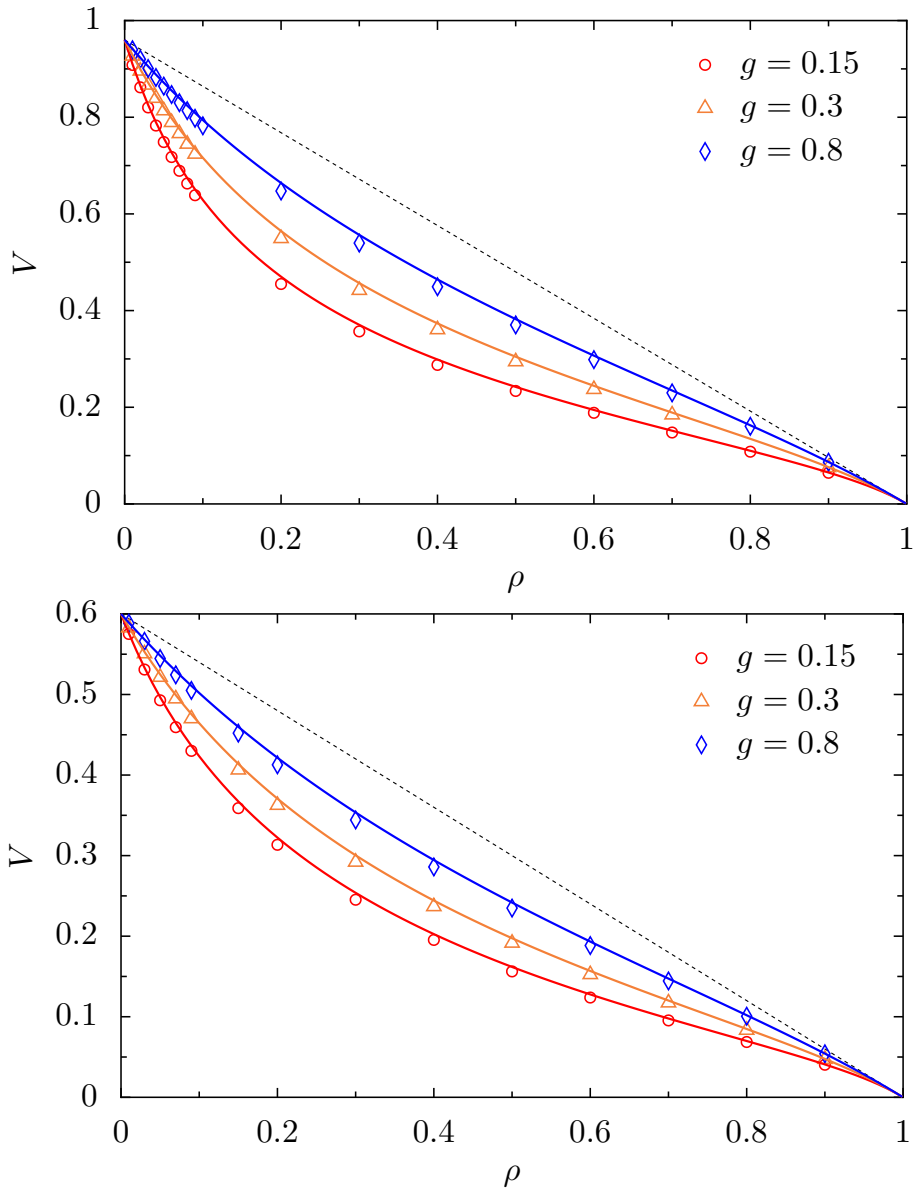

Figure 9.1: Stationary velocity V of the TP as a function of the density for different values of the desorption rate g obtained from numerical simulations (symbols) and from the decoupling approximation (lines). The bias is $p_1 - p_{-1} = 0.96$ (top) and $p_1 - p_{-1} = 0.6$ (bottom), the waiting times are $\tau = \tau^* = 1$. The dashed line is the trivial mean-field solution $V = \frac{\sigma}{\tau}(p_1 - p_{-1})(1 - \rho)$.

9.3.3 Diffusion coefficient

9.3.3.1 Results

In a similar way, we study the diffusion coefficient as a function of the density ρ, for different values of p_1 and g. We confront the analytical predictions to results from numerical simulations on Fig. 9.2. These results were first presented in [P1]. In the simulations presented in that publication, the quantity $t_{\max}$ was not sufficiently large, so that the numerical estimations of the cumulants were not accurate enough. We present here new simulations results.

The analytical predictions as well as the numerical simulations reveal the existence of a striking effect: the diffusion coefficient can be a non-monotonic function of the density of bath particles. Conterintuitively, increasing the density of particles surrounding the TP may increase the TP dispersion in some range of parameters. This result is surprising, since one naturally expects that the dispersion will be maximal when there are no hardcore bath particles (i.e., when $\rho = 0$). Consequently, this means that the diffusion of the TP may be enhanced by the presence of bath particles on the lattice. Moreover, we observe that for given values of p_1 and g, this extremum of the function $K(\rho)$ may appear if the bias $p_1 - p_{-1}$ is large enough. This effect could be investigated in experimental situations (e.g. in microrheology) and could have interesting applications.

The discrepancy between the results from numerical simulations, which correspond to an exact sampling of the master equation (8.2), and the solution obtained using the decoupling approximations (8.10), (8.22) is small, except in the domain $0.05 \lesssim \rho \lesssim 0.15$. However, the approximate solution still gives a good qualitative description of the evolution of K. The agreement is particularly good close to $\rho = 0$ and $\rho = 1$. We conclude that the decoupling approximation is accurate for the estimation of the diffusion coefficient of the TP.

In what follows, we find a criterion of the parameters g and p_1 allowing the emergence of a maximum for $K(\rho)$. We show that the non-monotonicity of the diffusion coefficient is actually correlated to the non-monotonicity of the cross-correlation functions $\widetilde{g}_n$ in the domain $n < 0$ (i.e. behind the TP).

9.3.3.2 Criterion for the existence of a maximum value of K

In this Section, we determine an explicit criterion for the existence of this maximum. This is equivalent to determine the parameters for which $K(\rho)$ has a positive derivative at the origin. We will then solve the equation:

$$\left.\frac{\mathrm{d}K}{\mathrm{d}\rho}\right|_{\rho=0} = 0. \tag{9.50}$$

If g is fixed, as the density ρ is related to f and g through $\rho = f/(f+g)$, this is equivalent to considering K as a function of f and solving

$$\left.\frac{\mathrm{d}K}{\mathrm{d}f}\right|_{f=0} = 0. \tag{9.51}$$

In what follows, we obtain the leading order term of K in an expansion in powers of f, the other parameters being constant. For simplicity, we introduce the quantities $\tau' \equiv \tau^*/\tau$ and $\delta \equiv p_1 - p_{-1}$. Assuming that the quantities $A_{\pm 1}$ have the following expansions

$$A_{\pm 1} \underset{f\to 0}{=} A_{\pm 1}^{(0)} + A_{\pm 1}^{(1)} f + \mathcal{O}(f^2), \tag{9.52}$$

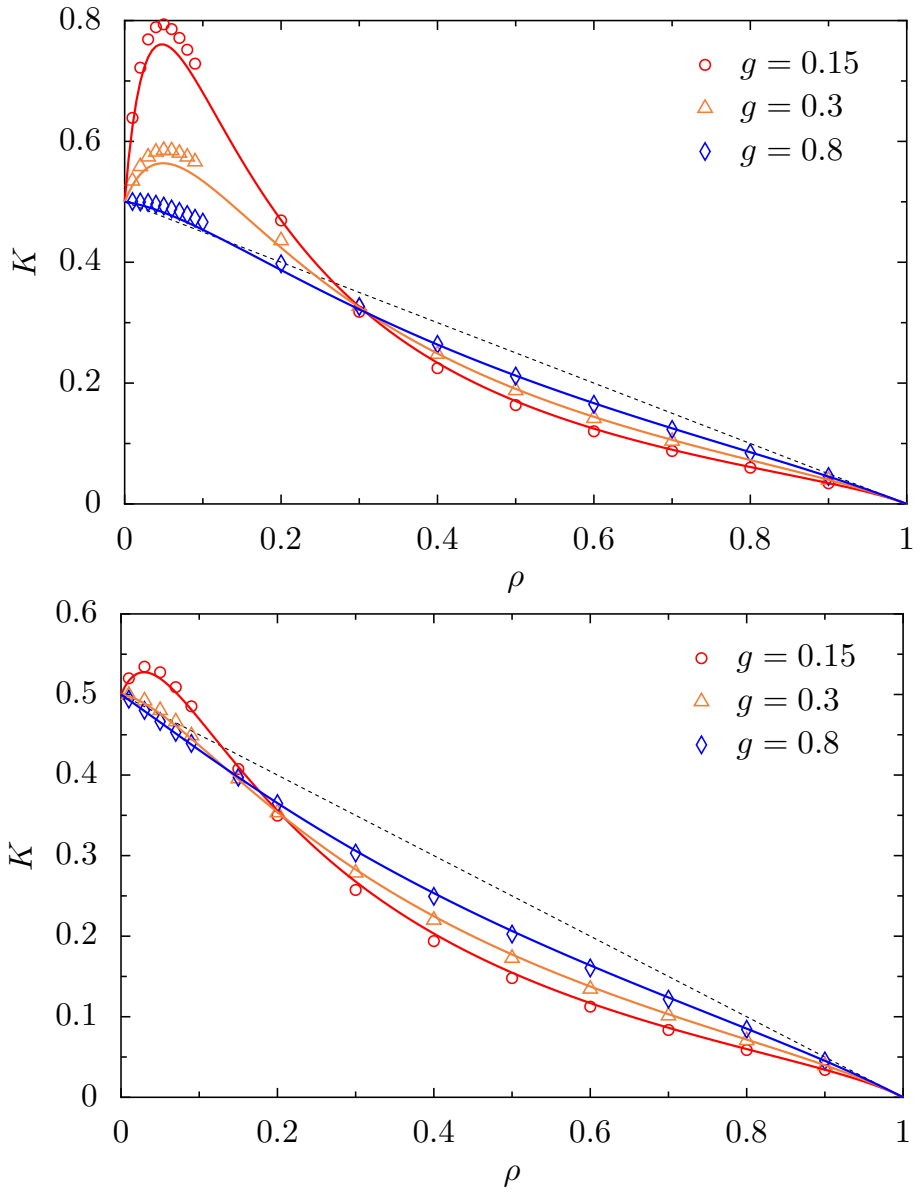

Figure 9.2: Stationary diffusion coefficient K of the TP as a function of the density for different values of the desorption rate g obtained from numerical simulations (symbols) and from the decoupling approximation (lines). The bias is $p_1 - p_{-1} = 0.96$ (top) and $p_1 - p_{-1} = 0.6$ (bottom), the waiting times are $\tau = \tau^* = 1$. The dashed line is the trivial mean-field solution $K = \frac{\sigma^2}{2\tau}(1-\rho)$.

and using (9.12) and (9.13), we obtain

$$A_{\pm 1} \underset{f\to 0}{=} 1+(1\pm\delta)\tau'-\frac{\tau'}{g^2}\frac{1\pm\delta}{1+\tau'(1\pm\delta)}\left(\delta^2\tau'^2+g(1+\tau')\pm\delta\sqrt{\delta^2\tau'^2+g^2+2g(1+\tau')}\right)f+\mathcal{O}(f^2). \tag{9.53}$$

We can deduce from the expansions of $A_{\pm 1}$ the expansions of $K_\pm$, r_1 and r_2. We then obtain the expansions of $k_{\pm 1}$ and $\widetilde{g}_{\pm 1}$, and finally an expansion of K. These general expressions are too lengthy to be reproduced here, but we give them in the case $\tau' = 1$, which is the case we considered in our simulations:

$$K \underset{f\to 0}{=} \frac{\sigma^2}{2\tau}\left[1+\frac{N(g,\delta)}{D(g,\delta)}f+\mathcal{O}(f^2)\right] \tag{9.54}$$

where

$$\begin{aligned} N(g,\delta) &= 2\left[(\delta^2-4)g^3+(3\delta^4-16)g^2+\delta^2(3\delta^4-5\delta^2+4)g+\delta^4(\delta^4-3\delta^2+4)\right] \\ &\quad -\sqrt{\delta^2+g^2+4g}\left[2(\delta^4-4)(\delta^2-3)g^2+\delta^2(\delta^4-\delta^2+4)g+4\delta^4(\delta^2-2)\right], \end{aligned} \tag{9.55}$$

$$D(g,\delta) = 2(\delta-2)^2(\delta+2)^2(\delta^2+g^2+4g)g^3. \tag{9.56}$$

For any value of δ and g, $D(g,\delta) > 0$. For a given value of the bias δ, the critical value of g (denoted by g_c) allowing K to reach a maximal value is then the solution of the equation:

$$N(g_c,\delta) = 0, \tag{9.57}$$

which can be determined numerically. We present the numerical solutions of (9.57) on Fig. 9.3 (curves in blue). On this figure, we also give the solutions obtained for other values of τ'. We conclude that, for a fixed value of the bias, K is nonmonotonic if the desorption rate g is large enough (or, for a fixed value of the desorption rate, if the bias is large enough).

9.3.3.3 Influence of the cross-correlations functions on the non-monotonicity

We now aim to give a first insight into a better understanding of the non-monotonicity of the diffusion coefficient. We first notice that the diffusion coefficient K (9.3) may be separated into three contributions:

$$K = K_{\mathrm{MF}} + K_1 + K_2, \tag{9.58}$$

with

$$K_{\mathrm{MF}} = \frac{\sigma^2}{\tau}(1-\rho) \tag{9.59}$$

$$K_1 = -\frac{\sigma^2}{\tau}[p_1(k_1-\rho)+p_{-1}(k_{-1}-\rho)] \tag{9.60}$$

$$K_2 = -\frac{2\sigma}{\tau}(p_1\widetilde{g}_1 - p_{-1}\widetilde{g}_{-1}). \tag{9.61}$$

The first term is the simplest mean-field approximation of the problem, obtained by taking the average local densities $k_{\boldsymbol{r}}$ equal to ρ and the cross-correlation functions $\langle \delta X_t \delta\eta_{X_t+\boldsymbol{r}}\rangle$ equal to zero. K_1 may be seen as a contribution from the inhomogeneous density profiles, and K_2 a contribution from the cross-correlations $\widetilde{g}_{\pm 1}$. For a given set of parameters which gives rise to a non-monotonic behavior

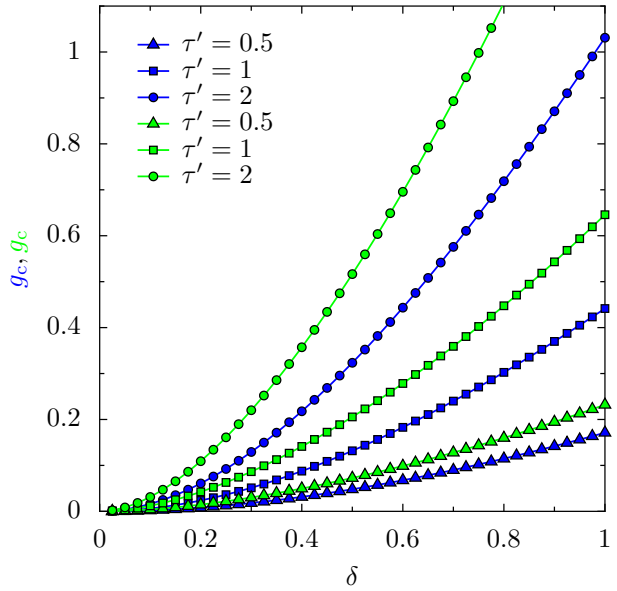

Figure 9.3: Critical value of the desorption rate g_c as a function of δ, for different values of the ratio $\tau' = \tau^*/\tau$, with $\sigma = 1$ and $\tau = 1$ obtained by the study of the behavior of K at $\rho \to 0$ (curves in blue). The region below the curves correspond to the range of parameters where $K(\rho)$ is nonmonotonic. The critical value of the desorption rate g'_c for which the cross-correlations $\widetilde{g}$ have the property $\widetilde{g}_{-1} > \widetilde{g}_{-2}$ is represented in green. The region below the curves correspond to the range of parameters where $\widetilde{g}_{-1} > \widetilde{g}_{-2}$.

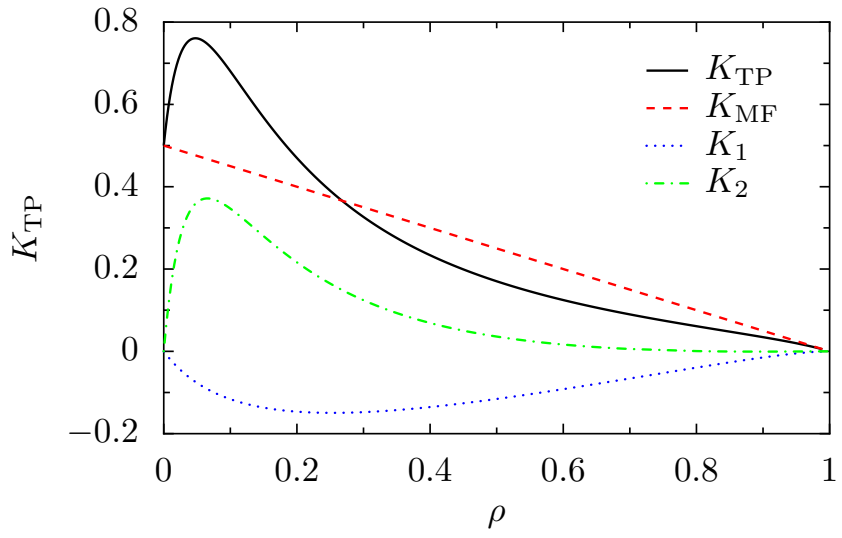

Figure 9.4: Contributions in the expressions of K as a function of the density, for the parameters $p_1 = 0.98$ and $g = 0.15$.

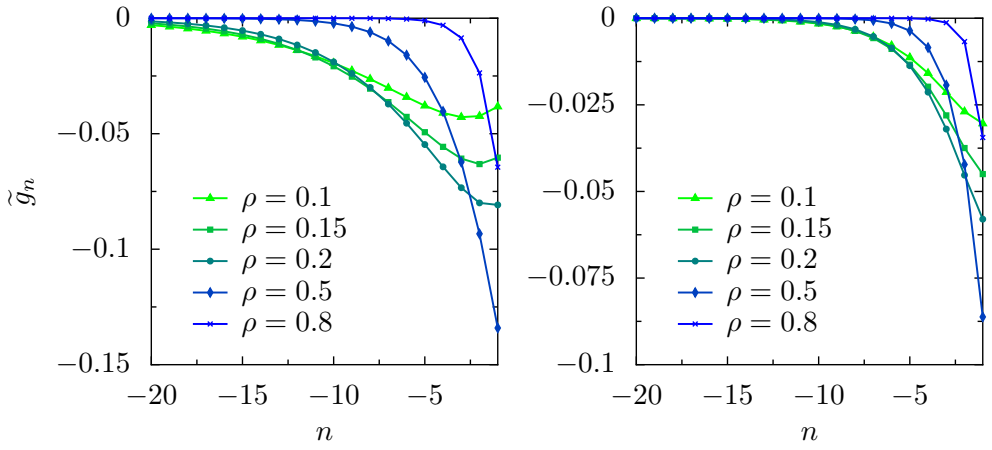

Figure 9.5: Cross-correlations functions $\widetilde{g}$ as a function of the distance to the tracer n for $g = 0.2$ (left) and $g = 0.6$ (right), and for different values of the density ρ. In both cases, we take $p_1 = 0.98$.

($p_1 = 0.98$ and $g = 0.15$), we plot on Fig. 9.4 K as well as the three contributions. The origin of the non-monotonicity of K with respect to the density ρ can then be attributed to K_2.

As it was stressed in [16], the cross-correlation functions $\widetilde{g}_n$ have nontrivial behaviors with respect to the distance n to the TP. In particular, they appear to have non-monotonous behavior in the domain $n < 0$, i.e. behind the TP,z for some values of the parameters. On Fig. 9.5, we plot the functions $\widetilde{g}_n$ for different values of the density ρ, for two sets of parameters: one for which the diffusion K is known to be a non-monotonic function of the density ($p_1 = 0.98$ and $g = 0.2$), and one for which it is monotonous ($p_1 = 0.98$ and $g = 0.6$). On Fig. 9.6, we plot the functions $\widetilde{g}_n$ for different values of the desorption parameter g, for $\rho = 0.01$, for $p_1 = 0.98$. The non-monotonicity of $\widetilde{g}_n$ then seems to be correlated with that of K, as it occurs for g small enough.

In order to get a more quantitative comparison of these two effects (the non-monotonicity of K with respect to the density ρ and that of $\widetilde{g}_n$ with respect to the distance to the TP n in the domain $n < 0$), we first determine, for a fixed value of the bias $p_1 - p_{-1}$, and at leading order in f, the critical value of $g'_{\rm c}$ giving a minimal value for $\widetilde{g}_n$, i.e. for which $\widetilde{g}_{-1} > \widetilde{g}_{-2}$.

Using the small f expansion of $A_{\pm 1}$ (9.53), we easily deduce from the definitions of $\widetilde{g}_n$ in the domain $n < 0$ (9.19) an expression for $\widetilde{g}_{-1} - \widetilde{g}_{-2}$ at leading order in f. The general expression is too lengthy to be given here. We present it in the particular case where $\tau' = 1$:

$$\widetilde{g}_{-1} - \widetilde{g}_{-2} \underset{f\to 0}{=} 2\sigma f \frac{N'(g,\delta)}{D'(g,\delta)} + \mathcal{O}(f^2) \tag{9.62}$$

with

$$\begin{aligned} N'(g,\delta) &= (\delta - g)\left[(1+\delta)g^2 - 2(\delta^2 - 2\delta - 2)g + \delta^2(\delta - 1)\right] \\ &\quad - \sqrt{\delta^2 + g^2 + 4g}\left[(1+\delta)g^2 - (3\delta + 2)(\delta - 1)g + \delta^2(\delta - 1)\right], \qquad (9.63) \\ D'(g,\delta) &= 2g\sqrt{\delta^2 + g^2 + 4g}\Big\{\left[2g^2 + (2\delta + 4)g + \delta(\delta + 2)\right]\sqrt{\delta^2 + g^2 + 4g} \\ &\quad + 2g^3 + 2(\delta + 4)g^2 + 2(\delta + 2)(\delta + 1)g + \delta^2(\delta + 2)\Big\}. \qquad (9.64) \end{aligned}$$

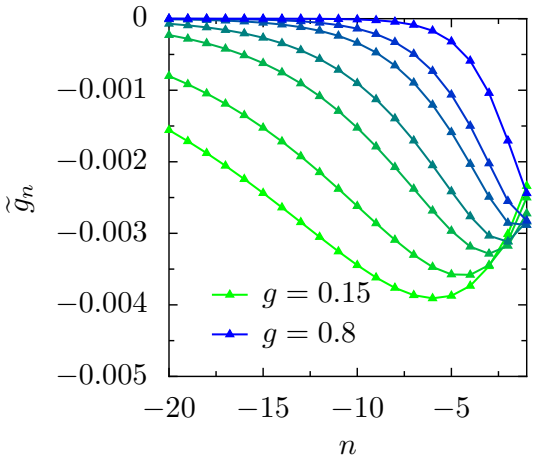

Figure 9.6: Cross-correlations functions $\widetilde{g}$ as a function of the distance to the tracer n for $\rho = 0.01$, $p_1 = 0.98$, and for different values of the desorption parameter g.

Then, for a fixed value of the bias δ, the critical value of g canceling $\widetilde{g}_{-1} - \widetilde{g}_{-2}$ is the solution of the equation

$$N'(g'_{\rm c}, \delta) = 0. \tag{9.65}$$

The numerical solutions for $g'_{\rm c}$ as a function of δ, for different values of the ratio τ' are represented on Fig. 9.3 and confronted to the values $g_{\rm c}$ obtained by the criterion on K. The two functions $g_{\rm c}$ and $g'_{\rm c}$ are comparable as long as τ' is not too large. We also show that their expansions for $\delta \to 0$ are identical at leading order, and that they go to zero as $(\sqrt{17}+1)\delta^2/8$.

This study indicates that the emergence of a maximal value for $K(\rho)$ for $\rho > 0$ is correlated to the observation of a minimal value in the cross-correlation functions $\widetilde{g}_n$ in the domain $n < 0$.

9.3.3.4 Range of parameters for which $K > 1/2$

In the previous sections, we determined the critical value of the desorption rate $g_{\rm c}$ allowing the emergence of a nontrivial maximum value for the function $K(\rho)$ for a given value of the bias δ. As a complementary approach, for a fixed value of the bias, we study the domain of the plane (g, ρ) in which the diffusion coefficient is greater than $1/2$, which is its value when there is no bath particle.

In the case where the curve $K(\rho)$ displays an extremum value, the value of the diffusion coefficient is greater than $1/2$ in the range $[0, \widetilde{\rho}]$, where $\widetilde{\rho}$ is a function of p_1 and g only. From the analytical curves $K(\rho)$, we can then deduce the values of $\widetilde{\rho}$ as a function of g for different values of p_1, which are plotted on Fig. 9.7.

As it was shown on Fig. 9.6, for a given value of p_1 and g, there exists a value of ρ below which the difference $\widetilde{g}_{-1} - \widetilde{g}_{-2}$ is negative, i.e. below which there is a minimum for $\widetilde{g}_n$ in the range $n < 0$. This critical value of ρ will be denoted by $\widetilde{\rho}'$. In order to compare the domain of parameters giving respectively $K > 1/2$ and $\widetilde{g}_{-1} - \widetilde{g}_{-2} \geq 0$, we also represent on Fig. 9.7 the curves of $\widetilde{\rho}'$ as a function of g for different values of p_1.

The domains in the plane (ρ, g) for which $K > 1/2$ and for which $\widetilde{g}_{-1} - \widetilde{g}_{-2} < 0$ then seem to be correlated.

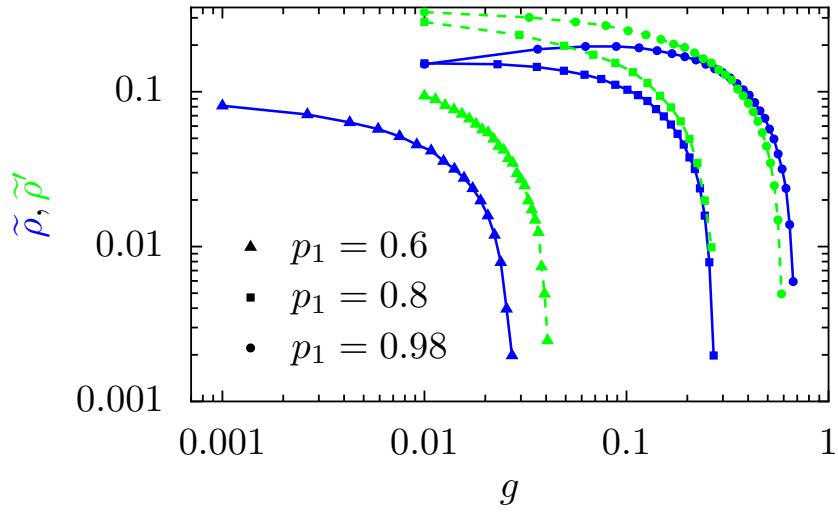

Figure 9.7: Critical value of the density $\widetilde{\rho}$ below which the diffusion coefficient is greater than $1/2$, as a function of g and for different values of the bias p_1 (curves in blue). Critical value of the density $\widetilde{\rho}'$ below which $\widetilde{g}_{-1} - \widetilde{g}_{-2} \geq 0$, as a function of g and for different values of the bias p_1 (curves in green).

This study shows that the non-monotonicity of the diffusion coefficient with respect to the density (emergence of a maximum value of K for $\rho > 0$) and the non-monotonicity of the cross-correlation function $\widetilde{g}_n$ behind the TP are correlated. A more detailed study of the cross-correlation functions $\widetilde{g}_n$, whose behavior affects the fluctuations of the TP position, could allow us to have a more physical understanding of the phenomenon highlighted in this Section.

9.3.4 Third cumulant

The third cumulant of the distribution of X_t gives information about its asymmetry. We introduced earlier the coefficient γ, defined by

$$\gamma = \lim_{t\to\infty} \frac{1}{6}\frac{\mathrm{d}}{\mathrm{d}t}\left\langle (X_t - \langle X_t\rangle)^3 \right\rangle . \tag{9.66}$$

With this definition, if $\gamma > 0$ (resp. $\gamma < 0$), the distribution of X_t is expected to be skewed to the right (resp. to the left). We take as an example a biased random walker on a lattice in the absence of exclusion interactions. If the particle is more likely to jump to the right ($p_1 > p_{-1}$), its third cumulant will be positive, indicating a distribution skewed to the right. Here, we study the influence of the presence of bath particles and of the different parameters of our model on the sign of the third cumulant of X_t.

We use the solutions for $\widetilde{m}_{\pm 1}$ (9.39) and (9.40) obtained from the decoupling approximation in order to compute the coefficient γ from its definition (9.5). For two values of the bias ($p_1 = 0.98$ and 0.8), we study the coefficient γ as a function of the density ρ, for different values of the desorption rate g. The curves are presented on Fig. 9.8. For high values of the desorption rate, $\gamma(\rho)$ is monotonic and decreases when the density of bath particles increases. However, for small values of the desorption rate, the function becomes nonmonotonic, and one observes the emergence of a minimum and a maximum

value, different from the trivial values $\rho = 0$ and $\rho = 1$. Finally, if g is small enough, there exists an interval of density for which γ becomes negative, which means that the distribution of X_t may actually be negatively skewed, in opposition with the situation where there is no bath particles on the lattice.

These results are preliminary, and will deserve future work in order to offer a better understanding, and to confront them with the results from numerical simulations.

9.4 Cumulant generating function and propagator

9.4.1 Calculation

We now turn to the computation of the cumulant generating function $\Psi(t)$, defined as $\Psi(t) = \ln \left\langle \mathrm{e}^{\mathrm{i}uX_t} \right\rangle$. It was shown in Chapter 8 that its derivative takes the form

$$\frac{\mathrm{d}\Psi(t)}{\mathrm{d}t} = \frac{p_1}{\tau}\left(\mathrm{e}^{\mathrm{i}u\sigma} - 1\right)\left(1 - \widetilde{w}_{\boldsymbol{e}_1}\right) + \frac{p_{-1}}{\tau}\left(\mathrm{e}^{-\mathrm{i}u\sigma} - 1\right)\left(1 - \widetilde{w}_{\boldsymbol{e}_{-1}}\right), \tag{9.67}$$

where we defined the correlation functions $\widetilde{w}_{\boldsymbol{r}} = \left\langle \mathrm{e}^{\mathrm{i}uX_t}\eta_{\boldsymbol{X}_t+\boldsymbol{r}} \right\rangle / \left\langle \mathrm{e}^{\mathrm{i}uX_t} \right\rangle$, which are solutions of the equations (8.57) and (8.58). In the long-time limit, if $\widetilde{w}_{\boldsymbol{e}_1}$ and $\widetilde{w}_{\boldsymbol{e}_{-1}}$ reach stationary value, one has

$$\Psi(t) \underset{t\to\infty}{\sim} \left[\frac{p_1}{\tau}\left(\mathrm{e}^{\mathrm{i}u\sigma} - 1\right)\left(1 - \widetilde{w}_{\boldsymbol{e}_1}\right) + \frac{p_{-1}}{\tau}\left(\mathrm{e}^{-\mathrm{i}u\sigma} - 1\right)\left(1 - \widetilde{w}_{\boldsymbol{e}_{-1}}\right)\right] t. \tag{9.68}$$

The p.d.f. of X_t can be deduced using the inverse Fourier transform

$$P_t(x) = \mathrm{Prob}[X_t = x] = \int_{-\pi}^{\pi} \frac{\mathrm{d}u}{2\pi} \mathrm{e}^{-iux}\mathrm{e}^{\Psi(t)}, \tag{9.69}$$

In this Section, we solve the equations on $\widetilde{w}_{\boldsymbol{r}}$ in the one-dimensional case, and deduce the cumulant generating function and the distribution $P_t(x)$.

In the one-dimensional case, starting from (8.57) and (8.58) and assuming that there exists non-trivial stationary solutions, one gets the following equations verified by $\widetilde{w}_n \equiv \widetilde{w}_{n\boldsymbol{e}_1}$:

$$B_1\widetilde{w}_{n+1} - B_2\widetilde{w}_n + B_3\widetilde{w}_{n-1} = -(B_4K_+r_1^n + B_5) \quad \text{for} \quad n > 1 \tag{9.70}$$

$$B_1\widetilde{w}_{n+1} - B_2\widetilde{w}_n + B_3\widetilde{w}_{n-1} = -(C_4K_-r_2^n + B_5) \quad \text{for} \quad n < -1 \tag{9.71}$$

$$D_1\widetilde{w}_2 - D_2\widetilde{w}_1 + D_3\widetilde{w}_{-1} + D_4 + D_5\widetilde{w}_1^2 + D_6\widetilde{w}_1\widetilde{w}_{-1} = 0 \quad \text{for} \quad n = 1 \tag{9.72}$$

$$E_1\widetilde{w}_1 - E_2\widetilde{w}_{-1} + E_3\widetilde{w}_{-2} + E_4 + D_6\widetilde{w}_{-1}^2 + D_5\widetilde{w}_1\widetilde{w}_{-1} = 0 \quad \text{for} \quad n = -1 \tag{9.73}$$

where the expressions of the different prefactors are given in Appendix K.2. (9.70) and (9.71) are associated to the characteristic equation

$$B_1X^2 - B_2X + B_3 = 0, \tag{9.74}$$

which has the solutions

$$q_{1,2} = \frac{B_2 \pm \sqrt{B_2^2 - 4B_1B_3}}{2B_1}. \tag{9.75}$$

A development in powers of u shows that

$$q_1 = r_1 + \mathcal{O}(u) \quad \text{and} \quad q_2 = r_2 + \mathcal{O}(u). \tag{9.76}$$

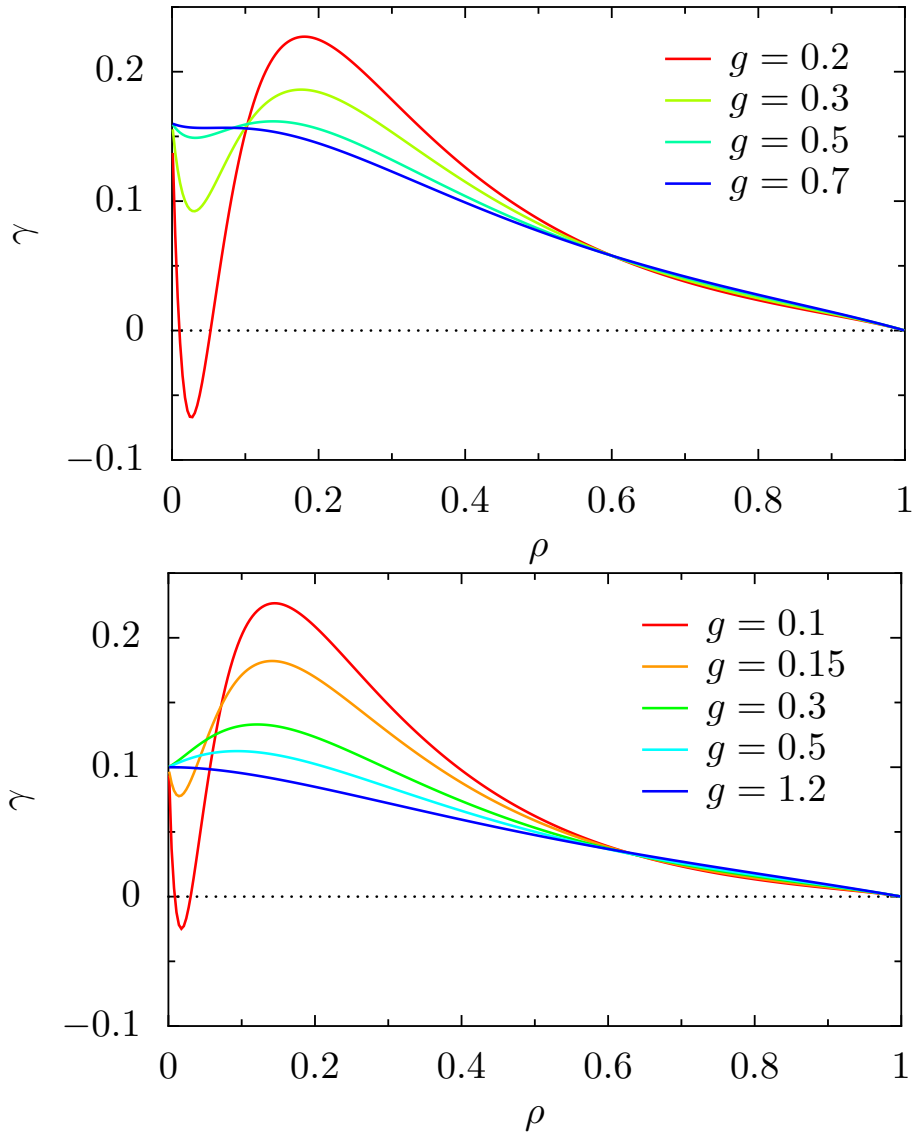

Figure 9.8: Coefficient γ defined in (9.66) as a function of the density for different values of the desorption rate g obtained from the decoupling approximation. The bias is $p_1 - p_{-1} = 0.96$ (top) and $p_1 - p_{-1} = 0.6$ (bottom). The waiting times are $\tau = \tau^* = 1$.

At order zero in u, (9.70) and (9.71) are equivalent to (8.11) and (8.12), so that their solutions must coincide at this order. Consequently, the general solution of (9.70) is of the form

$$\widetilde{w}_n = \alpha_+ q_1^n \tag{9.77}$$

The particular solution is easily calculated, and for $n > 0$, we find

$$\widetilde{w}_n = \alpha_+ q_1^n - \frac{B_4 K_+}{B_1 r_1 - B_2 + B_3 r_1^{-1}} r_1^n - \frac{B_5}{B_1 - B_2 + B_3}. \tag{9.78}$$

With similar arguments, we find for $n < 0$

$$\widetilde{w}_n = \alpha_- q_2^n - \frac{C_4 K_-}{B_1 r_2 - B_2 + B_3 r_2^{-1}} r_2^n - \frac{B_5}{B_1 - B_2 + B_3}. \tag{9.79}$$

Finally, writing (9.78) (resp. (9.79)) for $n = 1$ (resp. $n = -1$) and using (9.72) and (9.73), we find the following nonlinear system of four equations whose unknowns are $\widetilde{w}_1$, $\widetilde{w}_{-1}$, α_+ and α_- :

$$\begin{cases} \widetilde{w}_1 = \alpha_+ q_1 - \dfrac{B_4 K_+}{B_1 r_1 - B_2 + B_3 r_1^{-1}} r_1 - \dfrac{B_5}{B_1 - B_2 + B_3} \\ \widetilde{w}_{-1} = \alpha_- q_2^{-1} - \dfrac{C_4 K_-}{B_1 r_2 - B_2 + B_3 r_2^{-1}} r_2^{-1} - \dfrac{B_5}{B_1 - B_2 + B_3} \\ D_1 \left[\alpha_+ q_1^2 - \dfrac{B_4 K_+}{B_1 r_1 - B_2 + B_3 r_1^{-1}} r_1^2 - \dfrac{B_5}{B_1 - B_2 + B_3} \right] \\ -D_2 \widetilde{w}_1 + D_3 \widetilde{w}_{-1} + D_4 + D_5 \widetilde{w}_1^2 + D_6 \widetilde{w}_1 \widetilde{w}_{-1} = 0 \\ E_1 \widetilde{w}_1 - E_2 \widetilde{w}_{-1} + E_3 \left[\alpha_- q_2^{-2} - \dfrac{C_4 K_-}{B_1 r_2 - B_2 + B_3 r_2^{-1}} r_2^{-2} - \dfrac{B_5}{B_1 - B_2 + B_3} \right] \\ +E_4 + D_6 \widetilde{w}_{-1}^2 + D_5 \widetilde{w}_1 \widetilde{w}_{-1} = 0. \end{cases} \tag{9.80}$$

The numerical resolution of this system of equations for specific values of u allows us to calculate $\widetilde{w}_1$ and $\widetilde{w}_{-1}$, and to deduce the expression of $\Psi(t)$ as a function of u. Using (9.69), one can calculate the probability distribution $P_t(x)$, valid in the asymptotic regime $t \to \infty$.

9.4.2 Numerical simulations

We compare the results of this calculation with data obtained from Monte Carlo simulations for a given set of parameters (see Fig. 9.9).

We observe a good agreement between the analytical prediction obtained from the decoupling approximation and the results from numerical simulations. We see that the prediction from the decoupling approximation tends to be shifted to the right for large times: this is expected from the analysis of the velocity of the TP, which was shown to be overestimated by the approximation (Fig. 9.1).

As emphasized in Section 8.4.1, the rescaled variable $Z_t = (X_t - \langle X_t \rangle)/\sqrt{\mathrm{Var}(X_t)}$ is expected to be distributed accordingly to a Gaussian distribution in the long-time limit. A more detailed study of the distribution of X_t determined in the previous Section and of the results from numerical simulations could allow us to study and quantify the convergence of the distribution of Z_t to a Gaussian distribution.

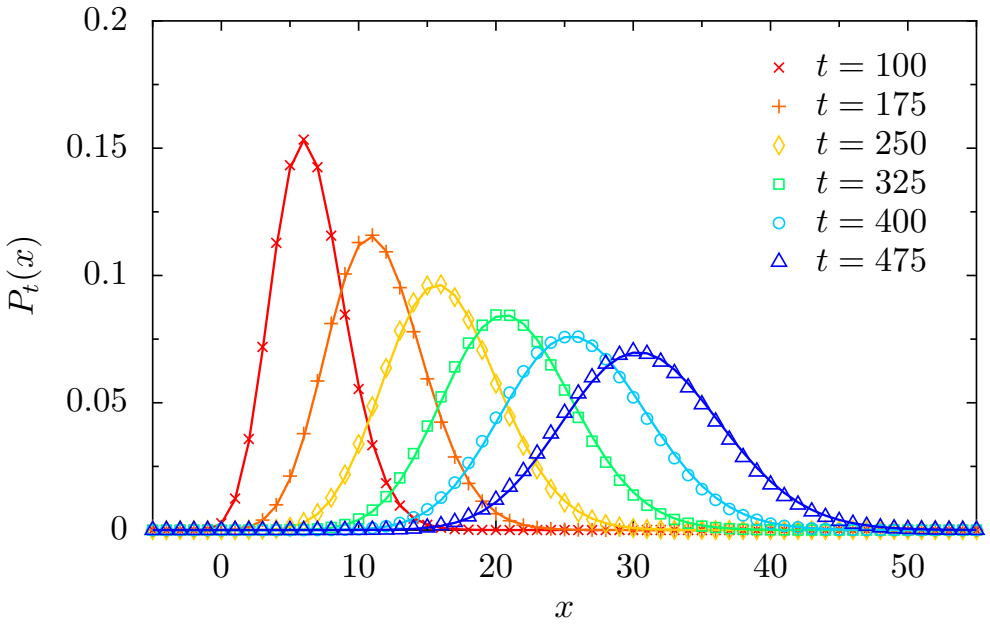

Figure 9.9: Probability distribution function of the TP position $P_t(x) = \mathrm{Prob}[X_t = x]$, for different times. The results from numerical simulations (symbols) are compared to the expression (9.69), the functions $\widetilde{w}_{\pm 1}(u)$ being numerically computed as solutions of the system (9.80). The parameters are $g = 0.15$, $p_1 = 0.98$, $\rho = 0.9$.

9.5 Conclusion

In this Chapter, we studied the one-dimensional version of the general model of a biased tracer in a hardcore lattice gas in contact with a reservoir of particles. We solved the equations verified by the different correlation functions introduced in Chapter 8 in order to obtain the long-time behavior of the first cumulants and of the distribution of the position of the TP.

First, we recalled the solutions of the equations verified by the mean density profiles $k_{\boldsymbol{r}} = \langle \eta_{\boldsymbol{r}} \rangle$, already presented in [15], and obtained using a decoupling approximation. In particular, the quantities $k_{\boldsymbol{e}_{\pm 1}}$, involved in the expression of the TP velocity, are the solution of an implicit system of equations, that can be solved numerically for a given set of parameters. The general solution for the TP velocity was confronted to Monte-Carlo simulations, which exactly sample the master equation of the problem. The agreement between the numerical simulations and the solution from the decoupling approximation was very good, in particular in the limits where $\rho \to 0$ and $\rho \to 1$.

We studied the solutions of the equations verified by the cross-correlation functions $\widetilde{g}_{\boldsymbol{r}} = \langle \delta X_t (\eta_{\boldsymbol{X}_t + \boldsymbol{r}} - \langle \eta_{\boldsymbol{X}_t + \boldsymbol{r}} \rangle) \rangle$, and obtained in particular an expression for the quantities $\widetilde{g}_1$ and $\widetilde{g}_{-1}$, involved in the computation of the diffusion coefficient of the TP, in terms of the density profiles $k_{\boldsymbol{r}}$. It is then possible to obtain numerically the value of the diffusion coefficient for a given set of parameters. The analysis of this general solution shows that the diffusion coefficient may be a nonmonotonic function of the density. Indeed, surprisingly, the diffusion coefficient may be increased by the presence of bath particles on the lattice for a wide range of parameters. This nonmonotonicity is not an artifact of the decoupling approximation, and we show that its existence is confirmed by Monte Carlo simulations, which confirm the accuracy of the approximation. This effect is shown to be related to an anomaly in the profiles of the cross-correlations $\widetilde{g}_{\boldsymbol{r}}$, which are nonmonotonic functions of the distance to the TP for values of the parameters similar to the ones leading to the existence of a maximum value for the diffusion coefficient. A further study could allow us to get a better physical understanding of this phenomenon.

We also studied the solutions of the equations governing the correlation functions $\widetilde{m}_{\boldsymbol{r}} = \big\langle (\delta X_t)^2 (\eta_{\boldsymbol{X}_t + \boldsymbol{r}} - \langle \eta_{\boldsymbol{X}_t + \boldsymbol{r}} \rangle) \big\rangle$, involved in the computation of the coefficient γ, which describes the skewness of the distribution. In the case of a one-dimensional lattice, we write the quantities $\widetilde{m}_{\pm 1}$ in terms of the correlation functions $\widetilde{g}_{\boldsymbol{r}}$ and $k_{\boldsymbol{r}}$. Consequently, one can determine numerically the values of the coefficients $\widetilde{m}_{\boldsymbol{e}_{\pm 1}}$. Surprisingly, we observe that the coefficient γ is a nonmonotonic function of the density and that it may take negative values, so that the distribution of the TP position may be negatively skewed for some values of the parameters.

Finally, we studied the solutions of the equations governing the correlation functions $\widetilde{w}_{\boldsymbol{r}} \equiv \big\langle \mathrm{e}^{\mathrm{i}uX_t} \eta_{\boldsymbol{X}_t + \boldsymbol{r}} \big\rangle / \big\langle \mathrm{e}^{\mathrm{i}uX_t} \big\rangle$, involved in the computation of the cumulant generating function of X_t and therefore in its distribution. In the case of the one-dimensional lattice, we showed that the quantities $\widetilde{w}_{\pm 1}$ were implicit solutions of a system of equations, so that the distribution of X_t could be determined and confronted to numerical simulations with a good agreement. The rescaled variable $(X_t - \langle X_t \rangle)/\sqrt{\mathrm{Var}(X_t)}$ is distributed accordingly to a Gaussian distribution in the long-time limit.

CHAPTER 10

Resolution on higher-dimensional lattices

Contents

In this Chapter, we consider lattices of dimension two and higher and solve the equations verified by the mean density profiles $k_{\boldsymbol{r}}$ and the cross-correlation functions $\widetilde{g}_{\boldsymbol{r}}$, which were established using a decoupling approximation in Chapter 8. We then deduce the velocity and diffusion coefficient of the TP. Surprisingly, the analysis of the velocity of the TP shows that it may decrease for increasing values of the applied force. We study quantitatively this phenomenon, known as negative differential mobility *in other contexts. We also show that in the limits of a very dilute or very dense bath of particles, the expressions of the velocity and of the diffusion coefficient become explicit. In the high-density limit, they correspond to the results obtained from the exact approach presented in the first part of this thesis. In the low-density limit, they correspond to exact results obtained by other authors. The decoupling approximation is then* exact *in the limits of very high and very low densities.*

10.1 Introduction

In Chapter 8, we introduced a model of hardcore lattice gas in contact with a reservoir of particles. Bath particles perform symmetric nearest-neighbor random walks with a mean waiting time τ^*, and may desorb to the reservoir with a given rate. Particles from the reservoir may adsorb on vacant lattice sites. A tracer particle (TP) performing a biased random walk of mean waiting time τ is also introduced. All the particles interact via hardcore interactions. Using a decoupling approximation, the velocity V and the diffusion coefficient K of the TP, defined by

$$V = \lim_{t\to\infty} \frac{\mathrm{d}}{\mathrm{d}t} \langle X_t \rangle \,, \tag{10.1}$$

$$K = \frac{1}{2d} \lim_{t\to\infty} \frac{\mathrm{d}}{\mathrm{d}t} \left(\langle {X_t}^2 \rangle - \langle X_t \rangle^2 \right), \tag{10.2}$$

were given as functions of the mean density at site $\boldsymbol{r}$ ($k_{\boldsymbol{r}} = \langle \eta_{\boldsymbol{r}} \rangle$) and of the correlation functions $\widetilde{g}_{\boldsymbol{r}} = \langle \delta X_t (\eta_{\boldsymbol{X}_t + \boldsymbol{r}} - \langle \eta_{\boldsymbol{X}_t + \boldsymbol{r}} \rangle) \rangle$. In turn, these quantities are the solutions of general equations given in Chapter 8 (see (8.11) and (8.12), (8.23) and (8.24)). The solutions of these equations were presented and studied in the particular of a one-dimensional lattice in Chapter 9.

In this Chapter, we present a method to compute the velocity and the diffusion coefficient of the tracer particle, in the case of a lattice of arbitrary dimension. We study the equations verified by $k_{\boldsymbol{r}}$ and $\widetilde{g}_{\boldsymbol{r}}$, and show that these quantities evaluated at $\boldsymbol{r} = \{\boldsymbol{e}_{\pm 1}, \ldots, \boldsymbol{e}_{\pm d}\}$ are solutions of nonlinear equations that can be solved numerically for a given set of parameters. We then obtain an *implicit* expression of V and K for an arbitrary set of parameters. In the particular limits where $\rho \to 0$ (resp. $\rho \to 1$), these equations become *explicit* and can be solved in order to obtain the expressions of V and K at leading order in ρ (resp. $1 - \rho$).

The computation of the velocity of the TP leads to several interesting results:

- in the limit where $\rho \to 0$, and in the particular situation where the bath particles are frozen (i.e. $\tau^* \to \infty$), we retrieve the expression of the velocity at leading order in ρ obtained exactly by Leitmann and Franosch [77].

- in the limit where $\rho \to 1$, the expression of the velocity correctly matches the expression we obtained with the exact approach at leading order in the density of vacancies (Chapter 5). This result together with the previous one actually show that the approximation used compute V is *exact* in the limits of low and high densities.

- for intermediate densities, we study the behavior of the TP velocity as a function of the force F applied on the TP, for different values of the relative time scales of the bath and the TP τ^*/τ. We show that for a certain range of parameters, the velocity is non-monotonous when F varies, i.e. it may be a decreasing function of the applied force. In other contexts, this phenomenon is known as *negative differential mobility*. We will investigate it quantitatively, and give a physical insight into these observations.

Finally, the study of the expression of the diffusion coefficient K in the limit $\rho \to 1$ allows us to retrieve the expressions obtained for the second cumulant of the position of the TP with the exact approach (Chapter 4). This shows that the decoupling approximation used to compute K is *exact* in the limit of high densities.

10.2 Mean position of the TP

In this Section, we aim to compute the velocity of the TP, defined as

$$V = \lim_{t\to\infty} \frac{\mathrm{d}}{\mathrm{d}t} \langle X_t \rangle . \tag{10.3}$$

In Chapter 8, we obtained the following expression for the derivative of the mean position:

$$\frac{\mathrm{d}}{\mathrm{d}t} \langle X_t \rangle = \frac{\sigma}{\tau} \left[p_1 \left(1 - k_{\boldsymbol{e}_1}\right) - p_{-1} \left(1 - k_{\boldsymbol{e}_{-1}}\right) \right], \tag{10.4}$$

were $k_{\boldsymbol{r}} = \langle \eta_{\boldsymbol{r}} \rangle$ is the average density at site $\boldsymbol{r}$, and is the solution of the equations (8.11) and (8.12). In this Section, we solve these equations for lattices of arbitrary dimension, and obtain an implicit expression for V. This method was first introduced in [13, 14]. The implicit expression of V was obtained in the case of a two-dimensional lattice. We extend this method to study the case of d-dimensional lattices and d-dimensional generalized capillaries (lattices which are infinite in one direction and finite with periodic boundary conditions in the other directions). We also study the limits $\rho \to 0$ and $\rho \to 1$ of this implicit solution, which becomes explicit, and which coincides with the expressions obtained with exact approaches.

10.2.1 Basic equations

It was shown in Chapter 8 that the density profiles $k_{\boldsymbol{r}}$ were the solutions of the equations (8.11) and (8.12) that we recall here:

- for $\boldsymbol{r} \notin \{\boldsymbol{0}, \pm\boldsymbol{e}_1, \ldots, \pm\boldsymbol{e}_d\}$
$$2d\tau^* \partial_t k_{\boldsymbol{r}} = \widetilde{L} k_{\boldsymbol{r}}, \tag{10.5}$$
- for $\boldsymbol{r} \in \{\pm\boldsymbol{e}_1, \ldots, \pm\boldsymbol{e}_d\}$
$$2d\tau^* \partial_t k_{\boldsymbol{e}_\nu} = (\widetilde{L} + A_\nu) k_{\boldsymbol{e}_\nu}, \tag{10.6}$$

where we defined the operator $\widetilde{L}$:

$$\widetilde{L} \equiv \sum_\mu A_\mu \nabla_\mu - 2d(f+g), \tag{10.7}$$

and the quantities

$$A_\mu \equiv 1 + \frac{2d\tau^*}{\tau} p_\mu (1 - k_{\boldsymbol{e}_\mu}). \tag{10.8}$$

Note that for symmetry reasons, the quantities $A_{\pm 2}, \ldots, A_{\pm d}$ are identical, and will be denoted by A_2. For simplicity, in this Chapter, we will use the following notational convention: for any space-dependent function $f_{\boldsymbol{r}}$, we will write $f_\nu \equiv f_{\boldsymbol{e}_\nu}$. Noticing that, far from the TP, $\lim_{|\boldsymbol{r}|\to\infty} k_{\boldsymbol{r}} = \rho$, we introduce the function

$$h_{\boldsymbol{r}} = k_{\boldsymbol{r}} - \rho. \tag{10.9}$$

This definition holds for $\boldsymbol{r} \neq \boldsymbol{0}$, and we choose $h_{\boldsymbol{0}} = 0$. Using the relation

$$\nabla_\mu k_{\boldsymbol{e}_\nu} = \begin{cases} \nabla_\mu h_{\boldsymbol{e}_\nu} & \text{if } \mu \neq -\nu \\ \nabla_\mu h_{\boldsymbol{e}_\nu} - \rho & \text{if } \mu = -\nu, \end{cases} \tag{10.10}$$

we finally get the following evolution equations :

- $\boldsymbol{r} \notin \{\boldsymbol{0}, \pm\boldsymbol{e}_1, \ldots, \pm\boldsymbol{e}_d\}$

$$2d\tau^* \partial_t h_{\boldsymbol{r}} = \widetilde{L} h_{\boldsymbol{r}}, \tag{10.11}$$

- $\boldsymbol{r} \in \{\pm\boldsymbol{e}_1, \ldots, \pm\boldsymbol{e}_d\}$

$$2d\tau^* \partial_t h_{\boldsymbol{e}_\nu} = (\widetilde{L} + A_\nu) h_{\boldsymbol{e}_\nu} + \rho(A_\nu - A_{-\nu}). \tag{10.12}$$

According to (10.4), the velocity of the TP in the stationary state is

$$V = \lim_{t\to\infty} \frac{\mathrm{d}}{\mathrm{d}t} \langle X_t \rangle = \frac{\sigma}{\tau} [p_1 (1 - k_{\boldsymbol{e}_1}) - p_{-1} \left(1 - k_{\boldsymbol{e}_{-1}}\right)]. \tag{10.13}$$

In order to compute the velocity of the TP in the stationary state and to apply the definition of V, we will first solve (10.11) and (10.12) to calculate $h_{\boldsymbol{e}_1}$ and $h_{\boldsymbol{e}_{-1}}$. In what follows, we will consider two geometries:

- generalized d-dimensional capillaries, infinite in direction 1 and finite of width L with periodic boundary conditions in directions $2, \ldots, d$.
- infinitely extended lattices of dimension d.

We introduce the auxiliary variable $\boldsymbol{w} = (w_1, \ldots, w_d)$, and define the generating function $H(\boldsymbol{w}; t)$ as

$$H(\boldsymbol{w}; t) = \begin{cases} \displaystyle\sum_{r_1=-\infty}^{\infty} \sum_{r_2,\ldots,r_d=0}^{L-1} h_{\boldsymbol{r}}(t) \prod_{j=1}^{d} {w_j}^{r_j} & \text{for a generalized capillary,} \\ \displaystyle\sum_{r_1,\ldots,r_d=-\infty}^{\infty} h_{\boldsymbol{r}}(t) \prod_{j=1}^{d} {w_j}^{r_j} & \text{for an infinitely extended lattice.} \end{cases} \tag{10.14}$$

From (10.11) and (10.12) we can show that $H(\boldsymbol{w}; t)$ is the solution of the following differential equation

$$2d\tau^* \partial_t H(\boldsymbol{w}; t) = \left[\frac{A_1(t)}{w_1} + A_{-1}(t) w_1 + A_2(t) \sum_{j=2}^{d} \left(\frac{1}{w_j} + w_j \right) - \mathcal{A}(t) \right] H(\boldsymbol{w}; t) + K(\boldsymbol{w}; t), \tag{10.15}$$

with $\mathcal{A}(t) = A_1(t) + A_{-1}(t) + 2(d-1)A_2(t) + 2d(f+g)$ and

$$\begin{aligned} K(\boldsymbol{w}; t) \;\equiv\; & A_1(t)(w_1 - 1)h_1(t) + A_{-1}(t) \left(\frac{1}{w_1} - 1 \right) h_{-1}(t) \\ + \; & A_2(t) \sum_{j=2}^{d} \left[(w_j - 1)h_j(t) + \left(\frac{1}{w_j} - 1 \right) h_{-j}(t) \right] + \rho[A_1(t) - A_{-1}(t)] \left(w_1 - \frac{1}{w_1} \right). \end{aligned} \tag{10.16}$$

The solution of (10.15) is formally represented as:

$$H(\boldsymbol{w}; t) = \frac{1}{2d\tau^*} \int_0^t \mathrm{d}t' K(\boldsymbol{w}; t') \mathrm{e}^{\frac{1}{2d\tau^*} \int_{t'}^{t} \mathrm{d}t'' \left[\frac{A_1(t'')}{w_1} + A_{-1}(t'') w_1 + A_2(t'') \sum_{j=2}^{d} \left(\frac{1}{w_j} + w_j \right) - \mathcal{A}(t'') \right]}. \tag{10.17}$$

This integral equation can in principle be solved in order to get the full time-dependence of the density profiles $h_{\boldsymbol{r}}$ and then the expression of the first cumulant $\langle X_t \rangle$ at any time. This will deserve a further study. Here, we focus on the stationary solution of (10.15), in which we take $\lim_{t\to\infty} \partial_t H(\boldsymbol{w};t)$ and in which we drop the time-dependence of the other quantities, assuming that the profiles $h_{\boldsymbol{r}}$ reach stationary values. We get

$$H(\boldsymbol{w}) = \frac{K(\boldsymbol{w})}{\mathcal{A}} \frac{1}{1 - \left[\frac{A_1}{\mathcal{A}}\frac{1}{w_1} + \frac{A_{-1}}{\mathcal{A}} w_1 + \frac{A_2}{\mathcal{A}} \sum_{j=2}^{d} \left(\frac{1}{w_j} + w_j\right)\right]}. \tag{10.18}$$

In what follows, the last step of the computation is made explicit on the two types of considered lattices.

10.2.2 Infinite lattices

We specialize the auxiliary variables as $w_j = \mathrm{e}^{\mathrm{i}q_j}$, and introduce the function

$$\mathcal{F}_{\boldsymbol{r}} = \frac{1}{(2\pi)^d} \int_{[-\pi,\pi]^d} \mathrm{d}q_1 \dots \mathrm{d}q_d \frac{\prod_{j=1}^{d} \mathrm{e}^{-\mathrm{i}r_j q_j}}{1 - \lambda(q_1, \dots, q_d)} \tag{10.19}$$

with

$$\lambda(q_1, \dots, q_d) = \frac{A_1}{\mathcal{A}} \mathrm{e}^{-\mathrm{i}q_1} + \frac{A_{-1}}{\mathcal{A}} \mathrm{e}^{\mathrm{i}q_1} + \frac{2A_2}{\mathcal{A}} \sum_{j=2}^{d} \cos q_j, \tag{10.20}$$

so that $H(\boldsymbol{w})$ becomes a function of $q_1, \dots, q_d$:

$$H(q_1, \dots, q_d) = \frac{K(q_1, \dots, q_d)}{\mathcal{A}} \frac{1}{1 - \lambda(q_1, \dots, q_d)}. \tag{10.21}$$

Note that λ is the structure function of the random walk of a particle going in direction -1 with probability $A_1/\mathcal{A}$, in direction 1 with probability $A_{-1}/\mathcal{A}$ and in any other direction with probability $A_2/\mathcal{A}$. Consequently, $\mathcal{F}_{\boldsymbol{r}}$ is the long-time limit of the generating function associated to the propagator of a biased random walker starting from $\mathbf{0}$ and arriving at site $\boldsymbol{r}$ on a d-dimensional infinite lattice, with the evolution rules specified by the structure function λ [58]. Using the definition of $\mathcal{F}_{\boldsymbol{r}}$ from (10.19), and taking the inverse Fourier transforms, we get

$$\frac{1}{1 - \lambda(q_1, \dots, q_d)} = \sum_{r_1, \dots, r_d = -\infty}^{\infty} \left(\prod_{j=1}^{d} \mathrm{e}^{\mathrm{i}\pi r_j q_j} \right) \mathcal{F}_{\boldsymbol{r}}. \tag{10.22}$$

Using (10.21),

$$H(q_1, \dots, q_d) = \frac{1}{\mathcal{A}} \sum_{r_1, \dots, r_d = -\infty}^{\infty} K(q_1, \dots, q_d) \mathcal{F}_{\boldsymbol{r}} \prod_{j=1}^{d} \mathrm{e}^{\mathrm{i}r_j q_j}. \tag{10.23}$$

Finally, using the definition of K in (10.16), writing $H(q_1, \dots, q_d)$ using (10.14) and identifying the terms from both sides of (10.23), one shows that $h_{\boldsymbol{r}}$ is given by the following equation:

$$\mathcal{A} h_{\boldsymbol{r}} = \sum_{\nu} A_\nu h_\nu \nabla_{-\nu} \mathcal{F}_{\boldsymbol{r}} - \rho(A_1 - A_{-1})(\nabla_1 - \nabla_{-1}) \mathcal{F}_{\boldsymbol{r}}, \tag{10.24}$$

The right-hand side of this equation involves the quantities $h_\nu = h_{\boldsymbol{e}_\nu}$. Noticing that $h_{\pm 2} = \cdots = h_{\pm d}$ for symmetry reasons, one actually needs to determine the expressions of h_1, h_{-1} and h_2 in order to deduce $h_{\boldsymbol{r}}$ for any $\boldsymbol{r}$. This can be done by evaluating (10.24) for $\boldsymbol{r} = \boldsymbol{e}_1$, $\boldsymbol{e}_{-1}$ and $\boldsymbol{e}_2$, which yields a system of three equations on h_1, h_{-1} and h_2. The functions $\mathcal{F}_{\boldsymbol{r}}$ are expressed in terms of the quantities A_μ, which are in turn expressed in terms of h_1, h_{-1} and h_2. The system of three equations is then highly nonlinear in the quantities h_ν, but can be solved numerically (see Section 10.2.4 for details). One can then deduce the value of the velocity using (10.13).

Note that the density profiles $h_{\boldsymbol{r}}$ for any value of $\boldsymbol{r}$ may also be deduced from (10.24), and would deserve a complete analysis.

10.2.3 Generalized capillaries

We now study the case where the considered d-dimensional lattice is infinite in direction 1 and finite of size L with periodic boundary conditions in the $(d-1)$ other directions. The calculation is similar to the case of infinite lattices. We specialize the auxiliary variables as $w_1 = \mathrm{e}^{\mathrm{i}q}$ and $w_j = \mathrm{e}^{2\mathrm{i}\pi k_j/L}$ (for $j \neq 1$), and introduce the function

$$\mathcal{F}_{\boldsymbol{r}} = \frac{1}{L^{d-1}} \sum_{k_2,\dots,k_d=0}^{L-1} \frac{1}{2\pi} \int_{-\pi}^{\pi} dq \frac{\mathrm{e}^{-\mathrm{i}r_1 q} \prod_{j=2}^{d} \mathrm{e}^{-2\mathrm{i}\pi r_j k_j/L}}{1 - \lambda(q, k_2, \dots, k_d)}, \tag{10.25}$$

with

$$\lambda(q, k_2, \dots, k_d) = \frac{A_1}{\mathcal{A}} \mathrm{e}^{-\mathrm{i}q} + \frac{A_{-1}}{\mathcal{A}} \mathrm{e}^{\mathrm{i}q} + \frac{2A_2}{\mathcal{A}} \sum_{j=2}^{d} \cos\left(\frac{2\pi k_j}{L}\right), \tag{10.26}$$

so that $H(\boldsymbol{w})$ becomes

$$H(q, k_2, \dots, k_d) = \frac{K(q, k_2, \dots, k_d)}{\mathcal{A}} \frac{1}{1 - \lambda(q, k_2, \dots, k_d)}. \tag{10.27}$$

Note that λ is the structure function of the random walk of a particle going in direction -1 with probability $A_1/\mathcal{A}$, in direction 1 with probability $A_{-1}/\mathcal{A}$ and in any other direction with probability $A_2/\mathcal{A}$. Consequently, $\mathcal{F}_{\boldsymbol{r}}$ is the long-time limit of the generating function associated to the propagator of a biased random walker starting from $\mathbf{0}$ and arriving at site $\boldsymbol{r}$ on a d-dimensional capillary, with the evolution rules specified by the structure function λ. Using the definition of $\mathcal{F}_{\boldsymbol{r}}$ from (10.25), and taking the inverse Fourier transforms, we get

$$\frac{1}{1 - \lambda(q, k_2, \dots, k_d)} = \sum_{n_1=-\infty}^{\infty} \sum_{n_2,\dots,n_d=0}^{L-1} \mathrm{e}^{\mathrm{i}n_1 q} \prod_{j=2}^{d} \mathrm{e}^{2\mathrm{i}\pi r_j k_j/L} \mathcal{F}_{\boldsymbol{r}}. \tag{10.28}$$

Using Eq. (10.75),

$$H(q, k_2, \dots, k_d) = \frac{1}{\alpha} \sum_{r_1=-\infty}^{\infty} \sum_{r_2,\dots,r_d=0}^{L-1} K(q, k_2, \dots, k_d) \mathcal{F}_{\boldsymbol{r}} \mathrm{e}^{\mathrm{i}r_1 q} \prod_{j=2}^{d} \mathrm{e}^{2\mathrm{i}\pi r_j k_j/L}. \tag{10.29}$$

Finally, as in the case of infinite lattices, the definition of K in (10.16) allows us to show that $h_{\boldsymbol{r}}$ is given by the equation

$$\mathcal{A} h_{\boldsymbol{r}} = \sum_{\nu} A_\nu h_\nu \nabla_{-\nu} \mathcal{F}_{\boldsymbol{r}} - \rho(A_1 - A_{-1})(\nabla_1 - \nabla_{-1}) \mathcal{F}_{\boldsymbol{r}}, \tag{10.30}$$

which may be solved with the method described in Section 10.2.2.

10.2.4 General solution

Finally, the quantities $h_{\boldsymbol{e}_1}$, $h_{\boldsymbol{e}_{-1}}$ and $h_{\boldsymbol{e}_2}$ are always given by the system of three equations obtained by evaluating

$$\mathcal{A}h_{\boldsymbol{r}} = \sum_{\nu} A_\nu h_\nu \nabla_{-\nu}\mathcal{F}_{\boldsymbol{r}} - \rho(A_1 - A_{-1})(\nabla_1 - \nabla_{-1})\mathcal{F}_{\boldsymbol{r}}, \tag{10.31}$$

at $\boldsymbol{r} = \boldsymbol{e}_1, \boldsymbol{e}_{-1}$, and $\boldsymbol{e}_2$. The functions $\mathcal{F}_{\boldsymbol{r}}$ are given by

$$\mathcal{F}_{\boldsymbol{r}} = \begin{cases} \dfrac{1}{L^{d-1}} \displaystyle\sum_{k_2,\ldots,k_d=0}^{L-1} \frac{1}{2\pi}\int_{-\pi}^{\pi} \mathrm{d}q \frac{\mathrm{e}^{-\mathrm{i}r_1 q}\prod_{j=2}^{d}\mathrm{e}^{-2\mathrm{i}\pi r_j k_j/L}}{1-\lambda(q,k_2,\ldots,k_d)} & \text{for a generalized capillary,} \\ \dfrac{1}{(2\pi)^d}\displaystyle\int_{[-\pi,\pi]^d} \mathrm{d}q_1\ldots\mathrm{d}q_d \frac{\prod_{j=1}^{d}\mathrm{e}^{-\mathrm{i}r_j q_j}}{1-\lambda(q_1,\ldots,q_d)} & \text{for an infinitely extended lattice.} \end{cases} \tag{10.32}$$

Explicitely, this system is

$$\mathcal{A}h_1 = \sum_{\nu} A_\nu h_\nu \nabla_{-\nu}\mathcal{F}_{\boldsymbol{e}_1} - \rho(A_1 - A_{-1})(\nabla_1 - \nabla_{-1})\mathcal{F}_{\boldsymbol{e}_1}, \tag{10.33}$$

$$\mathcal{A}h_{-1} = \sum_{\nu} A_\nu h_\nu \nabla_{-\nu}\mathcal{F}_{\boldsymbol{e}_{-1}} - \rho(A_1 - A_{-1})(\nabla_1 - \nabla_{-1})\mathcal{F}_{\boldsymbol{e}_{-1}}, \tag{10.34}$$

$$\mathcal{A}h_2 = \sum_{\nu} A_\nu h_\nu \nabla_{-\nu}\mathcal{F}_{\boldsymbol{e}_2} - \rho(A_1 - A_{-1})(\nabla_1 - \nabla_{-1})\mathcal{F}_{\boldsymbol{e}_2}. \tag{10.35}$$

This may be rewritten under a matricial form

$$\widetilde{C}\widetilde{h} = \rho(A_1 - A_{-1})\widetilde{\mathcal{F}} \tag{10.36}$$

with

$$\widetilde{h} = \begin{pmatrix} h_1 \\ h_{-1} \\ h_2 \end{pmatrix}, \widetilde{\mathcal{F}} = \begin{pmatrix} (\nabla_1 - \nabla_{-1})\mathcal{F}_{\boldsymbol{e}_1} \\ (\nabla_1 - \nabla_{-1})\mathcal{F}_{\boldsymbol{e}_{-1}} \\ (\nabla_1 - \nabla_{-1})\mathcal{F}_{\boldsymbol{e}_2} \end{pmatrix}, \tag{10.37}$$

and

$$\widetilde{C} = \begin{pmatrix} A_1\nabla_{-1}\mathcal{F}_{\boldsymbol{e}_1} - \mathcal{A} & A_{-1}\nabla_1\mathcal{F}_{\boldsymbol{e}_1} & A_2\nabla_{-2}\mathcal{F}_{\boldsymbol{e}_1} \\ A_1\nabla_{-1}\mathcal{F}_{\boldsymbol{e}_{-1}} & A_{-1}\nabla_1\mathcal{F}_{\boldsymbol{e}_{-1}} - \mathcal{A} & A_2\nabla_{-2}\mathcal{F}_{\boldsymbol{e}_{-1}} \\ A_1\nabla_{-1}\mathcal{F}_{\boldsymbol{e}_2} & A_{-1}\nabla_1\mathcal{F}_{\boldsymbol{e}_2} & A_2\nabla_{-2}\mathcal{F}_{\boldsymbol{e}_2} - \mathcal{A} \end{pmatrix}. \tag{10.38}$$

The solutions of this system are then

$$h_\nu = \rho(A_1 - A_{-1})\frac{\det\widetilde{C}_\nu}{\det\widetilde{C}} \tag{10.39}$$

where $\widetilde{C}_\nu$ stands for the matrix obtained from $\widetilde{C}$ by replacing the ν-th column by $\widetilde{\mathcal{F}}$. Expressing the quantities A_ν (10.8) in terms of h_ν, we get

$$A_\nu = 1 + \frac{2d\tau^*}{\tau}p_\nu(1 - \rho - h_\nu) \tag{10.40}$$

$$= 1 + \frac{2d\tau^*}{\tau}p_\nu\left[1 - \rho - \rho(A_1 - A_{-1})\frac{\det\widetilde{C}_\nu}{\det\widetilde{C}}\right]. \tag{10.41}$$

Writing this last equation for $\nu = 1, -1, 2$, we obtain a set of equations containing *implicitly* A_1, A_{-1} and A_2. It can be solved numerically for a given set of the parameters ρ, τ, τ^* and σ. Recalling the definition of V (10.3) and (10.4), the velocity is deduced from the relation

$$V = \frac{\sigma}{\tau}\left[p_1\left(1-\rho-h_1\right) - p_{-1}\left(1-\rho-h_{-1}\right)\right] \tag{10.42}$$

$$= \frac{1}{2d\tau^*}(A_1 - A_{-1}). \tag{10.43}$$

In what follows, we study the limits $\rho \to 0$ and $\rho \to 1$, in which the expression of the velocity V becomes *explicit*.

10.2.5 High-density limit

In this Section, we focus on the high-density limit, in which the density of particles ρ goes to 1. We introduce the notation $\rho_0 = 1 - \rho$, which denotes the density of vacancies on the lattice. We consider the case where the lattice is not in contact with a reservoir anymore, so that f and g are taken equal to zero with a fixed value of the density ρ. We intend to compute the expression of the velocity at leading order in ρ_0, and compare it with the exact approach at high density presented in Chapter 5.

10.2.5.1 Stationary regime

In the limit where $\rho \to 1$, the mean occupation number of each site tends to 1, and the quantity $h_{\boldsymbol{r}}$ is of order $\mathcal{O}(\rho_0)$. Recalling the expression of A_μ

$$A_\mu = 1 + \underbrace{\frac{2d\tau^*}{\tau} p_\mu(\rho_0 - h_\mu)}_{=\mathcal{O}(\rho_0)}, \tag{10.44}$$

we obtain the following useful expansions:

$$\mathcal{A} \underset{\rho_0\to 0}{=} 2d + \mathcal{O}(\rho_0), \tag{10.45}$$

$$A_1 - A_{-1} \underset{\rho_0\to 0}{=} \frac{2d\tau^*}{\tau}[p_1(\rho_0 - h_1) - p_{-1}(\rho_0 - h_{-1})] + \mathcal{O}({\rho_0}^2). \tag{10.46}$$

Expanded at order $\mathcal{O}(\rho_0)$, the general equation for $h_{\boldsymbol{r}}$ (10.31) evaluated at $\boldsymbol{r} = \boldsymbol{e}_\mu$ becomes

$$2dh_\mu = \sum_\nu h_\nu \nabla_{-\nu}\mathcal{F}_{\boldsymbol{e}_\mu} - \frac{2d\tau^*}{\tau}(1-\rho_0)[p_1(\rho_0 - h_1) - p_{-1}(\rho_0 - h_{-1})](\nabla_1 - \nabla_{-1})\mathcal{F}_{\boldsymbol{e}_\mu}. \tag{10.47}$$

As it was emphasized above, the functions $\mathcal{F}_{\boldsymbol{r}}$ actually correspond to the long-time limit of the generating function of the propagators of a biased random walk starting from $\mathbf{0}$ and arriving at site $\boldsymbol{r}$, which jumps in direction -1 with probability $A_1/\mathcal{A}$, in direction 1 with probability $A_{-1}/\mathcal{A}$ and in any other direction with probability $A_2/\mathcal{A}$. We can then use the following symmetry relations:

- $\nabla_\nu \mathcal{F}_{\boldsymbol{e}_1} = \nabla_2 \mathcal{F}_{\boldsymbol{e}_1}$ for all $\nu \neq \pm 1$,
- $\nabla_\nu \mathcal{F}_{\boldsymbol{e}_2} = \nabla_3 \mathcal{F}_{\boldsymbol{e}_1}$ for all $\nu \neq \pm 1, \pm 2$,

and write the resulting equations obtained for $\mu = 1, -1, 2$:

$$\begin{aligned}
2dh_1 &= h_1\nabla_{-1}\mathcal{F}_{\boldsymbol{e}_1} + h_{-1}\nabla_1\mathcal{F}_{\boldsymbol{e}_1} + 2(d-1)h_2\nabla_2\mathcal{F}_{\boldsymbol{e}_1} \\
&\quad -\frac{2d\tau^*}{\tau}[p_1(\rho_0 - h_1) - p_{-1}(\rho_0 - h_{-1})]\left[\nabla_1\mathcal{F}_{\boldsymbol{e}_1} - \nabla_{-1}\mathcal{F}_{\boldsymbol{e}_1}\right] \qquad (10.48)\\
2dh_{-1} &= h_1\nabla_{-1}\mathcal{F}_{\boldsymbol{e}_{-1}} + h_{-1}\nabla_1\mathcal{F}_{\boldsymbol{e}_{-1}} + 2(d-1)h_2\nabla_2\mathcal{F}_{\boldsymbol{e}_{-1}} \\
&\quad -\frac{2d\tau^*}{\tau}[p_1(\rho_0 - h_1) - p_{-1}(\rho_0 - h_{-1})]\left[\nabla_1\mathcal{F}_{\boldsymbol{e}_{-1}} - \nabla_{-1}\mathcal{F}_{\boldsymbol{e}_{-1}}\right] \qquad (10.49)\\
2dh_2 &= h_1\nabla_{-1}\mathcal{F}_{\boldsymbol{e}_2} + h_{-1}\nabla_1\mathcal{F}_{\boldsymbol{e}_2} + h_2\left[\nabla_{-2}\mathcal{F}_{\boldsymbol{e}_2} + \nabla_2\mathcal{F}_{\boldsymbol{e}_2}\right] + 2(d-2)h_2\nabla_3\mathcal{F}_{\boldsymbol{e}_2} \\
&\quad - \frac{2d\tau^*}{\tau}[p_1(\rho_0 - h_1) - p_{-1}(\rho_0 - h_{-1})]\left[\nabla_1\mathcal{F}_{\boldsymbol{e}_2} - \nabla_{-1}\mathcal{F}_{\boldsymbol{e}_2}\right]. \qquad (10.50)
\end{aligned}$$

We then need to compute the behavior of the functions $\mathcal{F}_{\boldsymbol{r}}$ when $\rho_0 \to 0$. This is made explicit in Appendix M. The main result is the following: defining $\widehat{P}(\boldsymbol{r}|\boldsymbol{0};\xi)$ as the generating function associated to the the propagator of a *symmetric* nearest-neighbor random walk of a particle starting from $\boldsymbol{0}$ and arriving at $\boldsymbol{r}$, the differences of functions $\mathcal{F}_{\boldsymbol{r}}$ may be simply expressed in terms of the differences of the generating functions $\widehat{P}$:

$$\lim_{\rho_0\to 0}\nabla_\nu\mathcal{F}_{\boldsymbol{r}} = \lim_{\xi\to 1}\left[\widehat{P}(\boldsymbol{r}+\boldsymbol{e}_\nu|\boldsymbol{0};\xi) - \widehat{P}(\boldsymbol{r}|\boldsymbol{0};\xi)\right] + \delta_\nu, \qquad (10.51)$$

with

$$\delta_\nu = \begin{cases} -\dfrac{d}{L^{d-1}} & \text{if } \nu = 1, \\ \dfrac{d}{L^{d-1}} & \text{if } \nu = -1, \\ 0 & \text{otherwise.} \end{cases} \qquad (10.52)$$

Note that for infinitely extended lattices, the quantities δ_ν vanish. Using (10.51), in the limit where $\rho_0 \to 0$, we rewrite (10.48), (10.49) and (10.50) in terms of the propagators $\widehat{P}(\boldsymbol{r}|\boldsymbol{r}_0;\xi)$. In order to reduce the number of propagators involved in this system, we use the symmetry relations for the quantities $\widehat{P}$ (4.48), (4.49) and (4.50) (see Appendix L for expressions of the differences $\nabla_\mu\mathcal{F}_{\boldsymbol{r}}$ that include the symmetry properties of $\widehat{P}$). We also use the relation

$$\widehat{P}(\boldsymbol{r}|\boldsymbol{r}_0;\xi) = \delta_{\boldsymbol{r},\boldsymbol{r}_0} + \frac{\xi}{2d}\sum_\mu \widehat{P}(\boldsymbol{r}|\boldsymbol{r}_0+\boldsymbol{e}_\mu;\xi). \qquad (10.53)$$

which was demonstrated and used in Chapter 4 (4.40). For $\boldsymbol{r}_0 = \boldsymbol{0}$, and $\boldsymbol{r} = \boldsymbol{0}, \boldsymbol{e}_1, \boldsymbol{e}_2$, we obtain

$$\begin{aligned}
\widehat{P}(\boldsymbol{0}|\boldsymbol{0},\xi) &= 1 + \frac{1}{d}\left[\widehat{P}(\boldsymbol{e}_1|\boldsymbol{0},\xi) + (d-1)\widehat{P}(\boldsymbol{e}_2|\boldsymbol{0},\xi)\right] \qquad (10.54)\\
\widehat{P}(\boldsymbol{e}_1|\boldsymbol{0},\xi) &= \frac{1}{2d}\left[\widehat{P}(\boldsymbol{0}|\boldsymbol{0},\xi) + \widehat{P}(2\boldsymbol{e}_1|\boldsymbol{0},\xi) + 2(d-1)\widehat{P}(\boldsymbol{e}_1+\boldsymbol{e}_2|\boldsymbol{0},\xi)\right] \qquad (10.55)\\
\widehat{P}(\boldsymbol{e}_2|\boldsymbol{0},\xi) &= \frac{1}{2d}\left[\widehat{P}(\boldsymbol{0}|\boldsymbol{0},\xi) + \widehat{P}(2\boldsymbol{e}_2|\boldsymbol{0},\xi) + \widehat{P}(2\boldsymbol{e}_1|\boldsymbol{0},\xi) + 2(d-2)\widehat{P}(\boldsymbol{e}_2+\boldsymbol{e}_3|\boldsymbol{0},\xi)\right] \qquad (10.56)
\end{aligned}$$

We can then rewrite the relations (10.48)-(10.49) in terms of the propagators $\widehat{P}(\mathbf{0}|\mathbf{0};\xi)$, $\widehat{P}(2\boldsymbol{e}_1|\mathbf{0};\xi)$ and $\widehat{P}(\boldsymbol{e}_1|\mathbf{0};\xi)$ only. Introducing finally the usual quantities

$$\beta = \lim_{\xi\to 1}\left[\widehat{P}(\mathbf{0}|\mathbf{0};\xi) - \widehat{P}(\boldsymbol{e}_1|\mathbf{0};\xi)\right], \tag{10.57}$$

$$\alpha = \lim_{\xi\to 1}\left[\widehat{P}(\mathbf{0}|\mathbf{0};\xi) - \widehat{P}(2\boldsymbol{e}_1|\mathbf{0};\xi)\right], \tag{10.58}$$

the system of linear equations (10.48)-(10.50) takes the simplified form:

$$\widetilde{M}(\delta)\begin{pmatrix} h_1 \\ h_{-1} \\ h_2 \end{pmatrix} = 2d\frac{\tau^*}{\tau}\rho_0(p_1-p_{-1})\begin{pmatrix} -\alpha-2\delta \\ \alpha-2\delta \\ -2\delta \end{pmatrix} \tag{10.59}$$

with $\delta = d/L^{d-1}$, and where $\widetilde{M}(\delta)$ is the following matrix:

$$\widetilde{M}(\delta) = \begin{pmatrix} -\left[2dp_1\frac{\tau^*}{\tau}(\alpha+2\delta)+2d-\beta-\delta\right] & 2dp_{-1}\frac{\tau^*}{\tau}(\alpha+2\delta)-\alpha+\beta-\delta & \alpha-2\beta \\ 2dp_1\frac{\tau^*}{\tau}(\alpha-2\delta)-\alpha+\beta+\delta & -\left[2dp_{-1}\frac{\tau^*}{\tau}(\alpha-2\delta)+2d-\beta+\delta\right] & \alpha-2\beta \\ \frac{1}{2(d-1)}\left[-8\delta p_1\frac{\tau^*}{\tau}(d-1)-2\beta(d+1)\right. & \frac{1}{2(d-1)}\left[-8\delta p_1\frac{\tau^*}{\tau}(d-1)-2\beta(d+1)\right. & \frac{1}{d-1}\left[2\beta(d+1)-2d^2-\alpha\right] \\ \left.+2\delta(d-1)+\alpha-2\beta+2d\right] & \left.-2\delta(d-1)+\alpha-2\beta+2d\right] & \end{pmatrix}. \tag{10.60}$$

The linear system (10.86) has the following solutions:

$$h_1 = \rho_0\frac{\frac{2d\tau^*}{\tau}(\alpha+\frac{2d}{L^{d-1}})(p_1-p_{-1})}{\frac{2d\tau^*}{\tau}\alpha(p_1+p_{-1})+\frac{4d^2}{L^{d-1}}\frac{\tau^*}{\tau}(p_1-p_{-1})+2d-\alpha} \tag{10.61}$$

$$h_{-1} = -\rho_0\frac{\frac{2d\tau^*}{\tau}(\alpha+\frac{2d}{L^{d-1}})(p_1-p_{-1})}{\frac{2d\tau^*}{\tau}\alpha(p_1+p_{-1})+\frac{4d^2}{L^{d-1}}\frac{\tau^*}{\tau}(p_1-p_{-1})+2d-\alpha} \tag{10.62}$$

$$h_2 = \rho_0\frac{\frac{4d^2}{L^{d-1}}\frac{\tau^*}{\tau}(p_1-p_{-1})}{\frac{2d\tau^*}{\tau}\alpha(p_1+p_{-1})+\frac{4d^2}{L^{d-1}}\frac{\tau^*}{\tau}(p_1-p_{-1})+2d-\alpha} \tag{10.63}$$

Finally, using again the definition of the velocity (10.13), we obtain

$$\boxed{\lim_{t\to\infty}\frac{\mathrm{d}}{\mathrm{d}t}\langle X_t\rangle \underset{\rho_0\to 0}{\sim} \rho_0\frac{\sigma}{\tau}\frac{p_1-p_{-1}}{1+\frac{2d\alpha}{2d-\alpha}\frac{\tau^*}{\tau}(p_1+p_{-1})+\frac{4d^2}{L^{d-1}(2d-\alpha)}\frac{\tau^*}{\tau}(p_1-p_{-1})}.} \tag{10.64}$$

With the values $\tau^* = \tau = \sigma = 1$, this expression matches the expression of the first cumulant obtained with the exact approach of the high-density limit (see Chapter 5 for the expressions of $\lim_{t\to\infty}\kappa_1^{(1)}(t)/t$ in the limit of $\rho_0 \to 0$, and in particular (5.7) and (5.22)). This expression was obtained in the case of generalized capillaries, but may be extended to infinite lattices. Indeed, taking the limit where L goes to infinity, one obtains

$$\lim_{t\to\infty}\frac{\mathrm{d}}{\mathrm{d}t}\langle X_t\rangle \underset{\rho_0\to 0}{\sim} \rho_0\frac{\sigma}{\tau}\frac{p_1-p_{-1}}{1+\frac{2d\alpha}{2d-\alpha}(p_1+p_{-1})}. \tag{10.65}$$

With $d = 2$, this corresponds to the result obtained for the two-dimensional lattice (5.29). With $d = 3$, one retrieves the result obtained for the three-dimensional lattice (6.43).

To conclude, the velocity is explicitly given by the decoupling approximation in the limit $\rho \to 1$. Moreover, we showed that the expression of the velocity at leading order in the vacancy density ρ_0 correctly matches the expression obtained by the exact approach presented in Chapter 5. This suggests that the decoupling approximation of the correlation functions $\left\langle \eta_{\boldsymbol{X}_t+\boldsymbol{r}} \eta_{\boldsymbol{X}_t+\boldsymbol{e}_\mu} \right\rangle$ (8.10) is exact in the high-density limit.

10.2.5.2 Transient regime

The calculation presented in the previous section yields the ultimate regime of the system in the long-time limit. It relied on the study of the stationary limit of the differential equation (10.15). By taking the limit where ρ_0 is going to zero first, it was shown in the exact approach (Chapters 4 and 5) that the stationary regime appears after a long-lived anomalous regime. We want to retrieve this observation with the formalism presented in this Chapter, and show explicitly that the limits $\rho_0 \to$ and $t \to \infty$ do not commute.

Technically, this is possible by starting again from the general differential equation (10.15), and taking first the limit where $\rho_0 \to 0$. Using again the expansions of $\mathcal{A}$ (10.45), A_μ (10.44) and $A_1 - A_{-1}$ (10.46), we obtain the following expression of (10.15) at leading order in ρ_0:

$$2d\tau^* \partial_t H(\boldsymbol{w};t) = \left[\sum_{j=1}^{d} \left(\frac{1}{w_j} + w_j \right) - 2d \right] H(\boldsymbol{w};t) + K(\boldsymbol{w};t), \tag{10.66}$$

where $H(\boldsymbol{w};t)$ is of order ρ_0, and where $K(\boldsymbol{w};t)$, defined by (10.16), has the expansion

$$\begin{aligned} K(\boldsymbol{w};t) \underset{\rho_0 \to 0}{=} & \sum_{j=1}^{d} \left[(w_j - 1) h_j(t) + \left(\frac{1}{w_j} - 1 \right) h_{-j}(t) \right] \\ & + \frac{2d\tau^*}{\tau} \left(w_1 - \frac{1}{w_1} \right) \{ p_1 [\rho_0 - h_1(t)] + p_{-1} [\rho_0 - h_{-1}(t)] \} + \mathcal{O}({\rho_0}^2). \end{aligned} \tag{10.67}$$

We then write the Laplace transform of (10.66):

$$2d\tau^* [s\widehat{H}(\boldsymbol{w};s) - H(\boldsymbol{w};t=0)] = \left[\sum_{j=1}^{d} \left(\frac{1}{w_j} + w_j \right) - \mathcal{A} \right] \widehat{H}(\boldsymbol{w};s) + \widehat{K}(\boldsymbol{w};s), \tag{10.68}$$

where we introduced the Laplace transform

$$\widehat{f}(s) = \int_0^\infty \mathrm{d}t \, \mathrm{e}^{-st} f(t), \tag{10.69}$$

so that

$$\widehat{H}(\boldsymbol{w};s) = \begin{cases} \displaystyle\sum_{r_1=-\infty}^{\infty} \sum_{r_2,\dots,r_d=0}^{L-1} \widehat{h}_{\boldsymbol{r}}(s) \prod_{j=1}^{d} {w_j}^{r_j} & \text{for a generalized capillary,} \\ \displaystyle\sum_{r_1,\dots,r_d=-\infty}^{\infty} \widehat{h}_{\boldsymbol{r}}(s) \prod_{j=1}^{d} {w_j}^{r_j} & \text{for an infinitely extended lattice,} \end{cases} \tag{10.70}$$

and

$$\widehat{K}(\boldsymbol{w};s) \underset{\rho_0\to 0}{=} \sum_{j=1}^{d}\left[(w_j-1)\widehat{h}_j(s)+\left(\frac{1}{w_j}-1\right)\widehat{h}_{-j}(s)\right] + \frac{2d\tau^*}{\tau}\left(w_1-\frac{1}{w_1}\right)\left\{p_1\left[\frac{\rho_0}{s}-\widehat{h}_1(s)\right]+p_{-1}\left[\frac{\rho_0}{s}-\widehat{h}_{-1}(s)\right]\right\}+\mathcal{O}({\rho_0}^2). \quad (10.71)$$

The system being initially at equilibrium, the mean density $k_{\boldsymbol{r}}$ is equal to ρ on every site at time $t=0$, so that $h_{\boldsymbol{r}}=\mathbf{0}$ and $H(\boldsymbol{w};t=0)=0$. We finally get from (10.67)

$$\widehat{H}(\boldsymbol{w};s)=\frac{\widehat{K}(\boldsymbol{w};s)}{2d(1+\tau^*s)}\frac{1}{1-\frac{1}{1+\tau^*s}\frac{1}{2d}\sum_{j=1}^{d}\left(\frac{1}{w_j}+w_j\right)}. \quad (10.72)$$

This equation is the equivalent of (10.18), which was obtained in the stationary limit. We can then follow the procedures presented for infinite lattices (Section 10.2.2) and generalized capillaries (Section 10.2.3). We present here the case of generalized capillaries. We specialize the auxiliary variables as $w_1=\mathrm{e}^{\mathrm{i}q}$ and $w_j=\mathrm{e}^{2\mathrm{i}\pi k_j/L}$ (for $j\neq 1$), and introduce the function

$$\mathcal{E}_{\boldsymbol{r}}=\frac{1}{L^{d-1}}\sum_{k_2,\dots,k_d=0}^{L-1}\frac{1}{2\pi}\int_{-\pi}^{\pi}\mathrm{d}q\frac{e^{-\mathrm{i}r_1q}\prod_{j=2}^{d}e^{-2\mathrm{i}\pi r_jk_j/L}}{1-\frac{1}{1+\tau^*s}\Lambda(q,k_2,\dots,k_d)}, \quad (10.73)$$

with

$$\Lambda(q,k_2,\dots,k_d)=\frac{1}{2d}\mathrm{e}^{-\mathrm{i}q}+\frac{1}{2d}\mathrm{e}^{\mathrm{i}q}+\frac{1}{d}\sum_{j=2}^{d}\cos\left(\frac{2\pi k_j}{L}\right), \quad (10.74)$$

so that $\widehat{H}(\boldsymbol{w};s)$ becomes

$$\widehat{H}(q,k_2,\dots,k_d;s)=\frac{\widehat{K}(q,k_2,\dots,k_d;s)}{2d(1+\tau^*s)}\frac{1}{1-\frac{1}{1+\tau^*s}\Lambda(q,k_2,\dots,k_d)}. \quad (10.75)$$

Note that $\mathcal{E}_{\boldsymbol{r}}$ may be easily related to the generating functions of the propagators $\widehat{P}$ of a symmetric random walk on a generalized capillaries, which write

$$\widehat{P}(\boldsymbol{r}|\mathbf{0};\xi)=\frac{1}{L^{d-1}}\sum_{k_2,\dots,k_d=0}^{L-1}\frac{1}{2\pi}\int_{-\pi}^{\pi}\mathrm{d}q\frac{e^{-\mathrm{i}r_1q}\prod_{j=2}^{d}e^{-2\mathrm{i}\pi r_jk_j/L}}{1-\xi\Lambda(q,k_2,\dots,k_d)}, \quad (10.76)$$

so that

$$\mathcal{E}_{\boldsymbol{r}}=\widehat{P}\left(\boldsymbol{r}|\mathbf{0};\frac{1}{1+\tau^*s}\right). \quad (10.77)$$

Using the definition of $\mathcal{E}_{\boldsymbol{r}}$ from (10.73), and taking its inverse Fourier transform, we get

$$\frac{1}{1-\frac{1}{1+\tau^*s}\Lambda(q,k_2,\dots,k_d)}=\sum_{r_1=-\infty}^{\infty}\sum_{r_2,\dots,r_d=0}^{L-1}e^{\mathrm{i}r_1q}\prod_{j=2}^{d}e^{2\mathrm{i}\pi r_jk_j/L}\mathcal{E}_{\boldsymbol{r}}. \quad (10.78)$$

Using (10.72), we then obtain

$$\widehat{H}(q,k_2,\dots,k_d;p)=\frac{1}{2d(1+\tau^* s)}\sum_{r_1=-\infty}^{\infty}\sum_{r_2,\dots,r_d=0}^{L-1}\widehat{K}(q,k_2,\dots,k_d;p)\mathcal{E}_{\boldsymbol{r}}e^{\mathrm{i}r_1 q}\prod_{j=2}^{d}e^{2\mathrm{i}\pi r_j k_j/L}. \tag{10.79}$$

Finally, using the definition of $\widehat{K}$ (10.71), recalling the definition of $\widehat{H}$ (10.70) and identifying the terms on both sides of the previous equation, we get

$$2d(1+\tau^* s)\widehat{h}_{\boldsymbol{r}}(s)=\sum_{\nu}\widehat{h}_\nu(s)\nabla_{-\nu}\mathcal{E}_{\boldsymbol{r}}-\frac{2d\tau^*}{\tau}\left\{p_1\left[\frac{\rho_0}{s}-\widehat{h}_1(s)\right]+p_{-1}\left[\frac{\rho_0}{s}-\widehat{h}_{-1}(s)\right]\right\}(\nabla_1-\nabla_{-1})\mathcal{E}_{\boldsymbol{r}}. \tag{10.80}$$

Note that reasoning on infinite lattices yields the same equation, with another definition of the functions $\mathcal{E}_{\boldsymbol{r}}$:

$$\mathcal{E}_{\boldsymbol{r}}=\frac{1}{(2\pi)^d}\int_{[-\pi,\pi]^d}\mathrm{d}q_1\dots\mathrm{d}q_d\frac{\prod_{j=1}^{d}e^{-\mathrm{i}q_i r_i}}{1-\frac{1}{1+\tau^* s}\Lambda(q_1,\dots,q_d)}, \tag{10.81}$$

Evaluating (10.80) for $\boldsymbol{r}=\boldsymbol{e}_1$, $\boldsymbol{e}_{-1}$ and $\boldsymbol{e}_2$, one obtains a closed system of three linear equations whose solutions are $\widehat{h}_1$, $\widehat{h}_{-1}$ and $\widehat{h}_2$. We are interested in the long-time limit of these solutions. In terms of the Laplace variable s, this is equivalent to taking the limit $s\to 0$. Using (10.77), we find that the limit $s\to 0$ of the quantities $\mathcal{E}_{\boldsymbol{r}}$ is identical to the limit $\xi\to 1$ of the propagators $\widehat{P}$. Consequently, we find the following system at leading order in s:

$$\begin{aligned}
2d\widehat{h}_1(s) &= \widehat{h}_1(s)\nabla_{-1}\widehat{P}_{\boldsymbol{e}_1}+\widehat{h}_{-1}(s)\nabla_1\widehat{P}_{\boldsymbol{e}_1}+2(d-1)\widehat{h}_2(s)\nabla_2\widehat{P}_{\boldsymbol{e}_1}\\
&\quad -\frac{2d\tau^*}{\tau}\left\{p_1\left[\frac{\rho_0}{s}-\widehat{h}_1(s)\right]-p_{-1}\left[\frac{\rho_0}{s}-\widehat{h}_{-1}(s)\right]\right\}\left[\nabla_1\widehat{P}_{\boldsymbol{e}_1}-\nabla_{-1}\widehat{P}_{\boldsymbol{e}_1}\right] &(10.82)\\
2d\widehat{h}_{-1}(s) &= \widehat{h}_1(s)\nabla_{-1}\widehat{P}_{\boldsymbol{e}_{-1}}+\widehat{h}_{-1}(s)\nabla_1\widehat{P}_{\boldsymbol{e}_{-1}}+2(d-1)\widehat{h}_2(s)\nabla_2\widehat{P}_{\boldsymbol{e}_{-1}}\\
&\quad -\frac{2d\tau^*}{\tau}\left\{p_1\left[\frac{\rho_0}{s}-\widehat{h}_1(s)\right]-p_{-1}\left[\frac{\rho_0}{s}-\widehat{h}_{-1}(s)\right]\right\}\left[\nabla_1\widehat{P}_{\boldsymbol{e}_{-1}}-\nabla_{-1}\widehat{P}_{\boldsymbol{e}_{-1}}\right] &(10.83)\\
2d\widehat{h}_2(s) &= \widehat{h}_1(s)\nabla_{-1}\widehat{P}_{\boldsymbol{e}_2}+\widehat{h}_{-1}(s)\nabla_1\widehat{P}_{\boldsymbol{e}_2}+\widehat{h}_2(s)\left[\nabla_{-2}\widehat{P}_{\boldsymbol{e}_2}+\nabla_2\widehat{P}_{\boldsymbol{e}_2}\right]+2(d-2)\widehat{h}_2(s)\nabla_3\widehat{P}_{\boldsymbol{e}_2}\\
&\quad - \frac{2d\tau^*}{\tau}\left\{p_1\left[\frac{\rho_0}{s}-\widehat{h}_1(s)\right]-p_{-1}\left[\frac{\rho_0}{s}-\widehat{h}_{-1}(s)\right]\right\}\left[\nabla_1\widehat{P}_{\boldsymbol{e}_2}-\nabla_{-1}\widehat{P}_{\boldsymbol{e}_2}\right] &(10.84)
\end{aligned}$$

where we wrote for convenience

$$\nabla_\nu\widehat{P}_{\boldsymbol{r}}=\lim_{\xi\to 1}\nabla_\nu\widehat{P}(\boldsymbol{r}|\boldsymbol{0};\xi). \tag{10.85}$$

Using the symmetry properties of the propagators $\widehat{P}$ (4.48), (4.49) and (4.50) as well as the relations (10.54), (10.55) and (10.56), we rewrite the system of equations (10.82)-(10.84) in terms of the propagators $\widehat{P}(\boldsymbol{0}|\boldsymbol{0};\xi)$, $\widehat{P}(2\boldsymbol{e}_1|\boldsymbol{0};\xi)$ and $\widehat{P}(\boldsymbol{e}_1|\boldsymbol{0};\xi)$ only. Defining α and β as previously, we show that the system of equations (10.82)-(10.84) is equivalent to the linear sytem

$$\widetilde{M}(\delta=0)\begin{pmatrix}s\widehat{h}_1(s)\\ s\widehat{h}_{-1}(s)\\ s\widehat{h}_2(s)\end{pmatrix}=2d\frac{\tau^*}{\tau}\rho_0(p_1-p_{-1})\begin{pmatrix}-\alpha\\ \alpha\\ 0\end{pmatrix}, \tag{10.86}$$

where $\widetilde{M}(\delta)$ is defined as previously (10.60). We obtain the following solutions

$$\lim_{\rho_0\to 0}\frac{\widehat{h}_1(s)}{\rho_0} \underset{s\to 0}{=} \frac{1}{s}\frac{\frac{2d\alpha\tau^*}{\tau}(p_1-p_{-1})}{\frac{2d\alpha\tau^*}{\tau}(p_1+p_{-1})+2d-\alpha} \tag{10.87}$$

$$\lim_{\rho_0\to 0}\frac{\widehat{h}_{-1}(s)}{\rho_0} \underset{s\to 0}{=} -\frac{1}{s}\frac{\frac{2d\alpha\tau^*}{\tau}(p_1-p_{-1})}{\frac{2d\alpha\tau^*}{\tau}(p_1+p_{-1})+2d-\alpha} \tag{10.88}$$

$$\lim_{\rho_0\to 0}\frac{\widehat{h}_2(s)}{\rho_0} \underset{s\to 0}{=} 0. \tag{10.89}$$

Recalling the expression of the velocity (10.13) and computing the inverse Laplace transforms of (10.87) and (10.88), we obtain

$$\boxed{\lim_{\rho_0\to 0}\frac{1}{\rho_0}\frac{\mathrm{d}}{\mathrm{d}t}\langle X_t\rangle \underset{t\to\infty}{=} \frac{\sigma}{\tau}\frac{p_1-p_{-1}}{1+\frac{2d\alpha}{2d-\alpha}\frac{\tau^*}{\tau}(p_1+p_{-1})}.} \tag{10.90}$$

With the values $\tau^* = \tau = \sigma = 1$, this expression matches the computation of the first cumulant with the exact description of the high-density limit (see Chapter 5 for the expressions of $\lim_{\rho_0\to 0}\kappa_1^{(1)}(t)/\rho_0$ in the long-time limit, and in particular the equations (5.4), (5.19) and (5.28)). The equation (10.15), obtained from the decoupling approximation, then yields the two limiting behaviors obtained from the exact calculation presented in Chapter 5, resulting of the non-interversion of the limits $t\to\infty$ and $\rho_0\to 0$. We showed in Chapter 5 that these two regimes were described by a scaling function (5.14) in the case of quasi-one-dimensional lattices. A further study of (10.15) in the joint limit of $t\to\infty$ and $\rho_0\to 0$ with the scaling $t\sim 1/{\rho_0}^2$ may yield the same scaling function.

The opposite limit, where the density of bath particles tends to zero, is also of interest as it was studied through exact approaches. In the next Section, we show that the decoupling approximation is exact in the limit where $\rho\to 0$ and where the bath particles are static.

10.2.6 Low-density limit and fixed obstacles

In a recent publication [77], Leitmann and Franosch studied the response of a tracer to an external force, on a two-dimensional lattice, with randomly distributed and fixed obstacles. The tracer waits an exponentially distributed time with mean 1, jumps in direction ± 1 with a probability $\mathrm{e}^{\pm F/2}/Z$, and in direction ± 2 with a probability $1/Z$, where $Z = 2(1+\cosh(F/2))$ is a normalization constant. Note that this corresponds to the evolution rules prescribed in our model in the particular situation where the TP is submitted to some external force $\boldsymbol{F} = F\boldsymbol{e}_1$ (8.1). The authors obtained an exact expression for the long-time limit of the tracer velocity at leading order in the density of obstacles ρ:

$$\lim_{t\to\infty} V \underset{\rho\to 0}{=} V_0 - \rho V_0\left\{\frac{\frac{Z}{4}(\pi-2\mathrm{E})}{\mathrm{E}-\left[1-\left(\frac{4}{Z}\right)^2\right]\mathrm{K}} - \frac{\left(1-\frac{Z}{4}\right)(\pi-2\mathrm{E})}{\frac{2\pi}{Z}-\mathrm{E}+\left(1-\frac{4}{Z}\right)\mathrm{K}}+1\right\} \tag{10.91}$$

where $V_0 = p_1 - p_{-1} = 2\sinh(F/2)/Z$ is the velocity of the tracer in the absence of obstacles, and where K and E are defined by the integrals

$$\mathrm{K} = \frac{\pi}{2}\int_0^\infty \mathrm{d}t\, \mathrm{e}^{-t}\mathrm{I}_0\left(\frac{2t}{Z}\right)^2, \tag{10.92}$$

$$\mathrm{E} = \int_0^\infty \mathrm{d}t\, \mathrm{e}^{-t}\left[\left(\frac{\pi}{2} - \frac{4\pi}{Z^2}\right)\mathrm{I}_0\left(\frac{2t}{Z}\right)^2 - \frac{4\pi}{Z^2}\mathrm{I}_1\left(\frac{2t}{Z}\right)^2\right], \tag{10.93}$$

and where I_n is the modified Bessel function of the first kind. In this Section, we show that the equations (10.31) verified by $h_{\boldsymbol{r}}$ under the decoupling approximation have explicit solutions, and that the resulting expression of the TP velocity corresponds to the the exact expression (10.91) in the limit where $\rho \to 0$ and $\tau^* \to \infty$. We start from (10.31):

$$\mathcal{A}h_{\boldsymbol{r}} = \sum_\nu A_\nu h_\nu \nabla_{-\nu}\mathcal{F}_{\boldsymbol{r}} - \rho(A_1 - A_{-1})(\nabla_1 - \nabla_{-1})\mathcal{F}_{\boldsymbol{r}}, \tag{10.94}$$

and study its limit when $\rho \to 0$. We study the expansions of the quantities $h_{\boldsymbol{r}}$, A_ν and $\mathcal{A}$ in this limit:

- Recalling the definition of $h_{\boldsymbol{r}}$:
$$h_{\boldsymbol{r}} = k_{\boldsymbol{r}} - \rho, \tag{10.95}$$
and noticing that the density profiles $k_{\boldsymbol{r}}$ are of order ρ when $\rho \to 0$, we define the quantities $v_{\boldsymbol{r}}$ as
$$h_{\boldsymbol{r}} \underset{\rho\to 0}{\sim} v_{\boldsymbol{r}}\rho. \tag{10.96}$$
Starting from its expression (10.13), the velocity V can then be expressed in terms of the quantities $v_{\pm 1}$:
$$\lim_{t\to\infty} V = \frac{\sigma}{\tau}\left[p_1(1-k_1) - p_{-1}(1-k_{-1})\right] \tag{10.97}$$
$$= \frac{\sigma}{\tau}\left[(p_1 - p_{-1}) - \rho(p_1 - p_{-1}) - (p_1h_1 - p_{-1}h_{-1})\right] \tag{10.98}$$
$$\underset{\rho\to 0}{=} \frac{\sigma}{\tau}\left[V_0 - \rho V_0 - \rho(p_1v_1 - p_{-1}v_{-1})\right]. \tag{10.99}$$
Consequently, it suffices to compute v_1 and v_{-1} in order to obtain $\lim_{t\to\infty} V$.
- The quantities A_ν are constant at leading order when $\rho \to 0$:
$$A_\nu \underset{\rho\to 0}{\sim} 1 + \frac{2d\tau^*}{\tau}p_\nu. \tag{10.100}$$
- From this expansion, one deduces the expansions of $\mathcal{A}$ and $A_1 - A_{-1}$:
$$\mathcal{A} = \sum_\mu A_\mu \underset{\rho\to 0}{\sim} 2d\left(1 + \frac{\tau^*}{\tau}\right), \tag{10.101}$$
$$A_1 - A_{-1} \underset{\rho\to 0}{\sim} \frac{2d\tau^*}{\tau}(p_1 - p_{-1}). \tag{10.102}$$

Finally, at leading order in ρ, (10.94) becomes

$$2d\left(1+\frac{\tau^*}{\tau}\right)v_{\boldsymbol{r}} = \sum_{\nu}\left(1+\frac{2d\tau^*}{\tau}p_\nu\right)v_\nu\nabla_{-\nu}\mathcal{F}_{\boldsymbol{r}} - \frac{2d\tau^*}{\tau}(p_1-p_{-1})(\nabla_1-\nabla_{-1})\mathcal{F}_{\boldsymbol{r}}. \tag{10.103}$$

In the limit where the bath particles are fixed, i.e. when their mean waiting time τ^* goes to ∞, we find at leading order the following equation for the quantities $v_{\boldsymbol{r}}$:

$$v_{\boldsymbol{r}} = \sum_{\nu} p_\nu v_\nu \nabla_{-\nu}\mathcal{F}_{\boldsymbol{r}} - (p_1-p_{-1})(\nabla_1-\nabla_{-1})\mathcal{F}_{\boldsymbol{r}}. \tag{10.104}$$

We now aim to evaluate the functions $\mathcal{F}_{\boldsymbol{r}}$ in the limit $\tau^* \to \infty$. In order to retrieve the result obtained by Leitmann and Franosch, we specialize our computation to the case of a two-dimensional lattice, in which these functions write

$$\mathcal{F}_{\boldsymbol{r}} = \frac{1}{(2\pi)^2}\int_{-\pi}^{\pi}\mathrm{d}q_1\int_{-\pi}^{\pi}\mathrm{d}q_2\frac{\mathrm{e}^{-\mathrm{i}(r_1q_1+r_2q_2)}}{1-\lambda(q_1,q_2)} \tag{10.105}$$

with

$$\lambda(q_1,q_2) = \frac{A_1}{\mathcal{A}}\mathrm{e}^{-\mathrm{i}q_1} + \frac{A_{-1}}{\mathcal{A}}\mathrm{e}^{\mathrm{i}q_1} + \frac{2A_2}{\mathcal{A}}\cos q_2. \tag{10.106}$$

Equivalently, the functions $\mathcal{F}_{\boldsymbol{r}}$ may be written

$$\mathcal{F}_{\boldsymbol{r}} = \frac{1}{(2\pi)^2}\int_0^\infty \mathrm{d}t\,\mathrm{e}^{-t}\int_{-\pi}^{\pi}\mathrm{d}q_1\int_{-\pi}^{\pi}\mathrm{d}q_2\,\mathrm{e}^{t\left(\frac{A_1}{\mathcal{A}}\mathrm{e}^{-\mathrm{i}q_1}+\frac{A_{-1}}{\mathcal{A}}\mathrm{e}^{\mathrm{i}q_1}+\frac{2A_2}{\mathcal{A}}\cos q_2\right)}\mathrm{e}^{-\mathrm{i}(r_1q_1+r_2q_2)}. \tag{10.107}$$

We use the generating function associated to the modified Bessel function of the first kind [1]:

$$\mathrm{e}^{\frac{z}{2}\left(t+\frac{1}{t}\right)} = \sum_{n=-\infty}^{\infty} t^n \mathrm{I}_n(z). \tag{10.108}$$

From this formula, it is straightforward to write the following expansion

$$\mathrm{e}^{t\left(\frac{A_1}{\mathcal{A}}\mathrm{e}^{-\mathrm{i}q_1}+\frac{A_{-1}}{\mathcal{A}}\mathrm{e}^{\mathrm{i}q_1}\right)} = \mathrm{e}^{t\frac{\sqrt{A_1A_{-1}}}{\mathcal{A}}\left(\sqrt{\frac{A_1}{A_{-1}}}\mathrm{e}^{-\mathrm{i}q_1}+\sqrt{\frac{A_{-1}}{A_1}}\mathrm{e}^{\mathrm{i}q_1}\right)} \tag{10.109}$$

$$= \sum_{n=-\infty}^{\infty}\left(\frac{A_{-1}}{A_1}\right)^{n/2}\mathrm{I}_n\left(\frac{2\sqrt{A_1A_{-1}}}{\mathcal{A}}t\right)\mathrm{e}^{-\mathrm{i}nq_1}. \tag{10.110}$$

Finally, the functions $\mathcal{F}_{\boldsymbol{r}}$ can be written

$$\mathcal{F}_{\boldsymbol{r}} = \left(\frac{A_{-1}}{A_1}\right)^{r_1/2}\int_0^\infty \mathrm{d}t\,\mathrm{e}^{-t}\mathrm{I}_{r_1}\left(\frac{2\sqrt{A_1A_{-1}}}{\mathcal{A}}t\right)\mathrm{I}_{r_2}\left(\frac{2A_2}{\mathcal{A}}t\right). \tag{10.111}$$

We are interested in the limit $\rho \to 0$ and $\tau^* \to \infty$ of these quantities. Recalling the expansions (10.100) and (10.101), we get at leading order in $\rho \to 0$ and $\tau^* \to \infty$,

$$\frac{A_{-1}}{A_1} \sim \frac{p_{-1}}{p_1} = \mathrm{e}^{-F}, \tag{10.112}$$

$$\frac{2\sqrt{A_1A_{-1}}}{\mathcal{A}} \sim 2\sqrt{p_1p_{-1}} = \frac{2}{Z}, \tag{10.113}$$

$$\frac{2A_2}{\mathcal{A}} \sim \frac{2}{Z}. \tag{10.114}$$

Finally, in this limit, we get:

$$\mathcal{F}_{\boldsymbol{r}} \sim \mathrm{e}^{-\frac{Fr_1}{2}} \int_0^\infty \mathrm{d}t\, \mathrm{e}^{-t} \mathrm{I}_{r_1}\left(\frac{2t}{Z}\right) \mathrm{I}_{r_2}\left(\frac{2t}{Z}\right). \tag{10.115}$$

Interestingly, denoting by $\widehat{P}(\boldsymbol{r}|\mathbf{0};\xi)$ the generating function associated to the propagator of a symmetric random walk starting from $\mathbf{0}$ and arriving at $\boldsymbol{r}$ on a two-dimensional lattice, and recalling its integral representation [58]:

$$\widehat{P}(\boldsymbol{r}|\mathbf{0};\xi) = \int_0^\infty \mathrm{d}t\, \mathrm{e}^{-t} \mathrm{I}_{r_1}\left(\frac{t\xi}{2}\right) \mathrm{I}_{r_2}\left(\frac{t\xi}{2}\right), \tag{10.116}$$

we show that the functions $\mathcal{F}_{\boldsymbol{r}}$ can be expressed straightforwardly in terms of these propagators:

$$\mathcal{F}_{\boldsymbol{r}} \sim \mathrm{e}^{-\frac{Fr_1}{2}} \widehat{P}(\boldsymbol{r}|\mathbf{0};4/Z). \tag{10.117}$$

We now go back to the equation on the quantities $v_{\boldsymbol{r}}$ (10.104), and obtain a closed system of equations for v_1, v_{-1} and v_2:

$$\widetilde{D}\widetilde{v} = (p_1 - p_{-1})\widetilde{\mathcal{F}}, \tag{10.118}$$

with

$$\widetilde{v} = \begin{pmatrix} v_1 \\ v_{-1} \\ v_2 \end{pmatrix}, \widetilde{\mathcal{F}} = \begin{pmatrix} (\nabla_1 - \nabla_{-1})\mathcal{F}_{\boldsymbol{e}_1} \\ (\nabla_1 - \nabla_{-1})\mathcal{F}_{\boldsymbol{e}_{-1}} \\ (\nabla_1 - \nabla_{-1})\mathcal{F}_{\boldsymbol{e}_2} \end{pmatrix}, \tag{10.119}$$

and

$$\widetilde{D} = \begin{pmatrix} p_1\nabla_{-1}\mathcal{F}_{\boldsymbol{e}_1} - 1 & p_{-1}\nabla_1\mathcal{F}_{\boldsymbol{e}_1} & 2p_2\nabla_2\mathcal{F}_{\boldsymbol{e}_1} \\ p_1\nabla_{-1}\mathcal{F}_{\boldsymbol{e}_{-1}} & p_{-1}\nabla_1\mathcal{F}_{\boldsymbol{e}_{-1}} - 1 & 2p_2\nabla_2\mathcal{F}_{\boldsymbol{e}_{-1}} \\ p_1\nabla_{-1}\mathcal{F}_{\boldsymbol{e}_2} & p_{-1}\nabla_1\mathcal{F}_{\boldsymbol{e}_2} & p_2(\nabla_2 + \nabla_{-2})\mathcal{F}_{\boldsymbol{e}_2} - 1 \end{pmatrix}. \tag{10.120}$$

Note that the quantities E (10.93) and K (10.92) are expressed in terms of the integrals $\int_0^\infty \mathrm{d}t\, \mathrm{e}^{-t}\mathrm{I}_0\,(2t/Z)^2 = \widehat{P}(\mathbf{0}|\mathbf{0};4/Z)$ and $\int_0^\infty \mathrm{d}t\, \mathrm{e}^{-t}\mathrm{I}_1\,(2t/Z)^2 = \widehat{P}(\boldsymbol{e}_1+\boldsymbol{e}_2|\mathbf{0};4/Z)$. Using the definitions of $\mathcal{F}_{\boldsymbol{r}}$ (10.117) and $\widehat{P}$ (10.116), as well as the usual symmetry properties of the propagators $\widehat{P}$ (4.49),(4.50), (4.93) and (4.94), one can express the gradients involved in $\widetilde{\mathcal{F}}$ and $\widetilde{D}$ in terms of the propagators $\widehat{P}(\boldsymbol{r}|\mathbf{0};\xi)$ evaluated at $\boldsymbol{r} = \mathbf{0}$, $\boldsymbol{e}_2$, $2\boldsymbol{e}_2$ and $\boldsymbol{e}_1 + \boldsymbol{e}_2$:

$$\widetilde{D} = Z \begin{pmatrix} \mathrm{e}^{F/2}(P_{\mathbf{0}} - \mathrm{e}^{-F/2}P_{\boldsymbol{e}_1}) - 1 & \mathrm{e}^{-F/2}(\mathrm{e}^{-F}P_{2\boldsymbol{e}_1} - \mathrm{e}^{-F/2}P_{\boldsymbol{e}_1}) & 2\mathrm{e}^{-F/2}(P_{\boldsymbol{e}_1+\boldsymbol{e}_2} - P_{\boldsymbol{e}_1}) \\ \mathrm{e}^{F/2}(\mathrm{e}^{F}P_{2\boldsymbol{e}_1} - \mathrm{e}^{F/2}P_{\boldsymbol{e}_1}) & \mathrm{e}^{-F/2}(P_{\mathbf{0}} - \mathrm{e}^{F/2}P_{\boldsymbol{e}_1}) - 1 & 2\mathrm{e}^{F/2}(P_{\boldsymbol{e}_1+\boldsymbol{e}_2} - P_{\boldsymbol{e}_1}) \\ \mathrm{e}^{F/2}(\mathrm{e}^{F/2}P_{\boldsymbol{e}_1+\boldsymbol{e}_2} - P_{\boldsymbol{e}_1}) - 1 & \mathrm{e}^{-F/2}(\mathrm{e}^{-F/2}P_{\boldsymbol{e}_1+\boldsymbol{e}_2} - P_{\boldsymbol{e}_1}) & P_{2\boldsymbol{e}_1} + P_{\mathbf{0}} - 2P_{\boldsymbol{e}_1} - 1 \end{pmatrix}, \tag{10.121}$$

$$\widetilde{\mathcal{F}} = \begin{pmatrix} \mathrm{e}^{-F}P_{2\boldsymbol{e}_1} - P_{\mathbf{0}} \\ P_{\mathbf{0}} - \mathrm{e}^{F}P_{2\boldsymbol{e}_1} \\ \mathrm{e}^{-F/2}P_{\boldsymbol{e}_1+\boldsymbol{e}_2} - \mathrm{e}^{F/2}P_{\boldsymbol{e}_1+\boldsymbol{e}_2} \end{pmatrix}, \tag{10.122}$$

where we defined

$$P_{\boldsymbol{r}} = \widehat{P}(\boldsymbol{r}|\mathbf{0};4/Z). \tag{10.123}$$

The usual relation on the propagators $\widehat{P}$

$$\widehat{P}(\boldsymbol{r}|\boldsymbol{r}_0;\xi) = \delta_{\boldsymbol{r},\boldsymbol{r}_0} + \frac{\xi}{4} \sum_{\mu=\pm1,\pm2} \widehat{P}(\boldsymbol{r}|\boldsymbol{r}_0 + \boldsymbol{e}_\mu;\xi) \tag{10.124}$$

yields the following relations

$$P_{\mathbf{0}} = 1 + \frac{4}{Z} P_{\boldsymbol{e}_1}, \tag{10.125}$$

$$P_{\boldsymbol{e}_1} = \frac{1}{Z}(P_{\mathbf{0}} + P_{2\boldsymbol{e}_1} + 2P_{\boldsymbol{e}_1+\boldsymbol{e}_2}), \tag{10.126}$$

which allow us to express $P_{\boldsymbol{e}_1}$ and $P_{2\boldsymbol{e}_1}$ in terms of $P_{\mathbf{0}}$ and $P_{\boldsymbol{e}_1+\boldsymbol{e}_2}$. Finally, we obtain an expression of v_1 and v_{-1} in terms of F and of the propagators $P_{\mathbf{0}}$ and $P_{\boldsymbol{e}_1+\boldsymbol{e}_2}$, and then, using (10.99) with $\tau = \sigma = 1$, an expression of $\lim_{t\to\infty} V$ in terms of the same quantities:

$$\lim_{t\to\infty} V = V_0 - \rho V_0 \left\{ 1 + \left(1 - P_{\mathbf{0}} + \frac{8}{Z^2} P_{\mathbf{0}} + \frac{8}{Z^2} P_{\boldsymbol{e}_1+\boldsymbol{e}_2} \right) \right. \tag{10.127}$$

$$\left. \times \left[\frac{\frac{Z}{4}}{\frac{8}{Z^2} P_{\mathbf{0}} - \frac{4}{Z^2}(P_{\mathbf{0}} + P_{\boldsymbol{e}_1+\boldsymbol{e}_2})} - \frac{1 - \frac{Z}{4}}{\frac{2}{Z}(1 - P_{\mathbf{0}}) + \frac{4}{Z^2}(P_{\mathbf{0}} + P_{\boldsymbol{e}_1+\boldsymbol{e}_2})} \right] \right\}. \tag{10.128}$$

Finally, rewriting K and E,

$$\mathrm{K} = \frac{\pi}{2} P_{\mathbf{0}} \tag{10.129}$$

$$\mathrm{E} = \left(\frac{\pi}{2} - \frac{4\pi}{Z^2} \right) P_{\mathbf{0}} - \frac{4\pi}{Z^2} P_{\boldsymbol{e}_1+\boldsymbol{e}_2}, \tag{10.130}$$

one can show that the expression obtained from the decoupling approximation (10.127) coincides with the exact expression obtained by Leitmann and Franosch (10.91).

From this calculation, we conclude that the decoupling approximation yields exact results in the limit of very dilute and fixed obstacles at leading order in the density ρ.

The situation where there is a small density of *mobile* obstacles (i.e. $\tau^* < \infty$) would also deserve attention. The exact calculation presented by Leitmann and Franosch may be extended in this situation, in order to obtain the exact expression of the velocity at leading order in ρ with finite τ^*. We expect the decoupling approximation to be exact in this situation too: indeed, this mean-field-type approximation is expected to more and more accurate as the mobility of the environment increases.

10.3 Negative differential mobility

The results from this Section were published in [P6].

10.3.1 Introduction

In the previous section, we obtained an approximated expression for the velocity of the TP in any dimension, defined by

$$V = \lim_{t\to\infty} \frac{\mathrm{d}\,\langle X_t \rangle}{\mathrm{d}t}. \tag{10.131}$$

It was shown (Section 10.2.4) that its value could be determined numerically for a given set of the parameters ρ, σ, τ, τ^* and $p_{\pm 1}$. In what follows, we will take the lattice spacing σ is taken equal to 1.

We consider the case where the number of particles on the lattice is conserved ($f = g = 0$). The jump probability of the TP in direction ν will be

$$p_\nu = \frac{\mathrm{e}^{\frac{1}{2}\boldsymbol{F}\cdot\boldsymbol{e}_\nu}}{\sum_\mu \mathrm{e}^{\frac{1}{2}\boldsymbol{F}\cdot\boldsymbol{e}_\mu}}, \tag{10.132}$$

where $\boldsymbol{F} = F\boldsymbol{e}_1$ is an external force applied on the TP.

In this section, we will study the behavior of the TP velocity as a function of the applied force $V(F)$, for different values of the characteristic times τ (mean waiting time between two jumps of the TP) and τ^* (mean waiting time between two jumps of a bath particle). We will show that for a given value of ρ, if the ratio τ^*/τ is small enough, V might be a non-monotonic function of the applied force. In other contexts, this phenomenon is known as negative differential mobility (NDM): the terminal drift velocity first grows as expected from linear response, reaches a peak value and eventually decreases. This means that the differential mobility of the driven particle becomes negative for F exceeding a certain threshold value. Such a counter-intuitive "getting more from pushing less" [121] behavior of the differential mobility (or of the differential conductivity) has been observed for a variety of physical systems and processes, e.g. for electron transfer in semiconductors at low temperatures [32, 93, 111, 76], hopping processes in disordered media [21], far-from-equilibrium quantum spin chains [12], some models of Brownian motors [107, 68], soft matter colloidal particles [39], different nonequilibrium systems [121], and also for the kinetically constrained models of glass formers [61].

Apart of these examples, negative differential mobility (NDM) has been shown to emerge in some particular limits of the minimal model of a driven lattice gas. In the case of immobile bath particles ($\tau^* \to \infty$), it has been argued that for a tracer subject to an external force and diffusing on an infinite percolation cluster, the drift velocity vanishes for large enough values of the force, and therefore NDM occurs [8]. More recently, NDM was also observed via numerical simulations for low density [77, 5] and analytically accounted for [77], but to the first order in ρ only. Surprisingly enough, it appears that NDM is not a specific feature of a frozen distribution of obstacles but also emerges in dynamical environments undergoing continuous reshuffling due to obstacles random motion ($\tau^* < \infty$). Indeed, very recently, numerical analysis performed in [9] at a specific value of the density revealed that NDM could occur in a 2D driven lattice gas for bath particles diffusing slow enough.

In general, the origin of the NDM has been attributed to the nonequilibrium (called "frenetic") contributions appearing in the fluctuation-dissipation relation [33, 6]. As shown earlier in [14, 13], due to its interactions with the environment, the TP drives such a crowded system to a nonequilibrium steady-state with a nonhomogeneous obstacles density profile. However, the "nonequilibrium" condition is clearly not the only necessary condition for the NDM to emerge - in simulations in [9] this phenomenon is apparent for some range of parameters but it definitely should be absent when the obstacles move sufficiently fast so that the TP sees the environment as a fluid.

Finally, NDM seems to be controlled by both the density ρ and the diffusion time scale τ^* of the bath particles. However, a microscopic theoretical analysis of this effect is still lacking. The only available analysis is restricted to the case of immobile obstacles in the low-density regime [77] where, by definition, the bath particles are not perturbed by the TP. In this Section, we reveal the complete scenario of this coupled dynamics providing:

- a scaling argument in the dilute regime that unveils the physical mechanism of NDM,

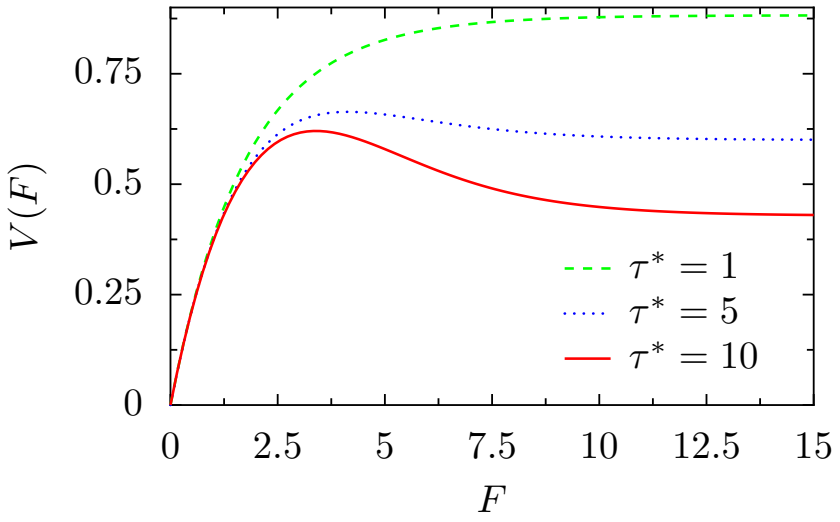

Figure 10.1: Expression of $V(F)$ from (10.133). The density is $\rho = 0.1$, the parameter τ is taken equal to 1. When τ^* is large enough, $V(F)$ is non-monotonic and is a decreasing function of F at large forces.

- an analytic analysis of the TP velocity for arbitrary values of system parameters,
- a criterion for the NDM effect to be observed, which shows in particular that for any ρ NDM exists if τ^* is large enough.

10.3.2 Simple physical mechanism

In this Section, we first obtain an approximate expression for $V(F)$ with simple physical arguments, and we show that it may be non-monotonic in some range of parameters.

Assuming a strong external force, one has $p_1 \simeq 1-\varepsilon$, $p_{-1} = \mathcal{O}(\varepsilon^2)$, with $\varepsilon = \exp(-F/2)$, so that the mean velocity in the absence of obstacles may be written $(1-\varepsilon)/\tau$. The stationary velocity in the presence of obstacles is then given by the mean distance $1/\rho$ traveled by the TP between two obstacles divided by the mean duration of this excursion, which is the sum of the mean time of free motion $\tau/[\rho(1-\varepsilon)]$ and of the mean trapping time $\tau_{\rm trap}$ per obstacle. The escape from a trap results from two alternative independent events: the TP steps in the transverse direction (with rate ε/τ) or the obstacle steps away (with rate $3/(4\tau^*)$ in two dimensions). This leads to $\tau_{\rm trap} = 3/(4\tau^*) + \varepsilon/\tau$, and finally

$$V(F) = \frac{1-\varepsilon}{\tau + 4\rho(1-\varepsilon)\frac{\tau^*}{3+4\varepsilon\tau^*/\tau}} = \frac{1-\mathrm{e}^{-F/2}}{\tau + 4\rho(1-\mathrm{e}^{-F/2})\frac{\tau^*}{3+4\mathrm{e}^{-F/2}\tau^*/\tau}} \tag{10.133}$$

From this formula, it can be seen that V is decreasing with F at large F (i.e. small ε) and therefore is nonmonotonic with F, as soon as $\tau^* \gtrsim \sqrt{\rho}$. On Fig. 10.1, we plot the expression of $V(F)$ from (10.133). We see that this function becomes non-monotonic when τ^* becomes large enough.

This unveils the physical origin of NDM in the dilute regime, where two effects compete. On the one hand, a large force reduces the travel time between two consecutive encounters with bath particles;

on the other hand it increases the escape time from traps created by surrounding particles. Eventually, for τ^* large enough, such traps are sufficiently long lived to slow down the TP when F is increased.

10.3.3 Method and results

In order to get a more quantitative picture, we calculate $V(F)$ for different values of the parameters. Using the decoupling approximation, it was shown in Section 10.2.4 that the velocity is the solution of an implicit equation that can be solved numerically. This solution is compared with results from numerical simulations. Our simulations exactly sample the master equation (8.2) using a Gillespie (or kinetic Monte-Carlo) algorithm, which is simply an extension of the algorithm presented in the case of a one-dimensional lattice in contact with a reservoir (Section 9.3.1). In all the simulations, we fix the TP mean waiting time τ to 1. We first study V as a function of F for a fixed value of the density and for increasing values of the parameter τ^* (on Fig. 10.2, we give the results obtained for three values of the density: $\rho = 0.05, 0.5, 0.999$).

We recall that the decoupling approximation is expected to be exact in the extreme density regimes $\rho \simeq 0$ and $\rho \simeq 1$. This is confirmed by the results from numerical simulations, which display an excellent agreement with the results obtained from the decoupling approximation (see Fig. 10.2(a) for $\rho = 0.05$ and Fig. 10.2(c) for $\rho = 0.999$). At intermediate values of the density, the quantitative agreement between the decoupling approximation and the simulations is still good and allows a good qualitative prediction of the behavior of the velocity.

We notice that the curve $V(F)$ becomes nonmonotonic when the parameter τ^* is large enough, and that the threshold value of τ^* yielding a negative mobility of the TP depends on the density of particles on the lattice: for $\rho = 0.05$, we observe that there exists a threshold value of τ^*, comprised between 3 and 5, above which NDM occurs. For $\rho = 0.5$, this value is close to 5, whereas for $\rho = 0.999$ it is greater than 30. Then, by using our analytical value of $V(F)$, the region for NDM in the plane $(\rho, \tau^*/\tau)$ can be determined (Fig. 10.3). This shows that for every density there exists a value of τ^*/τ above which NDM can be observed. This is consistent with the simple physical mechanism proposed in Section 10.3.2. This threshold value of the value diverges for both limits $\rho \to 0$ and $\rho \to 1$, in which NDM cannot be observed. In turn, for any value of $\tau^*/\tau \gtrsim 1$, there exists a range of density for which NDM occurs.

10.3.4 Summary

Consequently, with our minimal model of a driven TP in a hardcore lattice gas, we presented an analytic theory for NDM in a general driven lattice gas. We used the implicit equation verified by the TP velocity and obtained using a decoupling approximation. For values of τ^* large enough, a nonmonotonic behavior of the TP velocity as a function of the external force is indeed observed. Our study extends analytical results obtained in [77] and sheds light on recent numerical observations [5, 9].

Our solution reveals and quantifies a minimal physical mechanism responsible for NDM, which is based on the coupling between the density of obstacles and the diffusion time scales of the TP and obstacles. Our minimal model, which takes into account the repulsive part of the particle-particle interactions only, suggests that the phenomenon of the negative differential mobility could be a generic feature of biased transport in crowded environments.

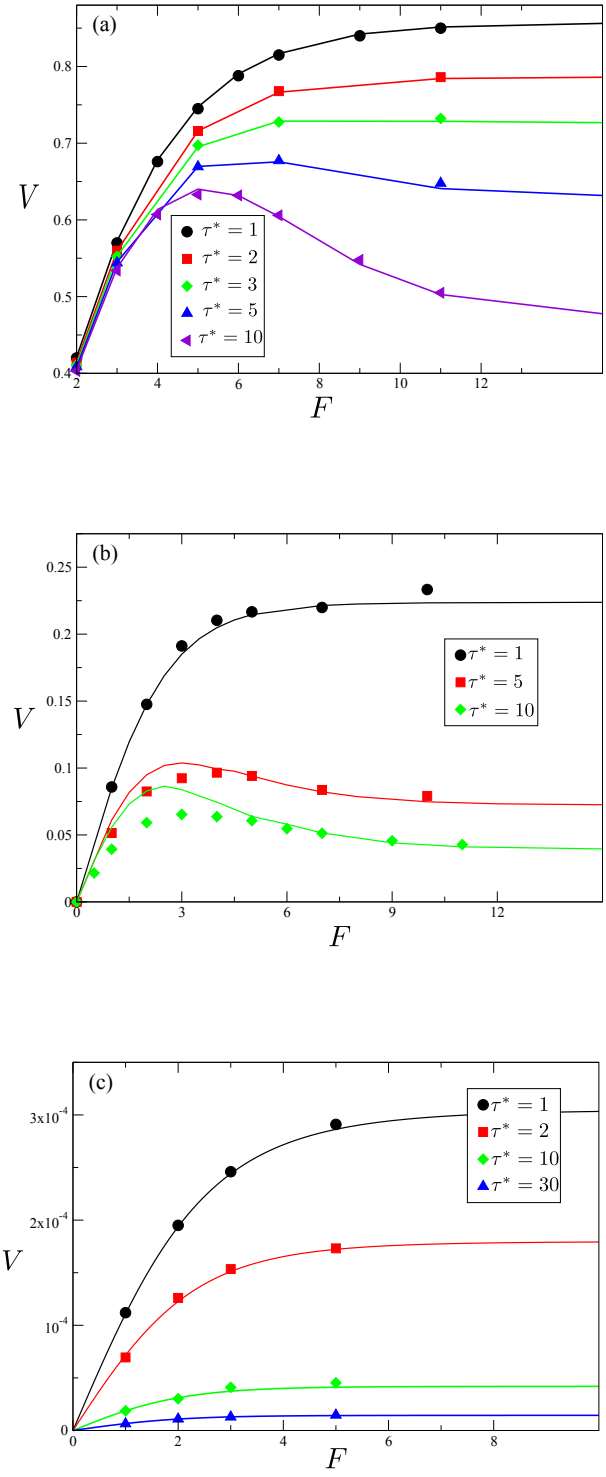

Figure 10.2: Velocity V of the TP on a 2D lattice as a function of the force F: (a) $\rho = 0.05$; (b) $\rho = 0.5$; (c) $\rho = 0.999$. For the three situations $\tau = 1$ and τ^* varies, results obtained from numerical simulations (symbols) are confronted with the predictions from the decoupling approximation. Numerical simulations performed by Alessandro Sarracino (postdoc in the group).

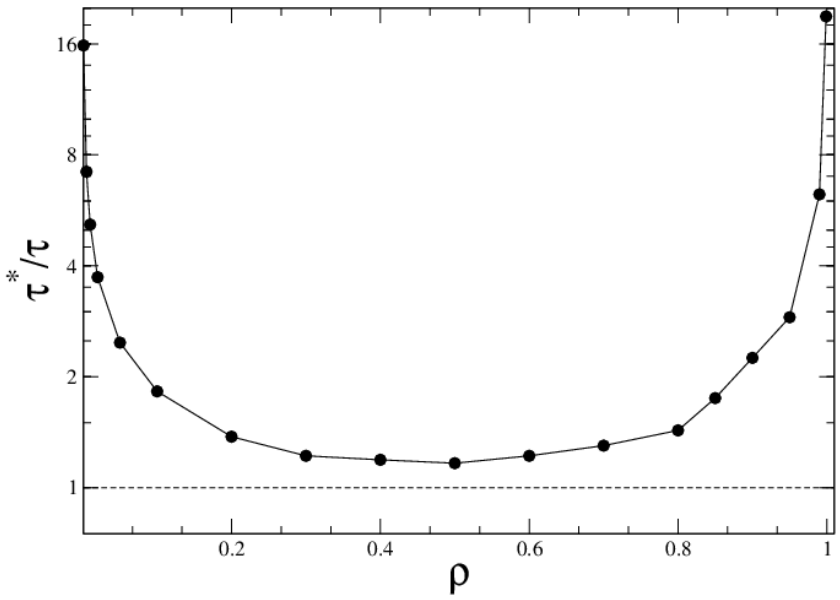

Figure 10.3: Region of negative differential mobility (above the curve) in the plane $(\rho, \tau^*/\tau)$ on a two-dimensional lattice, obtained by the decoupling approximation.

10.4 Fluctuations of the TP

In this Section, we aim to compute the fluctuations of the TP position $\langle {X_t}^2 \rangle - \langle X_t \rangle^2$. In Chapter 8, we obtained the following expression for the derivative of the fluctuations:

$$\frac{\mathrm{d}}{\mathrm{d}t}\left(\langle {X_t}^2 \rangle - \langle X_t \rangle^2\right) = -\frac{2\sigma}{\tau}\left[p_1 \widetilde{g}_{\boldsymbol{e}_1} - p_{-1}\widetilde{g}_{\boldsymbol{e}_{-1}}\right] + \frac{\sigma^2}{\tau}\left[p_1(1-k_{\boldsymbol{e}_1}) + p_{-1}(1-k_{\boldsymbol{e}_{-1}})\right], \quad (10.134)$$

were $k_{\boldsymbol{r}} = \langle \eta_{\boldsymbol{r}} \rangle$ is the average density at site $\boldsymbol{r}$ (a method to compute them was presented in Section 10.2), and where the cross-correlation functions $\widetilde{g}_{\boldsymbol{r}} = \langle \delta X_t \delta \eta_{\boldsymbol{X}_t + \boldsymbol{r}} \rangle$ are the solutions of the equations (8.23) and (8.24). We also recall the definition of the diffusion coefficient of the TP in the stationary limit:

$$K = \frac{1}{2}\lim_{t\to\infty} \frac{\mathrm{d}}{\mathrm{d}t}\left(\langle {X_t}^2 \rangle - \langle X_t \rangle^2\right). \quad (10.135)$$

In this Section, we obtain an equation verified by the quantities $\widetilde{g}_{\boldsymbol{r}}$, and involving the quantities h_ν, that can be determined numerically as shown in the previous Section. We also study the limit $\rho \to 1$ of this solution, which coincides with the expressions obtained with the exact approach presented in the first part of this thesis.

10.4.1 General equations

In what follows, we extend the method presented in Section 10.2 in order to solve the equations verified by the cross-correlation functions $\widetilde{g}_{\boldsymbol{r}}$. In Chapter 8 the functions $\widetilde{g}_{\boldsymbol{r}}$ were shown to be the solutions of (8.23) and (8.24). It then appears that $\widetilde{g}_{\boldsymbol{r}}$ will be determined in terms of the quantities $k_{\boldsymbol{r}}$. In Section 10.2, we solved the equation verified by the quantities $h_{\boldsymbol{r}} = k_{\boldsymbol{r}} - \rho$. For consistency, we first give the

evolution equations of $\widetilde{g}_{\boldsymbol{r}}$ in terms of the functions $h_{\boldsymbol{r}}$. Starting from (8.23) and (8.24), and using the definition of $h_{\boldsymbol{r}}$ (10.9), we get:

- for $\boldsymbol{r} \notin \{\boldsymbol{0}, \boldsymbol{e}_{\pm 1}, \dots, \boldsymbol{e}_{\pm d}\}$:

$$\begin{aligned} 2d\tau^* \partial_t \widetilde{g}_{\boldsymbol{r}} =& \widetilde{L}\widetilde{g}_{\boldsymbol{r}} + \frac{2d\tau^*}{\tau}\sigma \left\{ p_1(1-\rho-h_1)\nabla_1 h_{\boldsymbol{r}} - p_{-1}(1-\rho-h_{-1})\nabla_{-1} h_{\boldsymbol{r}} \right\} \\ & - \frac{2d\tau^*}{\tau} \sum_{\mu} p_\mu \widetilde{g}_\mu \nabla_\mu h_{\boldsymbol{r}}, \end{aligned} \tag{10.136}$$

- for $\boldsymbol{r} = \boldsymbol{e}_\nu$ with $\nu \neq \pm 1$:

$$\begin{aligned} 2d\tau^* \partial_t \widetilde{g}_\nu =& (\widetilde{L} + A_\nu)\widetilde{g}_\nu + \frac{2d\tau^*}{\tau}\sigma \left\{ p_1(1-\rho-h_1)\nabla_1 h_\nu - p_{-1}(1-\rho-h_{-1})\nabla_{-1} h_\nu \right\} \\ & - \frac{2d\tau^*}{\tau} \sum_{\mu} p_\mu \widetilde{g}_{\boldsymbol{e}_\mu} \nabla_\mu h_{\boldsymbol{e}_\nu} - \frac{2d\tau^*}{\tau} \left[p_\nu(\rho + h_\nu)\widetilde{g}_\nu - p_{-\nu}\rho \widetilde{g}_{-\nu} \right], \end{aligned} \tag{10.137}$$

- for $\boldsymbol{r} = \boldsymbol{e}_1$:

$$\begin{aligned} 2d\tau^* \partial_t \widetilde{g}_1 =& (\widetilde{L} + A_1)\widetilde{g}_\nu + \frac{2d\tau^*}{\tau}\sigma \left\{ p_1(1-\rho-h_1)\nabla_1 h_1 - p_{-1}(1-\rho-h_{-1})(\nabla_{-1} h_1 - \rho) \right\} \\ & - \frac{2d\tau^*}{\tau} \sum_{\mu} p_\mu \widetilde{g}_{\boldsymbol{e}_\mu} \nabla_\mu h_1 - \frac{2d\tau^*}{\tau} \left[p_1(\rho + h_1)\widetilde{g}_1 - p_{-1}\rho \widetilde{g}_{-1} \right], \end{aligned} \tag{10.138}$$

- for $\boldsymbol{r} = \boldsymbol{e}_{-1}$:

$$\begin{aligned} 2d\tau^* \partial_t \widetilde{g}_{-1} =& (\widetilde{L} + A_{-1})\widetilde{g}_{-1} + \frac{2d\tau^*}{\tau}\sigma \left\{ p_1(1-\rho-h_1)(\nabla_1 h_{-1} - \rho) - p_{-1}(1-\rho-h_{-1})\nabla_{-1} h_{-1} \right\} \\ & - \frac{2d\tau^*}{\tau} \sum_{\mu} p_\mu \widetilde{g}_{\boldsymbol{e}_\mu} \nabla_\mu h_{-1} - \frac{2d\tau^*}{\tau} \left[p_{-1}(\rho + h_{-1})\widetilde{g}_{-1} - p_1\rho \widetilde{g}_1 \right]. \end{aligned} \tag{10.139}$$

We then define the operators $\mathcal{L}$ and $\mathcal{L}'$ by

$$2d\tau^* \partial_t \widetilde{g}_{\boldsymbol{r}} \equiv \mathcal{L}(\boldsymbol{r}), \tag{10.140}$$

$$2d\tau^* \partial_t \widetilde{g}_\nu \equiv \mathcal{L}'(\nu). \tag{10.141}$$

We also introduce the generating function G, defined by

$$G(\boldsymbol{w}; t) = \begin{cases} \displaystyle\sum_{r_1=-\infty}^{\infty} \sum_{r_2,\dots,r_d=0}^{L-1} \widetilde{g}_{\boldsymbol{r}} \prod_{j=1}^{d} {w_j}^{r_j} & \text{for a generalized capillary,} \\ \displaystyle\sum_{r_1,\dots,r_d=-\infty}^{\infty} \widetilde{g}_{\boldsymbol{r}} \prod_{j=1}^{d} {w_j}^{r_j} & \text{for an infinitely extended lattice.} \end{cases} \tag{10.142}$$

Multiplying (10.136) by $\prod_{j=1}^{d} {w_j}^{r_j}$ and summing on every lattice sites, we find

$$\begin{aligned}2d\tau^*\partial_t G(\boldsymbol{w};t) = &\left[\frac{A_1}{w_1} + A_{-1}w_1 + A_2\sum_{\mu\neq\pm1} w_{|\mu|}^{\mathrm{sgn}(\mu)} - \mathcal{A}\right] G(\boldsymbol{w};t)\\ &+ \frac{2d\tau^*}{\tau}\sigma\left[p_1(1-\rho-h_1)\left(\frac{1}{w_1}-1\right) - p_{-1}(1-\rho-h_{-1})(w_1-1)\right] H(\boldsymbol{w};t)\\ &- \frac{2d\tau^*}{\tau}\left[\sum_\mu p_\mu\widetilde{g}_\mu\left(\frac{1}{w_{|\mu|}^{\mathrm{sgn}(\mu)}}-1\right)\right] H(\boldsymbol{w};t) - \mathcal{L}_0 + \sum_{\mu\neq\pm1} w_{|\mu|}^{\mathrm{sgn}(\mu)}\left[\mathcal{L}'(\mu)-\mathcal{L}(\mu)\right]\end{aligned} \tag{10.143}$$

where we used the symmetry relation $A_{\pm2} = \ldots A_{\pm d} = A_2$ and where we defined

$$\mathcal{L}_0 = \sum_\mu A_\mu\widetilde{g}_\mu + \frac{2d\tau^*}{\tau}\sigma\left[p_1(1-\rho-h_1)h_1 - p_{-1}(1-\rho-h_{-1})h_{-1}\right] - \frac{2d\tau^*}{\tau}\sum_\mu p_\mu\widetilde{g}_\mu h_\mu. \tag{10.144}$$

Replacing $\mathcal{L}'(\mu)$ and $\mathcal{L}'(\mu)$ by their expressions, we show that G is the solution of the following differential equation:

$$2d\tau^*\partial_t G(\boldsymbol{w};t) = \left[\frac{A_1}{w_1} + A_{-1}w_1 + A_2\sum_{\mu\neq\pm1} w_{|\mu|}^{\mathrm{sgn}(\mu)} - \mathcal{A}\right] G(\boldsymbol{w};t) + J_1(\boldsymbol{w};t)H(\boldsymbol{w};t) + J_0(\boldsymbol{w};t) \tag{10.145}$$

where we defined

$$\begin{aligned}J_0(\boldsymbol{w};t) \equiv &\sum_\mu\left(w_{|\mu|}^{\mathrm{sgn}(\mu)}-1\right)\left(A_\mu - \frac{2d\tau^*}{\tau}p_\mu h_\mu\right)\widetilde{g}_\mu - \frac{2d\tau^*}{\tau}\rho\left(w_1-\frac{1}{w_1}\right)(p_1\widetilde{g}_1 - p_{-1}\widetilde{g}_{-1})\\ &+ \frac{2d\tau^*}{\tau}\sigma\left[p_{-1}(1-\rho-h_{-1})\left(\rho w_1 + h_{-1}\right) - p_1(1-\rho-h_1)(\frac{\rho}{w_1}+h_1)\right],\end{aligned} \tag{10.146}$$

$$\begin{aligned}J_1(\boldsymbol{w};t) \equiv &\frac{2d\tau^*}{\tau}\left\{\sigma\left[p_1(1-\rho-h_1)\left(\frac{1}{w_1}-1\right) - p_{-1}(1-\rho-h_{-1})(w_1-1)\right]\right.\\ &\left.- \sum_\mu p_\mu\widetilde{g}_\mu\left(\frac{1}{w_{|\mu|}^{\mathrm{sgn}(\mu)}}-1\right)\right\}.\end{aligned} \tag{10.147}$$

The stationary solution of (10.145) is given by

$$G(\boldsymbol{w}) = \frac{J_1(\boldsymbol{w})K(\boldsymbol{w})}{\mathcal{A}^2[1-\lambda(\boldsymbol{w})]^2} + \frac{J_0(\boldsymbol{w})}{\mathcal{A}[1-\lambda(\boldsymbol{w})]} \tag{10.148}$$

where we defined λ as previously:

$$\lambda(\boldsymbol{w}) = \frac{A_1}{\mathcal{A}}\frac{1}{w_1} + \frac{A_{-1}}{\mathcal{A}}w_1 + \frac{A_2}{\mathcal{A}}\sum_{j=2}^{d}\left(\frac{1}{w_j}+w_j\right), \tag{10.149}$$

and where we used the relation

$$H(\boldsymbol{w}) = \frac{K(\boldsymbol{w})}{\mathcal{A}}\frac{1}{1-\lambda(\boldsymbol{w})} \tag{10.150}$$

from Section 10.2. Finally, we express the generating function variables $w_1, \dots, w_d$ in terms of the Fourier variables:

- $w_1 = \mathrm{e}^{\mathrm{i}q_1}$ and $w_j = \mathrm{e}^{\frac{2\mathrm{i}\pi k_j}{L}}$ $(j \geq 2)$ for a generalized capillary,
- $w_j = \mathrm{e}^{\mathrm{i}q_j}$ $(0 \leq j \leq d)$ for an infinitely extended lattice.

Then, we can compute the inverse Fourier transform of (10.148) in order to retrieve the functions $\widetilde{g}_{\boldsymbol{r}}$:

$$\begin{aligned}\widetilde{g}_{\boldsymbol{r}} =& \frac{1}{\mathcal{A}} \left\{ \sum_{\mu} \left(A_\mu - \frac{2d\tau^*}{\tau} p_\mu h_\mu \right) \widetilde{g}_\mu \nabla_{-\mu} \right. \\ &+ \frac{2d\tau^*}{\tau} \rho (p_1 \widetilde{g}_1 - p_{-1} \widetilde{g}_{-1})(\nabla_1 - \nabla_{-1}) \\ &\left. - \frac{2d\tau^*}{\tau} \sigma \left\{ p_1 (1-\rho-h_1)[\rho(\nabla_1 + 1) + h_1] - p_{-1}(1-\rho-h_{-1})[\rho(\nabla_{-1}+1)+h_{-1}] \right\} \right\} \mathcal{F}_{\boldsymbol{r}} \\ &- \frac{2d\tau^*}{\tau} \frac{1}{\mathcal{A}^2} \left\{ \sum_{\mu} A_\mu h_\mu \nabla_{-\mu} - \rho(A_1 - A_{-1})(\nabla_1 - \nabla_{-1}) \right\} \\ &\times \left\{ \sum_{\mu} p_\mu \widetilde{g}_\mu \nabla_\mu - \sigma \left[p_1 (1-\rho-h_1)\nabla_1 - p_{-1}(1-\rho-h_{-1})\nabla_{-1} \right] \right\} \mathcal{G}_{\boldsymbol{r}}, \end{aligned} \tag{10.151}$$

where we define

$$\mathcal{G}_{\boldsymbol{r}} = \begin{cases} \dfrac{1}{L^{d-1}} \displaystyle\sum_{k_2,\dots,k_d=0}^{L-1} \frac{1}{2\pi} \int_{-\pi}^{\pi} \mathrm{d}q_1 \frac{e^{-\mathrm{i}r_1 q_1} \prod_{j=2}^{d} e^{-2\mathrm{i}\pi r_j k_j / L}}{[1 - \lambda(q_1, k_2, \dots, k_d)]^2} & \text{for a generalized capillary,} \\ \dfrac{1}{(2\pi)^d} \displaystyle\int_{[-\pi,\pi]^d} \mathrm{d}q_1 \dots \mathrm{d}q_d \frac{\prod_{j=1}^{d} \mathrm{e}^{-\mathrm{i}r_j q_j}}{[1 - \lambda(q_1, \dots, q_d)]^2} & \text{for an infinitely extended lattice.} \end{cases} \tag{10.152}$$

The right-hand side of (10.151) involves the quantities $\widetilde{g}_\nu = \widetilde{g}_{\boldsymbol{e}_\nu}$. Noticing that $\widetilde{g}_{\pm 2} = \cdots = \widetilde{g}_{\pm d}$ for symmetry reasons, one actually needs to determine the expressions of $\widetilde{g}_1$, $\widetilde{g}_{-1}$ and $\widetilde{g}_2$ in order to deduce $\widetilde{g}_{\boldsymbol{r}}$ for any $\boldsymbol{r}$. This can be done by evaluating (10.151) for $\boldsymbol{r} = \boldsymbol{e}_1, \boldsymbol{e}_{-1}$ and $\boldsymbol{e}_2$, which yields a system of three equations on $\widetilde{g}_1$, $\widetilde{g}_{-1}$ and $\widetilde{g}_2$. The functions $\mathcal{F}_{\boldsymbol{r}}$ and $\mathcal{G}_{\boldsymbol{r}}$ are expressed in terms of the quantities A_μ, which are in turn expressed in terms of h_1, h_{-1} and h_2. They can be obtained numerically from (10.24). Finally, the system of three equations on the quantities $\widetilde{g}_1$, $\widetilde{g}_{-1}$ and $\widetilde{g}_2$ may be solved numerically for a given set of parameters. The value of the diffusion coefficient K in the stationary limit can be deduced from the relations (10.134) and (10.135).

The equation (10.151) is important, as it allows the calculation of $\widetilde{g}_{\pm 1}$, and therefore of the diffusion coefficient of the biased TP, for any set of parameters. A further study of the solutions of (10.151) would unveil the influence of the different parameters (bias, time scales τ^* and τ, density) on this diffusion coefficient. We could then check the robustness of the effects observed in the case of the one-dimensional lattice (Chapter 9) on higher-dimensional lattices. In particular, the dependence of the diffusion coefficient of the TP on ρ could be investigated, in order to see if there exists a non-zero value of the density that enhances the diffusion properties of the TP even on lattices of dimension greater than 1.

10.4.2 High-density limit

10.4.2.1 Stationary state

In this Section, we study the high-density limit of (10.151) and show that we retrieve the results obtained from the exact approach (Chapter 4). We assume that the lattice is not in contact with a reservoir of particles anymore, which corresponds to the limit where f and g go to zero with a fixed density $\rho = f/(f+g)$. When $\rho \to 1$, one has the following behaviors for the different quantities involved in (10.151):

$$A_\mu \underset{\rho_0\to 0}{=} 1 + \mathcal{O}(\rho_0), \tag{10.153}$$

$$\mathcal{A} \underset{\rho_0\to 0}{=} 2d + \mathcal{O}(\rho_0), \tag{10.154}$$

$$A_1 - A_{-1} \underset{\rho_0\to 0}{=} \frac{2d\tau^*}{\tau}[p_1(\rho_0 - h_1) - p_{-1}(\rho_0 - h_{-1})] + \mathcal{O}(rho_0), \tag{10.155}$$

$$h_\mu \underset{\rho_0\to 0}{=} \mathcal{O}(\rho_0), \tag{10.156}$$

$$\widetilde{g}_\mu \underset{\rho_0\to 0}{=} \mathcal{O}(\rho_0). \tag{10.157}$$

Using these expansions, we find the expansion of (10.151) at leading order in ρ_0:

$$\begin{aligned} 2d\widetilde{g}_{\boldsymbol{r}} = \Bigg\{ &\sum_\mu \widetilde{g}_\mu \nabla_{-\mu} + \frac{2d\tau^*}{\tau}(p_1\widetilde{g}_1 - p_{-1}\widetilde{g}_{-1})(\nabla_1 - \nabla_{-1}) \\ &- \frac{2d\tau^*}{\tau}\sigma\left\{p_1(\rho_0 - h_1)(\nabla_1 + 1) - p_{-1}(\rho_0 - h_{-1})(\nabla_{-1} + 1)]\right\}\Bigg\} \mathcal{F}_{\boldsymbol{r}}. \end{aligned} \tag{10.158}$$

In this limit, $\widetilde{g}_1$, $\widetilde{g}_{-1}$ and $\widetilde{g}_2$ are then the solutions of the linear system

$$\begin{aligned} 2d\widetilde{g}_1 &= \widetilde{g}_1\nabla_{-1}\mathcal{F}_{\boldsymbol{e}_1} + \widetilde{g}_{-1}\nabla_1\mathcal{F}_{\boldsymbol{e}_1} + 2(d-1)\widetilde{g}_2\nabla_2\mathcal{F}_{\boldsymbol{e}_1} \\ &\quad + \frac{2d\tau^*}{\tau}(p_1\widetilde{g}_1 - p_{-1}\widetilde{g}_{-1})\left[\nabla_1\mathcal{F}_{\boldsymbol{e}_1} - \nabla_{-1}\mathcal{F}_{\boldsymbol{e}_1}\right] \\ &\quad - \frac{2d\tau^*}{\tau}\sigma[p_1(\rho_0 - h_1)\mathcal{F}_{2\boldsymbol{e}_1} - p_{-1}(\rho_0 - h_{-1})\mathcal{F}_{\boldsymbol{0}}] \end{aligned} \tag{10.159}$$

$$\begin{aligned} 2d\widetilde{g}_{-1} &= \widetilde{g}_1\nabla_{-1}\mathcal{F}_{\boldsymbol{e}_{-1}} + \widetilde{g}_{-1}\nabla_1\mathcal{F}_{\boldsymbol{e}_{-1}} + 2(d-1)\widetilde{g}_2\nabla_2\mathcal{F}_{\boldsymbol{e}_{-1}} \\ &\quad + \frac{2d\tau^*}{\tau}(p_1\widetilde{g}_1 - p_{-1}\widetilde{g}_{-1})\left[\nabla_1\mathcal{F}_{\boldsymbol{e}_{-1}} - \nabla_{-1}\mathcal{F}_{\boldsymbol{e}_{-1}}\right] \\ &\quad - \frac{2d\tau^*}{\tau}\sigma[p_1(\rho_0 - h_1)\mathcal{F}_{\boldsymbol{0}} - p_{-1}(\rho_0 - h_{-1})\mathcal{F}_{2\boldsymbol{e}_{-1}}] \end{aligned} \tag{10.160}$$

$$\begin{aligned} 2d\widetilde{g}_2 &= \widetilde{g}_1\nabla_{-1}\mathcal{F}_{\boldsymbol{e}_2} + \widetilde{g}_{-1}\nabla_1\mathcal{F}_{\boldsymbol{e}_2} + \widetilde{g}_2\left[\nabla_{-2}\mathcal{F}_{\boldsymbol{e}_2} + \nabla_2\mathcal{F}_{\boldsymbol{e}_2}\right] + 2(d-2)\widetilde{g}_2\nabla_3\mathcal{F}_{\boldsymbol{e}_2} \\ &\quad + \frac{2d\tau^*}{\tau}(p_1\widetilde{g}_1 - p_{-1}\widetilde{g}_{-1})\left[\nabla_1\mathcal{F}_{\boldsymbol{e}_2} - \nabla_{-1}\mathcal{F}_{\boldsymbol{e}_2}\right] \\ &\quad - \frac{2d\tau^*}{\tau}\sigma[p_1(\rho_0 - h_1)\mathcal{F}_{\boldsymbol{e}_2+\boldsymbol{e}_1} - p_{-1}(\rho_0 - h_{-1})\mathcal{F}_{\boldsymbol{e}_2+\boldsymbol{e}_{-1}}]. \end{aligned} \tag{10.161}$$

In what follows, we study the $\rho_0 \to 0$ limit of these equations in the two situations where the lattice is a generalized capillary, and where it is a two-dimensional lattice.

Generalized capillaries We are interested in the limit where $\rho_0 \to 0$ of the equations (10.159)-(10.161). We will use again the relation (10.51), which was demonstrated in Appendix M:

$$\lim_{\rho_0\to 0} \nabla_\nu \mathcal{F}_{\boldsymbol{r}} = \lim_{\xi\to 1} \left[\widehat{P}(\boldsymbol{r}+\boldsymbol{e}_\nu|\mathbf{0};\xi) - \widehat{P}(\boldsymbol{r}|\mathbf{0};\xi)\right] + \delta_\nu. \tag{10.162}$$

Contrary to the system (10.48)-(10.50) verified by the quantities (h_1, h_{-1}, h_2) which only involved *differences* of the functions $\mathcal{F}_{\boldsymbol{r}}$, the system (10.159)-(10.161) also involves functions $\mathcal{F}_{\boldsymbol{r}}$ alone, which are known to diverge when $\rho_0 \to 0$. In the case of generalized capillaries, we showed in Appendix M that

$$\mathcal{F}_{\boldsymbol{r}} \underset{\rho_0\to 0}{\sim} \frac{1}{L^{d-1}V} \equiv \mathcal{G}(V), \tag{10.163}$$

where $\mathcal{G}$ is defined as in the first part of this thesis (Chapter 6), and where V is actually equal to the velocity of the TP:

$$V \underset{\rho_0\to 0}{\sim} \frac{\sigma}{\tau}\left[p_1(\rho_0 - h_1) - p_{-1}(\rho_0 - h_{-1})\right] \tag{10.164}$$

and then vanishes when $\rho_0 \to 0$. Using (10.163) and (10.162), we simplify the system (10.159)-(10.161). Finally, with the usual symmetry properties on the quantities $\widehat{P}$ (4.48)-(4.50) as well as the relations (10.54)-(10.56), we rewrite the system (10.159)-(10.161) in terms of the propagators $\widehat{P}(\mathbf{0}|\mathbf{0};\xi)$, $\widehat{P}(2\boldsymbol{e}_1|\mathbf{0};\xi)$ and $\widehat{P}(\boldsymbol{e}_1|\mathbf{0};\xi)$ only. Introducing the quantities α and β as previously and using the definition of the velocity V (10.164), we show that, at leading order in ρ_0, the equations (10.159)-(10.161) can be rewritten as

$$\widetilde{M}(\delta)\begin{pmatrix}\widetilde{g}_1\\ \widetilde{g}_{-1}\\ \widetilde{g}_2\end{pmatrix} = 2d\tau^* V\rho_0(p_1 - p_{-1})\mathcal{G}(V)\begin{pmatrix}1\\1\\1\end{pmatrix}, \tag{10.165}$$

where $\widetilde{M}(\delta)$ is defined as previously (10.60). We obtain the following solutions at leading order in $\rho_0 \to 0$:

$$\widetilde{g}_{\pm 1} \underset{\rho_0\to 0}{\sim} \frac{\tau^*}{L^{d-1}} \frac{\alpha - 2d - \frac{4d\alpha\tau^*}{\tau}p_{\mp 1}}{\left[2d - \alpha + \frac{2d\alpha\tau^*}{\tau}(p_1+p_{-1}) + \frac{4d^2}{L^{d-1}}\frac{\tau^*}{\tau}(p_1 - p_{-1})\right]^2}, \tag{10.166}$$

$$\widetilde{g}_2 \underset{\rho_0\to 0}{\sim} \frac{\tau^*}{L^{d-1}} \frac{\alpha - 2d - \frac{2d\alpha\tau^*}{\tau}(p_1+p_{-1})}{\left[2d - \alpha + \frac{2d\alpha\tau^*}{\tau}(p_1+p_{-1}) + \frac{4d^2}{L^{d-1}}\frac{\tau^*}{\tau}(p_1 - p_{-1})\right]^2}. \tag{10.167}$$

The expression of the second cumulant is deduced from the definition

$$\lim_{t\to\infty}\frac{\mathrm{d}}{\mathrm{d}t}\left(\langle {X_t}^2\rangle - \langle X_t\rangle^2\right) = -\frac{2\sigma}{\tau}\left\{p_1\widetilde{g}_1 - p_{-1}\widetilde{g}_{-1}\right\} + \frac{\sigma^2}{\tau}\left\{p_1(\rho_0 - h_1) + p_{-1}(\rho_0 - h_{-1})\right\}, \tag{10.168}$$

and recalling the expression of V (10.64), we finally obtain

$$\lim_{t\to\infty}\frac{\mathrm{d}}{\mathrm{d}t}\left(\langle {X_t}^2\rangle - \langle X_t\rangle^2\right) \underset{\rho_0\to 0}{\sim} \frac{2\sigma}{L^{d-1}}\frac{\tau^*}{\tau}\frac{p_1 - p_{-1}}{1 + \frac{2d\alpha}{2d-\alpha}\frac{\tau^*}{\tau}(p_1+p_{-1}) + \frac{4d^2}{L^{d-1}(2d-\alpha)}\frac{\tau^*}{\tau}(p_1 - p_{-1})}. \tag{10.169}$$

Taking $\tau^* = \tau = 1$, this corresponds to the result obtained through the exact approach in Chapter 4 for the asymptotic behavior of the second cumulant on stripes (4.168) and capillaries (4.198). In particular, we retrieve the fact that TP fluctuations in the ultimate regime grow linearly with time, and do not depend on the vacancy density.

Two-dimensional lattice Extending the relation (10.51) to an infinite two-dimensional lattice by taking $d = 2$ and $L \to \infty$, we get:

$$\lim_{\rho_0 \to 0} \nabla_\nu \mathcal{F}_{\boldsymbol{r}} = \lim_{\xi \to 1} \left[\widehat{P}(\boldsymbol{r} + \boldsymbol{e}_\nu | \mathbf{0}; \xi) - \widehat{P}(\boldsymbol{r} | \mathbf{0}; \xi) \right]. \tag{10.170}$$

We can extend the study presented in Appendix M to the case of a two dimensional lattice, and show that

$$\mathcal{F}_{\boldsymbol{r}} \underset{\rho_0 \to 0}{\sim} \frac{2}{\pi} \ln \frac{1}{V}, \tag{10.171}$$

where V is actually equal to the velocity of the TP (10.164), and vanishes when $\rho_0 \to 0$. The use of (10.163) and (10.162) then allows us to simplify the system (10.159)-(10.161). Once again, using the relations between the different propagators $\widehat{P}$, we express all the differences $\nabla_\nu \mathcal{F}_{\boldsymbol{r}}$ in terms of the quantities α and β. Finally, using the definition of the velocity V (10.164), we show that $\widetilde{g}_1$, $\widetilde{g}_{-1}$ and $\widetilde{g}_2$ are the solutions of the system (10.165), where we take $\mathcal{G}(V) = \frac{2}{\pi} \ln \frac{1}{V}$. We obtain the following solutions of the system at leading order in $\rho_0 \to 0$:

$$\widetilde{g}_{\pm 1} \underset{\rho_0 \to 0}{\sim} \rho_0 \frac{\tau^*}{\tau} \sigma \frac{(\alpha - 4)(p_1 - p_{-1}) \left(8\alpha p_{\mp 1} \frac{\tau^*}{\tau} + 4 - \alpha \right)}{\left[4 - \alpha + 4\alpha \frac{\tau^*}{\tau} (p_1 + p_{-1}) \right]^2} \frac{2}{\pi} \ln \frac{1}{V} \tag{10.172}$$

$$\widetilde{g}_2 \underset{\rho_0 \to 0}{\sim} \rho_0 \frac{\tau^*}{\tau} \sigma \frac{p_1 - p_{-1}}{1 + \frac{4\alpha}{4-\alpha} \frac{\tau^*}{\tau} (p_1 + p_{-1})} \frac{2}{\pi} \ln \frac{1}{V} \tag{10.173}$$

The expression of the second cumulant is deduced from the definition

$$\lim_{t \to \infty} \frac{\mathrm{d}}{\mathrm{d}t} \left(\langle {X_t}^2 \rangle - \langle X_t \rangle^2 \right) = -\frac{2\sigma}{\tau} \left\{ p_1 \widetilde{g}_1 - p_{-1} \widetilde{g}_{-1} \right\} + \frac{\sigma^2}{\tau} \left\{ p_1 (\rho_0 - h_1) + p_{-1} (\rho_0 - h_{-1}) \right\}. \tag{10.174}$$

Taking $\tau^* = \tau = \sigma = 1$, and using the expression of V (10.64) with $L \to \infty$, we finally obtain at leading order in ρ_0

$$\lim_{t \to \infty} \frac{\mathrm{d}}{\mathrm{d}t} \left(\langle {X_t}^2 \rangle - \langle X_t \rangle^2 \right) \underset{\rho_0 \to 0}{\sim} \rho_0 \frac{4 {a_0}^2}{\pi} \ln \frac{1}{\rho_0}, \tag{10.175}$$

where we introduced in the usual fashion the coefficient

$$a_0 = \frac{p_1 - p_{-1}}{1 + \frac{4\alpha}{4-\alpha} (p_1 - p_{-1})}. \tag{10.176}$$

This corresponds to the result obtained through the exact approach in Chapter 4 (4.214) for the asymptotic behavior of the second cumulant on a two-dimensional lattice (4.168). In particular, we retrieve the nontrivial behavior of the cumulant in the vacancy density $\rho_0 \ln(1/\rho_0)$.

In the limit $\rho \to 1$, the decoupling approximation then allows us to retrieve the results obtained in the high-density limit, in the cases of generalized capillaries and of a two-dimensional lattice. The decoupling approximations (8.10) and (8.22), on which rely the determinations of $h_{\pm 1}$ and $\widetilde{g}_{\pm 1}$ and therefore of the fluctuations of the TP position, are then exact in the high-density limit.

10.4.2.2 Transient regime

We now study the limit where $\rho_0 \to 0$ is taken first, and $t \to \infty$ ultimately, which allows us to calculate the transient regime preceding the ultimate diffusive regime. We start again from the differential equation (10.145):

$$2d\tau^*\partial_t G(\boldsymbol{w};t) = \left[\frac{A_1}{w_1} + A_{-1}w_1 + A_2\sum_\mu w_{|\mu|}^{\mathrm{sgn}(\mu)} - \mathcal{A}\right] G(\boldsymbol{w};t) + J_1(\boldsymbol{w};t)H(\boldsymbol{w};t) + J_0(\boldsymbol{w};t). \tag{10.177}$$

In the limit where $\rho_0 \to 0$, one notices from (10.147) that $J_1(\boldsymbol{w};t)$ is of order $\mathcal{O}(\rho_0)$, so that the term $J_1(\boldsymbol{w};t)H(\boldsymbol{w};t)$ is of order $\mathcal{O}({\rho_0}^2)$ and should be discarded at leading order. Then, the differential equation becomes

$$2d\tau^*\partial_t G(\boldsymbol{w};t) = \left[\frac{1}{w_1} + w_1 + \sum_\mu w_{|\mu|}^{\mathrm{sgn}(\mu)} - 2d\right] G(\boldsymbol{w};t) + J_0(\boldsymbol{w};t) \tag{10.178}$$

where $J_0(\boldsymbol{w};t)$ has the expansion:

$$\begin{aligned} J_0(\boldsymbol{w};t) \underset{\rho_0\to 0}{=} &\sum_\mu \left(w_{|\mu|}^{\mathrm{sgn}(\mu)} - 1\right) A_\mu \widetilde{g}_\mu - \frac{2d\tau^*}{\tau}\rho\left(w_1 - \frac{1}{w_1}\right)(p_1\widetilde{g}_1 - p_{-1}\widetilde{g}_{-1}) \\ &- \frac{2d\tau^*}{\tau}\sigma\left[p_1(\rho_0 - h_1)w_1) - p_{-1}(\rho_0 - h_{-1})\frac{1}{w_1}\right]. \end{aligned} \tag{10.179}$$

We rewrite the auxiliary variables as $w_1 = \mathrm{e}^{\mathrm{i}q}$ and $w_j = \mathrm{e}^{2\mathrm{i}\pi k_j/L}$ (for $j \neq 1$), and introduce again the functions $\mathcal{E}_{\boldsymbol{r}}$ (10.73) and $\Lambda(q, k_2, \ldots, k_d)$ (10.74). We then get

$$2d\tau^*\partial_t G(\boldsymbol{w};t) = 2d\left[\Lambda(q, k_2, \ldots, k_d) - 1\right] G(\boldsymbol{w};t) + J_0(\boldsymbol{w};t). \tag{10.180}$$

The Laplace transform of this equation allows us to compute $\widehat{G}(\boldsymbol{w};s)$:

$$\widehat{G}(q, k_2, \ldots, k_d; s) = \frac{1}{2d(1+\tau^* s)} \frac{\widehat{J_0}(q, k_2, \ldots, k_d; s)}{1 - \frac{1}{1+\tau^* s}\Lambda(q, k_2, \ldots, k_d)}. \tag{10.181}$$

With the definition of $\mathcal{E}_{\boldsymbol{r}}$, this is equivalent to

$$\widehat{G}(q, k_2, \ldots, k_d; s) = \frac{1}{2d(1+\tau^* s)} \sum_{r_1=-\infty}^{\infty} \sum_{r_2,\ldots,r_d=0}^{L-1} \widehat{J_0}(q, k_2, \ldots, k_d; p)\mathcal{E}_{\boldsymbol{r}}\mathrm{e}^{\mathrm{i}r_1 q} \prod_{j=2}^{d} \mathrm{e}^{2\mathrm{i}\pi r_j k_j/L}. \tag{10.182}$$

Recalling the definitions of G and J_0, and identifying the terms of the sums on both sides of the previous equation, one gets

$$\begin{aligned} \widehat{\widetilde{g}}_{\boldsymbol{r}}(s) = &\sum_\nu \widehat{\widetilde{g}}_\nu(s)\nabla_{-\nu}\mathcal{E}_{\boldsymbol{r}} + \frac{2d\tau^*}{\tau}[p_1\widehat{\widetilde{g}}_1(s) - p_{-1}\widehat{\widetilde{g}}_{-1}(s)](\nabla_1 - \nabla_{-1})\mathcal{E}_{\boldsymbol{r}} \\ &- \frac{2d\tau^*}{\tau}\left\{p_1\left[\frac{\rho_0}{s} - \widehat{h}_1(s)\right](\nabla_1 + 1) - p_{-1}\left[\frac{\rho_0}{s} - \widehat{h}_{-1}(s)\right](\nabla_{-1} + 1)\right\}\mathcal{E}_{\boldsymbol{r}}. \end{aligned} \tag{10.183}$$

Evaluating this equation for $\boldsymbol{r} = \boldsymbol{e}_1, \boldsymbol{e}_{-1}$ and $\boldsymbol{e}_2$, one gets a system of three equations that can be solved in order to get $\widetilde{g}_1$, $\widetilde{g}_{-1}$ and $\widetilde{g}_2$. As in Section 10.2.5.2, we find that the limit $s \to 0$ of the quantities $\mathcal{E}_{\boldsymbol{r}}$ are identical to the limit $\xi \to 1$ of the propagators $\widehat{P}$. Consequently, we find the following sytem:

$$\begin{aligned}
2d\widehat{\widetilde{g}}_1(s) &= \widehat{\widetilde{g}}_1(s)\nabla_{-1}\widehat{P}_{\boldsymbol{e}_1} + \widehat{\widetilde{g}}_{-1}(s)\nabla_1\widehat{P}_{\boldsymbol{e}_1} + 2(d-1)\widehat{\widetilde{g}}_2(s)\nabla_2\widehat{P}_{\boldsymbol{e}_1} \\
&\quad + \frac{2d\tau^*}{\tau}[p_1\widehat{\widetilde{g}}_1(s) - p_{-1}\widehat{\widetilde{g}}_{-1}(s)]\left[\nabla_1\widehat{P}_{\boldsymbol{e}_1} - \nabla_{-1}\widehat{P}_{\boldsymbol{e}_1}\right] \\
&\quad - \frac{2d\tau^*}{\tau}\sigma\left\{p_1\left[\frac{\rho_0}{s} - \widehat{h}_1(s)\right]\widehat{P}_{2\boldsymbol{e}_1} - p_{-1}\left[\frac{\rho_0}{s} - \widehat{h}_{-1}(s)\right]\widehat{P}_{\boldsymbol{0}}\right\} \qquad (10.184) \\
2d\widehat{\widetilde{g}}_{-1}(s) &= \widehat{\widetilde{g}}_1(s)\nabla_{-1}\widehat{P}_{\boldsymbol{e}_{-1}} + \widehat{\widetilde{g}}_{-1}(s)\nabla_1\widehat{P}_{\boldsymbol{e}_{-1}} + 2(d-1)\widehat{\widetilde{g}}_2(s)\nabla_2\widehat{P}_{\boldsymbol{e}_{-1}} \\
&\quad + \frac{2d\tau^*}{\tau}[p_1\widehat{\widetilde{g}}_1(s) - p_{-1}\widehat{\widetilde{g}}_{-1}(s)]\left[\nabla_1\widehat{P}_{\boldsymbol{e}_{-1}} - \nabla_{-1}\widehat{P}_{\boldsymbol{e}_{-1}}\right] \\
&\quad - \frac{2d\tau^*}{\tau}\sigma\left\{p_1\left[\frac{\rho_0}{s} - \widehat{h}_1(s)\right]\widehat{P}_{\boldsymbol{0}} - p_{-1}\left[\frac{\rho_0}{s} - \widehat{h}_{-1}(s)\right]\widehat{P}_{2\boldsymbol{e}_1}\right\} \qquad (10.185) \\
2d\widehat{\widetilde{g}}_2(s) &= \widehat{\widetilde{g}}_1(s)\nabla_{-1}\widehat{P}_{\boldsymbol{e}_2} + \widehat{\widetilde{g}}_{-1}(s)\nabla_1\widehat{P}_{\boldsymbol{e}_2} + \widehat{\widetilde{g}}_2(s)\left[\nabla_{-2}\widehat{P}_{\boldsymbol{e}_2} + \nabla_2\widehat{P}_{\boldsymbol{e}_2}\right] + 2(d-2)\widehat{\widetilde{g}}_2(s)\nabla_3\widehat{P}_{\boldsymbol{e}_2} \\
&\quad + \frac{2d\tau^*}{\tau}(p_1\widehat{\widetilde{g}}_1(s) - p_{-1}\widehat{\widetilde{g}}_{-1}(s))\left[\nabla_1\widehat{P}_{\boldsymbol{e}_2} - \nabla_{-1}\widehat{P}_{\boldsymbol{e}_2}\right] \\
&\quad - \frac{2d\tau^*}{\tau}\sigma\left\{p_1\left[\frac{\rho_0}{s} - \widehat{h}_1(s)\right]\widehat{P}_{\boldsymbol{e}_2+\boldsymbol{e}_1} - p_{-1}\left[\frac{\rho_0}{s} - \widehat{h}_{-1}(s)\right]\widehat{P}_{\boldsymbol{e}_2+\boldsymbol{e}_{-1}}\right\}. \qquad (10.186)
\end{aligned}$$

where we wrote for convenience

$$\nabla_\nu\widehat{P}_{\boldsymbol{r}} = \lim_{\xi\to 1}\nabla_\nu\widehat{P}(\boldsymbol{r}|\boldsymbol{0};\xi) \qquad (10.187)$$

With the usual symmetry properties on the quantities $\widehat{P}$ (4.48)-(4.50) as well as the relations (10.54)-(10.56), we rewrite the system (10.159)-(10.161) in terms of the propagators $\widehat{P}(\boldsymbol{0}|\boldsymbol{0};\xi)$, $\widehat{P}(2\boldsymbol{e}_1|\boldsymbol{0};\xi)$ and $\widehat{P}(\boldsymbol{e}_1|\boldsymbol{0};\xi)$ only. We introduce the quantities α and β as previously. At leading order when $s \to 0$, one can replace the propagators $\widehat{P}_{\boldsymbol{r}}$ by $G_0(1-s)$, where the function G_0 is defined as in Chapter 6 as the leading order term of the expansion of the propagators $\widehat{P}(\boldsymbol{r}|\boldsymbol{r}_0;\xi)$ when $\xi \to 1$:

$$\widehat{P}(\boldsymbol{r}|\boldsymbol{r}_0;\xi) \underset{\xi\to 1}{=} G_0(\xi) + \mathcal{O}(1). \qquad (10.188)$$

We write the Laplace transform of the TP velocity and use the main result of Section 10.2.5.2:

$$\begin{aligned}
\mathcal{L}\left[\frac{\mathrm{d}\langle X_t\rangle}{\mathrm{d}t}\right](s) &= \frac{\sigma}{\tau}\left[p_1\left(\frac{\rho_0}{s} - \widehat{h}_1(s)\right) - p_{-1}\left(\frac{\rho_0}{s} - \widehat{h}_{-1}(s)\right)\right], \qquad (10.189) \\
&\underset{s\to 0}{\sim} \frac{\rho_0}{s}\frac{\sigma}{\tau}\frac{p_1 - p_{-1}}{1 + \frac{2d\alpha}{2d-\alpha}\frac{\tau^*}{\tau}(p_1 + p_{-1})}. \qquad (10.190)
\end{aligned}$$

We deduce that at leading order when $s \to 0$, the system (10.184)-(10.186) may be written as

$$\widetilde{M}(\delta = 0)\begin{pmatrix}\widehat{\widetilde{g}}_1(s)\\ \widehat{\widetilde{g}}_{-1}(s)\\ \widehat{\widetilde{g}}_2(s)\end{pmatrix} = 2d\tau^*\rho_0\frac{p_1 - p_{-1}}{1 + \frac{2d\alpha}{2d-\alpha}\frac{\tau^*}{\tau}(p_1 + p_{-1})}\frac{G_0(1-s)}{s}\begin{pmatrix}1\\1\\1\end{pmatrix}, \qquad (10.191)$$

where $\widetilde{M}(\delta)$ is defined as previously (10.60). We finally obtain the expressions of $\widehat{\widetilde{g}}_1(s)$, $\widehat{\widetilde{g}}_{-1}(s)$ and $\widehat{\widetilde{g}}_2(s)$ in the limit $s \to 0$:

$$\widehat{\widetilde{g}}_{\pm 1}(s) \underset{s\to 0}{\sim} \rho_0 \frac{\sigma\tau^*}{\tau} \frac{(p_1 - p_{-1})(2d-\alpha)\left(\alpha - 2d - \frac{4d\alpha\tau^*}{\tau} p_{\mp 1}\right)}{\left[2d - \alpha + \frac{2d\alpha\tau^*}{\tau}(p_1 + p_{-1})\right]^2} \frac{G_0(1-s)}{s} \tag{10.192}$$

$$\widehat{\widetilde{g}}_2(s) \underset{s\to 0}{\sim} -\rho_0 \frac{\sigma\tau^*}{\tau} \frac{p_1 - p_{-1}}{1 + \frac{2d\alpha}{2d-\alpha}\frac{\tau^*}{\tau}(p_1 + p_{-1})} \frac{G_0(1-s)}{s}. \tag{10.193}$$

Recalling the expression of the second cumulant

$$\frac{\mathrm{d}\kappa_1^{(2)}(t)}{\mathrm{d}t} = -\frac{2\sigma}{\tau}\left\{p_1\widetilde{g}_1 - p_{-1}\widetilde{g}_{-1}\right\} + \frac{\sigma^2}{\tau}\left\{p_1(\rho_0 - h_1) + p_{-1}(\rho_0 - h_{-1})\right\}, \tag{10.194}$$

we write its Laplace transform

$$\mathcal{L}\left[\frac{\mathrm{d}\kappa_1^{(2)}(t)}{\mathrm{d}t}\right](s) = -\frac{2\sigma}{\tau}[p_1\widehat{\widetilde{g}}_1(s) - p_{-1}\widehat{\widetilde{g}}_{-1}(s)] + \frac{\sigma^2}{\tau}\left\{p_1\left[\frac{\rho_0}{s} - \widehat{h}_1(s)\right] + p_{-1}\left[\frac{\rho_0}{s} - \widehat{h}_{-1}(s)\right]\right\}. \tag{10.195}$$

Finally, using the solutions (10.192) as well as the Laplace transforms (10.87) and (10.88):

$$\lim_{\rho_0\to 0}\frac{\widehat{h}_1(s)}{\rho_0} \underset{s\to 0}{\sim} \frac{\rho_0}{s}\frac{\frac{2d\alpha\tau^*}{\tau}(p_1 - p_{-1})}{\frac{2d\alpha\tau^*}{\tau}(p_1 + p_{-1}) + 2d - \alpha} \tag{10.196}$$

$$\lim_{\rho_0\to 0}\frac{\widehat{h}_{-1}(s)}{\rho_0} \underset{s\to 0}{\sim} -\frac{\rho_0}{s}\frac{\frac{2d\alpha\tau^*}{\tau}(p_1 - p_{-1})}{\frac{2d\alpha\tau^*}{\tau}(p_1 + p_{-1}) + 2d - \alpha} \tag{10.197}$$

we get

$$\mathcal{L}\left[\frac{\mathrm{d}\kappa_1^{(2)}(t)}{\mathrm{d}t}\right](s) \underset{s\to 0}{\sim} 2\rho_0\frac{\tau^*\sigma^2}{\tau}\left[\frac{p_1 - p_{-1}}{1 + \frac{2d\alpha}{2d-\alpha}(p_1 + p_{-1})}\right]^2 \frac{G_0(1-s)}{s}. \tag{10.198}$$

Generalized capillaries For the stripe-like and capillary-like geometries, it was shown that

$$G_0(\xi) \underset{\xi\to 1}{\sim} \frac{\sqrt{d/2}}{L^{d-1}\sqrt{1-\xi}}, \tag{10.199}$$

so that (10.198) yields

$$\mathcal{L}\left[\frac{\mathrm{d}\kappa_1^{(2)}(t)}{\mathrm{d}t}\right](s) \underset{s\to 0}{\sim} 2\rho_0\frac{\tau^*\sigma^2}{\tau}{a_0}^2\frac{\sqrt{d/2}}{L^{d-1}s^{3/2}}, \tag{10.200}$$

where we introduced the usual definition of a_0:

$$a_0 = \frac{p_1 - p_{-1}}{1 + \frac{2d\alpha}{2d-\alpha}(p_1 + p_{-1})}. \tag{10.201}$$

An inverse Laplace transform yields the expression of the derivative of $\kappa_1^{(2)}(t)$

$$\frac{\mathrm{d}\kappa_1^{(2)}(t)}{\mathrm{d}t} \underset{t\to\infty}{\sim} \frac{4\rho_0{a_0}^2\sqrt{d/2}}{\sqrt{\pi}L^{d-1}}\frac{\tau^*\sigma^2}{\tau}\sqrt{t}, \tag{10.202}$$

and finally

$$\kappa_1^{(2)}(t) \underset{t\to\infty}{\sim} \frac{8\rho_0 {a_0}^2}{3L^{d-1}} \sqrt{\frac{d}{2\pi}} \frac{\tau^*\sigma^2}{\tau} t^{3/2}. \tag{10.203}$$

Taking $\tau = \tau^* = \sigma = 1$, this result matches the expressions of $\lim_{\rho_0\to 0} \kappa_1^{(2)}(t)/\rho_0$ in the long-time limit obtained on stripes (4.65) and capillaries (4.89).

Two-dimensional lattice In the case of the two-dimensional lattice, it was shown that

$$G_0(\xi) \underset{\xi\to 1}{\sim} \frac{1}{\pi} \ln \frac{1}{1-\xi}, \tag{10.204}$$

so that (10.198) yields

$$\mathcal{L}\left[\frac{\mathrm{d}\kappa_1^{(2)}(t)}{\mathrm{d}t}\right](s) \underset{s\to 0}{\sim} 2\rho_0 \frac{\tau^*\sigma^2}{\tau} \frac{{a_0}^2}{\pi} \frac{1}{s} \ln \frac{1}{s}, \tag{10.205}$$

where we introduced the usual definition of a_0. An inverse Laplace transform yields the expression of the derivative of $\kappa_1^{(2)}(t)$

$$\frac{\mathrm{d}\kappa_1^{(2)}(t)}{\mathrm{d}t} \underset{t\to\infty}{\sim} \frac{2\rho_0 {a_0}^2}{\pi} \frac{\tau^*\sigma^2}{\tau} \ln t, \tag{10.206}$$

and finally

$$\kappa_1^{(2)}(t) \underset{t\to\infty}{\sim} \frac{2\rho_0 {a_0}^2}{\pi} \frac{\tau^*\sigma^2}{\tau} t \ln t. \tag{10.207}$$

Taking $\tau = \tau^* = \sigma = 1$, this result matches the expressions of $\lim_{\rho_0\to 0} \kappa_1^{(2)}(t)/\rho_0$ in the long-time limit obtained on the two-dimensional lattice (4.101).

These results show that the decoupling approximation for the functions $\widetilde{g}_{\boldsymbol{r}}$ allows us to retrieve the long-time transient regime computed exactly at leading order in ρ_0 in Chapter 4.

The equation (10.145), obtained from the decoupling approximation, then yields the two limiting behaviors of the fluctuations of the TP position, obtained from the exact calculation presented in Chapter 4, resulting of the non-interversion of the limits $t \to \infty$ and $\rho_0 \to 0$. This confirms that the decoupling approximation is exact in the high-density limit. With a more detailed study of the general differential equation (10.145), we would like to obtain a scaling function in the joint limit $t \to \infty$ and $\rho_0 \to 0$ with the scaling $t \sim 1/{\rho_0}^2$ and confront it to the scaling functions obtained in Chapter 4 in the cases of quasi-one-dimensional lattices (4.183) and of the two-dimensional lattice (4.222).

10.5 Conclusion

In this Chapter, we considered the evolution of the velocity and of the diffusion coefficient of a biased TP in a hardcore lattice gas of arbitrary dimension. It was shown in Chapter 8 that these quantities can be expressed in terms of the density profiles $h_{\boldsymbol{r}} = \langle \eta_{\boldsymbol{r}} \rangle - \rho$ and in terms of the correlation functions $\widetilde{g}_{\boldsymbol{r}} = \langle \delta X_t (\eta_{\boldsymbol{X}_t+\boldsymbol{r}} - \langle \eta_{\boldsymbol{X}_t+\boldsymbol{r}} \rangle) \rangle$. Under a mean-field-type approximation, $h_{\boldsymbol{r}}$ and $\widetilde{g}_{\boldsymbol{r}}$ are given as solutions of equations which were established in Chapter 8. In this Chapter, we solve these equations, which yield implicit determinations of the velocity and diffusion coefficient of the TP.

The analysis of these solutions yields several interesting results. In particular, we studied the dependence of the terminal velocity of the TP with the applied force. If the bath particles are slow enough (i.e. if their mean waiting time τ^* is large enough), we show that the velocity can be a nonmonotonic function of the applied force, and that it may decrease for increasing values of the force. This counter-intuitive effect is known in other domains as *negative differential mobility* (NDM). It can be explained by the following simple physical arguments: increasing the applied force on the TP reduces its travel time between successive encounters with the bath particles, but increases the escape time from traps created by the bath particles when they are slow enough. The competition between these two effects controls the emergence of NDM. Our approach gives a new microscopic insight into this phenomenon. The analytical predictions are confirmed by Monte-Carlo simulations, which also confirm the accuracy of the decoupling approximation in a wide range of parameters.

We also show that in the extreme density regimes $\rho \to 0$ and $\rho \to 1$, the decoupling approximation yields explicit expressions for the velocity and the diffusion coefficient of the TP. The high-density limit, in the case where the lattice is not in contact with a reservoir, has been studied in the first part of this thesis, in which we obtained exact results for the mean position (Chapter 5) and the fluctuations (Chapter 4) of the TP at leading order in the density of vacancy ρ_0 . We show that the results from the decoupling approximation perfectly match the results obtained from the exact approach in the limit $\rho \to 1$. The opposite limit of a very dilute bath of immobile particles, was studied by Leitmann and Franosch [77] who obtained the velocity of the TP at leading order in the density of bath particles ρ. We show that our decoupling approximation yields the same result. This shows that the decoupling approximation is *exact* in these limits.

Our study shows that, in spite of the complexity of the initial problem, the decoupling approximation presented in Chapter 8 yields a very accurate estimation of the velocity and diffusion coefficient of the TP for a wide range of parameters, and is exact in the high and low density limits. In a future work, we would like to study the dependence of the diffusion coefficient on the different parameters of the problem, and in particular on the density, in order to see if it can be non-monotonic, and to test the robustness of the effect observed in one dimension. Finally, we could extend the methods presented in this Chapter in order to solve the evolution equations verified by $\widetilde{w}_{\boldsymbol{r}}$, in order to get the probability distribution of the TP position on lattices of arbitrary dimension.

CHAPTER 11

Conclusion

In this thesis, we studied the general model of a biased tracer particle (TP) in a bath of Brownian particles on a lattice. The bath particles perform symmetric nearest-neigbor random walks, whereas the TP performs a biased nearest-neighbor random walk, where the bias can originate from an external force applied on the TP. All the particles interact via hardcore interactions. This model has been studied in the past, but the results were limited to the behavior of the mean position of the TP and to the determination of the force-velocity relation. The aim of this work was to go beyond this force-velocity relation, and to study the fluctuations of the position of the TP, and more generally its whole distribution.

We first focused on the limit where the bath of particles is *very dense*. In this limit, there is only a small number of vacancies on the lattice. It is then more convenient to describe the dynamics of the vacancies rather than the dynamics of the whole bath of particles. The results at leading order in the density of vacancies ρ_0 can be obtained by assuming that each vacancy contributes independently to the motion of the TP, as the events involving two vacancies on the same site or on neighboring sites contribute only to order $\mathcal{O}({\rho_0}^2)$. We first considered the auxiliary problem where there is only one vacancy interacting with the TP. The propagator associated to the position of the TP was expressed in terms of conditional first-passage time densities (FPTD) associated to the random walk of a vacancy. Noticing that the vacancy performs a nearest-neighbor symmetric random walk on each site of the lattice except in the vicinity of the TP where it is perturbed by the bias undergone by the TP, the conditional FPTD can be expressed in terms of the propagators of a single symmetric random walker on the considered structure. The general propagator associated to a TP interacting with a small number of vacancies is finally expressed in terms of the single-vacancy propagators at leading order in ρ_0.

This general formalism was then used to study the fluctuations of the position of the TP, and to study the dependence of this quantity on the different parameters of the problem (time, force, vacancy density, lattice dimension). We first considered the one-dimensional situation. It was shown that the fluctuations of the TP grow subdiffusively and proportionally to $\sqrt{t}$, with a prefactor that is independent of the bias. Moreover, we showed that all the odd cumulants on the one hand and all the even cumulants on the other hand are equal to each other, and that they all grow as $\sqrt{t}$.

We considered higher-dimensional lattices (quasi-one-dimensional capillaries and two-dimensional lattice), on which the fluctuations of the TP were shown to grow superdiffusively. This anomalous regime is transient, and crosses over to a diffusive regime. In this ultimate regime, surprisingly, the diffusion coefficient of the TP is independent on the vacancy density in quasi-1D geometries. The crossover time to the diffusive regime was shown to scale as $1/{\rho_0}^2$. This indicates that the transient regime may actually be long-lived and that it may be the only one accessible in numerical simulations or in experimental realizations. We also showed that for quasi-one-dimensional geometries, the mean position of the TP itself may display an anomaly, as the velocity of the TP saturates to a high value before dropping to its ultimate value for the same crossover time that scales as $1/{\rho_0}^2$.

All these results were recast under a general formula that describes both regimes for the different geometries we considered. We also studied the higher-order cumulants of the position of the TP, both in the direction of the bias and in the transverse direction, which can be written under simple generic formulae. These expressions seem to be universal as they correctly predict the behavior of the TP in a hardcore lattice gas on a fractal lattice. Finally, the underlying physical mechanism was determined by considering a simplified model that correctly captures the results obtained through the exact approach.

In the second part of this thesis, we studied the general situation of a biased TP in a hardcore lattice gas of *arbitrary* density. The resolution method introduced in this part allows us to consider a more general situation than the one considered in the first part. We assume that the lattice is in contact with a reservoir of particles, which constitutes an experimentally relevant situation. We adopt a continuous-time description of the problem. The TP performs a biased random walk with a mean waiting time τ. The bath particles perform symmetric nearest-neighbor random walks with a mean waiting time τ^*, and may desorb back to the reservoir with a given rate. Particles from the reservoir may adsorb on vacant lattice sites. This problem is a many-body problem, for which we can write a master equation whose solution is the joint probability distribution of the position of the TP and of the configuration of the bath particles $\{\eta_{\boldsymbol{r}}\}$ (where $\eta_{\boldsymbol{r}}$ is an occupation variable equal to 1 if site $\boldsymbol{r}$ is occupied and 0 otherwise). From this master equation, one can obtain an expression of the mean position of the TP in terms of the mean density profiles $k_{\boldsymbol{r}} = \langle \eta_{\boldsymbol{r}} \rangle$. These density profiles are given in terms of the correlation functions $\langle \eta_{\boldsymbol{r}} \eta_{\boldsymbol{r}'} \rangle$, which in turn involve higher-order correlation functions, so that the initial master equation yields an infinite hierarchy of equations that cannot be solved unless it is closed by some approximation. We used a mean-field-type decoupling approximation which consists in discarding the quadratic corrections to the mean occupation numbers $\langle \eta_{\boldsymbol{r}} \rangle$. We then obtained an expression of the velocity of the TP in terms of the mean density profiles $k_{\boldsymbol{r}} = \langle \eta_{\boldsymbol{r}} \rangle$, which are given as the solutions of an implicit set of equations. Extending the decoupling approximation, the evolution equation for the fluctuations of the TP position is given in terms of the correlation functions $\widetilde{g}_{\boldsymbol{r}} = \langle \delta X_t \delta \eta_{\boldsymbol{X}_t + \boldsymbol{r}} \rangle$, and the evolution equations for the cumulant generating function of the TP position are given in terms of other correlation functions $\widetilde{w}_{\boldsymbol{r}} = \left\langle \mathrm{e}^{\mathrm{i}uX_t} \eta_{\boldsymbol{X}_t + \boldsymbol{r}} \right\rangle / \left\langle \mathrm{e}^{\mathrm{i}uX_t} \right\rangle$, where the functions $\widetilde{g}_{\boldsymbol{r}}$ and $\widetilde{w}_{\boldsymbol{r}}$ are the solutions of an closed set of equations.

We then studied the particular case of the one-dimensional geometry. We obtained the solutions of the equations verified by the functions $k_{\boldsymbol{r}}$, $\widetilde{g}_{\boldsymbol{r}}$ and $\widetilde{w}_{\boldsymbol{r}}$ in the stationary limit, and deduced the velocity, the fluctuations and the distribution of the position of the TP. Theses solutions were compared to Monte Carlo numerical simulations, which indicates that the mean-field-type approximation we used is accurate in a wide range of parameters. The fluctuations of the TP position display a striking behavior: for a given value of the bias, if the desorption rate is small enough, the diffusion coefficient of the TP is a nonmonotonic function of the density, so that its maximum is reached for nonzero value of the density of bath particles. This surprising effect is shown to be related to a nonmonotonic behavior of the cross-correlation functions $\widetilde{g}_{\boldsymbol{r}}$ past the TP. We showed that the third cumulant also has an anomalous behavior: in a large range of parameters, it is a nonmonotonic function of the density of bath particles, and it may have negative values. Finally, we solved the equations verified by the functions $\widetilde{w}_{\boldsymbol{r}}$ and obtained the distribution of the position of the TP.

We finally adapted the methods used in the one-dimensional case to obtain the solutions of the equations satisfied by $k_{\boldsymbol{r}}$ and $\widetilde{g}_{\boldsymbol{r}}$ on higher-dimensional lattices. We particularly studied the dependence of the velocity on the force applied on the TP. It was shown that it can be non-monotonic for some

values of the parameters: the velocity may be a decreasing function of the force for large forces if the displacement of the bath particles is slow enough (i.e. τ^* large enough). This phenomenon is an example of negative differential mobility (NDM), which was observed in other contexts. The decoupling approximation framework allowed us to give a microscopic description of NDM and to predict the range of parameters in which it occurs. Finally, in the limits where the bath of particles is very dilute or very dense ($\rho \to 0$ or 1), we showed that the equations verified by the correlation functions $k_{\boldsymbol{r}}$ and $\widetilde{g}_{\boldsymbol{r}}$ become explicit in the different parameters, so that we obtained explicit expressions of the mean and of the fluctuations of the TP position in these limits. In the high-density limit, these expressions are identical to the one we obtained with the exact approach at leading order in ρ_0. In the low-density limit, we retrieve the exact results at order ρ obtained by other authors. This shows that the decoupling approximation is exact in the low and high-density limits.

Our study shows that the initial very complex many-body problem can be studied by resorting to a mean-field-type decoupling approximation, which is very accurate in a wide range of parameters and exact in the low and high density limits. This approximation then constitues an appropriate approach to the study of the transport properties of a biased TP in a hardcore lattice gas.

The theoretical framework developed in this thesis could be extended to address several open questions.

- The evolution of the mean position of the TP is closely related to the densities of bath particles at the sites in the neighborhood of the TP, and it could be interesting to study in details these observables. The behavior of the density profiles at large distances away from the TP could also lead to interesting observations. On a one-dimensional lattice, when the number of particles on the lattice is conserved, there is no stationary density profile, and size of the perturbed domain grows as $\sqrt{t}$. On a two-dimensional lattice, the density profiles reach an inhomogeneous stationary state, and decrease algebraically with the distance to the TP [14, 13]. It would be interesting to investigate the long-distance behavior of the density profiles on confined quasi-one-dimensional lattices. This will be possible starting from the equations established in Chapter 10.

- The study of the behavior of a bath particle entrained in the wake of the biased TP could also give an interesting insight into the way the TP modifies its environment.

- The situation where two biased tracers are placed on the lattice was studied previously with numerical simulations [86], and it was shown that the biased tracers could interact and attract each other. This effect could be investigated analytically, and generalized to the case where several tracers interact.

- The response of the TP to time-dependent forces could be of interest in relation with experimental realizations. In particular, the case where the TP is submitted to an oscillatory force has been studied experimentally [102], and our model could possibly be extended to study such a situation.

- Finally, our lattice gas model could be the starting point to study more complex dynamics. The situation where identical hardcore particles perform persistent random walks on a lattice was considered recently with numerical simulations [108]. It was found that cooperative affects arise, and that the system forms clusters of particles. Extensions of our lattice gas model could give a theoretical approach to this observation.

Beyond these theoretical questions, the relevance of our lattice gas model to describe real systems could be investigated. Preliminary off-lattice simulations presented in the conclusion of Chapter 4 indicate that confinement-superdiffusion emerges in off-lattice systems of systems of hard particles. These numerical simulations could be extended to include more realistic interactions (soft colloidal repulsion, hydrodynamic interactions...). Such simulations could test the robustness of some effects described by our analytical framework: (i) the velocity anomaly in confined geometries and in the high-density limit; (ii) negative differential mobility; (iii) the non-monotonic behavior of the diffusion coefficient as a function of the density for a lattice in contact with a reservoir of particles.

Experimental realizations of biased tracer diffusion in granular media or colloidal suspensions could also be proposed to confront our theoretical predictions to real systems, and to investigate their impact on practical situations.

CHAPTER 12

Publications

[P1] O. Bénichou, P. Illien, G. Oshanin, R. Voituriez, *Fluctuations and correlations of a driven tracer in a hard-core lattice gas*, Phys. Rev. E **87**, 032164 (2013).

[P2] O. Bénichou, P. Illien, C. Mejía-Monasterio, G. Oshanin, *A biased intruder in a dense quiescent medium: looking beyond the force-velocity relation*, J. Stat. Mech., P05008 (2013).

[P3] P. Illien, O. Bénichou, C. Mejía-Monasterio, G. Oshanin, R. Voituriez, *Active transport in dense diffusive single-file systems*, Phys. Rev. Lett. **111**, 038102 (2013).

[P4] O. Bénichou, A. Bodrova, D. Chakraborty, P. Illien, A. Law, C. Mejía-Monasterio, G. Oshanin, R. Voituriez, *Geometry-induced superdiffusion in driven crowded systems*, Phys. Rev. Lett. **111**, 260601 (2013).

[P5] P. Illien, O. Bénichou, G. Oshanin, R. Voituriez, *Velocity anomaly of a driven tracer in a confined crowded environment*, Phys. Rev. Lett. **113**, 030603 (2014).

[P6] O. Bénichou, P. Illien, G. Oshanin, A. Sarracino, R. Voituriez, *Microscopic theory for negative differential mobility in crowded environments*, Phys. Rev. Lett. **113**, 268002 (2014).

APPENDIX A

Propagators of a random walk on a stripe-like lattice

In this Appendix, we consider a stripe-like lattice, which is infinite in a direction and finite of width L with periodic boundary conditions in the other direction (Fig. A.1). We compute the propagators associated to a symmetric nearest-neighbor random walk, and consider their long-time limit. We compute the propagators associated to a biased random walk (where the bias only affects the infinitely extended direction of the stripe), in the long-time limit and in the limit of a small bias. Finally, we study the biased propagators in a joint limit of long time and small bias.

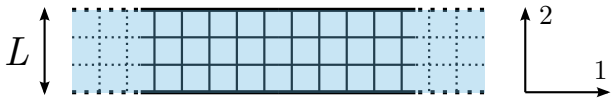

Figure A.1: Stripe-like geometry. The lattice is infinite in the a direction (which will be the direction of the external force imposed on the TP), and finite of width L with periodic boundary conditions in the other direction.

A.1 General expression of the propagators in terms of the structure function

Let $P_t(\boldsymbol{r}|\boldsymbol{r}_0)$ be the probability to find a walker at site $\boldsymbol{r}$ at time t knowing that it started from site $\boldsymbol{r}_0$ at time 0. Let $p(\boldsymbol{r}|\boldsymbol{r}')$ the probability for the walker to jump from $\boldsymbol{r}'$ to site $\boldsymbol{r}$ in a single step. On the considered lattice, the random walk is translation invariant, so that

$$P_t(\boldsymbol{r}|\boldsymbol{r}_0) = P_t(\boldsymbol{r}-\boldsymbol{r}_0|\boldsymbol{0}), \tag{A.1}$$

$$p(\boldsymbol{r}|\boldsymbol{r}') = p(\boldsymbol{r}-\boldsymbol{r}'|\boldsymbol{0}). \tag{A.2}$$

Therefore, we will only calculate $P_t(\boldsymbol{r}|\boldsymbol{0})$. Partitioning over the last step of the walk, we get

$$P_{t+1}(\boldsymbol{r}|\boldsymbol{0}) = \sum_{\boldsymbol{r}'} p(\boldsymbol{r}|\boldsymbol{r}')P_t(\boldsymbol{r}'|\boldsymbol{0}) = \sum_{\boldsymbol{r}'} p(\boldsymbol{r}-\boldsymbol{r}'|\boldsymbol{0})P_t(\boldsymbol{r}'|\boldsymbol{0}), \tag{A.3}$$

where the sum over $\boldsymbol{r}'$ runs over all lattice sites. Multiplying by ξ^t and summing for t going from 0 to infinity, we obtain the associated generating functions:

$$\frac{1}{\xi}\sum_{t=1}^{\infty}\xi^t P_t(\boldsymbol{r}|\boldsymbol{0}) = \sum_{\boldsymbol{r}'} p(\boldsymbol{r}-\boldsymbol{r}'|\boldsymbol{0})\widehat{P}(\boldsymbol{r}'|\boldsymbol{0};\xi). \tag{A.4}$$

Using $P_0(\boldsymbol{r}|\boldsymbol{0}) = \delta_{\boldsymbol{r},\boldsymbol{0}}$ and therefore $\frac{1}{\xi}\sum_{t=1}^{\infty}\xi^t P_t(\boldsymbol{r}|\boldsymbol{0}) = \widehat{P}(\boldsymbol{r}|\boldsymbol{0};\xi) - \delta_{\boldsymbol{r},\boldsymbol{0}}$, we obtain

$$\widehat{P}(\boldsymbol{r}|\boldsymbol{0};\xi) = \delta_{\boldsymbol{r},\boldsymbol{0}} + \xi\sum_{\boldsymbol{r}'} p(\boldsymbol{r}-\boldsymbol{r}'|\boldsymbol{0})\widehat{P}(\boldsymbol{r}'|\boldsymbol{0};\xi). \tag{A.5}$$

We introduce the Fourier transform of the propagators

$$\widehat{\widehat{P}}(\boldsymbol{k}|\mathbf{0};\xi) = \sum_{r_1=-\infty}^{\infty} \mathrm{e}^{\mathrm{i}k_1 r_1} \sum_{r_1=0}^{L-1} \mathrm{e}^{\frac{2\mathrm{i}\pi k_2 r_2}{L}} \widehat{P}(\boldsymbol{r}|\mathbf{0};\xi) \tag{A.6}$$

so that (A.5) becomes

$$\widehat{\widehat{P}}(\boldsymbol{k}|\mathbf{0};\xi) = 1 + \xi \left(\sum_{\boldsymbol{r}} \mathrm{e}^{\mathrm{i}k_1 r_1} \mathrm{e}^{\frac{2\mathrm{i}\pi k_2 r_2}{L}} p(\boldsymbol{r}|\mathbf{0}) \right) \widehat{\widehat{P}}(\boldsymbol{k}|\mathbf{0};\xi). \tag{A.7}$$

Finally,

$$\widehat{\widehat{P}}(\boldsymbol{k}|\mathbf{0};\xi) = \frac{1}{1-\xi\lambda(\boldsymbol{k})} \tag{A.8}$$

where the structure function $\lambda(\boldsymbol{k})$ is defined as

$$\lambda(\boldsymbol{k}) \equiv \sum_{\boldsymbol{r}} \mathrm{e}^{\mathrm{i}k_1 r_1} \mathrm{e}^{\frac{2\mathrm{i}\pi k_2 r_2}{L}} p(\boldsymbol{r}|\mathbf{0}). \tag{A.9}$$

Finally, writing the inverse Fourier transform, we retrieve the generating function:

$$\widehat{P}(\boldsymbol{r}|\mathbf{0};\xi) = \frac{1}{L} \sum_{k_2=0}^{L-1} \frac{1}{2\pi} \int_{-\pi}^{\pi} \mathrm{d}k_1 \frac{\mathrm{e}^{-\mathrm{i}k_1 r_1} \mathrm{e}^{-\frac{2\mathrm{i}\pi k_2 r_2}{L}}}{1-\xi\lambda(\boldsymbol{k})} \tag{A.10}$$

A.2 Propagators of a symmetric random walk

The case where the random walk is symmetric has already been studied in [22], and we recall the results for completeness. In this situation, the structure function becomes

$$\begin{aligned} \lambda(\boldsymbol{k}) &= \frac{1}{4}\mathrm{e}^{\mathrm{i}k_1} + \frac{1}{4}\mathrm{e}^{-\mathrm{i}k_1} + \frac{1}{4}\mathrm{e}^{\frac{2\mathrm{i}\pi k_2}{L}} + + \frac{1}{4}\mathrm{e}^{-\frac{2\mathrm{i}\pi k_2}{L}} && \text{(A.11)} \\ &= \frac{1}{2}\left(\cos k_1 + \cos\frac{2\pi k_2}{L}\right), && \text{(A.12)} \end{aligned}$$

and the propagators are

$$\widehat{P}(\boldsymbol{r}|\mathbf{0};\xi) = \frac{1}{L} \sum_{k_2=0}^{L-1} \frac{1}{2\pi} \int_{-\pi}^{\pi} \mathrm{d}k_1 \frac{\mathrm{e}^{-\mathrm{i}k_1 r_1} \mathrm{e}^{-\frac{2\mathrm{i}\pi k_2 r_2}{L}}}{1-\xi\left(\cos k_1 + \cos\frac{2\pi k_2}{L}\right)}. \tag{A.13}$$

This propagator can be computed explicitly. For a given site $\boldsymbol{r} = (r_1, r_2)$, we write

$$\widehat{P}(\boldsymbol{r}|\mathbf{0};\xi) = \frac{1}{L} \sum_{k_2=0}^{L-1} \frac{1}{2\pi} \mathrm{e}^{-\frac{2\mathrm{i}\pi k_2 r_2}{L}} f(r_1) \tag{A.14}$$

with

$$f(r_1) = \int_{-\pi}^{\pi} \mathrm{d}k_1 \frac{\mathrm{e}^{-\mathrm{i}k_1 r_1}}{1-\frac{\xi}{2}\left(\cos k_1 + \cos\frac{2\pi k_2}{L}\right)} \tag{A.15}$$

With the change of variable $u = \mathrm{e}^{-\mathrm{i}k_1}$, and denoting by $\mathcal{C}$ the unit circle, we get

$$\begin{aligned} f(r_1) &= -\oint_{\mathcal{C}} \frac{\mathrm{d}u}{-\mathrm{i}u} \frac{u^{r_1}}{1-\frac{\xi}{2}\left[\frac{1}{2}\left(u+\frac{1}{u}\right)+\cos\frac{2\pi k_2}{L}\right]} && \text{(A.16)} \\ &= \frac{4\mathrm{i}}{\xi} \oint_{\mathcal{C}} \mathrm{d}u \frac{u^{r_1}}{(u-U_1)(u-U_2)} && \text{(A.17)} \end{aligned}$$

where we defined

$$U_{\frac{1}{2}} = \frac{2}{\xi} - \cos\frac{2\pi k_2}{L} \pm \sqrt{\left(\frac{2}{\xi} - \cos\frac{2\pi k_2}{L}\right)^2 - 1} \tag{A.18}$$

For $0 < \xi < 1$ and $0 \leq k_2 \leq L-1$, one shows that U_2 is in the contour $\mathcal{C}$ and U_1 is outside. Depending on the value of r_1, we determine the singularities of f contained in $\mathcal{C}$, and we apply the residue theorem:

- if $r_1 \geq 0$, U_2 is the only singularity of the integrand contained in $\mathcal{C}$, so that

$$f(r_1) = \frac{4\mathrm{i}}{\xi} 2\mathrm{i}\pi \mathrm{Res}\left[\frac{u^{r_1}}{(u-U_1)(u-U_2)}, u=U_2\right] \tag{A.19}$$

$$= \frac{8\pi}{\xi}\frac{U_2^{r_1}}{U_1-U_2}. \tag{A.20}$$

- if $r_1 < 0$, U_2 and 0 are the singularities of the integrand contained in $\mathcal{C}$, so that

$$f(r_1) = \frac{4\mathrm{i}}{\xi} 2\mathrm{i}\pi \left\{\mathrm{Res}\left[\frac{u^{r_1}}{(u-U_1)(u-U_2)}, u=U_2\right] + \mathrm{Res}\left[\frac{u^{r_1}}{(u-U_1)(u-U_2)}, u=0\right]\right\}$$

$$= \frac{8\pi}{\xi}\frac{1}{U_1^{|r_1|}(U_1-U_2)}. \tag{A.21}$$

Finally, the propagators write

$$\widehat{P}(\boldsymbol{r}|\boldsymbol{0};\xi) = \frac{1}{L}\sum_{k=0}^{L-1} \mathrm{e}^{-\frac{2i\pi k r_2}{L}} f(r_1), \tag{A.22}$$

where we have the following new definition of f:

$$f(r_1) = \begin{cases} \frac{4}{\xi}\frac{U_2^{r_1}}{U_1-U_2} & \text{if } r_1 \geq 0, \\ \frac{4}{\xi}\frac{1}{U_1^{|r_1|}(U_1-U_2)} & \text{if } r_1 < 0. \end{cases} \tag{A.23}$$

The propagators needed for the calculation of the entries of the matrices $\boldsymbol{A}$ and $\boldsymbol{P}$ (Section 4.3.2) then write

$$\widehat{P}(\boldsymbol{0}|\boldsymbol{0};\xi) = C_{L,0}(\xi), \tag{A.24}$$

$$\widehat{P}(\boldsymbol{e}_1|\boldsymbol{0};\xi) = \frac{2}{\xi}\left[C_{L,0}(\xi)-1\right] - C_{L,1}(\xi), \tag{A.25}$$

$$\widehat{P}(\boldsymbol{e}_2|\boldsymbol{0};\xi) = C_{L,1}(\xi), \tag{A.26}$$

$$\widehat{P}(2\boldsymbol{e}_1|\boldsymbol{0};\xi) = -\frac{8}{\xi^2} + \left(\frac{8}{\xi^2}-1\right)C_{L,0}(\xi) - \frac{8}{\xi}C_{L,1}(\xi) + 2C_{L,2}(\xi), \tag{A.27}$$

$$\widehat{P}(2\boldsymbol{e}_2|\boldsymbol{0};\xi) = 2C_{L,2}(\xi) - C_{L,0}(\xi), \tag{A.28}$$

$$\widehat{P}(\boldsymbol{e}_1+\boldsymbol{e}_2|\boldsymbol{0};\xi) = \frac{2}{\xi}C_{L,1}(\xi) - C_{L,2}(\xi), \tag{A.29}$$

where we introduced the quantity

$$C_{L,n}(\xi) = \frac{1}{L}\sum_{k=0}^{L-1} \frac{\cos^n(2\pi k_2/L)}{\sqrt{\left[1-\frac{\xi}{2}\cos(2\pi k_2/L)\right]^2 - \frac{\xi^2}{4}}}. \tag{A.30}$$

In order to determine the $\xi \to 1$ expansions of the quantities $C_{L,n}(\xi)$, we write

$$C_{L,n}(\xi) = \frac{1}{L}\frac{1}{\sqrt{1-\xi}} + \frac{1}{L}\sum_{k=1}^{L-1} \frac{\cos^n(2\pi k_2/L)}{\sqrt{\left[1-\frac{\xi}{2}\cos(2\pi k_2/L)\right]^2 - \frac{\xi^2}{4}}}. \tag{A.31}$$

The first term of this expression diverges when $\xi \to 1$, whereas the second one is constant in this limit. For $0 \leq k_2 \leq L-1$, the argument of the sum over k_2 may be written:

$$\frac{\cos^n(2\pi k_2/L)}{\sqrt{\left[1-\frac{\xi}{2}\cos(2\pi k_2/L)\right]^2 - \frac{\xi^2}{4}}} \underset{\xi\to 1}{=} \frac{2\cos^n(2\pi k_2/L)}{\sqrt{\cos^2(2\pi k_2/L) - 4\cos(2\pi k_2/L) + 3}} + \mathcal{O}(1-\xi) \tag{A.32}$$

We then study the quantities $C_{L,0}(\xi)$, $C_{L,1}(\xi)$ and $C_{L,2}(\xi)$ needed for the computation of the propagators. Using elementary trigonometry relations, we find

$$C_{L,0}(\xi) = \frac{1}{L\sqrt{1-\xi}} + S^{(2)}_{L,-1} + \mathcal{O}(1-\xi) \tag{A.33}$$

$$C_{L,1}(\xi) = \frac{1}{L\sqrt{1-\xi}} + S^{(2)}_{L,-1} - 2S^{(2)}_{L,1} + \mathcal{O}(1-\xi) \tag{A.34}$$

$$C_{L,2}(\xi) = \frac{1}{L\sqrt{1-\xi}} + S^{(2)}_{L,-1} - 4S^{(2)}_{L,1} + 4S^{(2)}_{L,3} + \mathcal{O}(1-\xi) \tag{A.35}$$

Finally, in the limit where $\xi \to 1$ (which corresponds to the long-time limit), one gets

$$\widehat{P}(\mathbf{0}|\mathbf{0};\xi) \underset{\xi\to1}{=} \frac{1}{L\sqrt{1-\xi}} + S^{(2)}_{L,-1} + O(1-\xi) \tag{A.36}$$

$$\widehat{P}(\mathbf{e}_1|\mathbf{0};\xi) \underset{\xi\to1}{=} \frac{1}{L\sqrt{1-\xi}} + S^{(2)}_{L,-1} + 2S^{(2)}_{L,1} - 2 + \frac{2}{L}\sqrt{1-\xi} + O(1-\xi) \tag{A.37}$$

$$\widehat{P}(\mathbf{e}_2|\mathbf{0};\xi) \underset{\xi\to1}{=} \frac{1}{L\sqrt{1-\xi}} + S^{(2)}_{L,-1} - 2S^{(2)}_{L,1} + O(1-\xi) \tag{A.38}$$

$$\widehat{P}(2\mathbf{e}_1|\mathbf{0};\xi) \underset{\xi\to1}{=} \frac{1}{L\sqrt{1-\xi}} + S^{(2)}_{L,-1} + 8S^{(2)}_{L,1} + 8S^{(2)}_{L,3} - 8 + \frac{8}{L}\sqrt{1-\xi} + O(1-\xi) \tag{A.39}$$

$$\widehat{P}(2\mathbf{e}_2|\mathbf{0};\xi) \underset{\xi\to1}{=} \frac{1}{L\sqrt{1-\xi}} + S^{(2)}_{L,-1} - 8S^{(2)}_{L,1} + 8S^{(2)}_{L,3} + O(1-\xi) \tag{A.40}$$

$$\widehat{P}(\mathbf{e}_1+\mathbf{e}_2|\mathbf{0};\xi) \underset{\xi\to1}{=} \frac{1}{L\sqrt{1-\xi}} + S^{(2)}_{L,-1} - 4S^{(2)}_{L,3} + \frac{2}{L}\sqrt{1-\xi} + O(1-\xi) \tag{A.41}$$

where we defined the sums

$$S^{(2)}_{L,n} \equiv \frac{1}{L}\sum_{k_2=1}^{L-1} \frac{\sin^n(\pi k_2/L)}{\sqrt{1+\sin^2(\pi k_2/L)}}. \tag{A.42}$$

A.3 Propagators of a biased random walk

A.3.1 General formulation

When the vacancies are assumed to undergo a biased proportional to ε in the -1 direction (Fig. 4.7), the structure function of the walk writes:

$$\lambda(\boldsymbol{k}) = \widetilde{p}_1 \mathrm{e}^{\mathrm{i}k_1} + \widetilde{p}_{-1}\mathrm{e}^{-\mathrm{i}k_1} + 2\widetilde{p}_2 \cos\frac{2\pi k_2}{L}, \tag{A.43}$$

where the jump probabilities $\widetilde{p}_\nu$ are given by

$$\widetilde{p}_{-1} = \frac{1}{1+\varepsilon}\left(\frac{1}{4}+\varepsilon\right), \tag{A.44}$$

$$\widetilde{p}_1 = \widetilde{p}_{\pm2} = \frac{1}{4(1+\varepsilon)}. \tag{A.45}$$

The associated propagators are

$$\widehat{\mathcal{P}}(\boldsymbol{r}|\mathbf{0};\xi,\varepsilon) = \frac{1}{L}\sum_{k_2=0}^{L-1} \frac{1}{2\pi}\mathrm{e}^{-\frac{2\mathrm{i}\pi k_2 r_2}{L}} \int_{-\pi}^{\pi} \mathrm{d}k_1 \frac{\mathrm{e}^{-\mathrm{i}k_1 r_1}}{1-\xi\left(\widetilde{p}_1\mathrm{e}^{\mathrm{i}k_1} + \widetilde{p}_{-1}\mathrm{e}^{-\mathrm{i}k_1} + 2\widetilde{p}_2\cos\frac{2\pi k_2}{L}\right)}. \tag{A.46}$$

The explicit computation of the integral over k_1 is similar as the one performed in the case of non-biased propagators. With the change of variable $u = \mathrm{e}^{-\mathrm{i}k_1}$ and applying the residue theorem, one gets

$$\widehat{\mathcal{P}}(\boldsymbol{r}|\mathbf{0};\xi,\varepsilon) = \frac{1}{L}\sum_{k_2=0}^{L-1} \mathrm{e}^{-\frac{2\mathrm{i}\pi k_2 r_2}{L}} f(r_1,k_2). \tag{A.47}$$

with

$$f(r_1,k_2;\xi,\varepsilon) = \begin{cases} \frac{1}{\xi\widetilde{p}_{-1}} \frac{U_2(\xi,\varepsilon)^{r_1}}{U_1(\xi,\varepsilon)-U_2(\xi,\varepsilon)} & \text{if } r_1 \geq 0 \\ \frac{1}{\xi\widetilde{p}_{-1}} \frac{1}{U_1(\xi,\varepsilon)^{|r_1|}[U_1(\xi,\varepsilon)-U_2(\xi,\varepsilon)]} & \text{if } r_1 < 0. \end{cases} \tag{A.48}$$

and

$$U_{\frac{1}{2}}(\xi,\varepsilon) = \frac{1}{2\xi\widetilde{p}_{-1}}\left(1-2\xi\widetilde{p}_2\cos\frac{2\pi k_2}{L}\right) \pm \frac{1}{2}\sqrt{\frac{1}{(\xi\widetilde{p}_{-1})^2}\left(1-2\xi\widetilde{p}_2\cos\frac{2\pi k_2}{L}\right)^2 - 4\frac{\widetilde{p}_1}{\widetilde{p}_{-1}}} \tag{A.49}$$

We are interested in the limiting behavior of the propagators $\widehat{\mathcal{P}}$ when ε goes to 0 and ξ goes to one. In what follows, we show that these two limits do not commute. The case where the limit $\varepsilon \to 0$ is taken first actually corresponds with the study of the unbiased propagators $\widehat{P}$ in the long-time limit (see Section A.2).

A.3.2 Small bias expansion of the propagators in the long-time limit

The divergence of the propagators $\widehat{P}$ and $\widehat{\mathcal{P}}$ is due to the cancellation of the denominator $U_1 - U_2$. For any value of ξ and ε, we find that

$$U_1(\xi,\varepsilon) - U_2(\xi,\varepsilon) = \frac{1}{\sqrt{\frac{1}{4}+\varepsilon}} \sqrt{\frac{1}{\frac{1}{4}+\varepsilon}\left(\frac{1+\varepsilon}{\xi} - \frac{1}{2}\cos\frac{2\pi k_2}{L}\right)^2 - 1}. \tag{A.50}$$

Taking $\xi = 1$ and $\varepsilon = 0$ in this expression, one gets:

$$U_1(1,0) - U_2(1,0) = 4\sqrt{\left(1 - \frac{1}{2}\cos\frac{2\pi k_2}{L}\right)^2 - \frac{1}{4}}. \tag{A.51}$$

This quantity is equal to zero when $k_2 = 0$ and nonzero when $1 \geq k_2 \geq L-1$. In order to study the divergence of the propagators, we then write

$$\widehat{\mathcal{P}}(\boldsymbol{r}|\mathbf{0};\xi,\varepsilon) = \frac{1}{L} f(r_1, k_2 = 0; \xi, \varepsilon) + \phi(\boldsymbol{r};\xi,\varepsilon) \tag{A.52}$$

where the function ϕ is defined as

$$\phi(\boldsymbol{r};\xi,\varepsilon) \equiv \frac{1}{L}\sum_{k_2=1}^{L-1} \mathrm{e}^{-\frac{2\mathrm{i}\pi k_2 r_2}{L}} f(r_1, k_2), \tag{A.53}$$

and has the following property:

$$\lim_{\xi\to 1}\left[\lim_{\varepsilon\to 0}\phi(\boldsymbol{r};\xi,\varepsilon)\right] = \lim_{\varepsilon\to 0}\left[\lim_{\xi\to 1}\phi(\boldsymbol{r};\xi,\varepsilon)\right] \equiv \Phi(\boldsymbol{r}) \tag{A.54}$$

Using these notations, and the definition of f (A.48), we obtain the following expansions, where we carefully consider the two possible orders for the limits:

1. if we first take $\varepsilon \to 0$ and ultimately $\xi \to 1$, one obtains

$$\widehat{\mathcal{P}}(\boldsymbol{r}|\mathbf{0};\xi,\varepsilon=0) = \widehat{P}(\boldsymbol{r}|\mathbf{0};\xi) \underset{\xi\to 1}{=} \frac{1}{L\sqrt{1-\xi}} - \frac{2|r_1|}{L} + \Phi(\boldsymbol{r}) + \mathcal{O}(\sqrt{1-\xi}) \tag{A.55}$$

   Note that this corresponds to the random walk of an unbiased vacancy on the lattice, and that the following result is simply a rewriting of the results from Section A.2.

2. if we first take $\xi \to 1$ and ultimately $\varepsilon \to 0$, one obtains

$$\widehat{\mathcal{P}}(\boldsymbol{r}|\mathbf{0};\xi=1,\varepsilon) \underset{\varepsilon\to 0}{=} \begin{cases} \dfrac{1}{L\varepsilon} + \dfrac{1-4r_1}{L} + \Phi(\boldsymbol{r}) + \mathcal{O}(\varepsilon) & \text{if } r_1 \geq 0\,, \\ \dfrac{1}{L\varepsilon} + \dfrac{1}{L} + \Phi(\boldsymbol{r}) + \mathcal{O}(\varepsilon) & \text{if } r_1 < 0\,. \end{cases} \tag{A.56}$$

Then, the expansions of $\widehat{\mathcal{P}}(\boldsymbol{r}|\mathbf{0};\xi=1,\varepsilon)$ in the $\varepsilon \to 0$ limit are known as soon as the quantities $\Phi(\boldsymbol{r})$ are known. They can be computed from the expansions of $\widehat{P}$ (A.36)-(A.41): introducing the quantity

$$\Delta(\boldsymbol{r}) = \lim_{\xi\to 1}\left[\widehat{P}(\mathbf{0}|\mathbf{0};\xi) - \widehat{P}(\boldsymbol{r}|\mathbf{0};\xi)\right], \tag{A.57}$$

one gets

$$\Phi(\boldsymbol{r}) = \frac{2|r_1|}{L} + S^{(2)}_{L,-1} - \Delta(\boldsymbol{r}). \tag{A.58}$$

Combining with (B.52), we finally write:

$$\widehat{\mathcal{P}}(\boldsymbol{r}|\mathbf{0};\xi=1,\varepsilon) \underset{\varepsilon\to 0}{=} \frac{1}{L\varepsilon} + \frac{1}{L} - \frac{2r_1}{L} + S^{(2)}_{L,-1} - \Delta(\boldsymbol{r}) + \mathcal{O}(\varepsilon). \tag{A.59}$$

A.3.3 Joint expansion of the propagators

As it is suggested in Section 4.7.5, we study the propagators $\widehat{\mathcal{P}}$ in the limit where $\xi \to 1$ and $\varepsilon \to 0$ simultaneously, with the scaling

$$1 - \xi \sim \varepsilon^2. \tag{A.60}$$

We eliminate the variable ε by introducing a parameter λ such that

$$\varepsilon = \frac{1}{\lambda}\sqrt{1-\xi} \tag{A.61}$$

We then study the behavior of the propagators $\widehat{\mathcal{P}}$ in the $\xi \to 1$ limit assuming that λ is constant when $\xi \to 1$. We get

$$\widehat{\mathcal{P}}(\boldsymbol{r}|\mathbf{0};\xi,\varepsilon) \underset{\xi\to 1}{=} \begin{cases} \dfrac{\lambda}{L\sqrt{1+\lambda^2}\sqrt{1-\xi}} - \dfrac{2r_1}{L}\left(1+\dfrac{1}{L\sqrt{1+\lambda^2}}\right) + \dfrac{1}{2L\sqrt{1+\lambda^2}}\dfrac{2-\lambda^2}{1+\lambda^2} + \Phi(\boldsymbol{r}) + \mathcal{O}(\sqrt{1-\xi}) & \text{if } r_1 \geq 0\,, \\ \dfrac{\lambda}{L\sqrt{1+\lambda^2}\sqrt{1-\xi}} + \dfrac{2r_1}{L}\left(1-\dfrac{1}{L\sqrt{1+\lambda^2}}\right) + \dfrac{1}{2L\sqrt{1+\lambda^2}}\dfrac{2-\lambda^2}{1+\lambda^2} + \Phi(\boldsymbol{r}) + \mathcal{O}(\sqrt{1-\xi}) & \text{if } r_1 < 0\,. \end{cases} \tag{A.62}$$

Recalling the expression of $\Phi(\boldsymbol{r})$ (A.59), we finally obtain

$$\widehat{\mathcal{P}}(\boldsymbol{r}|\mathbf{0};\xi,\varepsilon) \underset{\xi\to 1}{=} \frac{\lambda}{L\sqrt{1+\lambda^2}\sqrt{1-\xi}} - \frac{2r_1}{L}\frac{1}{\sqrt{1+\lambda^2}} + \frac{1}{2L\sqrt{1+\lambda^2}}\frac{2-\lambda^2}{1+\lambda^2} + S^{(2)}_{L,-1} - \Delta(\boldsymbol{r}) + \mathcal{O}(\sqrt{1-\xi}) \tag{A.63}$$

where $\Delta(\boldsymbol{r})$ is given by (A.57).

APPENDIX B

Propagators of a random walk on a capillary-like lattice

In this Appendix, we consider a capillary-like lattice, which is infinite in a direction and finite of width L with periodic boundary conditions in the other directions (Fig. B.1). We compute the propagators associated to a symmetric nearest-neighbor random walk, and consider their long-time limit. We compute the propagators associated to a biased random walk (where the bias only affects the infinitely extended direction of the stripe), in the long-time limit and in the limit of a small bias. Finally, we study the biased propagators in a joint limit of long time and small bias.

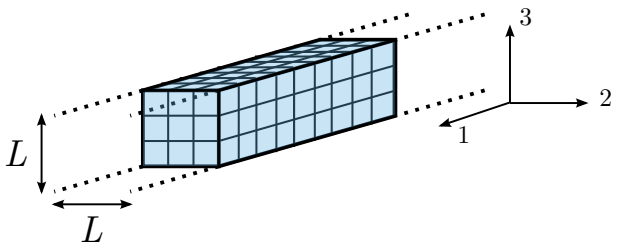

Figure B.1: Capillary-like geometry. The lattice is infinite in the first direction (which will be the direction of the external force imposed on the TP), and finite of width L with periodic boundary conditions in the other directions.

B.1 Propagators of a symmetric random walk

Adapting to the case of the three-dimensional capillaries the expressions used in the case of the stripe-like capillary (A.10), we write the general expression of the propagators:

$$\widehat{P}(\boldsymbol{r}|\boldsymbol{0};\xi) = \frac{1}{L^2}\sum_{k_2,k_3=0}^{L-1}\frac{1}{2\pi}\int_{-\pi}^{\pi}\mathrm{d}k_1\frac{\mathrm{e}^{-\mathrm{i}k_1 r_1}\mathrm{e}^{-\frac{2\mathrm{i}\pi k_2 r_2}{L}}\mathrm{e}^{-\frac{2\mathrm{i}\pi k_3 r_3}{L}}}{1-\xi\lambda(\boldsymbol{k})}, \tag{B.1}$$

where

$$\lambda(\boldsymbol{k}) = \frac{1}{3}\left(\cos k_1 + \cos\frac{2\pi k_2}{L} + \cos\frac{2\pi k_3}{L}\right). \tag{B.2}$$

This propagator can be computed explicitly. For a given site $\boldsymbol{r} = (r_1, r_2, r_3)$, we write

$$\widehat{P}(\boldsymbol{r}|\boldsymbol{0};\xi) = \frac{1}{L^2}\sum_{k_2,k_3=0}^{L-1}\frac{1}{2\pi}\mathrm{e}^{-\frac{2\mathrm{i}\pi k_2 r_2}{L}}\mathrm{e}^{-\frac{2\mathrm{i}\pi k_3 r_3}{L}}f(r_1), \tag{B.3}$$

with

$$f(r_1) = \int_{-\pi}^{\pi}\mathrm{d}k_1\frac{\mathrm{e}^{-\mathrm{i}k_1 r_1}}{1-\frac{\xi}{3}\left(\cos k_1 + \cos\frac{2\pi k_2}{L}\cos\frac{2\pi k_3}{L}\right)}. \tag{B.4}$$

With the change of variable $u = \mathrm{e}^{-\mathrm{i}k_1}$, and denoting by $\mathcal{C}$ the unit circle, we get

$$f(r_1) = -\oint_{\mathcal{C}} \frac{\mathrm{d}u}{-\mathrm{i}u} \frac{u^{r_1}}{1 - \frac{\xi}{3}\left[\frac{1}{2}\left(u + \frac{1}{u}\right) + \cos\frac{2\pi k_2}{L} + \cos\frac{2\pi k_3}{L}\right]}, \tag{B.5}$$

$$= \frac{6\mathrm{i}}{\xi} \oint_{\mathcal{C}} \mathrm{d}u \frac{u^{r_1}}{(u - U_1)(u - U_2)}, \tag{B.6}$$

where we defined

$$U_{\frac{1}{2}} = \frac{3}{\xi} - \left(\cos\frac{2\pi k_2}{L} + \cos\frac{2\pi k_3}{L}\right) \pm \sqrt{\left(\frac{3}{\xi} - \cos\frac{2\pi k_2}{L} - \cos\frac{2\pi k_3}{L}\right)^2 - 1}. \tag{B.7}$$

For $0 < \xi < 1$ and $0 \leq k_2 \leq L-1$, one shows that U_2 is in the contour $\mathcal{C}$ and U_1 is outside. Depending on the value of r_1, we determine the singularities of f contained in $\mathcal{C}$, and we apply the residue theorem. Finally, the propagators write:

- if $r_1 \geq 0$:

$$\widehat{P}(r_1, r_2, r_3|\mathbf{0};\xi) = \frac{1}{L^2} \sum_{k_2,k_3=0}^{L-1} \mathrm{e}^{-\frac{2i\pi(k_2 r_2 + k_3 r_3)}{L}} \frac{{U_2}^{r_1}}{\sqrt{\left[1 - \frac{\xi}{3}\left(\cos\frac{2\pi k_2}{L} + \cos\frac{2\pi k_3}{L}\right)\right]^2 - \frac{\xi^2}{9}}} \tag{B.8}$$

- if $r_1 < 0$:

$$\widehat{P}(r_1, r_2, r_3|\mathbf{0};\xi) = \frac{1}{L^2} \sum_{k_2,k_3=0}^{L-1} \mathrm{e}^{-\frac{2i\pi(k_2 r_2 + k_3 r_3)}{L}} \frac{1}{{U_1}^{|r_1|}} \frac{1}{\sqrt{\left[1 - \frac{\xi}{3}\left(\cos\frac{2\pi k_2}{L} + \cos\frac{2\pi k_3}{L}\right)\right]^2 - \frac{\xi^2}{9}}} \tag{B.9}$$

The propagators needed in Section 4.4.3 to compute the matrices $\boldsymbol{A}$ and $\boldsymbol{P}$ then write

$$\widehat{P}(\mathbf{0}|\mathbf{0};\xi) = C_{L,0}(\xi), \tag{B.10}$$

$$\widehat{P}(\boldsymbol{e}_1|\mathbf{0};\xi) = \frac{3}{\xi}\left[C_{L,0}(\xi) - 1\right] - C_{L,1}(\xi), \tag{B.11}$$

$$\widehat{P}(\boldsymbol{e}_2|\mathbf{0};\xi) = \frac{1}{2} C_{L,1}(\xi), \tag{B.12}$$

$$\widehat{P}(2\boldsymbol{e}_1|\mathbf{0};\xi) = -\frac{18}{\xi^2} + \left(\frac{18}{\xi^2} - 1\right) C_{L,0}(\xi) - \frac{12}{\xi} C_{L,1}(\xi) + 2C_{L,2}(\xi), \tag{B.13}$$

$$\widehat{P}(2\boldsymbol{e}_2|\mathbf{0};\xi) = C_{L,2}(\xi) - 2D_L(\xi) - C_{L,0}(\xi), \tag{B.14}$$

$$\widehat{P}(\boldsymbol{e}_1 + \boldsymbol{e}_2|\mathbf{0};\xi) = \frac{3}{2\xi} C_{L,1}(\xi) - \frac{1}{2} C_{L,2}(\xi), \tag{B.15}$$

$$\widehat{P}(\boldsymbol{e}_2 + \boldsymbol{e}_3|\mathbf{0};\xi) = D_L(\xi), \tag{B.16}$$

where we introduced the quantities

$$C_{L,n}(\xi) = \frac{1}{L^2} \sum_{k_2,k_3=0}^{L-1} \frac{\left(\cos\frac{2\pi k_2}{L} + \frac{2\pi k_3}{L}\right)^n}{\sqrt{\left[1 - \frac{\xi}{3}\left(\cos\frac{2\pi k_2}{L} + \frac{2\pi k_3}{L}\right)\right]^2 - \frac{\xi^2}{9}}}, \tag{B.17}$$

$$D_L(\xi) = \frac{1}{L^2} \sum_{k_2,k_3=0}^{L-1} \frac{\cos\frac{2\pi k_2}{L}\cos\frac{2\pi k_3}{L}}{\sqrt{\left[1 - \frac{\xi}{3}\left(\cos\frac{2\pi k_2}{L} + \frac{2\pi k_3}{L}\right)\right]^2 - \frac{\xi^2}{9}}}. \tag{B.18}$$

In the quantities $C_{L,n}(\xi)$, the term of the sum obtained for $(k_2, k_3) = (0, 0)$ diverges when $\xi \to 1$, whereas the other ones tend to finite values. We then write:

$$C_{L,n}(\xi) = \frac{1}{L^2} \frac{2^n}{\sqrt{\left(1 - \frac{2\xi}{3}\right)^2 - \frac{\xi^2}{9}}} + \frac{1}{L^2} \sum_{\substack{k_2,k_3=0 \\ (k_2,k_3)\neq(0,0)}}^{L-1} \frac{\left(\cos\frac{2\pi k_2}{L} + \cos\frac{2\pi k_3}{L}\right)^n}{\sqrt{\left[1 - \frac{\xi}{3}\left(\cos\frac{2\pi k_2}{L} + \frac{2\pi k_3}{L}\right)\right]^2 - \frac{\xi^2}{9}}}. \tag{B.19}$$

We write separately the expansions of these two terms:

$$frac1L^2 \frac{2^n}{\sqrt{\left(1 - \frac{2\xi}{3}\right)^2 - \frac{\xi^2}{9}}} = \frac{2^{n-1}\sqrt{6}}{L^2\sqrt{1-\xi}} - \frac{2^{n-3}\sqrt{6}}{L^2}\sqrt{1-\xi} + \mathcal{O}[(1-\xi)^{3/2}], \tag{B.20}$$

$$\frac{1}{L^2}\sum_{\substack{k_2,k_3=0\\(k_2,k_3)\neq(0,0)}}^{L-1}\frac{\left(\cos\frac{2\pi k_2}{L}+\cos\frac{2\pi k_3}{L}\right)^n}{\sqrt{\left[1-\frac{\xi}{3}\left(\cos\frac{2\pi k_2}{L}+\frac{2\pi k_3}{L}\right)^2\right]^2-\frac{\xi^2}{9}}}=S_{L,n}^{(3)}+\mathcal{O}(1-\xi), \tag{B.21}$$

where we defined

$$S_{L,n}^{(3)}\equiv\frac{1}{L^2}\sum_{\substack{k_2,k_3=0\\(k_2,k_3)\neq(0,0)}}^{L-1}\frac{\left(\cos\frac{2\pi k_2}{L}+\cos\frac{2\pi k_3}{L}\right)^n}{\sqrt{\left[1-\frac{1}{3}\left(\cos\frac{2\pi k_2}{L}+\frac{2\pi k_3}{L}\right)^2\right]^2-\frac{1}{9}}}. \tag{B.22}$$

Finally, we write the expansion of $C_{L,n}(\xi)$:

$$C_{L,n}(\xi)=\frac{2^{n-1}\sqrt{6}}{L^2\sqrt{1-\xi}}+S_{L,n}^{(3)}-\frac{2^{n-3}\sqrt{6}}{L^2}\sqrt{1-\xi}+\mathcal{O}(1-\xi). \tag{B.23}$$

Similarly, we show that

$$D_L(\xi)=\frac{\sqrt{6}}{2L^2\sqrt{1-\xi}}+T_L-\frac{\sqrt{6}}{8L^2}\sqrt{1-\xi}+\mathcal{O}(1-\xi), \tag{B.24}$$

where

$$T_L\equiv\frac{1}{L^2}\sum_{\substack{k_2,k_3=0\\(k_2,k_3)\neq(0,0)}}^{L-1}\frac{\cos\frac{2\pi k_2}{L}\cos\frac{2\pi k_3}{L}}{\sqrt{\left[1-\frac{1}{3}\left(\cos\frac{2\pi k_2}{L}+\frac{2\pi k_3}{L}\right)^2\right]^2-\frac{1}{9}}}. \tag{B.25}$$

Finally, the expansions of the propagators in the $\xi\to 1$ limit are found to be given by

$$\widehat{P}(\mathbf{0}|\mathbf{0};\xi) = \frac{\sqrt{6}}{2L^2\sqrt{1-\xi}}+S_{L,0}^{(3)}-\frac{\sqrt{6}}{8L^2}\sqrt{1-\xi}+\mathcal{O}(1-\xi), \tag{B.26}$$

$$\widehat{P}(\boldsymbol{e}_1|\mathbf{0};\xi) = \frac{\sqrt{6}}{2L^2\sqrt{1-\xi}}+3S_{L,0}^{(3)}-3-S_{L,1}^{(3)}+\frac{11\sqrt{6}}{8L^2}\sqrt{1-\xi}+\mathcal{O}(1-\xi), \tag{B.27}$$

$$\widehat{P}(\boldsymbol{e}_2|\mathbf{0};\xi) = \frac{\sqrt{6}}{2L^2\sqrt{1-\xi}}+\frac{1}{2}S_{L,1}^{(3)}\frac{\sqrt{6}}{8L^2}\sqrt{1-\xi}+\mathcal{O}(1-\xi), \tag{B.28}$$

$$\widehat{P}(2\boldsymbol{e}_1|\mathbf{0};\xi) = \frac{\sqrt{6}}{2L^2\sqrt{1-\xi}}-18+17S_{L,0}^{(3)}-12S_{L,1}^{(3)}+2S_{L,2}^{(3)}+\frac{47\sqrt{6}}{8L^2}\sqrt{1-\xi}+\mathcal{O}(1-\xi), \tag{B.29}$$

$$\widehat{P}(2\boldsymbol{e}_2|\mathbf{0};\xi) = \frac{\sqrt{6}}{2L^2\sqrt{1-\xi}}+S_{L,2}^{(3)}-2T_L-S_{L,0}^{(3)}-\frac{\sqrt{6}}{8L^2}\sqrt{1-\xi}+\mathcal{O}(1-\xi), \tag{B.30}$$

$$\widehat{P}(\boldsymbol{e}_1+\boldsymbol{e}_2|\mathbf{0};\xi) = \frac{\sqrt{6}}{2L^2\sqrt{1-\xi}}+\frac{3}{2}S_{L,1}^{(3)}-\frac{1}{2}S_{L,2}^{(3)}+\frac{11\sqrt{6}}{8L^2}\sqrt{1-\xi}+\mathcal{O}(1-\xi), \tag{B.31}$$

$$\widehat{P}(\boldsymbol{e}_2+\boldsymbol{e}_3|\mathbf{0};\xi) = \frac{\sqrt{6}}{2L^2\sqrt{1-\xi}}+T_L-\frac{\sqrt{6}}{8L^2}\sqrt{1-\xi}+\mathcal{O}(1-\xi). \tag{B.32}$$

B.2 Propagators of a biased random walk

B.2.1 General formulation

When the vacancies are assumed to undergo a biased proportional to ε in the -1 direction (Fig. 4.7), the structure function of the walk writes:

$$\lambda(\boldsymbol{k})=\widetilde{p}_1\mathrm{e}^{\mathrm{i}k_1}+\widetilde{p}_{-1}\mathrm{e}^{-\mathrm{i}k_1}+2\widetilde{p}_2\left(\cos\frac{2\pi k_2}{L}+\cos\frac{2\pi k_3}{L}\right). \tag{B.33}$$

where the jump probabilities $\widetilde{p}_\nu$ are given by

$$\widetilde{p}_{-1} = \frac{1}{1+\varepsilon}\left(\frac{1}{6}+\varepsilon\right) \tag{B.34}$$

$$\widetilde{p}_1=\widetilde{p}_{\pm 2}=\widetilde{p}_{\pm 3} = \frac{1}{6(1+\varepsilon)} \tag{B.35}$$

The associated propagators are

$$\widehat{\mathcal{P}}(\boldsymbol{r}|\mathbf{0};\xi,\varepsilon)=\frac{1}{L}\sum_{k_2,k_3=0}^{L-1}\frac{1}{2\pi}\mathrm{e}^{-\frac{2\mathrm{i}\pi k_2 r_2}{L}}\mathrm{e}^{-\frac{2\mathrm{i}\pi k_3 r_3}{L}}\int_{-\pi}^{\pi}\mathrm{d}k_1\frac{\mathrm{e}^{-\mathrm{i}k_1 r_1}}{1-\xi\left[\widetilde{p}_1\mathrm{e}^{\mathrm{i}k_1}+\widetilde{p}_{-1}\mathrm{e}^{-\mathrm{i}k_1}+2\widetilde{p}_2\left(\cos\frac{2\pi k_2}{L}+\cos\frac{2\pi k_3}{L}\right)\right]}. \tag{B.36}$$

The explicit computation of the integral over k_1 is similar as the one performed in the case of non-biased propagators. With the change of variable $u = \mathrm{e}^{-\mathrm{i}k_1}$ and applying the residue theorem, one gets

$$\widehat{\mathcal{P}}(\boldsymbol{r}|\mathbf{0};\xi,\varepsilon) = \frac{1}{L^2}\sum_{k_2,k_3=0}^{L-1} \mathrm{e}^{-\frac{2\mathrm{i}\pi k_2 r_2}{L}}\mathrm{e}^{-\frac{2\mathrm{i}\pi k_3 r_3}{L}} f(r_1,k_2,k_3). \tag{B.37}$$

with

$$f(r_1,k_2,k_3;\xi,\varepsilon) = \begin{cases} \frac{1}{\xi\widetilde{p}_{-1}}\frac{U_2(\xi,\varepsilon)^{r_1}}{U_1(\xi,\varepsilon)-U_2(\xi,\varepsilon)} & \text{if } r_1 \geq 0 \\ \frac{1}{\xi\widetilde{p}_{-1}}\frac{1}{U_1(\xi,\varepsilon)^{|r_1|}[U_1(\xi,\varepsilon)-U_2(\xi,\varepsilon)]} & \text{if } r_1 < 0. \end{cases} \tag{B.38}$$

and

$$\begin{aligned} U_{\frac{1}{2}}(\xi,\varepsilon) \quad = \quad & \frac{1}{2\xi\widetilde{p}_{-1}}\left[1-2\xi\widetilde{p}_2\left(\cos\frac{2\pi k_2}{L}+\cos\frac{2\pi k_3}{L}\right)\right] \\ & \pm\frac{1}{2}\sqrt{\frac{1}{(\xi\widetilde{p}_{-1})^2}\left[1-2\xi\widetilde{p}_2\left(\cos\frac{2\pi k_2}{L}+\cos\frac{2\pi k_3}{L}\right)\right]^2 - 4\frac{\widetilde{p}_1}{\widetilde{p}_{-1}}} \end{aligned} \tag{B.39}$$

We are interested in the limiting behavior of the propagators $\widehat{\mathcal{P}}$ when ε goes to 0 and ξ goes to one. In what follows, we show that these two limits do not commute. The case where the limit $\varepsilon \to 0$ is taken first actually corresponds with the study of the unbiased propagators $\widehat{P}$ in the long-time limit (see Section B.1).

B.2.2 Small bias expansion of the propagators in the long-time limit

The divergence of the propagators $\widehat{P}$ and $\widehat{\mathcal{P}}$ is due to the cancellation of the denominator $U_1 - U_2$. For any value of ξ and ε, we find that

$$U_1(\xi,\varepsilon)-U_2(\xi,\varepsilon) = \frac{2}{\sqrt{1+6\varepsilon}}\sqrt{\frac{9}{1+6\varepsilon}\left[\frac{1+\varepsilon}{\xi}-\frac{1}{3}\left(\cos\frac{2\pi k_2}{L}+\cos\frac{2\pi k_3}{L}\right)\right]^2-1}. \tag{B.40}$$

Taking $\xi = 1$ and $\varepsilon = 0$ in this expression, one gets:

$$U_1(1,0)-U_2(1,0) = 6\sqrt{\left[1-\frac{1}{3}\left(\cos\frac{2\pi k_2}{L}+\cos\frac{2\pi k_3}{L}\right)\right]^2-\frac{1}{9}}. \tag{B.41}$$

This quantity is equal to zero when $(k_2,k_3) = (0,0)$ and nonzero otherwise (as long as $0 \leq k_2, k_3 \leq L-1$). In order to study the divergence of the propagators, we then write

$$\widehat{\mathcal{P}}(\boldsymbol{r}|\mathbf{0};\xi,\varepsilon) = \frac{1}{L}f(r_1,k_2=0,k_3=0;\xi,\varepsilon)+\phi(\boldsymbol{r};\xi,\varepsilon) \tag{B.42}$$

where the function ϕ is defined as

$$\phi(\boldsymbol{r};\xi,\varepsilon) \equiv \frac{1}{L^2}\sum_{\substack{k_2,k_3=0 \\ (k_2,k_3)\neq(0,0)}}^{L-1} \mathrm{e}^{-\frac{2\mathrm{i}\pi k_2 r_2}{L}}\mathrm{e}^{-\frac{2\mathrm{i}\pi k_3 r_3}{L}} f(r_1,k_2,k_3), \tag{B.43}$$

and has the following property:

$$\lim_{\xi\to1}\left[\lim_{\varepsilon\to0}\phi(\boldsymbol{r};\xi,\varepsilon)\right] = \lim_{\varepsilon\to0}\left[\lim_{\xi\to1}\phi(\boldsymbol{r};\xi,\varepsilon)\right] \equiv \Phi(\boldsymbol{r}) \tag{B.44}$$

Using these notations, and the definition of f (B.38), we obtain the following expansions, where we carefully consider the two possible orders for the limits:

1. if we first take $\varepsilon \to 0$ and ultimately $\xi \to 1$, one obtains

$$\widehat{\mathcal{P}}(\boldsymbol{r}|\mathbf{0};\xi,\varepsilon=0) = \widehat{P}(\boldsymbol{r}|\mathbf{0};\xi) \underset{\xi\to1}{=} \frac{\sqrt{6}}{2L^2\sqrt{1-\xi}} - \frac{3|r_1|}{L^2} + \Phi(\boldsymbol{r}) + \mathcal{O}(\sqrt{1-\xi}) \tag{B.45}$$

   Note that this corresponds to the random walk of an unbiased vacancy on the lattice, and that the following result is simply a rewriting of the results from Section B.1.

2. if we first take $\xi \to 1$ and ultimately $\varepsilon \to 0$, one obtains

$$\widehat{\mathcal{P}}(\boldsymbol{r}|\mathbf{0};\xi=1,\varepsilon) \underset{\varepsilon\to 0}{=} \begin{cases} \dfrac{1}{L^2\varepsilon} + \dfrac{1-6r_1}{L} + \Phi(\boldsymbol{r}) + \mathcal{O}(\varepsilon) & \text{if } r_1 \geq 0\,, \\ \dfrac{1}{L^2\varepsilon} + \dfrac{1}{L^2} + \Phi(\boldsymbol{r}) + \mathcal{O}(\varepsilon) & \text{if } r_1 < 0\,. \end{cases} \tag{B.46}$$

Then, the expansions of $\widehat{\mathcal{P}}(\boldsymbol{r}|\mathbf{0};\xi=1,\varepsilon)$ in the $\varepsilon \to 0$ limit are known as soon as the quantities $\Phi(\boldsymbol{r})$ are knwon. They can be computed from the expansions of $\widehat{P}$ (B.26)-(B.32): introducing the quantity

$$\Delta(\boldsymbol{r}) = \lim_{\xi\to 1}\left[\widehat{P}(\mathbf{0}|\mathbf{0};\xi) - \widehat{P}(\boldsymbol{r}|\mathbf{0};\xi)\right], \tag{B.47}$$

one gets

$$\Phi(\boldsymbol{r}) = \frac{3|r_1|}{L^2} + S^{(3)}_{L,0} - \Delta(\boldsymbol{r}). \tag{B.48}$$

Combining with (B.46), we finally write:

$$\widehat{\mathcal{P}}(\boldsymbol{r}|\mathbf{0};\xi=1,\varepsilon) \underset{\varepsilon\to 0}{=} \frac{1}{L^2\varepsilon} + \frac{1}{L^2} - \frac{3r_1}{L^2} + S^{(3)}_{L,0} - \Delta(\boldsymbol{r}) \tag{B.49}$$

B.2.3 Joint expansion of the propagators

As it is suggested in Section 4.8.3, we study the propagators $\widehat{\mathcal{P}}$ in the limit where $\xi \to 1$ and $\varepsilon \to 0$ simultaneously, with the scaling

$$1-\xi \sim \varepsilon^2. \tag{B.50}$$

We eliminate the variable ε by introducing a parameter λ such that

$$\varepsilon = \frac{1}{\lambda}\sqrt{1-\xi}. \tag{B.51}$$

We then study the behavior of the propagators $\widehat{\mathcal{P}}$ in the $\xi \to 1$ limit assuming that λ is constant when $\xi \to 1$. We get

$$\widehat{\mathcal{P}}(\boldsymbol{r}|\mathbf{0};\varepsilon) \underset{\varepsilon\to 0}{=} \begin{cases} \dfrac{\lambda}{L^2\sqrt{1+2\lambda^2/3}\sqrt{1-\xi}} - \dfrac{3r_1}{L^2}\left(1+\dfrac{1}{\sqrt{1+2\lambda^2/3}}\right) \\ \qquad + \dfrac{1}{L^2\sqrt{1+2\lambda^2/3}}\dfrac{3-2\lambda^2}{3+2\lambda^2} + \Phi(\boldsymbol{r}) + \mathcal{O}(\sqrt{1-\xi}) & \text{if } r_1 \geq 0\,, \\ \dfrac{\lambda}{L^2\sqrt{1+2\lambda^2/3}\sqrt{1-\xi}} + \dfrac{3r_1}{L^2}\left(1-\dfrac{1}{\sqrt{1+2\lambda^2/3}}\right) \\ \qquad + \dfrac{1}{L^2\sqrt{1+2\lambda^2/3}}\dfrac{3-2\lambda^2}{3+2\lambda^2} + \Phi(\boldsymbol{r}) + \mathcal{O}(\sqrt{1-\xi}) & \text{if } r_1 < 0\,. \end{cases} \tag{B.52}$$

Recalling the expression of $\Phi(\boldsymbol{r})$ (B.48), we finally obtain

$$\widehat{\mathcal{P}}(\boldsymbol{r}|\mathbf{0};\varepsilon) \underset{\varepsilon\to 0}{=} \frac{\lambda}{L^2\sqrt{1+2\lambda^2/3}\sqrt{1-\xi}} - \frac{3r_1}{L^2}\frac{1}{\sqrt{1+2\lambda^2/3}} + \frac{1}{L^2\sqrt{1+2\lambda^2/3}}\frac{3-2\lambda^2}{3+2\lambda^2} + S^{(3)}_{L,0} - \Delta(\boldsymbol{r}) + \mathcal{O}(\sqrt{1-\xi}), \tag{B.53}$$

where $\Delta(\boldsymbol{r})$ is given by (B.47).

APPENDIX C

Propagators of a random walk on a two-dimensional lattice

C.1 Propagators of a symmetric random walk

Using the same definitions as in Section A.1, we have the following expression of the Fourier-Laplace transform of the propagator:

$$\widetilde{\widehat{P}}(\boldsymbol{k}|\mathbf{0};\xi) = \frac{1}{1-\xi\lambda(\boldsymbol{k})} \tag{C.1}$$

where the Fourier transform is defined as

$$\widetilde{\widehat{P}}(\boldsymbol{k}|\mathbf{0};\xi) = \sum_{r_1,r_2=-\infty}^{\infty} \mathrm{e}^{\mathrm{i}r_1k_1}\mathrm{e}^{\mathrm{i}r_2k_2}\widehat{P}(\boldsymbol{r}|\mathbf{0};\xi) \tag{C.2}$$

and the structure function of symmetric random walk is

$$\lambda(\boldsymbol{k}) = \frac{1}{2}(\cos k_1 + \cos k_2). \tag{C.3}$$

The general expression of a given propagator $\widehat{P}(\boldsymbol{r}|\mathbf{0};\xi)$ is then

$$\widehat{P}(\boldsymbol{r}|\mathbf{0};\xi) = \frac{1}{(2\pi)^2}\int_{-\pi}^{\pi}\mathrm{d}k_1\int_{-\pi}^{\pi}\mathrm{d}k_2\frac{\mathrm{e}^{-\mathrm{i}k_1r_1}\mathrm{e}^{-\mathrm{i}k_2r_2}}{1-\frac{\xi}{2}(\cos k_1+\cos k_2)} \tag{C.4}$$

As it was shown in Section 4.5.1, four propagators (with $\boldsymbol{r} = \mathbf{0}$, $\boldsymbol{e}_1$, $2\boldsymbol{e}_1$, $\boldsymbol{e}_1+\boldsymbol{e}_2$) are needed in order to perform the computation of the matrices $\mathbf{A}$ and $\mathbf{P}$. Using the general relation between propagators (4.40) for $\boldsymbol{r}_0 = \mathbf{0}$ and $\boldsymbol{r} = \mathbf{0}$, $\boldsymbol{e}_1$, we obtain the relations

$$\widehat{P}(\mathbf{0}|\mathbf{0};\xi) = 1+\xi\widehat{P}(\boldsymbol{e}_1|\mathbf{0};\xi), \tag{C.5}$$

$$\widehat{P}(\boldsymbol{e}_1|\mathbf{0};\xi) = \frac{\xi}{4}\left[\widehat{P}(2\boldsymbol{e}_1|\mathbf{0};\xi)+\widehat{P}(\mathbf{0}|\mathbf{0};\xi)+2\widehat{P}(\boldsymbol{e}_1+\boldsymbol{e}_2|\mathbf{0};\xi)\right]. \tag{C.6}$$

We then express $\widehat{P}(\boldsymbol{e}_1|\mathbf{0};\xi)$ and $\widehat{P}(\boldsymbol{e}_1+\boldsymbol{e}_2|\mathbf{0};\xi)$ in terms of $\widehat{P}(\mathbf{0}|\mathbf{0};\xi)$ and $\widehat{P}(2\boldsymbol{e}_1|\mathbf{0};\xi)$:

$$\widehat{P}(\boldsymbol{e}_1|\mathbf{0};\xi) = \frac{\widehat{P}(\mathbf{0}|\mathbf{0};\xi)-1}{\xi}, \tag{C.7}$$

$$\widehat{P}(\boldsymbol{e}_1+\boldsymbol{e}_2|\mathbf{0};\xi) = \left(\frac{2}{\xi^2}-\frac{1}{2}\right)\widehat{P}(\mathbf{0}|\mathbf{0};\xi)-\frac{1}{2}\widehat{P}(2\boldsymbol{e}_1|\mathbf{0};\xi)-\frac{2}{\xi^2}. \tag{C.8}$$

The propagator $\widehat{P}(\mathbf{0}|\mathbf{0};\xi)$ has been shown to be simply expressed as a special function [58]:

$$\widehat{P}(\mathbf{0}|\mathbf{0};\xi) = \frac{2}{\pi}\mathrm{K}(\xi) \tag{C.9}$$

where K is the complete elliptic integral of the first kind, defined by

$$\mathrm{K}(x) = \int_0^{\pi/2}\frac{\mathrm{d}\psi}{\sqrt{1-x^2\sin^2\psi}}. \tag{C.10}$$

Its expansion in powers of $(1-x)$ is known [1] to be

$$\mathrm{K}(x) \underset{x\to1}{=} \frac{1}{2}\ln\frac{1}{1-x}+\frac{1}{2}\ln 8+\frac{1}{4}(1-x)\ln\frac{1}{1-x}+\mathcal{O}(1-x). \tag{C.11}$$

We then get the expansion

$$\widehat{P}(\mathbf{0}|\mathbf{0};\xi) \underset{\xi\to 1}{=} \frac{1}{\pi}\ln\frac{1}{1-\xi} + \frac{\ln 8}{\pi} + \frac{1}{2\pi}(1-\xi)\ln\frac{1}{1-\xi} + \mathcal{O}(1-\xi). \tag{C.12}$$

The evaluation of $\widehat{P}(2\boldsymbol{e}_1|\mathbf{0};\xi)$ near $\xi = 1$ has been given in [85, 22]:

$$\widehat{P}(2\boldsymbol{e}_1|\mathbf{0};\xi) \underset{\xi\to 1}{=} \frac{1}{\pi}\ln\frac{1}{1-\xi} + \frac{\ln 8}{\pi} - 4 + \frac{8}{\pi} + \frac{9}{2\pi}(1-\xi)\ln\frac{1}{1-\xi} + \mathcal{O}(1-\xi) \tag{C.13}$$

C.2 Propagators of a biased random walk

C.2.1 Method

When the vacancies are assumed to undergo a biased proportional to ε in the -1 direction (Fig. 4.7), the structure function of the walk writes:

$$\lambda(\boldsymbol{k}) = \widetilde{p}_1 \mathrm{e}^{\mathrm{i}k_1} + \widetilde{p}_{-1}\mathrm{e}^{-\mathrm{i}k_1} + 2\widetilde{p}_2\cos k_2, \tag{C.14}$$

where the jump probabilities $\widetilde{p}_\nu$ are given by

$$\widetilde{p}_{-1} = \frac{1}{1+\varepsilon}\left(\frac{1}{4}+\varepsilon\right), \tag{C.15}$$

$$\widetilde{p}_1 = \widetilde{p}_{\pm 2} = \frac{1}{4(1+\varepsilon)}, \tag{C.16}$$

and the generating function associated to a propagator $\mathcal{P}_t(\boldsymbol{r}|\mathbf{0};\xi,\varepsilon)$ is

$$\widehat{\mathcal{P}}(\boldsymbol{r}|\mathbf{0};\xi,\varepsilon) = \frac{1}{(2\pi)^2}\int_{-\pi}^{\pi}\mathrm{d}k_1\int_{-\pi}^{\pi}\mathrm{d}k_2 \frac{\mathrm{e}^{-\mathrm{i}k_1 r_1}\mathrm{e}^{-\mathrm{i}k_2 r_2}}{1-\xi(\widetilde{p}_1\mathrm{e}^{\mathrm{i}k_1} + \widetilde{p}_{-1}\mathrm{e}^{-\mathrm{i}k_1 +} + 2\widetilde{p}_2\cos k_2)}. \tag{C.17}$$

In the limit where ξ is taken equal to 1 and $\varepsilon \to 0$, the method to compute the propagators is as follows. We will first write them in terms of the propagators $\widehat{\mathcal{P}}(\mathbf{0}|\mathbf{0};\xi,\varepsilon)$:

$$\widehat{\mathcal{P}}(\boldsymbol{r}|\mathbf{0};\xi=1,\varepsilon) = \widehat{\mathcal{P}}(\mathbf{0}|\mathbf{0};\xi=1,\varepsilon) - \Big[\widehat{\mathcal{P}}(\mathbf{0}|\mathbf{0};\xi=1,\varepsilon) - \widehat{\mathcal{P}}(\boldsymbol{r}|\mathbf{0};\xi=1,\varepsilon)\Big] \tag{C.18}$$

It will then be shown that the quantity $\widehat{\mathcal{P}}(\mathbf{0}|\mathbf{0};\xi,\varepsilon)$ diverges when $\varepsilon \to 0$, and we will compute its expansion up to order $\mathcal{O}(1)$. Then, we will show that the differences $\widetilde{\Delta}(\boldsymbol{r},\xi,\varepsilon) \equiv \Big[\widehat{\mathcal{P}}(\mathbf{0}|\mathbf{0};\xi,\varepsilon) - \widehat{\mathcal{P}}(\boldsymbol{r}|\mathbf{0};\xi,\varepsilon)\Big]$ are of order 1 when ξ is taken equal to 1 and when $\varepsilon \to 0$. Moreover, in Section C.2.3, we will show the relation

$$\lim_{\varepsilon\to 0}\Big[\widehat{\mathcal{P}}(\mathbf{0}|\mathbf{0};\xi=1,\varepsilon) - \widehat{\mathcal{P}}(\boldsymbol{r}|\mathbf{0};\xi=1,\varepsilon)\Big] = \lim_{\xi\to 1}\Big[\widehat{\mathcal{P}}(\mathbf{0}|\mathbf{0};\xi,\varepsilon=0) - \widehat{\mathcal{P}}(\boldsymbol{r}|\mathbf{0};\xi,\varepsilon=0)\Big] \tag{C.19}$$

$$= \lim_{\xi\to 1}\Big[\widehat{P}(\mathbf{0}|\mathbf{0};\xi) - \widehat{P}(\boldsymbol{r}|\mathbf{0};\xi)\Big] \tag{C.20}$$

$$= \Delta(\boldsymbol{r}) \tag{C.21}$$

Then, (C.18) will give an expansion of $\widehat{\mathcal{P}}(\boldsymbol{r}|\mathbf{0};\xi=1,\varepsilon)$ up to order $\mathcal{O}(1)$.

C.2.2 Calculation of $\widehat{\mathcal{P}}(\mathbf{0}|\mathbf{0};\xi=1,\varepsilon)$

Starting from the expression

$$\widehat{\mathcal{P}}(\mathbf{0}|\mathbf{0};\xi=1,\varepsilon) = \frac{1}{(2\pi)^2}\int_{-\pi}^{\pi}\mathrm{d}k_1\int_{-\pi}^{\pi}\mathrm{d}k_2 \frac{1}{1-(\widetilde{p}_1\mathrm{e}^{\mathrm{i}k_1} + \widetilde{p}_{-1}\mathrm{e}^{-\mathrm{i}k_1 +} + 2\widetilde{p}_2\cos k_2)}, \tag{C.22}$$

we first compute the integral over k_1. With the change of variable $u = \mathrm{e}^{-\mathrm{i}k_1}$, we get

$$\int_{-\pi}^{\pi}\mathrm{d}k_1 \frac{1}{1-(\widetilde{p}_1\mathrm{e}^{\mathrm{i}k_1} + \widetilde{p}_{-1}\mathrm{e}^{-\mathrm{i}k_1 +} + 2\widetilde{p}_2\cos k_2)} = \frac{\mathrm{i}}{\widetilde{p}_{-1}}\oint_{\mathcal{C}}\frac{\mathrm{d}u}{u^2 - \frac{u}{\widetilde{p}_{-1}}(1-2\widetilde{p}_2\cos k_2) + \frac{\widetilde{p}_1}{\widetilde{p}_{-1}}}, \tag{C.23}$$

where $\mathcal{C}$ is the unit circle. The roots of the denominator are

$$U_{\frac{1}{2}} = \frac{1}{2}\left[\frac{1-2\widetilde{p}_2\cos k_2}{\widetilde{p}_{-1}} \pm \sqrt{\frac{(1-2\widetilde{p}_2\cos k_2)^2}{\widetilde{p}_{-1}^2} - \frac{4\widetilde{p}_1}{\widetilde{p}_{-1}}}\right]. \tag{C.24}$$

Noticing that U_2 is in $\mathcal{C}$ and applying the residue theorem, we get

$$\int_{-\pi}^{\pi} \mathrm{d}k_1 \frac{1}{1-(\widetilde{p}_1 \mathrm{e}^{\mathrm{i}k_1} + \widetilde{p}_{-1}\mathrm{e}^{-\mathrm{i}k_1 +} + 2\widetilde{p}_2\cos k_2)} = \frac{2\pi}{\sqrt{(1-2\widetilde{p}_2\cos k_2)^2 - 4\widetilde{p}_1\widetilde{p}_{-1}}}, \tag{C.25}$$

and finally, with the parity of this quantity,

$$\widehat{\mathcal{P}}(\mathbf{0}|\mathbf{0};\xi=1,\varepsilon) = \frac{1}{\pi}\int_0^{\pi} \mathrm{d}k_2 \frac{1}{\sqrt{(1-2\widetilde{p}_2\cos k_2)^2 - 4\widetilde{p}_1\widetilde{p}_{-1}}}. \tag{C.26}$$

With the change of variable $t = \cos k_2$, we find

$$\begin{aligned}\widehat{\mathcal{P}}(\mathbf{0}|\mathbf{0};\xi=1,\varepsilon) &= \frac{1}{\pi}\int_{-1}^{1} \frac{\mathrm{d}t}{\sqrt{1-t^2}} \frac{1}{\sqrt{(1-2\widetilde{p}_2 t)^2 - 4\widetilde{p}_1\widetilde{p}_{-1}}}, &\text{(C.27)}\\ &= \frac{1}{2\pi\widetilde{p}_2}\int_{-1}^{1} \frac{\mathrm{d}t}{\sqrt{1-t}\sqrt{1+t}\sqrt{a_+ - t}\sqrt{a_- - t}}, &\text{(C.28)}\end{aligned}$$

with

$$a_\pm = \frac{1 \pm 2\sqrt{\widetilde{p}_1\widetilde{p}_{-1}}}{2\widetilde{p}_2}. \tag{C.29}$$

This integral can be expressed in terms of the complete elliptic integral of the first kind (Eq. C.10):

$$\widehat{\mathcal{P}}(\mathbf{0}|\mathbf{0};\xi=1,\varepsilon) = \frac{1}{2\pi\widetilde{p}_2}\frac{2}{\sqrt{a_- + 1}\sqrt{a_+ - 1}}\mathrm{K}\left(\sqrt{\frac{2(a_+ - a_-)}{(a_- + 1)(a_+ - 1)}}\right). \tag{C.30}$$

Recalling the definitions of $\widetilde{p}$ and the expansion of K (C.11), we finally get

$$\boxed{\widehat{\mathcal{P}}(\mathbf{0}|\mathbf{0};\xi=1,\varepsilon) \underset{\varepsilon\to 0}{=} \frac{2}{\pi}\ln\frac{1}{\varepsilon} + \frac{\ln 8}{\pi} + \mathcal{O}(\varepsilon^2 \ln\varepsilon)} \tag{C.31}$$

C.2.3 Calculation of the differences $\widetilde{\Delta}(\boldsymbol{r},\varepsilon)$

In this Section, we demonstrate the relation (C.19). We compute the difference between the propagators $\widehat{\mathcal{P}}(\mathbf{0}|\mathbf{0};\xi,\varepsilon)$ and $\widehat{\mathcal{P}}(\boldsymbol{r}|\mathbf{0};\xi,\varepsilon)$:

$$\begin{aligned}\widetilde{\Delta}(\boldsymbol{r},\xi,\varepsilon) &\equiv \left[\widehat{\mathcal{P}}(\mathbf{0}|\mathbf{0};\xi,\varepsilon) - \widehat{\mathcal{P}}(\boldsymbol{r}|\mathbf{0};\xi,\varepsilon)\right] &\text{(C.32)}\\ &= \frac{1}{(2\pi)^2}\int_{-\pi}^{\pi}\mathrm{d}k_2\int_{-\pi}^{\pi}\mathrm{d}k_1 \frac{\mathrm{e}^{-\mathrm{i}n_1k_1}\mathrm{e}^{-\mathrm{i}n_2k_2} - 1}{1-\xi(\widetilde{p}_1\mathrm{e}^{\mathrm{i}k_1} + \widetilde{p}_{-1}\mathrm{e}^{-\mathrm{i}k_1} + 2\widetilde{p}_2\cos k_2)} &\text{(C.33)}\end{aligned}$$

The integral over k_1 is evaluated by introducing the change of variable $u = \mathrm{e}^{-\mathrm{i}k_1}$. Denoting by $\mathcal{C}$ the unit circle, we get

$$\int_{-\pi}^{\pi}\mathrm{d}k_1 \frac{\mathrm{e}^{-\mathrm{i}n_1k_1}\mathrm{e}^{-\mathrm{i}n_2k_2} - 1}{1-\xi(\widetilde{p}_1\mathrm{e}^{\mathrm{i}k_1} + \widetilde{p}_{-1}\mathrm{e}^{-\mathrm{i}k_1} + 2\widetilde{p}_2\cos k_2)} = \mathrm{i}\oint_{\mathcal{C}}\frac{\mathrm{d}u}{\xi\widetilde{p}_{-1}}\frac{u^{n_1}\mathrm{e}^{-\mathrm{i}n_2k_2} - 1}{(u-U_1)(u-U_2)}, \tag{C.34}$$

with

$$U_{\frac{1}{2}} = \frac{1}{2}\left[\frac{1-2\xi\widetilde{p}_2\cos k_2}{\xi\widetilde{p}_{-1}} \pm \sqrt{\frac{(1-2\widetilde{p}_2\cos k_2)^2}{\xi^2\widetilde{p}_{-1}^2} - \frac{4\widetilde{p}_1}{\widetilde{p}_{-1}}}\right]. \tag{C.35}$$

Finally, noticing that U_2 is the only singularity in $\mathcal{C}$ and applying the residue theorem, we get

$$\begin{aligned}\widetilde{\Delta}(\boldsymbol{r},\xi,\varepsilon) &= \frac{1}{2\pi}\int_{-\pi}^{\pi}\frac{\mathrm{d}k_2}{\xi\widetilde{p}_{-1}}\frac{1-{U_2}^{n_1}\mathrm{e}^{-\mathrm{i}n_2k_2}}{U_2-U_1} &\text{(C.36)}\\ &= \frac{1}{\pi}\int_0^{\pi}\frac{\mathrm{d}k_2}{\xi\widetilde{p}_{-1}}\frac{1-{U_2}^{n_1}\cos(n_2k_2)}{U_2-U_1}. &\text{(C.37)}\end{aligned}$$

Taking $\xi = 1$ and $\varepsilon = 0$ (i.e. $p_\nu = 1/4$ for all ν), $\widetilde{\Delta}(\boldsymbol{r}, \xi, \varepsilon)$ becomes

$$\widetilde{\Delta}(\boldsymbol{r}, \xi = 1, \varepsilon = 0) = \frac{1}{\pi} \int_0^\pi \mathrm{d}k_2 \frac{2^{n_1} \cos(n_2 k_2) \left[1 - \frac{1}{2}\cos k_2 - \sqrt{\left(1 - \frac{1}{2}\cos k_2\right)^2 - \frac{1}{4}}\right]^{n_1} - 1}{\sqrt{\left(1 - \frac{1}{2}\cos k_2\right)^2 - \frac{1}{4}}}. \tag{C.38}$$

This integral is defined, so that $\widetilde{\Delta}(\boldsymbol{r}, \xi = 1, \varepsilon = 0)$ takes a finite value and the limits $\xi \to 1$ and $\varepsilon \to 0$ commute. We finally obtain (C.19):

$$\lim_{\varepsilon \to 0} \left[\widehat{\mathcal{P}}(\mathbf{0}|\mathbf{0}; \xi = 1, \varepsilon) - \widehat{\mathcal{P}}(\boldsymbol{r}|\mathbf{0}; \xi = 1, \varepsilon)\right] = \lim_{\xi \to 1} \left[\widehat{\mathcal{P}}(\mathbf{0}|\mathbf{0}; \xi, \varepsilon = 0) - \widehat{\mathcal{P}}(\boldsymbol{r}|\mathbf{0}; \xi, \varepsilon = 0)\right] \tag{C.39}$$

C.2.4 Joint limit of $\xi \to 1$ and $\varepsilon \to 0$

We finally obtain the expansion of $\widehat{\mathcal{P}}(\mathbf{0}|\mathbf{0}; \xi, \varepsilon)$ in the limit where $\xi \to 1$ and $\varepsilon \to 0$ with the scaling

$$1 - \xi \sim \varepsilon^2. \tag{C.40}$$

In the this limit, we will apply the same method as previously, and write

$$\widehat{\mathcal{P}}(\boldsymbol{r}|\mathbf{0}; \xi, \varepsilon) = \widehat{\mathcal{P}}(\mathbf{0}|\mathbf{0}; \xi, \varepsilon) - \left[\widehat{\mathcal{P}}(\mathbf{0}|\mathbf{0}; \xi, \varepsilon) - \widehat{\mathcal{P}}(\boldsymbol{r}|\mathbf{0}; \xi, \varepsilon)\right]. \tag{C.41}$$

The expansion of $\widehat{\mathcal{P}}(\mathbf{0}|\mathbf{0}; \xi, \varepsilon)$ in the joint limit will be computed. The quantity between the square brackets will be equal to $\Delta(\boldsymbol{r})$ at leading order in this joint limit. We will finally obtain an expansion of $\widehat{\mathcal{P}}(\mathbf{0}|\mathbf{0}; \xi, \varepsilon)$ in the joint limit up to order $\mathcal{O}(1)$. In order to compute an expansion for $\widehat{\mathcal{P}}(\mathbf{0}|\mathbf{0}; \xi, \varepsilon)$, we start from its expression

$$\widehat{\mathcal{P}}(\mathbf{0}|\mathbf{0}; \xi, \varepsilon) = \frac{1}{(2\pi)^2} \int_{-\pi}^{\pi} \mathrm{d}k_1 \int_{-\pi}^{\pi} \mathrm{d}k_2 \frac{1}{1 - \xi(\widetilde{p}_1 \mathrm{e}^{\mathrm{i}k_1} + \widetilde{p}_{-1} \mathrm{e}^{-\mathrm{i}k_1 +} + 2\widetilde{p}_2 \cos k_2)}, \tag{C.42}$$

The calculation of $\widehat{\mathcal{P}}(\mathbf{0}|\mathbf{0}; \xi = 1, \varepsilon)$ may then be simply extended, in order to obtain

$$\widehat{\mathcal{P}}(\mathbf{0}|\mathbf{0}; \xi = 1, \varepsilon) = \frac{1}{2\pi\widetilde{p}_2} \frac{2}{\sqrt{a'_- + 1}\sqrt{a'_+ - 1}} \mathrm{K}\left(\sqrt{\frac{2(a'_+ - a'_-)}{(a'_- + 1)(a'_+ - 1)}}\right) \tag{C.43}$$

with

$$a'_\pm = \frac{1 \pm 2\xi\sqrt{\widetilde{p}_1 \widetilde{p}_{-1}}}{2\xi\widetilde{p}_2} \tag{C.44}$$

The joint expansion is obtained as follows: we replace ε by $\sqrt{1-\xi}/\lambda$ where λ is a constant. After a cumbersome but straightforward computation, we get

$$\widehat{\mathcal{P}}(\mathbf{0}|\mathbf{0}; \xi, \varepsilon) \underset{\xi \to 1}{=} \frac{1}{\pi} \ln\left(\frac{1}{1-\xi} \frac{\lambda^2}{\lambda^2 + 1}\right) + \frac{\ln 8}{\pi} + \dots \tag{C.45}$$

We finally retrieve the ε-dependence:

$$\widehat{\mathcal{P}}(\mathbf{0}|\mathbf{0}; \xi, \varepsilon) \underset{\substack{\varepsilon \sim \sqrt{1-\xi} \\ \xi \to 1}}{=} \frac{1}{\pi} \ln \frac{1}{1 - \xi + \varepsilon^2} + \frac{\ln 8}{\pi} + \dots \tag{C.46}$$

Finally, using (C.41), we obtain the expansion of any propagator $\widehat{\mathcal{P}}(\boldsymbol{r}|\mathbf{0}; \xi, \varepsilon)$ in the joint limit with the formula

$$\widehat{\mathcal{P}}(\boldsymbol{r}|\mathbf{0}; \xi, \varepsilon) \underset{\substack{\varepsilon \sim \sqrt{1-\xi} \\ \xi \to 1}}{=} \frac{1}{\pi} \ln \frac{1}{1 - \xi + \varepsilon^2} + \frac{\ln 8}{\pi} - \Delta(\boldsymbol{r}) + \dots \tag{C.47}$$

where $\Delta(\boldsymbol{r})$ was defined in (C.21).

APPENDIX D

Capillary geometry: expression of $\widehat{\Omega}(k_1;\xi)$ and of the conditional FPTD $\widehat{F}^*$

D.1 Expression of $\widehat{\Omega}(k_1;\xi)$

Using this expression of $\boldsymbol{T}$ (4.72), we can express the determinant $\mathcal{D}(\boldsymbol{k};\xi)$,

$$\mathcal{D}(k_1;\xi) = -b_-^2 c_+ (\mathcal{D}_0 + \mathcal{D}_1 \mathrm{e}^{ik_1} + \mathcal{D}_{-1}\mathrm{e}^{-ik_1}) \tag{D.1}$$

where

$$\begin{aligned} \mathcal{D}_0 &= (F^*_{-1,-1}F^*_{1,1} - F^*_{-1,1}F^*_{1,-1} - 1)(b_+ + 2F^*_{2,3}) + 4(F^*_{2,-1}b_1 + F^*_{2,1}b_{-1}) && \text{(D.2)} \\ \mathcal{D}_{\pm 1} &= F^*_{\pm 1,\mp 1}b_+ - 4F^*_{2,\mp 1}F^*_{\pm 1,2} + 2F^*_{\pm 1,\mp 1}F^*_{2,3} && \text{(D.3)} \end{aligned}$$

and

$$\begin{aligned} b_\pm &= F^*_{2,-2} \pm F^*_{2,2} - 1 && \text{(D.4)} \\ b_{\pm 1} &= F^*_{\mp 1,\pm 1}F^*_{\pm 1,2} - F^*_{\pm 1,\pm 1}F^*_{\mp 1,2} && \text{(D.5)} \\ c_+ &= b_+ - 2F^*_{2,3}. && \text{(D.6)} \end{aligned}$$

Expressing $U_\mu(k_1;\xi)$ using (2.15), we can express the single-vacancy propagator

$$\widehat{\widetilde{P}}^{(1)}(k_1|\mathbf{Y_0};\xi) = \frac{1}{1-\xi}\frac{\mathcal{D}_0 - \sigma_1(\mathbf{Y_0}) - \sigma_{-1}(\mathbf{Y_0}) + [\mathcal{D}_1 + \sigma_1(\mathbf{Y_0})]\,\mathrm{e}^{ik_1} + [\mathcal{D}_{-1} + \sigma_{-1}(\mathbf{Y_0})]\,\mathrm{e}^{-ik_1}}{\mathcal{D}_0 + \mathcal{D}_1\mathrm{e}^{ik_1} + \mathcal{D}_{-1}\mathrm{e}^{-ik_1}} \tag{D.7}$$

with

$$\begin{aligned} \sigma_{\pm 1}(\mathbf{Y_0}) &= F^*_{\pm 1,\mathbf{Y_0}}[-b_+ - 2F^*_{2,3} + F^*_{\mp 1,\mp 1}b_+ - 4F^*_{2,\mp 1}F^*_{\mp 1,2} + 2F^*_{\mp 1,\mp 1}F^*_{2,3}] \\ &+ F^*_{\mp 1,\mathbf{Y_0}}[-F^*_{\pm 1,\mp 1}b_+ + 4F^*_{2,\mp 1}F^*_{\pm 1,2} - 2F^*_{\pm 1,\mp 1}F^*_{2,3}] \\ &+ \left(\sum_{\mu \neq \pm 1} F^*_{\mu,\mathbf{Y_0}}\right)(F^*_{\pm 1,2} + b_{\mp 1}). \end{aligned} \tag{D.8}$$

and

$$F^*_{\mu,\mathbf{Y_0}} = F^*(\mathbf{0}|\boldsymbol{e}_\mu|\mathbf{Y_0};\xi). \tag{D.9}$$

We finally obtain

$$\begin{aligned} \widehat{\Omega}(k_1;\xi) = \frac{1}{1-\xi}\sum_\nu &\left(\sum_{\mathbf{Y}\neq\mathbf{0}} F^*(\mathbf{0}|\boldsymbol{e}_\nu|\mathbf{Y};\xi)\right) \\ &\times \left\{1 - \mathrm{e}^{i\boldsymbol{k}\cdot\boldsymbol{e}_\nu}\frac{\mathcal{D}_0 - \sigma_1(-\boldsymbol{e}_\nu) - \sigma_{-1}(-\boldsymbol{e}_\nu) + [\mathcal{D}_1 + \sigma_1(-\boldsymbol{e}_\nu)]\,\mathrm{e}^{ik_1} + [\mathcal{D}_{-1} + \sigma_{-1}(-\boldsymbol{e}_\nu)]\,\mathrm{e}^{-ik_1}}{\mathcal{D}_0 + \mathcal{D}_1\mathrm{e}^{ik_1} + \mathcal{D}_{-1}\mathrm{e}^{-ik_1}}\right\}. \end{aligned} \tag{D.10}$$

D.2 Expression of $\boldsymbol{P}$

Using appropriate symmetry relations, the matrix $\boldsymbol{P}$ writes

$$\boldsymbol{P} = \begin{pmatrix} \widehat{P}_{0,0,0} & \widehat{P}_{1,0,0} & \widehat{P}_{1,0,0} & \widehat{P}_{0,1,0} & \widehat{P}_{0,1,0} & \widehat{P}_{0,1,0} & \widehat{P}_{0,1,0} \\ \widehat{P}_{0,1,0} & \widehat{P}_{1,0,0} & \widehat{P}_{2,0,0} & \widehat{P}_{1,1,0} & \widehat{P}_{1,1,0} & \widehat{P}_{1,1,0} & \widehat{P}_{1,1,0} \\ \widehat{P}_{1,0,0} & \widehat{P}_{2,0,0} & \widehat{P}_{0,0,0} & \widehat{P}_{1,1,0} & \widehat{P}_{1,1,0} & \widehat{P}_{1,1,0} & \widehat{P}_{1,1,0} \\ \widehat{P}_{0,1,0} & \widehat{P}_{1,1,0} & \widehat{P}_{1,1,0} & \widehat{P}_{0,0,0} & \widehat{P}_{0,2,0} & \widehat{P}_{0,1,1} & \widehat{P}_{0,1,1} \\ \widehat{P}_{0,1,0} & \widehat{P}_{1,1,0} & \widehat{P}_{1,1,0} & \widehat{P}_{0,2,0} & \widehat{P}_{0,0,0} & \widehat{P}_{0,1,1} & \widehat{P}_{0,1,1} \\ \widehat{P}_{0,1,0} & \widehat{P}_{1,1,0} & \widehat{P}_{1,1,0} & \widehat{P}_{0,1,1} & \widehat{P}_{0,1,1} & \widehat{P}_{0,0,0} & \widehat{P}_{0,2,0} \\ \widehat{P}_{0,1,0} & \widehat{P}_{1,1,0} & \widehat{P}_{1,1,0} & \widehat{P}_{0,1,1} & \widehat{P}_{0,1,1} & \widehat{P}_{0,2,0} & \widehat{P}_{0,0,0} \end{pmatrix} \tag{D.11}$$

where we used the short notation $\widehat{P}_{r_1,r_2,r_3} \equiv \widehat{P}(r_1\boldsymbol{e}_1 + r_2\boldsymbol{e}_2 + r_3\boldsymbol{e}_3|\boldsymbol{0};\xi)$. A computation of these propagators is given in Appendix B.

D.3 Expression of $\boldsymbol{A}$

Extending the calculation from Section 4.3.2.1, we obtain an expression for the coefficients of $\boldsymbol{A}$:

$$A(\boldsymbol{s}_i|\boldsymbol{0};\xi) = \delta_{i,0} - (1-\xi)\widehat{P}(\boldsymbol{s}_i|\boldsymbol{0};\xi), \tag{D.12}$$

$$A(\boldsymbol{s}_i|\boldsymbol{e}_\nu;\xi) = \left(\frac{1}{p_\nu + 5/6} - 1\right)\left[\widehat{P}(\boldsymbol{s}_i|\boldsymbol{e}_\nu;\xi) - \delta_{i,\nu} - \xi\widehat{P}(\boldsymbol{s}_i|\boldsymbol{0};\xi)\right], \tag{D.13}$$

so that $\boldsymbol{A}$ is the following 7×7 matrix:

$$\boldsymbol{A} = \begin{pmatrix} 1-(1-\xi)\widehat{P}_{0,0,0} & r_1(\xi\widehat{P}_{0,0,0} - \widehat{P}_{1,0,0}) & r_{-1}(\xi\widehat{P}_{0,0,0} - \widehat{P}_{1,0,0}) & r_2(\xi\widehat{P}_{0,0,0} - \widehat{P}_{0,1,0}) & \dots \\ -(1-\xi)\widehat{P}_{1,0,0} & r_1(\xi\widehat{P}_{1,0,0} - \widehat{P}_{0,0,0} + 1) & r_{-1}(\xi\widehat{P}_{1,0,0} - \widehat{P}_{2,0,0}) & r_2(\xi\widehat{P}_{1,0,0} - \widehat{P}_{1,1,0}) & \dots \\ -(1-\xi)\widehat{P}_{1,0,0} & r_1(\xi\widehat{P}_{1,0,0} - \widehat{P}_{2,0,0}) & r_{-1}(\xi\widehat{P}_{1,0,0} - \widehat{P}_{0,0,0} + 1) & r_2(\xi\widehat{P}_{1,0,0} - \widehat{P}_{1,1,0}) & \dots \\ -(1-\xi)\widehat{P}_{0,1,0} & r_1(\xi\widehat{P}_{0,1,0} - \widehat{P}_{1,1,0}) & r_{-1}(\xi\widehat{P}_{0,1,0} - \widehat{P}_{1,1,0}) & r_2(\xi\widehat{P}_{0,1,0} - \widehat{P}_{0,0,0} + 1) & \dots \\ -(1-\xi)\widehat{P}_{0,1,0} & r_1(\xi\widehat{P}_{0,1,0} - \widehat{P}_{1,1,0}) & r_{-1}(\xi\widehat{P}_{0,1,0} - \widehat{P}_{1,1,0}) & r_2(\xi\widehat{P}_{0,1,0} - \widehat{P}_{0,2,0}) & \dots \\ -(1-\xi)\widehat{P}_{0,1,0} & r_1(\xi\widehat{P}_{0,1,0} - \widehat{P}_{1,1,0}) & r_{-1}(\xi\widehat{P}_{0,1,0} - \widehat{P}_{1,1,0}) & r_2(\xi\widehat{P}_{0,1,0} - \widehat{P}_{0,1,0}) & \dots \\ -(1-\xi)\widehat{P}_{0,1,0} & r_1(\xi\widehat{P}_{0,1,0} - \widehat{P}_{1,1,0}) & r_{-1}(\xi\widehat{P}_{0,1,0} - \widehat{P}_{1,1,0}) & r_2(\xi\widehat{P}_{0,1,0} - \widehat{P}_{0,1,0}) & \dots \end{pmatrix}$$

$$\begin{pmatrix} \dots & r_2(\xi\widehat{P}_{0,0,0} - \widehat{P}_{0,1,0}) & r_2(\xi\widehat{P}_{0,0,0} - \widehat{P}_{0,1,0}) & r_2(\xi\widehat{P}_{0,0,0} - \widehat{P}_{0,1,0}) \\ \dots & r_2(\xi\widehat{P}_{1,0,0} - \widehat{P}_{1,1,0}) & r_2(\xi\widehat{P}_{1,0,0} - \widehat{P}_{1,1,0}) & r_2(\xi\widehat{P}_{1,0,0} - \widehat{P}_{1,1,0}) \\ \dots & r_2(\xi\widehat{P}_{1,0,0} - \widehat{P}_{1,1,0}) & r_2(\xi\widehat{P}_{1,0,0} - \widehat{P}_{1,1,0}) & r_2(\xi\widehat{P}_{1,0,0} - \widehat{P}_{1,1,0}) \\ \dots & r_2(\xi\widehat{P}_{0,1,0} - \widehat{P}_{0,2,0}) & r_2(\xi\widehat{P}_{0,1,0} - \widehat{P}_{0,1,0}) & r_2(\xi\widehat{P}_{0,1,0} - \widehat{P}_{0,1,0}) \\ \dots & r_2(\xi\widehat{P}_{0,1,0} - \widehat{P}_{0,0,0} + 1) & r_2(\xi\widehat{P}_{0,1,0} - \widehat{P}_{0,1,0}) & r_2(\xi\widehat{P}_{0,1,0} - \widehat{P}_{0,1,0}) \\ \dots & r_2(\xi\widehat{P}_{0,1,0} - \widehat{P}_{0,1,0}) & r_2(\xi\widehat{P}_{0,1,0} - \widehat{P}_{0,0,0} + 1) & r_2(\xi\widehat{P}_{0,1,0} - \widehat{P}_{0,2,0}) \\ \dots & r_2(\xi\widehat{P}_{0,1,0} - \widehat{P}_{0,1,0}) & r_2(\xi\widehat{P}_{0,1,0} - \widehat{P}_{0,2,0}) & r_2(\xi\widehat{P}_{0,1,0} - \widehat{P}_{0,0,0} + 1) \end{pmatrix}, \tag{D.14}$$

where we defined $r_\nu = \frac{1}{p_\nu + 5/6} - 1$.

APPENDIX E

Stripe-like geometry: intermediate quantities

In this Appendix, we give the expansions of the quantities $\sigma_{\pm1}(\boldsymbol{e}_\nu)$, $\mathcal{D}_0$, $\mathcal{D}_{\pm1}$ and $\sigma_{\pm1}(\boldsymbol{e}_\nu)$ involved in the calculation of the fluctuations (4.30) and mean (5.2) of the position of the TP in the case of a stripe-like lattice.

E.1 First limit

$\sigma_{\pm1}(\boldsymbol{e}_\nu)$	$-\frac{1}{\mathcal{S}}p_{\pm1}(\alpha-4)(4+\alpha-4\beta)+\dots$
$\mathcal{D}_0$	$-\frac{1}{\mathcal{S}}(p_1+p_{-1})(\alpha-4)(4+\alpha-4\beta)+\dots$
$\mathcal{D}_{\pm1}$	$\frac{1}{\mathcal{S}}p_{\pm1}(\alpha-4)(4+\alpha-4\beta)+\dots$
$\mathcal{D}_0+\mathcal{D}_1+\mathcal{D}_{-1}$	$\frac{1}{\mathcal{S}}(4+\alpha-4\beta)[4-\alpha+4\alpha(p_1+p_{-1})]L\sqrt{1-\xi}+\dots$
$F_1'+F_{-1}'$	$\frac{1}{\mathcal{S}}\frac{L}{\sqrt{1-\xi}}[8\alpha p_1p_{-1}-(\alpha-4)(p_1+p_{-1})][2(\alpha-6\beta+4)(p_1+p_{-1})-\alpha+8\beta-4]+\dots$
$F_1'-F_{-1}'$	$-\frac{L}{\mathcal{S}\sqrt{1-\xi}}(\alpha-4)(p_1-p_{-1})[2(\alpha-6\beta+4)(p_1+p_{-1})-\alpha+8\beta-4]$
$\sum_\nu F_\nu'(\xi)$	$\frac{L}{\sqrt{1-\xi}}+\dots$

$$\begin{aligned}\mathcal{S} \;=\;& 8\alpha(\alpha-4\beta+2)(p_1+p_{-1})^3-4(3\alpha-4)(\alpha-4\beta+2)(p_1+p_{-1})^2\\ &+\left[6\alpha^2-24\alpha\beta+64\beta-32-8\alpha(\alpha-4\beta+2)(p_1-p_{-1})^2\right](p_1+p_{-1})\\ &+2\alpha(3\alpha-12\beta+4)(p_1-p_{-1})^2-(\alpha-4)(4+\alpha-4\beta),\end{aligned} \tag{E.1}$$

E.2 Second limit

$\sigma_{\pm1}(\boldsymbol{e}_\nu)$	$-\frac{1}{\mathcal{S}}p_{\pm1}(\alpha-4)(4+\alpha-4\beta)+\dots$
$\mathcal{D}_0$	$-\frac{1}{\mathcal{S}}(p_1+p_{-1})(\alpha-4)(4+\alpha-4\beta)+\dots$
$\mathcal{D}_{\pm1}$	$\frac{1}{\mathcal{S}}p_{\pm1}(\alpha-4)(4+\alpha-4\beta)+\dots$
$\mathcal{D}_0+\mathcal{D}_1+\mathcal{D}_{-1}$	$\frac{1}{\mathcal{S}}\varepsilon(4+\alpha-4\beta)[L(4-\alpha)+4L\alpha(p_1+p_{-1})+16(p_1-p_{-1})]+\dots$
$F_1'+F_{-1}'$	$\mathcal{O}\left(\frac{\varepsilon}{1-\xi}\right)$
$F_1'-F_{-1}'$	$\mathcal{O}\left(\frac{\varepsilon}{1-\xi}\right)$
$\sum_\nu F_\nu'(\xi)$	$\frac{\varepsilon L}{1-\xi}+\dots$

E.3 Joint limit

$\sigma_{\pm1}(\boldsymbol{e}_\nu)$	$-\frac{1}{\mathcal{S}}p_{\pm1}(\alpha-4)(4+\alpha-4\beta)+\dots$
$\mathcal{D}_0$	$-\frac{1}{\mathcal{S}}(p_1+p_{-1})(\alpha-4)(4+\alpha-4\beta)+\dots$
$\mathcal{D}_{\pm1}$	$\frac{1}{\mathcal{S}}p_{\pm1}(\alpha-4)(4+\alpha-4\beta)+\dots$
$\mathcal{D}_0+\mathcal{D}_1+\mathcal{D}_{-1}$	$\frac{\sqrt{1-\xi}}{\mathcal{S}\lambda\sqrt{1+\lambda^2}}(4+\alpha-4\beta)[L(4-\alpha)(1+\lambda^2)+4L\alpha(1+\lambda^2)(p_1+p_{-1})$ $+16(p_1-p_{-1})\sqrt{1+\lambda^2}]+\dots$
$F_1'+F_{-1}'$	$\mathcal{O}\left(\frac{1}{\sqrt{1-\xi}}\right)$
$F_1'-F_{-1}'$	$\mathcal{O}\left(\frac{1}{\sqrt{1-\xi}}\right)$
$\sum_\nu F_\nu'(\xi)$	$\frac{L\sqrt{1+\lambda^2}}{\lambda\sqrt{1-\xi}}+\dots$

APPENDIX F

Capillary-like geometry: intermediate quantities

In this Appendix, we give the expansions of the quantities $\sigma_{\pm 1}(\boldsymbol{e}_\nu)$, $\mathcal{D}_0$, $\mathcal{D}_{\pm 1}$ and $\sigma_{\pm 1}(\boldsymbol{e}_\nu)$ involved in the calculation of the fluctuations (4.80) and mean (5.18) of the position of the TP in the case of a capillary-like lattice.

F.1 First limit

$\sigma_{\pm 1}(\boldsymbol{e}_\nu)$	$-\frac{2}{\mathcal{S}} p_{\pm 1}(\alpha-6)(6+\alpha-6\beta)+\dots$
$\mathcal{D}_0$	$-\frac{2}{\mathcal{S}}(p_1+p_{-1})(\alpha-6)(6+\alpha-4\beta)+\dots$
$\mathcal{D}_{\pm 1}$	$\frac{2}{\mathcal{S}} p_{\pm 1}(\alpha-6)(6+\alpha-4\beta)+\dots$
$\mathcal{D}_0+\mathcal{D}_1+\mathcal{D}_{-1}$	$\frac{2\sqrt{6}L^2}{3\mathcal{S}}\sqrt{1-\xi}(6+\alpha-4\beta)[6-\alpha+6\alpha(p_1+p_{-1})]+\dots$
$F_1'+F_{-1}'$	$\frac{\sqrt{6}L^2}{3\mathcal{S}\sqrt{1-\xi}}[12\alpha p_1 p_{-1}+(6-\alpha)(p_1+p_{-1})][3(\alpha-8\beta+6)(p_1+p_{-1})-\alpha+12\beta-6]+\dots$
$F_1'-F_{-1}'$	$\frac{\sqrt{6}L^2}{3\mathcal{S}\sqrt{1-\xi}}(\alpha-6)(p_1-p_{-1})[3(\alpha-8\beta+6)(p_1+p_{-1})-\alpha+12\beta-6]+\dots$
$\sum_\nu F_\nu'(\xi)$	$\frac{\sqrt{6}}{3}\frac{L^2}{\sqrt{1-\xi}}+\dots$

$$
\begin{aligned}
\mathcal{S} \;=\;& 27\alpha(\alpha-4\beta+2)(p_1+p_{-1})^3-18(2\alpha-3)(\alpha-4\beta+2)(p_1+p_{-1})^2\\
&+3\left[5\alpha^2-20\alpha\beta+72\beta-36-9\alpha(\alpha-4\beta+2)(p_1-p_{-1})^2\right](p_1+p_{-1})\\
&+3\alpha(7\alpha-28\beta+6)(p_1-p_{-1})^2-(\alpha-6)(6+\alpha-6\beta),
\end{aligned}
\tag{F.1}
$$

F.2 Second limit (for $p_1 = 1$)

$\sigma_1(\boldsymbol{e}_\nu)$	$-\frac{2}{\mathcal{S}} p_{\pm 1}(\alpha-6)(6+\alpha-6\beta)+\dots$
$\sigma_{-1}(\boldsymbol{e}_\nu)$	0
$\mathcal{D}_0$	$-\frac{2}{\mathcal{S}}(\alpha-6)(6+\alpha-4\beta)+\dots$
$\mathcal{D}_1$	$\frac{2}{\mathcal{S}}(\alpha-6)(6+\alpha-4\beta)+\dots$
$\mathcal{D}_{-1}$	0
$\mathcal{D}_0+\mathcal{D}_1+\mathcal{D}_{-1}$	$\frac{2\varepsilon}{\mathcal{S}}(6+\alpha-4\beta)[L^2(6-\alpha)+6L^2\alpha+36]+\dots$
$F_1'+F_{-1}'$	$\mathcal{O}\left(\frac{\varepsilon}{1-\xi}\right)$
$F_1'-F_{-1}'$	$\mathcal{O}\left(\frac{\varepsilon}{1-\xi}\right)$
$\sum_\nu F_\nu'(\xi)$	$\frac{L^2\varepsilon}{1-\xi}+\dots$

F.3 Joint limit (for $p_1 = 1$)

$\sigma_1(\boldsymbol{e}_\nu)$	$-\frac{2}{\mathcal{S}}(\alpha-6)(6+\alpha-6\beta)+\dots$
$\sigma_{-1}(\boldsymbol{e}_\nu)$	0
$\mathcal{D}_0$	$-\frac{2}{\mathcal{S}}(\alpha-6)(6+\alpha-4\beta)+\dots$
$\mathcal{D}_1$	$\frac{2}{\mathcal{S}}(\alpha-6)(6+\alpha-4\beta)+\dots$
$\mathcal{D}_{-1}$	0
$\mathcal{D}_0+\mathcal{D}_1+\mathcal{D}_{-1}$	$\frac{2\sqrt{1-\xi}}{\mathcal{S}\lambda\sqrt{1+2\lambda^2/3}}(6+\alpha-4\beta)[L^2(6-\alpha)(1+2\lambda^2/3)+6L^2\alpha(1+2\lambda^2/3)+36\sqrt{1+2\lambda^2/3}]+\dots$
$F_1'+F_{-1}'$	$\mathcal{O}\left(\frac{1}{\sqrt{1-\xi}}\right)$
$F_1'-F_{-1}'$	$\mathcal{O}\left(\frac{1}{\sqrt{1-\xi}}\right)$
$\sum_\nu F_\nu'(\xi)$	$\frac{L^2\sqrt{1+2\lambda^2/3}}{\lambda\sqrt{1-\xi}}+\dots$

APPENDIX G

Two-dimensional geometry: intermediate quantities

In this Appendix, we give the expansions of the quantities $\sigma_{\pm 1}(\boldsymbol{e}_\nu)$, $\mathcal{D}_0$, $\mathcal{D}_{\pm 1}$ and $\sigma_{\pm 1}(\boldsymbol{e}_\nu)$ involved in the calculation of the fluctuations (4.30) and mean (5.2) of the position of the TP in the case of a two-dimensional lattice. We only give the leading order terms. Note that it is necessary to compute the subdominant terms of the intermediate quantities in order to get the subdominant term of the second cumulant.

G.1 First limit

$\sigma_{\pm 1}(\boldsymbol{e}_\nu)$	$-\frac{1}{\mathcal{S}} p_{\pm 1}\alpha(\alpha-4)+\dots$
$\mathcal{D}_0$	$-\frac{1}{\mathcal{S}}(p_1+p_{-1})\alpha(\alpha-4)+\dots$
$\mathcal{D}_{\pm 1}$	$\frac{1}{\mathcal{S}} p_{\pm 1}\alpha(\alpha-4)+\dots$
$\mathcal{D}_0+\mathcal{D}_1+\mathcal{D}_{-1}$	$\frac{\pi}{\ln\frac{1}{1-\xi}}\frac{1}{\mathcal{S}}\alpha[4-\alpha+4\alpha(p_1+p_{-1})]+\dots$
$F_1'+F_{-1}'$	$\mathcal{O}\left(\frac{1}{(1-\xi)\ln\frac{1}{1-\xi}}\right)$
$F_1'-F_{-1}'$	$\mathcal{O}\left(\frac{1}{(1-\xi)\ln\frac{1}{1-\xi}}\right)$
$\sum_\nu F_\nu'(\xi)$	$\frac{1}{1-\xi}\frac{\pi}{\ln\frac{1}{1-\xi}}+\dots$

$$\begin{aligned}\mathcal{S} &= 8\alpha(\alpha-2)(p_1+p_{-1})^3-4(3\alpha-4)(\alpha--2)(p_1+p_{-1})^2\\ &\quad -2\left[4\alpha(\alpha-2)(p_1-p_{-1})^2-3\alpha+12\alpha-16\right](p_1+p_{-1})\\ &\quad +2\alpha(3\alpha-8)(p_1-p_{-1})^2-\alpha(\alpha-4),\end{aligned} \tag{G.1}$$

G.2 Second limit

$\sigma_{\pm 1}(\boldsymbol{e}_\nu)$	$-\frac{1}{\mathcal{S}} p_{\pm 1}\alpha(\alpha-4)+\dots$
$\mathcal{D}_0$	$-\frac{1}{\mathcal{S}}(p_1+p_{-1})\alpha(\alpha-4)+\dots$
$\mathcal{D}_{\pm 1}$	$\frac{1}{\mathcal{S}} p_{\pm 1}\alpha(\alpha-4)+\dots$
$\mathcal{D}_0+\mathcal{D}_1+\mathcal{D}_{-1}$	$\frac{\pi}{2\ln\frac{1}{\varepsilon}}\frac{1}{\mathcal{S}}\alpha[4-\alpha+4\alpha(p_1+p_{-1})]+\dots$
$F_1'+F_{-1}'$	$\mathcal{O}\left(\frac{1}{(1-\xi)\ln\frac{1}{\varepsilon}}\right)$
$F_1'-F_{-1}'$	$\mathcal{O}\left(\frac{1}{(1-\xi)\ln\frac{1}{\varepsilon}}\right)$
$\sum_\nu F_\nu'(\xi)$	$\frac{\pi}{2(1-\xi)\ln\frac{1}{\varepsilon}}+\dots$

G.3 Joint limit

The quantity λ only appears in the subdominant terms.

$\sigma_{\pm1}(\boldsymbol{e}_\nu)$	$-\frac{1}{\mathcal{S}}p_{\pm1}\alpha(\alpha-4)+\dots$
$\mathcal{D}_0$	$-\frac{1}{\mathcal{S}}(p_1+p_{-1})\alpha(\alpha-4)+\dots$
$\mathcal{D}_{\pm1}$	$\frac{1}{\mathcal{S}}p_{\pm1}\alpha(\alpha-4)+\dots$
$\mathcal{D}_0+\mathcal{D}_1+\mathcal{D}_{-1}$	$\frac{\pi}{\ln\frac{1}{1-\xi}}\frac{1}{\mathcal{S}}\alpha[4-\alpha+4\alpha(p_1+p_{-1})]+\dots$
$F_1'+F_{-1}'$	$\mathcal{O}\left(\frac{1}{(1-\xi)\ln\frac{1}{1-\xi}}\right)$
$F_1'-F_{-1}'$	$\mathcal{O}\left(\frac{1}{(1-\xi)\ln\frac{1}{1-\xi}}\right)$
$\sum_\nu F_\nu'(\xi)$	$\frac{1}{1-\xi}\frac{\pi}{\ln\frac{1}{1-\xi}}+\dots$

APPENDIX H

Cumulant generating function: general expressions

In this Appendix, we give the general expression of $\widehat{\Omega}(\boldsymbol{k};\xi)$, defined by (2.55). This expression involves of the generating functions associated to the conditional first-passage time densities (FPTD) $F_t^*(\mathbf{0}|\boldsymbol{e}_\mu \boldsymbol{Y}_0)$ (probability to reach the origin for the first time at time t, starting from $\boldsymbol{Y}_0$ and being at site $\boldsymbol{e}_\mu$ at time $t-1$). This expression also involves the single-vacancy propagators defined by (2.11). The aim of this Appendix is to provide an explicit expression of $\widehat{\Omega}(\boldsymbol{k};\xi)$ in terms of the conditional FPTD.

H.1 Expression of $\widehat{\Omega}(\boldsymbol{k};\xi)$ in the longitudinal direction

The determination of the single-vacancy propagators (2.11) and therefore of $\widehat{\Omega}(\boldsymbol{k};\xi)$ requires the study of the matrix $\boldsymbol{T}(\boldsymbol{k};\xi)$ defined by (2.13). If we first study the behavior of the TP in the longitudinal direction, it suffices to take the Fourier variable reduced to its first component: $\boldsymbol{k} = (k_1, 0, \dots, 0)$. Taking advantage of the problem symmetries (the directions $\pm 2, \pm 3, \dots, \pm d$ are equivalent), we find that the matrix $\boldsymbol{T}$ takes the simplified block form

$$\boldsymbol{T}(k_1;\xi) = \begin{pmatrix} Q_1 & Q_{1,2} & Q_{1,2} & Q_{1,2} & \cdots & Q_{1,2} \\ Q_{2,1} & Q_{2,2} & Q_{2,3} & Q_{2,3} & \cdots & Q_{2,3} \\ Q_{2,1} & Q_{2,3} & Q_{2,2} & Q_{2,3} & \cdots & Q_{2,3} \\ Q_{2,1} & Q_{2,3} & Q_{2,3} & Q_{2,2} & \cdots & Q_{2,3} \\ \vdots & \vdots & \vdots & \vdots & \ddots & \vdots \\ Q_{2,1} & Q_{2,3} & Q_{2,3} & Q_{2,3} & \cdots & Q_{2,2} \end{pmatrix} \tag{H.1}$$

where the matrices Q are the following 2×2 matrices :

$$Q_1 = \begin{pmatrix} \mathrm{e}^{ik_1} F^*_{1,-1} & \mathrm{e}^{ik_1} F^*_{1,1} \\ \mathrm{e}^{-ik_1} F^*_{-1,-1} & \mathrm{e}^{-ik_1} F^*_{-1,1} \end{pmatrix}, Q_{1,2} = \begin{pmatrix} \mathrm{e}^{ik_1} F^*_{1,2} & \mathrm{e}^{ik_1} F^*_{1,2} \\ \mathrm{e}^{-ik_1} F^*_{-1,2} & \mathrm{e}^{-ik_1} F^*_{-1,2} \end{pmatrix}, Q_{2,1} = \begin{pmatrix} F^*_{2,-1} & F^*_{2,1} \\ F^*_{2,-1} & F^*_{2,1} \end{pmatrix}$$

$$Q_{2,2} = \begin{pmatrix} F^*_{2,-2} & F^*_{2,2} \\ F^*_{2,2} & F^*_{2,-2} \end{pmatrix}, Q_{2,3} = F^*_{2,3} \begin{pmatrix} 1 & 1 \\ 1 & 1 \end{pmatrix}$$

Using this expression of $\mathbf{T}$, we can express the determinant $\mathcal{D}(\boldsymbol{k};\xi)$ defined by (2.12),

$$\mathcal{D}(k_1;\xi) = -b_-^{d-1} c_+^{d-2} (\mathcal{D}_0 + \mathcal{D}_1 \mathrm{e}^{ik_1} + \mathcal{D}_{-1} \mathrm{e}^{-ik_1}) \tag{H.2}$$

where

$$\mathcal{D}_0 = (F^*_{-1,-1}F^*_{1,1} - F^*_{-1,1}F^*_{1,-1} - 1)(b_+ + 2(d-2)F^*_{2,3}) + 2(d-1)(F^*_{2,-1}b_1 + F^*_{2,1}b_{-1}) \tag{H.3}$$

$$\mathcal{D}_{\pm 1} = F^*_{\pm 1,\mp 1} b_+ - 2(d-1) F^*_{2,\mp 1} F^*_{\pm 1,2} + 2(d-2) F^*_{\pm 1,\mp 1} F^*_{2,3} \tag{H.4}$$

and

$$b_\pm = F^*_{2,-2} \pm F^*_{2,2} - 1 \tag{H.5}$$

$$b_{\pm 1} = F^*_{\mp 1,\pm 1} F^*_{\pm 1,2} - F^*_{\pm 1,\pm 1} F^*_{\mp 1,2} \tag{H.6}$$

$$c_+ = b_+ - 2F^*_{2,3}. \tag{H.7}$$

Expressing $U_\mu(k_1;\xi)$ using (2.15), we can express the single-vacancy propagator with its expression (2.11), which takes the form

$$\widehat{\widetilde{P}}^{(1)}(k_1|\mathbf{Y_0};\xi) = \frac{1}{1-\xi}\frac{\mathcal{D}_0 - \sigma_1(\mathbf{Y_0}) - \sigma_{-1}(\mathbf{Y_0}) + [\mathcal{D}_1 + \sigma_1(\mathbf{Y_0})]\,\mathrm{e}^{ik_1} + [\mathcal{D}_{-1} + \sigma_{-1}(\mathbf{Y_0})]\,\mathrm{e}^{-ik_1}}{\mathcal{D}_0 + \mathcal{D}_1\mathrm{e}^{ik_1} + \mathcal{D}_{-1}\mathrm{e}^{-ik_1}} \tag{H.8}$$

with

$$\begin{aligned}\sigma_{\pm1}(\mathbf{Y_0}) &= F^*_{\pm1,\mathbf{Y_0}}[-b_+ - 2(d-2)F^*_{2,3} + F^*_{\mp1,\mp1}b_+ - 2(d-1)F^*_{2,\mp1}F^*_{\mp1,2} + 2(d-2)F^*_{\mp1,\mp1}F^*_{2,3}]\\ &+ F^*_{\mp1,\mathbf{Y_0}}[-F^*_{\pm1,\mp1}b_+ + 2(d-1)F^*_{2,\mp1}F^*_{\pm1,2} - 2(d-2)F^*_{\pm1,\mp1}F^*_{2,3}]\\ &+ \left(\sum_{\mu\neq\pm1} F^*_{\mu,\mathbf{Y_0}}\right)(F^*_{\pm1,2} + b_{\mp1}).\end{aligned} \tag{H.9}$$

and

$$F^*_{\mu,\mathbf{Y_0}} = F^*(\mathbf{0}|\boldsymbol{e}_\mu|\mathbf{Y_0};\xi). \tag{H.10}$$

We finally obtain an expression for $\Omega(k_1;\xi)$ from (2.55)

$$\begin{aligned}\widehat{\Omega}(k_1;\xi) = \frac{1}{1-\xi}\sum_\nu &\left(\sum_{\mathbf{Y}\neq\mathbf{0}} F^*(\mathbf{0}|\boldsymbol{e}_\nu|\mathbf{Y};\xi)\right)\\ &\times\left\{1 - \mathrm{e}^{i\boldsymbol{k}\cdot\boldsymbol{e}_\nu}\frac{\mathcal{D}_0 - \sigma_1(-\boldsymbol{e}_\nu) - \sigma_{-1}(-\boldsymbol{e}_\nu) + [\mathcal{D}_1 + \sigma_1(-\boldsymbol{e}_\nu)]\,\mathrm{e}^{ik_1} + [\mathcal{D}_{-1} + \sigma_{-1}(-\boldsymbol{e}_\nu)]\,\mathrm{e}^{-ik_1}}{\mathcal{D}_0 + \mathcal{D}_1\mathrm{e}^{ik_1} + \mathcal{D}_{-1}\mathrm{e}^{-ik_1}}\right\}.\end{aligned} \tag{H.11}$$

H.2 Expression of $\widehat{\Omega}(\boldsymbol{k};\xi)$ in the transverse direction

To study the behavior of the position of the TP in a transverse direction, it suffices to take $\boldsymbol{k} = (0, k_2, 0, \ldots, 0)$. Using a block-type description of the matrix $\boldsymbol{T}(k_2;\xi)$ as in the previous section, we obtain the following expression of $\Omega(k_2;\xi)$:

$$\begin{aligned}\Omega(k_2;\xi) = \frac{1}{1-\xi}\sum_\nu &\left(\sum_{\mathbf{Y}\neq\mathbf{0}} F^*(\mathbf{0}|\boldsymbol{e}_\nu|\mathbf{Y};\xi)\right)\\ &\times\left\{1 - \mathrm{e}^{i\boldsymbol{k}\cdot\boldsymbol{e}_\nu}\frac{\mathcal{D}_0 + 2\mathcal{D}_1\cos k_2 - \sigma_2(-\boldsymbol{e}_\nu) - \sigma_{-2}(-\boldsymbol{e}_\nu) + \sigma_2(-\boldsymbol{e}_\nu)\mathrm{e}^{ik_2} + \sigma_{-2}(-\boldsymbol{e}_\nu)\mathrm{e}^{-ik_2}}{\mathcal{D}_0 + 2\mathcal{D}_1\cos k_2}\right\}.\end{aligned} \tag{H.12}$$

The different quantities are defined as follows :

- $d \geq 3$

$$\begin{aligned}\mathcal{D}_0 &= 2B\left[(d-1)({F^*_{2,-2}}^2 - {F^*_{2,2}}^2) - (2(d-1)F^*_{2,3} + 1)(F^*_{2,-2} - F^*_{2,2}) + d - 2\right]\\ &+ A_1\left[{F^*_{2,-2}}^3 - {F^*_{2,2}}^3 + ({F^*_{2,-2}}^2 - {F^*_{2,2}}^2 + 1)(2(d-3)F^*_{2,3} - 1)\right.\\ &\left. + (F^*_{2,2}F^*_{2,-2} + 4(d-2){F^*_{2,3}}^2)(F^*_{2,-2} - F^*_{2,2}) + F^*_{2,-2} + F^*_{2,2}\right]\end{aligned} \tag{H.13}$$

$$\begin{aligned}\mathcal{D}_1 &= -B\left[(2d-3)F^*_{2,-2} + F^*_{2,2} - 2(d-1)F^*_{2,3} - 1\right]\\ &- A_1\left[{F^*_{2,-2}}^2 + (2(d-3)F^*_{2,3} - 1)F^*_{2,-2} + F^*_{2,-2}F^*_{2,2} - 2(d-2){F^*_{2,3}}^2\right]\end{aligned} \tag{H.14}$$

$$\begin{aligned}\sigma_2(\mathbf{Y_0}) &= F^*_{1,\mathbf{Y_0}}c_+(F^*_{2,-1} - \beta_{-1})(F^*_{2,2} - F^*_{2,-2} - 1)\\ &+ F^*_{-1,\mathbf{Y_0}}c_+(F^*_{2,1} - \beta_1)(F^*_{2,2} - F^*_{2,-2} - 1)\\ &+ F^*_{2,\mathbf{Y_0}}\left[\mathcal{D}'_1 - A_1(2(d-3)F^*_{2,3} + F^*_{2,2} + F^*_{2,-2} - 1) - 2B(d-2)\right]\\ &- F^*_{-2,\mathbf{Y_0}}\mathcal{D}_1\\ &+ \left(\sum_{\mu\neq\pm1,\pm2} F^*_{\mu,\mathbf{Y_0}}\right)(B + A_1F^*_{2,3})(F^*_{2,2} - F^*_{2,-2} - 1)\end{aligned} \tag{H.15}$$

$$\begin{aligned}
\sigma_{-2}(\mathbf{Y_0}) &= F^*_{1,\mathbf{Y_0}} c_+ (F^*_{2,-1} - \beta_{-1})(F^*_{2,2} - F^*_{2,-2} - 1) \\
&+ F^*_{-1,\mathbf{Y_0}} c_+ (F^*_{2,1} - \beta_1)(F^*_{2,2} - F^*_{2,-2} - 1) \\
&- F^*_{2,\mathbf{Y_0}} \mathcal{D}_1 \\
&+ F^*_{-2,\mathbf{Y_0}} \left[\mathcal{D}'_1 - A_1(2(d-3)F^*_{2,3} + F^*_{2,2} + F^*_{2,-2} - 1) - 2B(d-2)\right] \\
&+ \left(\sum_{\mu \neq \pm 1, \pm 2} F^*_{\mu,\mathbf{Y_0}}\right)(B + A_1 F^*_{2,3})(F^*_{2,2} - F^*_{2,-2} - 1) \qquad \text{(H.16)}
\end{aligned}$$

where we defined

$$\begin{aligned}
A_1 &= F^*_{1,1}F^*_{-1,-1} - (F^*_{1,-1} - 1)(F^*_{-1,1} - 1) && \text{(H.17)} \\
B &= (b_{-1} - F^*_{-1,2})F^*_{2,1} + (b_1 - F^*_{1,2})F^*_{2,-1} && \text{(H.18)} \\
\beta_1 &= F^*_{1,-1}F^*_{2,1} - F^*_{1,1}F^*_{2,-1} && \text{(H.19)} \\
\beta_{-1} &= F^*_{-1,1}F^*_{2,-1} - F^*_{-1,-1}F^*_{2,1} && \text{(H.20)} \\
\mathcal{D}'_1 &= -B\left[(2d-3)F^*_{2,2} + F^*_{2,-2} - 2(d-1)F^*_{2,3} - 1\right] \\
&- A_1\left[{F^*_{2,2}}^2 + (2(d-3)F^*_{2,3} - 1)F^*_{2,2} + F^*_{2,-2}F^*_{2,2} - 2(d-2){F^*_{2,3}}^2\right] && \text{(H.21)}
\end{aligned}$$

- $d = 2$

$$\mathcal{D}_0 = 2B(F^*_{2,-2} - F^*_{2,2}) + A_1({F^*_{2,-2}}^2 - {F^*_{2,2}}^2 + 1) \qquad \text{(H.22)}$$

$$\mathcal{D}_1 = -B - A_1 F^*_{2,-2} \qquad \text{(H.23)}$$

$$\begin{aligned}
\sigma_2(\mathbf{Y_0}) &= F^*_{1,\mathbf{Y_0}}(F^*_{2,-1} - \beta_{-1})(F^*_{2,2} - F^*_{2,-2} - 1) \\
&+ F^*_{-1,\mathbf{Y_0}}(F^*_{2,1} - \beta_1)(F^*_{2,2} - F^*_{2,-2} - 1) \\
&+ F^*_{2,\mathbf{Y_0}}(\mathcal{D}'_1 + A_1) - F^*_{-2,\mathbf{Y_0}}\mathcal{D}_1 \qquad \text{(H.24)}
\end{aligned}$$

$$\begin{aligned}
\sigma_{-2}(\mathbf{Y_0}) &= F^*_{1,\mathbf{Y_0}}(F^*_{2,-1} - \beta_{-1})(F^*_{2,2} - F^*_{2,-2} - 1) \\
&+ F^*_{-1,\mathbf{Y_0}}(F^*_{2,1} - \beta_1)(F^*_{2,2} - F^*_{2,-2} - 1) \\
&- F^*_{2,\mathbf{Y_0}}\mathcal{D}_1 + F^*_{-2,\mathbf{Y_0}}(\mathcal{D}'_1 + A_1) \qquad \text{(H.25)}
\end{aligned}$$

where we defined

$$\mathcal{D}'_1 = -B - A_1 F^*_{2,2}. \qquad \text{(H.26)}$$

APPENDIX I

Higher-order cumulants: case of the stripe-like geometry

In this Appendix, we present the calculation of the higher-order cumulants in the longitudinal and transverse direction in the particular case of a stripe-like geometry. General results are presented in Chapter 6 (Sections 6.3 and 6.4).

I.1 Higher-order cumulants in the longitudinal direction

I.1.1 A remark on the large-time expansion

We start from the general expression of $\widehat{\Omega}(k_1;\xi)$ (H.11) in terms of the generating functions associated to the conditional first-passage time densities (FPTD). In order to obtain the time dependance of Ω_t (and of the cumulants), we will have to calculate the inverse Laplace transform of $\widehat{\Omega}$, given by

$$\Omega_t(k_1) = \frac{1}{2\mathrm{i}\pi}\oint_\gamma \frac{\mathrm{d}\xi}{\xi^{t+1}}\widehat{\Omega}(k_1;\xi). \tag{I.1}$$

where γ is a simple closed contour encircling $\xi = 0$ once, which lies within the circle of convergence of $\widehat{\Omega}(k_1;\xi)$ and which is traversed anti-clockwise. From the structure of $\widehat{\Omega}(k_1;\xi)$ (H.11), we see that the behavior of this integral is controlled by the zeros of $\mathcal{D}(k_1;\xi)$ nearest to $\xi = 0$, which cannot be computed explicitly. We then focus on the long-time expansion, that is the behavior of $\mathcal{D}(k_1;\xi)$ around its singular point nearest to $\xi = 0$.

In what follows, we show that this is the point $(k_1,\xi) = (0,1)$. For recurrent lattices, one has the relation

$$\sum_\nu \widehat{F}^*(\mathbf{0}|\boldsymbol{e}_\nu|\mathbf{Y}_0;\xi=1) = 1. \tag{I.2}$$

This relation means that the vacancy is certain to reach the origin in the long-time limit. Using the symmetry properties of the problem (directions $\pm 2,\dots,\pm d$ are equivalent), we obtain the three following equations:

$$F_{-1,1}(\xi=1) + F_{1,1}(\xi=1) + 2(d-1)F_{2,1}(\xi=1) = 1 \tag{I.3}$$

$$F_{-1,-1}(\xi=1) + F_{1,-1}(\xi=1) + 2(d-1)F_{2,-1}(\xi=1) = 1 \tag{I.4}$$

$$F_{-1,2}(\xi=1) + F_{1,2}(\xi=1) + F_{2,2}(\xi=1) + F_{2,-2}(\xi=1) + 2(d-2)F_{2,3}(\xi=1) = 1. \tag{I.5}$$

Using these relations in the definitions of $\mathcal{D}_0$, $\mathcal{D}_1$ and $\mathcal{D}_{-1}$ (H.3) and (H.4), we get

$$\lim_{\xi\to 1}\left[\mathcal{D}_0 + \mathcal{D}_1 + \mathcal{D}_{-1}\right] = 0 \tag{I.6}$$

which implies $\mathcal{D}(k_1 = 0;\xi = 1) = 0$. The point $(k_1,\xi) = (0,1)$ is singular and must be approached by a joint limit of $k_1 \to 0$ and $\xi \to 1$ with an appropriate scaling to be determined.

I.1.2 First limit

We use the expression of $\widehat{\Omega}(k_1;\xi)$ in terms of the conditional FPTD (H.11). These quantities are computed using the method presented in Chapter 4 (Section 4.3.2). With a computer algebra software, we expand $\widehat{\Omega}(k_1;\xi)$ in powers of both $(1-\xi)$ and k_1, and we find

$$\widehat{\Omega}(k_1;\xi) = \frac{1}{(1-\xi)^2}\left[L\sqrt{1-\xi} - \frac{p_1 - p_{-1}}{1 + \frac{4\alpha}{4-\alpha}(p_1+p_{-1})}\mathrm{i}k_1 + \dots\right] \tag{I.7}$$

where the dots indicate terms of higher order in k_1 or $\sqrt{1-\xi}$. Consequently, these two terms are of comparable magnitude when

$$k_1 \sim \sqrt{1-\xi}. \tag{I.8}$$

This relation gives the appropriate scaling to expand $\widehat{\Omega}(k_1;\xi)$ in the joint limit of $k_1 \to 0$ and $\xi \to 1$. Expanding $\widehat{\Omega}(k_1;\xi)$ with this scaling gives

$$\widehat{\Omega}(k_1;\xi) = \frac{1}{(1-\xi)^2}\left\{ \frac{-\mathrm{i}a_0 k_1}{1-\frac{\mathrm{i}a_0 k_1}{L\sqrt{1-\xi}}} \right. \tag{I.9}$$

$$\left. + \frac{1}{2}k_1 \frac{1}{\left(1-\frac{\mathrm{i}a_0 k_1}{L\sqrt{1-\xi}}\right)^2}\left[(2S^{(2)}_{L,-1}{a_0}^2 + 2{a_0}^2 c + a_1)k_1 - \mathrm{i}2L\sqrt{1-\xi}a_0 c_1'\right] + \mathcal{O}({k_1}^3)\right\}, \tag{I.10}$$

where

$$c_1' = \frac{4(\alpha(\alpha-4)(p_1-p_{-1})^2 - 32(p_1+p_{-1}))}{L^2(\alpha-4)(4\alpha(p_1+p_{-1})-\alpha+4)}. \tag{I.11}$$

Using the notation $\widehat{\kappa}_1^{(n)}(\xi)$ to denote the generating function associated to the n-th cumulant of X_t, and recalling (2.54), we know that

$$\lim_{\rho_0\to 0}\frac{\widehat{\kappa}_1^{(n)}(\xi)}{\rho_0} = -\frac{1}{\mathrm{i}^n}\left.\frac{\partial^n \widehat{\Omega}(k_1;\xi)}{\partial k_1^n}\right|_{k_1=0}. \tag{I.12}$$

Expanding $\widehat{\Omega}(k_1;\xi)$ in powers of k_1 (with fixed ξ), we obtain the coefficients $\omega_n(\xi)$ defined by:

$$\widehat{\Omega}(k_1;\xi) = \sum_{n=0}^{\infty}\omega_n(\xi){k_1}^n. \tag{I.13}$$

Using (I.12), it is straightforward to show that

$$\lim_{\rho_0\to 0}\frac{\widehat{\kappa}_1^{(n)}(\xi)}{\rho_0} = -\frac{n!}{i^n}\omega_n(\xi). \tag{I.14}$$

Using the following usual series expansion (valid for $|ax|<1$),

$$\frac{1}{1-ax} = \sum_{n=0}^{\infty} a^n x^n, \tag{I.15}$$

$$\frac{1}{(1-ax)^2} = \frac{1}{a}\sum_{n=0}^{\infty}(n+1)a^{n+1}x^n, \tag{I.16}$$

we finally obtain

$$\lim_{\rho_0\to 0}\frac{\widehat{\kappa}_1^{(n)}(\xi)}{\rho_0} \underset{\xi\to 1}{=} \frac{a_0^n n!}{(1-\xi)^2}\left\{\left(\frac{1}{L\sqrt{1-\xi}}\right)^{n-1}\right.$$

$$\left. +(n-1)\left(\frac{1}{L\sqrt{1-\xi}}\right)^{n-2}\left[S^{(2)}_{L,-1} + \frac{a_1}{2a_0^2} + c + \frac{n}{n-1}c_1'\right] + \cdots\right\}. \tag{I.17}$$

This expression can be generalized in other geometries (capillary-like geometry, two-dimensional lattice). The general relation is given in the main text (6.38).

I.1.3 Second limit

As it was shown in Chapter 4, in these geometries, the limits $t\to\infty$ (i.e. $\xi\to 1$) and $\rho_0\to 0$ cannot be inverted. The ultimate regime reached by the cumulants of the TP position (i.e. their long-time limit for a fixed value of ρ_0) is obtained by assuming that the vacancies do not perform symmetric random walks anymore, but undergo an effective bias ε equal to the velocity of the TP, which depends on ρ_0 and vanishes when $\rho_0\to 0$ (see Chapter 4, Section 4.7.2.1 for a more precise definition of the evolution rules of the vacancies).

In this situation, the expression of $\widehat{\Omega}(k_2;\xi)$ in terms of the conditional FPTD given in Appendix H (Section H.1) is still valid, but the conditional FPTD must be replaced by the ones computed with the new evolution rules of the vacancies (see Chapter 4, Section 4.7.2). Consequently, $\widehat{\Omega}$ is now a function of k_1, ξ and ε. Expanding $\lim_{\xi\to 1}\left[(1-\xi)^2\Omega(k_1;\xi,\varepsilon)\right]$ in powers of both k_1 and ε, one gets

$$\lim_{\xi\to 1}\left[(1-\xi)^2\Omega(k_1;\xi,\varepsilon)\right] = L\varepsilon - \frac{p_1-p_{-1}}{1+\frac{4\alpha}{4-\alpha}(p_1+p_{-1})+\frac{16}{L(4-\alpha)}(p_1-p_{-1})}\mathrm{i}k_1+\dots \tag{I.18}$$

In the limit $k_1\to 0$ and $\varepsilon\to 0$ and with the scaling $k_1\sim\varepsilon$, we find the leading order term of $\Omega(k_1;\varepsilon)$ in this limit:

$$\lim_{\xi\to 1}\left[(1-\xi)^2\Omega(k_1;\xi,\varepsilon)\right] = \frac{1}{(1-\xi)^2}\frac{-\mathrm{i}a_0'k_1}{1-\frac{\mathrm{i}a_0'k_1}{L\varepsilon}}+\mathcal{O}({k_1}^2) \tag{I.19}$$

with

$$a_0' = \frac{p_1-p_{-1}}{1+\frac{4\alpha}{4-\alpha}(p_1+p_{-1})+\frac{16}{L(4-\alpha)}(p_1-p_{-1})}. \tag{I.20}$$

We can deduce the cumulants:

$$\lim_{\xi\to 1}\left[(1-\xi)^2\widehat{\kappa}_1^{(n)}(\xi)\right] = \rho_0 n!{a_0'}^n\left(\frac{1}{L\varepsilon}\right)^{n-1} = \rho_0 n!{a_0'}^n\mathcal{G}(\varepsilon)^{n-1}, \tag{I.21}$$

where $\mathcal{G}$ was defined by (6.28). ε is equal to the velocity of the TP in the ultimate regime, which can be computed from the expressions demonstrated in Chapter 5,

$$\lim_{\xi\to 1}\left[(1-\xi)^2\widehat{\langle X_t\rangle}(\xi)\right] = \lim_{\xi\to 1}\left[(1-\xi)^2\widehat{\kappa}_1^{(1)}(\xi)\right] = \rho_0 a_0' \tag{I.22}$$

so that $\langle X_t\rangle = \rho_0 a_0' t$ and $\varepsilon = \rho_0 a_0'$. We can deduce the cumulants $\widehat{\kappa}_1^{(n)}(\xi)$ in this limit:

$$\lim_{\xi\to 1}\left[(1-\xi)^2\widehat{\kappa}_1^{(n)}(\xi)\right] = \rho_0 n!{a_0'}^n\mathcal{G}(\rho_0 a_0')^{n-1}, \tag{I.23}$$

and, using a Tauberian theorem,

$$\lim_{t\to\infty}\frac{\kappa_1^{(n)}(t)}{t} \underset{\rho_0\to 0}{\sim} \rho_0 n!{a_0'}^n\mathcal{G}(\rho_0 a_0')^{n-1}. \tag{I.24}$$

This expression can be shown to hold for other geometries (three-dimensional capillary, two-dimensional lattice). Its general form is given in the main text (6.40).

I.2 Cumulants in the transverse direction

I.2.1 First limit

We use the expression of $\widehat{\Omega}(k_2;\xi)$ in terms of the conditional FPTD (H.12). These quantities are computed using the method presented in Chapter 4 (Section 4.3.2). With a computer algebra software, we expand $\lim_{\xi\to 1}\left[(1-\xi)^2\widehat{\Omega}(k_2;\xi)\right]$ in powers of k_2 and $1-\xi$ simultaneously, we find

$$\widehat{\Omega}(k_2;\xi) = \frac{1}{(1-\xi)^2}\left[L\sqrt{1-\xi}+\frac{2p_2}{1+\frac{4\alpha}{4-\alpha}2p_2}\frac{{k_2}^2}{2}+\dots\right] \tag{I.25}$$

Consequently, the appropriate scaling to expand $\widehat{\Omega}(k_2;\xi)$ in the joint limit of $k_2\to 0$ and $\xi\to 1$ is

$$k_2\sim(1-\xi)^{1/4}. \tag{I.26}$$

We get

$$\begin{aligned}\widehat{\Omega}(k_2;\xi) =& \frac{1}{(1-\xi)^2}\left\{\frac{\frac{1}{2}a_2{k_2}^2}{1+\frac{a_2{k_2}^2}{2L\sqrt{1-\xi}}}\right.\\ &\left.-\frac{{k_2}^2}{\left(1+\frac{a_2{k_2}^2}{2L\sqrt{1-\xi}}\right)^2}\left[\left(S_{L,-1}{a_2}^2+c{a_2}^2+\frac{a_2}{6}\right)\frac{{k_2}^2}{4}-\frac{1}{2}a_2c_2'L\sqrt{1-\xi}\right]+\mathcal{O}({k_2}^6)\right\}.\end{aligned} \tag{I.27}$$

where we defined

$$c_2' = \frac{4(\alpha_2 - 8\beta_2 + 8)(p_1 - p_{-1})^2}{L^2[4(\alpha_2 - 8\beta_2 + 8)(p_1 + p_{-1}) - \alpha_2 + 8\beta_2 - 4]} \tag{I.28}$$

Since $\widehat{\Omega}(k_2;\xi)$ is an even function of k_2, all the cumulants of odd order are equal to zero. Expanding $\widehat{\Omega}(k_2;\xi)$ in powers of k_2 using (I.27), and using the following relation, deduced from (2.54),

$$\lim_{\rho_0\to 0} \frac{\widehat{\kappa}_2^{(n)}(\xi)}{\rho_0} = -\frac{1}{\mathrm{i}^n} \left.\frac{\partial^n \widehat{\Omega}(k_2;\xi)}{\partial {k_2}^n}\right|_{k_2=0}, \tag{I.29}$$

we find that the even cumulants are given by

$$\lim_{\rho_0\to 0} \frac{\widehat{\kappa}_2^{(2n)}(\xi)}{\rho_0} = \frac{(2n)!}{(1-\xi)^2}\left(\frac{a_2}{2}\right)^n \left[\left(\frac{1}{L\sqrt{1-\xi}}\right)^{n-1} + (n-1)\left(\frac{1}{L\sqrt{1-\xi}}\right)^{n-2}\left(S_{L,-1} + c + \frac{1}{6a_2} + \frac{n}{n-1}c_2'\right)\right]. \tag{I.30}$$

This expression can be generalized to the case of a two-dimensional lattice. The general expression is given in the main text (6.48).

I.2.2 Second limit

As it was shown in Chapter 4, in these geometries, the limits $t \to \infty$ (i.e. $\xi \to 1$) and $\rho_0 \to 0$ cannot be inverted. The ultimate regime reached by the cumulants of the TP position (i.e. their long-time limit for a fixed value of ρ_0) is obtained by assuming that the vacancies do not perform symmetric random walks anymore, but undergo an effective bias ε equal to the velocity of the TP, which depends on ρ_0 and vanishes when $\rho_0 \to 0$ (see Chapter 4, Section 4.7.2.1 for a more precise definition of the evolution rules of the vacancies).

In this situation, the expression of $\widehat{\Omega}(k_2;\xi)$ in terms of the conditional FPTD given in Appendix H (Section H.2) is still valid, but the conditional FPTD must be replaced by the ones computed with the new evolution rules of the vacancies (see Chapter 4, Section 4.7.2). Consequently, $\widehat{\Omega}$ is now a function of k_2, ξ and ε. Expanding $\lim_{\xi\to 1}\left[(1-\xi)^2\Omega(k_2;\xi,\varepsilon)\right]$ in powers of both k_1 and ε, one gets

$$\lim_{\xi\to 1}\left[(1-\xi)^2\widehat{\Omega}(k_2;\xi,\varepsilon)\right] = L\varepsilon + \frac{1}{2}a_2'{k_2}^2 + \dots \tag{I.31}$$

with

$$a_2' = a_2\left[1 + \frac{16(p_1 - p_{-1})}{L[4(p_1+p_{-1})(\alpha - 8\beta + 8) - \alpha + 8\beta - 4]}\right]^{-1} \tag{I.32}$$

In the limit $k_2 \to 0$ and $\varepsilon \to 0$ and with the scaling $k_2 \sim \sqrt{\varepsilon}$, we find the leading order term of $\lim_{\xi\to 1}\left[(1-\xi)^2\widehat{\Omega}(k_2;\xi,\varepsilon)\right]$ in this limit:

$$\lim_{\xi\to 1}\left[(1-\xi)^2\widehat{\Omega}(k_2;\xi,\varepsilon)\right] = \frac{\frac{1}{2}a_2'{k_2}^2}{1 + \frac{a_2'{k_2}^2}{2L\varepsilon}} + \mathcal{O}(k_2^4) \tag{I.33}$$

Using again the relation $\varepsilon = \rho_0 a_0'$, we obtain

$$\lim_{\xi\to 1}\left[(1-\xi)^2\widehat{\Omega}(k_2;\xi,\varepsilon)\right] = \frac{1}{(1-\xi)^2}\frac{\frac{1}{2}a_2'{k_2}^2}{1 + \frac{a_2'{k_2}^2}{2L\rho_0 a_0'}} + \mathcal{O}(k_2^4). \tag{I.34}$$

We can deduce the cumulants in this limit using the general relation between the derivatives of $\widehat{\Omega}$ and the cumulants (I.29):

$$\lim_{\xi\to 1}\left[(1-\xi)^2\widehat{\kappa}_2^{(2n)}(\xi)\right] \underset{\rho_0\to 0}{\sim} \frac{(2n)!{a_2'}^n}{2^n L^{n-1}\rho_0^{n-2}{a_0'}^{n-1}}. \tag{I.35}$$

Using a Tauberian theorem, this is equivalent to

$$\lim_{t\to\infty}\frac{\kappa_2^{(2n)}(t)}{t} \underset{\rho_0\to 0}{\sim} \frac{(2n)!{a_2'}^n}{2^n L^{n-1}\rho_0^{n-2}{a_0'}^{n-1}}. \tag{I.36}$$

This expression can be generalized to the case of a two-dimensional lattice. Its general form is given in the main text (6.54).

APPENDIX J

Evolution equations of $\left\langle {X_t}^2 \right\rangle$ and of the correlation functions $\widetilde{g}_{\boldsymbol{r}}$

In this Appendix, we give the details of the derivation of the evolution equations of the second moment of the position of the TP $\left\langle {X_t}^2 \right\rangle$ (8.15) and of the correlation functions $\widetilde{g}_{\boldsymbol{r}}$ (8.20).

J.1 Evolution equation of $\left\langle {X_t}^2 \right\rangle$

In this Section, we start from the master equation (8.2) in order to derive the evolution equation verified by $\left\langle {X_t}^2 \right\rangle = \left\langle (\boldsymbol{X} \cdot \boldsymbol{e}_1)^2 \right\rangle$. We multiply the master equation (8.2) by $(\boldsymbol{X}_t \cdot \boldsymbol{e}_1)^2$ and average over all the bath configurations η and all the positions of the TP $\boldsymbol{X}$. We consider separately each term of the master equation:

- the left-hand-side term of (8.2) gives the contribution:

$$C_{\mathrm{L}} = \sum_{\boldsymbol{X},\eta} (\boldsymbol{X} \cdot \boldsymbol{e}_1)^2 2d\tau^* \partial_t P(\boldsymbol{X},\eta;t) \tag{J.1}$$

$$= 2d\tau^* \partial_t \left(\sum_{\boldsymbol{X},\eta} (\boldsymbol{X} \cdot \boldsymbol{e}_1)^2 P(\boldsymbol{X},\eta;t) \right) \tag{J.2}$$

$$= 2d\tau^* \frac{\mathrm{d}\left\langle {X_t}^2 \right\rangle}{\mathrm{d}t} \tag{J.3}$$

- the first term of the right-hand-side yields

$$C_1 = \sum_{\boldsymbol{X},\eta} (\boldsymbol{X} \cdot \boldsymbol{e}_1)^2 \sum_{\mu=1}^{d} \sum_{\boldsymbol{r} \neq \boldsymbol{X}-\boldsymbol{e}_\mu, \boldsymbol{X}} \left[P(\boldsymbol{X},\eta^{\boldsymbol{r},\mu};t) - P(\boldsymbol{X},\eta;t) \right] \tag{J.4}$$

$$= \sum_{\boldsymbol{X}} (\boldsymbol{X} \cdot \boldsymbol{e}_1)^2 \sum_{\mu=1}^{d} \sum_{\boldsymbol{r} \neq \boldsymbol{X}-\boldsymbol{e}_\mu, \boldsymbol{X}} \sum_{\eta} \left[P(\boldsymbol{X},\eta^{\boldsymbol{r},\mu};t) - P(\boldsymbol{X},\eta;t) \right]. \tag{J.5}$$

  Recalling that $\eta^{\boldsymbol{r},\mu}$ a configuration obtained from η by exchanging the occupation variables of two neighboring sites $\boldsymbol{r}$ and $\boldsymbol{r}+\boldsymbol{e}_\mu$, we obtain

$$\sum_{\eta} P(\boldsymbol{X},\eta^{\boldsymbol{r},\mu};t) = \sum_{\eta} P(\boldsymbol{X},\eta;t), \tag{J.6}$$

  and we conclude that $C_1 = 0$.

- the second term of the right-hand-side of (8.2) gives the contribution:

$$C_2 = \frac{2d\tau^*}{\tau} \sum_{\mu} p_\mu \left[\sum_{\boldsymbol{X},\eta} (\boldsymbol{X} \cdot \boldsymbol{e}_1)^2 \left(1 - \eta_{\boldsymbol{X}}\right) P(\boldsymbol{X} - \boldsymbol{e}_{\boldsymbol{\mu}},\eta;t) - \sum_{\boldsymbol{X},\eta} (\boldsymbol{X} \cdot \boldsymbol{e}_1)^2 \left(1 - \eta_{\boldsymbol{X}+\boldsymbol{e}_\mu}\right) P(\boldsymbol{X},\eta;t) \right]. \tag{J.7}$$

  We consider for instance the term corresponding to $\mu = 1$, and consider the first sum over $\boldsymbol{X}$ and η, in which we make the change of variable $\boldsymbol{X} \leftarrow \boldsymbol{X} + \boldsymbol{e}_1$:

$$\sum_{\boldsymbol{X},\eta} (\boldsymbol{X} \cdot \boldsymbol{e}_1)^2 \left(1 - \eta_{\boldsymbol{X}}\right) P(\boldsymbol{X} - \boldsymbol{e}_1,\eta;t) = \sum_{\boldsymbol{X},\eta} (\boldsymbol{X} \cdot \boldsymbol{e}_1 + \sigma)^2 \left(1 - \eta_{\boldsymbol{X}+\boldsymbol{e}_1}\right) P(\boldsymbol{X},\eta;t) \tag{J.8}$$

$$= \sum_{\boldsymbol{X},\eta} \left[(\boldsymbol{X} \cdot \boldsymbol{e}_1)^2 + \sigma^2 + 2\sigma(\boldsymbol{X} \cdot \boldsymbol{e}_1) \right]^2 \left(1 - \eta_{\boldsymbol{X}+\boldsymbol{e}_1}\right) P(\boldsymbol{X},\eta;t). \tag{J.9}$$

Finally, we get

$$\begin{aligned} & \sum_{\boldsymbol{X},\eta} (\boldsymbol{X}\cdot\boldsymbol{e}_1)^2 \left(1-\eta_{\boldsymbol{X}}\right) P(\boldsymbol{X}-\boldsymbol{e}_\mu,\eta;t) - \sum_{\boldsymbol{X},\eta} (\boldsymbol{X}\cdot\boldsymbol{e}_1)^2 \left(1-\eta_{\boldsymbol{X}+\boldsymbol{e}_\mu}\right) P(\boldsymbol{X},\eta;t) \\ = \;& \sigma^2 \sum_{\boldsymbol{X},\eta} (1-\eta_{\boldsymbol{X}+\boldsymbol{e}_1}) P(\boldsymbol{X},\eta;t) + 2\sigma \sum_{\boldsymbol{X},\eta} (\boldsymbol{X}\cdot\boldsymbol{e}_1)(1-\eta_{\boldsymbol{X}+\boldsymbol{e}_1}) P(\boldsymbol{X},\eta;t). \end{aligned} \tag{J.10}$$

Following the same procedure for the term $\mu = 1$ and noticing that the terms obtained for $\mu = \pm 2, \ldots, \pm d$ in (J.7) cancel, we finally get

$$C_2 = \frac{2d\tau^*}{\tau} \left\{ p_1[\sigma^2(1-k_{\boldsymbol{e}_1}) + 2\sigma(\langle X_t\rangle - g_{\boldsymbol{e}_1})] + p_{-1}[\sigma^2(1-k_{\boldsymbol{e}_{-1}}) - 2\sigma(\langle X_t\rangle - g_{\boldsymbol{e}_{-1}})] \right\}, \tag{J.11}$$

where we define

$$g_{\boldsymbol{r}} = \langle X_t \eta_{\boldsymbol{X}_t+\boldsymbol{r}} \rangle . \tag{J.12}$$

- the third term of the right-hand-side of (8.2) will give

$$\begin{aligned} C_3 &= 2dg \sum_{\boldsymbol{X},\eta} (\boldsymbol{X}\cdot\boldsymbol{e}_1)^2 \sum_{\boldsymbol{r}\neq\boldsymbol{X}} \left[\left(1-\eta_{\boldsymbol{r}}\right) P(\boldsymbol{X},\hat{\eta}^{\boldsymbol{r}};t) - \eta_{\boldsymbol{r}} P(\boldsymbol{X},\eta;t) \right] && \text{(J.13)} \\ &= 2dg \sum_{\boldsymbol{X}} (\boldsymbol{X}\cdot\boldsymbol{e}_1)^2 \sum_{\boldsymbol{r}\neq\boldsymbol{X}} \sum_{\eta} \left[\left(1-\eta_{\boldsymbol{r}}\right) P(\boldsymbol{X},\hat{\eta}^{\boldsymbol{r}};t) - \eta_{\boldsymbol{r}} P(\boldsymbol{X},\eta;t) \right]. && \text{(J.14)} \end{aligned}$$

Recalling that $\hat{\eta}^{\boldsymbol{r}}$ is the configuration obtained from η with the change $\eta_{\boldsymbol{r}} \leftarrow 1-\eta_{\boldsymbol{r}}$, we have the following equality

$$\sum_{\eta} \left(1-\eta_{\boldsymbol{r}}\right) P(\boldsymbol{X},\hat{\eta}^{\boldsymbol{r}};t) = \sum_{\eta} \eta_{\boldsymbol{r}} P(\boldsymbol{X},\eta;t), \tag{J.15}$$

which yields $C_3 = 0$.

- for the same reason, the fourth term will have a zero contribution after multiplying by $(\boldsymbol{X}\cdot\boldsymbol{e}_1)^2$ and averaging over $\boldsymbol{X}$ and η.

Finally, bringing together the different contributions originating from the different terms of (8.2), we obtain

$$2d\tau^* \frac{\mathrm{d}}{\mathrm{d}t} \langle {X_t}^2 \rangle = \frac{2d\tau^*}{\tau} \left\{ p_1[\sigma^2(1-k_{\boldsymbol{e}_1}) + 2\sigma(\langle X_t\rangle - g_{\boldsymbol{e}_1})] + p_{-1}[\sigma^2(1-k_{\boldsymbol{e}_{-1}}) - 2\sigma(\langle X_t\rangle - g_{\boldsymbol{e}_{-1}})] \right\}, \tag{J.16}$$

which is equivalent to (8.15):

$$\frac{\mathrm{d}}{\mathrm{d}t} \langle {X_t}^2 \rangle = \frac{2\sigma}{\tau} \left[p_1 \left(\langle X_t\rangle - g_{\boldsymbol{e}_1} \right) - p_{-1} \left(\langle X_t\rangle - g_{\boldsymbol{e}_{-1}} \right) \right] + \frac{\sigma^2}{\tau} \left[p_1 \left(1-k_{\boldsymbol{e}_1}\right) + p_{-1} \left(1-k_{\boldsymbol{e}_{-1}}\right) \right]. \tag{J.17}$$

J.2 Evolution equation of $\widetilde{g}_{\boldsymbol{r}}$

In this Section, we start from the master equation (8.2) in order to derive the evolution equation verified by $\widetilde{g}_{\boldsymbol{r}} = \langle (X_t - \langle X_t\rangle) \eta_{\boldsymbol{X}_t+\boldsymbol{r}} \rangle$. We multiply the master equation (8.2) by $(X - \langle X_t\rangle)\eta_{\boldsymbol{X}+\boldsymbol{r}}$ and average over all the bath configurations η and all the positions of the TP $\boldsymbol{X}$. We consider separately each term of the master equation:

- the left-hand-side term of (8.2) gives the contribution:

$$\begin{aligned} C_{\mathrm{L}} &= \sum_{\boldsymbol{X},\eta} (X - \langle X_t\rangle) \eta_{\boldsymbol{X}_t+\boldsymbol{r}} 2d\tau^* \partial_t P(\boldsymbol{X},\eta;t) && \text{(J.18)} \\ &= 2d\tau^* \sum_{\boldsymbol{X},\eta} (X - \langle X_t\rangle) \eta_{\boldsymbol{X}_t+\boldsymbol{r}} \partial_t P(\boldsymbol{X},\eta;t) && \text{(J.19)} \\ &= \sum_{\boldsymbol{X},\eta} \eta_{\boldsymbol{X}_t+\boldsymbol{r}} \left[\partial_t \left((X - \langle X_t\rangle) P(\boldsymbol{X},\eta;t) \right) - P(\boldsymbol{X},\eta;t) \partial_t (X - \langle X_t\rangle) \right] && \text{(J.20)} \\ &= 2d\tau^* \partial_t \left[\sum_{\boldsymbol{X},\eta} \eta_{\boldsymbol{X}_t+\boldsymbol{r}} (X - \langle X_t\rangle) P(\boldsymbol{X},\eta;t) + \frac{\mathrm{d}\langle X_t\rangle}{\mathrm{d}t} \sum_{\boldsymbol{X},\eta} \eta_{\boldsymbol{X}_t+\boldsymbol{r}} P(\boldsymbol{X},\eta;t) \right] && \text{(J.21)} \\ &= 2d\tau^* \left(\partial_t \widetilde{g}_{\boldsymbol{r}} + k_{\boldsymbol{r}} \frac{\mathrm{d}\langle X_t\rangle}{\mathrm{d}t} \right), && \text{(J.22)} \end{aligned}$$

where we defined $\widetilde{g}_{\boldsymbol{r}}$ as in the main text (8.18).

- the first term of the right-hand-side of the master equation becomes

$$C_1 = \sum_{\boldsymbol{X}} (X - \langle X_t \rangle) \sum_{\mu=1}^{d} \sum_{\boldsymbol{r}' \neq \boldsymbol{X} - \boldsymbol{e}_\mu, \boldsymbol{X}} \sum_{\eta} \eta_{\boldsymbol{X}+\boldsymbol{r}} \left[P(\boldsymbol{X}, \eta^{\boldsymbol{r}',\mu}; t) - P(\boldsymbol{X}, \eta; t) \right] \tag{J.23}$$

With an appropriate change of variable in the sum over η, we obtain

$$\sum_{\eta} \eta_{\boldsymbol{X}+\boldsymbol{r}} P(\boldsymbol{X}, \eta^{\boldsymbol{r}',\mu}; t) = \sum_{\eta} \left(\eta^{\boldsymbol{r}',\mu} \right)_{\boldsymbol{X}+\boldsymbol{r}} P(\boldsymbol{X}, \eta; t), \tag{J.24}$$

so that C_1 is written

$$C_1 = \sum_{\boldsymbol{X}} (X - \langle X_t \rangle) \sum_{\mu=1}^{d} \sum_{\boldsymbol{r}' \neq \boldsymbol{X} - \boldsymbol{e}_\mu, \boldsymbol{X}} \sum_{\eta} \left[\left(\eta^{\boldsymbol{r}',\mu} \right)_{\boldsymbol{X}+\boldsymbol{r}} - \eta_{\boldsymbol{X}+\boldsymbol{r}} \right] P(\boldsymbol{X}, \eta; t) \tag{J.25}$$

We consider the sum over $\boldsymbol{r}'$

$$\begin{aligned} &\sum_{\boldsymbol{r}' \neq \boldsymbol{X} - \boldsymbol{e}_\mu, \boldsymbol{X}} \left[\left(\eta^{\boldsymbol{r}',\mu} \right)_{\boldsymbol{X}+\boldsymbol{r}} - \eta_{\boldsymbol{X}+\boldsymbol{r}} \right] \\ &= \sum_{\boldsymbol{r}'} \left[\left(\eta^{\boldsymbol{r}',\mu} \right)_{\boldsymbol{X}+\boldsymbol{r}} - \eta_{\boldsymbol{X}+\boldsymbol{r}} \right] - \left[\left(\eta^{\boldsymbol{X}-\boldsymbol{e}_\mu,\mu} \right)_{\boldsymbol{X}+\boldsymbol{r}} - \eta_{\boldsymbol{X}+\boldsymbol{r}} \right] - \left[\left(\eta^{\boldsymbol{X},\mu} \right)_{\boldsymbol{X}+\boldsymbol{r}} - \eta_{\boldsymbol{X}+\boldsymbol{r}} \right]. \end{aligned} \tag{J.26}$$

Recalling that $\eta^{\boldsymbol{r},\mu}$ a configuration obtained from η by exchanging the occupation variables of two neighboring sites $\boldsymbol{r}$ and $\boldsymbol{r} + \boldsymbol{e}_\mu$, we obtain the general relation

$$(\eta^{\boldsymbol{r}',\mu})_{\boldsymbol{x}} = \begin{cases} \eta_{\boldsymbol{x}} & \text{if } \boldsymbol{r}' \neq \boldsymbol{x}, \boldsymbol{x} - \boldsymbol{e}_\mu \ , \\ \eta_{\boldsymbol{x}-\boldsymbol{e}_\mu} & \text{if } \boldsymbol{r}' = \boldsymbol{x} - \boldsymbol{e}_\mu \ , \\ \eta_{\boldsymbol{x}+\boldsymbol{e}_\mu} & \text{if } \boldsymbol{r}' = \boldsymbol{x} \ . \end{cases} \tag{J.27}$$

We then consider separately the two cases:

- if $\boldsymbol{r} = \boldsymbol{e}_\nu$ ($\nu \in \{\pm 1, \ldots, \pm d\}$), using (J.26) and (J.27), we obtain

$$\sum_{\boldsymbol{r}' \neq \boldsymbol{X} - \boldsymbol{e}_\mu, \boldsymbol{X}} \left[\left(\eta^{\boldsymbol{r}',\mu} \right)_{\boldsymbol{X}+\boldsymbol{r}} - \eta_{\boldsymbol{X}+\boldsymbol{r}} \right] = \nabla_\mu \eta_{\boldsymbol{X}+\boldsymbol{r}} + \nabla_{-\mu} \eta_{\boldsymbol{X}+\boldsymbol{r}} \tag{J.28}$$

  where the operator ∇_μ was defined in the main text (8.7). We finally obtain

$$\begin{aligned} C_1 &= \sum_{\boldsymbol{X}, \eta} (X - \langle X_t \rangle) \sum_{\mu=1}^{d} \left(\nabla_\mu \eta_{\boldsymbol{X}+\boldsymbol{r}} + \nabla_{-\mu} \eta_{\boldsymbol{X}+\boldsymbol{r}} \right) P(\boldsymbol{X}, \eta; t) && \text{(J.29)} \\ &= \sum_{\mu} \langle (X - \langle X_t \rangle) \nabla_\mu \eta_{\boldsymbol{X}+\boldsymbol{r}} \rangle && \text{(J.30)} \\ &= \sum_{\mu} \nabla_\mu \widetilde{g}_{\boldsymbol{r}}, && \text{(J.31)} \end{aligned}$$

  where the sum over μ runs over $\{\pm 1, \ldots, \pm d\}$.

- if $\boldsymbol{r} = \boldsymbol{e}_\nu$, using again (J.26) and (J.27), we obtain

$$\sum_{\mu=1}^{d} \sum_{\boldsymbol{r}' \neq \boldsymbol{X} - \boldsymbol{e}_\mu, \boldsymbol{X}} \left[\left(\eta^{\boldsymbol{r}',\mu} \right)_{\boldsymbol{X}+\boldsymbol{e}_\nu} - \eta_{\boldsymbol{X}+\boldsymbol{e}_\nu} \right] = \sum_{\mu} \nabla_\mu \eta_{\boldsymbol{X}+\boldsymbol{e}_\nu} - \nabla_{-\nu} \eta_{\boldsymbol{X}+\boldsymbol{e}_\nu}. \tag{J.32}$$

  Then, C_1 becomes

$$\begin{aligned} C_1 &= \left\langle (X_t - \langle X_t \rangle) \left(\sum_{\mu} \nabla_\mu - \nabla_{-\nu} \right) \eta_{\boldsymbol{X}+\boldsymbol{e}_\nu} \right\rangle && \text{(J.33)} \\ &= \sum_{\mu} \nabla_\mu \widetilde{g}_{\boldsymbol{e}_\nu} - \nabla_{-\nu} \widetilde{g}_{\boldsymbol{e}_\nu} && \text{(J.34)} \end{aligned}$$

Finally, for any value of $\boldsymbol{r}$, (J.31) and (J.34) are recast under the equation

$$C_1 = \left(\sum_{\mu} \nabla_{\mu} - \delta_{\boldsymbol{r},\boldsymbol{e}_{\mu}} \nabla_{-\mu} \right) \widetilde{g}_{\boldsymbol{r}}. \tag{J.35}$$

- we then study the second term of the right-hand-side of the master equation (8.2), which yields the contribution

$$\begin{aligned} C_2 &= \frac{2d\tau^*}{\tau} \sum_{\boldsymbol{X},\eta} \sum_{\mu} p_{\mu} (X - \langle X_t \rangle) \eta_{\boldsymbol{X}+\boldsymbol{r}} \left[(1-\eta_{\boldsymbol{X}}) \, P(\boldsymbol{X} - \boldsymbol{e}_{\mu}, \eta; t) - \left(1 - \eta_{\boldsymbol{X}+\boldsymbol{e}_{\mu}}\right) P(\boldsymbol{X}, \eta; t) \right] && \text{(J.36)} \\ &= \frac{2d\tau^*}{\tau} \left\{ \sum_{\boldsymbol{X},\eta} \sum_{\mu} p_{\mu} (X - \langle X_t \rangle) \eta_{\boldsymbol{X}+\boldsymbol{r}} \, (1-\eta_{\boldsymbol{X}}) \, P(\boldsymbol{X} - \boldsymbol{e}_{\mu}, \eta; t) \right. \\ &\quad \left. - \sum_{\boldsymbol{X},\eta} \sum_{\mu} p_{\mu} (X - \langle X_t \rangle) \eta_{\boldsymbol{X}+\boldsymbol{r}} \left(1 - \eta_{\boldsymbol{X}+\boldsymbol{e}_{\mu}}\right) P(\boldsymbol{X}, \eta; t) \right\} && \text{(J.37)} \end{aligned}$$

With the change of variable $\boldsymbol{X} \leftarrow \boldsymbol{X} + \boldsymbol{e}_{\mu}$ in the first sum, and recalling that $X = \boldsymbol{X} + \boldsymbol{e}_1$, we obtain

$$\begin{aligned} C_2 &= \frac{2d\tau^*}{\tau} \left\{ \sum_{\boldsymbol{X},\eta} \sum_{\mu} p_{\mu} [X + \sigma(\boldsymbol{e}_{\mu} \cdot \boldsymbol{e}_1) - \langle X_t \rangle] \eta_{\boldsymbol{X}+\boldsymbol{r}+\boldsymbol{e}_{\mu}} \left(1 - \eta_{\boldsymbol{X}+\boldsymbol{e}_{\mu}}\right) P(\boldsymbol{X}, \eta; t) \right. \\ &\quad \left. - \sum_{\boldsymbol{X},\eta} \sum_{\mu} p_{\mu} (X - \langle X_t \rangle) \eta_{\boldsymbol{X}+\boldsymbol{r}} \left(1 - \eta_{\boldsymbol{X}+\boldsymbol{e}_{\mu}}\right) P(\boldsymbol{X}, \eta; t) \right\} && \text{(J.38)} \\ &= \frac{2d\tau^*}{\tau} \left\{ \sum_{\boldsymbol{X},\eta} \sum_{\mu} p_{\mu} (X - \langle X_t \rangle) \nabla \eta_{\boldsymbol{X}+\boldsymbol{r}} \left(1 - \eta_{\boldsymbol{X}+\boldsymbol{e}_{\mu}}\right) P(\boldsymbol{X}, \eta; t) \right. \\ &\quad \left. + \sigma \sum_{\boldsymbol{X},\eta} \sum_{\mu} p_{\mu} (\boldsymbol{e}_{\mu} \cdot \boldsymbol{e}_1) \eta_{\boldsymbol{X}+\boldsymbol{r}+\boldsymbol{e}_{\mu}} \left(1 - \eta_{\boldsymbol{X}+\boldsymbol{e}_{\mu}}\right) P(\boldsymbol{X}, \eta; t) \right\} && \text{(J.39)} \end{aligned}$$

As $\boldsymbol{e}_{\mu} \cdot \boldsymbol{e}_1$ is equal to ± 1 for $\mu = \pm 1$ and 0 otherwise, we finally obtain

$$\begin{aligned} C_2 &= \frac{2d\tau^*}{\tau} \sum_{\mu} p_{\mu} \left\langle (X_t - \langle X_t \rangle)(1 - \eta_{\boldsymbol{X}-t+\boldsymbol{e}_{\mu}}) \nabla_{\boldsymbol{X}_t+\boldsymbol{r}} \right\rangle \\ &\quad + \frac{2d\tau^*}{\tau} \sigma \left[p_1 \left\langle (1 - \eta_{\boldsymbol{X}_t+\boldsymbol{e}_1}) \eta_{\boldsymbol{X}_t+\boldsymbol{r}+\boldsymbol{e}_1} \right\rangle - p_{-1} \left\langle (1 - \eta_{\boldsymbol{X}_t+\boldsymbol{e}_{-1}}) \eta_{\boldsymbol{X}_t+\boldsymbol{r}+\boldsymbol{e}_{-1}} \right\rangle \right] && \text{(J.40)} \end{aligned}$$

- the third term yields the contribution C_3:

$$\begin{aligned} C_3 &= 2dg \sum_{\boldsymbol{X},\eta} (X - \langle X_t \rangle) \eta_{\boldsymbol{X}_t+\boldsymbol{r}} \sum_{\boldsymbol{r}' \neq \boldsymbol{X}} \left[(1 - \eta_{\boldsymbol{r}'}) \, P(\boldsymbol{X}, \hat{\eta}^{\boldsymbol{r}'}; t) - \eta_{\boldsymbol{r}'} P(\boldsymbol{X}, \eta; t) \right] && \text{(J.41)} \\ &= 2dg \sum_{\boldsymbol{X}} \sum_{\boldsymbol{r}' \neq \boldsymbol{X}} (X - \langle X_t \rangle) \sum_{\eta} \eta_{\boldsymbol{r}'} \left[\left(\hat{\eta}^{\boldsymbol{r}'} \right)_{\boldsymbol{X}+\boldsymbol{r}} - \eta_{\boldsymbol{X}+\boldsymbol{r}} \right] P(\boldsymbol{X}, \eta; t), && \text{(J.42)} \\ & && \text{(J.43)} \end{aligned}$$

where we used again (J.24). By the definition of $\hat{\eta}^{\boldsymbol{r}'}$ (configuration obtained from η with the change $\eta_{\boldsymbol{r}'} \leftarrow 1 - \eta_{\boldsymbol{r}'}$), we write

$$\left(\hat{\eta}^{\boldsymbol{r}'} \right)_{\boldsymbol{x}} \begin{cases} \eta_{\boldsymbol{x}} & \text{if } \boldsymbol{x} \neq \boldsymbol{r}', \\ 1 - \eta_{\boldsymbol{x}} & \text{if } \boldsymbol{x} \neq \boldsymbol{r}'. \end{cases} \tag{J.44}$$

The expression of C_3 becomes

$$C_3 = 2dg \sum_{\boldsymbol{X}} (X - \langle X_t \rangle) \sum_{\eta} \eta_{\boldsymbol{X}+\boldsymbol{r}} (1 - 2\eta_{\boldsymbol{X}+\boldsymbol{r}}) P(\boldsymbol{X}, \eta; t). \tag{J.45}$$

As $\eta_{\boldsymbol{X}+\boldsymbol{r}} \in \{0, 1\}$, then $(\eta_{\boldsymbol{X}+\boldsymbol{r}})^2 = \eta_{\boldsymbol{X}+\boldsymbol{r}}$, and we finally obtain

$$C_3 = -2dg \widetilde{g}_{\boldsymbol{r}} \tag{J.46}$$

- the computation of the contribution C_4 of the fourth term of the master equation is similar to that of C_3, and we obtain

$$C_4 = 2df \sum_{\boldsymbol{X}} (X - \langle X_t \rangle) \sum_{\eta} (1 - \eta_{\boldsymbol{X}+\boldsymbol{r}})(1 - 2\eta_{\boldsymbol{X}+\boldsymbol{r}}) P(\boldsymbol{X}, \eta; t). \tag{J.47}$$

  Using again $(\eta_{\boldsymbol{X}+\boldsymbol{r}})^2 = \eta_{\boldsymbol{X}+\boldsymbol{r}}$, we obtain

$$(1 - \eta_{\boldsymbol{X}+\boldsymbol{r}})(1 - 2\eta_{\boldsymbol{X}+\boldsymbol{r}}) = 1 - \eta_{\boldsymbol{X}+\boldsymbol{r}}, \tag{J.48}$$

  and, finally,

$$C_4 = -2df \widetilde{g}_{\boldsymbol{r}}. \tag{J.49}$$

Finally, writing from the master equation (8.2) the relation

$$C_{\mathrm{L}} = C_1 + C_2 + C_3 + C_4, \tag{J.50}$$

and using (J.35), (J.40), (J.46) and (J.49), we get

$$\begin{aligned} 2d\tau^* \partial_t \widetilde{g}_{\boldsymbol{r}} = & \sum_{\mu} \left(\nabla_\mu - \delta_{\boldsymbol{r}, \boldsymbol{e}_\mu} \nabla_{-\mu} \right) \widetilde{g}_{\boldsymbol{r}} - 2d(f+g) \widetilde{g}_{\boldsymbol{r}} \\ & + \frac{2d\tau^*}{\tau} \sum_{\mu} p_\mu \left\langle \delta X_t (1 - \eta_{\boldsymbol{X}_t + \boldsymbol{e}_\mu}) \nabla_\mu \eta_{\boldsymbol{X}_t + \boldsymbol{r}} \right\rangle \\ & + \frac{2d\tau^*}{\tau} \sigma \left[p_1 \left\langle (1 - \eta_{\boldsymbol{X}_t + \boldsymbol{e}_1}) \eta_{\boldsymbol{X}_t + \boldsymbol{r} + \boldsymbol{e}_1} \right\rangle - p_{-1} \left\langle (1 - \eta_{\boldsymbol{X}_t + \boldsymbol{e}_{-1}}) \eta_{\boldsymbol{X}_t + \boldsymbol{r} + \boldsymbol{e}_{-1}} \right\rangle \right] \\ & - \frac{2d\tau^*}{\tau} \sigma \left[p_1 (1 - k_{\boldsymbol{e}_1}) - p_{-1} (1 - k_{\boldsymbol{e}_{-1}}) \right] k_{\boldsymbol{r}}. \end{aligned} \tag{J.51}$$

which is equivalent to the relation (8.20) presented in the main text.

APPENDIX K

1D lattice in contact with a reservoir: additional equations

Contents

K.1 Explicit expressions of $\widetilde{g}_1$ and $\widetilde{g}_{-1}$ in one dimension

It is finally found that:

$$\widetilde{g}_1 = \frac{CE - BF}{AE - BD} \text{ and } \widetilde{g}_{-1} = \frac{AF - CD}{AE - BD}, \tag{K.1}$$

where

$$A \equiv \frac{2\tau^*}{\tau}\sigma p_1 K_+(r_1 - 1)\frac{A_1 r_1^2}{A_1 r_1 - A_{-1} r_1^{-1}} + A_1 r_1 - \left(A_{-1} + 2(f+g) + \frac{2\tau^*}{\tau}p_1(\rho + K_+ r_1^2)\right), \tag{K.2}$$

$$B \equiv \frac{2\tau^*}{\tau}\sigma p_{-1} K_+(r_1^{-1} - 1)\frac{A_1 r_1^2}{A_1 r_1 - A_{-1} r_1^{-1}} + \frac{2\tau^*}{\tau}p_{-1}(\rho + K_+ r_1), \tag{K.3}$$

$$\begin{aligned} C \equiv{}& \frac{2\tau^*}{\tau}\sigma(p_1(1-\rho-K_+r_1) - p_{-1}(1-\rho-K_-r_2^{-1}))(\rho + K_+ r_1) - \frac{2\tau^*}{\tau}\sigma p_1(1-\rho-K_+r_1)(\rho + K_+ r_1^2) \\ &+ \frac{2\tau^*}{\tau}\sigma\left(p_1(1-\rho-K_+r_1)K_+ r_1 - p_{-1}\left(1-\rho-\frac{K_-}{r_2}\right)\frac{K_+}{r_1}\right)\frac{A_1 r_1^2}{A_1 r_1 - A_{-1} r_1^{-1}}, \end{aligned} \tag{K.4}$$

$$D \equiv -\frac{2\tau^*}{\tau}\sigma p_1 K_-(r_2 - 1)\frac{A_{-1} r_2^{-2}}{A_1 r_2 - A_{-1} r_2^{-1}} + \frac{2\tau^*}{\tau}p_1(\rho + K_- r_2^{-1}), \tag{K.5}$$

$$E \equiv -\frac{2\tau^*}{\tau}\sigma p_{-1} K_-(r_2^{-1} - 1)\frac{A_{-1} r_2^{-2}}{A_1 r_2 - A_{-1} r_2^{-1}} + A_{-1} r_2^{-1} - \left(A_1 + 2(f+g) + \frac{2\tau^*}{\tau}p_{-1}(\rho + K_- r_2^{-2})\right) \tag{K.6}$$

and

$$\begin{aligned} F \equiv{}& \frac{2\tau^*}{\tau}\sigma(p_1(1-\rho-K_+r_1) - p_{-1}(1-\rho-K_-r_2^{-1}))(\rho + K_- r_2^{-1}) + \frac{2\tau^*}{\tau}\sigma p_{-1}(1-\rho-K_-r_2^{-1})(\rho + K_- r_2^{-2}) \\ &- \frac{2\tau^*}{\tau}\sigma\left(p_1(1-\rho-K_+r_1)K_- r_2 - p_{-1}\left(1-\rho-\frac{K_-}{r_2}\right)\frac{K_-}{r_2}\right)\frac{A_{-1} r_2^{-2}}{A_1 r_2 - A_{-1} r_2^{-1}}, \end{aligned} \tag{K.7}$$

K_+, K_-, A_1 and A_{-1} have been determined in Section 9.2.1. Using their expressions, we compute $\widetilde{g}_1$ and $\widetilde{g}_{-1}$, and finally compute K with the formula:

$$K = \frac{\sigma^2}{2\tau}\left(p_1(1-\rho-K_+r_1) + p_{-1}\left(1-\rho-K_-r_2^{-1}\right)\right) - \frac{\sigma}{\tau}\left(p_1\widetilde{g}_1 - p_{-1}\widetilde{g}_{-1}\right). \tag{K.8}$$

K.2 Detailed expressions of (9.70) to (9.73)

$$B_1 = A_1 + \frac{2\tau^*}{\tau} p_1 (\mathrm{e}^{iu\sigma} - 1)(1 - k_1) \tag{K.9}$$

$$B_2 = A_1 + A_{-1} + 2(f+g) + \frac{2\tau^*}{\tau} p_1 (\mathrm{e}^{iu\sigma} - 1)(1 - \widetilde{w}_1) + \frac{2\tau^*}{\tau} p_{-1} (\mathrm{e}^{-iu\sigma} - 1)(1 - \widetilde{w}_{-1}) \tag{K.10}$$

$$B_3 = A_{-1} + \frac{2\tau^*}{\tau} p_{-1} (\mathrm{e}^{-iu\sigma} - 1)(1 - k_{-1}) \tag{K.11}$$

$$B_4 = \frac{2\tau^*}{\tau} \Big[p_1 (k_1 - \widetilde{w}_1)(r_1 \mathrm{e}^{iu\sigma} - 1) + p_{-1} (k_{-1} - \widetilde{w}_{-1})(r_1^{-1} \mathrm{e}^{-iu\sigma} - 1) \Big] \tag{K.12}$$

$$B_5 = 2f + \frac{2\tau^*}{\tau} \rho \Big[p_1 (k_1 - \widetilde{w}_1)(\mathrm{e}^{iu\sigma} - 1) + p_{-1} (k_{-1} - \widetilde{w}_{-1})(\mathrm{e}^{-iu\sigma} - 1) \Big] \tag{K.13}$$

$$C_4 = \frac{2\tau^*}{\tau} \Big[p_1 (k_1 - \widetilde{w}_1)(r_2 \mathrm{e}^{iu\sigma} - 1) + p_{-1} (k_{-1} - \widetilde{w}_{-1})(r_2^{-1} \mathrm{e}^{-iu\sigma} - 1) \Big] \tag{K.14}$$

$$D_1 = A_1 + \frac{2\tau^*}{\tau} p_1 (\mathrm{e}^{iu\sigma} - 1)(1 - k_1) \tag{K.15}$$

$$D_2 = A_{-1} + 2(f+g) + \frac{2\tau^*}{\tau} p_1 \mathrm{e}^{iu\sigma} k_2 + \frac{2\tau^*}{\tau} \Big[p_1 (\mathrm{e}^{iu\sigma} - 1) + p_{-1} (\mathrm{e}^{-iu\sigma} - 1) \Big] \tag{K.16}$$

$$D_3 = \frac{2\tau^*}{\tau} p_{-1} k_1 \tag{K.17}$$

$$D_4 = 2f + \frac{2\tau^*}{\tau} \Big[p_1 \mathrm{e}^{iu\sigma} k_1 k_2 - p_{-1} k_1 k_{-1} \Big] \tag{K.18}$$

$$D_5 = \frac{2\tau^*}{\tau} p_1 (\mathrm{e}^{iu\sigma} - 1) \tag{K.19}$$

$$D_6 = \frac{2\tau^*}{\tau} p_{-1} (\mathrm{e}^{-iu\sigma} - 1) \tag{K.20}$$

$$E_1 = \frac{2\tau^*}{\tau} p_1 k_{-1} \tag{K.21}$$

$$E_2 = A_1 + 2(f+g) + \frac{2\tau^*}{\tau} p_{-1} \mathrm{e}^{-iu\sigma} k_{-2} + \frac{2\tau^*}{\tau} \Big[p_1 (\mathrm{e}^{iu\sigma} - 1) + p_{-1} (\mathrm{e}^{-iu\sigma} - 1) \Big] \tag{K.22}$$

$$E_3 = A_{-1} + \frac{2\tau^*}{\tau} p_{-1} (\mathrm{e}^{-iu\sigma} - 1)(1 - k_{-1}) \tag{K.23}$$

$$E_4 = 2f + \frac{2\tau^*}{\tau} \Big[p_{-1} \mathrm{e}^{-iu\sigma} k_{-1} k_{-2} - p_1 k_1 k_{-1} \Big] \tag{K.24}$$

K.3 Detailed expression of (9.38)

$$M_{13} = \frac{2\tau^*}{\tau} \frac{r_1}{A_1 r_1 - A_{-1} r_1^{-1}} [p_1 K_+ (r_1 - 1) - 1] \tag{K.25}$$

$$M_{14} = \frac{2\tau^*}{\tau} \frac{r_1}{A_1 r_1 - A_{-1} r_1^{-1}} p_1 K_+ (r_1^{-1} - 1) \tag{K.26}$$

$$M_{23} = -\frac{2\tau^*}{\tau} \frac{1}{r_2} \frac{1}{A_1 r_2 - A_{-1} r_2^{-1}} p_1 K_- (r_2 - 1) \tag{K.27}$$

$$M_{24} = -\frac{2\tau^*}{\tau} \frac{1}{r_2} \frac{1}{A_1 r_2 - A_{-1} r_2^{-1}} [p_{-1} K_- (r_2^{-1} - 1) + 1] \tag{K.28}$$

$$M_{33} = -\left(A_{-1} + 2(f+g) + \frac{2\tau^*}{\tau} p_1 k_2 \right) + \frac{2\tau^*}{\tau} \frac{2A_1}{A_1 r_1 - A_{-1} r_1^{-1}} p_1 K_+ (r_1 - 1) \tag{K.29}$$

$$M_{34} = \frac{2\tau^*}{\tau} p_{-1} k_1 + \frac{2\tau^*}{\tau} \frac{2A_1}{A_1 r_1 - A_{-1} r_1^{-1}} p_{-1} K_+ (r_1^{-1} - 1) \tag{K.30}$$

$$M_{43} = \frac{2\tau^*}{\tau} p_{-1} k_1 - \frac{2\tau^*}{\tau} \frac{2A_{-1}}{A_1 r_2 - A_{-1} r_2^{-1}} p_1 K_- (r_2 - 1) \tag{K.31}$$

$$M_{44} = -\left(A_1 + 2(f+g) + \frac{2\tau^*}{\tau} p_{-1} k_{-2}\right) - \frac{2\tau^*}{\tau} \frac{2A_{-1}}{A_1 r_2 - A_{-1} r_2^{-1}} p_{-1} K_-(r_2^{-1} - 1) \tag{K.32}$$

$$Y_1 = \frac{2a_+ A_{-1} - \psi_+ r_1}{A_1 r_1 - A_{-1} r_1^{-1}} \tag{K.33}$$

$$Y_2 = -\frac{2a_- A_1 - \psi_- r_2^{-1}}{A_1 r_2 - A_{-1} r_2^{-1}} \tag{K.34}$$

$$Y_3 = -\varphi_1 - 2A_1 \frac{a_+(A_1 r_1 - 3A_{-1} r_1^{-1}) + \psi_-}{A_1 r_1 - A_{-1} r_1^{-1}} \tag{K.35}$$

$$Y_4 = -\varphi_{-1} - 2A_{-1} \frac{a_-(3A_1 r_2 - A_{-1} r_2^{-1}) + \psi_-}{A_1 r_2 - A_{-1} r_2^{-1}} \tag{K.36}$$

APPENDIX L

Simplified expressions of the quantities $\nabla_\nu \mathcal{F}_{\boldsymbol{r}}$

$$\nabla_{-1}\mathcal{F}_{\boldsymbol{e}_1} = \mathcal{F}_{\boldsymbol{0}} - \mathcal{F}_{\boldsymbol{e}_1} = \lim_{\xi\to 1}\left[\widehat{P}(\boldsymbol{0}|\boldsymbol{0};\xi) - \widehat{P}(\boldsymbol{e}_1|\boldsymbol{0};\xi)\right] \tag{L.1}$$

$$\nabla_{1}\mathcal{F}_{\boldsymbol{e}_1} = \mathcal{F}_{2\boldsymbol{e}_1} - \mathcal{F}_{\boldsymbol{e}_1} = \lim_{\xi\to 1}\left[\widehat{P}(2\boldsymbol{e}_1|\boldsymbol{0};\xi) - \widehat{P}(\boldsymbol{e}_1|\boldsymbol{0};\xi)\right] \tag{L.2}$$

$$\nabla_{2}\mathcal{F}_{\boldsymbol{e}_1} = \mathcal{F}_{\boldsymbol{e}_1+\boldsymbol{e}_2} - \mathcal{F}_{\boldsymbol{e}_1} = \lim_{\xi\to 1}\left[\widehat{P}(\boldsymbol{e}_1+\boldsymbol{e}_2|\boldsymbol{0};\xi) - \widehat{P}(\boldsymbol{e}_1|\boldsymbol{0};\xi)\right] \tag{L.3}$$

$$\nabla_{-1}\mathcal{F}_{\boldsymbol{e}_{-1}} = \mathcal{F}_{2\boldsymbol{e}_{-1}} - \mathcal{F}_{\boldsymbol{e}_{-1}} = \lim_{\xi\to 1}\left[\widehat{P}(2\boldsymbol{e}_1|\boldsymbol{0};\xi) - \widehat{P}(\boldsymbol{e}_1|\boldsymbol{0};\xi)\right] \tag{L.4}$$

$$\nabla_{1}\mathcal{F}_{\boldsymbol{e}_{-1}} = \mathcal{F}_{\boldsymbol{0}} - \mathcal{F}_{\boldsymbol{e}_{-1}} = \lim_{\xi\to 1}\left[\widehat{P}(\boldsymbol{0}|\boldsymbol{0};\xi) - \widehat{P}(\boldsymbol{e}_1|\boldsymbol{0};\xi)\right] \tag{L.5}$$

$$\nabla_{2}\mathcal{F}_{\boldsymbol{e}_{-1}} = \mathcal{F}_{\boldsymbol{e}_{-1}+\boldsymbol{e}_2} - \mathcal{F}_{\boldsymbol{e}_{-1}} = \lim_{\xi\to 1}\left[\widehat{P}(\boldsymbol{e}_1+\boldsymbol{e}_2|\boldsymbol{0};\xi) - \widehat{P}(\boldsymbol{e}_1|\boldsymbol{0};\xi)\right] \tag{L.6}$$

$$\nabla_{-1}\mathcal{F}_{\boldsymbol{e}_2} = \mathcal{F}_{\boldsymbol{e}_{-1}+\boldsymbol{e}_2} - \mathcal{F}_{\boldsymbol{e}_2} = \lim_{\xi\to 1}\left[\widehat{P}(\boldsymbol{e}_1+\boldsymbol{e}_2|\boldsymbol{0};\xi) - \widehat{P}(\boldsymbol{e}_2|\boldsymbol{0};\xi)\right] \tag{L.7}$$

$$\nabla_{1}\mathcal{F}_{\boldsymbol{e}_2} = \mathcal{F}_{\boldsymbol{e}_1+\boldsymbol{e}_2} - \mathcal{F}_{\boldsymbol{e}_2} = \lim_{\xi\to 1}\left[\widehat{P}(\boldsymbol{e}_1+\boldsymbol{e}_2|\boldsymbol{0};\xi) - \widehat{P}(\boldsymbol{e}_2|\boldsymbol{0};\xi)\right] \tag{L.8}$$

$$\nabla_{2}\mathcal{F}_{\boldsymbol{e}_2} = \mathcal{F}_{2\boldsymbol{e}_2} - \mathcal{F}_{\boldsymbol{e}_2} = \lim_{\xi\to 1}\left[\widehat{P}(2\boldsymbol{e}_2|\boldsymbol{0};\xi) - \widehat{P}(\boldsymbol{e}_2|\boldsymbol{0};\xi)\right] \tag{L.9}$$

$$\nabla_{-2}\mathcal{F}_{\boldsymbol{e}_2} = \mathcal{F}_{\boldsymbol{0}} - \mathcal{F}_{\boldsymbol{e}_2} = \lim_{\xi\to 1}\left[\widehat{P}(\boldsymbol{0}|\boldsymbol{0};\xi) - \widehat{P}(\boldsymbol{e}_2|\boldsymbol{0};\xi)\right] \tag{L.10}$$

$$\nabla_{3}\mathcal{F}_{\boldsymbol{e}_2} = \mathcal{F}_{\boldsymbol{e}_2+\boldsymbol{e}_3} - \mathcal{F}_{\boldsymbol{e}_2} = \lim_{\xi\to 1}\left[\widehat{P}(\boldsymbol{e}_2+\boldsymbol{e}_3|\boldsymbol{0};\xi) - \widehat{P}(\boldsymbol{e}_2|\boldsymbol{0};\xi)\right] \tag{L.11}$$

APPENDIX M

High-density expansion of the functions $\mathcal{F}_{\boldsymbol{r}}$

In this Appendix, we study the quantities

$$\mathcal{F}_{\boldsymbol{r}} = \frac{1}{L^{d-1}} \sum_{k_2,\dots,k_d=0}^{L-1} \frac{1}{2\pi} \int_{-\pi}^{\pi} dq \frac{e^{-ir_1 q} \prod_{j=2}^{d} e^{-2i\pi r_j k_j/L}}{1-\lambda(q,k_2,\dots,k_d)} \tag{M.1}$$

where

$$\lambda(q,k_2,\dots,k_d) = \frac{A_1}{\alpha}\mathrm{e}^{-iq} + \frac{A_{-1}}{\alpha}\mathrm{e}^{iq} + \frac{2A_2}{\alpha}\sum_{j=2}^{d}\cos\left(\frac{2\pi k_j}{L}\right), \tag{M.2}$$

and

$$A_\mu \equiv 1 + \frac{2d\tau^*}{\tau} p_\mu(\rho_0 - h_\mu) \tag{M.3}$$

$$\mathcal{A} = A_1 + A_{-1} + 2(d-1)A_2 \tag{M.4}$$

For clarity, we specify here that the quantities $\mathcal{F}_{\boldsymbol{r}}$ actually depends on ρ_0. Defining $\widetilde{p}_{-1} \equiv A_1/\mathcal{A}$, $\widetilde{p}_1 \equiv A_{-1}/\mathcal{A}$ and $\widetilde{p}_2 \equiv A_2/\mathcal{A}$, the functions $\mathcal{F}_{\boldsymbol{r}}$ write

$$\mathcal{F}_{\boldsymbol{r}}(\rho_0) = \frac{1}{L^{d-1}} \sum_{k_2,\dots,k_d=0}^{L-1} \frac{1}{2\pi} \int_{-\pi}^{\pi} dq \frac{e^{-in_1 q} \prod_{j=2}^{d} e^{-2i\pi n_j k_j/L}}{1-\left(\widetilde{p}_1 \mathrm{e}^{iq} + \widetilde{p}_{-1}\mathrm{e}^{-iq} + 2\widetilde{p}_2 \sum_{j=2}^{d}\cos\frac{2\pi k_j}{L}\right)} \tag{M.5}$$

As it was emphasized in Section 10.2.5, they in fact correspond to the long-time limit of the generating function of the propagators of a biased random walk starting from $\mathbf{0}$ and arriving at site $\boldsymbol{r}$, which jumps in direction 1 with probability $\widetilde{p}_1$, in direction -1 with probability $\widetilde{p}_{-1}$ and in any other direction with probability $\widetilde{p}_2$. We introduce the functions $\mathcal{F}'_{\boldsymbol{r}}(\rho_0,\xi)$, defined by

$$\mathcal{F}'_{\boldsymbol{r}}(\rho_0,\xi) = \frac{1}{L^{d-1}} \sum_{k_2,\dots,k_d=0}^{L-1} \frac{1}{2\pi} \int_{-\pi}^{\pi} dq \frac{e^{-in_1 q} \prod_{j=2}^{d} e^{-2i\pi n_j k_j/L}}{1-\xi\left(\widetilde{p}_1 \mathrm{e}^{\mathrm{i}q} + \widetilde{p}_{-1}\mathrm{e}^{-\mathrm{i}q} + 2\widetilde{p}_2 \sum_{j=2}^{d}\cos\frac{2\pi k_j}{L}\right)} \tag{M.6}$$

so that $\mathcal{F}_{\boldsymbol{r}} = \mathcal{F}'_{\boldsymbol{r}}(1)$. Note that this quantity diverges when $\xi \to 1$ and $\widetilde{p}_\mu \to 1/(2d)$ for all μ (the denominator of the integrand then cancels for $(q,k_2,\dots,k_d) = (0,0,\dots,0)$).

The integral over q may be computed with the change of variable $u = \mathrm{e}^{-\mathrm{i}q}$ and using the residue theorem. Extending the methods used in Appendices A and B for the computations of the biased propagators on the stripe and capillary geometry, we find the following expression of $\mathcal{F}'_{\boldsymbol{r}}(\rho_0,\xi)$:

$$\mathcal{F}'_{\boldsymbol{r}}(\rho_0,\xi) = \frac{1}{L^{d-1}} \sum_{k_2,\dots,k_d=0}^{L-1} f(r_1,k_2,\dots,k_d;\rho_0,\xi) \prod_{j=2}^{d} \mathrm{e}^{-\frac{2\mathrm{i}\pi k_j r_j}{L}}. \tag{M.7}$$

with

$$f(r_1,k_2,\dots,k_d;\rho_0,\xi) = \begin{cases} \frac{1}{\widetilde{p}_{-1}} \frac{{U_2}^{r_1}}{U_1-U_2} & \text{if } r_1 \geq 0 \\ \frac{1}{\widetilde{p}_{-1}} \frac{1}{{U_1}^{|r_1|}[U_1-U_2]} & \text{if } r_1 < 0. \end{cases} \tag{M.8}$$

and

$$U_{\frac{1}{2}} = \frac{1}{2\xi\widetilde{p}_{-1}}\left(1 - 2\xi\widetilde{p}_2\sum_{j=2}^{d}\cos\frac{2\pi k_j}{L}\right) \pm \frac{1}{2}\sqrt{\frac{1}{(\xi\widetilde{p}_{-1})^2}\left(1-2\widetilde{p}_2\xi\sum_{j=2}^{d}\cos\frac{2\pi k_j}{L}\right)^2 - 4\frac{\widetilde{p}_1}{\widetilde{p}_{-1}}} \tag{M.9}$$

We recall that the quantities $A_\nu/\mathcal{A}$ write

$$\frac{A_\nu}{\mathcal{A}} = \frac{1+\frac{2d\tau^*}{\tau}p_\nu(\rho_0-h_\nu)}{2d+\frac{2d\tau^*}{\tau}\sum_\mu p_\mu(\rho_0-h_\mu)} \tag{M.10}$$

so that the quantities $\widetilde{p}_\mu$ all tend to $1/(2d)$ when $\rho_0 \to 0$. In order to compute the expansions of $\mathcal{F}_{\boldsymbol{r}}(\rho_0)$, we are then interested in the behavior of $\mathcal{F}'_{\boldsymbol{r}}(\rho_0,\xi)$ when ξ goes to 1 and $\widetilde{p}_\mu \to 1/(2d)$ (or $\rho_0 \to 0$) for all μ. These two limits do not commute, and in the case where the limit $\widetilde{p}_\mu \to 1/(2d)$ (or $\rho_0 \to 0$) is taken first the quantities $\mathcal{F}'_{\boldsymbol{r}}(\rho_0,\xi)$ are actually equal to the propagators $\widehat{P}(\boldsymbol{r}|\boldsymbol{0};\xi)$ computed for the stripe and capillary like geometries.

The divergence of $\mathcal{F}'_{\boldsymbol{r}}(\rho_0,\xi)$ is due to the cancellation of the quantities U_1-U_2, which occurs at the point $(k_2,\dots,k_d)=(0,\dots,0)$ in the limits $\xi\to 1$ and $\rho_0\to 0$. We then write

$$\mathcal{F}_{\boldsymbol{r}}(\rho_0) = \frac{1}{L^{d-1}} f(r_1,0,\dots,0;\rho_0,\xi) + \phi(\boldsymbol{r}) \tag{M.11}$$

where the function ϕ is defined as

$$\phi(\boldsymbol{r};\rho_0,\xi) \equiv \frac{1}{L^{d-1}} {\sum_{k_2,\dots,k_d}}' f(r_1,k_2,\dots,k_d;\rho_0,\xi) \prod_{j=2}^{d} \mathrm{e}^{-\frac{2\mathrm{i}\pi k_j r_j}{L}} \tag{M.12}$$

where the prime denotes a sum for $k_2,\dots,k_d$ going from 0 to $L-1$ with the point $(k_2,\dots,k_d)=(0,\dots,0)$ excluded. The function ϕ has the property

$$\lim_{\xi\to 1}\left[\lim_{\rho_0\to 0}\phi(\boldsymbol{r};\rho_0,\xi)\right] = \lim_{\rho_0\to 0}\left[\lim_{\xi\to 1}\phi(\boldsymbol{r};\rho_0,\xi)\right] \equiv \Phi(\boldsymbol{r}) \tag{M.13}$$

Using these notations, and the definition of f, we obtain the following expansions, where we carefully consider the two possible orders for the limits:

1. if we first take $\rho_0\to 0$ and ultimately $\xi\to 1$, one obtains

$$\mathcal{F}'_{\boldsymbol{r}}(\xi,\rho_0=0) = \widehat{P}(\boldsymbol{r}|\boldsymbol{0};\xi) \underset{\xi\to 1}{=} \frac{\sqrt{d/2}}{L^{d-1}\sqrt{1-\xi}} - \frac{(d+1)|r_1|}{L^{d-1}} + \Phi(\boldsymbol{r}) + \mathcal{O}(\sqrt{1-\xi}) \tag{M.14}$$

2. the case where we first take $\xi\to 1$ and ultimately $\rho_0\to 0$ must be considered with attention. Indeed, taking $\rho_0\to 0$ in fact implies that $\widetilde{p}_1$, $\widetilde{p}_{-1}$ and $\widetilde{p}_2$ tend to $1/(2d)$ simultaneously. We can eliminate $\widetilde{p}_2$ using the normalization condition $\widetilde{p}_1+\widetilde{p}_{-1}+2(d-1)\widetilde{p}_2=1$. We then define $v\equiv\widetilde{p}_{-1}-\widetilde{p}_1$ so that we replace $\widetilde{p}_1$ by $\widetilde{p}_{-1}-v$. Setting $\xi=1$, we get

$$U_{\frac{1}{2}}(k_2=0,\dots,k_d) = 1-\frac{v}{2\widetilde{p}_{-1}} \pm \frac{v}{2\widetilde{p}_{-1}} \tag{M.15}$$

and

$$f(r_1,0,\dots,0) = \begin{cases} \dfrac{1}{v}\left(1-\dfrac{v}{\widetilde{p}_{-1}}\right)^{r_1} & \text{if } r_1\geq 0\,, \\ \dfrac{1}{v} & \text{if } r_1<0\,. \end{cases} \tag{M.16}$$

When $\rho_0\to 0$, $v\to 0$ and $\widetilde{p}_{-1}\to 1/(2d)$, so that we get

$$\mathcal{F}_{\boldsymbol{r}} = \begin{cases} \dfrac{1}{L^{d-1}v} - \dfrac{2dr_1}{L^{d-1}} + \Phi(\boldsymbol{r}) + \dots & \text{if } r_1\geq 0\,, \\ \dfrac{1}{L^{d-1}v} + \Phi(\boldsymbol{r}) + \dots & \text{if } r_1<0\,. \end{cases} \tag{M.17}$$

Then, the expansions of $\widehat{\mathcal{P}}(\boldsymbol{r}|\boldsymbol{0};\xi=1,\varepsilon)$ in the $\varepsilon\to 0$ limit are known as soon as the quantities $\Phi(r_1,r_2)$, which can be easily deduced from the expansions of $\widehat{P}$ (see Appendices A and B). We introduce the quantity

$$\Delta(\boldsymbol{r}) = \lim_{\xi\to 1}\left[\widehat{P}(\boldsymbol{0}|\boldsymbol{0};\xi) - \widehat{P}(\boldsymbol{r}|\boldsymbol{0};\xi)\right]. \tag{M.18}$$

One gets

$$\Phi(\boldsymbol{r}) = \frac{2d|r_1|}{L^{d-1}} + \Phi_0 - \Delta(\boldsymbol{r}), \tag{M.19}$$

where Φ_0 is such that

$$\widehat{P}(\mathbf{0}|\mathbf{0};\xi) \underset{\xi\to 1}{=} \frac{\sqrt{d/2}}{L^{d-1}\sqrt{1-\xi}} + \Phi_0 + \mathcal{O}(\sqrt{1-\xi}) \tag{M.20}$$

Combining with Eq. M.17, we finally write:

$$\mathcal{F}_{\boldsymbol{r}} \underset{\rho_0\to 0}{=} \frac{1}{L^{d-1}v} - \frac{(d+1)r_1}{L^d} + S^{(d)}_{L,0} - \Delta(\boldsymbol{r}) \tag{M.21}$$

where v is simply related to the velocity of the TP, and goes to zero as $\rho_0 \to 0$:

$$v = \widetilde{p}_{-1} - \widetilde{p}_1 \tag{M.22}$$

$$= \frac{A_1 - A_{-1}}{\mathcal{A}} \tag{M.23}$$

$$\underset{\rho_0\to 0}{=} \frac{\tau^*}{\tau}\left[p_1(\rho_0 - h_1) - p_{-1}(\rho_0 - h_{-1})\right] \tag{M.24}$$

$$= \frac{\tau^*}{\sigma}V \tag{M.25}$$

Finally, the main interesting result is about the gradients of $\mathcal{F}_{\boldsymbol{r}}$, which are simply expressed in terms of the gradients of the known propagators $\widehat{P}$:

$$\nabla_\nu \mathcal{F}_{\boldsymbol{r}} = \lim_{\xi\to 1}\left[\widehat{P}(\boldsymbol{r} + \boldsymbol{e}_\nu|\mathbf{0};\xi) - \widehat{P}(\boldsymbol{r}|\mathbf{0};\xi)\right] + \delta_\nu, \tag{M.26}$$

with

$$\delta_\nu = \begin{cases} -\dfrac{d}{L^{d-1}} & \text{if } \nu = 1, \\ \dfrac{d}{L^{d-1}} & \text{if } \nu = -1, \\ 0 & \text{otherwise.} \end{cases} \tag{M.27}$$

Bibliography

[1] M. Abramowitz and I. Stegun. *Handbook of Mathematical Functions: with Formulas, Graphs, and Mathematical Tables*. Dover Publications, 1965. (Cited on pages 51, 125, 184 and 221.)

[2] F. Agulló-López, C. R. A. Catlow, and P. D. Townsend. *Point defects in materials*. Academic Press, academic p edition, 1988. (Cited on page 28.)

[3] S. Alexander and P. Pincus. Diffusion of labeled particles on one-dimensional chains. *Physical Review B*, 18(4):2011–2012, 1978. (Cited on pages 21 and 42.)

[4] R. Arratia. The motion of a tagged particle in the simple symmetric exclusion system on Z. *The Annals of Probability*, 11(2):362–373, 1983. (Cited on pages 5, 21 and 42.)

[5] P. Baerts, U. Basu, C. Maes, and S. Safaverdi. Frenetic origin of negative differential response. *Physical Review E*, 88:052109, 2013. (Cited on pages 187 and 189.)

[6] M. Baiesi, C. Maes, and B. Wynants. Fluctuations and response of nonequilibrium states. *Physical Review Letters*, 103:010602, 2009. (Cited on page 187.)

[7] E. Barkai and R. Silbey. Diffusion of tagged particle in an exclusion process. *Physical Review E*, 81:041129, 2010. (Cited on pages 21 and 42.)

[8] M. Barma and D. Dhar. Directed diffusion in a percolation network. *Journal of Physics C: Solid State Physics*, 16:1451–1458, 1983. (Cited on page 187.)

[9] U. Basu and C. Maes. Mobility transition in a dynamic environment. *Journal of Physics A: Mathematical and Theoretical*, 47:255003, 2014. (Cited on pages 187 and 189.)

[10] A. R. Bausch, F. Ziemann, A. A. Boulbitch, K. Jacobson, and E. Sackmann. Local measurements of viscoelastic parameters of adherent cell surfaces by magnetic bead microrheometry. *Biophysical journal*, 75:2038–2049, 1998. (Cited on pages 1 and 19.)

[11] D. Ben-avraham and S. Havlin. *Diffusion and reactions in fractals and disordered systems*. Cambridge University Press, 2005. (Cited on page 117.)

[12] G. Benenti, G. Casati, T. Prosen, and D. Rossini. Negative differential conductivity in far-from-equilibrium quantum spin chains. *Europhysics Letters*, 85:37001, 2009. (Cited on page 187.)

[13] O. Benichou, A. M. Cazabat, J. De Coninck, M. Moreau, and G. Oshanin. Stokes formula and density perturbances for driven tracer diffusion in an adsorbed monolayer. *Physical Review Letters*, 84:511, 2000. (Cited on pages 1, 12, 20, 22, 134, 138, 171, 187 and 205.)

[14] O. Bénichou, A. M. Cazabat, J. De Coninck, M. Moreau, and G. Oshanin. Force-velocity relation and density profiles for biased diffusion in an adsorbed monolayer. *Physical Review B*, 63(23):235413, May 2001. (Cited on pages 1, 12, 20, 22, 134, 138, 171, 187 and 205.)

[15] O. Bénichou, A. M. Cazabat, A. Lemarchand, M. Moreau, and G. Oshanin. Biased diffusion in a one-dimensional adsorbed monolayer. *Journal of Statistical Physics*, 97:351–371, 1999. (Cited on pages 1, 12, 14, 20, 22, 134, 138, 149, 155 and 168.)

[16] O. Bénichou, P. Illien, G. Oshanin, and R. Voituriez. Fluctuations and correlations of a driven tracer in a hard-core lattice gas. *Physical Review E*, 87:032164, 2013. (Cited on page 161.)

[17] O. Bénichou and G. Oshanin. Ultraslow vacancy-mediated tracer diffusion in two dimensions: The Einstein relation verified. *Physical Review E*, 66:031101, 2002. (Cited on pages 22, 29 and 44.)

[18] L. Berthier and G. Biroli. Theoretical perspective on the glass transition and amorphous materials. *Reviews of Modern Physics*, 83:587–645, 2011. (Cited on page 19.)

[19] L. Berthier, D. Chandler, and J. P. Garrahan. Length scale for the onset of Fickian diffusion in supercooled liquids. *Europhysics Letters*, 69(3):320, 2005. (Cited on page 55.)

[20] R. Blüher, P. Scharwaechter, W. Frank, and H. Kronmüller. First low-temperature radiotracer studies of diffusion in icosahedral quasicrystals. *Physical Review Letters*, 80:1014–1017, 1998. (Cited on page 28.)

[21] H. Böttger and V. V. Bryksin. Hopping Conductivity in Ordered and Disordered Systems (III). *Physica Status Solidi (B)*, 113:9–49, 1982. (Cited on page 187.)

[22] M. J. A. M. Brummelhuis and H. J. Hilhorst. Single-vacancy induced motion of a tracer particle in a two-dimensional lattice gas. *Journal of Statistical Physics*, 53(1-2):249–278, 1988. (Cited on pages 3, 21, 22, 29, 33, 210 and 222.)

[23] M. J. A. M. Brummelhuis and H. J. Hilhorst. Tracer particle motion in a two-dimensional lattice gas with low vacancy density. *Physica A: Statistical Mechanics and its Applications*, 156:575–598, 1989. (Cited on pages 3, 21, 22, 29 and 36.)

[24] S. F. Burlatsky, G. Oshanin, A. M. Cazabat, and M. Moreau. Microscopic Model of Upward Creep of an Ultrathin Wetting Film. *Physical Review Letters*, 76:86–89, 1996. (Cited on page 134.)

[25] S. F. Burlatsky, G. Oshanin, M. Moreau, and W. P. Reinhardt. Motion of a driven tracer particle in a one-dimensional symmetric lattice gas. *Physical Review E*, 54(4):3165, 1996. (Cited on pages 5, 22, 43, 48, 51 and 52.)

[26] S. F. Burlatsky, G. S. Oshanin, A. V. Mogutov, and M. Moreau. Directed walk in a one-dimensional lattice gas. *Physics Letters A*, 166:230–234, 1992. (Cited on pages 22 and 43.)

[27] R. Candelier and O. Dauchot. Creep Motion of an Intruder within a Granular Glass Close to Jamming. *Physical Review Letters*, 103:128001, 2009. (Cited on pages 1 and 19.)

[28] C. Cercignani. *The Boltzmann equation and its applications*. Springer New York, 1988. (Cited on page 19.)

[29] B. S. Chae and E. M. Furst. Probe surface chemistry dependence and local polymer network structure in F-actin microrheology. *Langmuir*, 21:3084–3089, 2005. (Cited on pages 1 and 19.)

[30] D. T. Chen, E. R. Weeks, J. C. Crocker, M. F. Islam, R. Verma, J. Gruber, A. J. Levine, T. C. Lubensky, and a. G. Yodh. Rheological Microscopy: Local Mechanical Properties from Microrheology. *Physical Review Letters*, 90:108301, 2003. (Cited on pages 1 and 19.)

[31] T. Chou, K. Mallick, and R. K. P. Zia. Non-equilibrium statistical mechanics: from a paradigmatic model to biological transport. *Reports on Progress in Physics*, 74:116601, 2011. (Cited on pages 1 and 19.)

[32] E. M. Conwell. Negative Differential Conductivity. *Physics Today*, 23(6):35, 1970. (Cited on page 187.)

[33] F. Corbieri, E. Lippiello, A. Sarracino, and M. Zannetti. Fluctuation-dissipation relations and field-free algorithms for the computation of response functions. *Physical Review E*, 81:011124, 2010. (Cited on page 187.)

[34] L. F. Cugliandolo. The effective temperature. *Journal of Physics A: Mathematical and Theoretical*, 44:483001, 2011. (Cited on page 54.)

[35] H. J. De Bruin and G. E. Murch. Diffusion correlaiton effects in non-stoichiometric solids. *Philosophical Magazine*, 27:1475, 1973. (Cited on page 21.)

[36] D. S. Dean. Langevin equation for the density of a system of interacting Langevin processes. *Journal of Physics A: Mathematical and General*, 29:L613, 1996. (Cited on page 19.)

[37] V. Démery. Mean-field microrheology of a very soft colloidal suspension : inertia induces shear-thickening. *arXiv:1503.00988*, 2015. (Cited on page 20.)

[38] V. Démery, O. Bénichou, and H. Jacquin. Generalized Langevin equations for a driven tracer in dense soft colloids: sonstruction and applications. *New Journal of Physics*, 16:053032, 2014. (Cited on page 20.)

[39] R. Eichhorn, J. Regtmeier, D. Anselmetti, and P. Reimann. Negative mobility and sorting of colloidal particles. *Soft Matter*, 6:1858, 2010. (Cited on page 187.)

[40] A. Einstein. Über die von der molekularkinetischen Theorie der Wärme geforderte Bewegung von in ruhenden Flüssigkeiten suspendierten Teilchen. *Annalen der Physik*, 17:549, 1905. (Cited on page 19.)

[41] M. H. Ernst, T. M. Nieuwenhuizen, and P. F. J. V. Velthoven. Density expansion of transport coefficients on a 2D site-disordered lattice. II. *Journal of Physics A: Mathematical and General*, 20:5335–5350, 1987. (Cited on page 21.)

[42] M. R. Evans and T. Hanney. Nonequilibrium statistical mechanics of the zero-range process and related models. *Journal of Physics A: Mathematical and General*, 38(19):R195–R240, May 2005. (Cited on pages 1 and 20.)

[43] W. Feller. *An Introduction to Probability Theory and Its Applications, Vol. 2*. Wiley, 2nd edition, 1971. (Cited on page 47.)

[44] D. Frenkel. Velocity auto-correlation functions in a 2d lattice Lorentz gas: Comparison of theory and computer simulation. *Physics Letters A*, 121:385–389, 1987. (Cited on page 21.)

[45] I. Gazuz and M. Fuchs. Nonlinear microrheology of dense coloidal suspensions: A mode-coupling theory. *Physical Review E*, 87:032304, 2013. (Cited on page 19.)

[46] I. Gazuz, A. M. Puertas, T. Voigtmann, and M. Fuchs. Active and Nonlinear Microrheology in Dense Colloidal Suspensions. *Physical Review Letters*, 102:248302, 2009. (Cited on page 19.)

[47] D. T. Gillespie. A General Method for Numerically Simulating the Stochastic Time Evolution of Coupled Chemical Reactions. *Journal of computational physics*, 22:403–434, 1976. (Cited on page 154.)

[48] T. Gisler and D. A. Weitz. Scaling of the Microrheology of Semidilute F-Actin Solutions. *Physical Review Letters*, 82:1606–1609, 1999. (Cited on pages 1 and 19.)

[49] R. J. Glauber. Time-Dependent Statistics of the Ising Model. *J. Math. Phys.*, 4(2):294–307, 1963. (Cited on page 136.)

[50] V. Gupta, S. S. Nivarthi, A. V. McCormick, and H. Ted Davis. Evidence for single file diffusion of ethane in the molecular sieve AlPO4-5. *Chemical Physics Letters*, 247:596–600, 1995. (Cited on page 42.)

[51] P. Habdas, D. Schaar, A. C. Levitt, and E. R. Weeks. Forced motion of a probe particle near the colloidal glass transition. *Europhysics Letters*, 67(3):477–483, 2004. (Cited on pages 1 and 19.)

[52] K. Hahn, J. Kärger, and V. Kukla. Single-File Diffusion Observation. *Physical Review Letters*, 76:2762, 1996. (Cited on page 42.)

[53] C. J. Harrer, D. Winter, J. Horbach, M. Fuchs, and T. Voigtmann. Force-induced diffusion in microrheology. *Journal of Physics: Condensed Matter*, 24:464105, 2012. (Cited on pages 54 and 55.)

[54] T. Harris. Diffusion with 'collisions' between particles. *Journal of Applied Probability*, 2:323–338, 1965. (Cited on pages 5, 21 and 42.)

[55] R. Hawkins, M. Piel, G. Faure-Andre, A. M. Lennon-Dumenil, J. F. Joanny, J. Prost, and R. Voituriez. Pushing off the Walls: A Mechanism of Cell Motility in Confinement. *Physical Review Letters*, 102:058103, 2009. (Cited on page 42.)

[56] F. Höfling and T. Franosch. Anomalous transport in the crowded world of biological cells. *Reports on Progress in Physics*, 76:046602, 2013. (Cited on page 54.)

[57] J. Howard. *Mechanics of Motor Proteins and the Cytoskeleton*. Sinauer Associates, Inc., 2005. (Cited on page 134.)

[58] B. D. Hughes. *Random Walks and Random Environments: Random walks, Volume 1*. Oxford University, New York, 1995. (Cited on pages 4, 31, 35, 45, 75, 76, 106, 108, 117, 129, 173, 185 and 221.)

[59] B. D. Hughes and M. F. Shlesinger. Lattice dynamics, random walks, and nonintegral effective dimensionality. *Journal of Mathematical Physics*, 23(1982):1688, 1982. (Cited on page 117.)

[60] S. Ishioka and M. Koiwa. On the correlation effect in self-diffusion via the vacancy mechanism. *Philosophical Magazine A*, 41:385, 1980. (Cited on page 21.)

[61] R. L. Jack, D. Kelsey, J. P. Garrahan, and D. Chandler. Negative differential mobility of weakly driven particles in models of glass formers. *Physical Review E*, 78:011506, 2008. (Cited on pages 55 and 187.)

[62] K. Kawasaki. Diffusion Constants near the Critical Point for Time-Dependent Ising Models. I. *Physical Review*, 145:224–230, 1966. (Cited on page 135.)

[63] K. W. Kehr and K. Binder. Simulation of Diffusion in Lattice Gases and Related Kinetic Phenomena. In *Applications of the Monte Carlo Method in Statistical Physics*, pages 181–221. Springer, Berlin, 1984. (Cited on page 20.)

[64] K. W. Kehr, R. Kutner, and K. Binder. Diffusion in concentrated lattice gases. Self-diffusion of noninteracting particles in three-dimensional lattices. *Physical Review B*, 23:4931–4945, 1981. (Cited on pages 21 and 29.)

[65] P. Klugkist, K. Rätzke, and F. Faupel. Evidence of Defect-Mediated Zirconium Self-Diffusion in Amorphous Co92Zr8. *Physical Review Letters*, 81:614, 1998. (Cited on page 28.)

[66] M. Koiwa. On the possible effect of the vacancy concentration on the correlation factor for tracer diffusion via vacancy mechanism. *J. Phys. Soc. Jpn.*, 45:1327, 1978. (Cited on page 21.)

[67] T. Komorowski and S. Olla. On Mobility and Einstein Relation for Tracers in Time-Mixing Random Environments. *Journal of Statistical Physics*, 118:407–435, 2005. (Cited on pages 22 and 134.)

[68] M. Kostur, L. Machura, P. Hänggi, J. Luczka, and P. Talkner. Forcing inertial Brownian motors: Efficiency and negative differential mobility. *Physica A: Statistical Mechanics and its Applications*, 371:20–24, 2006. (Cited on page 187.)

[69] P. L. Krapivsky, K. Mallick, and T. Sadhu. Large Deviations in Single-File Diffusion. *Physical Review Letters*, 113:078101, 2014. (Cited on page 42.)

[70] K. Kruse and K. Sekimoto. Growth of fingerlike protrusions driven by molecular motors. *Physical Review E*, 66:031904, 2002. (Cited on page 134.)

[71] R. Kubo. The fluctuation-dissipation theorem. *Reports on Progress in Physics*, 29:255, 1966. (Cited on page 19.)

[72] C. Landim, S. Olla, and S. B. Volchan. Driven Tracer Particle in One Dimensional Symmetric Simple Exclusion. *Communications in Mathematical Physics*, 192:287–307, 1998. (Cited on pages 5, 22, 43, 48 and 52.)

[73] P. Langevin. Sur la théorie du mouvement brownien. *Comptes rendus de l'Académie des Sciences (Paris)*, 146:530, 1908. (Cited on page 19.)

[74] A. W. C. Lau, B. D. Hoffman, A. Davies, J. C. Crocker, and T. C. Lubensky. Microrheology, Stress Fluctuations, and Active Behavior of Living Cells. *Physical review letters*, 91:198101, 2003. (Cited on pages 1 and 19.)

[75] A. D. Le Claire. Correlation Effects in Diffusion in Solids. In *Physical Chemistry - an Advanced Treatise, Vol. X*, chapter 5. Academic Press, 1970. (Cited on page 20.)

[76] X. L. Lei, N. J. M. Horing, and H. L. Cui. Theory of negative differential conductivity in a superlattice miniband. *Physical Review Letters*, 66:3277–3280, 1991. (Cited on page 187.)

[77] S. Leitmann and T. Franosch. Nonlinear Response in the Driven Lattice Lorentz Gas. *Physical Review Letters*, 111:190603, 2013. (Cited on pages 17, 23, 170, 182, 187, 189 and 202.)

[78] D. G. Levitt. Dynamics of a Single-File Pore: Non-Fickian Behavior. *Physical Review A*, 8:3050–3054, 1973. (Cited on pages 21 and 42.)

[79] B. Lin, M. Meron, B. Cui, S. A. Rice, and H. Diamant. From Random Walk to Single-File Diffusion. *Physical Review Letters*, 94:216001, 2005. (Cited on page 42.)

[80] L. Lizana and T. Ambjörnsson. Single-File Diffusion in a Box. *Physical Review Letters*, 100:200601, 2008. (Cited on pages 21 and 42.)

[81] C. Loverdo, O. Bénichou, M. Moreau, and R. Voituriez. Enhanced reaction kinetics in biological cells. *Nature Physics*, 4:134–137, 2008. (Cited on page 42.)

[82] K. Mallick. The exclusion process: A paradigm for non-equilibrium behaviour. *Physica A*, 418:17–48, 2015. (Cited on pages 1 and 20.)

[83] M. C. Marchetti, J. F. Joanny, S. Ramaswamy, T. B. Liverpool, J. Prost, M. Rao, and R. A. Simha. Hydrodynamics of soft active matter. *Reviews of Modern Physics*, 85:1143–1189, 2013. (Cited on pages 1 and 19.)

[84] U. M. B. Marconi, A. Puglisi, L. Rondoni, and A. Vulpiani. Fluctuation-dissipation: Response theory in statistical physics. *Physics Reports*, 461:111–195, 2008. (Cited on pages 1, 19 and 54.)

[85] W. H. McCrea and F. J. W. Whipple. Random Paths in Two and Three Dimensions. *Proceedings of the Royal Society of Edinburgh*, 60(03):281–298, 1940. (Cited on page 222.)

[86] C. Mejia-Monasterio and G. Oshanin. Bias- and bath-mediated pairing of particles driven through a quiescent medium. *Soft Matter*, 7:993, 2010. (Cited on page 205.)

[87] A. Meyer, A. Marshall, B. G. Bush, and E. M. Furst. Laser tweezer microrheology of a colloidal suspension. *Journal of Rheology*, 50:77, 2006. (Cited on pages 1 and 19.)

[88] G. L. Montet. Integral Methods in the Calculation of Correlation Factors in Diffusion. *Physical Review B*, 7:650–662, 1973. (Cited on page 21.)

[89] E. W. Montroll. Random walks on lattices. *Proceedings of Symposia on Applied Mathematics*, 16:193–220, 1964. (Cited on page 35.)

[90] E. W. Montroll. Random Walks on Lattices. III. Calculation of First-Passage Times with Application to Exciton Trapping on Photosynthetic Units. *Journal of Mathematical Physics*, 10(4):753, 1969. (Cited on page 117.)

[91] G. Murch and R. Thorn. Interstitial solute diffusion in metals. *J. Phys. Chem. Solids*, 38:789, 1977. (Cited on page 21.)

[92] K. Nakazato and K. Kitahara. Site blocking effect in tracer diffusion on a lattice. *Progress of Theoretical Physics*, 64(6):2261, 1980. (Cited on pages 21 and 22.)

[93] F. Nava, C. Canali, F. Catellani, G. Gavioli, and G. Ottaviani. Electron drift velocity in high-purity Ge between 8 and 240K. *Journal of Physics C: Solid State Physics*, 9:1685–1689, 1676. (Cited on page 187.)

[94] T. J. Newman. Continuum theory of vacancy-mediated diffusion. *Physical Review B*, 59:754–763, 1999. (Cited on page 29.)

[95] T. M. Nieuwenhuizen, P. F. J. van Velthoven, and M. H. Ernst. Diffusion and Long-Time Tails in a Two-Dimensional Site-Percolation Model. *Physical Review Letters*, 57:2477, 1986. (Cited on page 21.)

[96] T. M. Nieuwenhuizen, P. F. J. van Velthoven, and M. H. Ernst. Density expansion of transport properties on 2D site-disordered lattices: I. General theory. *Journal of Physics A: Mathematical and General*, 20:4001–4015, 1987. (Cited on page 21.)

[97] G. Oshanin, J. De Coninck, A. M. Cazabat, and M. Moreau. Dewetting, partial wetting and spreading of a two-dimensional monolayer on solid surface. *Physical Review E*, 58:20(R), 1998. (Cited on page 134.)

[98] A. Parmeggiani, T. Franosch, and E. Frey. Phase Coexistence in Driven One-Dimensional Transport. *Physical Review Letters*, 90:086601, 2003. (Cited on page 134.)

[99] A. Parmeggiani, T. Franosch, and E. Frey. Totally asymmetric simple exclusion process with Langmuir kinetics. *Physical Review E*, 70:046101, Oct. 2004. (Cited on page 134.)

[100] B. N. J. Persson and E. Tosatti. Layering transition in confined molecular thin films: Nucleation and growth. *Physical Review B*, 50:5590–5599, 1994. (Cited on page 134.)

[101] G. Pólya. Über eine Aufgabe der Wahrscheinlichkeitsrechnung betreffend die Irrfahrt im Straßennetz. *Mathematische Annalen*, 84(1-2):149–160, 1921. (Cited on page 29.)

[102] A. M. Puertas and T. Voigtmann. Microrheology of colloidal systems. *Journal of Physics: Condensed Matter*, 26:243101, 2014. (Cited on pages 1, 19, 20 and 205.)

[103] O. F. Sankey and P. A. Fedders. Correlation functions for simple hopping in a face-centered-cubic lattice. *Physical Review B*, 20:39–45, 1979. (Cited on page 21.)

[104] C. F. E. Schroer and A. Heuer. Anomalous Diffusion of Driven Particles in Supercooled Liquids. *Physical Review Letters*, 110:067801, 2013. (Cited on pages 55 and 93.)

[105] C. A. Sholl. Diffusion correlation factors and atomic displacements for the vacancy mechanism. *Journal of Physics C: Solid State Physics*, 14:2723–2729, 1981. (Cited on pages 21 and 29.)

[106] J. G. Skellam. The Frequency Distribution of the Difference Between Two Poisson Variates Belonging to Different Populations. *Journal of the Royal Statistical Society*, 109(3):296, 1946. (Cited on page 51.)

[107] G. W. Slater, H. L. Guo, and G. I. Nixon. Bidirectional Transport of Polyelectrolytes Using Self-Modulating Entropic Ratchets. *Physical Review Letters*, 78:1170–1173, 1997. (Cited on page 187.)

[108] R. Soto and R. Golestanian. Run-and-tumble dynamics in a crowded environment: Persistent exclusion process for swimmers. *Physical Review E*, 89:012706, 2014. (Cited on page 205.)

[109] T. M. Squires and J. F. Brady. A simple paradigm for active and nonlinear microrheology. *Physics of Fluids*, 17:073101, 2005. (Cited on page 19.)

[110] T. M. Squires and T. G. Mason. Fluid Mechanics of Microrheology. *Annual Review of Fluid Mechanics*, 42:413–438, 2010. (Cited on pages 1 and 19.)

[111] C. J. Stanton, H. U. Baranger, and J. W. Wilkins. Analytic Boltzmann equation approach for negative differential mobility in two-valley semiconductors. *Applied Physics Letters*, 49:176–178, 1986. (Cited on page 187.)

[112] R. A. Tahir-Kheli and R. J. Elliott. Correlated random walk in lattices: Tracer diffusion at general concentration. *Physical Review B*, 27:844, 1983. (Cited on page 21.)

[113] R. van Gastel, E. Somfai, S. B. Van Albada, W. Van Saarloos, and J. W. M. Frenken. Nothing moves a surface: Vacancy mediated surface diffusion. *Physical Review Letters*, 86:1562–1565, 2001. (Cited on page 28.)

[114] R. van Gastel, E. Somfai, W. van Saarloos, and J. W. M. Frenken. A giant atomic slide-puzzle. *Nature*, 408:665, 2000. (Cited on page 28.)

[115] Q. Wei, C. Bechinger, and P. Leiderer. Single-File Diffusion of Colloids in One-Dimensional Channels. *Science*, 287(5453):625–627, 2000. (Cited on page 42.)

[116] L. G. Wilson, A. W. Harrison, W. C. K. Poon, and A. M. Puertas. Microrheology and the fluctuation theorem in dense colloids. *Europhysics Letters*, 93:58007, 2011. (Cited on page 19.)

[117] L. G. Wilson and W. C. K. Poon. Small-world rheology: an introduction to probe-based active microrheology. *Physical Chemistry Chemical Physics*, 13:10617–10630, 2011. (Cited on page 42.)

[118] D. Winter, J. Horbach, P. Virnau, and K. Binder. Active Nonlinear Microrheology in a Glass-Forming Yukawa Fluid. *Physical Review Letters*, 108:028303, 2012. (Cited on pages 54, 55 and 93.)

[119] R. Würschum, P. Farber, R. Dittmar, P. Scharwaechter, W. Frank, and H. E. Schaefer. Thermal Vacancy Formation and Self-Diffusion in Intermetallic Fe3Si Nanocrystallites of Nanocomposite Alloys. *Physical Review Letters*, 79:4918–4921, 1997. (Cited on page 28.)

[120] W. M. Young and E. W. Elcock. Monte Carlo studies of vacancy migration in binary ordered alloys: I. *Proceedings of the Physical Society*, 89:735, 1966. (Cited on page 154.)

[121] R. K. P. Zia, E. L. Praestgaard, and O. G. Mouritsen. Getting more from pushing less: Negative specific heat and conductivity in nonequilibrium steady states. *American Journal of Physics*, 70(4):384, 2002. (Cited on page 187.)

[122] F. Ziemann, J. Rädler, and E. Sackmann. Local Measurements of Viscoelastic Moduli of Entangled Actin Networks Using an Oscillating Magnetic Bead Micro-Rheometer. *Biophysical Journal*, 66:2210–2216, 1994. (Cited on pages 1 and 19.)

Remerciements

Je remercie tout d'abord David Dean et Ludovic Berthier, qui ont accepté d'être rapporteurs de ce manuscrit. Je remercie également les autres membres du jury, Leticia Cugliandolo, Kirone Mallick et Andrea Parmeggiani, qui ont accepté de s'intéresser à mon travail et de l'évaluer.

Je suis très reconnaissant envers Olivier Bénichou, qui m'a initié à la physique des marches aléatoires dès le début du M2 Physique des Liquides, et qui m'a accueilli comme doctorant quelques mois plus tard. Pendant ces trois années, j'ai bénéficié de ses connaissances et de sa pédagogie. Il m'a proposé de nombreux projets très intéressants, et il a su me guider et m'apprendre de nombreuses techniques. Sa gentillesse, sa disponibilité, et son optimisme sans faille sont pour beaucoup dans la réussite de cette thèse. J'ai également bénéficié de la co-direction de Raphaël Voituriez, que je remercie pour son encadrement attentif, ses remarques et questions qui m'ont donné à réfléchir, et l'éclairage différent qu'il a apporté à certains résultats.

Je remercie Gleb Oshanin, qui a suivi attentivement mon travail, qui m'a donné de nombreux conseils, et qui m'a fait rencontrer beaucoup d'autres physiciens. Je le remercie en particulier de m'avoir donné la chance de présenter mon travail à Singapour en mai 2015.

Un grand merci à Alessandro Sarracino, avec qui j'ai eu le plaisir de travailler pendant la deuxième moitié de ma thèse. Merci également à Carlos Mejía-Monasterio avec qui j'ai collaboré pour une partie des travaux présentés dans ce manuscrit.

J'ai eu la chance d'enseigner pendant ma thèse, et je remercie les enseignants de l'UPMC et du Lycée Saint-Louis qui m'ont donné cette opportunité.

J'ai beaucoup apprécié ces trois années au LPTMC. Merci à Pascal Viot, dont la disponibilité était très précieuse, que ce soit pour discuter de questions scientifiques, informatiques ou administratives ! Merci à Bertrand Delamotte, parrain auprès de l'école doctorale (et parrain du commerce de café interne au labo), dont j'ai eu le plaisir de suivre les cours de renormalisation non-perturbative à Saclay en janvier-février 2014. Merci à Annie Lemarchand, pour ses conseils relatifs à la rédaction du manuscrit et à la soutenance. Merci à Hélène Berthoumieux, organisatrice des séminaires de doctorants, auxquels j'ai participé avec plaisir. Enfin, merci à l'équipe administrative, Diane Domand, Sylvie Dalla Foglia et Liliane Cruzel, pour leur aide et leur gentillesse.

Un grand merci à mes "grands frères" de thèse, Thibaut Calandre et Jean-François Rupprecht, pour tous les bons moments passés entre le labo, la piscine Pontoise et l'incontournable boulangerie Cocherel. Merci à Marie Chupeau et Nicolas Levernier, qui prennent le relais en pièce 519, et avec qui j'ai beaucoup apprécié discuter et partager des déjeuners. Merci aux post-docs de l'équipe que j'ai eu le plaisir de côtoyer : Thomas Guérin, Clément Touya et Simon Moulieras. Merci aux autres thésard-e-s et post-docs du labo, pour toutes les pauses café et les soirées autour d'une bière.

Un immense merci à mes ami-e-s, qui m'ont permis d'avoir une vie sociale plus que nécessaire en dehors du labo, et avec qui j'ai eu le plaisir de partager des soirées, des restaus, des pique-niques, des séances de ciné, des débats animés, des week-ends, des vacances... Je ne me risquerai pas à les énumérer de peur d'en oublier, mais ils et elles se reconnaitront et savent l'amitié que je leur porte. Merci également à mes partenaires musicaux, avec qui j'ai partagé des moments très épanouissants.

Enfin, mes derniers remerciements vont à mes parents et à ma soeur, à qui je dois énormément. Ils m'ont beaucoup appris, et ils m'ont toujours soutenu.

Fluctuations et corrélations d'un traceur biaisé dans un gaz de coeurs durs

Résumé:

Nous étudions la dynamique d'un traceur soumis à une force extérieure dans un bain de particules. Nous proposons un modèle qui prend en compte explicitement la dynamique du bain, et qui décrit les corrélations entre la dynamique du traceur et la réponse du bain. Nous considérons un traceur biaisé dans un gaz de coeurs durs sur réseau : le traceur réalise une marche aléatoire biaisée tandis que les particules du bain réalisent des marches aléatoires symétriques. Nous étudions plus particulièrement les fluctuations de la position du traceur.

Dans la limite de haute densité, nous obtenons des résultats exacts à l'ordre dominant en la densité de lacunes. En géométrie confinée, un calcul analytique des fluctuations de la position du traceur prévoit un long régime superdiffusif, et une transition vers un régime diffusif final. Nous proposons une description simplifiée du système qui révèle le mécanisme physique à l'origine de ce comportement anormal. Nous montrons l'existence d'une anomalie de la vitesse du traceur dans les systèmes quasi-1D.

Nous étudions également le cas général d'une densité arbitraire de particules sur un réseau en contact avec un réservoir. Cette situation constitue un problème à N corps décrit par une équation maîtresse, qui ne peut être résolue qu'en recourant à une approximation de type champ moyen consistant en le découplage de certaines fonctions de corrélation. Il est alors possible de déterminer des valeurs approchées de la vitesse, de coefficient de diffusion du traceur ainsi que de la distribution de position du traceur. Nous montrons enfin que l'approximation de découplage est exacte dans les limites de basse et de haute densité.

Mots-clés :

gaz sur réseau, diffusion de traceur, fluctuations, diffusion anormale, processus stochastiques, marches aléatoires

Fluctuations and correlations of a driven tracer in a hardcore lattice gas

Abstract:

We study the dynamics of a tracer submitted to an external force in a bath of particles. We propose a model which takes explicitly into account the dynamics of the bath, and which describes the correlations between the dynamics of the tracer and the response of the bath. We consider a biased tracer in a lattice gas of hardcore particles: the tracer performs a biased random walk whereas the bath particles perform symmetric random walks. We study in particular the fluctuations of the position of the tracer.

In the high-density limit, we obtain exact results at leading order in the density of vacancies. In confined geometries, an analytical calculation of the fluctuations of tracer position predicts a long superdiffusive regime, and a crossover to an ultimate diffusive regime. We give a simplified description of the system that unveils the physical mechanism explaining this anomalous behavior. We show the existence of a velocity anomaly in quasi-1D systems.

We also study the general case of an arbitrary density of particles on a lattice in contact with a reservoir. This situation is a N-body problem described by a master equation, that can be solved by resorting to a mean-field-type approximation, which consists in the decoupling of relevant correlation functions. It is then possible to determine approximate values of the velocity, the diffusion coefficient and the distribution of the position of the tracer. We finally show that the decoupling approximation is exact in the high-density and low-density limits.

Keywords:

lattice gas, tracer diffusion, fluctuations, anomalous diffusion, stochastic processes, random walks